UNIVERSITÀ DELLA CALABRIA

UNIVERSITÀ DELLA CALABRIA

Dipartimento di Fisica

Dottorato di Ricerca in

Scienze e Tecnologie Fisiche, Chimiche e dei Materiali

XXXV CICLO

TITOLO TESI

Probing the high-energy dynamics of QCD: selected theoretical and phenomenological studies

Settore Scientifico Disciplinare

FIS/02 – FISICA TEORICA, MODELLI E METODI MATEMATICI

Coordinatore: Ch.ma Prof.ssa Gabriella Cipparrone

Firma 

Supervisore: Ch.mo Prof. Alessandro Papa

Firma 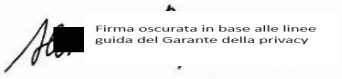

Dottorando: Dott. Michael Fucilla

Firma 

I wish to report you, that I am still doing physics, but, I must admit, that only nine hours per day. I still enjoy doing physics, I think, that we made a correct decision, choosing physics as the way of life. At least I have not felt bored even a minute in my life. Every time when I put my formulae on the sheet of paper I feel myself as a young guy from Gribov's department, who is hurrying up to meet you and discuss, what I have understood. All our hopes, all our ideas, all our dreams are still with me and I am trying to share them with young physicists.

Eugene M. Levin [1, 2]

Acknowledgements

First of all, I want to thank my supervisor Alessandro immensely for his availability, his attention and for all the knowledge he shared with me. I am sure that the passion for this field that he has passed on to me will never fade. I could not have written this manuscript without Alessandro's guidance and his inspiring way of approaching physics: strongly, formally and deeply.

A big thank you also goes to Samuel and Lech. During my visiting periods, I had the opportunity to work with them and with their young collaborators. I could not have had a more beautiful experience, from the professional and the personal point of view. Benefiting from their vast knowledge, I had the opportunity to expand my research interests and learn about multiple aspects of QCD, ranging from saturation physics to exclusive processes. I am proud to have the opportunity to continue my path in physics collaborating with them. I am grateful to the IJCLAB and NCBJ Warsaw for their hospitality and support.

I would also like to thank some colleagues I have worked and interacted with over the years. First of all, Francesco for having stimulated my interest in numerical analysis and phenomenology, sharing with me his experience and his tools. Subsequently, I would like to thank Emilie and Saad with whom I have had innumerable discussions, which have helped me grow enormously as a physicist. With Emilie we already have a nice paper together, with Saad I'm sure we will soon. It is a pleasure to thank Victor S. Fadin, Dmitry Yu. Ivanov, Andrey Grabovsky, Mohammed M.A. Mohammed and Andrèe Dafne Bolognino for their collaboration in the devolpment of some of the papers on which this thesis is based. For interesting and inspiring discussions, I want also to thank: Renaud Boussarie, Maxim Nefedov, Valerio Bertone, Benoît Blossier, Cédric Mezrag, Jean-Philippe Lansberg, Michael Winn, Charlotte Van Hulse, Ronan McNulty,

Marco Rossi, Jamal Jalilian-Marian and Michel Fontannaz.

I would like to thank Leszek Motyka and Tuomas Lappi for accepting to be the referee of this work and for inspiring comments.

I want to thank all my family and friends who have supported me over the years. A special thanks to my friend Mario, who has been close to me, like a brother, in many difficult moments of these years.

I want to thank my mum, dad and Mattia from deep in my heart. Without their support, this journey and my life in general would have been much more difficult.

Last but not least, I dedicate this thesis and my efforts in writing it to Laura, love of my life and my *place to be*.

Abstract

The center-of-mass energies available at modern accelerators, such as the Large Hadron Collider (LHC), and at future generation accelerators, such as the Electron-Ion Collider (EIC) and Future Circular Collider (FCC), offer us a unique opportunity to investigate hadronic matter under the most extreme conditions ever reached. In particular, we can access the *Regge-Gribov* (or *semi-hard*) limit of QCD, characterized by the scale hierarchy $s \gg \{Q^2\} \gg \Lambda^2_{\rm QCD}$, where $\sqrt{s}$ is the center-of-mass energy, $\{Q\}$ a set of hard scales characterizing the process and $\Lambda_{\rm QCD}$ is the QCD mass scale. In this limit, large logarithmic corrections can affect both parton densities and hard scattering cross sections. The Balitsky-Fadin-Kuraev-Lipatov (BFKL) approach represents the established tool to resum to all orders, both in the leading (LLA) and the next-to-leading (NLA) approximation, these large-energy logarithmic contributions. However, it is well known that at very low values of the Bjorken-x, the density of partons, per unit transverse area, in hadronic wavefunctions becomes very large leading to the so-called *saturation effects*. The evolution of densities is then described by non-linear generalizations of the BFKL equation. Among these, the most general is represented by the Balitsky-JIMWLK hierarchy of equations, which is needed to describe the scattering of a dilute projectile on a dense target, or also the scattering of two dense systems. The dense system condition can be achieved by a very small-x proton, but is more easily achieved for large nuclei.

It is clear that a detailed comparison with experimental data requires precision predictions that can only be achieved in the next-to-leading logarithmic approximation or beyond. We face this task from two different perspectives. On the one hand developing analytical calculations that allow to increase the theoretical accuracy that can be reached in predictions, and on the other, by proposing phenomenological analyzes that can be directly tested experimentally. In particular, within the BFKL approach we calculate the full NLO impact factor for the Higgs production. This is the necessary ingredient to

study the inclusive forward emissions of a Higgs boson in association with a backward identified jet. We claim that this result should necessarily supplement pure fixed-order calculations entering in the collinear factorization framework, which cannot be able to describe the entire kinematic spectrum in the Higgs-plus-jet channel. The result can be as well used to describe the inclusive hadroproduction of a forward Higgs in the limit of small Bjorken x. Moreover, using the knowledge of already known impact factors we propose a series of new semi-hard reactions that can be used to investigate BFKL dynamics at the LHC. We investigate all observables used so far to study BFKL, including: total cross sections, azimuthal coefficients, azimuthal distributions and p_T-differential distributions. In the context of linear evolution, we consider also the problem of extending BFKL beyond the NLLA. To this aim, we compute the Lipatov vertex in QCD with higher ϵ-accuracy, where $\epsilon = (D-4)/2$. This ingredient enters the BFKL kernel at next-to-NLA (NNLLA) accuracy. In fact, the NNLLA formulation of BFKL requires not only two and three-loop calculations, but also higher ϵ-accuracy of the one-loop results, for instance, in the part of the kernel containing the product of two one-loop Lipatov vertices. Finally, in the saturation framework, and more specifically in the Shockwave approach, we calculate the diffractive double hadron photo- or electroproduction cross sections with full NLL accuracy. These results are usable to detect saturation effects, at both the future EIC or already at LHC, using Ultra Peripheral Collisions.

Sintesi in lingua italiana

Le energie nel centro di massa disponibili ai moderni acceleratori, come il Large Hadron Collider (LHC), e a gli acceleratori di futura generazione, come l'Electron-Ion Collider (EIC) e il Future Circular Collider (FCC), ci offrono un'opportunità unica di indagare la materia adronica nelle condizioni più estreme mai raggiunte. In particolare, possiamo accedere al limite di *Regge-Gribov* (o *semi-duro*) della QCD, caratterizzato dalla gerarchia di scale $s \gg \{Q^2\} \gg \Lambda^2_{\rm QCD}$, dove $\sqrt{s}$ è l'energia nel centro di massa, $\{Q\}$ un insieme di scale dure che caratterizzano il processo e $\Lambda_{\rm QCD}$ è la scala di massa della QCD. In questo limite, grandi correzioni logaritmiche entrano in gioco sia nelle funzioni di distribuzione partoniche che nelle sezioni d'urto dure. L'approccio BFKL è lo strumento appropriato per risommare a tutti gli ordini, sia nell'approssimazione dei logaritmi dominanti (LLA) che nell'approssimazione dei logaritmi sottodominanti (NLA), questi contributi logaritmici. Tuttavia, è ben noto che a valori molto bassi della variabile di Bjorken x, la densità dei partoni, per unità di area trasversale, nelle funzioni d'onda adroniche diventa molto grande conducendo ai cosiddetti *effetti di saturazione*. L'evoluzione delle densità deve essere allora descritta da generalizzazioni non lineari dell'equazione BFKL. Tra queste, la più generale è rappresentata dalla gerarchia di equazioni di Balitsky-JIMWLK, necessaria per descrivere la diffusione di un proiettile "diluito" su un bersaglio denso, o anche la diffusione di due sistemi densi. La condizione di sistema denso può essere raggiunta da un protone ad x molte piccole, ma è più facilmente raggiungibile per grandi nuclei.

Risulta chiaro che, un confronto dettagliato con i dati sperimentali richiede delle predizioni di precisione che possono essere raggiunte solo nell'approssimazione dei logaritmi sottodominanti o oltre. Affrontiamo questo compito da due diverse prospettive. Da un lato sviluppando calcoli analitici che consentano di aumentare l'accuratezza teorica raggiungibile nelle previsioni e, dall'altro, proponendo analisi fenomenologiche direttamente verificabili sperimentalmente. In particolare, nell'ambito dell'approccio BFKL calcoliamo

il fattore di impatto per la produzione di un bosone di Higgs, nell'approssimazione sottodominante. Questo è l'ingrediente necessario per studiare le emissioni inclusive di un bosone di Higgs in associazione ad un jet identificato. Crediamo che questo risultato dovrebbe necessariamente supportare i puri calcoli ad ordine fissato che entrano nella fattorizzazione collineare, che non posso descrivere l'intero spettro cinematico nel canale di Higgs più jet. Il risultato può essere utilizzato anche per descrivere l'adroproduzione inclusiva di un Higgs nel limite di basso x. Inoltre, utilizzando la conoscenza dei fattori di impatto già noti, proponiamo una serie di nuove reazioni semi-dure che possono essere utilizzate per studiare la dinamica BFKL ad LHC. Indaghiamo tutte le osservabili utilizzate finora per studiare BFKL, tra cui: sezioni d'urto totali, coefficienti azimutali, distribuzioni azimutali e distribuzioni differenziali nel p_T. Nel contesto dell'evoluzione lineare, consideriamo anche il problema dell'estensione di BFKL oltre l'approssimazione dei logaritmi sottodominanti. A tale scopo, calcoliamo il vertice di Lipatov in QCD con maggiore accuratezza in ϵ. Questo ingrediente entra nel kernel BFKL con precisione successiva a quella sottodominante. Infatti, a questo grado di accuratezza, la formulazione di BFKL richiede non solo calcoli a due e tre loop, ma anche una maggiore accuratezza in ϵ dei risultati a un loop, per esempio, nella parte del kernel che contiene il prodotto di due vertici di Lipatov ad un loop. Infine, nel quadro della saturazione, e più specificamente nell'approccio Shockwave, calcoliamo le sezioni d'urto diffrattive della foto- o elettroproduzione di due adroni con precisione sottodominante. Questi risultati sono utilizzabili per rilevare effetti di saturazione, sia al futuro EIC che già ad LHC, utilizzando collisioni ultra-periferiche.

List of Publications

Regular articles

- V. S. Fadin, M. Fucilla and A. Papa, *One-loop Lipatov vertex in QCD with higher ϵ-accuracy*, JHEP **04** (2023), 137
  arXiv:2302.09868, DOI: 10.1007/JHEP04(2023)137.

- M. Fucilla, A. V. Grabovsky, E. Li, L. Szymanowski and S. Wallon, *NLO computation of diffractive di-hadron production in a saturation framework*, JHEP **03** (2023), 159
  arXiv:2211.05774, DOI: 10.1007/JHEP03(2023)159

- F. G. Celiberto, M. Fucilla, D. Y. Ivanov, M. M. A. Mohammed and A. Papa, *The next-to-leading order Higgs impact factor in the infinite top-mass limit*, JHEP **08** (2022), 092
  arXiv:2205.02681, DOI:10.1007/JHEP08(2022)092.

- F. G. Celiberto, M. Fucilla, M. M. A. Mohammed and A. Papa, *Ultraforward production of a charmed hadron plus a Higgs boson in unpolarized proton collisions*, Phys. Rev. **D 105** (2022) no.11, 114056
  arXiv:2205.13429, DOI:10.1103/PhysRevD.105.114056.

- F. G. Celiberto and M. Fucilla, *Diffractive semi-hard production of a J/ψ or a Υ from single-parton fragmentation plus a jet in hybrid factorization*, Eur. Phys. J. C **82** (2022) no.10, 929
  arXiv:2202.12227, DOI:10.1140/epjc/s10052-022-10818-8.

- F. G. Celiberto, M. Fucilla, D. Y. Ivanov, M. M. A. Mohammed and A. Papa, *Bottom-flavored inclusive emissions in the variable-flavor number scheme: A high-*

energy analysis, Phys. Rev. **D 104** (2021) no.11, 114007
arXiv:2109.11875, DOI:10.1103/PhysRevD.104.114007.

- F. G. Celiberto, M. Fucilla, D. Y. Ivanov and A. Papa, *High-energy resummation in Λ_c baryon production*, Eur. Phys. J. C **81** (2021) no.8, 780
arXiv:2105.06432, DOI:10.1140/epjc/s10052-021-09448-3.

- A. D. Bolognino, F. G. Celiberto, M. Fucilla, D. Y. Ivanov and A. Papa, *"Inclusive production of a heavy-light dijet system in hybrid high-energy and collinear factorization,"* Phys. Rev. **D 103** (2021) no.9, 094004
arXiv:2103.07396, DOI:10.1103/PhysRevD.103.094004.

- A. D. Bolognino, F. G. Celiberto, M. Fucilla, D. Y. Ivanov and A. Papa, *"High-energy resummation in heavy-quark pair hadroproduction,"* Eur. Phys. J. C **79** (2019) no.11, 939
arXiv:1909.03068, DOI:10.1140/epjc/s10052-019-7392-1.

Review, community and white papers

- M. Begel, S. Hoeche, M. Schmitt, H. W. Lin, P. M. Nadolsky, C. Royon, Y. J. Lee, S. Mukherjee, C. Baldenegro and J. Campbell, *et al.* *"Precision QCD, Hadronic Structure & Forward QCD, Heavy Ions: Report of Energy Frontier Topical Groups 5, 6, 7 submitted to Snowmass 2021,"*
arXiv:2209.14872, .

- M. Hentschinski, C. Royon, M. A. Peredo, C. Baldenegro, A. Bellora, R. Boussarie, F. G. Celiberto, S. Cerci, G. Chachamis and J. G. Contreras, *et al.* *"White Paper on Forward Physics, BFKL, Saturation Physics and Diffraction,"* Acta Phys.Polon.B 54 (2023)
arXiv:2203.08129. DOI:10.5506/APhysPolB.54.3-A2

- J. L. Feng, F. Kling, M. H. Reno, J. Rojo, D. Soldin, L. A. Anchordoqui, J. Boyd, A. Ismail, L. Harland-Lang and K. J. Kelly, *et al.* *"The Forward Physics Facility at the High-Luminosity LHC,"* J. Phys. **G 50** (2023) no.3, 030501
arXiv:2203.05090, DOI: 10.1016/j.physrep.2022.04.004.

- L. A. Anchordoqui, A. Ariga, T. Ariga, W. Bai, K. Balazs, B. Batell, J. Boyd, J. Bramante, M. Campanelli and A. Carmona, *et al.* *"The Forward Physics Facility: Sites, experiments, and physics potential,"* Phys. Rept. **968** (2022), 1-50 arXiv:2109.10905, DOI:10.1088/1361-6471/ac865e.

Conference papers

- M. Fucilla, *"The Higgs impact factor at next-to-leading order,"* Difflowx2022. arXiv:2212.01794.

- A. D. Bolognino, F. G. Celiberto, M. Fucilla, D. Y. Ivanov, M. M. A. Mohammed and A. Papa, *"High-energy signals from heavy-flavor physics,"* Difflowx2022. arXiv:2211.16818.

- M. Fucilla, A. V. Grabovsky, L. Szymanowski, E. Li and S. Wallon, *"Diffractive di-hadron production at NLO within the shockwave formalism,"* Difflowx2022. arXiv:2211.04390.

- F. G. Celiberto, M. Fucilla and A. Papa, *"The high-energy limit of perturbative QCD: Theory and phenomenology,"* EPJ Web Conf. **270** (2022) 00001 arXiv:2209.01372, DOI:https://doi.org/10.1051/epjconf/202227000001.

- F. G. Celiberto and M. Fucilla, *"Inclusive J/ψ and Υ emissions from single-parton fragmentation in hybrid high-energy and collinear factorization,"* DIS2022. arXiv:2208.07206, DOI:10.48550/arXiv.2208.07206.

- A. D. Bolognino, F. G. Celiberto, M. Fucilla, D. Y. Ivanov, A. Papa, W. Schäfer and A. Szczurek, *"Hadron structure at small-x via unintegrated gluon densities,"* Rev. Mex. Fis. Suppl. **3** (2022) no.3, 0308109 arXiv:2202.02513, DOI:10.31349/SuplRevMexFis.3.0308109.

- F. G. Celiberto, M. Fucilla, D. Y. Ivanov, M. M. A. Mohammed and A. Papa, "Higgs boson production in the high-energy limit of pQCD," PoS **PANIC2021** (2022), 352 arXiv:2111.13090, DOI:10.22323/1.380.0352.

- A. D. Bolognino, F. G. Celiberto, M. Fucilla, D. Y. Ivanov and A. Papa, *"Heavy flavored emissions in hybrid collinear/high energy factorization,"* PoS **EPS-HEP2021** (2022), 389
arXiv:2110.12772, DOI:10.48550/arXiv.2110.12772.

- F. G. Celiberto, M. Fucilla, A. Papa, D. Y. Ivanov and M. M. A. Mohammed, *"Higgs-plus-jet inclusive production as stabilizer of the high-energy resummation,"* PoS **EPS-HEP2021** (2022), 589
arXiv:2110.09358, DOI:10.22323/1.398.0589.

- F. G. Celiberto, M. Fucilla, D. Y. Ivanov, M. M. A. Mohammed and A. Papa, *"BFKL phenomenology: resummation of high-energy logs in inclusive processes,"* SciPost Phys. Proc. **10** (2022), 002
arXiv:2110.12649, DOI:10.21468/SciPostPhysProc.10.002.

- A. D. Bolognino, F. G. Celiberto, M. Fucilla, D. Y. Ivanov and A. Papa, *"Hybrid high-energy/collinear factorization in a heavy-light dijets system reaction,"* SciPost Phys. Proc. **8** (2022), 068
arXiv:2107.12120, DOI:10.21468/SciPostPhysProc.8.068.

- A. D. Bolognino, F. G. Celiberto, M. Fucilla, D. Y. Ivanov, B. Murdaca and A. Papa, *"Inclusive production of two rapidity-separated heavy quarks as a probe of BFKL dynamics,"* PoS **DIS2019** (2019), 067
arXiv:1906.05940, DOI:10.22323/1.352.0067.

Contents

Introduction

QCD is the most perfect and non-trivial of the established microscopic theories of physics.
John C. Collins [3]

Quantum chromodynamics (QCD) is a quantum field theory describing the *Strong interaction*, one of the four fundamental forces of Nature. It is based on the non-Abelian gauge group $SU(N_c)$, where $N_c = 3$ is the number of quark colors [4]. Although QCD is a theory that has developed over a long period through a combination of theoretical and experimental efforts, its birth year is usually considered to be 1973, when David Gross and Frank Wilczek, and independently David Politzer, discovered the *Asymptotic freedom*, *i.e.* the remarkable property for which interactions between color sources become asymptotically weaker as the energy scale increases and the corresponding length scale decreases. From that point on, the continued predictive successes of the theory definitely established QCD as the theory of strong interactions. However, to date, a full understanding of the theory has not been achieved.

One of the main aspects that makes the theory tremendously complicated is the *Color confinement*: the phenomenon that color-charged particles (such as quarks and gluons) cannot be isolated, and therefore cannot be directly observed. There is not yet an analytic proof of color confinement in any non-Abelian gauge theory, but it is well established from lattice QCD calculations and decades of experiments. The phenomenon can be understood qualitatively by noting that the force-carrying gluons of QCD have color charge, unlike the photons of *Quantum electrodynamics* (QED). Whereas the electric field between electrically charged particles decreases rapidly as those particles are separated, the gluon field between a pair of color charges forms a narrow flux tube (or string) between them. Because of this behavior of the gluon field, the strong force between the particles is constant regardless of their separation. Therefore, as two color charges are separated, at some

point it becomes energetically favorable for a new quark–antiquark pair to appear, rather than extending the tube further. This tells us that the theory, which is asymptotically free at high-energy (short distance), is strongly coupled at low-energy (large distance). At high-energy, since the coupling of the theory is small, the interaction processes can be described through the perturbation theory, we speak in this case of *pertutbative* QCD (pQCD). On the other hand, at low energies a perturbative approach is not possible; in this case, the most common approach is the *Lattice* QCD (LQCD), based on numerical calculations on a discretized space-time lattice.

It is clear that, when collision processes involving hadronic particles are experimentally investigated, both dynamics (long and short distance) are involved. Among the greatest achievements of pQCD, there are the so-called *factorization theorems*, which allow us to separate the total process into a *hard part*, a cross-section for the scattering of partons computable in perturbation theory, and some non-perturbative parts, encoding the long-distance dynamics. In the factorization approach, the proton beams are treated as collections of so-called partons: quasi-free quarks and gluons, whose (non-perturbative) distributions, the parton densities contain the long distance dynamics and have to be either fit from experimental data or evaluated using LQCD. Factorization implies that these quantities must be universal, so that, extracted in a process, they can then be used for the description of other reactions. Concerning the hard part, in any scattering process, at least two scales are involved: the center-of-mass of the whole process, $\sqrt{s}$, and the so-called hard scale, Q. The hard scale must satisfy the relation

$$Q^2 > \Lambda^2_{\mathrm{QCD}} \ ,$$

where Λ_{QCD} is the QCD mass scale, to ensure a perturbative treatment in $\alpha_s(Q^2)$. Although the perturbative approach is a very powerful tool, it also presents some pitfalls. Among these, one of the most important is related to the appearance of logarithmic corrections, depending on the kinematic scales involved and entering the perturbative series with a power increasing along with the order. It is clear that, if in certain kinematics these logarithms are large, they can compensate the smallness of the strong coupling, α_s. In these cases, a resummation to all orders of the perturbative series becomes mandatory.

An important example of this phenomenon is related to the cancellation of infrared (IR) divergences in QCD for IR-safe observables. These are typically dealt with through

the *dimensional regularization* procedure, which leads us to divergent quantities of the type

$$\frac{1}{\epsilon}\left(Q^2\right)^{\epsilon} = \frac{1}{\epsilon} + \ln Q^2 + \mathcal{O}(\epsilon) \ , \tag{1}$$

which appear when considering collinear gluon dynamics in the massless quark limit. Here, $\epsilon = (D-4)/2\epsilon$. In an IR-safe observable, the pole cancels but the logarithm remain. At any order in perturbation theory we thus have corrections of the type $\alpha_s^n \ln^p Q^2$. In the the so-called *Bjorken* limit, $Q^2 \to \infty$ and moderately small Bjorken x, given by $x = (Q^2/s)$, the logarithms can compensate the smallness of the coupling constant. The resummation of such logarithms leads to the Dokshitzer-Gribov-Lipatov-Altarelli-Parisi [5, 6, 7] (DGLAP) evolution equations.

Another situation that can lead to the appearance of large logarithmic corrections is the existence of a hierarchy among the scales involved. A very famous case is that of the so-called *Regge-Gribov* or *semi-hard* region, where

$$s \gg Q^2 \gg \Lambda^2_{\rm QCD} \ .$$

In this case, the logarithmic corrections are of the type $\ln(s/Q^2)$. Suppose we consider a proton-proton collision, where the partonic center-of-mass energy is $\sqrt{\hat{s}} = \sqrt{x_1 x_2 s}$, with $x_{1,2}$ the Bjorken fraction associated to the two colliding protons, we then have

$$\ln\left(\frac{s}{Q^2}\right) = \ln\left(\frac{1}{x_1}\right) + \ln\left(\frac{\hat{s}}{Q^2}\right) + \ln\left(\frac{1}{x_2}\right) \ .$$

All logarithms on the right-hand side can be potentially large. Those of small-x appear in the evolution of parton densities, while those of the ratio $\hat{s}/Q^2$ in the partonic cross sections. As we will see, from a physical point of view, they are always related to the occurrence of large rapidity intervals. The Balitsky-Fadin-Kuraev-Lipatov (BFKL) [8, 9, 10, 11] approach represents the established tool to resum to all orders, both in the leading (LLA) and the next-to-leading (NLLA) approximation, these large-energy logarithmic contributions. In the BFKL framework, the cross section of hadronic processes can be expressed as the convolution of two impact factors, related to the transition from each colliding particle to the respective final-state object, and a process-independent Green's function. The BFKL approach has proven to be very robust as it is able to predict rapid growth of the $\gamma^* p$ cross section at increasing energy and its consistent with pre-QCD results from Regge theory. It is also very powerful, being able to be applied in many different contexts.

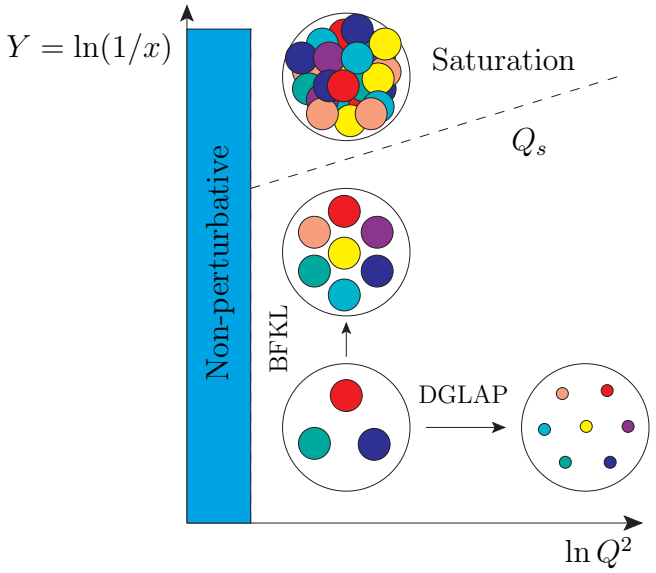

Figure 1: The parton distribution in the transverse plane as a function of $\ln(1/x)$ and $\ln Q^2$.

One of the major theoretical problems of the BFKL formalism is its inconsistency with the Froissart bound, which states that the total cross sections cannot grow in s faster than $k \times \ln^2 s$, with k a constant. This limit is explicitly violated by the power-like behavior in s of BFKL-resummed total cross sections. When we refer to the small-x logarithms, the violation of Froissart bound is physically interpretable as an infinite growth of the gluon density at small-x. The hadronic systems appears to become a denser and denser gluon medium, until at some point it becomes infinitely dense. This scenario seems to suggest that at a certain point some *saturation effects* must intervene to slow this growth. As we shall see, these effects are theoretically described by non-linear generalizations of the BFKL equation. Among these, the most general is represented by the *Balitsky-JIMWLK hierarchy of equations*, derived, in the so-called Shockwave approach, by Balitsky [12, 13, 14, 15] and, in the so-called Color Glass Condensate (CGC) approach, by Jalilian-Marian, Iancu, McLerran, Weigert, Leonidov and Kovner (JIMWLK) [16, 17, 18, 19, 20, 21, 22, 23, 24]. These approaches are needed to describe the scattering of a dilute projectile on a dense target, or also the scattering of two dense systems. The dense system condition can be achieved by a very small-x proton, but is more easily achieved for nuclei. A schematic representation of the proton/nucleus structure in terms of its constituents is shown in Fig. 1.

The center-of-mass energies available at modern accelerators, such as the Large Hadron Collider (LHC), and at future generation accelerators, such as the Electron-Ion Collider (EIC) and Future Circular Collider (FCC), offer us a unique opportunity to test the theoretical framework illustrated above, investigating hadronic matter under the most extreme conditions ever reached. This requires making theoretical predictions that are as accurate as possible and this is exactly the aim of this work. The thesis is divided into three parts. In the first and in the second part we consider the linear regime, well described by the BFKL approach. In the first part, we focus on aspects more related to phenomenology, such as calculations of next-to-leading order impact factors and numerical studies. In the second part, we focus on more formal aspects related to the extension of BFKL beyond the NLLA. The third and final part is entirely dedicated to saturation in which we investigate a new process with full NLL accuracy. More specifically, the thesis is organized as follows:

- In the first chapter, we introduce the problem of scattering in the Regge limit of QCD. We briefly describe the pre-QCD approach and then move on to the formulation of the BFKL approach. We first develop the approach pedagogically in the leading logarithmic approximation (LLA), and then, the chapter closes with a discussion of the approach in the next-to-leading logarithm approximation (NLLA).

- In the second chapter, we present an example of full NLO computation of an impact factor. In particular, we consider the forward Higgs boson impact factor, obtained in the infinite top-mass limit. This is the necessary ingredient to describe the inclusive hadroproduction of a forward Higgs in the limit of small Bjorken x, as well to study the inclusive forward emissions of a Higgs boson in association with a backward identified jet. We claim that this result should necessarily supplement pure fixed-order calculations entering in the collinear factorization framework, which cannot be able to describe the entire kinematic spectrum in the Higgs-plus-jet channel. We corroborate this claim in the third chapter, showing a comparison between fixed-order results and resummed predictions, in the case of Higgs p_T-distribution.

- The third chapter is devoted to the BFKL phenomenology and, in particular, to the study, in the NLLA, of processes featuring a forward-plus-backward two particle final state configuration. With particular reference to processes involving the production of the Higgs boson or of bound states of heavy quarks, we will show which observables are useful for testing the dynamics of high-energy QCD and what

are the phenomenological challenges. We will present numerical predictions for all these observables that can compared with data coming from the LHC.

- The fourth chapter focuses on more formal aspects. In particular, we briefly discuss the NNLLA formulation of the BFKL approach and then we compute one of the ingredient needed in this construction, *i.e.* the one-loop Lipatov vertex with higher accuracy in the dimensional regularization parameter $\epsilon = (D-4)/2$.

- In the fifth chapter, we briefly introduce the saturation picture and discuss the non-linear extension of the BFKL approach in the so-called Shockwave formalism. We derive, in this context, the B-JIMWLK evolution equation for the dipole operator.

- In the sixth and last chapter, we apply the Shockwave approach to the study, in the full next-to-leading logarithmic approximation, of the cross-sections of diffractive double hadron photo- or electroproduction, on a nucleon or a nucleus. The results are usable, to detect saturation effects, at both the future Electron-Ion-Collider (EIC) or already at LHC, using Ultra Peripheral Collisions (UPC).

Part I
BFKL in the NLLA: theory and phenomenology

Chapter 1

High-energy scattering in the Regge limit

The effort to understand the universe is one of the very few things that lifts human life a little above the level of farce, and gives it some of the grace of tragedy.
Steven Weinberg [25]

In the first section of this chapter the Regge theory will be introduced, following the standard presentations in books [26, 27]; it represents a very general framework in which to discuss the scattering of particles at high center-of-mass energies. The successive section is focused on the discussion of the BFKL approach [8, 9, 10, 11], which gives the description of pQCD-scattering amplitudes in the region of large s and fixed momentum transfer t, $s \gg |t|$ (Regge region), with various colour states in the t-channel. For this part, we will follow Refs. [26, 28].

1.1 Regge theory and the Pomeron

Before the advent of the field-theoretical approach to strong interactions, physicists sought to extract as much information as possible about scattering amplitudes of strongly interacting particles by studying the consequences of a number of postulates on the S-matrix, whose ab_{th} element is the overlap between the *in*-state (free particles state as $t \longrightarrow -\infty$), $|a\rangle$, and the *out*-state (free particles state as $t \longrightarrow +\infty$), $|b\rangle$,

$$S_{ab} = \langle b_{out} | a_{in} \rangle \, . \tag{1.1}$$

This type of approach is known as *S-matrix bootstrap*.

1.1.1 The S-matrix bootstrap

The most general postulates, which can be imposed on the S-matrix, are

1. **The S-matrix is Lorentz invariant**.
   This implies that can be expressed as a function of the (Lorentz invariant) scalar products of the incoming and outgoing momenta. For a two-particle scattering the most natural choice is to use the Mandelstam variables s, t, u. Since only two of them are independent, a two-particle scattering amplitude can be expressed as $\mathcal{A}(s,t)$, *i.e.* a function of only s, t (obviously, also other choices are possible).

2. **The S-matrix is unitary**.
   This means that
   $$SS^\dagger = S^\dagger S = \mathbb{1}. \tag{1.2}$$
   As known, this is a statement of conservation of probability. The scattering amplitude, A_{ab}, for scattering from an *in*-state $|a\rangle$ to an *out*-state $|b\rangle$ is related to the S-matrix element by
   $$S_{ab} = \delta_{ab} + i\ 2\pi\delta^4\left(\sum_a p_a - \sum_b p_b\right) A_{ab}\ .$$
   An immediate consequence of the unitary of the scattering matrix are the Cutkosky rules, which read
   $$2\Im m\mathcal{A}_{ab} = (2\pi)^4\delta^4\left(\sum_a p_a - \sum_b p_b\right)\sum_c \mathcal{A}_{ac}\mathcal{A}^\dagger_{cb}\ , \tag{1.3}$$
   where p_a, p_b are the 4-momenta of the particles in the states $|a\rangle, |b\rangle$, respectively. The Cutkosky rules allow to determine the imaginary part of an amplitude by considering the scattering amplitudes of the incoming and outgoing states into all possible "intermediate" states. When we consider the special case of forward elastic amplitude, $\mathcal{A}_{aa}$, we get the famous *optical theorem*. It states that the total cross-section for the scattering of two particles in the state $|a\rangle$ is related to the imaginary of the elastic scattering amplitude by the relation
   $$2\Im m\mathcal{A}_{aa}(s,0) = (2\pi)^4\sum_n \delta^4\left(\sum_f p_f - \sum_b p_b\right)|\mathcal{A}_{a\longrightarrow n}|^2 = F\sigma_{tot}, \tag{1.4}$$
   where F is the flux factor.

3. **Analyticity**
   The S-matrix is an analytic function of Lorentz invariants (regarded as complex variables), with only those singularities required by unitarity [26].
   It can be shown that this property is a consequence of causality[1]. Analiticity has a number of important and useful consequences. One is that, combined with unitarity, it allows to establish the existence of an s-plane singularity structure of the amplitude $\mathcal{A}(s,t)$ (there are s-plane cuts with branch points corresponding to the physical thresholds). Moreover, it enables to reconstruct the real part of an amplitude from its imaginary part using dispersion relations.

From these postulates, coupled with the spectrum of elementary particles, one can develop a set of conditions for amplitudes. In fact, unitarity relates the imaginary parts of amplitudes to sums of the products of other amplitudes, and dispersion relations then allow to determine the corresponding real parts. To underline the beauty of this approach, we want to observe that no assumptions about the underlying quantum field theory are made. All this information descend from fundamental principles of Nature.
As mentioned earlier, this approach uses dispersion relations to reconstruct the amplitudes, which involve integrations over the complex s variable, extending to infinity. This means that we need to know the asymptotic behavior in s of the amplitudes; this is the goal of *Regge theory*.

1.1.2 Regge theory

The Italian physicist T. Regge showed that it is useful to regard the angular momenta, l, as a complex variable, when discussing solutions of the Schrödinger equation for non-relativistic potential scattering [30]. He has demonstrated that, for a wide class of potentials, the only singularities of the scattering amplitude in the complex l plane are poles, called "Regge poles" after him. When these poles occur for positive integer values of l, they correspond to bound states or resonances, and they are also important for determining dispersion properties of the amplitudes.

His methods is also applicable in high-energy elementary particle physics. Regge theory predicts that, for a great variety of processes, the high-energy behaviour of a

[1]This connection has a very deep meaning and is discussed, for instance, in the section 6.6 of [29].

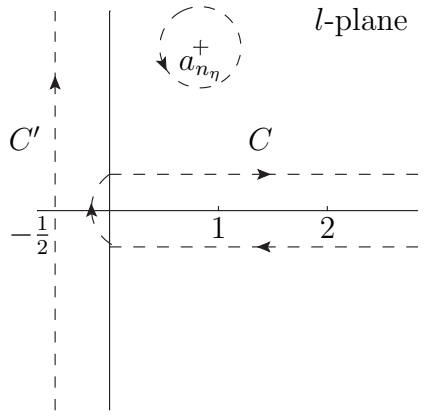

Figure 1.1: Sommerfeld-Watson transformation.

scattering amplitude $\mathcal{A}(s,t)$ will be

$$\mathcal{A}(s,t) \sim s^{\alpha(t)}. \tag{1.5}$$

To find this high-energy behaviour, one must consider the partial-wave expansion of the amplitude. Through this expansion, the amplitude can be expressed as a series of Legendre polynomials $P_l\left(1+\frac{2s}{t}\right)$,

$$\mathcal{A}(s,t) = \sum_{l=0}^{\infty} (2l+1)\, a_l(t)\, P_l\left(1+\frac{2s}{t}\right), \tag{1.6}$$

where $a_l(t)$ are called partial-wave amplitudes. Sommerfeld [31] rewrote this partial-wave expansion in terms of a contour integral in the complex angular momentum (l) plane as

$$\mathcal{A}(s,t) = \frac{1}{2i}\oint_C dl \frac{(2l+1)}{\sin\pi l} \sum_{\eta=\pm 1} \frac{\eta + e^{-i\pi l}}{2} a^{(\eta)}(l,t)\, P_l\left(l, 1+\frac{2s}{t}\right), \tag{1.7}$$

where $a(l,t)$ and $P\left(l,1+\frac{2s}{t}\right)$ are the analytic continuations in l of the partial waves $a_l(t)$, and of the Legendre polynomials $P_l\left(1+\frac{2s}{t}\right)$, respectively. The contour C surrounds the positive real axis as shown in Fig. 1.1.

It is important to note the presence of the index η, called *signature*, which assumes the two possible values 1 and -1. The signature means parity with respect to the substitution $\cos\theta_t \leftrightarrow -\cos\theta_t$, where θ_t is the t-channel-scattering angle. As we will see, the separation into partial waves with a definite signature represents an important operation for the development of the BFKL approach.

Now, we need to carry out the so-called *Sommerfeld-Watson transformation*, *i.e.* to

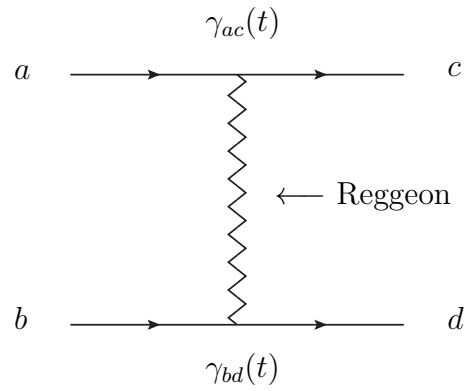

Figure 1.2: A Regge exchange diagram.

deform the path C into the path C', which runs parallel to the imaginary axis with $\Re\, l = -1/2$, encircling any poles[2] that the function $a^{(\eta)}(l,t)$ may have at $l = a_{n_\eta}(t)$ and picking up $2\pi i \times$ the residue of that pole (see Fig. 1.1). After this transformation, for the particular case of simple poles (in the l-plane) and in the Regge kinematical region $|s| \gg t$, one finds that

$$\mathcal{A}(s,t) \xrightarrow{s\to\infty} \frac{\eta + e^{-i\pi\alpha(t)}}{2}\beta(t)s^{\alpha(t)}, \tag{1.8}$$

where $\alpha(t)$ represents the position of the leading Regge pole in the l-plane; it is not a fixed value, but rather a function of the transferred momentum t. More in general, in the case of non-simple poles and cuts, the expression of the amplitude in Eq. (1.8) will be different.

The amplitude given by Eq. (1.8) can be seen as the exchange in the t-channel of an object with an effective "angular momentum" equal to $\alpha(t)$. It is called a Reggeon, and $\alpha(t)$ is called "Regge trajectory". A Reggeon-exchange amplitude can be thought as the superposition of amplitudes for the exchange of all possible particles in the t-channel, with quantum number determined by those of colliding particles. The amplitude can be factorized as shown in Fig. 1.2 into a coupling $\gamma_{ac}(t)$ of the Reggeon between the particles a and c, a similar coupling $\gamma_{bd}(t)$ between particles b and d, and a universal contribution from the Reggeon exchange. The couplings γ are functions of t only, and hence, the Reggeon exchange determines completely the behaviour in s of the whole amplitude.

[2]In principles also cuts can be presented.

1.1.3 Reggeization and Pomeron

Now, it is possible to give a formal definition of Reggeization. A particle of mass M and spin J is said to "Reggeize" if the amplitude, $\mathcal{A}$, for a process involving the exchange in the t-channel of the quantum numbers of that particle, behaves asymptotically in s as

$$\mathcal{A} \propto s^{\alpha(t)},$$

where $\alpha(t)$ is the trajectory and $\alpha(M^2) = J$, so that the particles itself lies on the trajectory.

In the large-s limit, a hadronic process is governed by the exchange of one or more Reggeons in the t-channel. The exchange of Reggeons instead of particles gives rise to scattering amplitudes of the type of Eq. (1.5). Using the optical theorem together with the Eq. (1.5) we can obtain the asymptotic behaviour of the total cross section of that process, which reads

$$\sigma_{\text{tot}} \propto s^{(\alpha(0)-1)}. \tag{1.9}$$

In 1965 Pomeranchuk proved from general assumptions that in any scattering process in which there is charge exchange, the cross section vanishes asymptotically (the Pomeranchuk's theorem [32]). Foldy and Peierls proved the converse, that is, if for a particular scattering process the cross section does not fall as s increases, then that process must be dominated by the exchange of vacuum quantum numbers [33]. It is observed experimentally that the total cross sections do not vanish asymptotically. In fact they rise slowly as s increases. If we are to attribute this rise to the exchange of a single Regge pole, then it follows that the exchange is that of a Reggeon which carries the quantum numbers of the vacuum, called Pomeron ($\alpha_P(0) > 1$) in honour of its inventor Pomeranchuk. The physical particles which would provide the resonances for integer values of the Pomeron trajectory have not been identified, but in QCD, natural candidates are hypothetical bound states of gluons (glueballs).

We want to remark once again that the notions of Reggeon and Pomeron that we have introduced are not linked to the perturbative approach. From now on, we will be interested in studying the so-called semi-hard processes in pQCD, *i.e.* those processes characterized by the scale hierarchy[3]

$$s \gg t \gg \Lambda^2_{QCD}\ . \tag{1.10}$$

[3]Here t plays the role of a generic hard scale of the process.

In this context, we will talk about gluon Reggeization in pQCD and we will construct the so-called hard Pomeron (or BFKL Pomeron). These objects, which allow us to find the asymptotic behavior of the scattering amplitudes in pQCD, should not be confused with the corresponding soft objects which are of non-perturbative origin. The connection between the two objects concerns only the quantum numbers exchanged in the t-channel and the first condition in (1.10).

1.2 BFKL approach

The BFKL equation is an integral equation that determines the behaviour at high energy $\sqrt{s}$ of the perturbative QCD amplitudes in which vacuum quantum numbers are exchanged in the t-channel. It was derived in the LLA, which means collection of all terms of the type $\alpha_s^n \ln^n s$. This approximation leads to an increase of cross sections. In fact, calculated in LLA, the total cross σ_{tot}^{LLA} grows at large center-of-mass energies as

$$\sigma_{tot}^{LLA} \sim \frac{s^{\omega_0}}{\sqrt{\ln s}}, \tag{1.11}$$

where $\omega_0 = (g^2 N \ln 2)/\pi^2$, with N the number of colors in QCD, is the LLA position of the rightmost singularity in the complex momentum plane of the t-channel partial wave with vacuum quantum numbers (Pomeron singularity). The BFKL equation works also in the NLLA (next-to-leading logarithmic approximation), in which one has to resum also all the terms of the type $\alpha_s^{n+1} \ln^n s$ in the perturbative series. To derive the BFKL equation, the Reggeization of the gluon in QCD is fundamental. In this section, first, the BFKL equation will be treated in the LLA, then the NLLA case will be discussed.

1.2.1 Reggeization of the gluon in pQCD

Reggeization of the gluon in QCD has a very deep meaning. Obviously, it means that there exists a Reggeon with gluon quantum numbers, negative signature and trajectory

$$\alpha(t) = 1 + \omega(t) \ , \tag{1.12}$$

passing through one at $t = 0$, but it also establishes that only this Reggeon gives the leading contribution, in each order of the perturbation theory, to amplitudes with the gluon quantum numbers exchanged in the t-channel.
Considering an elastic scattering process $A + B \longrightarrow A' + B'$ with $s \gg |t|$, in which

$$s = (p_A + p_B)^2 \ , \qquad t = q^2 \ , \qquad q = p_A - p_{A'} \ , \tag{1.13}$$

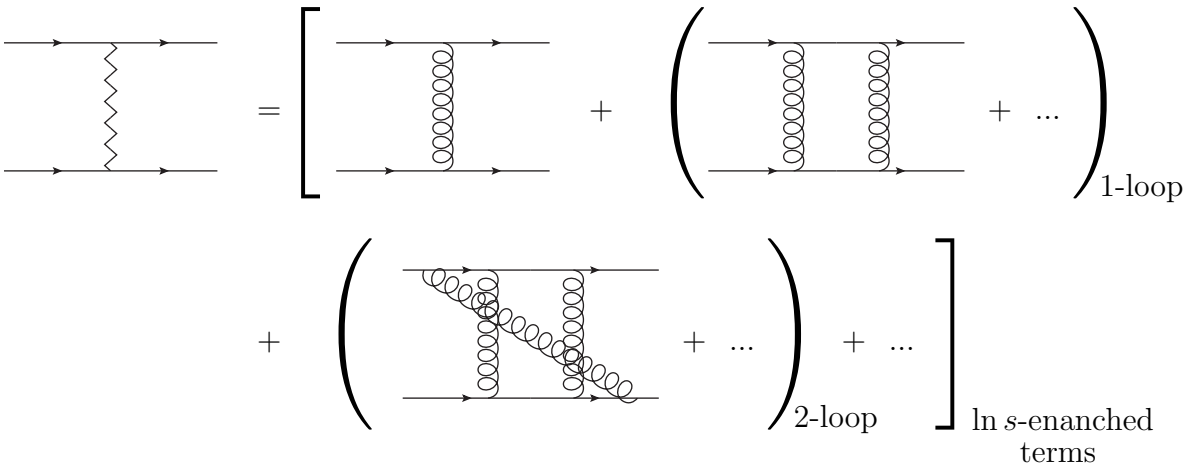

Figure 1.3: Schematic representation of the Reggeized gluon in pQCD. At Born level it is given by the exchange of a single gluon in the t-channel, while, at higher orders, it is represented by the exchange of a certain number of gluons which combine in such a way as to give the exchange of an octet Reggeized gluon in the t-channel.

the Reggeization implies that the amplitude with the gluon quantum numbers in t-channel has the factorized form

$$\mathcal{A}_{AB}^{A'B'} = \Gamma_{A'A}^{i} \left(\frac{s}{-t}\right)^{\alpha(t)} \left[-1 + e^{-i\pi\alpha(t)}\right] \Gamma_{B'B}^{i} = \Gamma_{A'A}^{i} \frac{s}{t} \left[\left(\frac{s}{-t}\right)^{\omega(t)} + \left(\frac{-s}{-t}\right)^{\omega(t)}\right] \Gamma_{B'B}^{i} \,, \tag{1.14}$$

where $\Gamma_{P'P}^{i}$ (with $P = A, B$) represent the particle-particle-Reggeon (PPR) vertices (they do not depend on s) and i is the colour index. It is not difficult to observe that the amplitude in Eq. (1.14) is exactly of the form shown in Figure 1.2, in fact, there are two couplings of particles with the Reggeon and a universal contribution which behaves as $s^{\alpha(t)}$. The second term between square brackets comes from the contribution of the u-channel[4]. It can also be seen that this amplitude is antisymmetric under the transformation $s \to u \simeq -s$, which, in the Regge limit, is equivalent to negative signature.

The analytic form in Eq. (1.14) is the result of an infinite resummation of diagrams, this means that the pQCD Reggeized gluon possesses a perturbative expansion in terms of normal gluons (see Fig. 1.3). Each of the terms in the expansion in Fig. 1.3 represents a term in the $\omega(t)$-expansion (or equivalently α_s-expansion) of the expression in Eq. (1.14). To give a clearer idea of the Reggeization, we will now extract the Regge trajectory at

[4]Since $s + u + t \simeq s + u = \sum_i m_i^2 \simeq 0$, we have $u \simeq -s$.

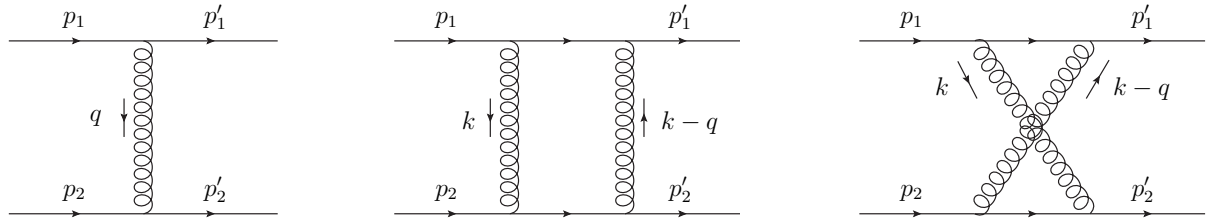

Figure 1.4: In (a) the leading order diagram contributing to the quark-quark scattering; (b) and (c) are the two next-leading order diagrams contributing to the Regge trajectory in the LLA.

one-loop accuracy. To do this, we need to consider a "reference" amplitude, compute it at least up to 1-loop accuracy in the high-energy limit and then compare it with the following expanded version of Eq. (1.14):

$$(\mathcal{A})_{12}^{1'2'} = \Gamma^a_{1'1}\frac{s}{t}\left[2+\omega(t)\ln\left(\frac{-s}{-t}\right)+\omega(t)\ln\left(\frac{s}{-t}\right)\right]\Gamma^a_{2'2}+\dots\,. \tag{1.15}$$

Let us consider the quark-quark scattering amplitude with gluon quantum number exchange in the t-channel (see Fig. 1.4). We choose the momenta of the two incoming quarks as

$$p_1^\mu = \frac{\sqrt{s}}{2}\left(1,\vec{0},1\right)\ , \quad p_2^\mu = \frac{\sqrt{s}}{2}\left(1,\vec{0},-1\right)\ , \tag{1.16}$$

and use q to denote the exchanged momentum carried by the gluon in the t-channel, so that

$$q = p_1 - p_{1'} = p_{2'} - p_2 \quad \text{and} \quad t = q^2\ . \tag{1.17}$$

We are interested in studying the process in the Regge kinematical region, where

$$2p_1\cdot p_2 = s \gg |t| = \vec{q}^{\,2}\ . \tag{1.18}$$

We choose to work in the covariant Feynman gauge and the form of the leading order contribution to the amplitude is

$$\mathcal{A}_{12}^{1'2'} = (-i)igt^a_{ji}\bar{u}(p_1-q)\gamma^\mu u(p_1)\left(\frac{-ig_{\mu\nu}\delta^{ab}}{q^2}\right)igt^b_{kn}\bar{u}(p_2+q)\gamma^\nu u(p_2)\ . \tag{1.19}$$

Now, it is important to stress that in the Regge kinematical region, any components of q is small compared to $\sqrt{s}$, and we can make the replacement[5]

$$\bar{u}(p_1-q)\gamma^\mu u(p_1) \simeq \bar{u}(p_1)\gamma^\mu u(p_1) = 2\delta_{\lambda_{1'},\lambda_1}p_1^\mu\ . \tag{1.20}$$

[5]The normalization of spinors is $u^\dagger(p_1)u(p_1) = 2E_{p_1}\delta_{\lambda_{1'},\lambda_1}$.

This is called *eikonal approximation* and it is correct when the gauge exchanged particle is relatively soft. The final result for the amplitude can be written as

$$\mathcal{A}_{12}^{1'2'} = \Gamma_{1'1}^{a} \left(\frac{2s}{t}\right) \Gamma_{2'2}^{a} \,, \tag{1.21}$$

where

$$\Gamma_{1'1}^{a} = g t_{ji}^{a} \delta_{\lambda_{1'}\lambda_1} \,, \qquad \Gamma_{2'2}^{a} = g t_{kn}^{a} \delta_{\lambda_{2'}\lambda_2} \tag{1.22}$$

are the effective quark-quark-Reggeon vertices.

At this point it is interesting to note that this result could also be obtained starting from Eq. (1.19) and performing the following replacement in the gluon propagator

$$\frac{g^{\mu\nu}}{t} = \frac{1}{t}\left(g_{\perp\perp}^{\mu\nu} + \frac{2p_1^\mu p_2^\nu + 2p_1^\nu p_2^\mu}{s}\right) \to \frac{1}{t}\frac{2p_1^\nu p_2^\mu}{s} = \frac{2s}{t}\left(-\frac{p_2^\mu}{s}\right)\left(-\frac{p_1^\nu}{s}\right) \,. \tag{1.23}$$

This replacement is known as *Gribov trick* and represents a general method for extracting the high-energy behavior of QCD amplitudes in which relatively soft gluons are exchanged in the t-channel. The application of Gribov's trick produces an overall factor $2s/t$ and it causes the upper (lower) vertex to contract with a term $-p_2^\mu/s$ ($-p_1^\nu/s$). These contractions generate the effective vertices mentioned above, which are energy-independent. If we look only at the upper part of the diagram (a) in Fig. 1.4 it is as if the effective vertex can be obtained by writing the normal quark-quark-gluon vertex and assigning an "effective polarization" (usually called *nonsense polarization*), $-p_2^\mu/s$, to the t-channel gluon.

In order to compute the Regge trajectory, we need to compute one-loop corrections the $\mathcal{A}_{12}^{1'2'}$. In the LLA and in a covariant gauge there are no contributions from one-loop graphs which contain corrections to propagators or vertices, but only from the two diagrams denoted by (b) and (c) in Fig. 1.4. We will denote the first as $\mathcal{A}_{12,\mathrm{box}}^{1'2'}$ and the second as $\mathcal{A}_{12,\mathrm{cross}}^{1'2'}$. The "cross" diagram will be obtained form the "box" one by using the crossing symmetry, *i.e.*

$$\mathcal{A}_{12,\mathrm{cross}}^{1'2'} = -\mathcal{A}_{12,\mathrm{box}}^{1'2'}(s \to u \simeq -s) \,. \tag{1.24}$$

Eq. (1.24) requires a number of remarks. As it is easy to observe, when we calculate the "box" and the "cross" diagram, in general, they have a different color structure. If the "box" is proportional to

$$(t^b t^a)_{ji}(t^b t^a)_{kn} \,, \tag{1.25}$$

the "cross" is proportional to

$$(t^a t^b)_{ji}(t^b t^a)_{kn} \,. \tag{1.26}$$

With these structures, in general the two amplitudes have no definite signature and Eq. (1.24) is not valid. What is convenient to do is to separate each of the two amplitudes into two parts with a definite signature, using the identities

$$(t^b t^a)_{ji} = \frac{1}{2}[t^b, t^a]_{ji} + \frac{1}{2}\{t^b, t^a\}_{ji} \,, \tag{1.27}$$

$$(t^a t^b)_{ji} = \frac{1}{2}[t^a, t^b]_{ji} + \frac{1}{2}\{t^a, t^b\}_{ji} = -\frac{1}{2}[t^b, t^a]_{ji} + \frac{1}{2}\{t^b, t^a\}_{ji} \,. \tag{1.28}$$

Now, the parts of the amplitudes depending on the commutator, as far as the color structure is concerned, differ by one sign, while those depending on the anticommutator are equal. If we strip off the color factors, the amplitude of the "cross" diagram is obtained from the "box" through the substitution $s \to u \simeq -s$ which produces a global minus sign of difference in the real part of the two amplitudes. This last minus sign is compensated with that which comes from the color structure only for the part of amplitude proportional to the commutator. In the part of amplitude proportional to the anticommutator, it generates a "fatal" cancellation of the dominant ($\ln(s)$-enhanced) contribution. The part of amplitude containing the commutator, which we will henceforth refer to as *negative signature* contributions, dominate in the high-energy approximation and satisfies the relation in Eq. (1.24). To all orders it produces the behavior in Eq. (1.14). From now on, speaking of gluon quantum numbers, we will always refer to the part of the octet with negative signature and will therefore make use of definite parity with respect to $s \to u$ transformation of this contribution.

The "box" diagram can be easily calculated using dispersive techniques. Cutting the diagram in the s-channel and using Cutkosky rules we have[6]

$$\Im \mathcal{A}^{1'2'}_{12,\text{box}} = \frac{1}{2}\sum_{\{f\}} \int d\Phi_2 \mathcal{A}^{1'2'}_{12}(k) \mathcal{A}^{1'2'\dagger}_{12}(q-k) \,, \tag{1.29}$$

where[7]

$$d\Phi_2 = \frac{d^D l_1}{(2\pi)^{D-1}} \frac{d^D l_2}{(2\pi)^{D-1}} \delta(l_1^2)\delta(l_2^2)(2\pi)^D \delta^D(p_1 + p_2 - l_1 - l_2) \tag{1.30}$$

is the two-body phase space. In Eq. (1.30), l_1 and l_2 represent the momenta of the two "cut" particles. Because of the $\delta^D(p_1+p_2-l_1-l_2)$, one integration can be done immediately and we can change variables from the remaining one to the momenta k exchanged in the

[6] We will always use $\sum_{\{f\}}$ to denote the summation over all relevant quantum numbers of the intermediate state.

[7] We work in dimension $D = 4 + 2\epsilon$. A non-zero ϵ is introduced to regularize IR-divergences.

t-channel; we obtain

$$d\Phi_2 = \frac{1}{(2\pi)^{D-2}} d^D k \delta((p_1-k)^2)\delta((p_2+k)^2) \; . \tag{1.31}$$

Now, it is convenient to introduce the *Sudakov decomposition* for the momentum k:

$$k^\mu = \beta p_1^\mu + \alpha p_2^\mu + k_\perp^\mu \; , \tag{1.32}$$

where $k_\perp = (0, \vec{k}, 0)$ is a four-vector, completely transverse with respect to the plane identified by the two light-cone vectors p_1 and p_2. In terms of these variables, the phase space becomes

$$\begin{aligned} d\Phi_2 &= \frac{s}{2(2\pi)^{D-2}} d\alpha d\beta d^{D-2} k_\perp \delta(-s(1-\beta)\alpha + k_\perp^2)\delta(s(1+\alpha)\beta + k_\perp^2) \\ &\simeq \frac{s}{2(2\pi)^{D-2}} d\alpha d\beta d^{D-2} k_\perp \delta(-s\alpha + k_\perp^2)\delta(s\beta + k_\perp^2) \; , \end{aligned} \tag{1.33}$$

where, in the last step, we have used that in the kinematics we are interested in

$$\alpha \ll 1 \; , \quad \beta \ll 1 \; , \quad k^2 = k_\perp^2 = -\vec{k}^2, \quad (k+q)^2 = (k+q)_\perp^2 = -(\vec{k}+\vec{q}\,)^2 \; . \tag{1.34}$$

Now, it is very simple to see that $\Im \mathcal{A}_{12,\mathrm{box}}^{1'2'}$ takes the form

$$\Im \mathcal{A}_{12,\mathrm{box}}^{1'2'} = g\delta_{\lambda_1\lambda_{1'}} g\delta_{\lambda_2\lambda_{2'}} (t^a_{li} t^a_{mn})(t^b_{jl} t^b_{km}) \left(\frac{s}{t}\right) \frac{g^2}{(2\pi)^{D-2}} \int d^{D-2} k_\perp \frac{t}{k_\perp^2 (k-q)_\perp^2} \; . \tag{1.35}$$

Since we are interested in gluon quantum numbers we have to perform the projection on the negative signature and the octet colour state in the t-channel. This is easily achieved through the replacement

$$(t^b t^a)_{ji} \to \frac{1}{2}(t^b t^a - t^a t^b)_{ji} = \frac{1}{2}(T^c)_{ab} t^c_{ji} \; . \tag{1.36}$$

After this, the color structure becomes

$$\frac{1}{2}(T^c)_{ab} t^c_{ji} (t^b t^a)_{kn} = -\frac{C_A}{4} t^a_{ji} t^a_{kn} \; , \tag{1.37}$$

and hence we obtain

$$\Im \mathcal{A}_{12,\mathrm{box}}^{1'2'} = \Gamma^a_{1'1} \frac{s}{t} \Gamma^a_{2'2} (-\pi) \left[\frac{g^2 t}{(2\pi)^{(D-1)}} \frac{N}{2} \int \frac{d^{D-2} k_\perp}{k_\perp^2 \, (q-k)_\perp^2} \right] \; . \tag{1.38}$$

The mere existence of this imaginary part tells us that the full amplitude must be proportional to

$$\ln\left(\frac{-s}{-t}\right) = \ln\left(\frac{s}{-t}\right) - i\pi \; , \tag{1.39}$$

and hence, we have

$$\mathcal{A}_{12,\text{box}}^{1'2'} = \Gamma_{1'1}^{a} \frac{s}{t} \Gamma_{2'2}^{a} \ln\left(\frac{s}{t}\right) \left[\frac{g^2 t}{(2\pi)^{(D-1)}} \frac{N}{2} \int \frac{d^{D-2}k_\perp}{k_\perp^2 \, (q-k)_\perp^2} \right] . \tag{1.40}$$

Using the Eq. (1.24) we can immediately write down the full (LO+NLO) amplitude, which reads

$$\begin{aligned} \mathcal{A}_{12}^{1'2'} + \mathcal{A}_{12,\text{box}}^{1'2'} + \mathcal{A}_{12,\text{cross}}^{1'2'} &= \mathcal{A}_{12}^{1'2'} + \mathcal{A}_{12,\text{box}}^{1'2'} - \mathcal{A}_{12,\text{box}}^{1'2'}(s \to u \simeq -s) \\ &= \Gamma_{1'1}^{a} \frac{s}{t} \left[2 + \omega^{(1)}(t) \ln\left(\frac{-s}{-t}\right) + \omega^{(1)}(t) \ln\left(\frac{s}{-t}\right) \right] \Gamma_{2'2}^{a} \, , \end{aligned} \tag{1.41}$$

where

$$\omega^{(1)}(t) \equiv \frac{g^2 t}{(2\pi)^{(D-1)}} \frac{N}{2} \int \frac{d^{D-2}k_\perp}{k_\perp^2 \, (q-k)_\perp^2} \, . \tag{1.42}$$

The last definition is not casual. By comparing (1.41) and (1.15), we understand immediately that, the deviation from one of the gluon trajectory is

$$\omega(t) \simeq \omega^{(1)}(t) = \frac{g^2 t}{(2\pi)^{(D-1)}} \frac{N}{2} \int \frac{d^{D-2}k_\perp}{k_\perp^2 \, (q-k)_\perp^2} \, . \tag{1.43}$$

A curious reader might reasonably wonder why the relation $\omega(t) \simeq \omega^{(1)}(t)$. It indicates that we have extracted only the one-loop contribution, $\omega^{(1)}(t)$, to the complete Regge trajectory, $\omega(t)$. What are the sub-dominant contributions to Regge trajectory, it will become clear in the next sections when we will discuss BFKL in the NLLA. For the moment, is important to remind that, although we have made a resummation to all orders, we have collected, order by order, only those terms in which the number of powers of α_s is compensated by an equal number of logarithms of the ratio s/t.
The integral in Eq. (1.43) can be evaluated by using standard techniques for Feynman integrals, we get

$$\omega^{(1)}(t) = \frac{g^2 t}{(2\pi)^{(D-1)}} \frac{N}{2} \int \frac{d^{D-2}k_\perp}{k_\perp^2 \, (q-k)_\perp^2} = -\frac{g^2 N \Gamma(1-\epsilon)}{(4\pi)^{2+\epsilon}} \frac{[\Gamma(\epsilon)]^2}{\Gamma(2\epsilon)} (\vec{q}^{\,2})^{\epsilon} \, . \tag{1.44}$$

From Eq. (1.44), it is easy to observe that, for the gluon, $\omega(0) = 0$, hence $\alpha(0) = 1$; this shows that the gluon lies on the Reggeon trajectory with its quantum numbers.

1.2.2 The Lipatov vertex

The second key ingredient to build the BFKL approach in the leading-logarithmic approximation is the so-called *Lipatov vertex*. It is an effective non-local vertex. To understand

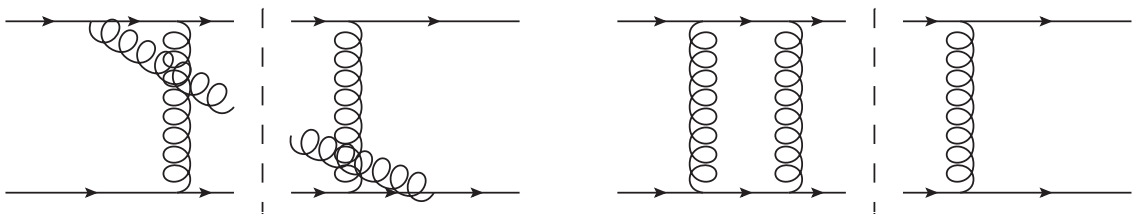

(a) (b)

Figure 1.5: The two types of diagram which contribute to the imaginary part of the elastic amplitude, $\Im \mathcal{A}_{12}^{1'2'}$, at this perturbative order.

its nature, Let us consider the quark-quark scattering again. Let us imagine we want to demonstrate explicitly that the form (1.14) is correct at two-loop level. If we want to use again dispersive techniques, cutting diagrams in the s-channel, we should compute a series of diagrams that we can split into two categories[8]:

- Diagrams in which the cut goes through one gluon line and two quark lines (see diagram (a) in Fig. 1.5); we have 25 diagrams of this kind.
- Diagrams in which the cut only goes through the two quark lines (see diagram (b) in Fig. 1.5); we have 4 diagrams of this kind.

Let us concentrate on the first class for the moment. It is clear that, for this class of diagram, the contribution to the imaginary part of the elastic amplitude will read[9]

$$\Im \mathcal{A}_{12,\text{ladder}}^{1'2'} = \frac{1}{2} \sum_{\{f\}} \int d\Phi_3 \mathcal{A}_{12}^{1'2'3,\sigma}(q_1, q_2)(\mathcal{A}_{12}^{1'2'3,\gamma}(q_1 - q, q_2 - q))^\dagger \,, \tag{1.45}$$

where 3 is labelling the additional particle (gluon in this case). Since the gluon can be emitted by one of the four quark lines or by the t-channel gluon, the inelastic amplitude $\mathcal{A}_{12}^{1'2'3,\sigma}$ has five contributions. These contributions are shown in Fig. 1.6. Let us start by computing the diagram (a). Using the Gribov trick for the t-channel gluons, it can be immediately written as

$$\mathcal{A}_{12,(a)}^{1'2'3} = -2s\Gamma_{1'1}^{a} \frac{1}{t_1} g(T^c)_{ab} \left[2\frac{p_{1,\rho} p_{2,\delta}}{s} A^{\rho\delta\sigma}(q_2, q_1 - q_2)\varepsilon_\sigma^* \right] \frac{1}{t_2} \Gamma_{2'2}^{b} \,, \tag{1.46}$$

[8] In analogy with before, we do not get contribution of the form $\alpha_s^2 \ln^2(s/t)$ from graph which consist of vertex or self-energy corrections on the one-loop diagrams.

[9] I denoted this contribution with the label "ladder" because (within this order), as we will see, this contributions are organizable as an effective ladder of pure gluons.

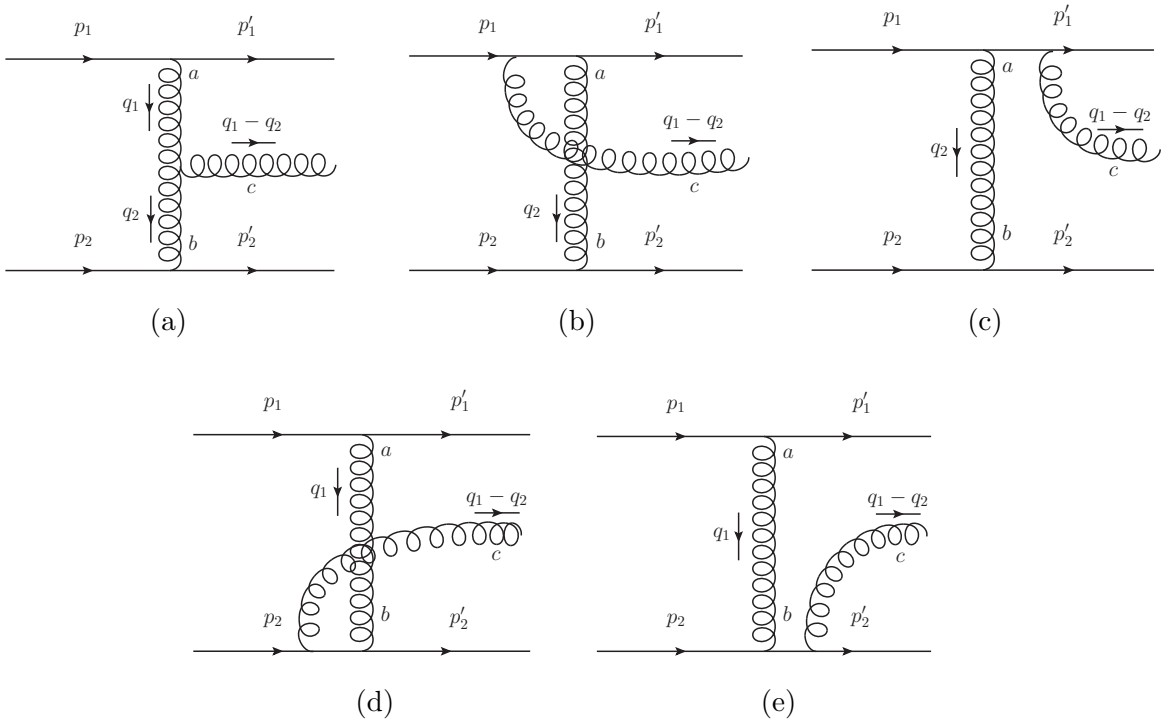

Figure 1.6: The five diagrams contributing to the inelastic process $q + q \to q + g + q$.

where

$$A^{\rho\delta\sigma}(q_2, q_1 - q_2) = g^{\rho\sigma}(q_1 - 2q_2)^\rho + g^{\rho\delta}(q_1 + q_2)^\sigma - g^{\rho\sigma}(2q_1 - q_2)^\delta$$

is the tensor structure appearing in the triple-gluon vertex. Now, we introduce the usual Sudakov decomposition for gluons momenta:

$$q_1 = \beta_{q_1} p_1 + \alpha_{q_1} p_2 + q_{1,\perp} \ , \qquad q_2 = \beta_{q_2} p_1 + \alpha_{q_2} p_2 + q_{2,\perp} \ . \tag{1.47}$$

The dominant logarithms come from the region where

$$1 \gg \beta_{q_1} \gg \beta_{q_2} \ , \quad 1 \gg |\alpha_{q_2}| \gg |\alpha_{q_1}| \ , \quad t_1 = q_1^2 = -\vec{q}_1^{\,2} \ , \quad t_2 = q_2^2 = -\vec{q}_2^{\,2} \ . \tag{1.48}$$

It is easy to understand that the first three conditions automatically imply also that

$$1 \gg \beta_{q_1} - \beta_{q_2} > 0, \quad 1 \gg \alpha_{q_1} - \alpha_{q_2} > 0 \ , \tag{1.49}$$

and hence the three particles through the cut are strongly ordered in rapidity. This kinematical constraint is very important and it is known as *multi-Regge kinematics*. From the on-shell condition of the emitted gluon, we also have

$$(q_1 - q_2)^2 = -\beta_{q_1}\alpha_{q_2} s - (\vec{q}_1 - \vec{q}_2)^2 = 0 \implies \beta_{q_1}\alpha_{q_2} s = -(\vec{q}_1 - \vec{q}_2)^2 \ . \tag{1.50}$$

That said, we understand that

$$2\frac{p_{1,\rho}p_{2,\delta}}{s}A^{\rho\delta\sigma}(q_2,q_1-q_2)\simeq-\alpha_{q_2}p_2^\sigma-\beta_{q_1}p_1^\sigma+(q_1+q_2)_\perp^\sigma \tag{1.51}$$

and hence

$$\mathcal{A}^{1'2'3}_{12,(a)}=2s\Gamma^a_{1'1}\frac{1}{t_1}g(T^c)_{ab}\varepsilon^*_\sigma\left[\alpha_{q_2}p_2^\sigma+\beta_{q_1}p_1^\sigma-(q_1+q_2)_\perp^\sigma\right]\frac{1}{t_2}\Gamma^b_{2'2}\,. \tag{1.52}$$

Let us now consider diagram (b), we first observe that the quark propagator appearing in this diagram, in the multi-Regge kinematics, can be approximated as

$$\frac{i(\hat{p}_1-\hat{q}_1+\hat{q}_2)}{(p_1-q_1+q_2)^2}\simeq\frac{i\hat{p}_1}{\alpha_{q_2}s}\,, \tag{1.53}$$

where $\hat{p}=\gamma^\mu p_\mu$. The approximation in (1.53) is justified by the fact that any components of q_1-q_2 is negligible compared to the longitudinal component of p_1. After this observation is clear that, by using again the Gribov trick for the t-channel gluon propagator, we get

$$\mathcal{A}^{1'2'3}_{12,(b)}=(t^at^c)_{ji}t^a_{kn}2sg\bar{u}(p_1-q_1)\frac{\hat{p}_2}{s}u(p_1)\frac{1}{t_1}g\varepsilon^*_\sigma\left[\frac{2p_1^\sigma t_1}{\alpha_{q_2}s}\right]\frac{1}{t_2}\bar{u}(p_2+q_2)\frac{\hat{p}_2}{s}u(p_2)\,. \tag{1.54}$$

The diagram (c) is computed in the same way, but with respect to the previous one it has a minus sign and the color structure in front is $(t^ct^a)_{ji}t^a_{kn}$. The sum of the two gives

$$\begin{aligned}\mathcal{A}^{1'2'3}_{12,(b)}+\mathcal{A}^{1'2'3}_{12,(c)}&=(t^at^c-t^ct^a)_{ji}t^a_{kn}2sg\bar{u}(p_1-q_1)\frac{\hat{p}_2}{s}u(p_1)\frac{1}{t_1}g\varepsilon^*_\sigma\left[\frac{2p_1^\sigma t_1}{\alpha_{q_2}s}\right]\frac{1}{t_2}\bar{u}(p_2+q_2)\frac{\hat{p}_2}{s}u(p_2)\\&=2s\Gamma^a_{1'1}\frac{1}{t_1}g\,(T^c)_{ab}\,\varepsilon^*_\sigma\left[-\frac{2p_1^\sigma t_1}{\alpha_{q_2}s}\right]\frac{1}{t_2}\Gamma^b_{2'2}\,.\end{aligned} \tag{1.55}$$

The sum of the two remaining diagrams, $\mathcal{A}^{1'2'3}_{12,(d)}+\mathcal{A}^{1'2'3}_{12,(e)}$, can be obtained from (1.55) by adding a minus sign and performing the substitution: $p_1\leftrightarrow p_2,\ t_1\leftrightarrow t_2,\alpha_2\leftrightarrow-\beta_1$. The contribution is

$$\mathcal{A}^{1'2'3}_{12,(d)}+\mathcal{A}^{1'2'3}_{12,(e)}=2s\Gamma^a_{1'1}\frac{1}{t_1}g\,(T^c)_{ab}\,\varepsilon^*_\sigma\left[-\frac{2p_2^\sigma t_2}{\beta_{q_1}s}\right]\frac{1}{t_2}\Gamma^b_{2'2}\,. \tag{1.56}$$

Hence, the complete inelastic amplitude $\mathcal{A}^{1'2'3}_{12}$ is

$$\begin{aligned}\mathcal{A}^{1'2'3}_{12}&=2s\Gamma^a_{1'1}\frac{1}{t_1}g(T^c)_{ab}\varepsilon^*_\sigma\left[p_2^\sigma\left(\alpha_{q_2}-\frac{2t_2}{\beta_{q_1}s}\right)+p_1^\sigma\left(\beta_{q_1}-\frac{2t_1}{\alpha_{q_2}s}\right)-(q_1+q_2)_\perp^\sigma\right]\frac{1}{t_2}\Gamma^b_{2'2}\\&\equiv2s\Gamma^a_{1'1}\frac{1}{t_1}g(T^c)_{ab}\varepsilon^*_\sigma C^\sigma(q_2,q_1)\frac{1}{t_2}\Gamma^b_{2'2}\,.\end{aligned} \tag{1.57}$$

The structure in the middle of the two propagators,

$$\gamma^c_{ab}(q_1, q_2) = g(T^c)_{ab}\varepsilon^*_\sigma C^\sigma(q_2, q_1) \ , \tag{1.58}$$

is the previously mentioned Lipatov effective vertex and its structure is schematically represented in Fig. 1.7. Defining $k = q_1 - q_2$ and re-expressing the Lorentz structure inside the Lipatov vertex in terms of scalar products, we obtain

$$\begin{aligned} C^\sigma(q_2, q_1) &= -q^\sigma_{1\perp} - q^\sigma_{2\perp} - \frac{p^\sigma_1}{2p_1 \cdot k}\left(k^2_\perp - 2q^2_{1\perp}\right) + \frac{p^\sigma_2}{2p_2 \cdot k}\left(k^2_\perp - 2q^2_{2\perp}\right) \\ &= -q^\sigma_1 - q^\sigma_2 + p^\sigma_1\left(\frac{q^2_1}{p_1 \cdot k} + \frac{2p_2 \cdot k}{p_1 \cdot p_2}\right) - p^\sigma_2\left(\frac{q^2_2}{p_2 \cdot k} + \frac{2p_1 \cdot k}{p_1 \cdot p_2}\right) \ . \end{aligned} \tag{1.59}$$

Before proceeding further, let us take a little digression to discuss some properties of the vertex. It is simple to observe that

$$C^\sigma(q_2, q_1)k_\sigma = 0 \ , \tag{1.60}$$

which means that the vertex is gauge invariant.
In physical light-cone gauges, the vertex simplifies considerably. Let us choose the following gauge:

$$\varepsilon(k) \cdot p_2 = \varepsilon(k) \cdot k = 0 \ . \tag{1.61}$$

From the first condition $\varepsilon(k)$ has no p_1 component, the second automatically fixes the one along p_2 and we have

$$\varepsilon_\sigma(k) = \varepsilon_{\perp\sigma}(k) - p_{2\sigma}\frac{\varepsilon_\perp \cdot k_\perp}{p_2 \cdot k} \ . \tag{1.62}$$

Using (1.62), we find the form of the Lipatov vertex in this gauge,

$$\gamma^c_{ab}(q_1, q_2) = g(T^c)_{ab}\varepsilon^*_\sigma\left[q^\sigma_{1\perp} - k^\mu_\perp\frac{2q^2_{1\perp}}{k^2_\perp}\right] \ . \tag{1.63}$$

In the light-cone gauge defined by

$$\varepsilon(k) \cdot p_1 = \varepsilon(k) \cdot k = 0 \ , \tag{1.64}$$

the vertex becomes

$$\gamma^c_{ab}(q_1, q_2) = g(T^c)_{ab}\varepsilon^*_\sigma\left[q^\sigma_{2\perp} + k^\mu_\perp\frac{2q^2_{2\perp}}{k^2_\perp}\right] \ . \tag{1.65}$$

Let us now return to the calculation of the imaginary part of the elastic amplitude

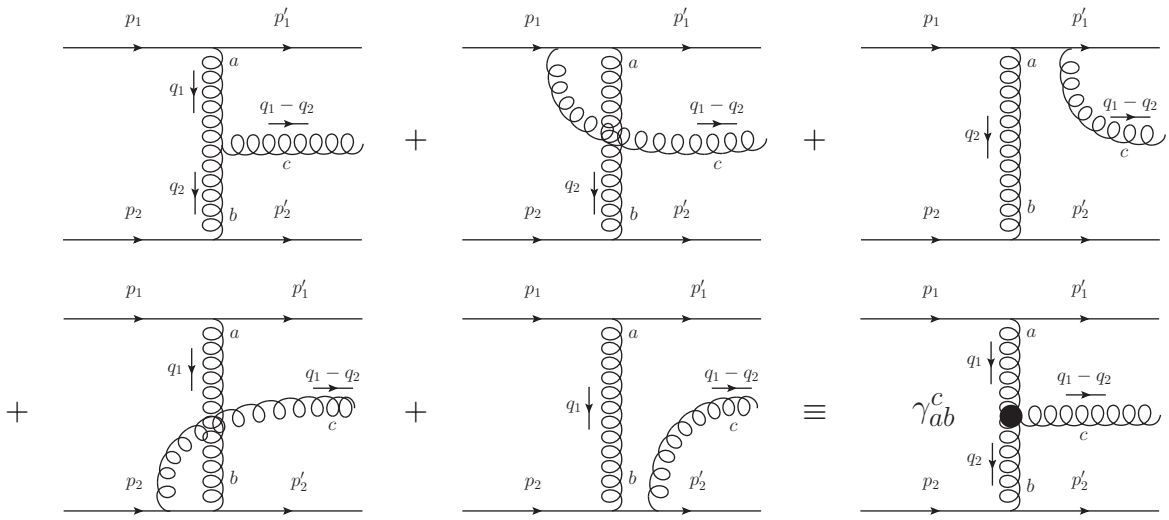

Figure 1.7: Schematic representation of the Lipatov effective vertex.

(Eq. (1.45)). First of all, we have to compute the contraction between the two Lorentz structures appearing in the Lipatov vertex[10],

$$C^\sigma(q_2,q_1)C_\sigma(q-q_2,q-q_1) = 2q_\perp^2 - 2\frac{(q_2-q)_\perp^2 q_{1\perp}^2}{(q_1-q_2)_\perp^2} - 2\frac{(q_1-q)_\perp^2 q_{2\perp}^2}{(q_1-q_2)_\perp^2} \ . \tag{1.66}$$

In the last equation we have neglected the longitudinal component $\beta_q(\alpha_q)$ of the net transverse momentum exchanged in the q-q scattering, with respect to $\beta_{q_1}(\alpha_{q_2})$. As for the color structure and other factors, we have

$$\frac{2s^2 g^6 \delta_{\lambda_1\lambda_{1'}}\delta_{\lambda_2\lambda_{2'}}}{q_{1\perp}^2 q_{2\perp}^2 (q_1-q)_\perp^2 (q_2-q)_\perp^2} f_{abc} f_{dec} (t^d t^a)_{ji} (t^e t^b)_{kn} \ . \tag{1.67}$$

Performing again the projection on negative signature and t-channel color octet through the substitution:

$$(t^e t^b)_{kn} \to \frac{1}{2}(t^e t^b - t^b t^e)_{kn} \ , \tag{1.68}$$

we get

$$-\frac{s^2 g^6 \delta_{\lambda_1\lambda_{1'}}\delta_{\lambda_2\lambda_{2'}} C_A^2}{4q_{1\perp}^2 q_{2\perp}^2 (q_1-q)_\perp^2 (q_2-q)_\perp^2} (t^a)_{ji} (t^a)_{kn} \ . \tag{1.69}$$

For the imaginary part of the elastic amplitude, we get

$$\Im\mathcal{A}^{1'2'}_{12,\text{ladder}} = -\frac{s^2 g^6 \delta_{\lambda_1\lambda_{1'}}\delta_{\lambda_2\lambda_{2'}}}{2} C_A^2 (t^a)_{ji} (t^a)_{kn}$$

[10]Recall that Hermitian conjugation requires the reversal of the direction of momentum in the right hand effective vertex.

$$\times \int d\Phi_3 \frac{1}{q_{1\perp}^2 q_{2\perp}^2 (q_1-q)_\perp^2 (q_2-q)_\perp^2} \left[q_\perp^2 - \frac{(q_2-q)_\perp^2 q_{1\perp}^2}{(q_1-q_2)_\perp^2} - \frac{(q_1-q)_\perp^2 q_{2\perp}^2}{(q_1-q_2)_\perp^2} \right] . \tag{1.70}$$

Now, we can write down the three-particles phase space in terms of Sudakov variables of q_1 and q_2,

$$\begin{aligned} d\Phi_3 = {} & \frac{1}{(2\pi)^{2D-3}} \left(\frac{s}{2}\right)^2 d\beta_{q_1} d\beta_{q_2} d\alpha_{q_1} d\alpha_{q_2} d^{D-2} q_{1\perp} d^{D-2} q_{2\perp} \\ & \times \delta(-\alpha_{q_1} s + q_{1\perp}^2) \delta(\beta_{q_2} s + q_{2\perp}^2) \delta(-\beta_{q_1}\alpha_{q_2} s + (q_1-q_2)_\perp^2) , \end{aligned} \tag{1.71}$$

and obtain[11]

$$\Im \mathcal{A}_{12,\text{ladder}}^{1'2'} = -\frac{s g^6 \delta_{\lambda_1\lambda_{1'}} \delta_{\lambda_2\lambda_{2'}} C_A^2 (t^a)_{ji} (t^a)_{kn}}{8(2\pi)^{2D-3}} \int_{-t/s}^1 \frac{d\beta_{q_1}}{\beta_{q_1}} d^{D-2} q_{1\perp} d^{D-2} q_{2\perp}$$

$$\times \left[\frac{q_\perp^2}{q_{1\perp}^2 q_{2\perp}^2 (q_1-q)_\perp^2 (q_2-q)_\perp^2} - \frac{1}{q_{1\perp}^2 (q_2-q)_\perp^2 (q_1-q_2)_\perp^2} - \frac{1}{q_{2\perp}^2 (q_1-q)_\perp^2 (q_1-q_2)_\perp^2} \right] . \tag{1.72}$$

The first term in the previous expression looks promising, in fact, since the two transverse momentum integration are decoupled, we can easily obtain a factor $\omega^2(t)$. The other two terms, on the other hand, are far from promising, but we still have to include the contributions that come from the second family of diagrams (see (b) of Fig. 1.5). Let us consider the diagram (b) of Fig. 1.5, we have

$$\Im A_{12,(b)}^{1'2'} = \frac{1}{2} \sum_{\{f\}} \int d\Phi_2 \mathcal{A}_{12,\text{box}}^{1'2'}(q_2) \mathcal{A}_{12}^{1'2'}(q-q_2)$$

$$= -\frac{s g^6 \delta_{\lambda_1\lambda_{1'}} \delta_{\lambda_2\lambda_{2'}} C_A^2 t_{ji}^a t_{kn}^a}{16(2\pi)^{2D-3}} \ln\left(\frac{s}{-t}\right) \int d^{D-2} q_{1\perp} d^{D-2} q_{2\perp} \left[\frac{1}{q_{1\perp}^2 (q_2-q)_\perp^2 (q_1-q_2)_\perp^2} \right] . \tag{1.73}$$

The last equality in Eq. (1.73) is obtained by exploiting the expression for $d\Phi_2$, as in Eq. (1.33), but in terms of the Sudakov variables of q_2 and expressing the Regge trajectory $\omega(q_2^2)$, contained in $\mathcal{A}_{12,\text{box}}^{1'2'}(q_2)$, as an integral over the variable q_1[12]. Another point that needs to be clarified concerns $\ln(s/(-t))$. We have only considered the real part of the $\mathcal{A}_{12,\text{box}}^{1'2'}$ amplitude, which is dominant in the high-energy limit. However, the reader may be confused by the fact that, if we keep full amplitude, it seems that $\Im \mathcal{A}_{12}^{1'2'}$ acquires an imaginary part, which is absurd since it is real by definition. The illusory presence of this imaginary part is due to the fact that we are taking all contributions through the cut separately. If we put all the diagrams together, a contribution will also appear where the

[11] The motivation for the bounds in the integration over β_1 is that, in the kinematic region we are interested in, $1 \gg \beta_1 \gg \beta_2 > 0$.

[12] As usual, we also project on negative signature and t-channel color octet.

box is to the right of the cut and its imaginary part will remove exactly the one previously mentioned.

The diagram in which the "box" is replaced by the "cross" gives exactly the same contribution, while, it is simple to observe that the contribution of the two diagrams in which the single gluon is at the right of the cut are obtained by the exchange $q_1 \leftrightarrow q_2$. In this way, we obtain that the total contribution due to the four diagrams in which the cut crosses only the quark lines is

$$\Im A^{1'2'}_{12,\text{unladder}} = -\frac{sg^6\delta_{\lambda_1\lambda_{1'}}\delta_{\lambda_2\lambda_{2'}}C_A^2 t^a_{ji}t^a_{kn}}{8(2\pi)^{2D-3}}\ln\left(\frac{s}{-t}\right)$$

$$\times\int d^{D-2}q_{1\perp}d^{D-2}q_{2\perp}\left[\frac{1}{q_{1\perp}^2(q_2-q)_\perp^2(q_1-q_2)_\perp^2}+\frac{1}{q_{2\perp}^2(q_1-q)_\perp^2(q_1-q_2)_\perp^2}\right]. \tag{1.74}$$

This contribution exactly cancels the "unwanted" part in Eq. (1.72). Finally, we obtain that the imaginary part of the two-loop correction to the amplitude $\mathcal{A}_{12}^{1'2'}$ is

$$\Im A_{12}^{1'2'(2)} = -\frac{sg^6\delta_{\lambda_1\lambda_{1'}}\delta_{\lambda_2\lambda_{2'}}C_A^2 (t^a)_{ji}(t^a)_{kn}}{8(2\pi)^{2D-3}}$$

$$\times\int_{-t/s}^1\frac{d\beta_{q_1}}{\beta_{q_1}}d^{D-2}q_{1\perp}d^{D-2}q_{2\perp}\left[\frac{q_\perp^2}{q_{1\perp}^2q_{2\perp}^2(q_1-q)_\perp^2(q_2-q)_\perp^2}\right]. \tag{1.75}$$

With few efforts, we can rewrite this as

$$\Im A_{12}^{1'2'(2)} = \Gamma^a_{1'1}\frac{s}{t}\Gamma^a_{2'2}\frac{\omega(t)^2}{2}\left[-2\pi\ln\left(\frac{s}{-t}\right)\right]. \tag{1.76}$$

We can use dispersion relation to reconstruct the full amplitude. First, we observe that the term in the square bracket is the imaginary part of $\ln^2((-s)/(-t))$ and then we add the contribution coming from the crossed diagrams in which s is replaced by u[13]:

$$A_{12}^{1'2'(2)} = \Gamma^a_{1'1}\frac{s}{t}\Gamma^a_{2'2}\frac{\omega(t)^2}{2}\left[\ln^2\left(\frac{-s}{-t}\right)+\ln^2\left(\frac{s}{-t}\right)\right]. \tag{1.77}$$

This is exactly the third term in the $\omega(t)$ (or equivalently α_s)-expansion of Eq. (1.14) and it therefore confirms the Reggeization ansatz up to 2-loop. It is important to note that it was necessary to include the contribution of diagrams in which the gluon does not pass through the cut. In the context of this dispersive technique, the contributions obtained when the gluon is cut, are generated by the interference of two inelastic amplitudes at tree level, while the contributions in which the gluon is not cut can be interpreted as

[13]As usual, the minus we get from the factor s t hat goes in $u = -s$ is compensated by a color factor and hence the net effect is only in the sign inside the logarithm.

coming from radiative corrections to the inelastic amplitude at the previous perturbative order. The systematic inclusion of these terms, to all orders in perturbation theory, will be discussed in the next section.

1.2.3 Multi-Regge form of the inelastic $2 \to 2+n$ amplitude

In this section, we want to establish the last ingredient that allows to construct the BFKL approach, *i.e.* the general form of the inelastic $2 \to 2+n$ amplitude in the Regge limit. This form is a generalization of the one appearing in Eq. (1.57).

A useful gauge trick

Let us once again consider the five diagrams that contribute to the Lipatov vertex, Fig. 1.6. Let us imagine that we remove the lower quark line, we are left with the three diagrams corresponding to the emission of a gluon either from the upper quark lines or from the central gluon. In the sum of these three diagrams, all but the bottom gluon are on-shell and this means that we have the Ward identity

$$q_2^\nu \mathcal{M}_\nu^\sigma(q_1,q_2) = 0 \implies \mathcal{A}_{12,(a)+(b)+(c)}^{1'2'3(\text{w. l. l.})} \sim p_2^\nu \mathcal{M}_\nu^\sigma(q_1,q_2) = -\frac{1}{\alpha_{q_2}} q_{2\perp}^\nu \mathcal{M}_\nu^\sigma(q_1,q_2)\ . \tag{1.78}$$

The second implication is correct as the p_2-component of $\mathcal{M}$ is negligible. Now, since in the eikonal approximation $\mathcal{M}$ has no transverse component from diagrams (b) and (c) in Fig. 1.6, the only diagram contributing is (a). Now, we can repeat the discussion removing the upper part of the diagram and obtain

$$q_1^\mu \mathcal{N}_\mu^\sigma(q_1,q_2) = 0 \implies \mathcal{A}_{12,(a)+(e)+(d)}^{1'2'3(\text{w. u. l.})} \sim p_1^\mu \mathcal{N}_\mu^\sigma(q_1,q_2) = -\frac{1}{\beta_{q_1}} q_{1\perp}^\mu \mathcal{N}_\mu^\sigma(q_1,q_2)\ , \tag{1.79}$$

where $\mathcal{N}$ is the analog of $\mathcal{M}$ for the lower line. Now, since in the eikonal approximation $\mathcal{N}$ has no transverse component from diagrams of the type (b) and (c) in Fig. 1.6, again, the only diagram contributing is of the type (a). This observation is very important, because it means that we can organize the structure of the amplitude in (1.57), in such a way to make only the genuine ladder-type diagram contributing. Let us be more precise, the amplitude is

$$\mathcal{A}_{12}^{1'2'3} = 2s\Gamma_{1'1}^a \frac{1}{t_1} g(T^c)_{ab} \varepsilon_\sigma^* C^\sigma(q_2,q_1) \frac{1}{t_2} \Gamma_{2'2}^b = 2s \left(\frac{2p_1^\mu p_2^\nu}{s}\right) \Gamma_{1'1}^a \frac{1}{t_1} g(T^c)_{ab} \varepsilon_\sigma^* \Gamma_{\mu\nu}^\sigma(q_1,q_2) \frac{1}{t_2} \Gamma_{2'2}^b\ , \tag{1.80}$$

where we have defined the quantity

$$\Gamma_{\mu\nu}^\sigma(q_1,q_2) \equiv \frac{2p_{2,\mu}p_{1,\nu}}{s} C^\sigma(q_2,q_1)\ . \tag{1.81}$$

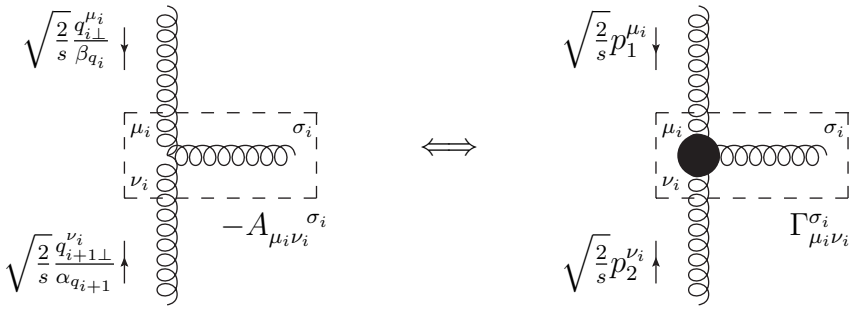

Figure 1.8: Schematic representation of the gauge trick.

In the last equality in Eq. (1.80), we have isolated the factors $p_{1,\mu}$ and $p_{2,\nu}$ appearing in the previous Ward identities. From the previous discussion, it is clear that, the same amplitude must be obtained considering only the diagram involving the triple gluon vertex (*i.e.* $-A_{\mu\nu}{}^{\sigma}(q_2, q_1 - q_2)$ instead of $\Gamma^{\sigma}_{\mu\nu}(q_1, q_2)$ in Eq. (1.80)), but performing at the same time the replacement

$$\left(\frac{2p_1^{\mu}p_2^{\nu}}{s}\right) \longrightarrow \left(\frac{2q_{1\perp}^{\mu}q_{2\perp}^{\nu}}{\beta_{q_1}\alpha_{q_2}s}\right) . \tag{1.82}$$

Hence, we must have

$$\mathcal{A}_{12}^{1'2'3} = -2s\left(\frac{2q_{1\perp}^{\mu}q_{2\perp}^{\nu}}{\beta_{q_1}\alpha_{q_2}s}\right)\Gamma^{a}_{1'1}\frac{1}{t_1}g(T^c)_{ab}\varepsilon^{*}_{\sigma}A_{\mu\nu}{}^{\sigma}(q_2, q_1 - q_2)\frac{1}{t_2}\Gamma^{b}_{2'2} .$$

By substituting the explicit expression of $A_{\mu\nu}{}^{\sigma}$ and using the Sudakov decomposition for momenta q_1 and q_2, we can verify the relation explicitly. After a bit of algebra, we find

$$\mathcal{A}_{12}^{1'2'3} = 2s\Gamma^{a}_{1'1}\frac{1}{t_1}g(T^c)_{ab}$$

$$\times\varepsilon^{*}_{\sigma}\left[p_2^{\sigma}\left(\alpha_{q_2} - \frac{2t_2}{\beta_{q_1}s}\right) + p_1^{\sigma}\left(\beta_{q_1} - \frac{2t_1}{\alpha_{q_2}s}\right) - (q_1 + q_2)_{\perp}^{\sigma} + \frac{(q_{1\perp}^2 - q_{2\perp}^2)}{\beta_{q_1}\alpha_{q_2}s}(q_1 - q_2)^{\sigma}\right]\frac{1}{t_2}\Gamma^{b}_{2'2} .$$

We recover exactly the same expression, apart for a gauge term that evidently vanishes because

$$\varepsilon^{*}_{\sigma}(q_1 - q_2)^{\sigma} = \varepsilon^{*}_{\sigma}(q_1 - q_2)(q_1 - q_2)^{\sigma} = 0 . \tag{1.83}$$

We have therefore established that, apart from a gauge term, the following equality

$$\frac{2p_1^{\mu}p_2^{\nu}}{s}\Gamma^{\sigma}_{\mu\nu}(q_1, q_2) = -\frac{2q_{1\perp}^{\mu}q_{2\perp}^{\nu}}{\beta_{q_1}\alpha_{q_2}s}A_{\mu\nu}{}^{\sigma}(q_2, q_1 - q_2) \tag{1.84}$$

holds. In the next section, we will need this relation applied to the i-th vertex of the scale, *i.e.*

$$\frac{2p_1^{\mu_i}p_2^{\nu_i}}{s}\Gamma^{\sigma_i}_{\mu_i\nu_i}(q_1, q_2) = -\frac{2q_{i\perp}^{\mu_i}q_{i+1\perp}^{\nu_i}}{\beta_{q_i}\alpha_{q_{i+1}}s}A_{\mu_i\nu_i}{}^{\sigma_i}(q_{i+1}, q_i - q_{i+1}) . \tag{1.85}$$

A schematic representation of this trick is shown in Fig. 1.8.

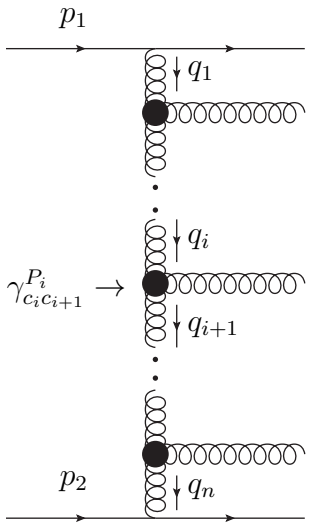

Figure 1.9: Schematic representation of $\mathcal{A}_{12}^{1'2'\ldots n+2}$.

Proof of multiperipheral form of inelastic amplitude à la Gribov-Levin-Ryskin

In this section, we want to prove that the inelastic $2 \to 2+n$ amplitude, generalizing Eq. (1.57), assumes the following form:

$$\mathcal{A}_{12}^{1'2'+n} = 2s\Gamma^{c_1}_{1'1}\left(\prod_i^n \gamma^{P_i}_{c_i c_{i+1}}(q_i, q_{i+1})\frac{1}{t_i}\right)\frac{1}{t_{n+1}}\Gamma^{c_{n+1}}_{2'2}\ , \tag{1.86}$$

which is schematically represented in Fig. 1.9. As a first observation, we note that the eikonal approximation we have illustrated in the section 1.2.1 holds for particles of any spin and therefore also for gluons. In this case, it is still valid at every central vertex due to the strong ordering in rapidity required by the multi-Regge kinematics, *i.e.*

$$1 \gg \beta_{q_i} \gg \beta_{q_{i+1}} \gg \frac{-t}{s}\ , \quad 1 \gg |\alpha_{q_{i+1}}| \gg |\alpha_{q_i}| \gg \frac{-t}{s}\ . \tag{1.87}$$

To prove the form (1.86), we will follow the elegant derivation in [34]. Consider the amplitude for two quarks to scatter into two quarks plus n gluons. As described before, if we cut the i_{th} vertical propagator the amplitude is split into an upper part $\mathcal{M}_\mu(p_1, q_1, ..., q_i)$ and a lower part $\mathcal{N}_\nu(p_2, q_i, ..., q_n)$ (see Fig. 1.10). As seen in the previous sections, the following two Ward identities

$$q^\mu_{i\perp}\mathcal{M}_\mu = -\beta_{q_i}p_2^\mu\mathcal{M}_\mu\ , \qquad q^\nu_{i\perp}\mathcal{N}_\nu = -\alpha_{q_i}p_1^\nu\mathcal{N}_\mu \tag{1.88}$$

hold. This means that we can replace the numerator of the cut gluon propagator by

$$\frac{2q^\mu_{i\perp}q^\nu_{i\perp}}{\beta_{q_i}\alpha_{q_i}s}\ . \tag{1.89}$$

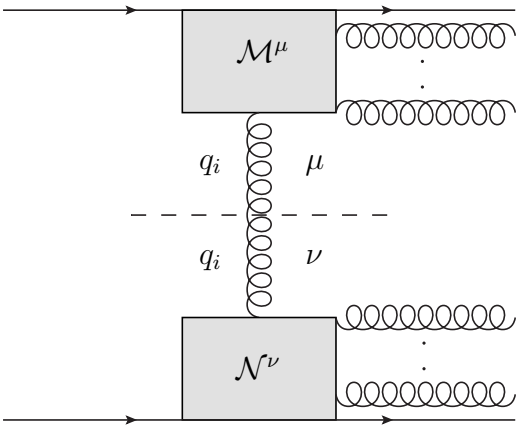

Figure 1.10: t-channel cut of the amplitude $\mathcal{A}_{12}^{1'2'+n}$.

It is evident that this procedure can be repeated for all vertical gluon lines and we can perform the same manipulations. Therefore, we end up with an amplitude that is a genuine uncrossed ladder in which the metric tensor in the propagator (approximated à la Gribov) can be written as (1.89).
We can associate a factor $\sqrt{\frac{2}{s}}q_{i\perp}^{\mu_i}/\alpha_{q_i}$ to the top of the i_{th} vertical gluon line and a factor $\sqrt{\frac{2}{s}}q_{i\perp}^{\nu_i}/\beta_{q_i}$ to the bottom of the same line. In this way, the amplitude immediately becomes

$$\mathcal{A}_{12}^{1'2'+n} = 2s\Gamma_{1'1}^{c_1}\left(\prod_i^n(-g)\varepsilon_{\sigma_i}^* T_{c_ic_{i+1}}^{P_i}\frac{2q_{i\perp}^{\mu_i}q_{i+1\perp}^{\nu_i}}{\alpha_{q_{i+1}}\beta_{q_i}s}A_{\mu_i\nu_i}^{\ \ \sigma_i}(q_{i+1}, q_i - q_{i+1})\frac{1}{t_i}\right)\frac{1}{t_{n+1}}\Gamma_{2'2}^{c_{n+1}}\ . \quad (1.90)$$

Using Eqs. (1.81, 1.85), we obtain exactly the result (1.86).

Genuine gluon ladders only

Everything we have shown works if, when the gauge trick is applied to the t-channel gluons, the only dominant diagrams are the genuine gluon ladder contributions (see Fig. (1.11)). Each of the diagrams contains multiple terms, we focus on a few of these to demonstrate the suppression mechanism of non-genuine contributions. Since they are useless for the purposes of the discussion below, we neglect color factors.
Let us start by considering the diagram (a), we are going to focus on terms proportional to $p_1^{\sigma_{i-1}}p_2^{\sigma_i}$ and $q_{i-1\perp}^{\sigma_{i-1}}q_{i+1\perp}^{\sigma_i}$. The upper vertex of the diagram has a contribution proportional to

$$-\frac{2q_{i-1\perp}^{\mu}q_{i\perp}^{\tau}}{\beta_{q_{i-1}}\alpha_{q_i}s}g_{\mu\tau}(q_{i-1}+q_i)^{\sigma_{i-1}} \sim \frac{t}{\beta_{q_{i-1}}\alpha_{q_i}s}(\beta_{q_{i-1}}p_1^{\sigma_{i-1}}) = \beta_{q_{i-1}}p_1^{\sigma_{i-1}}\ ,$$

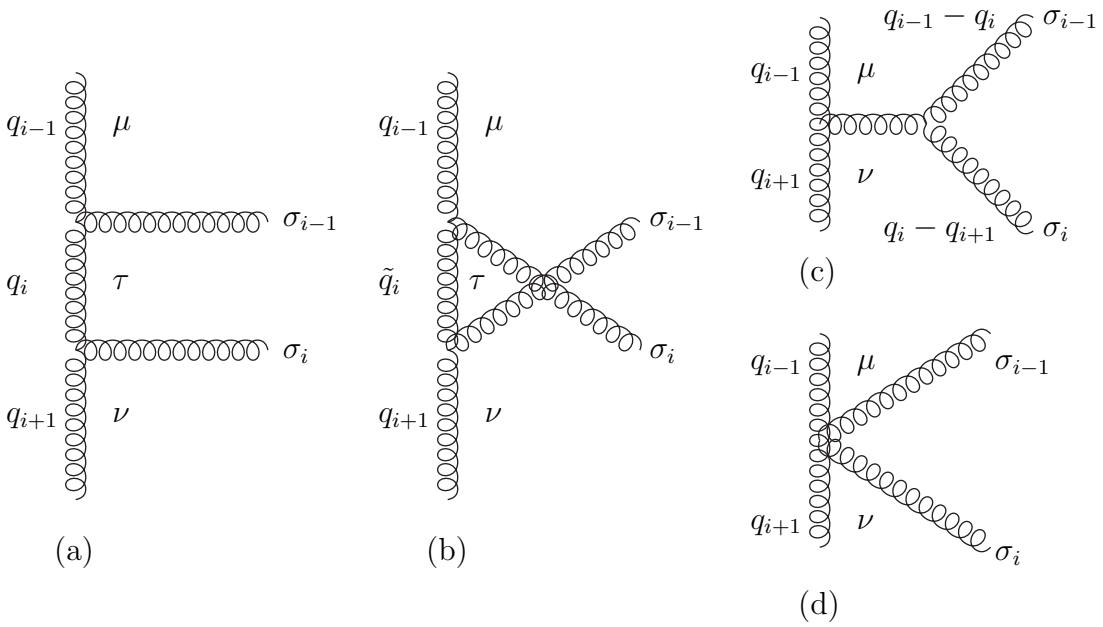

Figure 1.11: The diagram (a) represents the genuine ladder contribution, while, all other contributions are the non-genuine ones.

while the lower has a term of the form

$$-\frac{2q_{i\perp}^{\tau}q_{i+1\perp}^{\nu}}{\beta_{q_i}\alpha_{q_{i+1}}s}g_{\tau\nu}(q_i+q_{i+1})^{\sigma_i} \sim \frac{t}{\beta_{q_i}\alpha_{q_{i+1}}s}(\alpha_{q_{i+1}}p_2^{\sigma_i}) = \alpha_{q_{i+1}}p_2^{\sigma_i} \ .$$

In the last two equalities of previous expressions we have used that $\beta_{q_{i-1}} \sim \frac{t}{\alpha_{q_i}s}$[14]. The total contribution goes like

$$\beta_{q_{i-1}}\alpha_{q_{i+1}}p_1^{\sigma_{i-1}}p_2^{\sigma_i} \ . \tag{1.91}$$

The transverse contribution can be immediately extracted and goes like

$$\left(\frac{t}{\beta_{q_{i-1}}\alpha_{q_i}s}\right)\left(\frac{t}{\beta_{q_i}\alpha_{q_{i+1}}s}\right)q_{i-1\perp}^{\sigma_{i-1}}q_{i+1\perp}^{\sigma_i} \sim q_{i-1\perp}^{\sigma_{i-1}}q_{i+1\perp}^{\sigma_i} \ . \tag{1.92}$$

We must also note that we have a propagator of the order

$$\frac{1}{q_i^2} \sim \frac{1}{t} \sim \frac{1}{\beta_{q_{i-1}}\alpha_{q_i}s} \ . \tag{1.93}$$

Let us move to diagram (b). We observe that, when we work on a genuine ladder, we are always dealing with terms of type

$$-\frac{2q_{i\perp}^{\mu_i}q_{i+1\perp}^{\nu_i}}{\beta_{q_i}\alpha_{q_{i+1}}s}A_{\mu_i\nu_i}{}^{\sigma_i}(q_{i+1}, q_i - q_{i+1})$$

[14]Please note that these relations come from the on-shell conditions of outgoing particles.

$$= \frac{2q_{i\perp}^{\mu_i} q_{i+1\perp}^{\nu_i}}{\beta_{q_i}\alpha_{q_{i+1}} s} \left[-g_{\mu_i\nu_i}(q_i + q_{i+1})^{\sigma_i} + g_{\mu_i}^{\sigma_i}(2q_i - q_{i+1})_{\nu_i} + g_{\nu_i}^{\sigma_i}(2q_{i+1} - q_i)_{\mu_i} \right] . \tag{1.94}$$

Unlike this, when we work with crossed ladders, the momenta entering the upper and lower vertex are not simply the "closest neighbors" q_i and q_{i+1}. The generalization of formula (1.94) in this latter case is

$$-\frac{2q_{i\perp}^{\mu} q_{j\perp}^{\nu}}{\beta_{q_i}\alpha_{q_j} s} A_{\mu\nu}{}^{\sigma}(q_j, q_i - q_j)$$

$$= \frac{2q_{i\perp}^{\mu} q_{j\perp}^{\nu}}{\beta_{q_i}\alpha_{q_j} s} \left[-g_{\mu\nu}(q_i + q_j)^{\sigma} + g_{\mu}^{\sigma}(2q_i - q_j)_{\nu} + g_{\nu}^{\sigma}(2q_j - q_i)_{\mu} \right] . \tag{1.95}$$

By using this formula, we are able to see that the diagram (b) has a contribution proportional to

$$\left(\frac{\beta_{q_i}}{\beta_{q_{i-1}}} \right)^2 \beta_{q_{i-1}}\alpha_{q_{i+1}} p_1^{\sigma_{i-1}} p_2^{\sigma_i} . \tag{1.96}$$

We immediately realize that Eq. (1.96) has a suppressing[15] factor $(\beta_{q_i}/\beta_{q_{i-1}})^2$ with respect to the corresponding term in Eq. (1.91). Furthermore, also the propagator is strongly suppressed, in fact

$$\frac{1}{\tilde{q}_i^{\,2}} = \frac{1}{(q_{i-1} + q_{i+1} - q_i)^2} \sim \frac{1}{\beta_{q_{i-1}}\alpha_{q_{i+1}} s} \ll \frac{1}{\beta_{q_{i-1}}\alpha_{q_i} s} . \tag{1.97}$$

We now pass to diagram (c), it is obtained by the contraction of two triple gluon vertices and the usual "effective" polarization of t-channel gluons. We can easily find that it has a contribution proportional to

$$\frac{\beta_{q_i}}{\beta_{q_{i-1}}} q_{i-1\perp}^{\sigma_{i-1}} q_{i+1\perp}^{\sigma_i} , \tag{1.98}$$

which again has a suppression factor and, moreover, the gluon propagator in this case gives

$$\frac{1}{(q_{i-1} - q_{i+1})^2} = \frac{1}{\alpha_{q_{i+1}}\beta_{q_{i-1}} s} \ll \frac{1}{\beta_{q_i}\alpha_{q_{i+1}} s} . \tag{1.99}$$

The last diagram is (d); since in this case we do not have a propagator, we can multiply and divide by a factor t in such a way as to make the factor related to the denominator equal to that of (a). In this way, we obtain a term of the form

$$\frac{t}{\beta_{q_{i-1}}\alpha_{q_{i+1}} s} q_{i-1\perp}^{\mu} q_{i-1\perp}^{\nu} \sim \frac{\beta_{q_i}}{\beta_{q_{i-1}}} q_{i-1\perp}^{\mu} q_{i-1\perp}^{\nu} , \tag{1.100}$$

which has the usual suppression factor.

[15] Remind the strong order in the Sudakov variables in Eq. (1.87).

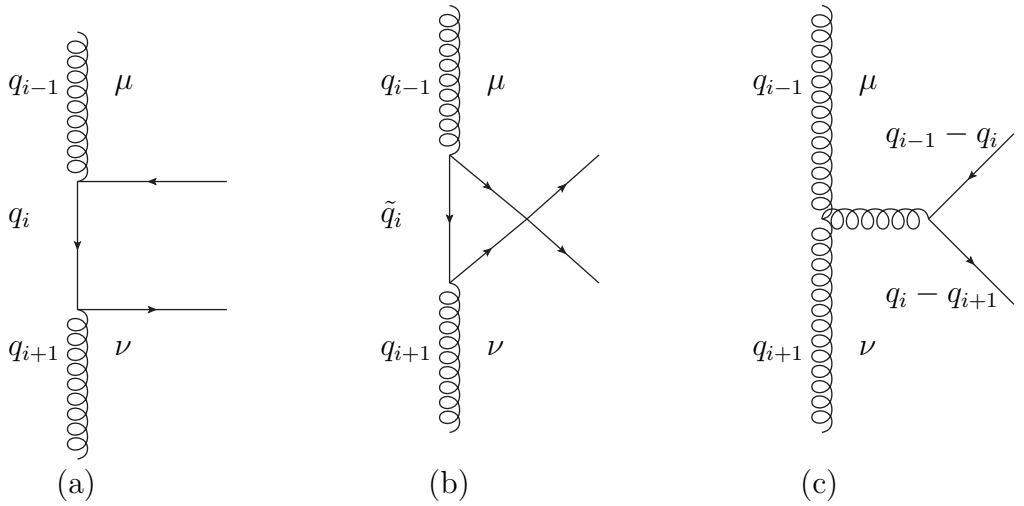

Figure 1.12: Diagrams involving fermions.

Absence of fermions

Another important point is the absence of diagrams containing fermions (see Fig. 1.12). The reason for this absence is to be found in the fact that a particle of spin 1/2 is being exchanged in the t-channel. A particle of this spin generates a less strong s-dependence than that of a spin one boson such as the gluon.

We can understand this suppression as before. In the case where fermions cross, (b) in Fig. 1.12, or are produced by the splitting of a single outgoing gluon, (c) in Fig. 1.12, we certainly have a suppression factor coming from a propagator. For the diagram (a) in Fig. 1.12 a simple computation shows that we have again a suppression factor of $\beta_{q_i}/\beta_{q_{i-1}}$.

Reggeization in all sub-channels

In the previous subsection, we constructed the tree-level amplitude for two quarks to scatter to two quarks and n gluons in the multi-Regge kinematics. This amplitude, multiplied by its complex conjugate and integrated over the phase space of $n+2$ particles will contribute to the imaginary part of the amplitude of the Reggeized gluon. Obviously, as seen explicitly in the section 1.2.2, this is not sufficient to reconstruct all the dominant part of the amplitude in the high-energy limit. In fact, in the two-loop calculation it is necessary to insert some corrections in which the cut only goes through the two quark lines. It is important to find a systematic method of including these loop corrections in

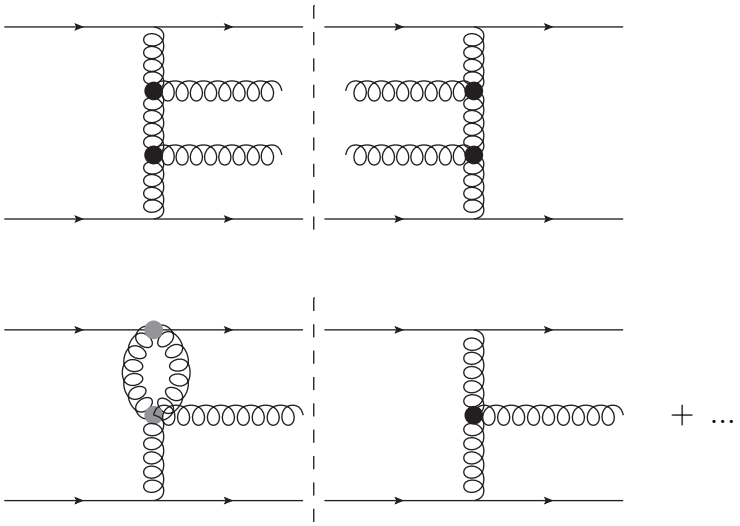

Figure 1.13: In the upper diagram the contribution to the order g^8 which is obtained from the square of the amplitude $\mathcal{A}_{12}^{1'2'+2}$. In the bottom diagram, the contribution to the order g^8 in which one gluon is not cut. This contribution can be included by reggeizing the corresponding propagator in the amplitude $\mathcal{A}_{12}^{1'2'3}$.

our generalized form for the amplitude in Eq. (1.86).

Let us start with a very simple observation. If we focus only on the real part of the amplitude $\mathcal{A}_{AB}^{A'B'}$ (which is dominant in the high-energy approximation), the Reggeization ansatz in Eq. (1.14) becomes

$$\Re\mathcal{A}_{AB}^{A'B'} = \Gamma^i_{A'A}\frac{2s}{t}\left(\frac{s}{-t}\right)^{\omega(t)}\Gamma^i_{B'B}\ . \tag{1.101}$$

Basically, it can be obtained by the following replacement in the t-channel gluon propagator

$$\frac{-ig_{\mu\nu}\delta^{ab}}{t} \to \frac{-ig_{\mu\nu}\delta^{ab}}{t}\left(\frac{s}{-t}\right)^{\omega(t)}\ . \tag{1.102}$$

Now, the crucial point of the whole Reggeization is that, including these loop corrections is equivalent to Reggeize all the t-channel gluons in the inelastic amplitude $\mathcal{A}_{12}^{1'2'+n}$, *i.e.* performing the replacement

$$\frac{1}{t_i} \to \frac{1}{t_i}\left(\frac{s_i}{s_R}\right)^{\omega(t_i)} \tag{1.103}$$

in Eq. (1.86), where s_i is the center-of-mass energy coming into the $i_{\rm th}$ section of the gluon ladder and we have introduced a scale s_R which is of the order of $-t$. The scale s_R is irrelevant in LLA as its variation produces sub-leading effects.

Therefore, the final **multi-Regge exchange** amplitude for $2 \to 2+n$ is[16]

$$\Re\mathcal{A}_{12}^{1'2'+n} = 2s\Gamma_{1'1}^{c_1}\left(\prod_{i=1}^{n}\gamma_{c_ic_{i+1}}^{P_i}(q_i,q_{i+1})\left(\frac{s_i}{s_R}\right)^{\omega(t_i)}\frac{1}{t_i}\right)\frac{1}{t_{n+1}}\left(\frac{s_{n+1}}{s_R}\right)^{\omega(t_{n+1})}\Gamma_{2'2}^{c_{n+1}}\ . \quad (1.104)$$

A proof can be achieved, in the LLA, using Regge theory techniques, exploiting unitarity in all possible final state sub-channels. We will not delve into the intricacies of this proof, but we want just to give some intuitive arguments. Previously, we proved the Regge form of the scattering amplitude for two quarks to two quarks up to the order g^6 (2-loop). Suppose we want to consider the order g^8 (3-loop), for sure we will have to consider the inelastic amplitude

$$\mathcal{A}_{12}^{1'2'34} = 2s\Gamma_{1'1}^{c_1}\frac{1}{t_1}\left(\frac{s_1}{s_R}\right)^{\omega(t_1)}\gamma_{c_1c_2}^{P_1}(q_1,q_2)\frac{1}{t_2}\left(\frac{s_2}{s_R}\right)^{\omega(t_2)}\gamma_{c_2c_3}^{P_2}(q_2,q_3)\frac{1}{t_3}\left(\frac{s_3}{s_R}\right)^{\omega(t_3)}\Gamma_{2'2}^{c_3}\ . \quad (1.105)$$

An immediate observation is that, if we perturbatively expand the Regge factors up to the non-trivial first order, we find a term of order g^4 plus three terms of order g^6. When we square and integrate over the phase space this $2 \to 4$ amplitude to reconstruct the contribution to the imaginary part of the $2 \to 2$ amplitude, only the term of order g^4 in Eq. (1.105) will produce a term contributing within g^8 (see top diagram in Fig. 1.13). Hence, the Reggeization of this contribution will only impact the next perturbative order. Now, let us take a step back and look at the form of the inelastic $2 \to 3$ amplitude, we have

$$\mathcal{A}_{12}^{1'2'3} = 2s\Gamma_{1'1}^{c_1}\frac{1}{t_1}\left(\frac{s_1}{s_R}\right)^{\omega(t_1)}\gamma_{c_1c_2}^{P_1}(q_1,q_2)\frac{1}{t_2}\left(\frac{s_2}{s_R}\right)^{\omega(t_2)}\Gamma_{2'2}^{c_2}\ . \quad (1.106)$$

Obviously, as before, this form contains a factor g^3 as well as two factors g^5; this means that, when we square we produce four interference terms which are of the order g^8 and will impact in our 3-loop computation. A schematic representation of some of these terms is presented in the bottom diagram of Fig. 1.13. These terms reproduce exactly the corrections of order g^8 which, using this dispersive technique, would have been obtained from diagrams in which a gluon is not cut. There is therefore a reshuffle, which allows us to automatically generate the contributions in which there are loops that are not cut when the $2 \to 2$ amplitude is dispersively reconstructed using Cutkosky's rules.

Let us look more closely at the contribution in the bottom of Fig. 1.13 and study the

[16]It is important to observe that this simple factorized form is strictly valid only for the real part of the amplitudes. However, as we will see, only the real part is important within LLA and NLLA accuracy. The real part will be implied in subsequent formulas in which we remove the symbol $\Re$.

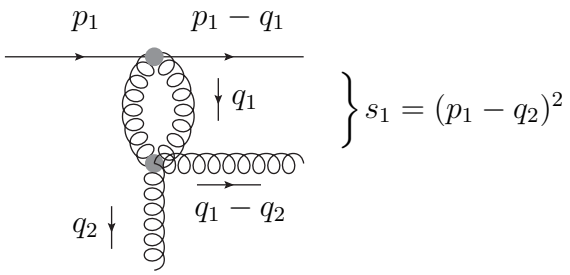

Figure 1.14: Upper section of the diagram in which one gluon is not cut.

section of the diagram shown in Fig. 1.14. In this section of the diagram, the momentum exchanged is q_1 and the energy available in the center of mass is

$$s_1 = (p_1 - q_2)^2 \simeq -\alpha_{q_2} s \; . \tag{1.107}$$

This energy is much lower than s, but is much greater than the typical transverse scale s_R that we introduced, in fact

$$s_1 \simeq -\alpha_{q_2} s = \frac{1}{\beta_{q_1}} \left(-\beta_{q_1} \alpha_{q_2} s\right) \sim \frac{1}{\beta_{q_1}} (-t) \sim \frac{1}{\beta_{q_1}} s_R \; . \tag{1.108}$$

We therefore have a scale hierarchy which, in the spirit of Reggeization, will produce logarithmic corrections of the ratio s_1/s_R. To all orders in perturbation theory, the effect will be to Reggeize the propagator with momenta q_1, *i.e.*

$$\frac{1}{t_1} \to \frac{1}{t_1} \left(\frac{s}{s_R}\right)^{\omega(t_1)} \; . \tag{1.109}$$

Obviously, the same reasoning extended to all subsections of the ladder, leads us precisely to the form in Eq. (1.104). The final form of the inelastic amplitude, schematized in Fig. (1.15), it is therefore a "half ladder", whose vertical gluons are themselves Reggeized gluons (and therefore they are themselves an infinite superposition of diagrams).

1.2.4 BFKL equation

Let us now consider the BFKL equation in the LLA. Instead of directly considering the Pomeron channel, *i.e.* imaginary part of the forward-scattering amplitude ($t = 0$ and vacuum quantum numbers in the t-channel), we will keep more general. Indeed, it should be noted that the BFKL approach gives the description of QCD-scattering amplitudes in the region of large s, for any fixed momentum transfer t (*i.e.* not growing with s) and for

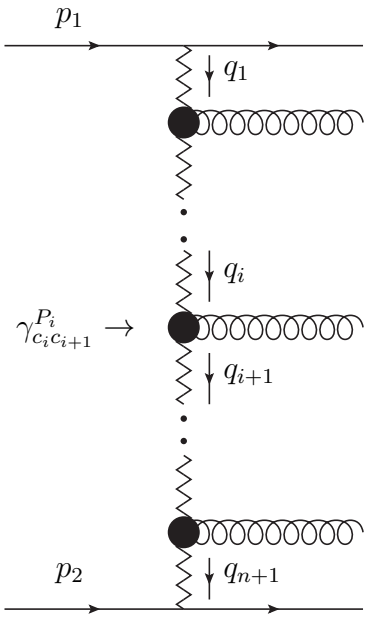

Figure 1.15: Schematic representation of $\mathcal{A}_{12}^{1'2'+n}$ after we include the Reggeization in all sub-channels.

various color state exchanges in the t-channel.
The imaginary part of the scattering amplitude $\mathcal{A}_{12}^{1'2'}$ (of the process $1+2 \longrightarrow 1'+2'$) in the s-channel can be written, using the Cutkosky rules (1.3), as

$$\Im_s \mathcal{A}_{12}^{1'2'} = \frac{1}{2} \sum_{n=0}^{\infty} \sum_{\{f\}} \int \mathcal{A}_{12}^{\tilde{1}\tilde{2}+n} \left(\mathcal{A}_{1'2'}^{\tilde{1}\tilde{2}+n} \right)^* d\Phi_{n+2} \, , \tag{1.110}$$

where $\mathcal{A}_{AB}^{\tilde{A}\tilde{B}+n}$ is the amplitude introduced in Eq. (1.104) for the production of $n+2$ particles having momenta k_i, with $i = 0, 1, ..., n, n+1$ (we set $p_{\tilde{1}} = k_0$ and $p_{\tilde{2}} = k_{n+1}$), $d\Phi_{n+2}$ is the element of the intermediate particle phase of space, $\sum_f$ means sum over all the discrete quantum numbers of the intermediate particles (see Figure 1.16).

Kinematics

As before, we introduce the light-cone vectors p_1 and p_2 ($p_1^2 = p_2^2 = 0$), so that the center-of-mass energy is $s = 2p_1 \cdot p_2$. Using the Sudakov decomposition, the momenta k_i can be parametrized as

$$k_i = \beta_i p_1 + \alpha_i p_2 + k_{i\perp}, \qquad\qquad s\alpha_i\beta_i = k_i^2 - k_{i\perp}^2 = k_i^2 + \vec{k}_i^{\,2}. \tag{1.111}$$

To extract the dominant contribution ($\sim s$) in Eq. (1.110) we should rely on the MRK. By definition, in this kinematics, transverse momenta of produced particles are limited

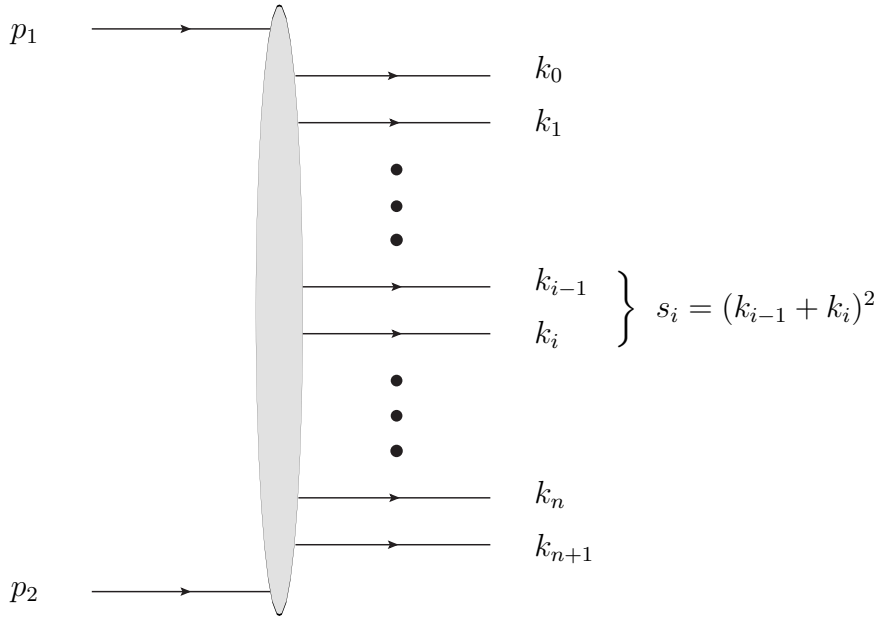

Figure 1.16: Production of $n+2$ particles in the multi-Regge kinematics

and their Sudakov variables α_i and β_i are strongly ordered in the rapidity space, having so[17]

$$\alpha_{n+1} \gg \alpha_n \gg \alpha_{n-1} ... \gg \alpha_0 \ , \qquad \beta_0 \gg \beta_1 \gg \beta_2 ... \gg \beta_{n+1} \ . \tag{1.112}$$

In this case, we have that

$$\alpha_{n+1} \simeq 1, \ \beta_0 \simeq 1 \ , \qquad \text{and} \qquad \alpha_0 \simeq \frac{\vec{k}_0^{\,2}}{s}, \ \beta_{n+1} \simeq \frac{\vec{k}_{n+1}^{\,2}}{s} \ . \tag{1.113}$$

In the MRK the squared invariant masses $s_{i,j} = (k_i + k_j)^2$ of any pair of produced particles i and j are large (see Fig. 1.16). In particular we have

$$s_{i-1,i} \equiv s_i = (k_{i-1} + k_i)^2 \simeq s\beta_{i-1}\alpha_i = \frac{\beta_{i-1}}{\beta_i}(k_i^2 + \vec{k}_i^{\,2}) \ . \tag{1.114}$$

The momenta q_i of the t-channel Reggeons can be expressed as follows:

$$\begin{aligned} q_i &= p_1 - \sum_{j=0}^{i-1} k_j = \left(1 - \sum_{j=0}^{i-1} \beta_j\right) p_1 - \left(\sum_{j=0}^{i-1} \alpha_j\right) p_2 - \sum_{j=0}^{i-1} k_{j\perp} \\ &= \left(\sum_{j=i}^{n+1} \beta_j\right) p_1 - \left(\sum_{j=0}^{i-1} \alpha_j\right) p_2 - \sum_{j=0}^{i-1} k_{j\perp} \simeq \beta_i p_1 - \alpha_{i-1} p_2 - \sum_{j=0}^{i-1} k_{j\perp} \ , \end{aligned} \tag{1.115}$$

[17] Differently from the previous section, we give the definition of multi-Regge kinematics in terms of the longitudinal Sudakov variables of the outgoing particles. The two sets of conditions are fully equivalent.

where we first used the conservation of momenta along p_1-direction,

$$1 = \sum_{j=0}^{n+1} \beta_j \tag{1.116}$$

and then conditions of MRK in Eq. (1.112) to simplify the expression. The $i_{\rm th}$ momentum squared is $t_i = q_i^2 \simeq q_{i\perp}^2 = -\vec{q}_i^{\,2}$ and is predominantly transverse.
We now recall the form of the inelastic amplitude $2 \to 2+n$, introduced in the previous section (see Fig. 1.15):

$$\mathcal{A}_{12}^{\tilde{1}\tilde{2}+n} = 2s\Gamma_{\tilde{1}1}^{c_1} \left(\prod_{i=1}^{n} \gamma_{c_i c_{i+1}}^{P_i}(q_i, q_{i+1}) \left(\frac{s_i}{s_R} \right)^{\omega(t_i)} \frac{1}{t_i} \right) \frac{1}{t_{n+1}} \left(\frac{s_{n+1}}{s_R} \right)^{\omega(t_{n+1})} \Gamma_{\tilde{2}2}^{c_{n+1}}, \tag{1.117}$$

where

$$\gamma_{c_i c_{i+1}}^{G_i}(q_i, q_{i+1}) = g T_{c_i c_{i+1}}^{d_i} \varepsilon_\mu^*(k_i) C^\mu(q_{i+1}, q_i), \tag{1.118}$$

and the Lorentz structure (C^μ) is

$$C^\mu(q_{i+1}, q_i) = -q_i^\mu - q_{i+1}^\mu + p_1^\mu \left(\frac{q_i^2}{k_i \cdot p_1} + 2\frac{k_i \cdot p_2}{p_1 \cdot p_2} \right) - p_2^\mu \left(\frac{q_{i+1}^2}{k_i \cdot p_2} + 2\frac{k_i \cdot p_1}{p_1 \cdot p_2} \right). \tag{1.119}$$

The current conservation property $(k_i)_\mu C^\mu$ (see Eq. (1.60)) permits us to choose an arbitrary gauge for each of the produced gluons. It is easy to observe that the other amplitude appearing in the Eq. (1.110) ($\mathcal{A}_{1'2'}^{\tilde{1}\tilde{2}+n}$) can be obtained from Eq. (1.117) by the substitutions

$$1 \longrightarrow 1' \,, \quad 2 \longrightarrow 2' \,, \quad q_i \longrightarrow q_i' \equiv q_i - q,$$

with

$$q = p_1 - p_{1'} \simeq q_\perp. \tag{1.120}$$

Color decomposition

Of all the possible color states exchanged in the t-channel, we would like to extract the two cases of greatest physical relevance, that of singlet (Pomeron channel) and that of anti-symmetrical octet (Reggeized gluon channel). For this purpose, we have to decompose the product of two adjoint $SU(3)$ representations (the two gluons in t-channel) into sum of irreducible representations, *i.e.*

$$8 \otimes 8 = 1^+ \oplus 8_A^- \oplus 8_S^+ \oplus (10 \oplus \overline{10})^- \oplus 27^+ \,, \tag{1.121}$$

where the superscript denotes the signature of the representation and the symmetric and anti-symmetric parts of the color octet have been decoupled. In practice, this corresponds

to decomposing the product of two matrices in the adjoint representation of $SU(3)$ in the following way:

$$T^{d_i}_{c_i c_{i+1}} \left(T^{d_i}_{c'_i c'_{i+1}}\right)^* = \sum_R c_R \, \langle c_i c'_i | \hat{\mathcal{P}}_R | c_{i+1} c'_{i+1} \rangle \, , \tag{1.122}$$

where $\hat{\mathcal{P}}_R$ are the projection operators of two-gluon colour states in the t-channel in the unitary condition (1.110) on the irreducible representation R of the colour group. For the singlet representation, we have

$$c_0 = N \, , \qquad \langle c_i c'_i | \hat{\mathcal{P}}_0 | c_{i+1} c'_{i+1} \rangle = \frac{\delta^{c_i c'_i} \delta^{c_{i+1} c'_{i+1}}}{N^2 - 1} \, , \tag{1.123}$$

while for the color octet

$$c_8 = \frac{N}{2} \, , \qquad \langle c_i c'_i | \hat{\mathcal{P}}_8 | c_{i+1} c'_{i+1} \rangle = \frac{f_{a c_i c'_i} f_{a c_{i+1} c'_{i+1}}}{N} \, . \tag{1.124}$$

It is easy to check that these are the correct projectors; for example, in the case of singlet we have

$$c_0 \, \langle c_i c'_i | \hat{\mathcal{P}}_0 | c_{i+1} c'_{i+1} \rangle = N \frac{\delta^{c_i c'_i} \delta^{c_{i+1} c'_{i+1}}}{N^2 - 1} = \begin{cases} 2 C_A^2 C_F & \text{if } c_i = c'_i \text{ and } c_{i+1} = c'_{i+1} \\ 0 & \text{otherwise} \end{cases} \, , \tag{1.125}$$

where in the upper term the summation is taken over c_i and c_{i+1}. On the other hand, if we are exchanging a singlet ($c_i = c'_i$ and $c_{i+1} = c'_{i+1}$), on the right side of the equation (1.122) we have

$$T^{d_i}_{c_i c_{i+1}} \left(T^{d_i}_{c_i c_{i+1}}\right)^* = f_{d_i c_i c_{i+1}} f_{d_i c_i c_{i+1}} = 2 C_A^2 C_F \, . \tag{1.126}$$

The octet case can be verified in a similar way by remembering that in Eq. (1.124) we are referring to the anti-symmetric part and that therefore this component must be extracted. To do this, we can apply the substitution (1.36) to the $SU(3)$ matrices in the adjoint representation. The introduced decomposition brings us to

$$\sum_{G_i} \gamma^{G_i}_{c_i c_{i+1}} (q_i, q_{i+1}) \left(\gamma^{G_i}_{c'_i c'_{i+1}} (q_i, q_{i+1})\right)^* = \sum_R \langle c_i c'_i | \hat{\mathcal{P}}_R | c_{i+1} c'_{i+1} \rangle \, 2 (2\pi)^{D-1} \mathcal{K}_r^{(R)} (\vec{q}_i, \vec{q}_{i+1}; \vec{q}) \, , \tag{1.127}$$

where the sum is taken over color and polarization states of the produced gluon and

$$\begin{aligned} \mathcal{K}_r^{(R)} (\vec{q}_i, \vec{q}_{i+1}; \vec{q}) &= - \frac{g^2 c_R}{2 (2\pi)^{D-1}} C^\mu (q_{i+1}, q_i) C_\mu (q_{i+1} - q, q_i - q) \\ &= \frac{g^2 c_R}{(2\pi)^{D-1}} \left(\frac{\vec{q}_i^{\,2} (\vec{q}_{i+1} - \vec{q})^2 + \vec{q}_{i+1}^{\,2} (\vec{q}_i - \vec{q})^{\,2}}{(\vec{q}_i - \vec{q}_{i+1})^2} - \vec{q}^{\,2} \right) . \end{aligned} \tag{1.128}$$

Therefore, from Eq. (1.122) it is possible to decompose the scattering amplitude $\mathcal{A}_{12}^{1'2'}$ as

$$\mathcal{A}_{12}^{1'2'} = \sum_R (\mathcal{A}_R)_{12}^{1'2'}, \tag{1.129}$$

where $(\mathcal{A}_R)_{12}^{1'2'}$ is the part of the scattering amplitude corresponding to the definite irreducible representation R of the colour group in the t-channel.

Partial wave expansion

Now, it is necessary to introduce the Mellin transformation $f_R(\omega, \vec{q})_{AB}^{A'B'}$ (partial wave) of the imaginary part of the amplitude, that following [28], we define by

$$f_R(\omega, \vec{q})_{12}^{1'2'} = \int_{s_0}^{\infty} \frac{ds}{s} \left(\frac{s}{s_0}\right)^{-\omega} \left[\frac{\Im_s(\mathcal{A}_R)_{12}^{1'2'}}{s}\right] . \tag{1.130}$$

Its inverse is given by

$$\Im_s(\mathcal{A}_R)_{12}^{1'2'} = \frac{s}{2\pi i} \int_{\delta - i\infty}^{\delta + i\infty} d\omega \left(\frac{s}{s_0}\right)^{\omega} f_R(\omega, \vec{q})_{12}^{1'2'} = \frac{s}{2\pi i} \oint_C d\omega \left(\frac{s}{s_0}\right)^{\omega} f_R(\omega, \vec{q})_{12}^{1'2'} , \tag{1.131}$$

where $\delta + i\Im(\omega)$ is an axis, on the real axis of the complex plane of the variable ω, which lies to the right of all singularities of $f_R(\omega, \vec{q})$ and the closed surfaces C is obtained by adding to this axis an infinite semicircle which extends in the left region of the complex plane (which is in the direction in which the real part of ω becomes negative). The second equality holds due to the fact that the contribution on the semicircle is zero since the integrand vanishes exponentially when the real part of ω tends to minus infinity.
Using dispersion relations it is possible to reconstruct the total amplitude. Hence, the expression for the total amplitude in the form of a partial wave expansion is

$$(\mathcal{A}_R)_{12}^{1'2'} = \frac{s}{2\pi} \int_{\delta - i\infty}^{\delta + i\infty} \frac{d\omega}{\sin(\pi\omega)} \left[\left(\frac{-s}{s_0}\right)^{\omega} - \eta \left(\frac{s}{s_0}\right)^{\omega}\right] f_R(\omega, \vec{q})_{AB}^{A'B'}, \tag{1.132}$$

where η is the signature and coincides with the symmetry of the representation R.
It is important to observe that in the octet representation we have to add the Born contribution to the dispersion relation, *i.e.*

$$(\mathcal{A}_R)_{12}^{1'2'} = (\mathcal{A}_R^B)_{12}^{1'2'} + \frac{s}{2\pi} \int_{\delta - i\infty}^{\delta + i\infty} \frac{d\omega}{\sin(\pi\omega)} \left[\left(\frac{-s}{s_0}\right)^{\omega} - \eta \left(\frac{s}{s_0}\right)^{\omega}\right] f_R(\omega, \vec{q})_{AB}^{A'B'} . \tag{1.133}$$

Phase space

From Eq. (1.114), imposing the on-shellness of outgoing gluons, we have

$$\left(\prod_{i=1}^{n}\vec{k}_i^{\,2}\right)^{-1}=\left(\prod_{i=1}^{n}\frac{\beta_i}{\beta_{i-1}}s_i\right)^{-1}\implies\left(\prod_{i=1}^{n+1}s_i\right)\left(\prod_{i=1}^{n}\vec{k}_i^{\,2}\right)^{-1}=s_{n+1}\frac{\beta_0}{\beta_n}\simeq s\ . \tag{1.134}$$

We can manipulate this further to get

$$s=\left(\prod_{i=1}^{n+1}s_i\right)\left(\prod_{i=1}^{n}\vec{k}_i^{\,2}\right)^{-1}=\left(\prod_{i=1}^{n+1}\frac{s_i}{\sqrt{\vec{k}_{i-1}^{\,2}\vec{k}_i^{\,2}}}\right)\sqrt{\vec{q}_1^{\,2}\vec{q}_{n+1}^{\,2}}\ . \tag{1.135}$$

The phase of space element of $n+2$ particles reads

$$\begin{aligned}
d\Phi_{n+2}&=(2\pi)^D\delta^D\left(p_1+p_2-\sum_{i=0}^{n+1}k_i\right)\left(\prod_{i=0}^{n+1}\delta(k_i^2)\frac{d^Dk_i}{(2\pi)^{D-1}}\right)\\
&=\frac{2}{s}(2\pi)^D\delta\left(1-\sum_{i=0}^{n+1}\alpha_i\right)\delta\left(1-\sum_{i=0}^{n+1}\beta_i\right)\delta^{(D-2)}\left(\sum_{i=0}^{n+1}k_{i\perp}\right)\frac{s}{2}\delta(\alpha_0\beta_0 s+k_{0\perp}^2)d\alpha_0d\beta_0\frac{d^{D-2}k_{0\perp}}{(2\pi)^{D-1}}\\
&\times\left(\prod_{i=1}^{n}\frac{s}{2}\delta(\alpha_i\beta_i s+k_{i\perp}^2)d\alpha_id\beta_i\frac{d^{D-2}k_{i\perp}}{(2\pi)^{D-1}}\right)\frac{s}{2}\delta(\alpha_{n+1}\beta_{n+1}s+k_{n+1\perp}^2)d\alpha_{n+1}d\beta_{n+1}\frac{d^{D-2}k_{n+1\perp}}{(2\pi)^{D-1}}\\
&=\frac{2}{s}(2\pi)^D\delta\left(1-\sum_{i=0}^{n+1}\alpha_i\right)\delta\left(1-\sum_{i=0}^{n+1}\beta_i\right)\delta^{(D-2)}\left(\sum_{i=0}^{n+1}k_{i\perp}\right)\frac{d\beta_0}{2\beta_0}\frac{d\alpha_{n+1}}{2\alpha_{n+1}}\prod_{i=1}^{n}\frac{d\beta_i}{2\beta_i}\prod_{i=0}^{n+1}\frac{d^{D-2}k_{i\perp}}{(2\pi)^{D-1}}\ .
\end{aligned} \tag{1.136}$$

In performing the integration over phase space, exploiting the MRK, the limits of integration in the variables β_i's must be restricted according to the condition $\beta_i<\beta_{i-1}$. In the following, we need to consider

$$\frac{ds}{s}d\Phi_{n+2}=\frac{ds}{2s^2}(2\pi)^D\prod_{i=1}^{n}\frac{d\beta_i}{2\beta_i}\prod_{i=0}^{n}\frac{d^{D-2}k_{i\perp}}{(2\pi)^{D-1}}\ . \tag{1.137}$$

We perform the following changes of variables

$$\{\beta_1,...,\beta_n,s\}\to\{s_1,...,s_n,s_{n+1}\}\ ,\qquad\{k_{0\perp},...,k_{n\perp}\}\to\{q_1,...,q_{n+1}\} \tag{1.138}$$

by making use of relations

$$\left\{s_i=\frac{\beta_{i-1}}{\beta_i}s_R\ ,i=1,...,n\right\}\ ,\ \ s_{n+1}=\beta_n s\ ,\ \ k_{0\perp}=-q_{1\perp}\ ,\ \ \left\{k_{i\perp}=q_{i\perp}-q_{i+1\perp}\ ,i=1,...,n\right\} \tag{1.139}$$

and get

$$\frac{ds}{s}d\Phi_{n+2}=\frac{2\pi}{s}\left(\prod_{i=1}^{n+1}\frac{ds_i}{s_i}\right)\left(\prod_{i=1}^{n+1}\frac{d^{D-2}q_i}{(2\pi)^{D-1}}\right)\ , \tag{1.140}$$

where the integration over variables s_i is extended between s_R and infinity.

Generalized BFKL equation

We can consider the $n_{\rm th}$ contribution to the partial wave amplitude, implicitly defined by the relation

$$f_R(\omega,\vec{q})_{12}^{1'2'} = \sum_{n=0}^{\infty} f_R^{(n)}(\omega,\vec{q})_{12}^{1'2'} \ , \tag{1.141}$$

which reads

$$f_R^{(n)}(\omega,\vec{q})_{12}^{1'2'} = \frac{1}{2}\int_{s_0}^{\infty}\frac{ds}{s}d\Phi_{n+2}\left(\frac{s}{s_0}\right)^{-\omega}\frac{1}{s}\sum_f \mathcal{A}_{12}^{\tilde{1}\tilde{2}+n}\left(\mathcal{A}_{1'2'}^{\tilde{1}\tilde{2}+n}\right)^*$$

$$= 2\int_{s_0}^{\infty}\frac{ds}{s}d\Phi_{n+2}\left(\frac{s}{s_0}\right)^{-\omega} s\left(\prod_{i=1}^{n}\langle c_i c_i'|\hat{\mathcal{P}}_R|c_{i+1}c_{i+1}'\rangle\, 2(2\pi)^{D-1}\mathcal{K}_r^{(R)}(\vec{q}_i,\vec{q}_{i+1};\vec{q})\right)$$
$$\times\left(\prod_{i=1}^{n+1}\left(\frac{s_i}{s_R}\right)^{\omega(t_i)+\omega(t_i')}\frac{1}{\vec{q}_i^{\,2}(\vec{q}_i-\vec{q})^2}\right)\left(\sum_{\tilde{1}}\Gamma^*_{\tilde{1}1'}\Gamma_{\tilde{1}1}\right)\left(\sum_{\tilde{2}}\Gamma^*_{\tilde{2}2'}\Gamma_{\tilde{2}2}\right) \ . \tag{1.142}$$

Now, we observe that

$$\langle c_i c_i'|\hat{\mathcal{P}}_R|c_{i+1}c_{i+1}'\rangle = \langle c_i c_i'|\hat{\mathcal{P}}_R\hat{\mathcal{P}}_R|c_{i+1}c_{i+1}'\rangle = \sum_\nu \langle c_i c_i'|\hat{\mathcal{P}}_R|\nu\rangle\,\langle\nu|\hat{\mathcal{P}}_R|c_{i+1}c_{i+1}'\rangle \ , \tag{1.143}$$

where the sum over the index ν is extended to all states of the irreducible representation R. Using this, we can write

$$\begin{aligned}&\sum_{\nu,\nu'}\langle c_1c_1'|\hat{\mathcal{P}}_R|\nu\rangle\left[\langle\nu|\hat{\mathcal{P}}_R|c_2c_2'\rangle\,\langle c_2c_2'|\hat{\mathcal{P}}_R|c_3c_3'\rangle\,...\,\langle c_nc_n'|\hat{\mathcal{P}}_R|\nu'\rangle\right]\langle\nu'|\hat{\mathcal{P}}_R|c_{n+1}c_{n+1}'\rangle\\ &=\sum_{\nu,\nu'}\langle c_1c_1'|\hat{\mathcal{P}}_R|\nu\rangle\,\langle\nu|\nu'\rangle\,\langle\nu'|\hat{\mathcal{P}}_R|c_{n+1}c_{n+1}'\rangle = \sum_\nu\langle c_1c_1'|\hat{\mathcal{P}}_R|\nu\rangle\,\langle\nu|\hat{\mathcal{P}}_R|c_{n+1}c_{n+1}'\rangle \ .\end{aligned} \tag{1.144}$$

Starting from (1.142), using Eqs. (1.135, 1.144) and performing the change of variables (1.140), we obtain

$$f_R^{(n)}(\omega,\vec{q})_{12}^{1'2'} = \frac{1}{(2\pi)^{D-2}}\int\left(\prod_i^{n+1}\frac{d^{D-2}q_{i\perp}}{\vec{q}_i^{\,2}(\vec{q}_i-\vec{q})^2}d\left(\frac{s_i}{s_R}\right)\left(\frac{s_i}{s_R}\right)^{\omega(t_i)+\omega(t_i')-\omega-1}\right)\left(\frac{s_0}{\sqrt{\vec{q}_1^{\,2}\vec{q}_{n+1}^{\,2}}}\right)^{\omega}$$
$$\times\sum_\nu I_{1'1}^{(R,\nu)}\left(\prod_{i=1}^{n}\mathcal{K}_r^{(R)}(\vec{q}_i,\vec{q}_{i+1};\vec{q})\right)I_{2'2}^{(R,\nu)} \ , \tag{1.145}$$

where

$$I_{1'1}^{(R,\nu)} = \sum_{\tilde{1}}\langle c_1c_1'|\hat{\mathcal{P}}_R|\nu\rangle\,\Gamma_{\tilde{1}1}^{c_1}\left(\Gamma_{\tilde{1}1}^{c_1'*}\right) \ , \qquad I_{2'2}^{(R,\nu)} = \sum_{\tilde{2}}\Gamma_{\tilde{2}2}^{c_{n+1}}\Gamma_{\tilde{2}2}^{c_{n+1}'*}\,\langle\nu|\hat{\mathcal{P}}_R|c_{n+1}c_{n+1}'\rangle \ . \tag{1.146}$$

The quantity $I_{i'i}^{(R,\nu)}$ in (1.146) are usually called *impact factors*. It is important to keep in mind that for the singlet representation the index ν takes only one value, hence it can be omitted and

$$\langle cc'|\hat{\mathcal{P}}_0|0\rangle = \frac{\delta_{cc'}}{\sqrt{N^2-1}}, \tag{1.147}$$

whereas for the antisymmetrical octet (gluon) representation ν coincides with the gluon colour index and

$$\langle cc'|\hat{\mathcal{P}}_8|a\rangle = \frac{f_{acc'}}{\sqrt{N}}. \tag{1.148}$$

We can now perform the integration over the variables (s_i/s_R)'s to find

$$f_R^{(n)}(\omega,\vec{q})_{12}^{1'2'} = \frac{1}{(2\pi)^{D-2}}\int\left(\prod_i^{n+1}\frac{d^{D-2}q_{i\perp}}{\vec{q}_i^{\,2}(\vec{q}_i-\vec{q})^2}\frac{1}{\omega-\omega(t_i)+\omega(t_i')}\right)$$

$$\times\sum_\nu I_{1'1}^{(R,\nu)}\left(\prod_{i=1}^n \mathcal{K}_r^{(R)}(\vec{q}_i,\vec{q}_{i+1};\vec{q})\right)I_{2'2}^{(R,\nu)}\,, \tag{1.149}$$

where we neglected terms of order $\omega\ln s_R$, since the essential integration region in (1.131) is the one where $\omega\sim(\ln s)^{-1}$. In particular, the exact lower bound of integration in the invariant masses has been neglected as it produces sub-dominant effects. Finally, from the last expression, we can reconstruct the complete partial wave and cast it in the form

$$f_R(\omega,\vec{q})_{12}^{1'2'} = \sum_{n=0}^\infty f_R^{(n)}(\omega,\vec{q})_{12}^{1'2'}$$

$$= \frac{1}{(2\pi)^{D-2}}\int\frac{d^{D-2}q_{A\perp}}{\vec{q}_A^{\,2}(\vec{q}_A-\vec{q})^2}\frac{d^{D-2}q_{B\perp}}{\vec{q}_B^{\,2}(\vec{q}_B-\vec{q})^2}\sum_\nu I_{1'1}^{(R,\nu)}G_\omega^{(R)}(\vec{q}_A,\vec{q}_B;\vec{q})I_{2'2}^{(R,\nu)}\,. \tag{1.150}$$

The function $G_\omega^{(R)}$, called Green function for the scattering of two Reggeized gluons, is defined as

$$G_\omega^{(R)}(\vec{q}_A,\vec{q}_B;\vec{q}) = \sum_{n=0}^\infty\int\left(\prod_{i=1}^{n+1}\frac{d^{D-2}q_{i\perp}}{\vec{q}_i^{\,2}(\vec{q}_i-\vec{q})^2\left(\omega-\omega(t_i)-\omega(t_i')\right)}\right)$$

$$\times\left(\prod_{i=1}^n\mathcal{K}_r^{(R)}(\vec{q}_i,\vec{q}_{i+1};\vec{q})\right)\vec{q}_A^{\,2}(\vec{q}_A-\vec{q})^2\vec{q}_B^{\,2}(\vec{q}_B-\vec{q})^2\delta^{D-2}(q_{1\perp}-q_{A\perp})\delta^{D-2}(q_{n+1\perp}-q_{B\perp}). \tag{1.151}$$

The function $G_\omega^{(R)}$ is the only quantity depending on ω, and hence it determines the s-behaviour of the scattering amplitude. It is the perturbative solution of the integral equation (see Fig. 1.17):

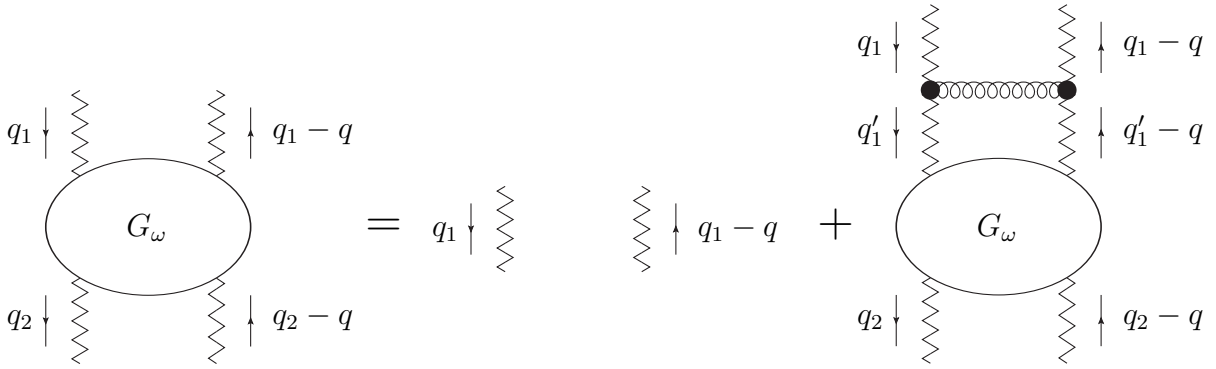

Figure 1.17: Schematic representation of the BFKL equation.

$$\omega G_\omega^{(R)}(\vec{q}_1,\vec{q}_2;\vec{q}) = \vec{q}_1^{\,2}(\vec{q}_1-\vec{q})^2\delta^{(D-2)}(\vec{q}_1-\vec{q}_2) + \int \frac{d^{D-2}q'_{1\perp}}{\vec{q}_1^{\,\prime 2}(\vec{q}_1^{\,\prime}-\vec{q})^2}\mathcal{K}^{(R)}(\vec{q}_1,\vec{q}_1^{\,\prime};\vec{q})G_\omega^{(R)}(\vec{q}_1^{\,\prime},\vec{q}_2;\vec{q}), \tag{1.152}$$

where the function $\mathcal{K}^{(R)}(\vec{q}_1,\vec{q}_1^{\,\prime};\vec{q})$, called kernel of the integral function, has the following expression:

$$\mathcal{K}^{(R)}(\vec{q}_1,\vec{q}_2;\vec{q}) = \left[\omega(q_{1\perp}^2)+\omega((q_1-q)_\perp^2)\right]\vec{q}_1^{\,2}\left(\vec{q}_1-\vec{q}\right)^2\delta^{(D-2)}(\vec{q}_1-\vec{q}_2) + \mathcal{K}_r^{(R)}(\vec{q}_1,\vec{q}_2;\vec{q})\ . \tag{1.153}$$

Two terms can be distinguished in Eq. (1.153); the first of them is called "virtual" and it is expressed in terms of the Regge trajectory of the gluon, while the second, which is related to the production of real particles, is given by the Eq. (1.128) (see the Fig. 1.18). The Eq. (1.152), in case of $R = 0$ (singlet) and $t = 0$, is called *BFKL equation*. In the most general case, it is called *generalized BFKL equation*. It is an iterative equation. The kernel $\mathcal{K}^{(R)}$ and the Green function $G_\omega^{(R)}$ can be seen as operators which act on the space of the transverse momentum defined by

$$\hat{\vec{q}}\,|\vec{q}_i\rangle = \vec{q}_i\,|\vec{q}_i\rangle\,,$$

$$\langle\vec{q}_1\,|\vec{q}_2\rangle = \delta^{(2)}\left(\vec{q}_1-\vec{q}_2\right), \qquad \langle A|B\rangle = \langle A|\vec{k}\,\rangle\,\langle\,\vec{k}\,|B\rangle = \int d^2\vec{k}\,A(\vec{k}\,)B(\vec{k}\,). \tag{1.154}$$

In this representation, the equation (1.152) can be written in the operator form:

$$\omega\hat{G}_\omega^{(R)} = 1 + \hat{\mathcal{K}}^{(R)}\hat{G}_\omega^{(R)}\ , \tag{1.155}$$

which implies

$$\hat{G}_\omega^{(R)} = \frac{1}{\omega-\hat{\mathcal{K}}^{(R)}}\ . \tag{1.156}$$

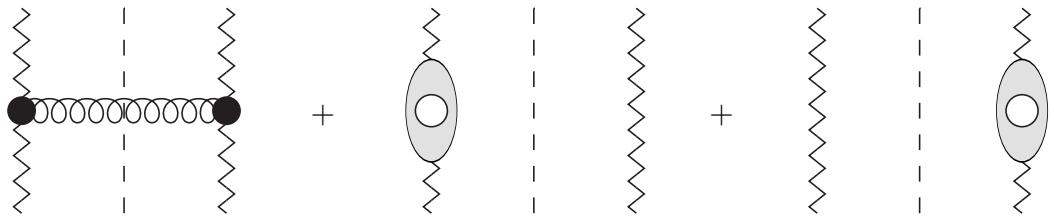

Figure 1.18: Schematic representation of the LO BFKL kernel.

1.2.5 Introduction to BFKL cross section and impact factors

We now focus on the case of the exchange of vacuum quantum numbers in the t-channel, considering an elastic process, $A + B \to A + B$, with the additional simplification of forward scattering ($q = 0$). We can relate the imaginary part of this amplitude to the total cross section of the process $A + B \to X$ by using the optical theorem (1.4)[18],

$$\sigma_{AB}(s) = \frac{\Im_s \mathcal{A}_{AB}^{AB}}{s} \, . \tag{1.157}$$

From Eqs. (1.131) and (1.2.4),

$$\sigma_{AB}(s) = \int_{\delta - i\infty}^{\delta + i\infty} \frac{d\omega}{2\pi i} \frac{1}{(2\pi)^{D-2}} \int d^{D-2} q_{A\perp} d^{D-2} q_{B\perp} \left(\frac{s}{s_0}\right)^{\omega} \frac{\Phi_A(\vec{q}_A)}{(\vec{q}_A^{\,2})^2} G_\omega(\vec{q}_A, \vec{q}_B) \frac{\Phi_B(-\vec{q}_B)}{(\vec{q}_B^{\,2})^2}, \tag{1.158}$$

where $\Phi_A(\vec{q}_A) \equiv I_{AA}^{(0)}$, $\Phi_B(\vec{q}_B) \equiv I_{BB}^{(0)}$ are the impact factors projected on the color singlet representation. Their expressions are obtained from (1.146), remembering that in the singlet representation and in the case of an elastic process, the color projector are given by the Eq. (1.147) with $c = c'$; hence:

$$\Phi_A(\vec{q}_A) = \frac{1}{\sqrt{N^2 - 1}} \sum_{\tilde{A}, c} |\Gamma^c_{\tilde{A}A}|^2; \quad \vec{q}_A = -\vec{p}_{\tilde{A}} \, , \tag{1.159}$$

$$\Phi_B(\vec{q}_B) = \frac{1}{\sqrt{N^2 - 1}} \sum_{\tilde{B}, c} |\Gamma^c_{\tilde{B}B}|^2; \quad \vec{q}_B = -\vec{p}_{\tilde{B}} \, . \tag{1.160}$$

At this point, it is very interesting to understand that in the BFKL approach the amplitude for a diffusion process at high energy can be written as the convolution of the Green function G for two Reggeized gluon with the impact factors $\Phi_{A'A}$ and $\Phi_{B'B}$ of the

[18] Note that the flux factor, for $\sqrt{s}$ much larger than the masses of the incoming particles, becomes $F \approx 2s$.

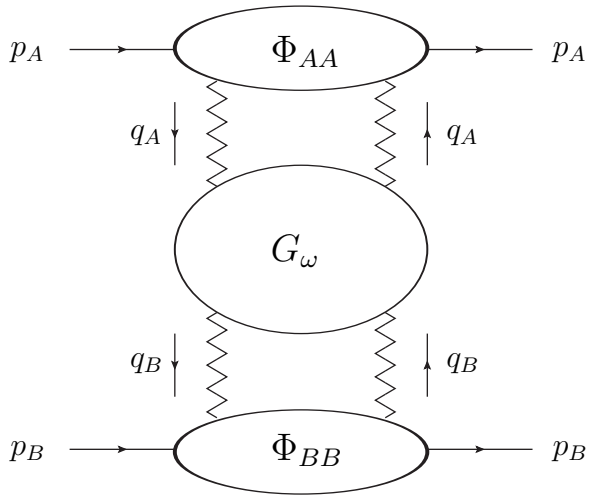

Figure 1.19: Schematic representation of the factorized amplitude.

colliding particles (see Fig. 1.19). The BFKL Green function is universal and completely governs the s-behavior of the amplitude, instead the impact factors depend on the particular process under analysis and they are s-independent.
It is important to make a clarification on the definition of impact factor. The one given above is not the most general possible, in fact, only one particle of the intermediate state across the s-channel cut has been included in its definition. In general the intermediate state can be a system of particles, and in this case, within the LLA, the definition generalizes to [35]

$$\Phi_{AA}(\vec{q}_A) = \langle cc|\hat{\mathcal{P}}_0|0\rangle \sum_{\{f\}} \int \frac{ds_{PR}}{2\pi} d\rho_f \Gamma^c_{\{f\}A} \left(\Gamma^{c'}_{\{f\}A}\right)^* . \tag{1.161}$$

In the case of a single particle in the intermediate state the integration becomes completely trivial and the expression (1.161) reduces to the one in Eq. (1.159).

1.2.6 Solution of BFKL equation at $t = 0$

The s-behaviour of the total cross section (1.11) is determined by solving the BFKL equation (1.152) and finding the leading singularity ω_0. Then, performing the anti-Mellin transformation, it is possible to get the asymptotic behaviour of cross sections. First of all, the Eqs. (1.152, 1.153) must be taken in the case of $R = 0$ (singlet) and $t = 0$. Redefining

$$\frac{G^{(0)}_\omega(\vec{q}_1, \vec{q}_2; \vec{0})}{\vec{q}_1^{\,2}\vec{q}_2^{\,2}} \equiv G_\omega\left(\vec{q}_1, \vec{q}_2\right), \tag{1.162}$$

$$\frac{\mathcal{K}^{(0)}(\vec{q}_1,\vec{q}_2,\vec{0})}{\vec{q}_1^{\,2}\vec{q}_2^{\,2}} \equiv \mathcal{K}(\vec{q}_1,\vec{q}_2), \tag{1.163}$$

and hence

$$\frac{\mathcal{K}_r^{(0)}(\vec{q}_1,\vec{q}_2,\vec{0})}{\vec{q}_1^{\,2}\vec{q}_2^{\,2}} \equiv \mathcal{K}_r(\vec{q}_1,\vec{q}_2) = \frac{g^2N}{(2\pi)^{D-1}}\frac{2}{(\vec{q}_1-\vec{q}_2)^2}\ , \tag{1.164}$$

it straightforward to find that the BFKL equation takes the following form:

$$\omega G_\omega\left(\vec{q}_1,\vec{q}_2\right) = \delta^{(2)}\left(\vec{q}_1-\vec{q}_2\right) + \int d^{D-2}k\ \mathcal{K}(\vec{q}_1,\vec{k})G_\omega(\vec{k},\vec{q}_2), \tag{1.165}$$

that can be rewritten as

$$\omega G_\omega\left(\vec{q}_1,\vec{q}_2\right) = \delta^{(2)}\left(\vec{q}_1-\vec{q}_2\right) + \mathcal{K}\bullet G_\omega\left(\vec{q}_1,\vec{q}_2\right)\ , \tag{1.166}$$

where we have defined the convolution operator as

$$A\bullet B\ (q_1,q_2) = \int d^{D-2}k\ A(q_1,k)B(k,q_2)\ . \tag{1.167}$$

The expression of the kernel function reads

$$\mathcal{K}(\vec{q}_1,\vec{q}_2) = \frac{\mathcal{K}^{(0)}(\vec{q}_1,\vec{q}_2)}{\vec{q}_1^{\,2}\vec{q}_2^{\,2}} = 2\omega(-\vec{q}_1^{\,2})\delta^{D-2}(\vec{q}_1-\vec{q}_2) + \frac{g^2N}{(2\pi)^{D-1}}\frac{2}{(\vec{q}_1-\vec{q}_2)^2}\ . \tag{1.168}$$

Finding the Green function G_ω means solving the eigenvalue problem for the kernel $\mathcal{K}$. In fact, if the equation

$$\mathcal{K}\bullet\phi_i(\vec{q}) = \lambda_i\phi_i(\vec{q}), \tag{1.169}$$

is solved, then, the Green function can be reconstructed through the spectral representation

$$G_\omega\left(\vec{q}_1,\vec{q}_2\right) = \sum_i \frac{\phi_i(\vec{q}_1)\phi_i^*(\vec{q}_2)}{\omega-\lambda_i}\ . \tag{1.170}$$

It is important to stress that the BFKL kernel can be seen as an operator acting on a space of complex functions, defined on a vectorial space, $\mathcal{V}$. Now, it is easy to see that the kernel is rotationally invariant[19], *i.e.*

$$\mathcal{K}(R\vec{q}_1,R\vec{q}_2) = \mathcal{K}(\vec{q}_1,\vec{q}_2)\ ,\quad \vec{q}_1,\vec{q}_2\in\mathcal{V}\ , \tag{1.171}$$

with R a generic rotation operator in $\mathcal{V}$. The consequence of rotational invariance is that the kernel admits a set of eigenfunctions of the type

$$\phi_\gamma^n(\vec{q}) = f_\gamma(|\vec{q}\,|)Y_n(\phi)\ , \tag{1.172}$$

[19]Please note that the Jacobian of a rotation is one.

where ϕ on the right hand side denotes the set of angular variables and Y_n is a spherical harmonic which, in dimension two, is nothing more than an exponential function $e^{in\phi}$. The kernel is also a scale invariant operator, in fact, given a $\lambda \in \mathbb{R}$,

$$\mathcal{K}(\lambda\vec{q}_1, \lambda\vec{q}_2) = \lambda^{-2}\mathcal{K}(\vec{q}_1, \vec{q}_2) \ , \quad \vec{q}_1, \vec{q}_2 \in \mathcal{V} \ . \tag{1.173}$$

The scale invariance forces the radial function $f_\gamma(|\vec{q}\,|)$ to be a power of $|\vec{q}\,|$, we will take them as

$$f_\gamma(|\vec{q}\,|) = (\vec{q}^{\,2})^\gamma \ . \tag{1.174}$$

The last step is to fix the value of γ and the overall normalization by requiring that these functions form an orthonormal complete sets, *i.e.*

$$\int d^2\vec{q}\ \phi^n_\nu(\vec{q})\phi^{n'}_{\nu'}(\vec{q}) = \delta(\nu - \nu')\delta(n - n'). \tag{1.175}$$

By imposing this last condition, it is simple to see that γ must be equal to $i\nu - 1/2$ with $\nu \in \mathbb{R}$ and hence, the set of eigenfunctions that solves the problem is

$$\left\{ \phi^n_\nu(\vec{q}\,) = \frac{1}{\pi\sqrt{2}}(\vec{q}^{\,2})^{-\frac{1}{2}+i\nu}e^{in\theta} \ : \ \nu \in \mathbb{R}\ ,\ n \in \mathbb{Z} \right\}. \tag{1.176}$$

To find the corresponding eigenvalues we have to make the kernel act on a test eigenfunction. We consider separately virtual corrections and real emissions in dimensional regularization with $d = 2 + 2\epsilon$. To this purpose, we introduce the "continuation" of the LO BFKL eigenfunctions to non-integer dimensions,

$$\left(\vec{q}^{\,2}\right)^\gamma e^{in\theta} \to \left(\vec{q}^{\,2}\right)^{\gamma-\frac{n}{2}} \left(\vec{q}\cdot\vec{l}\right)^n \ , \tag{1.177}$$

where $\vec{l}$ lies only in the first two of the $2+2\epsilon$ transverse space dimensions, *i.e.* $\vec{l} = \vec{e}_1 + i\vec{e}_2$ with $\vec{e}^{\,2}_{1,2} = 1$, $\vec{e}_1 \cdot \vec{e}_2 = 0$. In the limit $\epsilon \to 0$ the r.h.s. of Eq. (1.177) reduces to the LO BFKL eigenfunction, since we have

$$e^{in\theta} = (\cos\theta + i\sin\theta)^n = \left(\frac{q_x + iq_y}{|q|}\right)^n = \left(\frac{(\vec{q}\cdot\vec{l})^n}{(\vec{q}^{\,2})^{n/2}}\right) \ . \tag{1.178}$$

For the virtual part we have

$$\begin{aligned}\mathcal{K}_v \bullet \phi^n_\nu(\vec{q}) &= \int \frac{d^{D-2}k}{\pi\sqrt{2}}(\vec{k}^{\,2})^{-1/2+i\nu}\left(\frac{(\vec{k}\cdot\vec{l})^n}{(\vec{k}^{\,2})^{n/2}}\right) 2\omega(-\vec{q}^{\,2})\delta^{D-2}(\vec{q}-\vec{k}) \\ &= -\frac{2g^2N(\vec{q}^{\,2})^\epsilon}{(4\pi)^{2+\epsilon}}\frac{\Gamma(1-\epsilon)\Gamma^2(\epsilon)}{\Gamma(2\epsilon)}\phi^n_\nu(\vec{q}) \ . \end{aligned} \tag{1.179}$$

We see that the virtual part contains a pole in ϵ; this will be cancelled by the real part, ensuring the infrared finiteness in the singlet case. For the real part, we have

$$\mathcal{K}_r \bullet \phi_\nu^n(\vec{q}) = \int \frac{d^{D-2}k}{\pi\sqrt{2}} (\vec{k}^{\,2})^{-1/2+i\nu} \left(\frac{(\vec{k}\cdot\vec{l})^n}{(\vec{k}^{\,2})^{n/2}} \right) \frac{g^2 N}{(2\pi)^D} \frac{2}{(\vec{q}-\vec{k})^2} \, .$$

To solve this integral, we perform a Feynman parametrization to obtain

$$\mathcal{K}_r \bullet \phi_\nu^n(\vec{q}) = \frac{2g^2N}{(2\pi)^{3+2\epsilon}} \frac{\Gamma(\frac{3}{2}+\frac{n}{2}-i\nu)}{\Gamma(\frac{1}{2}+\frac{n}{2}-i\nu)} \int_0^1 dx \int \frac{d^{D-2}k}{\pi\sqrt{2}} \frac{(1-x)^{-1/2+n/2-i\nu} (\vec{k}\cdot\vec{l})^n}{\left[\vec{k}^{\,2} - 2x\vec{q}\cdot\vec{k} + x\vec{q}^{\,2}\right]^{3/2+n/2-i\nu}} \, . \tag{1.180}$$

If we perform the shift $\vec{k} \to \vec{k} + x\vec{q}$, in the numerator we obtain a factor

$$(\vec{k}\cdot\vec{l} + x\vec{q}\cdot\vec{l})^n = \sum_j \binom{n}{j} (\vec{k}\cdot\vec{l})^j x^{n-j} (\vec{q}\cdot\vec{l})^{n-j} \, . \tag{1.181}$$

Only the $j = 0$ term in Eq. (1.181) gives a non-vanishing contribution to the integral and therefore,

$$\mathcal{K}_r \bullet \phi_\nu^n(\vec{q}) = \frac{2g^2N}{(2\pi)^{3+2\epsilon}} \frac{\Gamma(\frac{3}{2}+\frac{n}{2}-i\nu)}{\Gamma(\frac{1}{2}+\frac{n}{2}-i\nu)} (\vec{q}^{\,2})^{n/2} e^{in\phi} \int_0^1 dx \; x^n (1-x)^{-1/2+n/2-i\nu}$$
$$\times \int \frac{d^{D-2}k}{\pi\sqrt{2}} \frac{1}{\left[\vec{k}^{\,2} + x(1-x)\vec{q}^{\,2}\right]^{3/2+n/2-i\nu}} \, . \tag{1.182}$$

Both integrations are now simple and we get

$$\mathcal{K}_r \bullet \phi_\nu^n(\vec{q}) = \frac{2g^2N(\vec{q}^{\,2})^\epsilon}{(4\pi)^{2+\epsilon}} \frac{2\Gamma(\epsilon)\Gamma(\frac{1}{2}+\frac{n}{2}-i\nu-\epsilon)\Gamma(\frac{1}{2}+\frac{n}{2}+i\nu+\epsilon)}{\Gamma(\frac{1}{2}+\frac{n}{2}-i\nu)\Gamma(\frac{1}{2}+\frac{n}{2}+i\nu+2\epsilon)} \phi_\nu^n(\vec{q}) \, . \tag{1.183}$$

Combining real and virtual parts, we get the full action of the kernel on its eigenfunctions:

$$\mathcal{K}\bullet\phi_\nu^n(\vec{q}) = \frac{2g^2N(\vec{q}^{\,2})^\epsilon}{(4\pi)^{2+\epsilon}} \left(\frac{2\Gamma(\epsilon)\Gamma(\frac{1}{2}+\frac{n}{2}-i\nu-\epsilon)\Gamma(\frac{1}{2}+\frac{n}{2}+i\nu+\epsilon)}{\Gamma(\frac{1}{2}+\frac{n}{2}-i\nu)\Gamma(\frac{1}{2}+\frac{n}{2}+i\nu+2\epsilon)} - \frac{\Gamma(1-\epsilon)\Gamma^2(\epsilon)}{\Gamma(2\epsilon)} \right) \phi_\nu^n(\vec{q}) \, .$$

Expanding in ϵ and up to constant order, we get

$$\mathcal{K} \bullet \phi_\nu^n = \bar{\alpha}_s \chi(n,\nu) \equiv \omega_n(\nu) \, , \tag{1.184}$$

where

$$\bar{\alpha}_s = \frac{\alpha_s N}{\pi} \tag{1.185}$$

and

$$\chi(n,\nu) = 2\psi(1) - \psi(1/2+n/2+i\nu) - \psi(1/2+n/2-i\nu)$$

$$= 2(-\gamma_E - \Re[\psi((n+1)/2 + i\nu)]). \tag{1.186}$$

The function $\chi(n,\nu)$ in Eq. (1.186) characterizes the behavior predicted by the BFKL approach in the leading-logarithmic approximation, it is a remarkable achievement of L. Lipatov and it is therefore known as *Lipatov characteristic function*.

As anticipated, from the knowledge of the eigenvalues and the eigenfunctions, we can immediately write a spectral representation for the Green, $G_\omega(\vec{q}_1, \vec{q}_2)$, which reads

$$G_\omega(\vec{q}_1, \vec{q}_2) = \sum_n^\infty \int_{-\infty}^{\infty} d\nu \left(\frac{q_1^2}{q_2^2}\right)^{i\nu} \frac{e^{in(\theta_1-\theta_2)}}{2\pi^2 q_1 q_2} \frac{1}{\omega - \bar{\alpha}_s \chi(n,\nu)}. \tag{1.187}$$

Since ν is a continuous variable, we do not obtain an isolated pole which we can associate with the intercept of the Pomeron. One is interested in the leading $\ln s$ behaviour which means the singularity with the largest real part in the ω-plane. This allows to make a number of simplifications. Since the function $\chi(n,\nu)$ decreases with increasing n, it is possible to restrict the sum over n in Eq. (1.187) to the case where $n = 0$. Furthermore, $\chi(0,\nu)$ decreases with increasing $|\nu|$, so one can expand $\chi(0,\nu)$ as a power series in ν and keep only the first two terms. One obtains

$$\chi(0,\nu) = 4\ln 2 - 14\zeta(3)\nu^2 + \dots . \tag{1.188}$$

In this approximation

$$G_\omega(\vec{q}_1, \vec{q}_2) \approx \frac{1}{\pi q_1 q_2} \int_{-\infty}^{\infty} \frac{d\nu}{2\pi} \left(\frac{q_1^2}{q_2^2}\right)^{i\nu} \frac{1}{(\omega - \omega_0 + a^2\nu^2)}, \tag{1.189}$$

with

$$\omega_0 = 4\bar{\alpha}_s \ln 2 \tag{1.190}$$

being the position of the leading singularity (the branch point of the cut) and

$$a^2 = 14\bar{\alpha}_s \zeta(3). \tag{1.191}$$

Eq. (1.189) can be inverted, performing the anti-Mellin transform,

$$\tilde{G}_s(\vec{q}_1, \vec{q}_2) = \frac{1}{2\pi i} \oint_C d\omega \left(\frac{s}{s_0}\right)^\omega \frac{1}{\pi q_1 q_2} \int_{-\infty}^{+\infty} \frac{d\nu}{2\pi} \left(\frac{q_1^2}{q_2^2}\right)^{i\nu} \frac{1}{\omega - \omega_0 + a^2\nu^2}, \tag{1.192}$$

where the contour C is to the right of the ω-plane singularity of the integrand function. Using the residue theorem, one finds

$$\begin{aligned} \tilde{G}_s(\vec{q}_1, \vec{q}_2) &= \frac{1}{2\pi^2 q_1 q_2} \int_{-\infty}^{+\infty} d\nu \left(\frac{s}{s_0}\right)^{\omega_0 - a^2\nu^2} \left(\frac{q_1^2}{q_2^2}\right)^{i\nu} \\ &= \frac{1}{2\pi^2 q_1 q_2} \int_{-\infty}^{+\infty} d\nu e^{\left(\omega_0 - a^2\nu^2\right)\ln\left(\frac{s}{s_0}\right) + i\nu \ln\left(\frac{q_1^2}{q_2^2}\right)} . \end{aligned} \tag{1.193}$$

An exponential factor, independent from ν, can be taken out the integral, while, in the remaining term one can complete the square to obtain:

$$\begin{aligned}\tilde{G}_s(\vec{q}_1,\vec{q}_2) =& \frac{1}{2\pi^2 q_1 q_2}\left(\frac{s}{s_0}\right)^{\omega_0}\int_{-\infty}^{+\infty} d\nu \\ & \times \exp\left(-a^2\ln\left(\frac{s}{s_0}\right)\nu^2 + i\ln\left(\frac{q_1}{q_2}\right)\nu + \frac{\ln^2\left(\frac{q_1^2}{q_2^2}\right)}{4a^2\ln\left(\frac{s}{\vec{q}_2^{\,2}}\right)} - \frac{\ln^2\left(\frac{q_1^2}{q_2^2}\right)}{4a^2\ln\left(\frac{s}{\vec{q}_2^{\,2}}\right)}\right) \\ =& \frac{1}{2\pi^2 q_1 q_2}\left(\frac{s}{s_0}\right)^{\omega_0}\int_{-\infty}^{+\infty} d\nu \\ & \times \exp\left(-\frac{\ln^2\left(\frac{q_1^2}{q_2^2}\right)}{4a^2\ln\left(\frac{s}{\vec{q}_2^{\,2}}\right)}\right)\exp\left(-\left(a\sqrt{\ln\left(\frac{s}{s_0}\right)}\nu - \frac{i\ln\left(\frac{q_1^2}{q_2^2}\right)}{2a\sqrt{\ln\left(\frac{s}{s_0}\right)}}\right)^2\right) .\end{aligned} \tag{1.194}$$

Applying the substitution

$$z = \nu - i\frac{\ln\left(\frac{q_1^2}{q_2^2}\right)}{2a^2\ln\left(\frac{s}{s_0}\right)} , \tag{1.195}$$

and remembering the solution of the Gaussian integral,

$$\int_{-\infty}^{\infty} dz e^{-Az^2} = \sqrt{\frac{\pi}{A}} , \tag{1.196}$$

the result is

$$\tilde{G}_s(\vec{q}_1,\vec{q}_2) \approx \frac{1}{\sqrt{\vec{q}_1^{\,2}\vec{q}_2^{\,2}}}\left(\frac{s}{s_0}\right)^{\omega_0}\frac{1}{\sqrt{\pi\ln(s/s_0)}}\frac{1}{2\pi a}\exp\left(-\frac{\ln^2(\vec{q}_1^{\,2}/\vec{q}_2^{\,2})}{4a^2\ln(s/s_0)}\right). \tag{1.197}$$

The predicted s-behaviour (1.11) of the cross sections appears from this expression[20], in fact, using the power series expansion of the exponential, one has:

$$\begin{aligned}\tilde{G}_s(\vec{q}_1,\vec{q}_2) \approx & \frac{1}{\sqrt{\vec{q}_1^{\,2}\vec{q}_2^{\,2}}}\left(\frac{s}{s_0}\right)^{\omega_0}\frac{1}{\sqrt{\pi\ln(s/s_0)}} \\ & \frac{1}{2\pi a}\left[1 + \left(-\frac{\ln^2(\vec{q}_1^{\,2}/\vec{q}_2^{\,2})}{4a^2\ln(s/s_0)}\right) + \frac{1}{2}\left(-\frac{\ln^2(\vec{q}_1^{\,2}/\vec{q}_2^{\,2})}{4a^2\ln(s/s_0)}\right)^2 + ...\right].\end{aligned} \tag{1.198}$$

α_s is fixed, increasing s, all terms of the expansion are suppressed with respect to one, and the leading contribution is

$$\tilde{G}_s(\vec{q}_1,\vec{q}_2) \approx \frac{1}{\sqrt{\vec{q}_1^{\,2}\vec{q}_2^{\,2}}}\left(\frac{s}{s_0}\right)^{\omega_0}\frac{1}{\sqrt{\pi\ln(s/s_0)}}\frac{1}{2\pi a}, \tag{1.199}$$

that shows exactly the behaviour in Eq. (1.11).

[20]Note that the s-dependences appear only in this "piece" of the cross section.

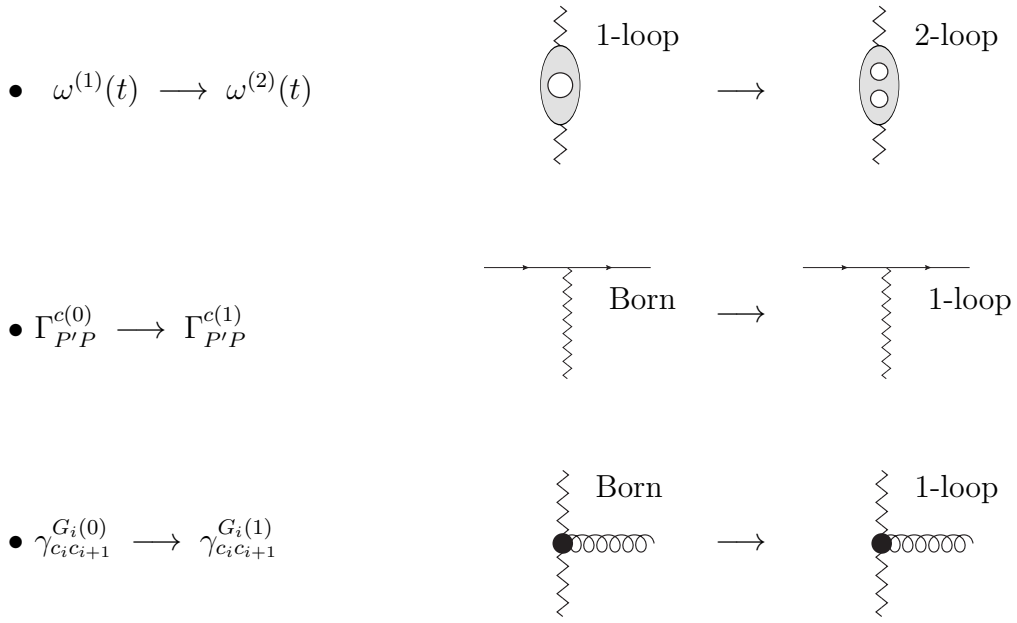

Figure 1.20: Next-to-leading corrections to Regge trajectory, PPR vertices, and central gluon production vertex in the multi-Regge kinematics.

1.2.7 BFKL equation in the NLLA

In the previous sections, we built the BFKL approach in the LLA; the goal of this section, is instead to describe the approach in the NLLA. In this approximation we can use an approach which coincides in the main features with that used in the LLA [36]. In general, the program of the calculations is analogous to that in LLA. The final goal is the elastic scattering amplitude, which has to be restored from its s- and u-channel imaginary parts. The s-channel imaginary part is given by the unitarity relation (1.110). It can be shown that, Eqs. (1.129)-(1.132), expressing the elastic scattering amplitudes in terms of their s-channel imaginary parts, remain unchanged.

Although conceptually the approach does not differ much from what has been described previously, the technical effort to complete the calculation program is enormous. For this reason, in the following, we will limit ourselves to a simple introductory description, referring to [28] (and reference therein) for all the details.

Gluon Reggeization in the NLLA

In the NLLA, Eq. (1.14) has been proved in the first three orders of perturbation theory and assumed to be valid to all orders. Only later, it has been proved to all orders of perturbation theory. Demonstrating Reggeization in the NLLA is again a very challenging topic, we refer to [37] (and reference therein) for full details on this topic.
Instead, we want to focus on how the Regge trajectory can be extracted in this approximation. To this scope, Let us consider again the quark-quark scattering and let us expand the Eq. (1.14) up to α_s^3:

$$\Gamma^a_{1'1}\frac{s}{t}\left[\left(\frac{s}{-t}\right)^{\omega(t)}+\left(\frac{-s}{-t}\right)^{\omega(t)}\right]\Gamma^a_{2'2}\simeq\left\{\Gamma^{a(0)}_{1'1}\frac{2s}{t}\Gamma^{a(0)}_{2'2}\right\}_{LLA}$$
$$+\left\{\Gamma^{a(0)}_{1'1}\frac{s}{t}\left[\omega^{(1)}(t)\ln\left(\frac{s}{-t}\right)+\omega^{(1)}(t)\ln\left(\frac{-s}{-t}\right)\right]\Gamma^{a(0)}_{2'2}\right\}_{LLA}+\left\{\Gamma^{a(1)}_{1'1}\frac{2s}{t}\Gamma^{a(0)}_{2'2}+\Gamma^{a(0)}_{1'1}\frac{2s}{t}\Gamma^{a(1)}_{2'2}\right\}_{NLLA}$$
$$+\left\{\Gamma^{a(0)}_{1'1}\frac{s}{t}\left[\frac{(\omega^{(1)}(t))^2}{2}\ln^2\left(\frac{s}{-t}\right)+\frac{(\omega^{(1)}(t))^2}{2}\ln^2\left(\frac{-s}{-t}\right)\right]\Gamma^{a(0)}_{2'2}\right\}_{LLA}$$
$$+\left\{\Gamma^{a(1)}_{1'1}\frac{s}{t}\omega^{(1)}(t)\left[\ln\left(\frac{s}{-t}\right)+\ln\left(\frac{-s}{-t}\right)\right]\Gamma^{a(0)}_{2'2}+\Gamma^{a(0)}_{1'1}\frac{s}{t}\omega^{(1)}(t)\left[\ln\left(\frac{s}{-t}\right)+\ln\left(\frac{-s}{-t}\right)\right]\Gamma^{a(1)}_{2'2}\right.$$
$$\left.+\Gamma^{a(0)}_{1'1}\frac{s}{t}\left[\omega^{(2)}(t)\ln\left(\frac{s}{-t}\right)+\omega^{(2)}(t)\ln\left(\frac{-s}{-t}\right)\right]\Gamma^{a(0)}_{2'2}\right\}_{NLLA}+\left\{\Gamma^{a(2)}_{1'1}\frac{2s}{t}\Gamma^{a(0)}_{2'2}+...\right\}_{NNLLA}. \tag{1.200}$$

In Eq. (1.200) we have restored the superscript (i) to denote the i-loops correction to a certain quantity and we have introduced a subscript to clarify within which approximation a given term contributes. Analyzing the Eq. (1.200), we have that

- In the first line we have the only contribution of order α_s, which is proportional to the Born effective vertices and obviously contributes within the LLA.

- In the second line we have three terms of order α_s^2. The first is proportional to the 1-loop Regge trajectory and contains a logarithm of the energy which compensates the additional α_s factor, hence it contributes within the LLA. The second and the third are both proportional to the 1-loop correction to one of the two effective vertices; compared to the Born contribution they have an extra α_s power and no large energy logarithm to compensate; they contribute within the NLLA.

- In the remaining lines we have a collection of terms of order α_s^3. The first is proportional to the squared of the 1-loop Regge trajectory and contains two logarithms of

the energy which compensate the additional α_s^2 factor, hence it contributes within the LLA. The second and the third contain the 1-loop Regge trajectory, the 1-loop correction of one of the two effective vertices and a logarithm of the energy which compensates one α_s factor; they contribute within the NLLA. The fourth term is proportional to the so called 2-loop correction to the Regge trajectory and contains a large logarithm of the energy; it contributes within NLLA. Finally, we have terms proportional to the product of 1-loop corrections to the effective vertices or terms proportional to the 2-loops correction to one of the two effective vertices. They contribute within the NNLLA.

At this point, it is clear how to proceed. First, we have to go back to our 1-loop computation of the quark-quark scattering and we have to include also those corrections that we have discarded in LLA since they do not generate large logarithms of energy. Among these we have contributions from the box and cross diagrams in Fig. 1.4 which come from regions of the phase space which we have ignored previously, but also vertex corrections which, in Feynman gauge, do not produce large logarithms of the energy.
By comparing this result with the correction of order α_s in Eq. (1.200), we can extract the effective vertices up to 1-loop accuracy. In general, they assume the following form[21]

$$\Gamma_{P'P} = \delta_{\lambda_P,\lambda_{P'}}\Gamma^{(+)}_{P'P} + \delta_{\lambda_P,-\lambda_{P'}}\Gamma^{(-)}_{P'P} \,, \tag{1.201}$$

where in the first term of Eq. (1.201), as before, the helicity is conserved, but there is a second term in which the helicity is not conserved [38, 39, 40, 41, 42].
Once these vertex corrections are found, the only ingredient to extract is $\omega^{(2)}(t)$. To do this, we need to compute the 2-loop correction to the quark-quark scattering amplitude, in the high-energy limit, and select those contributions that give rise to energy logarithms and compare it with Eq. (1.200). The result can be found in [28], it was derived in [42, 43, 44, 45, 46].

Multi-Regge kinematics

In the MRK and NLLA, as well as in LLA, only the amplitudes with the gluon quantum numbers in the channels with momentum transfers q_i do contribute. The appearance in the right hand side of Eq. (1.110) of amplitudes with quantum numbers in t_i-channels

[21] As always, we are thinking in terms of the quark-quark scattering amplitude, but nothing prevents us from considering the case of quark-gluon or gluon-gluon. The agreement of results extracted from different amplitudes is a further confirmation of the Reggeization.

different from the gluon ones leads to loss of at least two large logarithms and therefore can be ignored in NLLA. As before, the key point in the calculation of the amplitudes contributing in the unitarity relation (1.110) is the gluon Reggeization. In MRK the real parts of the contributing amplitudes (only these parts are relevant in NLLA because the LLA amplitudes are real) are presented in the same form (1.132) as in LLA.
In this kinematics, we need the two-loop contribution $\omega^{(2)}(t)$ to the gluon Regge trajectory $\omega(t)$ and the corrections to the real parts of the PPR-vertices that we discussed previously. Moreover, we need also to compute the one-loop corrections to the Lipatov vertex [39, 47]. The calculation program for these corrections is schematized in Fig. 1.20.

Quasi-multi-Regge kinematics

Probably, the most interesting feature of the NLLA is the appearance of a new kinematics, in fact, in the NLLA, MRK is not the only kinematics that contributes to the unitarity relation (1.110). Since we have the possibility to "lose" one large logarithm (in comparison with LLA), the limitation of the strong ordering (1.112) in the rapidity space cannot be implied more. Any (but only one) pair of the produced particles can have a fixed (not increasing with s) invariant mass, *i.e.* components of this pair can have rapidities of the same order. This kinematics was called quasi-multi-Regge kinematics (QMRK). We can deal with this kinematics by including, together with the production of a gluon, the production of more complicated states in Reggeon-Reggeon (RR) and Reggeon-particle (RP) collisions, which were neglected in the LLA. In particular, we must

- Include the possibility of producing gluon-gluon (GG) [36, 48, 49] and quark-antiquark ($\bar{Q}Q$) [50, 51, 52, 53, 54] states in Reggeon-Reggeon collisions.

- Include the possibility of producing states with larger number of particles in the Reggeon-particle collisions in the fragmentation region of one of the initial particles.

The calculation program for these corrections is schematized in Fig. 1.21.

BFKL kernel and impact factors in the NLLA

As already mentioned above, the partial wave (1.130) can be presented in the same form (1.2.4), but with modified impact factors and Green function. This fact is very important because it confirms that also in NLLA the amplitudes can be factorized as in Fig. 1.19.

In the definition of the impact factors (1.146) we have to include radiative corrections

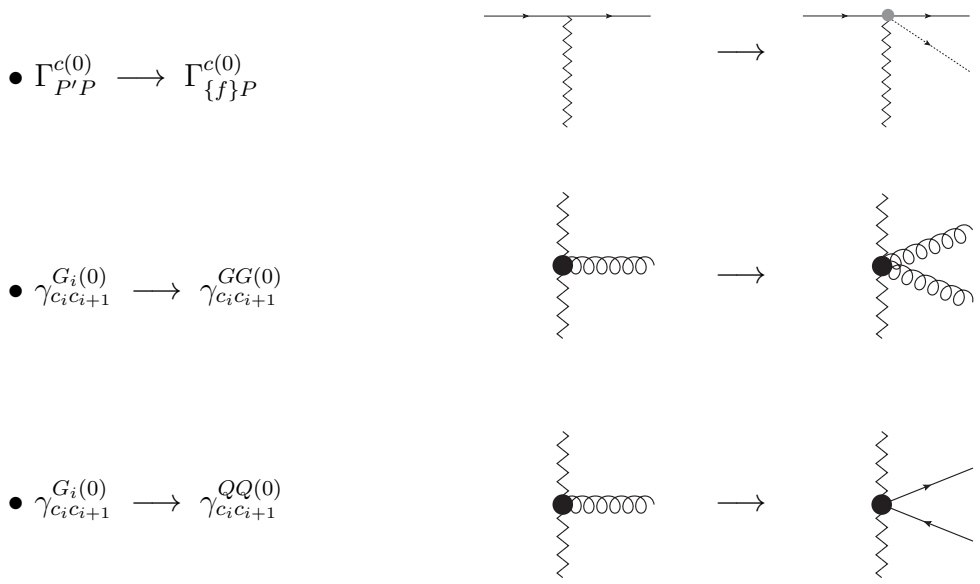

Figure 1.21: Next-to-leading corrections to the vertices PPR and RRG in the quasi-multi-Regge kinematics.

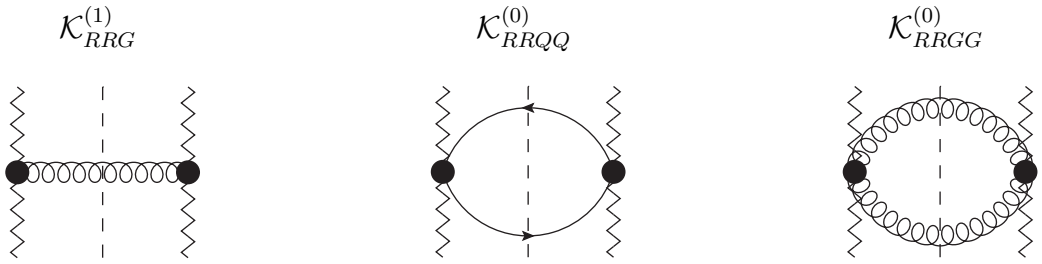

Figure 1.22: Schematic representation of the real part of the NLO BFKL kernel. In the first contribution, one Lipatov vertex is to be taken at one-loop.

to the PPR vertices and the contribution of the "excited" states in the fragmentation region. Eq. (1.152) for the Green function remains unchanged, as well as the representation (1.153) of the kernel, but the gluon trajectory has to be taken in the two-loop approximation:

$$\omega(t) = \omega^{(1)}(t) + \omega^{(2)}(t), \tag{1.202}$$

and the part, related with the real particle production, must contain, together with the contribution from the one-gluon production in the RR collisions (calculated to one-loop level), contributions from the two-gluon and quark-antiquark productions. The one-gluon contribution must be calculated with the one-loop accuracy, whereas the two-gluon and quark-antiquark contributions have to be taken in the Born approximation. For the forward scattering case the real production takes the form (see Fig. 1.22)

$$\mathcal{K}_r\left(\vec{q}_1, \vec{q}_2\right) = \mathcal{K}^{(1)}_{RRG}\left(\vec{q}_1, \vec{q}_2\right) + \mathcal{K}^{(0)}_{RRGG}\left(\vec{q}_1, \vec{q}_2\right) + \mathcal{K}^{(0)}_{RRQ\bar{Q}}\left(\vec{q}_1, \vec{q}_2\right). \tag{1.203}$$

There is an important point to stress, the appearance of a new kinematics introduces technical problems. Calculating the two-gluon production contribution to the kernel and the contribution to the impact factor from the gluon production in the fragmentation region, we meet divergencies of the integrals over invariant masses of the produced particles at upper limits[22]. The reason for the divergencies is the absence of a natural bound between MRK and QMRK. In order to give a precise meaning to the corresponding contributions and to treat them carefully, an artificial bound, which we denote as s_Λ, is introduced [35]. Obviously, the dependence on this artificial parameter disappears in final results.

As a consequence of what has just been explained, the definition of impact factor at the next-to-leading order, in the singlet case, reads

$$\Phi_{AA}(\vec{q}_1; s_0) = \left(\frac{s_0}{\vec{q}_1^{\,2}}\right)^{\omega(-\vec{q}_1^{\,2})} \sum_{\{f\}} \int \theta(s_\Lambda - s_{AR}) \frac{ds_{AR}}{2\pi}\, d\rho_f\, \Gamma^c_{\{f\}A} \left(\Gamma^{c'}_{\{f\}A}\right)^* \langle cc'|\hat{\mathcal{P}}_0|0\rangle$$

$$-\frac{1}{2}\int d^{D-2}q_2\, \frac{\vec{q}_1^{\,2}}{\vec{q}_2^{\,2}}\, \Phi^{(0)}_{AA}(\vec{q}_2)\, \mathcal{K}^{(0)}_r(\vec{q}_2, \vec{q}_1)\, \ln\left(\frac{s_\Lambda^2}{s_0(\vec{q}_2 - \vec{q}_1)^2}\right). \tag{1.204}$$

The first term in Eq. (1.204) is very similiar to that in Eq. (1.161); the important difference with respect to the leading-order definition is the Heaviside theta that creates the separation between MRK and QMRK and automatically regularizes the aforementioned rapidity divergence (s_{AR} goes to infinity). In this scheme, a contribution in which there is the emission of an additional gluon is included in the "QMRK part" of the impact factor

[22] In the next chapter we will refer to these as *rapidity divergences*.

only if $s_{AR} < s_\Lambda$, *i.e.* only if the particle (or the system of particle) that we had at the leading order and the additional emitted gluon are not strongly separated in rapidity.
The second term comes instead from the MRK contribution to the partial wave amplitude Eq. (1.145) in the NLLA. Consistently with how we define the QMRK kinematics using the cut-off s_Λ, we must now impose that the integration over invariant masses s_i in MRK kinematics is performed by imposing $s_i > s_\Lambda$. When we compute in the LLA, the lower bound of integration over invariant masses produces negligible contributions within this approximation. Within the NLLA, terms from the lower bound of integration must be included. In the specific case of the invariant mass s_{AR}, the produced term is exactly the one in the second line of Eq. (1.204).
The s_Λ parameter introduced must be understood as tending to infinity. Both expressions in the first and second line of Eq. (1.204) are divergent, but in their combination any dependence from s_Λ disappears and the result is finite. As it is easy to understand, also the contribution to the kernel from the emission of two gluons has a term similar to the second in Eq. (1.204). For the complete calculation of the separation between MRK and QMRK see [28].

Chapter 2

Next-leading order forward Higgs impact factor

We have made the discovery of a new particle, a completely new particle, which is most probably very different from all the other particles.
Rolf-Dieter Heuer

Precision physics in the Higgs sector has been one of the main challenges in recent years. The pure fixed-order calculations entering the collinear factorization framework, which have been pushed up to N^3LO, are not able to describe the entire kinematic spectrum. In particular conditions, they must be necessarily supplemented by all-order resummations. In the Regge kinematical region, large energy-type logarithms spoil the perturbative behavior of the series and must be resummed to all orders. The BFKL approach, that we have presented in the previous chapter, allows us to achive this resummation, in the NLLA, but, as already said, it requires the knowledge of impact factors. In this chapter, we calculate the next-to-leading order correction to the impact factor (vertex) for the production of a forward Higgs boson, in the infinite top-mass limit. We obtain the result both in the momentum representation and as superposition of the eigenfunctions of the leading-order BFKL kernel. As already mentioned earlier, this impact factor allows to describe the inclusive hadroproduction of a forward Higgs in the limit of small Bjorken x, as well as for the more interesting study of the inclusive forward emissions of a Higgs boson in association with a backward identified object.

The chapter contains five sections. In the first section, we introduce the necessary ingredients and the program of computations. In the second and third section, we calculate

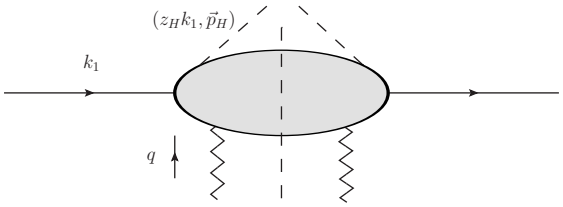

Figure 2.1: Schematic description of the Higgs impact factor: z_H is the fraction of longitudinal momentum of the initial parton carried by the outgoing Higgs and $\vec{p}_H$ is its transverse momentum.

real and virtual corrections, respectively. In the fourth, we perform the projection onto the eigenfunctions of the LO BFKL kernel and we show the cancellation of divergences. Lastly, in the fifth section we summarize and discuss future perspectives. The material in this chapter is based on Ref. [55, 56].

2.1 LO and NLO in a nutshell

2.1.1 The leading-order impact factor for forward Higgs production

Since we are interested in the description of the inclusive production of a Higgs in proton-proton collisions, say in the forward region, the setup sketched in the previous chapter must be suitably modified. First of all, we need to consider processes in which the parton A can be a gluon or any of the active quarks and must then take the convolution of the partonic impact factor with the corresponding PDF. Secondly, the integration over the intermediate states $\{f\}$ in (1.204) must exclude the state of the Higgs, so that the resulting impact factor will be differential in the Higgs kinematics (see Fig. 2.1).

Let us illustrate the procedure in the simplest case of the leading-order (LO) contribution. In the infinite top-mass approximation, the Higgs field couples to QCD *via* the effective Lagrangian [57, 58],

$$\mathcal{L}_{ggH} = -\frac{g_H}{4} F^a_{\mu\nu} F^{\mu\nu,a} H \,, \tag{2.1}$$

where H is the Higgs field, $F^a_{\mu\nu} = \partial_\mu A^a_\nu - \partial_\nu A^a_\mu + g f^{abc} A^b_\mu A^c_\nu$ is the field strength tensor,

$$g_H = \frac{\alpha_s}{3\pi v}\left(1 + \frac{11}{4}\frac{\alpha_s}{\pi}\right) + \mathcal{O}(\alpha_s^3) \tag{2.2}$$

is the effective coupling [59, 60] and $v^2 = 1/(G_F\sqrt{2})$ with G_F the Fermi constant. Feynman rules deriving from this theory can be found in Appendix A.1. We introduce the Sudakov decomposition for the Higgs and Reggeon momenta:

$$p_H = z_H k_1 + \frac{m_H^2 + \vec{p}_H^{\,2}}{z_H s} k_2 + p_{H\perp} \ , \quad p_H^2 = m_H^2 \ , \tag{2.3}$$

$$q = -\alpha_q k_2 + q_\perp \ , \quad q^2 = -\vec{q}^{\,2} \ . \tag{2.4}$$

At LO, the impact factor takes contribution only from the case when the initial-state parton (particle A) is a gluon, for which $k_A = k_1$. For the polarization vector of all gluons in the external lines involved in the calculation we will use the light-cone gauge,

$$\varepsilon(k) \cdot k_2 = 0 \ , \tag{2.5}$$

which leads to the following Sudakov decomposition:

$$\varepsilon(k) = -\frac{(k_\perp \cdot \varepsilon_\perp(k))}{(k \cdot k_2)} k_2 + \varepsilon_\perp(k) \ , \tag{2.6}$$

so that for the initial-state gluon we have $\varepsilon(k_1) = \varepsilon_\perp(k_1)$. The transverse polarization vectors have the properties

$$(\varepsilon_\perp^*(k_1, \lambda_1) \cdot \varepsilon_\perp(k_1, \lambda_2)) = (\varepsilon^*(k_1, \lambda_1) \cdot \varepsilon(k_1, \lambda_2)) = -\delta_{\lambda_1, \lambda_2},$$

$$\sum_\lambda \varepsilon_\perp^{*\mu}(k, \lambda) \varepsilon_\perp^\nu(k, \lambda) = -g_{\perp\perp}^{\mu\nu} \ , \tag{2.7}$$

where the index λ enumerates the independent polarizations of gluon (sometimes it will be omitted for simplicity, but it should be always understood), $g^{\mu\nu}$ is the metric tensor in the full space and $g_{\perp\perp}^{\mu\nu}$ the one in the transverse subspace,

$$g_{\perp\perp}^{\mu\nu} = g^{\mu\nu} - \frac{k_1^\mu k_2^\nu + k_2^\mu k_1^\nu}{(k_1 \cdot k_2)} \ . \tag{2.8}$$

The LO impact factor before differentiation in the kinematic variables of the Higgs is given by

$$\Phi_{gg}^{\{H\}(0)}(\vec{q}\,) = \frac{\langle cc'|\hat{\mathcal{P}}_0|0\rangle}{2(N^2-1)} \sum_{a,\lambda} \int \frac{ds_{gR}}{2\pi} d\rho_H \Gamma_{\{H\}g}^{ac(0)}(q) \left(\Gamma_{\{H\}g}^{ac'(0)}(q)\right)^* \ , \tag{2.9}$$

where the only state contributing to the intermediate state $\{f\}$ is the Higgs boson and the particle A is identified with an on-shell gluon. Here,

$$\Gamma_{\{H\}g}^{ac(0)}(q) = \frac{g_H}{2} \delta^{ac} \left(q_\perp \cdot \varepsilon_\perp(k_1)\right) \ , \tag{2.10}$$

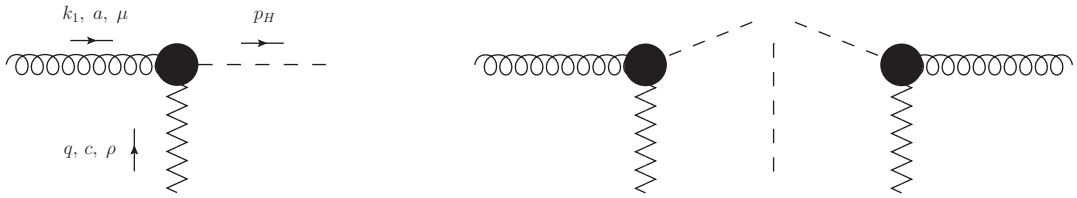

Figure 2.2: Born gluon-Reggeon-Higgs effective vertex (left) and schematic description of the single contribution to the impact factor LO (right). We draw the Higgs boson above the cut to emphasize that we do not integrate over its kinematic variables.

is the high-energy gluon-Reggeon-Higgs (gRH) Born vertex (see Fig. 2.2). The overall factor $1/2(N^2-1)$ comes from the average over the polarization and color states of the incoming gluon. The vertex in Eq. (2.10) is obtained from the Higgs effective theory Feynman rules, taking for the Reggeon in the t-channel the "nonsense" polarization $(-k_2^\rho/s)$. We stress again that this effective polarization arises from the fact that, for gluons in the t-channel that connect strongly separated regions in rapidity, the Gribov trick,

$$g^{\rho\nu} = g^{\rho\nu}_{\perp\perp} + 2\frac{k_1^\rho k_2^\nu + k_2^\rho k_1^\nu}{s} \longrightarrow 2\frac{k_2^\rho k_1^\nu}{s} = 2s\left(\frac{-k_2^\rho}{s}\right)\left(\frac{-k_1^\nu}{s}\right) \ , \tag{2.11}$$

can be used in the kinematic region relevant for the "upper" impact factor. Since the integration over the invariant mass s_{PR} and over the phase space is completely trivial, we simply obtain

$$\Phi_{gg}^{\{H\}(0)}(\vec{q}\,) = \frac{g_H^2}{8\sqrt{N^2-1}}\vec{q}^{\,2} \ . \tag{2.12}$$

Hence, it is straightforward to construct the differential (in the kinematic variables of the Higgs) LO order impact factor. This is the only chapter of the thesis in which, to adapt our notation to Ref. [55], we work in $D = 4-2\epsilon$ dimensions. The impact factor in this dimension reads[23]

$$\frac{d\Phi_{gg}^{\{H\}(0)}(\vec{q}\,)}{dz_H d^2\vec{p}_H} = \frac{g_H^2}{8(1-\epsilon)\sqrt{N^2-1}}\vec{q}^{\,2}\delta(1-z_H)\delta^{(2)}(\vec{q}-\vec{p}_H) \ . \tag{2.13}$$

[23]Not to burden our formulas, we write $\delta^{(2)}$ instead of $\delta^{(D-2)}$ in the R.H.S. and $d^2\vec{p}_H$ instead of $d^{D-2}\vec{p}_H$ in the L.H.S.; the latter convention will apply also in the following. Moreover, if g_H is meant to have dimension of an inverse mass, then in D-dimension it should be replaced by $g_H\mu^{-\epsilon}$, where μ is an arbitrary mass scale.

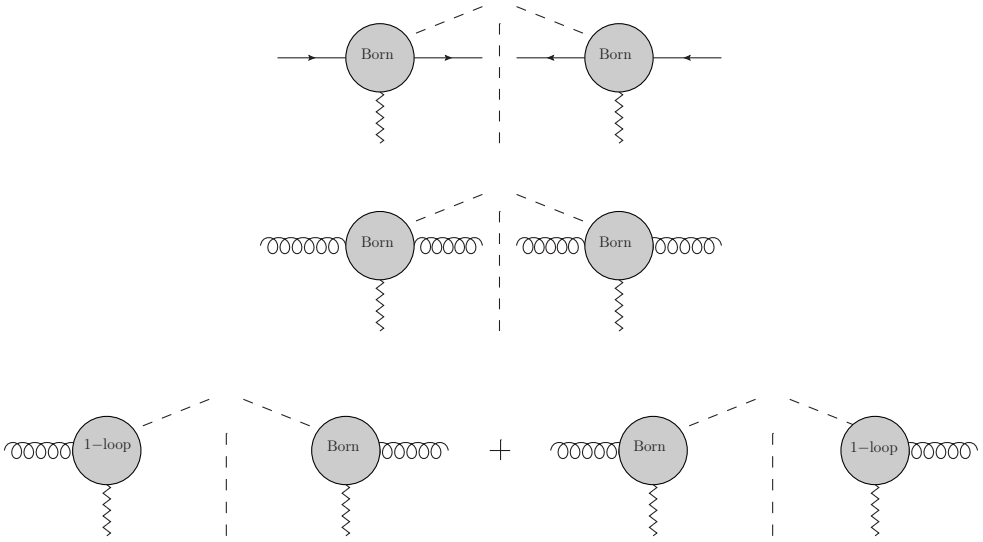

Figure 2.3: Schematic description of the calculation of the impact factor at the NLO. In the first figure from above the hard process is initiated by a quark, and an additional quark is produced through the cut. Note that this quark "crosses" the cut to indicate that we will integrate on its kinematic variables.

After convolution with the gluon PDF, we obtain the proton-initiated LO impact factor,

$$\frac{d\Phi_{PP}^{\{H\}(0)}(x_H,\vec{p}_H,\vec{q})}{dx_H d^2\vec{p}_H} = \int_{x_H}^1 \frac{dz_H}{z_H} f_g\left(\frac{x_H}{z_H}\right) \frac{d\Phi_{gg}^{\{H\}(0)}(z_H,\vec{p}_H,\vec{q})}{dz_H d^2\vec{p}_H} = \frac{g_H^2 \vec{q}^{\,2} f_g(x_H)\delta^{(2)}(\vec{q}-\vec{p}_H)}{8(1-\epsilon)\sqrt{N^2-1}} \,. \tag{2.14}$$

2.1.2 NLO computation in a nutshell

The program for calculating the NLO Higgs impact factor is the following:

- **Real corrections**
  At NLO the process can be initiated either by a gluon or by a quark extracted from the proton. Moreover, the Higgs must be accompanied by an additional parton (see the first two diagrams from the top of Fig. 2.3). These corrections will be calculated in section 2.2, separating the quark-initiated case (subsection 2.2.1) and the gluon-initiated one (subsection 2.2.2).

- **Virtual corrections**
  Another NLO order correction is obtained when we take one of the two effective vertices Γ that appear in the definition of the impact factor at one loop and the

other at Born level (see diagrams in the last line of Fig. 2.3). This correction is trivial to compute once the 1-loop correction to the vertex (2.10) has been extracted. This problem will be addressed in the section 2.3.

- **Projection onto the eigenfunctions of the LO BFKL kernel and cancellation of divergences**
  In section 2.4 we perform the convolution with the PDFs for the previously calculated contributions and show that, after (i) carrying out the UV renormalization of the strong coupling, (ii) introducing the counterterms associated with the PDFs, (iii) performing the projection on the eigenfunctions of the LO BFKL kernel (more details in section 2.4), the final result is free from any kind of divergence.

2.2 NLO impact factor: Real corrections

In this section, we compute real corrections to the Higgs impact factor. At NLO both initial-state gluon and quark can contribute: if the process is initiated by a quark (gluon), then the intermediate state $\{f\}$ will contain the Higgs and a quark (gluon). The Sudakov decomposition of the momentum of the produced parton reads

$$p_p = z_p k_1 + \frac{\vec{p}_p^{\,2}}{z_p s} k_2 + p_{p\perp} \,, \quad p_p^2 = 0 \,, \tag{2.15}$$

where the subscript p is equal to q (g) in the quark (gluon) case. We have then

$$s_{pR} = (p_p + p_H)^2 = \frac{z_p(z_H + z_p)m_H^2 + (z_p\vec{p}_H - z_H\vec{p}_p)^2}{z_H z_p} \,, \tag{2.16}$$

$$\frac{ds_{pR}}{2\pi} d\rho_{pH} = \delta(1 - z_p - z_H)\delta^{(2)}(\vec{p}_p + \vec{p}_H - \vec{q}\,)\frac{dz_p dz_H}{z_p z_H}\frac{d^{D-2}p_p d^{D-2}p_H}{2(2\pi)^{D-1}} \,. \tag{2.17}$$

The integration over the kinematic variables of the produced parton is trivial due to the presence of the delta functions and results in the constraints

$$z_p = 1 - z_H \,, \quad \vec{p}_p \equiv \vec{q} - \vec{p}_H \,. \tag{2.18}$$

The integration over z_H and $\vec{p}_H$ is not performed, since our target is an impact factor differential in the kinematic variables of the Higgs.

In the gluon case we will use the Sudakov decompositions of the polarization vectors of the initial-state gluon with momentum k_1 and of the produced gluon with momentum p_g,

$$\varepsilon(k_1) = \varepsilon_\perp(k_1) \,, \quad \varepsilon(p_g) = -\frac{(p_{g,\perp}\cdot\varepsilon_\perp(p_g))}{(p_g\cdot k_2)}k_2 + \varepsilon_\perp(p_g) \,, \tag{2.19}$$

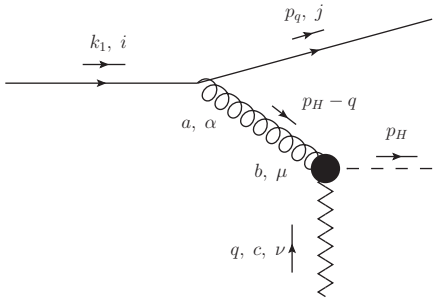

Figure 2.4: Feynman diagram contributing to the $q\ R \to q\ H$ amplitude.

which encode the gauge condition $\varepsilon \cdot k_2 = 0$ for both gluons.

We observe that, when calculating NLO real corrections, the s_0-dependent factor in the definition (1.204) can be taken at the lowest order in the perturbative expansion and therefore put equal to one. Moreover, in the quark case there is no rapidity divergence for $s_{pR} \to \infty$, therefore the regulator s_Λ can be sent to infinity in the argument of the theta function and the second term in Eq. (1.204) (the so-called "BFKL counterterm") can be omitted.

2.2.1 Quark-initiated contribution

In the case of incoming quark, the contribution to the impact factor reads

$$d\Phi_{qq}^{\{Hq\}}(\vec{q}) = \langle cc'|\hat{\mathcal{P}}_0|0\rangle \frac{1}{2N} \sum_{\substack{i,j \\ \lambda,\lambda'}} \int \frac{ds_{qR}}{2\pi} d\rho_{\{Hq\}} \Gamma^{c(0)}_{\{Hq\}q}(q) \left(\Gamma^{c'(0)}_{\{Hq\}q}(q)\right)^* . \tag{2.20}$$

where color and spin states have been averaged for the initial-state quark and summed over for the produced one. There is only one Feynman diagram to consider, shown in Fig. 2.4, leading to

$$\Gamma^{c(0)}_{\{Hq\}q} = -g g_H t^c_{ij} \frac{1 - z_H}{(\vec{q} - \vec{p}_H)^2} \bar{u}(p_q) \left(\frac{\not{k}_2}{s} (p_H - q) \cdot q - \not{q} \left((p_H - q) \cdot \frac{k_2}{s} \right) \right) u(k_1) . \tag{2.21}$$

Substituting Eq. (2.21) into Eq. (2.20), one easily gets the quark initiated contribution to the impact factor,

$$\frac{d\Phi_{qq}^{\{Hq\}}(z_H, \vec{p}_H, \vec{q})}{dz_H d^2\vec{p}_H} = \frac{\sqrt{N^2-1}}{16N(2\pi)^{D-1}} \frac{g^2 g_H^2}{[(\vec{q} - \vec{p}_H)^2]^2} \times \left[\frac{4(1 - z_H)\left[(\vec{q} - \vec{p}_H) \cdot \vec{q}\,\right]^2 + z_H^2 \vec{q}^{\,2} (\vec{q} - \vec{p}_H)^2}{z_H} \right] . \tag{2.22}$$

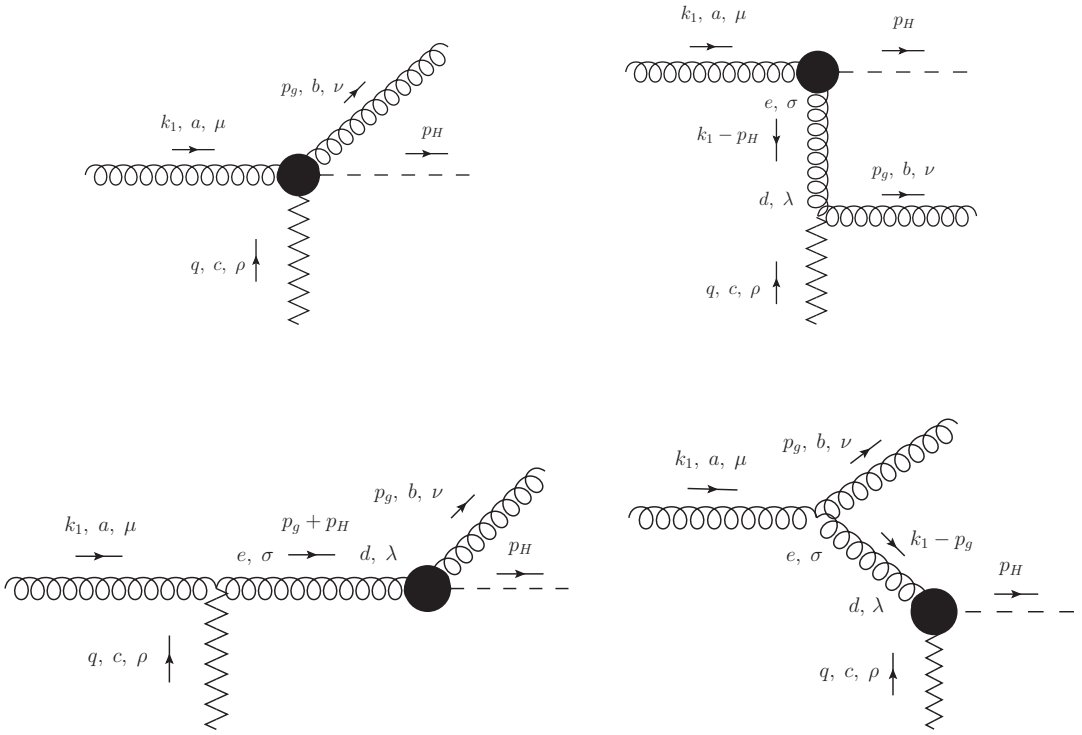

Figure 2.5: Feynman diagrams contributing to the $gR \to gH$ amplitude. In the text we label them from (1) to (4) starting from the top left.

We observe that this contribution to the impact factor vanishes in the limit $\vec{q} \to 0$, as required by gauge invariance.

2.2.2 Gluon-initiated contribution

In the case of gluon in the initial state, the NLO real corrections, which are given, up to the BFKL counterterm, by the first term in Eq. (1.204), take the following form

$$d\Phi_{gg}^{\{Hg\}}(\vec{q}) = \frac{\langle cc'|\mathcal{P}|0\rangle}{2(1-\epsilon)(N^2-1)} \sum_{\substack{a,b \\ \lambda,\lambda'}} \int \frac{ds_{gR}}{2\pi} d\rho_{\{Hg\}} \Gamma^{abc(0)}_{\{Hg\}g}(q) \left(\Gamma^{abc'(0)}_{\{Hg\}g}(q)\right)^* \theta(s_\Lambda - s_{gR}) \,, \tag{2.23}$$

where color and polarization states have been averaged for the initial-state gluon and summed over for the produced one. The Feynman diagrams contributing to the amplitude $\Gamma^{abc(B)}_{\{Hg\}g}$ of the $gR \to gH$ process are shown in Fig. 2.5, and give

$$\Gamma_1 = -igg_H f^{abc} \varepsilon_\mu(k_1) \varepsilon^*_\nu(p_g) \frac{2 - z_H}{2} g^{\mu\nu} \,, \tag{2.24}$$

$$\Gamma_2 = \frac{-igg_H f^{abc}\varepsilon_\mu(k_1)\varepsilon^*_\nu(p_g)}{2[(z_H-1)m_H^2-\vec{p}_H^{\,2}]}\left[(1-z_H)(m_H^2+\vec{p}_H^{\,2})g^{\mu\nu}-2z_H p_H^\mu(p_H^\nu-z_H k_1^\nu)\right] , \quad (2.25)$$

$$\Gamma_3 = \frac{igg_H f^{abc}\varepsilon_\mu(k_1)\varepsilon^*_\nu(p_g)}{2\left[(1-z_H)m_H^2+(\vec{p}_H-z_H\vec{q}\,)^2\right]}$$
$$\times\left[g^{\mu\nu}\left((1-z_H)^2m_H^2+(\vec{p}_H-z_H\vec{q}\,)^2\right)+2z_H(1-z_H)^2p_H^\mu p_H^\nu-2z_H^2(1-z_H)p_g^\mu p_H^\nu\right] , \quad (2.26)$$

$$\Gamma_4 = -igg_H f^{abc}\varepsilon_\mu(k_1)\varepsilon^*_\nu(p_g)\frac{(1-z_H)}{(\vec{q}-\vec{p}_H)^2}\left[-g^{\mu\nu}(\vec{q}-\vec{p}_H)\cdot\vec{q}-z_H(p_H^\mu k_1^\nu+p_g^\mu p_H^\nu)\right] , \quad (2.27)$$

which sum up to

$$\Gamma^{abc(0)}_{\{Hg\}g} = igg_H f^{abc}\varepsilon_\mu(k_1)\varepsilon^*_\nu(p_g)\left[\frac{[(1-z_H)(m_H^2+\vec{p}_H^{\,2})g^{\mu\nu}-2z_Hp_H^\mu(p_H^\nu-z_Hk_1^\nu)]}{2[(1-z_H)m_H^2+\vec{p}_H^{\,2}]}\right.$$
$$+\frac{\left[g^{\mu\nu}\left((1-z_H)^2m_H^2+(\vec{p}_H-z_H\vec{q}\,)^2\right)+2z_H(1-z_H)^2p_H^\mu p_H^\nu-2z_H^2(1-z_H)p_g^\mu p_H^\nu\right]}{2\left[(1-z_H)m_H^2+(\vec{p}_H-z_H\vec{q}\,)^2\right]}$$
$$\left.-\frac{2-z_H}{2}g^{\mu\nu}+\frac{(1-z_H)\left[g^{\mu\nu}(\vec{q}-\vec{p}_H)\cdot\vec{q}+z_H(p_H^\mu k_1^\nu+p_g^\mu p_H^\nu)\right]}{(\vec{q}-\vec{p}_H)^2}\right] . \quad (2.28)$$

Using Eqs. (2.19), we can decouple longitudinal and transverse degrees of freedom and get

$$\Gamma^{abc(0)}_{\{Hg\}g} = -igg_H f^{abc}\varepsilon_{\mu\perp}(k_1)\varepsilon^*_{\nu\perp}(p_g)\left[\frac{2z_Hp_{H\perp}^\mu p_{H\perp}^\nu-z_H(1-z_H)m_H^2g^{\mu\nu}}{2\left[(1-z_H)m_H^2+\vec{p}_H^{\,2}\right]}\right.$$
$$\left.-\frac{2z_H\Delta_\perp^\mu\Delta_\perp^\nu-z_H(1-z_H)m_H^2g^{\mu\nu}}{2\left[(1-z_H)m_H^2+\vec{\Delta}^2\right]}+\frac{z_H(q_\perp^\mu r_\perp^\nu-(1-z_H)r_\perp^\mu q_\perp^\nu)-(1-z_H)\vec{r}\cdot\vec{q}\,g^{\mu\nu}}{\vec{r}^{\,2}}\right] , \quad (2.29)$$

where we have defined, similarly to [61],

$$\Delta_\perp^\mu \equiv p_{H,\perp}^\mu - z_H q_\perp^\mu , \qquad r_\perp \equiv q_\perp^\mu - p_{H,\perp}^\mu . \quad (2.30)$$

We can finally plug this expression into Eq. (2.23) and get the gluon-initiated contribution to the impact factor,

$$\frac{d\Phi_{gg}^{\{Hg\}}(z_H,\vec{p}_H,\vec{q})}{dz_Hd^2p_H} = \frac{g^2g_H^2C_A}{8(2\pi)^{D-1}(1-\epsilon)\sqrt{N^2-1}}\left\{\frac{2}{z_H(1-z_H)}\right.$$
$$\left[2z_H^2+\frac{(1-z_H)z_Hm_H^2(\vec{q}\cdot\vec{r})[z_H^2-2(1-z_H)\epsilon]+2z_H^3(\vec{p}_H\cdot\vec{r})(\vec{p}_H\cdot\vec{q})}{\vec{r}^{\,2}\left[(1-z_H)m_H^2+\vec{p}_H^{\,2}\right]}-\frac{2z_H^2(1-z_H)m_H^2}{\left[(1-z_H)m_H^2+\vec{p}_H^{\,2}\right]}\right.$$
$$\left.-\frac{(1-z_H)z_Hm_H^2(\vec{q}\cdot\vec{r})[z_H^2-2(1-z_H)\epsilon]+2z_H^3(\vec{\Delta}\cdot\vec{r})(\vec{\Delta}\cdot\vec{q})}{\vec{r}^{\,2}\left[(1-z_H)m_H^2+\vec{\Delta}^2\right]}-\frac{2z_H^2(1-z_H)m_H^2}{\left[(1-z_H)m_H^2+\vec{\Delta}^2\right]}\right.$$

$$+\frac{(1-\epsilon)z_H^2(1-z_H)^2m_H^4}{2}\left(\frac{1}{[(1-z_H)m_H^2+\Delta^2]}+\frac{1}{[(1-z_H)m_H^2+\vec{p}_H^{\,2}]}\right)^2$$
$$-\frac{2z_H^2(\vec{p}_H\cdot\vec{\Delta})^2-2\epsilon(1-z_H)^2z_H^2m_H^4}{[(1-z_H)m_H^2+\vec{p}_H^{\,2}]\,[(1-z_H)m_H^2+\Delta^2]}\Bigg]$$
$$+\frac{2\vec{q}^{\,2}}{\vec{r}^{\,2}}\left[\frac{z_H}{1-z_H}+z_H(1-z_H)+2(1-\epsilon)\frac{(1-z_H)}{z_H}\frac{(\vec{q}\cdot\vec{r})^2}{\vec{q}^{\,2}\vec{r}^{\,2}}\right]\Bigg\}\theta\left(s_\Lambda-\frac{(1-z_H)m_H^2+\vec{\Delta}^2}{z_H(1-z_H)}\right)\,. \tag{2.31}$$

We notice that this expression is compatible with gauge invariance, since it vanishes for $\vec{q}\to 0$. We have presented our result for $\Phi_{gg}^{\{Hg\}}$ in a form similar to that given in Eq. (46) of Ref. [61] to facilitate the comparison. One can see that the expression in Ref. [61] agrees with ours[24], except for:

- two terms which are proportional to $z_H(1-z_H)^2$ instead of $z_H^2(1-z_H)$;
- two terms, proportional to z_H^3, which have a sign different from ours.

These little discrepancies are due to misprints in Ref. [61], as privately communicated to us by the authors of that paper.

2.3 NLO impact factor: Virtual corrections

In this section, we compute the contribution to the impact factor coming from virtual corrections. The basic ingredient we need is the 1-loop correction to the high-energy vertex in Eq. (2.10), that we indicate as[25]

$$\Gamma^{ac(1)}_{\{H\}g}(q)=\Gamma^{ac(0)}_{\{H\}g}(q)\,[1+\delta_{\rm NLO}]\,. \tag{2.32}$$

Thereafter, the virtual contribution to the impact factor can be calculated as

$$\Phi_{gg}^{\{H\}(1)}(\vec{q};s_0)=\frac{\langle cc'|\hat{\mathcal{P}}_0|0\rangle}{2(1-\epsilon)(N^2-1)}$$

[24] We stress that in Ref. [61] authors work in $D=4+2\epsilon$, while we work in $D=4-2\epsilon$

[25] We remind that this is the effective vertex for the coupling of the initial-state gluon with the final-state Higgs and a t-channel Reggeized gluon, which is an object in the octet color representation with negative signature. Up to the NLO, the effective vertex takes contribution from the exchange in the t-channel of either one or two gluons; in the latter case, the projection onto the octet color representation with negative signature should be taken; in our calculation this projection is automatic in presence of an initial-state gluon, since the Higgs is a color singlet state.

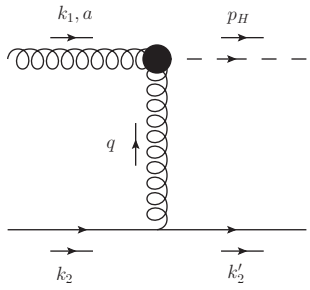

Figure 2.6: $gq \to Hq$ amplitude.

$$\times \sum_{a,\lambda} \int \frac{ds_{gR}}{2\pi} d\rho_H \Gamma^{ac(0)}_{\{H\}g}(q) \left(\Gamma^{ac'(0)}_{\{H\}g}(q)\right)^* \left[\omega^{(1)}(-\vec{q}^{\,2}) \ln\left(\frac{s_0}{\vec{q}^{\,2}}\right) + \delta_{\rm NLO} + \delta^*_{\rm NLO}\right] , \quad (2.33)$$

where the s_0-dependent term comes from the expansion of $(s_0/\vec{q}^{\,2})^{\omega^{(1)}(-\vec{q}^{\,2})}$ in (1.204).

The general strategy to find a NLO high-energy effective vertex is to compute, in the NLO and in the high-energy limit, a suitable amplitude and to compare it with the expected Regge form, written in terms of the needed effective vertex and of another known one. For our purposes, we consider the diffusion of a gluon off a quark to produce a Higgs plus a quark, whose amplitude $\mathcal{A}_{gq\to Hq}$, for the octet colour state and the negative signature in the t-channel has the following Reggeized form (see Fig. 2.6):

$$\mathcal{A}^{(8,-)}_{gq\to Hq} = \Gamma^{ac}_{\{H\}g} \frac{s}{t} \left[\left(\frac{s}{-t}\right)^{\omega(t)} + \left(\frac{-s}{-t}\right)^{\omega(t)}\right] \Gamma^c_{qq} \approx \Gamma^{ac(0)}_{\{H\}g} \frac{2s}{t} \Gamma^{c(0)}_{qq}$$

$$+\Gamma^{ac(0)}_{\{H\}g} \frac{s}{t} \omega^{(1)}(t) \left[\ln\left(\frac{s}{-t}\right) + \ln\left(\frac{-s}{-t}\right)\right] \Gamma^{c(0)}_{qq} + \Gamma^{ac(0)}_{\{H\}g} \frac{2s}{t} \Gamma^{c(1)}_{qq} + \Gamma^{ac(1)}_{\{H\}g} \frac{2s}{t} \Gamma^{c(0)}_{qq} , \quad (2.34)$$

where

$$\Gamma^{c(0)}_{qq} = g t^c_{ji} \bar{u}(k_2 - q) \frac{\not{k}_1}{s} u(k_2) \quad (2.35)$$

is the LO quark-quark-Reggeon effective vertex and $\Gamma^{c(1)}_{qq}$ its 1-loop correction, known since long [40, 42], and $t = q^2 = -\vec{q}^{\,2}$.

Let us now split the 1-loop contributions to this amplitude into three pieces, related to 2-gluon (2g) or 1-gluon (1g) exchange or self-energy (se) diagrams in the t-channel:

$$\mathcal{A}^{(2g)(8,-)(1)}_{gq\to Hq} + \mathcal{A}^{(se)(1)}_{gq\to Hq} + \mathcal{A}^{(1g)(1)}_{gq\to Hq} = \left\{\Gamma^{(2g)ac(1)}_{\{H\}g} \frac{2s}{t} \Gamma^{c(0)}_{qq} + \Gamma^{ac(0)}_{\{H\}g} \frac{2s}{t} \Gamma^{(2g)c(1)}_{qq}\right.$$

$$\left. +\Gamma^{c(0)}_{\{H\}g} \frac{s}{t} \omega^{(1)}(t) \left[\ln\left(\frac{s}{-t}\right) + \ln\left(\frac{-s}{-t}\right)\right] \Gamma^{c(0)}_{qq}\right\}$$

$$+\left\{\Gamma^{(se)ac(1)}_{\{H\}g}\frac{2s}{t}\Gamma^{c(0)}_{qq}+\Gamma^{ac(0)}_{\{H\}g}\frac{2s}{t}\Gamma^{(se)c(1)}_{qq}\right\}+\left\{\Gamma^{(1g)ac(1)}_{\{H\}g}\frac{2s}{t}\Gamma^{c(0)}_{qq}+\Gamma^{c(0)}_{\{H\}g}\frac{2s}{t}\Gamma^{(1g)c(1)}_{qq}\right\}, \quad (2.36)$$

where the self-energy diagrams and 1-gluon exchange diagrams are automatically in the 8^- color representation.

We stress that we will use a unique regulator $\epsilon \equiv \epsilon_{\rm UV} \equiv \epsilon_{\rm IR}$ for both ultraviolet (UV) and infrared (IR) divergences. As a consequences, scaleless integrals such as

$$\int \frac{d^Dk}{i(2\pi)^D}\frac{1}{k^2(k+k_1)^2} \quad (2.37)$$

are equal to zero due to the exact cancellation between IR- and UV-divergence. In our case of massless partons, this implies that the contribution from the renormalization of the external quark and gluon lines is absent in dimensional regularization.

The 1-gluon-exchange contribution $\Gamma^{(1g)ac(1)}_{gH}$ can be calculated in a straightforward way by taking the radiative corrections to the amplitude of Higgs production in the collision of an on-shell gluon with an off-shell one (the gluon in the t-channel) having momentum q, colour index c and "nonsense" polarization vector $-k_2/s$. In a similar manner one could calculate the 1-gluon-exchange contribution to the quark-quark-Reggeon effective vertex; in this case, the t-channel off-shell gluon must be taken with "nonsense" polarization vector $-k_1/s$. This is the consequence of the Gribov trick on the t-channel gluon propagator, valid in the high-energy limit. The 1-gluon-exchange contribution does not include self-energy corrections to the t-channel gluon, which must be calculated separately and assigned with weight equal to one half to both $\Gamma^{(se)ac(1)}_{\{H\}g}$ and $\Gamma^{(se)c(1)}_{qq}$.

For the 2-gluon exchange contributions we have the relation

$$\Gamma^{(2g)ac(1)}_{\{H\}g}\frac{2s}{t}\Gamma^{c(0)}_{qq}+\Gamma^{ac(0)}_{\{H\}g}\frac{2s}{t}\Gamma^{(2g)c(1)}_{qq}$$

$$=\mathcal{A}^{(2g)(8,-)(1)}_{gq\to Hq}-\Gamma^{ac(0)}_{\{H\}g}\frac{s}{t}\omega^{(1)}(t)\left[\ln\left(\frac{s}{-t}\right)+\ln\left(\frac{-s}{-t}\right)\right]\Gamma^{c(0)}_{qq}, \quad (2.38)$$

which shows that we need to know the correction $\Gamma^{(2g)c(1)}_{qq}$. This correction has been obtained in Ref. [62] and reads

$$\Gamma^{(2g)c(1)}_{qq}=\delta^{(2g)}_{qq}(t)\Gamma^{c(0)}_{qq}\ , \quad (2.39)$$

with

$$\delta^{(2g)}_{qq}(t)=\frac{1}{2}\omega^{(1)}(t)\left[-\frac{1}{\epsilon}+\psi(1)+\psi(1+\epsilon)-2\psi(1-\epsilon)\right]$$

$$=g^2N\frac{\Gamma(2+\epsilon)}{(4\pi)^{2-\epsilon}}\frac{1}{\epsilon}(-t)^{-\epsilon}\left(-\frac{1}{\epsilon}+1-\epsilon+4\epsilon\psi'(1)\right)+\mathcal{O}(\epsilon). \quad (2.40)$$

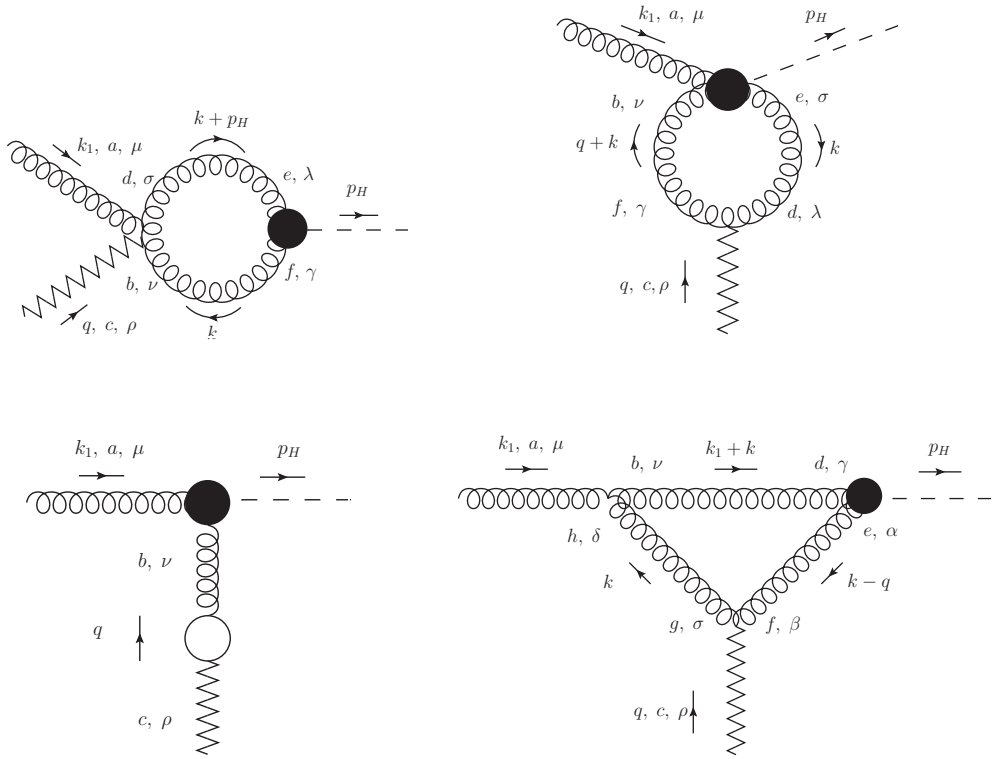

Figure 2.7: 1-gluon in the t-channel exchange diagrams. In the text we label them from (1) to (4) starting from the top left.

2.3.1 The 1-loop correction: 1-gluon exchange and self-energy diagrams

There are four non-vanishing diagrams with 1-gluon exchange in the t-channel, including the one with self-energy corrections to the exchanged gluon; they are shown in Fig. 2.7, where, the blob in the third diagram means the sum of gluon, ghost and quark loop contributions.

Let's start by considering the first diagram; it gives

$$\Gamma^{(1g)}_{1,V} = \frac{1}{2} i g^2 g_H \epsilon_\mu(k_1) \frac{k_{2,\rho}}{s} \int \frac{d^D k}{(2\pi)^D} \frac{\Gamma^{\mu\rho\nu\sigma}_{abcb} H_{\sigma\nu}(-k-p_H, k)}{k^2 (k+p_H)^2} \ , \tag{2.41}$$

where

$$\Gamma^{\mu\rho\nu\sigma}_{abcd} = [(T^g)_{ab}(T^g)_{cd}(g^{\mu\rho}g^{\nu\sigma} - g^{\mu\sigma}g^{\nu\rho}) + (T^g)_{ac}(T^g)_{bd}(g^{\mu\nu}g^{\rho\sigma} - g^{\mu\sigma}g^{\nu\rho})$$

$$+(T^g)_{ad}(T^g)_{cb}(g^{\mu\rho}g^{\nu\sigma} - g^{\mu\nu}g^{\sigma\rho})] \ , \qquad (T^a)_{bc} = -i f_{abc} \ , \tag{2.42}$$

and $H_{\sigma\nu}$ is defined in (A.1). After a trivial computation, we obtain

$$\Gamma^{(1g)}_{1,V} = \Gamma^{ac(0)}_{\{H\}g} N g^2 \frac{(D-2)}{4(D-1)} B_0(m_H^2) \equiv \Gamma^{ac(0)}_{\{H\}g} \delta^{(1g)}_{1,V} \ . \tag{2.43}$$

The definition and the value of the integral $B_0(m_H^2)$, together with all the other integrals that appear in the calculation of the virtual corrections, can be found in the Appendix A.2.

The second diagram gives the following contribution

$$\Gamma^{(1g)}_{2,V} = \frac{-i}{2}\epsilon_\mu(k_1)\frac{k_{2,\rho}}{s} N \delta^{ac} g^2 g_H \int \frac{d^D k}{(2\pi)^D} \frac{V^{\mu\nu\sigma}(-k_1, -k-q, k) A^{\rho}_{\sigma\nu}(-k, k+q)}{k^2 (q+k)^2} \ , \tag{2.44}$$

where

$$A^{\mu\rho\nu}(p,q) = g^{\nu\rho}(q-p)^\mu + g^{\rho\mu}(2p+q)^\nu - g^{\mu\nu}(p+2q)^\rho \tag{2.45}$$

and $V^{\mu\nu\sigma}$ is defined in (A.2). We find

$$\Gamma^{(1g)}_{2,V} = \Gamma^{ac(0)}_{\{H\}g} \left[-\frac{3}{2} N g^2 B_0(-\vec{q}^{\,2}) \right] \equiv \Gamma^{ac(0)}_{\{H\}g} \delta^{(1g)}_{2,V} \ . \tag{2.46}$$

The correction due to the Reggeon self-energy is universal and reads (see, *e.g.*, Ref. [63])

$$\Gamma^{(1g)}_{3,V} = \Gamma^{ac(0)}_{\{H\}g} \left[\omega^{(1)}(t) \frac{(5-3\epsilon)N - 2(1-\epsilon) n_f}{4(1-2\epsilon)(3-2\epsilon)N} \right] \equiv \Gamma^{ac(0)}_{\{H\}g} \delta^{(1g)}_{3,V} \ . \tag{2.47}$$

The last correction is the one associated with the "triangular" diagram,

$$\Gamma^{(1g)}_{4,V} = g^2 N \epsilon_\mu(k_1) \frac{k_{2,\rho}}{s} \delta^{ac} g_H$$

$$\times \int \frac{d^D k}{i(2\pi)^D} \frac{A^{\mu\ \nu}_{\ \sigma}(-k, k+k_1) A^{\ \sigma\rho\beta}(-q, q-k) H_{\nu\beta}(-k_1-k, k-q)}{k^2 (k+k_1)^2 (k-q)^2} \ . \tag{2.48}$$

This correction is less trivial and we made use of the FeynCalc [64, 65] package to perform some analytic steps; up to terms power-suppressed in s, we end up with

$$\Gamma^{(1g)}_{4,V} \equiv \Gamma^{ac(0)}_{Hg} \delta^{(1g)}_{4,V} = \Gamma^{ac(0)}_{Hg} \frac{N g^2}{4(D-2)(1-D)\left(m_H^2 + \vec{q}^{\,2}\right)^2}$$

$$\times \Big\{ 2(D-1) \left[\left(-5(D-2) m_H^4 - 4(3D-8) m_H^2 \vec{q}^{\,2} + (16-7D)(\vec{q}_2^{\,2})^2 \right) B_0(-\vec{q}^{\,2}) \right.$$

$$\left. + 2(D-2) m_H^2 \left(2m_H^4 + 3 m_H^2 \vec{q}^{\,2} + (\vec{q}^{\,2})^2 \right) C_0\left(0, -\vec{q}^{\,2}, m_H^2\right) \right] + \left(-D(D-2)(\vec{q}^{\,2})^2 \right.$$

$$\left. + \left(D(D(4D-35)+92) - 60 \right) m_H^4 - 2\left(D(-2(D-9)D - 41) + 24 \right) m_H^2 \vec{q}^{\,2} \right) B_0\left(m_H^2\right) \Big\} \ . \tag{2.49}$$

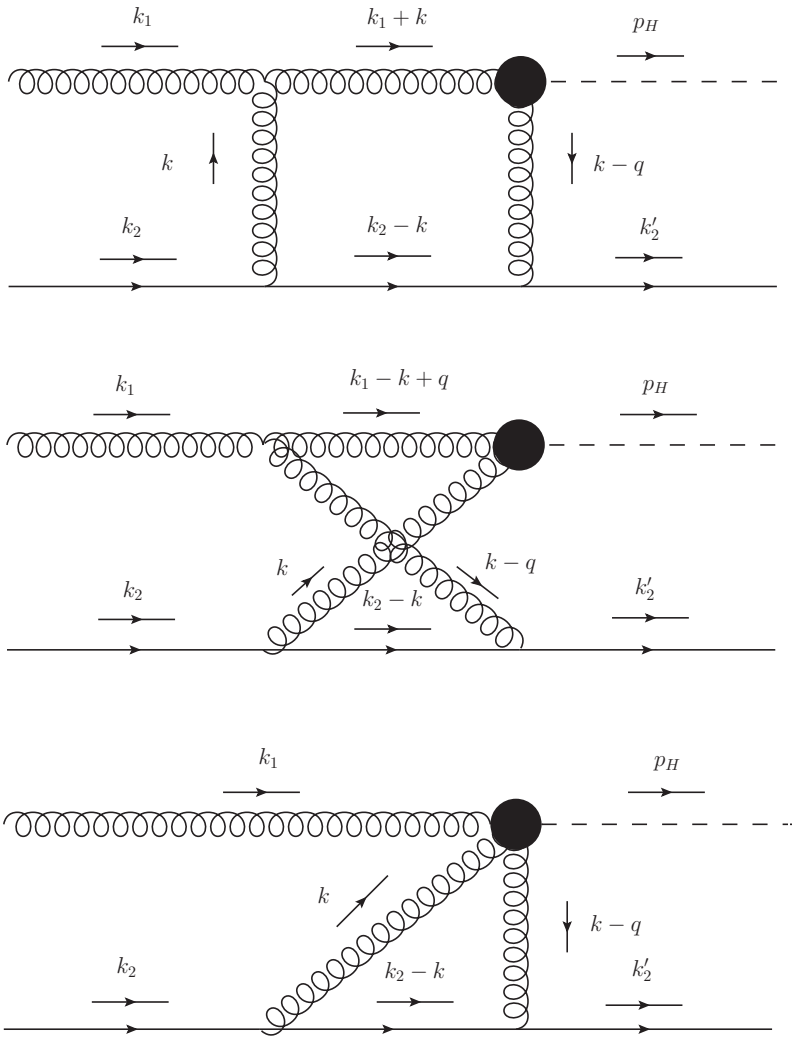

Figure 2.8: Feynman diagrams contributing to the $gR \to gH$ amplitude.

2.3.2 The 1-loop correction: 2-gluon exchange diagrams

As already mentioned, to extract this contribution we need to compute $\mathcal{A}^{(2g)(8,-)(1)}_{gq\to Hq}$ and use Eq. (2.38). There are three diagrams contributing to this amplitude (see Fig. 2.8). If all vertices involved in these diagrams were from QCD, one could use the Gribov trick (2.11) on both gluons in the t-channel and adopt the powerful technique explained in Refs. [66, 63] to simplify the calculation. Instead, it is interesting to note that, the use of an effective Lagrangian containing an operator of dimension 5, requires a modification of the technique introduced in renormalizable theories for extracting the high-energy behaviour of amplitudes. In particular, for diagrams where a single gluon connects the two rapidity regions, the trick can be safely applied, while for diagrams with two gluons exchanged in the t-channel, the transverse part of the metric tensor should be kept in any gluon propagator directly connected to the effective vertex. For those propagators, one should use the modified Gribov prescription,

$$g^{\mu\nu} = g^{\mu\nu}_{\perp\perp} + 2\frac{k_1^\mu k_2^\nu + k_2^\mu k_1^\nu}{s} \quad \to \quad g^{\mu\nu}_{\perp\perp} + 2\frac{k_2^\mu k_1^\nu}{s} \,. \tag{2.50}$$

We begin by computing the first diagram; the second one can be obtained from the first by analytic continuation from the s-channel to the u-channel, namely

$$\mathcal{A}^{(2g)(8,-)(1)}_{gq\to Hq,\,2}(s) = -\mathcal{A}^{(2g)(8,-)(1)}_{gq\to Hq,\,1}(-s) \,. \tag{2.51}$$

The amplitude relative to the first diagram is

$$\mathcal{A}^{(2g)(8,-)(1)}_{gq\to Hq,\,1} = \epsilon_\mu(k_1) g^3 g_H f^{abc}(t^b t^c)_{ji} \int \frac{d^D k}{(2\pi)^D} \frac{A^{\mu\rho\nu}(-k, k+k_1) H_\nu^\sigma(-k-k_1, k-q)}{k^2 (k+k_1)^2 (k_2-k)^2 (k-q)^2}$$
$$\times g_{\sigma\xi} g_{\rho\gamma} \bar{u}(k_2-q)\gamma^\xi(\not{k}_2 - \not{k})\gamma^\gamma u(k_2) \,. \tag{2.52}$$

Observing that

$$f^{abc}(t^b t^c)_{ji} = \frac{1}{2} f^{abc}(t^b t^c - t^c t^b)_{ji} = \frac{i}{2} C_A t^a_{ji} = \frac{i}{2} C_A \delta^{ac} t^c_{ji}$$

and then using FeynCalc [64, 65], we obtain

$$\mathcal{A}^{(2g)(8,-)(1)}_{gq\to\{H\}q,\,1} + \mathcal{A}^{(2g)(8,-)(1)}_{gq\to Hq,\,2} = \Gamma^{ac(0)}_{Hg} \left[\frac{g^2 N}{(-4)} \left(\frac{2\vec{q}^{\,2}\left((5D-12)m_H^2 + (D-2)\vec{q}^{\,2}\right) B_0\left(m_H^2\right)}{(D-2)\left(m_H^2 + \vec{q}^{\,2}\right)^2} \right.\right.$$
$$\left.\left. + \frac{4\left((D-2)m_H^4 + (D-2)m_H^2\vec{q}^{\,2} + (2D-5)(\vec{q}^{\,2})^2\right) B_0(-\vec{q}^{\,2})}{(D-2)\left(m_H^2 + \vec{q}^{\,2}\right)^2} + 2sC_0\left(m_H^2, 0, -s\right) \right.$$

$$-2sC_0\left(m_H^2,0,s\right)-\frac{4\left(m_H^4-m_H^2\vec{q}^{\,2}-\vec{q}^{\,2}\right)C_0\left(m_H^2,0,-\vec{q}^{\,2}\right)}{m_H^2+\vec{q}^{\,2}}+4\vec{q}^{\,2}C_0(0,0,-\vec{q}^{\,2})$$
$$-2sC_0(0,0,-s)+2sC_0(0,0,s)+2\vec{q}^{\,2}sD_0\left(m_H^2,0,0,0;-\vec{q}^{\,2},-s\right)$$
$$-2\vec{q}^{\,2}sD_0\left(m_H^2,0,0,0;-\vec{q}^{\,2},s\right)\Bigg)\Bigg]\frac{2s}{t}\Gamma_{qq}^{c(0)}\,. \tag{2.53}$$

The third diagram gives a much simpler contribution:

$$\mathcal{A}_{gq\to Hq,\,3}^{(2g)(8,-)(1)}=\Gamma_{\{H\}g}^{ac(0)}\left[Ng^2B_0(-\vec{q}^{\,2};0,0)\right]\frac{2s}{t}\Gamma_{qq}^{c(0)}\,. \tag{2.54}$$

At this point, using Eq. (2.38), we are able to extract the contribution to the gRH vertex from the exchange of two gluons in the t-channel:

$$\delta_{Hg}^{(2g)}=\frac{\mathcal{A}_{gq\to Hq,\,1}^{(2g)(8,-)(1)}+\mathcal{A}_{gq\to Hq,\,2}^{(2g)(8,-)(1)}+\mathcal{A}_{gq\to Hq,\,3}^{(2g)(8,-)(1)}}{\Gamma_{\{H\}g}^{ac(0)}\frac{2s}{t}\Gamma_{qq}^{c(0)}}-\delta_{qq}^{(2g)}-\frac{\omega^{(1)}(t)}{2}\left[\ln\left(\frac{s}{-t}\right)+\ln\left(\frac{-s}{-t}\right)\right]\,. \tag{2.55}$$

2.3.3 Full 1-loop correction to the impact factor

Adding $\delta_{Hg}^{(2g)}$ to $\delta_{1,V}^{(1g)}$, $\delta_{2,V}^{(1g)}$, $\delta_{3,V}^{(1g)}$, and $\delta_{4,V}^{(1g)}$ as defined in Eqs. (2.43), (2.46), (2.47), and (2.49), respectively, we obtain

$$\delta_{\rm NLO}\simeq\frac{\bar{\alpha}_s}{4\pi}\left(\frac{\vec{q}^{\,2}}{\mu^2}\right)^{-\epsilon}\left\{-\frac{C_A}{\epsilon^2}+\frac{11C_A-2n_f}{6\epsilon}-\frac{5n_f}{9}+C_A\left(2\mathrm{Li}_2\left(1+\frac{m_H^2}{\vec{q}^{\,2}}\right)+\frac{\pi^2}{3}+\frac{67}{18}\right)\right\}\,, \tag{2.56}$$

where we have kept only terms non-vanishing in the limit $\epsilon\to 0$ and have used

$$\bar{\alpha}_s=\frac{g^2\Gamma(1+\epsilon)\mu^{-2\epsilon}}{(4\pi)^{1-\epsilon}}\,,\quad C_A=N\,. \tag{2.57}$$

Substituting (2.56) into Eq. (2.33), we finally get the virtual correction to the Higgs impact factor:

$$\frac{d\Phi_{gg}^{\{H\}(1)}(z_H,\vec{p}_H,\vec{q};s_0)}{dz_Hd^2\vec{p}_H}=\frac{d\Phi_{gg}^{\{H\}(0)}(z_H,\vec{p}_H,\vec{q})}{dz_Hd^2\vec{p}_H}\,\frac{\bar{\alpha}_s}{2\pi}\left(\frac{\vec{q}^{\,2}}{\mu^2}\right)^{-\epsilon}\Bigg[-\frac{C_A}{\epsilon^2}$$
$$+\frac{11C_A-2n_f}{6\epsilon}-\frac{C_A}{\epsilon}\ln\left(\frac{\vec{q}^{\,2}}{s_0}\right)-\frac{5n_f}{9}+C_A\left(2\,\Re e\left(\mathrm{Li}_2\left(1+\frac{m_H^2}{\vec{q}^{\,2}}\right)\right)+\frac{\pi^2}{3}+\frac{67}{18}\right)+11\Bigg]\,. \tag{2.58}$$

where g_H has to be taken at leading order, while the last term equal to 11 takes into account its next-to-leading contribution (see Eq. (2.2)). The result in Eq. (2.58) can be

also obtained from Ref. [67], by taking the high-energy limit and using crossing symmetry. We used this alternative strategy as an independent check, finding perfect agreement.[26] The comparison with Ref. [61], whose virtual part contribution is based on Ref. [68], is not immediate, since their calculation is based on the Lipatov effective action and on a different definition of the impact factor. This implies, for instance, that in their purely virtual result, Eq. (43) of Ref. [61], the rapidity regulator is still present, which cancels when one combines the impact factor with their definition of the unintegrated gluon distribution[27].

2.4 Projection onto the eigenfunctions of the BFKL kernel

In this section we will carry out the projection of the Higgs impact factor onto the eigenfunctions of the LO BFKL kernel. There are two main reasons for performing this procedure.

First, being our impact factor differential in the Higgs kinematic variables, IR divergences do not appear in the real corrections and, therefore, it is not possible to observe their cancellation in the final result for the impact factor, as it would happen for a fully inclusive *hadronic* one (see Ref. [66]). The cancellation must of course be observed at the level of the cross section: the projection onto the LO BFKL eigenfunctions is an effective way to anticipate the integrations needed to get the cross section and, therefore, the projected impact factor, when all counterterms are taken into account, turns to be IR- and UV-finite. This procedure has been already successfully applied in Refs. [69, 70]. The second reason is more practical: moving from the momentum representation to the representation in terms of the LO BFKL kernel eigenfunctions makes the numeric implementation somewhat simpler.

To understand the idea behind the projection, it is enough to consider the *partonic*

[26] To perform the comparison, we first used crossing symmetry to obtain from Ref. [67] the NLO amplitude for the Higgs plus quark production in the collision of a gluon with a quark, then we took the high-energy limit of this amplitude and confronted with the BFKL-factorized form of the same amplitude, taking advantage of the known expression for the NLO quark-quark-Reggeon vertex.

[27] We recall that they considered the single-forward Higgs boson production.

amplitude in the LL,

$$\Im m_s\left((\mathcal{A}^{(0)})_{AB}^{AB}\right) = \frac{s}{(2\pi)^{D-2}}\int\frac{d^{D-2}q_1}{\vec{q}_1^{\,2}}\int\frac{d^{D-2}q_2}{\vec{q}_2^{\,2}}$$

$$\times\Phi_{AA}^{(0)}\left(\vec{q}_1;s_0\right)\int_{\delta-i\infty}^{\delta+i\infty}\frac{d\omega}{2\pi i}\left[\left(\frac{s}{s_0}\right)^{\omega}G_{\omega}^{(0)}\left(\vec{q}_1,\vec{q}_2\right)\right]\Phi_{BB}^{(0)}\left(-\vec{q}_2;s_0\right)\ ,$$

and the spectral representation for the BFKL Green's function (1.187),

$$G_{\omega}^{(0)}\left(\vec{q}_1,\vec{q}_2\right) = \sum_{n=-\infty}^{\infty}\int_{-\infty}^{+\infty}d\nu\frac{\phi_\nu^n(\vec{q}_1^{\,2})\phi_\nu^{n*}(\vec{q}_2^{\,2})}{\omega-\frac{\alpha_s C_A}{\pi}\chi(n,\nu)}\ . \tag{2.59}$$

If we use it, then, integrations over transverse momenta decouple and each impact factor can be separately projected onto the eigenfunctions of the BFKL kernel, so that

$$\int\frac{d^{2-2\epsilon}q}{\pi\sqrt{2}}(\vec{q}^{\,2})^{i\nu-\frac{3}{2}}e^{in\phi}\Phi_{AA}^{(0)}(\vec{q}\,) \equiv \Phi_{AA}^{(0)}(n,\nu)\ . \tag{2.60}$$

and similarly for the Φ_{BB}. The extension of the procedure to the NLL is straightforward (see the next chapter). Since we work in $D=4-2\epsilon$, we rely again on the "continuation" of the LO BFKL kernel eigenfunctions to non-integer dimensions,

$$(\vec{q}^{\,2})^{\gamma}e^{in\phi}\ \to(\vec{q}^{\,2})^{\gamma-\frac{n}{2}}(\vec{q}\cdot\vec{l})^n\ ,\qquad \gamma\equiv i\nu-\frac{1}{2}\ .$$

As already discussed in subsection 2.1.1, to get the Higgs impact factor for a proton-initiated process, we must take the convolution with the initial-state PDFs. This brings along initial-state collinear singularities, which must be canceled by suitable counterterms. In the rest of this section we will construct the (n,ν)-projection of all contributions to the hadronic Higgs impact factor, including the PDF counterterms, and will check the explicit cancellation of all IR divergences. The residual UV divergence will be taken care of by the renormalization of the QCD coupling. To perform the (n,ν)-projection, according to Eq. (2.60), we will make use of the integrals computed in Appendix A.3.

2.4.1 Projection of the LO impact factor

Recalling the expression of the LO impact factor,

$$\frac{d\Phi_{PP}^{\{H\}(0)}(x_H,\vec{p}_H,\vec{q})}{dx_H d^2\vec{p}_H} = \int_{x_H}^1\frac{dz_H}{z_H}f_g\left(\frac{x_H}{z_H}\right)\frac{d\Phi_{gg}^{\{H\}(0)}(z_H,\vec{p}_H,\vec{q})}{dz_H d^2\vec{p}_H} = \frac{g_H^2\vec{q}^{\,2}f_g(x_H)\delta^{(2)}(\vec{q}-\vec{p}_H)}{8(1-\epsilon)\sqrt{N^2-1}}\ , \tag{2.14}$$

we get immediately from Eq. (2.60) its projected counterpart,

$$\frac{d\Phi_{PP}^{\{H\}(0)}(x_H,\vec{p}_H,n,\nu)}{dx_H d^2\vec{p}_H} = \frac{g_H^2}{8(1-\epsilon)\sqrt{N^2-1}}\frac{(\vec{p}_H^{\,2})^{i\nu-\frac{1}{2}}e^{in\phi_H}}{\pi\sqrt{2}}f_g(x_H)\ . \tag{2.61}$$

Here ϕ_H is the azimuthal angle of the vector $\vec{p}_H$ counted from the fixed direction in the transverse space. The projected LO impact factor is the starting point for the calculation of the NLO contribution to the projected impact factor from the gluon PDF and QCD coupling counterterms. From now on, we will omit the apex $^{(1)}$, since all contributions to the projected impact factor are NLO.

2.4.2 Projection of gluon PDF and coupling counterterms

Taking into account the running of α_s,

$$\alpha_s(\mu^2) = \alpha_s(\mu_R^2)\left[1+\frac{\alpha_s(\mu_R^2)}{4\pi}\left(\frac{11C_A}{3}-\frac{2n_f}{3}\right)\left(-\frac{1}{\epsilon}-\ln(4\pi e^{-\gamma_E})+\ln\left(\frac{\mu_R^2}{\mu^2}\right)\right)\right]\ , \tag{2.62}$$

and the running of the gluon PDF,

$$f_g(x,\mu) = f_g(x,\mu_F) - \frac{\alpha_s(\mu_F)}{2\pi}\left(-\frac{1}{\epsilon}-\ln(4\pi e^{-\gamma_E})+\ln\left(\frac{\mu_F^2}{\mu^2}\right)\right)$$
$$\times\int_x^1\frac{dz}{z}\left[P_{gq}(z)\sum_{a=q\bar{q}}f_a\left(\frac{x}{z},\mu_F\right)+P_{gg}(z)f_g\left(\frac{x}{z},\mu_F\right)\right]\ , \tag{2.63}$$

where

$$P_{gq}(z) = C_F\frac{1+(1-z)^2}{z}\ , \tag{2.64}$$

$$P_{gg}(z) = 2C_A\left(\frac{z}{(1-z)_+}+\frac{(1-z)}{z}+z(1-z)\right)+\frac{11C_A-2n_f}{6}\delta(1-z)\ , \tag{2.65}$$

with plus prescription defined as

$$\int_a^1 dx\frac{F(x)}{(1-x)_+} = \int_a^1 dx\frac{F(x)-F(1)}{(1-x)} - \int_0^a dx\frac{F(1)}{1-x}\ , \tag{2.66}$$

we obtain the following projected counterterms,

$$\left.\frac{d\Phi_{PP}^{\{H\}}(x_H,\vec{p}_H,n,\nu)}{dx_H d^2\vec{p}_H}\right|_{\text{coupling c.t.}} = \frac{d\Phi_{PP}^{\{H\}(0)}(x_H,\vec{p}_H,n,\nu)}{dx_H d^2\vec{p}_H}\frac{\bar{\alpha}_s}{2\pi}\left(\frac{\vec{p}_H^{\,2}}{\mu^2}\right)^{-\epsilon}$$
$$\times\left(\frac{11C_A}{3}-\frac{2n_f}{3}\right)\left(-\frac{1}{\epsilon}+\ln\left(\frac{\mu_R^2}{\vec{p}_H^{\,2}}\right)\right)$$

$$\equiv \left.\frac{d\Phi^{\{H\}}_{PP,\mathrm{div}}(x_H,\vec{p}_H,n,\nu)}{dx_H d^2\vec{p}_H}\right|_{\text{coupling c.t.}} + \left.\frac{d\Phi^{\{H\}}_{PP,\mathrm{fin}}(x_H,\vec{p}_H,n,\nu)}{dx_H d^2\vec{p}_H}\right|_{\text{coupling c.t.}}, \tag{2.67}$$

$$\left.\frac{d\Phi^{\{H\}}_{PP}(x_H,\vec{p}_H,n,\nu)}{dx_H d^2\vec{p}_H}\right|_{\text{P}_{\text{qg}}\text{ c.t.}} = -\frac{1}{f_g(x_H)}\frac{d\Phi^{\{H\}(0)}_{PP}(x_H,\vec{p}_H,n,\nu)}{dx_H d^2\vec{p}_H}\frac{\bar{\alpha}_s}{2\pi}\left(\frac{\vec{p}_H^{\,2}}{\mu^2}\right)^{-\epsilon}$$
$$\times\left(-\frac{1}{\epsilon}+\ln\left(\frac{\mu_F^2}{\vec{p}_H^{\,2}}\right)\right)\int_{x_H}^1\frac{dz_H}{z_H}\left[P_{gq}(z_H)\sum_{a=q\bar{q}}f_a\left(\frac{x_H}{z_H},\mu_F\right)\right]$$
$$\equiv \left.\frac{d\Phi^{\{H\}}_{PP,\mathrm{div}}(x_H,\vec{p}_H,n,\nu)}{dx_H d^2\vec{p}_H}\right|_{\text{P}_{\text{qg}}\text{ c.t.}} + \left.\frac{d\Phi^{\{H\}}_{PP,\mathrm{fin}}(x_H,\vec{p}_H,n,\nu)}{dx_H d^2\vec{p}_H}\right|_{\text{P}_{\text{qg}}\text{ c.t.}} \tag{2.68}$$

and

$$\left.\frac{d\Phi^{\{H\}}_{PP}(x_H,\vec{p}_H,n,\nu)}{dx_H d^2\vec{p}_H}\right|_{\text{P}_{\text{gg}}\text{ c.t.}} = -\frac{1}{f_g(x_H)}\frac{d\Phi^{\{H\}(0)}_{PP}(x_H,\vec{p}_H,n,\nu)}{dx_H d^2\vec{p}_H}\frac{\bar{\alpha}_s}{2\pi}\left(\frac{\vec{p}_H^{\,2}}{\mu^2}\right)^{-\epsilon}$$
$$\times\left(-\frac{1}{\epsilon}+\ln\left(\frac{\mu_F^2}{\vec{p}_H^{\,2}}\right)\right)\int_{x_H}^1\frac{dz_H}{z_H}\left[P_{gg}(z_H)f_g\left(\frac{x_H}{z_H},\mu_F\right)\right]$$
$$\equiv \left.\frac{d\Phi^{\{H\}}_{PP,\mathrm{div}}(x_H,\vec{p}_H,n,\nu)}{dx_H d^2\vec{p}_H}\right|_{\text{P}_{\text{gg}}\text{ c.t.}} + \left.\frac{d\Phi^{\{H\}}_{PP,\mathrm{fin}}(x_H,\vec{p}_H,n,\nu)}{dx_H d^2\vec{p}_H}\right|_{\text{P}_{\text{gg}}\text{ c.t.}}. \tag{2.69}$$

With obvious notation, we have implicitly defined divergent ("div") and finite ("fin") part of each contribution. We will keep adopting this notation in the following.

2.4.3 Projection of high-rapidity real gluon contribution and BFKL counterterm

The contribution from a real gluon emission has a divergence for $z_H \to 1$ or $(z_g \to 0)$ at any value of the gluon momenta $\vec{q}-\vec{p}_H$. This divergence is regulated by the parameter s_Λ and, in the final result, cancelled by the BFKL counterterm appearing in the definition of the NLO impact factor. In this section we make the cancellation of s_Λ explicit and give the (n,ν)-projection of the high-rapidity part of the real gluon production impact factor combined with the BFKL counterterm.

First of all, let's take the convolution of the impact factor for real gluon production, given in (2.31), with the gluon PDF and rewrite it in an equivalent form, by adding and subtracting three terms, for later convenience:

$$\frac{d\Phi^{\{Hg\}}_{PP}(x_H,\vec{p}_H,\vec{q};s_0)}{dx_H d^2p_H} = \frac{d\tilde{\Phi}^{\{Hg\}}_{PP}(x_H,\vec{p}_H,n,\vec{q};s_0)}{dx_H d^2p_H}$$
$$+\frac{d\Phi^{\{Hg\}(1-x_H)}_{PP}(x_H,\vec{p}_H,\vec{q};s_0)}{dx_H d^2p_H} + \frac{d\Phi^{\{Hg\}\mathrm{plus}}_{PP}(x_H,\vec{p}_H,\vec{q};s_0)}{dx_H d^2p_H}$$

$$+\int_{x_H}^1 dz_H f_g(x_H)\frac{d\Phi_{gg}^{\{Hg\}}(z_H,\vec{p}_H,\vec{q};s_0)}{dz_H d^2\vec{p}_H}\bigg|_{z_H\to 1}, \tag{2.70}$$

where

$$\frac{d\tilde{\Phi}_{PP}^{\{Hg\}}(x_H,\vec{p}_H,\vec{q};s_0)}{dx_H d^2p_H}=\int_{x_H}^1\frac{dz_H}{z_H}f_g\left(\frac{x_H}{z_H}\right)\frac{d\Phi_{gg}^{\{Hg\}}(z_H,\vec{p}_H,\vec{q};s_0)}{dz_H d^2\vec{p}_H}$$
$$-\int_{x_H}^1 dz_H f_g\left(\frac{x_H}{z_H}\right)\left[\frac{d\Phi_{gg}^{\{Hg\}}(z_H,\vec{p}_H,\vec{q};s_0)}{dz_H d^2\vec{p}_H}\right]_{z_H=1}, \tag{2.71}$$

$$\frac{d\Phi_{PP}^{\{Hg\}(1-x_H)}(x_H,\vec{p}_H,\vec{q};s_0)}{dx_H d^2p_H}=\int_0^{x_H} dz_H f_g(x_H)\frac{d\Phi_{gg}^{\{Hg\}}(z_H,\vec{p}_H,\vec{q};s_0)}{dz_H d^2\vec{p}_H}\bigg|_{z_H=1} \tag{2.72}$$

and

$$\frac{d\Phi_{PP}^{\{Hg\}\mathrm{plus}}(x_H,\vec{p}_H,\vec{q};s_0)}{dx_H d^2p_H}=-\int_0^{x_H} dz_H f_g(x_H)\frac{d\Phi_{gg}^{\{Hg\}}(z_H,\vec{p}_H,\vec{q};s_0)}{dz_H d^2\vec{p}_H}\bigg|_{z_H=1}$$
$$+\int_{x_H}^1 dz_H\left(f_g\left(\frac{x_H}{z_H}\right)-f_g(x_H)\right)\left[\frac{d\Phi_{gg}^{\{Hg\}}(z_H,\vec{p}_H,\vec{q};s_0)}{dz_H d^2\vec{p}_H}\right]_{z_H=1}. \tag{2.73}$$

The pieces $d\tilde{\Phi}$, $d\Phi^{\{Hg\}(1-x_H)}$, and $d\Phi^{\{Hg\}\mathrm{plus}}$ are free from the divergence for $z_H\to 1$ and therefore in their expressions the limit $s_\Lambda\to\infty$ can be safely taken, which means that $\theta(s_\Lambda-s_{PR})$ can be set to one. The projection of these terms will be considered in subsection 2.4.5. The last term in Eq. (2.70) can be easily calculated, since

$$\frac{d\Phi_{gg}^{\{Hg\}}(z_H,\vec{p}_H,\vec{q};s_0)}{dz_H d^2\vec{p}_H}\bigg|_{z_H\to 1}=\frac{\langle cc'|\hat{\mathcal{P}}|0\rangle}{2(1-\epsilon)(N^2-1)}$$
$$\times\left[\sum_{\{f\}}\int\frac{ds_{PR}d\rho_f}{2\pi}\Gamma^c_{P\{f\}}\left(\Gamma^c_{P\{f\}}\right)^*\theta\left(s_\Lambda-s_{PR}\right)\right]_{z_H\to 1}$$
$$=\frac{g^2g_H^2C_A}{4(1-\epsilon)\sqrt{N^2-1}(2\pi)^{D-1}}\frac{\vec{q}^{\,2}}{(\vec{q}-\vec{p}_H)^2}\frac{1}{(1-z_H)}\theta\left(s_\Lambda-\frac{(\vec{q}-\vec{p}_H)^2}{(1-z_H)}\right). \tag{2.74}$$

We get

$$\int_{x_H}^1 dz_H f_g(x_H)\frac{d\Phi_{gg}^{\{Hg\}}(z_H,\vec{p}_H,\vec{q};s_0)}{dz_H d^2\vec{p}_H}\bigg|_{z_H\to 1}$$
$$=\frac{g^2g_H^2C_A}{4(1-\epsilon)\sqrt{N^2-1}(2\pi)^{D-1}}\frac{\vec{q}^{\,2}}{(\vec{q}-\vec{p}_H)^2}\int_{x_H}^1 dz_H\frac{1}{(1-z_H)}f_g(x_H)\theta\left(s_\Lambda-\frac{(\vec{q}-\vec{p}_H)^2}{(1-z_H)}\right)$$
$$=\frac{g^2g_H^2C_A}{4(1-\epsilon)\sqrt{N^2-1}(2\pi)^{D-1}}\frac{\vec{q}^{\,2}}{(\vec{q}-\vec{p}_H)^2}f_g(x_H)\left[\ln(1-x_H)-\frac{1}{2}\ln\left(\frac{\left[(\vec{q}-\vec{p}_H)^2\right]^2}{s_\Lambda^2}\right)\right]. \tag{2.75}$$

Let's consider now the BFKL counterterm

$$\frac{d\Phi_{gg}^{\text{BFKL c.t.}}(z_H,\vec{p}_H,\vec{q};s_0)}{dz_H d^2p_H} = -\frac{1}{2}\int d^{D-2}q' \frac{\vec{q}^{\,2}}{\vec{q}^{\,\prime 2}} \frac{d\Phi_{gg}^{\{H\}(0)}(\vec{q}^{\,\prime})}{dz_H d^2p_H} \mathcal{K}_r^{(0)}(\vec{q}^{\,\prime},\vec{q}\,) \ln\left(\frac{s_\Lambda^2}{(\vec{q}^{\,\prime}-\vec{q}\,)^2 s_0}\right) . \tag{2.76}$$

Using Eq. (2.13) and Eq. (1.164), we find

$$\frac{d\Phi_{gg}^{\text{BFKL c.t.}}(z_H,\vec{p}_H,\vec{q};s_0)}{dz_H d^2p_H} = \frac{-g^2 g_H^2 C_A}{8(2\pi)^{D-1}(1-\epsilon)\sqrt{N^2-1}} \frac{\vec{q}^{\,2}}{(\vec{q}-\vec{p}_H)^2} \ln\left(\frac{s_\Lambda^2}{(\vec{q}-\vec{p}_H)^2 s_0}\right) \delta(1-z_H) \tag{2.77}$$

and, after convolution with the gluon PDF, we get

$$\begin{aligned}\frac{d\Phi_{PP}^{\text{BFKL c.t.}}(x_H,\vec{p}_H,\vec{q};s_0)}{dx_H d^2p_H} &= \int_{x_H}^1 \frac{dz_H}{z_H} f_g\left(\frac{x_H}{z_H}\right) \frac{d\Phi_{gg}^{\text{BFKL c.t.}}(z_H,\vec{p}_H,\vec{q})}{dz_H d^2\vec{p}_H} \\ &= -\frac{g^2 g_H^2 C_A}{8(2\pi)^{D-1}\sqrt{N^2-1}} \frac{\vec{q}^{\,2}}{(\vec{q}-\vec{p}_H)^2} \frac{f_g(x_H)}{(1-\epsilon)} \ln\left(\frac{s_\Lambda^2}{(\vec{q}-\vec{p}_H)^2 s_0}\right) . \end{aligned} \tag{2.78}$$

When we combine the last term of Eq. (2.70), given in (2.75), with the BFKL counterterm, given in (2.78), we obtain

$$\frac{d\Phi_{PP}^{\text{BFKL}}(x_H,\vec{p}_H,\vec{q};s_0)}{dx_H d^2p_H} \equiv \frac{g^2 g_H^2 C_A}{4(2\pi)^{D-1}(1-\epsilon)\sqrt{N^2-1}} \frac{\vec{q}^{\,2}}{(\vec{q}-\vec{p}_H)^2} f_g(x_H) \ln\left(\frac{(1-x_H)\sqrt{s_0}}{|\vec{q}-\vec{p}_H|}\right) . \tag{2.79}$$

Note that this term is finite as far as the high-energy divergence is concerned. The remaining divergences can be isolated after the projection,

$$\begin{aligned}\frac{d\Phi_{PP}^{\text{BFKL}}(x_H,\vec{p}_H,n,\nu;s_0)}{dx_H d^2p_H} &= \frac{d\Phi_{PP}^{\{H\}(0)}(x_H,\vec{p}_H,n,\nu)}{dx_H d^2\vec{p}_H} \frac{\bar{\alpha}_s}{2\pi} \left(\frac{\vec{p}_H^{\,2}}{\mu^2}\right)^{-\epsilon} \left\{ \frac{C_A}{\epsilon^2} + \frac{C_A}{\epsilon} \ln\left(\frac{\vec{p}_H^{\,2}}{s_0}\right) \right. \\ &-2\frac{C_A}{\epsilon}\ln(1-x_H) + C_A \left[\ln\left(\frac{\vec{p}_H^{\,2}}{s_0(1-x_H)^2}\right) \left(2\gamma_E + \psi\left(\frac{1}{2}+\frac{n}{2}-i\nu\right)\right.\right. \\ &\left.\left. +\psi\left(\frac{1}{2}+\frac{n}{2}+i\nu\right)\right) - 2\gamma_E^2 - \zeta(2) - \frac{1}{2}\left(\psi'\left(\frac{1}{2}+\frac{n}{2}-i\nu\right) - \psi'\left(\frac{1}{2}+\frac{n}{2}+i\nu\right)\right) \right. \\ &-2\gamma_E\left(\psi\left(\frac{1}{2}+\frac{n}{2}-i\nu\right)+\psi\left(\frac{1}{2}+\frac{n}{2}+i\nu\right)\right) \\ &\left.\left. -\frac{1}{2}\left(\psi\left(\frac{1}{2}+\frac{n}{2}-i\nu\right)+\psi\left(\frac{1}{2}+\frac{n}{2}+i\nu\right)\right)^2 \right] \right\} \\ &\equiv \frac{d\Phi_{PP,\text{div}}^{\text{BFKL}}(x_H,\vec{p}_H,n,\nu;s_0)}{dx_H d^2p_H} + \frac{d\Phi_{PP,\text{fin}}^{\text{BFKL}}(x_H,\vec{p}_H,n,\nu;s_0)}{dx_H d^2p_H} . \end{aligned} \tag{2.80}$$

2.4.4 Projection of virtual and real quark contributions

Since the virtual contribution is proportional to the LO impact factor, the convolution with the gluon PDF and the (n,ν)-projection are trivial and give

$$\frac{d\Phi_{PP}^{\{H\}(1)}(x_H,\vec{p}_H,n,\nu;s_0)}{dx_H d^2\vec{p}_H} = \frac{d\Phi_{PP}^{\{H\}(0)}(x_H,\vec{p}_H,n,\nu)}{dx_H d^2\vec{p}_H}\,\frac{\bar{\alpha}_s}{2\pi}\left(\frac{\vec{p}_H^{\,2}}{\mu^2}\right)^{-\epsilon}\left[-\frac{C_A}{\epsilon^2}\right.$$

$$\left.+\frac{11C_A-2n_f}{6\epsilon}-\frac{C_A}{\epsilon}\ln\left(\frac{\vec{p}_H^{\,2}}{s_0}\right)-\frac{5n_f}{9}+C_A\left(2\,\Re e\left(\mathrm{Li}_2\left(1+\frac{m_H^2}{\vec{p}_H^{\,2}}\right)\right)+\frac{\pi^2}{3}+\frac{67}{18}\right)+11\right]$$

$$\equiv \frac{d\Phi_{PP,\mathrm{div}}^{\{H\}(1)}(x_H,\vec{p}_H,n,\nu;s_0)}{dx_H d^2\vec{p}_H}+\frac{d\Phi_{PP,\mathrm{fin}}^{\{H\}(1)}(x_H,\vec{p}_H,n,\nu)}{dx_H d^2\vec{p}_H}\,. \tag{2.81}$$

We recall that the real quark contribution is

$$\frac{d\Phi_{qq}^{\{Hq\}}(z_H,\vec{p}_H,\vec{q})}{dz_H d^2\vec{p}_H} = \frac{\sqrt{N^2-1}}{16N(2\pi)^{D-1}}\frac{g^2 g_H^2}{[(\vec{q}-\vec{p}_H)^2]^2}$$

$$\times\left[\frac{4(1-z_H)\left[(\vec{q}-\vec{p}_H)\cdot\vec{q}\,\right]^2+z_H^2\vec{q}^{\,2}(\vec{q}-\vec{p}_H)^2}{z_H}\right]\,. \tag{2.22}$$

Using

$$(\vec{q}-\vec{p}_H)\cdot\vec{q}=\frac{1}{2}\left[\vec{q}^{\,2}+(\vec{q}-\vec{p}_H)^2-\vec{p}_H^{\,2}\right]\,,$$

this contribution can be projected using the integral $I_1(\gamma_1,\gamma_2,n,\nu)$, defined in (A.31), and suitably choosing γ_1 and γ_2 for the different terms. The projected quark contribution gives

$$\frac{d\Phi_{qq}^{\{Hq\}}(z_H,\vec{p}_H,n,\nu)}{dz_H d^2\vec{p}_H} = \frac{\sqrt{N^2-1}}{16N(2\pi)^{D-1}}g^2 g_H^2\left\{\left(z_H+2\,\frac{1-z_H}{z_H}\right)I_1(-1,1,n,\nu)\right.$$

$$+\frac{1-z_H}{z_H}\left[(\vec{p}_H^{\,2})^2 I_1(0,2,n,\nu)\right.$$

$$\left.\left.-2\vec{p}_H^{\,2}\Big(I_1(0,1,n,\nu)+I_1(-1,2,n,\nu)\Big)+I_1(-2,2,n,\nu)\right]\right\}\,.$$

If we replace $I_1(\gamma_1,\gamma_2,n,\nu)$ by its explicit expression (A.31), perform a partial ϵ-expansion and take the convolution with the quark PDFs, we obtain

$$\frac{d\Phi_{PP}^{\{Hq\}}(x_H,\vec{p}_H,n,\nu)}{dx_H d^2\vec{p}_H} = \frac{1}{f_g(x_H)}\frac{d\Phi_{PP}^{\{H\}(0)}(x_H,\vec{p}_H,n,\nu)}{dx_H d^2 p_H}\frac{\bar{\alpha}_s}{2\pi}\left(\frac{\vec{p}_H^{\,2}}{\mu^2}\right)^{-\epsilon}$$

$$\times\int_{x_H}^1\frac{dz_H}{z_H}\sum_{a=q\bar{q}}f_a\left(\frac{x_H}{z_H},\mu_F\right)\left\{-\frac{1}{\epsilon}C_F\left(\frac{1+(1-z_H)^2}{z_H}\right)+(1-\gamma_E)C_F\left(\frac{1+(1-z_H)^2}{z_H}\right)\right.$$

$$+\frac{C_F}{z_H}\Bigg[4(z_H-1)-\frac{(1+n)(z_H-1)}{(\frac{1}{2}+\frac{n}{2}-i\nu)}-\frac{(1+(1-z_H)^2)}{(-\frac{3}{2}+\frac{n}{2}+i\nu)}-\frac{3+n(z_H-1)+z_H(z_H-3)}{(-\frac{1}{2}+\frac{n}{2}+i\nu)}$$

$$-(1+(1-z_H)^2)\left(H_{-1/2+n/2-i\nu}+\psi(-\frac{3}{2}+\frac{n}{2}+i\nu)\right)\Bigg]\Bigg\}$$

$$\equiv\frac{d\Phi^{\{Hq\}}_{PP,\rm div}(x_H,\vec{p}_H,n,\nu)}{dx_H d^2\vec{p}_H}+\frac{d\Phi^{\{Hq\}}_{PP,\rm fin}(x_H,\vec{p}_H,n,\nu)}{dx_H d^2\vec{p}_H}\,. \tag{2.82}$$

We observe that the ϵ-singularity is cancelled when we combine this object with the counterterm containing $P_{gq}(z_H)$, which appears in (2.68). We emphasize that the limits $n\to 1$ or $n\to 3$, $\nu\to 0$ are safe from divergences.

2.4.5 Projection of the real gluon contribution

In this subsection we discuss the projection of all terms appearing in (2.70), but the last, which was already treated in subsection 2.4.3.

We start with the terms labeled "plus", which, after (n,ν)-projection, gives

$$\frac{d\Phi^{\{Hg\}\rm plus}_{PP}(x_H,\vec{p}_H,n,\nu;s_0)}{dx_H d^2\vec{p}_H}=-\frac{1}{f_g(x_H)}\frac{d\Phi^{\{H\}(0)}_{PP}(x_H,\vec{p}_H,n,\nu)}{dx_H d^2\vec{p}_H}\frac{\bar{\alpha}_s}{2\pi}\left(\frac{\vec{p}_H^{\,2}}{\mu^2}\right)^{-\epsilon}$$

$$\times\int_{x_H}^1\frac{dz_H}{z_H}f_g\left(\frac{x_H}{z_H}\right)2C_A\frac{z_H}{(1-z_H)_+}\left[\frac{1}{\epsilon}+\left(H_{-1/2+n/2-i\nu}+H_{-1/2+n/2+i\nu}\right)\right]$$

$$\equiv\frac{d\Phi^{\{Hg\}\rm plus}_{PP,\rm div}(x_H,\vec{p}_H,n,\nu)}{dx_H d^2\vec{p}_H}+\frac{d\Phi^{\{Hg\}\rm plus}_{PP,\rm fin}(x_H,\vec{p}_H,n,\nu)}{dx_H d^2\vec{p}_H}\,. \tag{2.83}$$

The divergence in this term is cancelled by the term containing the plus prescription in $P_{gg}(z_H)$, which appears in (2.69).

Then, we project the term labeled "$(1-x_H)$" and find

$$\frac{d\Phi^{\{Hg\}(1-x_H)}_{PP}(x_H,\vec{p}_H,n,\nu)}{dx_H d^2\vec{p}_H}=\frac{d\Phi^{\{H\}(0)}_{PP}(x_H,\vec{p}_H,n,\nu)}{dx_H d^2\vec{p}_H}\frac{\bar{\alpha}_s}{2\pi}\left(\frac{\vec{p}_H^{\,2}}{\mu^2}\right)^{-\epsilon}$$

$$\times 2C_A\ln(1-x_H)\left[\frac{1}{\epsilon}+\left(H_{-1/2+n/2-i\nu}+H_{-1/2+n/2+i\nu}\right)\right]$$

$$\equiv\frac{d\Phi^{\{Hg\}(1-x_H)}_{PP,\rm div}(x_H,\vec{p}_H,n,\nu)}{dx_H d^2\vec{p}_H}+\frac{d\Phi^{\{Hg\}(1-x_H)}_{PP,\rm fin}(x_H,\vec{p}_H,n,\nu)}{dx_H d^2\vec{p}_H}\,. \tag{2.84}$$

The divergence cancels with an analogous term present in $d\Phi^{\rm BFKL}_{PP}$, given in (2.80).

We are left with the first term in Eq. (2.70), *i.e.*

$$\frac{d\tilde{\Phi}_{PP}^{\{Hg\}}(x_H,\vec{p}_H,\vec{q};s_0)}{dx_H d^2p_H} \tag{2.85}$$

$$= \int_{x_H}^1 \frac{dz_H}{z_H} f_g\left(\frac{x_H}{z_H}\right)\left[\frac{d\Phi_{gg}^{\{Hg\}}(z_H,\vec{p}_H,\vec{q})}{dz_H d^2\vec{p}_H} - z_H \frac{d\Phi_{gg}^{\{Hg\}}(z_H,\vec{p}_H,\vec{q})}{dz_H d^2\vec{p}_H}\bigg|_{z_H=1}\right].$$

The effect of this subtraction is to remove the first term of the last line in Eq. (2.31), which in fact represents the only true divergence for $z_H \to 1$, and we obtain

$$\frac{d\Phi_{gg}^{\{Hg\}}(z_H,\vec{p}_H,\vec{q})}{dz_H d^2\vec{p}_H} - z_H \frac{d\Phi_{gg}^{\{Hg\}}(z_H,\vec{p}_H,\vec{q};s_0)}{dz_H d^2\vec{p}_H}\bigg|_{z_H=1} = \frac{g^2 g_H^2 C_A}{8(2\pi)^{D-1}(1-\epsilon)\sqrt{N^2-1}}$$

$$\times\left\{\frac{2}{z_H(1-z_H)}\left[2z_H^2 + \frac{(1-z_H)z_H m_H^2(\vec{q}\cdot\vec{r})[z_H^2-2(1-z_H)\epsilon] + 2z_H^3(\vec{p}_H\cdot\vec{r})(\vec{p}_H\cdot\vec{q})}{\vec{r}^{\,2}\left[(1-z_H)m_H^2+\vec{p}_H^{\,2}\right]}\right.\right.$$

$$-\frac{2z_H^2(1-z_H)m_H^2}{[(1-z_H)m_H^2+\vec{p}_H^{\,2}]} - \frac{(1-z_H)z_H m_H^2(\vec{q}\cdot\vec{r})[z_H^2-2(1-z_H)\epsilon] + 2z_H^3(\vec{\Delta}\cdot\vec{r})(\vec{\Delta}\cdot\vec{q})}{\vec{r}^{\,2}\left[(1-z_H)m_H^2+\vec{\Delta}^2\right]}$$

$$-\frac{2z_H^2(1-z_H)m_H^2}{\left[(1-z_H)m_H^2+\vec{\Delta}^2\right]} + \frac{(1-\epsilon)z_H^2(1-z_H)^2m_H^4}{2}\left(\frac{1}{[(1-z_H)m_H^2+\Delta^2]}\right.$$

$$\left.\left.+\frac{1}{[(1-z_H)m_H^2+\vec{p}_H^{\,2}]}\right)^2 - \frac{2z_H^2(\vec{p}_H\cdot\vec{\Delta})^2 - 2\epsilon(1-z_H)^2z_H^2m_H^4}{[(1-z_H)m_H^2+\vec{p}_H^{\,2}]\,[(1-z_H)m_H^2+\Delta^2]}\right]$$

$$\left.+\frac{2\vec{q}^{\,2}}{\vec{r}^{\,2}}\left[z_H(1-z_H) + 2(1-\epsilon)\frac{(1-z_H)}{z_H}\frac{(\vec{q}\cdot\vec{r})^2}{\vec{q}^{\,2}\vec{r}^{\,2}}\right]\right\}$$

$$\equiv \frac{d\Phi_{gg}^{\{Hg\}\mathrm{coll}}(z_H,\vec{p}_H,\vec{q})}{dz_H d^2\vec{p}_H} + \frac{d\Phi_{gg}^{\{Hg\}(1-z_H)}(z_H,\vec{p}_H,\vec{q})}{dz_H d^2\vec{p}_H} + \frac{d\Phi_{gg}^{\{Hg\}\mathrm{rest}}(z_H,\vec{p}_H,\vec{q})}{dz_H d^2\vec{p}_H}. \tag{2.86}$$

In the last equality, we split this term in three contributions: 1) $d\Phi_{gg}^{\{Hg\}\mathrm{coll}}$ contains the pure collinear divergence remained, 2) $d\Phi_{gg}^{\{Hg\}(1-z_H)}$ contains terms that taken alone are singular for $z_H \to 1$, but when combined are safe from divergences, 3) $d\Phi_{gg}^{\{Hg\}\mathrm{rest}}$ is the rest.

Collinear term

$$\frac{d\Phi_{gg}^{\{Hg\}\mathrm{coll}}(z_H,\vec{p}_H,\vec{q})}{dz_H d^2\vec{p}_H} = \frac{g^2 g_H^2 C_A}{8(2\pi)^{D-1}(1-\epsilon)\sqrt{N^2-1}}\frac{2\vec{q}^{\,2}}{\vec{r}^{\,2}}$$

$$\times\left[z_H(1-z_H) + 2(1-\epsilon)\frac{(1-z_H)}{z_H}\frac{(\vec{q}\cdot\vec{r})^2}{\vec{q}^{\,2}\vec{r}^{\,2}}\right]. \tag{2.87}$$

This term can be projected and taken in convolution with the gluon PDF in a way quite analogous to the quark case; we find

$$\begin{aligned}
\frac{d\Phi_{PP}^{\{Hg\}\text{coll}}(x_H,\vec{p}_H,n,\nu)}{dx_H d^2\vec{p}_H} &\equiv \frac{1}{f_g(x_H)}\frac{d\Phi_{PP}^{\{H\}(0)}(x_H,\vec{p}_H,n,\nu)}{dx_H d^2\vec{p}_H}\frac{\bar{\alpha}_s}{2\pi}\left(\frac{\vec{p}_H^{\,2}}{\mu^2}\right)^{-\epsilon}\int_{x_H}^1\frac{dz_H}{z_H}f_g\left(\frac{x_H}{z_H}\right)\\
&\times\left\{-\frac{1}{\epsilon}2\,C_A\left(z_H(1-z_H)+\frac{(1-z_H)}{z_H}\right)-2\gamma_E C_A\left(z_H(1-z_H)+\frac{(1-z_H)}{z_H}\right)\right.\\
&-\frac{2C_A(1-z_H)}{z_H}\left[1+\gamma_E+\gamma_E z_H^2-\frac{1+n}{2(\frac{1}{2}+\frac{n}{2}-i\nu)}+\frac{1+z_H^2}{(-\frac{3}{2}+\frac{n}{2}+i\nu)}+\frac{3-n+2z_H^2}{2(-\frac{1}{2}+\frac{n}{2}+i\nu)}\right.\\
&\left.\left.+(1+z_H^2)\left(\psi\left(\frac{1}{2}+\frac{n}{2}-i\nu\right)+\psi\left(-\frac{3}{2}+\frac{n}{2}+i\nu\right)\right)\right]\right\}\\
&\equiv \frac{d\Phi_{PP,\text{div}}^{\{Hg\}\text{coll}}(x_H,\vec{p}_H,n,\nu)}{dx_H d^2\vec{p}_H}+\frac{d\Phi_{PP,\text{fin}}^{\{Hg\}\text{coll}}(x_H,\vec{p}_H,n,\nu)}{dx_H d^2\vec{p}_H}\,.
\end{aligned}\tag{2.88}$$

We observe that the ϵ-singularity is cancelled by a terms contained in the counterterm with $P_{gg}(z_H)$, which is given in (2.69). As in the quark case, the above expression is safe from divergences in $n=1$ or $n=3$, $\nu=0$.

$(1-z_H)$-term

$$\begin{aligned}
\frac{d\Phi_{gg}^{\{Hg\}(1-z_H)}(z_H,\vec{p}_H,\vec{q})}{dz_H d^2\vec{p}_H} &= \frac{g^2 g_H^2 C_A}{4(2\pi)^{D-1}(1-\epsilon)\sqrt{N^2-1}}\frac{1}{z_H(1-z_H)}\left[2z_H^2\right.\\
&+\frac{2z_H^3(\vec{p}_H\cdot\vec{r})(\vec{p}_H\cdot\vec{q})}{\vec{r}^{\,2}\left[(1-z_H)m_H^2+\vec{p}_H^{\,2}\right]}-\frac{2z_H^3(\vec{\Delta}\cdot\vec{r})(\vec{\Delta}\cdot\vec{q})}{\vec{r}^{\,2}\left[(1-z_H)m_H^2+\vec{\Delta}^2\right]}\\
&\left.-\frac{2z_H^2(\vec{p}_H\cdot\vec{\Delta})^2}{\left[(1-z_H)m_H^2+\vec{p}_H^{\,2}\right]\left[(1-z_H)m_H^2+\Delta^2\right]}\right]\,.
\end{aligned}\tag{2.89}$$

Here, and in the rest of the calculation, we will use the following formula,

$$\vec{q}\cdot\vec{p}_H=(\vec{q}^{\,2})^{\frac{1}{2}}(\vec{p}_H^{\,2})^{\frac{1}{2}}\cos(\phi-\phi_H)=(\vec{q}^{\,2})^{\frac{1}{2}}(\vec{p}_H^{\,2})^{\frac{1}{2}}\left(\frac{e^{i(\phi-\phi_H)}+e^{-i(\phi-\phi_H)}}{2}\right)\,.\tag{2.90}$$

Let us first observe that the term in square bracket gives zero in the limit $z_H\to 1$, so that there is no singularity in this limit. Now, using (2.90), we perform the projection and convolution with the gluon PDF and obtain, up to vanishing terms in the $\epsilon\to 0$ limit

$$\frac{d\Phi_{PP}^{\{Hg\}(1-z_H)}(x_H,\vec{p}_H,n,\nu)}{dx_H d^2\vec{p}_H}=\frac{1}{f_g(x_H)}\frac{d\Phi_{PP}^{\{H\}(0)}(x_H,\vec{p}_H,n,\nu)}{dx_H d^2\vec{p}_H}\frac{2\sqrt{2}C_A}{(\vec{p}_H^{\,2})^{i\nu-\frac{1}{2}}e^{in\phi_H}}\frac{\alpha_s}{2\pi}$$

$$\times\int_{x_H}^1\frac{dz_H}{z_H}f_g\left(\frac{x_H}{z_H}\right)\frac{1}{z_H(1-z_H)}\left\{\frac{2z_H^3}{[(1-z_H)m_H^2+\vec{p}_H^{\,2}]}\left[\frac{\vec{p}_H^{\,2}}{4}\left(e^{-2i\phi_H}I_1(-1,1,n+2,\nu)\right.\right.\right.$$
$$\left.+e^{2i\phi_H}I_1(-1,1,n-2,\nu)+2I_1(-1,1,n,\nu)\right)-\frac{(\vec{p}_H^{\,2})^{\frac{3}{2}}}{2}\left(e^{-i\phi_H}I_1\left(-\frac{1}{2},1,n+1,\nu\right)\right.$$
$$\left.\left.\left.+e^{i\phi_H}I_1\left(-\frac{1}{2},1,n-1,\nu\right)\right)\right]-\frac{2z_H^2}{[(1-z_H)m_H^2+\vec{p}_H^{\,2}]}\left[(\vec{p}_H^{\,2})^2I_3(0,1,n,\nu)\right.$$
$$+\frac{z_H^2\vec{p}_H^{\,2}}{4}\left(e^{-2i\phi_H}I_3(-1,1,n+2,\nu)+e^{2i\phi_H}I_3(-1,1,n-2,\nu)+2I_3(-1,1,n,\nu)\right)$$
$$\left.-z_H(\vec{p}_H^{\,2})^{\frac{3}{2}}\left(e^{-i\phi_H}I_3\left(-\frac{1}{2},1,n+1,\nu\right)+e^{i\phi_H}I_3\left(-\frac{1}{2},1,n-1,\nu\right)\right)\right]$$
$$-2z_H^3\left[\frac{(\vec{p}_H^{\,2})^{\frac{1}{2}}}{2}\left(e^{-i\phi_H}I_3\left(-\frac{1}{2},1,n+1,\nu\right)+e^{i\phi_H}I_3\left(-\frac{1}{2},1,n-1,\nu\right)\right)-z_HI_3(-1,1,n,\nu)\right]$$
$$-2z_H^3(1-z_H)\left[\frac{(\vec{p}_H^{\,2})^{\frac{1}{2}}}{2}(1+z_H)\left(e^{-i\phi_H}I_2\left(-\frac{3}{2},n+1,\nu\right)+e^{i\phi_H}I_2\left(-\frac{3}{2},n-1,\nu\right)\right)-z_H\right.$$
$$\left.\left.\times I_2(-2,n,\nu)-\frac{\vec{p}_H^{\,2}}{4}\left(e^{-2i\phi_H}I_2(-1,n+2,\nu)+e^{2i\phi_H}I_2(-1,n-2,\nu)+2I_2(-1,n,\nu)\right)\right]\right\}\,.$$

Setting $\epsilon=0$ and using the limits (A.17), (A.18), it is easy to show that the result is safe from $z_H\to 1$ divergences. In this result, there are combinations of integrals, which are safe from ϵ-divergences, even if single integrals, taken alone, are divergent. In particular, we note that if we use Eq. (A.31) for the integrals of the type I_1, the first five terms vanish up to $\mathcal{O}(\epsilon)$. Moreover, if we apply the replacement (A.30), we see that the "asymptotic" counterparts of the last six integrals cancel completely and therefore any I_2 integral in the previous expression can be replaced by $I_{2,\mathrm{reg}}$. The final form for this contribution is

$$\frac{d\Phi_{PP}^{\{Hg\}(1-z_H)}(x_H,\vec{p}_H,n,\nu)}{dx_Hd^2\vec{p}_H}=\frac{1}{f_g(x_H)}\frac{d\Phi_{PP}^{\{H\}}(x_H,\vec{p}_H,n,\nu)}{dx_Hd^2\vec{p}_H}\frac{2\sqrt{2}C_A}{(\vec{p}_H^{\,2})^{i\nu-\frac{1}{2}}e^{in\phi_H}}\frac{\alpha_s}{2\pi}$$
$$\times\int_{x_H}^1\frac{dz_H}{z_H}f_g\left(\frac{x_H}{z_H}\right)\frac{1}{z_H(1-z_H)}\left\{-\frac{2z_H^2}{[(1-z_H)m_H^2+\vec{p}_H^{\,2}]}\left[(\vec{p}_H^{\,2})^2I_3(0,1,n,\nu)\right.\right.$$
$$+\frac{z_H^2\vec{p}_H^{\,2}}{4}\left(e^{-2i\phi_H}I_3(-1,1,n+2,\nu)+e^{2i\phi_H}I_3(-1,1,n-2,\nu)+2I_3(-1,1,n,\nu)\right)$$
$$\left.\left.-z_H(\vec{p}_H^{\,2})^{\frac{3}{2}}\left(e^{-i\phi_H}I_3\left(-\frac{1}{2},1,n+1,\nu\right)+e^{i\phi_H}I_3\left(-\frac{1}{2},1,n-1,\nu\right)\right)\right]\right.$$
$$\left.-2z_H^3\left[\frac{(\vec{p}_H^{\,2})^{\frac{1}{2}}}{2}\left(e^{-i\phi_H}I_3\left(-\frac{1}{2},1,n+1,\nu\right)+e^{i\phi_H}I_3\left(-\frac{1}{2},1,n-1,\nu\right)\right)-z_HI_3(-1,1,n,\nu)\right]\right.$$

$$-2z_H^3(1-z_H)\left[\frac{(\vec{p}_H^{\,2})^{\frac{1}{2}}}{2}(1+z_H)\left(e^{-i\phi_H}I_{2,\mathrm{reg}}\left(-\frac{3}{2},n+1,\nu\right)+e^{i\phi_H}I_{2,\mathrm{reg}}\left(-\frac{3}{2},n-1,\nu\right)\right)\right.$$
$$-z_H I_{2,\mathrm{reg}}(-2,\nu,n)-\frac{\vec{p}_H^{\,2}}{4}\left(e^{-2i\phi_H}I_{2,\mathrm{reg}}(-1,n+2,\nu)\right.$$
$$\left.\left.+e^{2i\phi_H}I_{2,\mathrm{reg}}(-1,n-2,\nu)+2I_{2,\mathrm{reg}}(-1,n,\nu)\right)\right]\Bigg\}. \tag{2.91}$$

Rest term

$$\frac{d\Phi_{gg}^{\{Hg\}\mathrm{rest}}(z_H,\vec{p}_H,\vec{q})}{dz_H d^2\vec{p}_H}\equiv\frac{g^2g_H^2C_A}{4(2\pi)^{D-1}(1-\epsilon)\sqrt{N^2-1}}\left\{\frac{m_H^2(\vec{q}\cdot\vec{r})[z_H^2-2(1-z_H)\epsilon]}{\vec{r}^{\,2}\left[(1-z_H)m_H^2+\vec{p}_H^{\,2}\right]}\right.$$
$$+\frac{(1-\epsilon)z_H(1-z_H)m_H^4}{2}\left(\frac{1}{[(1-z_H)m_H^2+\Delta^2]}+\frac{1}{[(1-z_H)m_H^2+\vec{p}_H^{\,2}]}\right)^2$$
$$+\frac{2\epsilon(1-z_H)z_Hm_H^4}{[(1-z_H)m_H^2+\vec{p}_H^{\,2}]\,[(1-z_H)m_H^2+\Delta^2]}-2z_Hm_H^2\left(\frac{1}{[(1-z_H)m_H^2+\vec{p}_H^{\,2}]}\right.$$
$$\left.\left.+\frac{1}{\left[(1-z_H)m_H^2+\vec{\Delta}^2\right]}\right)-\frac{m_H^2(\vec{q}\cdot\vec{r})[z_H^2-2(1-z_H)\epsilon]}{\vec{r}^{\,2}\left[(1-z_H)m_H^2+\vec{\Delta}^2\right]}\right\}. \tag{2.92}$$

We perform the projection and convolution with gluon PDF and, finally, we find, up to terms $\mathcal{O}(\epsilon)$,

$$\frac{d\Phi_{PP}^{\{Hg\}\mathrm{rest}}(x_H,\vec{p}_H,n,\nu)}{dx_Hd^2\vec{p}_H}=\frac{1}{f_g(x_H)}\frac{d\Phi_{PP}^{\{H\}(0)}(x_H,\vec{p}_H,n,\nu)}{dx_Hd^2\vec{p}_H}\frac{\sqrt{2}C_A}{(\vec{p}_H^{\,2})^{i\nu-\frac{1}{2}}e^{in\phi_H}}\frac{\alpha_s}{2\pi}\int_{x_H}^1\frac{dz_H}{z_H}f_g\left(\frac{x_H}{z_H}\right)$$
$$\times\left\{\frac{2m_H^2\left[z_H^2-2(1-z_H)\epsilon\right]}{[(1-z_H)m_H^2+\vec{p}_H^{\,2}]}\left[I_1(-1,1,n,\nu)-\frac{(\vec{p}_H^{\,2})^{\frac{1}{2}}}{2}\left(e^{-i\phi_H}I_1\left(-\frac{1}{2},1,n+1,\nu\right)\right.\right.\right.$$
$$\left.\left.\left.+e^{i\phi_H}I_1\left(-\frac{1}{2},1,n-1,\nu\right)\right)\right]-2m_H^2[z_H^2-2(1-z_H)\epsilon]\left[I_2\left(-1,n,\nu\right)\right.\right.$$
$$\left.\left.-\frac{(\vec{p}_H^{\,2})^{\frac{1}{2}}}{2}\left(e^{-i\phi_H}I_2\left(-\frac{1}{2},n+1,\nu\right)+e^{i\phi_H}I_2\left(-\frac{1}{2},n-1,\nu\right)\right)\right]-4z_Hm_H^2I_3(0,1,n,\nu)\right.$$
$$\left.+(1-\epsilon)z_H(1-z_H)m_H^4\left[I_3(0,2,n,\nu)+\left(2+\frac{4\epsilon}{1-\epsilon}\right)\frac{I_3(0,1,n,\nu)}{[(1-z_H)m_H^2+\vec{p}_H^{\,2}]}\right]\right.\Bigg\}.$$

Using the explicit result for the integral I_1 and applying the same ideas as befor, after the ϵ-expansion we end up with

$$\frac{d\Phi_{PP}^{\{Hg\}\mathrm{rest}}(x_H,\vec{p}_H,n,\nu)}{dx_Hd^2\vec{p}_H}=\frac{1}{f_g(x_H)}\frac{d\Phi_{PP}^{\{H\}(0)}(x_H,\vec{p}_H,n,\nu)}{dx_Hd^2\vec{p}_H}\frac{\sqrt{2}C_A}{(\vec{p}_H^{\,2})^{i\nu-\frac{1}{2}}e^{in\phi_H}}\frac{\alpha_s}{2\pi}\int_{x_H}^1\frac{dz_H}{z_H}f_g\left(\frac{x_H}{z_H}\right)$$

$$\times \Bigg\{ \frac{2m_H^2 z_H^2}{[(1-z_H)m_H^2+\vec{p}_H^{\,2}]} \left[\frac{(\vec{p}_H^{\,2})^{i\nu-\frac{1}{2}-\epsilon} e^{in\phi_H}}{2\sqrt{2}} \left(\frac{1}{\left(\frac{1}{2}+\frac{n}{2}-i\nu\right)} - \frac{1}{\left(-\frac{1}{2}+\frac{n}{2}+i\nu\right)} \right) \right]$$

$$-2m_H^2 z_H^2 \Bigg[I_{2,\mathrm{reg}}\left(-1,n,\nu\right)$$

$$-\frac{(\vec{p}_H^{\,2})^{\frac{1}{2}}}{2} \left(e^{-i\phi_H} I_{2,\mathrm{reg}}\left(-\frac{1}{2},n+1,\nu\right) + e^{i\phi_H} I_{2,\mathrm{reg}}\left(-\frac{1}{2},n-1,\nu\right) \right) \Bigg]$$

$$-4z_H m_H^2 I_3(0,1,n,\nu) + z_H(1-z_H)m_H^4 \left[I_3(0,2,n,\nu) + \frac{2I_3(0,1,n,\nu)}{[(1-z_H)m_H^2+\vec{p}_H^{\,2}]} \right]. \qquad (2.93)$$

2.4.6 Final result

In this subsection we present the final result. First of all, we observe that if we sum all the ϵ-divergent contributions in Eqs. (2.67)-(2.69), (2.80), (2.81), (2.82)-(2.84), (2.88), we get that they cancel completely. The finite parts in the same equations, together with the contributions in Eqs. (2.91), (2.93) represent the final result. Setting $\epsilon = 0$, we can cast the final result in the sum of three terms,

$$\frac{d\Phi_{PP}^{\{H\},\mathrm{NLO}}(x_H,\vec{p}_H,n,\nu)}{dx_H d^2\vec{p}_H} = \frac{d\Phi_{PP,1}^{\{H\},\mathrm{NLO}}(x_H,\vec{p}_H,n,\nu;s_0)}{dx_H d^2\vec{p}_H}$$

$$+\frac{d\Phi_{PP,2}^{\{H\},\mathrm{NLO}}(x_H,\vec{p}_H,n,\nu)}{dx_H d^2\vec{p}_H} + \frac{d\Phi_{PP,3}^{\{H\},\mathrm{NLO}}(x_H,\vec{p}_H,n,\nu)}{dx_H d^2\vec{p}_H}\,, \qquad (2.94)$$

where the first term is given by the sum of all contributions purely proportional to $f_g(x_H)$, *i.e.*

$$\frac{d\Phi_{PP,1}^{\{H\},\mathrm{NLO}}(x_H,\vec{p}_H,n,\nu;s_0)}{dx_H d^2\vec{p}_H} \equiv \frac{d\Phi_{PP,\mathrm{fin}}^{\mathrm{BFKL}}(x_H,\vec{p}_H,n,\nu;s_0)}{dx_H d^2 p_H}$$

$$+\frac{d\Phi_{PP,\mathrm{fin}}^{\{H\}}(x_H,\vec{p}_H,n,\nu)}{dx_H d^2\vec{p}_H}\bigg|_{\text{coupling c.t.}} + \frac{d\Phi_{PP,\mathrm{fin}}^{\{H\}(1)}(x_H,\vec{p}_H,n,\nu)}{dx_H d^2\vec{p}_H}\,; \qquad (2.95)$$

the second is the sum of all contributions that are taken in convolution with $\sum_a f_a(x_H/z_H)$, *i.e.*

$$\frac{d\Phi_{PP,2}^{\{H\},\mathrm{NLO}}(x_H,\vec{p}_H,n,\nu;s_0)}{dx_H d^2\vec{p}_H} \equiv \frac{d\Phi_{PP,\mathrm{fin}}^{\{H\}}(x_H,\vec{p}_H,n,\nu)}{dx_H d^2\vec{p}_H}\bigg|_{\mathrm{P_{qg}\ c.t.}} + \frac{d\Phi_{PP,\mathrm{fin}}^{\{Hq\}}(x_H,\vec{p}_H,n,\nu)}{dx_H d^2\vec{p}_H}\,;$$

the third is the sum of all contributions that are taken in convolution with $f_g(x_H/z_H)$, *i.e.*

$$\frac{d\Phi_{PP,3}^{\{H\},\mathrm{NLO}}(x_H,\vec{p}_H,n,\nu;s_0)}{dx_H d^2\vec{p}_H} \equiv \frac{d\Phi_{PP,\mathrm{fin}}^{\{H\}}(x_H,\vec{p}_H,n,\nu)}{dx_H d^2\vec{p}_H}\bigg|_{\mathrm{P_{gg}\ c.t.}} + \frac{d\Phi_{PP,\mathrm{fin}}^{\{Hg\}\mathrm{plus}}(x_H,\vec{p}_H,n,\nu)}{dx_H d^2\vec{p}_H}$$

$$+\frac{d\Phi_{PP,\mathrm{fin}}^{\{Hg\}(1-x_H)}(x_H,\vec{p}_H,n,\nu)}{dx_H d^2\vec{p}_H}+\frac{d\Phi_{PP,\mathrm{fin}}^{\{Hg\}\mathrm{coll}}(x_H,\vec{p}_H,n,\nu)}{dx_H d^2\vec{p}_H}$$
$$+\frac{d\Phi_{PP}^{\{Hg\}(1-z_H)}(x_H,\vec{p}_H,n,\nu)}{dx_H d^2\vec{p}_H}+\frac{d\Phi_{PP}^{\{Hg\}\mathrm{rest}}(x_H,\vec{p}_H,n,\nu)}{dx_H d^2\vec{p}_H}\,. \tag{2.96}$$

2.5 Summary and outlook

We calculated the full NLO correction to the impact factor for the production of a Higgs boson emitted by a proton in the forward rapidity region. Its analytic expression was obtained both in the momentum and in the Mellin representations. The latter is particularly relevant to clearly observe a complete cancellation of NLO singularities, and it is useful for future numeric studies. We relied on the large top-mass limit approximation, thus we employed the gluon-Higgs effective field theory. We have found that the Gribov trick (see Eq. (2.11)) cannot be applied to both the t-channel gluon legs connected to the effective gluon-Higgs vertex. This prevents the use of the technique outlined in Refs. [66, 63] to simplify calculations. Formal studies on the generalization of that procedure to non-QCD vertices are underway [71]. As a first step forward towards phenomenology, we plan to extend the analysis on high-energy resummed distributions for the inclusive Higgs-plus-jet hadroproduction done in Ref. [72]. Our forward-Higgs NLO impact factor is a key ingredient to conduct a precise matching between BFKL and fixed-order approach.

From a more formal perspective, there are different natural developments of this work. One is the calculation of the Higgs impact factor *via* gluon fusion in the central-rapidity region. At the LO level it takes the form of a doubly off-shell coefficient function [73], where the top-quark loop connects two incoming Reggeized gluons with the outgoing scalar-boson line. Moving to NLO, the computation of contribution due to real emissions is not complicated, while technical issues are expected to emerge from the extraction of the vertex at 1-loop accuracy, due to the presence of an additional scale in the off-shellness of the incoming Reggeon. Once calculated, this doubly off-shell impact factor will be employed in the description of the central inclusive Higgs production in a pure high-energy factorization scheme, given as a κ_T-convolution between two UGDs describing the incoming protons and the aforementioned g^*g^*H vertex. Another interesting development, that is under development is the inclusion of top-mass corrections in the forward case. Even in this case, real corrections are quite straightforward, while the biggest problems emerge from virtual corrections that require two-loop calculations.

Chapter 3

BFKL phenomenology

Fermi's inclination toward concrete questions verifiable by direct experiment was due, at least in part, to his desire to check the soundness of his work by Nature, the infallible judge.
Emilio Segrè [74]

In this chapter, we propose a number of new semi-hard reactions as testfield of BFKL dynamics. We focus on a class of partially inclusive processes featuring a forward-plus-backward two-particle final-state configuration. We investigate processes that can be studied at the LHC in proton-proton collisions, in particular, reactions involving, in the final state jets, Higgs bosons and identified heavy-flavored hadrons. This will require the use of a hybrid approach in which both collinear and BFKL ingredients are encoded, to which we will refer as *hybrid high-energy/collinear factorization*. In the previous chapter, we have already seen a specific example by considering the Higgs impact factor. In the case of jets, in addition to a PDF for the description of the initial state in the impact factor, it is necessary to consider a jet algorithm for the final state, while, in the case of production of identified hadrons, it is necessary to make a further convolution with a fragmentation function (FF). The impact factors of the forward jets were calculated in [75, 76, 77], while the impact factors of forward hadrons in [70]. For our analyses, we use the expressions present in [77, 70], where the jet algorithm used is the *small-cone* one [78, 79].

The chapter contains four sections. In the first section, we introduce the hybrid factorization and construct the generic cross section within the NLLA. In the second, we describe the processes under investigation. In particular, we give details about the framework in which we study heavy-flavor production, the so-called *variable-flavor number*

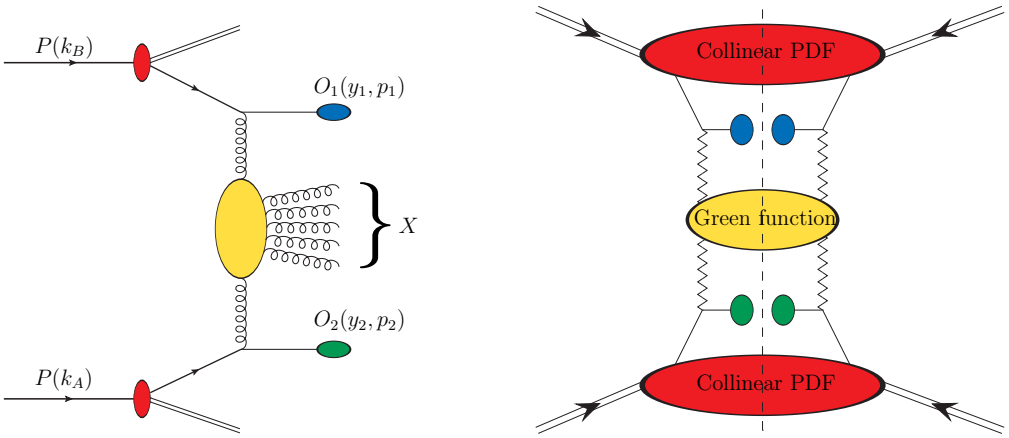

Figure 3.1: (a) Picture of the generic inclusive forward/backward reaction. (b) Schematic representation of the hybrid collinear/high-energy factorization.

scheme (VFNS). We also give details concerning the production of the Higgs in association with a jet or a charmed hadron. In the third section, we present numerical results, while in the fourth we summarize and discuss future perspectives. The material of this chapter is based on Refs. [72, 80, 81, 82, 83], where the numerical elaboration of all the considered observables is done by making use of the `JETHAD` modular work package [84, 85].

3.1 Theoretical framework

We want to study the high-energy behavior of interesting observables for the following type of semi-hard reactions:

$$P(k_A) + P(k_B) \longrightarrow O_1(y_1, p_1) + X + O_2(y_2, p_2) \; . \tag{3.1}$$

Here, two objects (O_1 and O_2) are emitted in proton-proton (P) collisions with large transverse momenta, $|\vec{p}_1|$ and $|\vec{p}_2|$, and wide separation in rapidity, $\Delta Y = y_1 - y_2$, together with the radiation of an undetected system, X. A schematic representation of the process is given in Fig. 3.1. The hybrid factorization that we use in this section was firstly introduced in the context of Mueller-Navelet jets [86] (two jets separated in rapidity) and then successfully extended and investigated at the next-to-leading order [75, 76, 77, 89, 90, 91, 92, 93, 94, 87, 88].

We begin by observing that the BFKL factorization allows us to construct cross sections as convolutions of two impact factors as defined in Eq. (1.161), and the Green's function for the scattering of two Reggeons. In the case of hadroproductions, this is sufficient to describe the parton collision only, but when we want to move on to the description of the whole physical process, we have to introduce some non-perturbative information on the distribution of partons inside protons[28]. This is done exactly the way it was shown in the chapter 2 for the Higgs impact factor. The hybrid factorization is schematically depicted in Fig. 3.1.

At this point, a clarification is in order. In literature, hybrid factorization can have slightly different meanings. For instance, recently a general hybrid k_T-factorization formula, in which one initial-state parton is light-like, and its associated PDF only depends on the longitudinal momentum fraction, while the other is space-like and its associated PDF also depends on k_T, has been established at NLO [95], using the auxiliary parton method. Through this chapter, although our impact factors are obtained considering the collisions of a parton extracted from a PDF (on-shell) and a Reggeon that comes from the BFKL Green's function (off-shell), we never introduce a k_T-dependent PDF. This latter object is necessary, for example, if we want to describe single-forward productions. The formalism on which we rely can be adapted to such a situation considering the convolution of a single forward impact factor with an unintegrated gluon distribution (UGD). In this case, however, leaving out the PDF in the impact factor, this would look more like a pure k_T-factorization, in which the impact factor and the unintegrated gluon distribution are linked only through the factorization in the transverse momentum.

Another important clarification concerns the use of the optical theorem. As we know, in the forward elastic case, the BFKL approach allows us to construct the imaginary part of the amplitude of an elastic process, $A + B \longrightarrow A + B$. Through the optical theorem, Eq. (1.157), we can immediately obtain the total cross section of the process $A + B \to X$. Since in this case we want to study partially inclusive processes of the type (3.1), we actually need to use one of the generalizations of the optical theorem[29] and adjust the imaginary amplitude constructed via the BFKL approach accordingly. For this

[28] In the case of identified hadrons in the final state, also the hadronization phase must be taken into account.

[29] The generalization we need is due to A. H. Mueller and it can be found in [27].

purpose, it is necessary to consider differential impact factors in which the kinematical variables of the tagged particles are left unintegrated and where the sum over all possible intermediate states in the s-channel cut is restricted to the final states compatible with the process (3.1).

3.1.1 Next-to-leading order BFKL cross section

In this subsection, we build the differential cross section of the generic process, (3.1), within the NLLA. We recall the representation introduced in Eq. (1.154), which allows us to represent the BFKL cross section as

$$\frac{d\hat{\sigma}_{AB}(z_1,\vec{p}_1,z_2,\vec{p}_2,s)}{dz_1 d^2\vec{p}_1 dz_2 d^2\vec{p}_2} = \frac{1}{(2\pi)^2}\int_{\delta-i\infty}^{\delta+i\infty}\frac{d\omega}{2\pi i}\left(\frac{\hat{s}}{s_0}\right)^{\omega}\langle\frac{d\Phi_{AA}}{\vec{q}_A^{\,2}}|\hat{G}_\omega|\frac{d\Phi_{BB}}{\vec{q}_B^{\,2}}\rangle\ , \tag{3.2}$$

where z_1, z_2 are the longitudinal Sudakov fractions with respect to the proton momenta k_A of the two detected particles. In this representation, the Green's function solving the BFKL equation is

$$\hat{G}_\omega = \left(\omega - \hat{K}\right)^{-1}. \tag{3.3}$$

The NLO kernel can be expanded in the strong coupling,

$$\hat{K} = \bar{\alpha}_s\hat{K}^0 + \bar{\alpha}_s^2\hat{K}^1, \tag{3.4}$$

where $\bar{\alpha}_s$ is defined as in Eq. (1.185), $\hat{K}^0$ is the BFKL kernel in the LLA and $\hat{K}^1$ represents the NLLA correction. To determine a cross section with next-to-leading accuracy we need an approximate solution of Eq. (3.3). With the required accuracy, this solution is

$$\hat{G}_\omega = \left(\omega-\bar{\alpha}_s\hat{K}^0\right)^{-1} + \left(\omega-\bar{\alpha}_s\hat{K}^0\right)^{-1}\left(\bar{\alpha}_s^2\hat{K}^1\right)\left(\omega-\bar{\alpha}_s\hat{K}^0\right)^{-1} + \mathcal{O}\left[\left(\bar{\alpha}_s^2\hat{K}^1\right)^2\right]\ . \tag{3.5}$$

In this representation the eigenfunctions of the LO BFKL kernel are denoted by the set of kets $\{|n,\nu\rangle\ :\ \nu\in\mathbb{R}\ ,\ n\in\mathbb{Z}\}$, defined by the relation

$$\langle\vec{q}\,|n,\nu\rangle = \frac{1}{\pi\sqrt{2}}\left(\vec{q}^{\,2}\right)^{i\nu-\frac{1}{2}}e^{in\theta}\ . \tag{3.6}$$

The action of the LLA kernel is

$$\hat{K}^0\,|n,\nu\rangle = \chi\,(n,\nu)\,|n,\nu\rangle\,, \tag{3.7}$$

where the function $\chi\,(n,\nu)$ is the Lipatov characteristic function defined in Eq. (1.186). For the basis introduced, the orthonormality conditions

$$\langle n',\nu'|n,\nu\rangle = \int\frac{d^2\vec{q}_A}{2\pi^2}\left(\vec{q}_A^{\,2}\right)^{i\nu-i\nu'-1}e^{i(n-n')\theta_A} = \delta\,(\nu-\nu')\,\delta_{nn'} \tag{3.8}$$

hold and the identity operator, with respect to this basis, can be written as

$$\hat{1} = \sum_{n=-\infty}^{\infty} \int_{-\infty}^{+\infty} d\nu \, |n,\nu\rangle \langle n,\nu| \, . \tag{3.9}$$

The action of the full NLA BFKL kernel on these functions may be expressed as follows:

$$\hat{K} \, |n,\nu\rangle = \bar{\alpha}_s \left(\mu_R\right) \chi \left(n,\nu\right) |n,\nu\rangle + \bar{\alpha}_s^2 \left(\mu_R\right) \left(\chi^{(1)} \left(n,\nu\right) + \frac{\beta_0}{4N_c} \chi \left(n,\nu\right) \ln\left(\mu_R^2\right) \right) |n,\nu\rangle$$

$$+ \bar{\alpha}_s^2 \left(\mu_R\right) \frac{\beta_0}{4N_c} \chi \left(n,\nu\right) \left(i \frac{\partial}{\partial \nu} \right) |n,\nu\rangle \, , \tag{3.10}$$

where μ_R is the renormalization scale of the QCD coupling, while

$$\beta_0 = \frac{11}{3} N_c - \frac{2}{3} n_f \tag{3.11}$$

is the first coefficient of the QCD β-function. The first term of Eq. (3.10) represents the action of LLA kernel, while the second term and the third ones stand for the diagonal and non-diagonal parts of the NLA kernel. For the calculation of $\chi^{(1)}\left(n,\nu\right)$ see [96, 97]. Here, only the final expression is presented:

$$\chi^{(1)}(n,\nu) = -\frac{\beta_0}{8N_c} \left(\chi^2(n,\nu) - \frac{10}{3} \chi(n,\nu) - i\chi'(n,\nu) \right) + \bar{\chi}(n,\nu), \tag{3.12}$$

where

$$\bar{\chi}(n,\nu) = -\frac{1}{4} \left[\frac{\pi^2-4}{3} \chi(n,\nu) - 6\zeta(3) - \chi''(n,\nu) + 2\phi(n,\nu) + 2\phi(n,-\nu) \right.$$

$$\left. + \frac{\pi^2 \sinh(\pi\nu)}{2\nu \cosh^2(\pi\nu)} \left(\left(3 + \left(1 + \frac{n_f}{N_c^3} \right) \frac{11+12\nu^2}{16(1+\nu^2)} \right) \delta_{n0} - \left(1 + \frac{n_f}{N_c^3} \right) \frac{1+4\nu^2}{32(1+\nu^2)} \delta_{n2} \right) \right] , \tag{3.13}$$

$$\phi(n,\nu) = -\int_0^1 dx \frac{x^{-1/2+i\nu+n/2}}{1+x} \left[\frac{1}{2} \left(\psi' \left(\frac{n+1}{2} \right) - \zeta(2) \right) + \mathrm{Li}_2(x) + \mathrm{Li}_2(-x) \right.$$

$$\left. + \ln x \left(\psi(n+1) - \psi(1) + \ln(1+x) + \sum_{k=1}^{\infty} \frac{(-x)^k}{k+n} \right) \sum_{k=1}^{\infty} \frac{x^k}{(k+n)^2} (1-(-1)^k) \right]$$

$$= \sum_{k=0}^{\infty} \frac{(-1)^{k+1}}{k+(n+1)/2+i\nu} \left[\psi'(k+n+1) - \psi'(k+1) + (-1)^{k+1} (\beta'(k+n+1) + \beta'(k+1)) \right.$$

$$\left. - \frac{1}{k+(n+1)/2+i\nu} (\psi(k+n+1) - \psi(k+1)) \right] , \tag{3.14}$$

and

$$\beta'(z) = \frac{1}{4} \left[\psi' \left(\frac{z+1}{2} \right) - \psi' \left(\frac{z}{2} \right) \right] , \quad \mathrm{Li}_2(x) = -\int_0^x dt \frac{\ln(1-t)}{t} \, . \tag{3.15}$$

Here $\chi'(n,\nu) = d\chi(n,\nu)/d\nu$ and $\chi''(n,\nu) = d^2\chi(n,\nu)/d\nu^2$.
Starting from the expression (3.2) for the differential cross section and inserting two identity operators in the form of Eq. (3.9), one obtains

$$\frac{d\hat{\sigma}_{AB}(z_1,\vec{p}_1,z_2,\vec{p}_2,s)}{dz_1 d^2\vec{p}_1 dz_2 d^2\vec{p}_2} = \frac{1}{(2\pi)^2}\sum_{n=-\infty}^{\infty}\int d\nu \sum_{n'=-\infty}^{\infty}\int d\nu'$$

$$\times \int_{\delta-i\infty}^{\delta+i\infty}\frac{d\omega}{2\pi i}\left(\frac{\hat{s}}{s_0}\right)^{\omega}\langle\frac{d\Phi_{AA}}{\vec{q}_A^{\,2}}|n,\nu\rangle\,\langle n,\nu|\hat{G}_\omega|n',\nu'\rangle\,\langle n',\nu'|\frac{d\Phi_{BB}}{\vec{q}_B^{\,2}}\rangle\,. \tag{3.16}$$

In Eq. (3.16), we have the projection of the impact factors onto the LO order BFKL eigenfunctions

$$\frac{d\Phi_{AA}\left(z_1,\vec{p}_1,n,\nu\right)}{dz_1 d^2\vec{p}_1} = \langle\frac{d\Phi_{AA}}{\vec{q}_A^{\,2}}|n,\nu\rangle = \int d^2\vec{q}_A\frac{1}{\vec{q}_A^{\,2}}\frac{d\Phi_{AA}\left(z_1,\vec{p}_1,\vec{q}_A\right)}{dz_1 d^2\vec{p}_1}\frac{1}{\pi\sqrt{2}}\left(\vec{q}_A^{\,2}\right)^{i\nu-\frac{1}{2}}e^{in\theta_A}, \tag{3.17}$$

$$\frac{d\Phi^*_{BB}(z_2,\vec{p}_2,n,\nu)}{dz_2 d^2\vec{p}_2} = \langle n',\nu'|\frac{d\Phi_{BB}}{\vec{q}_B^{\,2}}\rangle = \int d^2\vec{q}_B\frac{1}{\vec{q}_B^{\,2}}\frac{d\Phi_{BB}\left(z_2,\vec{p}_2,-\vec{q}_B\right)}{dz_2 d^2\vec{p}_2}\frac{1}{\pi\sqrt{2}}\left(\vec{q}_B^{\,2}\right)^{-i\nu'-\frac{1}{2}}e^{-in'\theta_B}\,, \tag{3.18}$$

and the matrix element of the BFKL Green's function, which is obtained by substituting the expansion for $\hat{G}_\omega$ (Eq. (3.5)) in the braket $\langle n,\nu|\hat{G}_\omega|n',\nu'\rangle$:

$$\langle n,\nu|\hat{G}_\omega|n',\nu'\rangle = \langle n,\nu|\left[\left(\omega-\bar{\alpha}_s\hat{K}^0\right)^{-1}+\left(\omega-\bar{\alpha}_s\hat{K}^0\right)^{-1}\left(\bar{\alpha}_s^2\hat{K}^1\right)\left(\omega-\bar{\alpha}_s\hat{K}^0\right)^{-1}\right]|n',\nu'\rangle\,. \tag{3.19}$$

Since one knows how the operators $\hat{K}_0$, $\hat{K}_1$ act on the states $|n,\nu\rangle$, this final expression can be easily calculated:

$$\langle n,\nu|\hat{G}_\omega|n',\nu'\rangle = \delta_{nn'}\left[\delta\left(\nu-\nu'\right)\left(\frac{1}{\omega-\bar{\alpha}_s\left(\mu_R\right)\chi\left(n,\nu\right)}\right.\right.$$

$$\left.+\frac{\bar{\alpha}_s^2(\mu_R)\left(\bar{\chi}\left(n,\nu\right)+\frac{\beta_0}{8N_c}\left(-\chi^2\left(n,\nu\right)+\frac{10}{3}\chi\left(n,\nu\right)+2\chi\left(n,\nu\right)\ln\mu_R^2+i\frac{\partial}{\partial\nu}\chi\left(n,\nu\right)\right)\right)}{\left(\omega-\bar{\alpha}_s\left(\mu_R\right)\chi\left(n,\nu\right)\right)^2}\right)$$

$$\left.+\frac{\frac{\beta_0}{4N_c}\bar{\alpha}_s^2\left(\mu_R\right)\chi\left(n,\nu'\right)}{\left(\omega-\bar{\alpha}_s\left(\mu_R\right)\chi\left(n,\nu\right)\right)\left(\omega-\bar{\alpha}_s\left(\mu_R\right)\chi\left(n,\nu'\right)\right)}\left(i\frac{d}{d\nu'}\delta\left(\nu-\nu'\right)\right)\right]. \tag{3.20}$$

The projected impact factors can be written as

$$\frac{d\Phi_{AA}\left(z_1,\vec{p}_1,n,\nu\right)}{dz_1 d^2\vec{p}_1} = \alpha_s\left(\mu_R\right)\left[\tilde{c}_1\left(z_1,\vec{p}_1,n,\nu\right)+\alpha_s(\mu_R)\tilde{c}_1^{(1)}\left(z_1,\vec{p}_1,n,\nu\right)\right]\,, \tag{3.21}$$

$$\frac{d\Phi^*_{BB}\left(z_2,\vec{p}_2,n',\nu'\right)}{dz_2 d^2\vec{p}_2} = \alpha_s\left(\mu_R\right)\left[\tilde{c}_2\left(z_2,\vec{p}_2,n',\nu'\right)+\alpha_s(\mu_R)\tilde{c}_2^{(1)}\left(z_1,\vec{p}_1,n',\nu'\right)\right]\,. \tag{3.22}$$

Inserting the expression for the matrix element, (3.20), together with the expressions for the impact factors projected onto the eigenfunctions of the kernel, (3.21, 3.22), in Eq. (3.16), one obtains

$$\frac{d\hat{\sigma}_{AB}(z_1,\vec{p}_1,z_2,\vec{p}_2,s)}{dz_1d^2\vec{p}_1dz_2d^2\vec{p}_2}=\frac{1}{(2\pi)^2}\sum_{n=-\infty}^{\infty}\int\frac{d\nu}{2\pi i}\int d\nu'\int_{\delta-i\infty}^{\delta+i\infty}d\omega\left(\frac{\hat{s}}{s_0}\right)^{\omega}\alpha_s^2(\mu_R)\tilde{c}_1(z_1,\vec{p}_1,n,\nu)\tilde{c}_2(z_2,\vec{p}_2,n',\nu')$$
$$\times\left[\delta\left(\nu-\nu'\right)\left(\frac{1}{\omega-\bar{\alpha}_s\left(\mu_R\right)\chi\left(n,\nu\right)}\left(1+\alpha_s(\mu_R)\left(\frac{\tilde{c}_1^{(1)}\left(z_1,\vec{p}_1,n,\nu\right)}{\tilde{c}_1\left(z_1,\vec{p}_1,n,\nu\right)}+\frac{\tilde{c}_2^{(1)}\left(z_1,\vec{p}_1,n',\nu'\right)}{\tilde{c}_2\left(z_1,\vec{p}_1,n',\nu'\right)}\right)\right)\right.\right.$$
$$\left.+\frac{\bar{\alpha}_s^2\left(\bar{\chi}\left(n,\nu\right)+\frac{\beta_0}{8N_c}\left(-\chi^2\left(n,\nu\right)+\frac{10}{3}\chi\left(n,\nu\right)+2\chi\left(n,\nu\right)\ln\mu_R^2+i\frac{\partial}{\partial\nu}\chi\left(n,\nu\right)\right)\right)}{\left(\omega-\bar{\alpha}_s\left(\mu_R\right)\chi\left(n,\nu\right)\right)^2}\right)$$
$$\left.+\frac{\frac{\beta_0}{4N_c}\bar{\alpha}_s^2\left(\mu_R\right)\chi\left(n,\nu'\right)}{\left(\omega-\bar{\alpha}_s\left(\mu_R\right)\chi\left(n,\nu\right)\right)\left(\omega-\bar{\alpha}_s\left(\mu_R\right)\chi\left(n,\nu'\right)\right)}\left(i\frac{d}{d\nu}\delta\left(\nu-\nu'\right)\right)\right]. \tag{3.23}$$

In Eq. (3.23) there are three terms. The first term is

$$\frac{1}{(2\pi)^2}\sum_{n=-\infty}^{\infty}\int d\nu\int_{\delta-i\infty}^{\delta+i\infty}\frac{d\omega}{2\pi i}\left(\frac{\hat{s}}{s_0}\right)^{\omega}\alpha_s^2(\mu_R)\tilde{c}_1(z_1,\vec{p}_1,n,\nu)\tilde{c}_2(z_2,\vec{p}_2,n,\nu)$$
$$\times\frac{1}{\omega-\bar{\alpha}_s\left(\mu_R\right)\chi\left(n,\nu\right)}\left(1+\alpha_s(\mu_R)\left(\frac{\tilde{c}_1^{(1)}\left(z_1,\vec{p}_1,n,\nu\right)}{\tilde{c}_1\left(z_1,\vec{p}_1,n,\nu\right)}+\frac{\tilde{c}_2^{(1)}\left(z_1,\vec{p}_1,n',\nu'\right)}{\tilde{c}_2\left(z_1,\vec{p}_1,n',\nu'\right)}\right)\right), \tag{3.24}$$

that, using the residue theorem, becomes

$$\frac{1}{(2\pi)^2}\sum_{n=-\infty}^{\infty}\int d\nu\;\alpha_s^2(\mu_R)\tilde{c}_1(z_1,\vec{p}_1,n,\nu)\tilde{c}_2(z_2,\vec{p}_2,n,\nu)\left(\frac{\hat{s}}{s_0}\right)^{\bar{\alpha}_s\chi(n,\nu)}$$
$$\times\left(1+\alpha_s(\mu_R)\left(\frac{\tilde{c}_1^{(1)}\left(z_1,\vec{p}_1,n,\nu\right)}{\tilde{c}_1\left(z_1,\vec{p}_1,n,\nu\right)}+\frac{\tilde{c}_2^{(1)}\left(z_1,\vec{p}_1,n',\nu'\right)}{\tilde{c}_2\left(z_1,\vec{p}_1,n',\nu'\right)}\right)\right), \tag{3.25}$$

The second term is

$$\frac{1}{(2\pi)^2}\sum_{n=-\infty}^{\infty}\int d\nu\int_{\delta-i\infty}^{\delta+i\infty}\frac{d\omega}{2\pi i}\left(\frac{\hat{s}}{s_0}\right)^{\omega}\alpha_s^2(\mu_R)\tilde{c}_1(z_1,\vec{p}_1,n,\nu)\tilde{c}_2(z_2,\vec{p}_2,n,\nu)$$
$$\times\frac{\bar{\alpha}_s^2\left[\bar{\chi}(n,\nu)+\frac{\beta_0}{8N_c}\left(-\chi(n,\nu)^2+\frac{10}{3}\chi(n,\nu)+2\chi(n,\nu)\ln\mu_R^2+i\chi'(n,\nu)\right)\right]}{\left(\omega-\bar{\alpha}_s\left(\mu_R\right)\chi\left(n,\nu\right)\right)^2}, \tag{3.26}$$

that, using the residue theorem, becomes

$$\frac{1}{(2\pi)^2}\sum_{n=-\infty}^{\infty}\int d\nu\;\alpha_s^2(\mu_R)\tilde{c}_1(z_1,\vec{p}_1,n,\nu)\tilde{c}_2(z_2,\vec{p}_2,n,\nu)\bar{\alpha}_s^2(\mu_R)\left(\frac{\hat{s}}{s_0}\right)^{\bar{\alpha}_s(\mu_R)\chi(n,\nu)}\ln\left(\frac{\hat{s}}{s_0}\right)$$
$$\times\left[\bar{\chi}(n,\nu)+\frac{\beta_0}{8N_c}\left(-\chi(n,\nu)^2+\frac{10}{3}\chi(n,\nu)+2\chi(n,\nu)\ln\mu_R^2+i\chi'(n,\nu)\right)\right]. \tag{3.27}$$

The third term is

$$\frac{1}{(2\pi)^2}\sum_{n=-\infty}^{\infty}\int d\nu\int d\nu'\int_{\delta-i\infty}^{\delta+i\infty}\frac{d\omega}{2\pi i}\left(\frac{\hat{s}}{s_0}\right)^{\omega}\alpha_s^2(\mu_R)\tilde{c}_1(z_1,\vec{p}_1,n,\nu)\tilde{c}_2(z_2,\vec{p}_2,n,\nu') \\ \times\frac{\beta_0}{4N_C}\bar{\alpha}_s^2(\mu_R)\frac{\chi(n,\nu')}{(\omega-\bar{\alpha}_s(\mu_R)\chi(n,\nu))(\omega-\bar{\alpha}_s(\mu_R)\chi(n,\nu'))}\left(i\frac{d}{d\nu'}\delta(\nu-\nu')\right). \tag{3.28}$$

Let us focus the attention only on the integration in ν and ν'. One can use the following symmetrization:

$$\int d\nu\int d\nu'\frac{\tilde{c}_1(z_1,\vec{p}_1,n,\nu)\tilde{c}_2(z_2,\vec{p}_2,n,\nu')\chi(n,\nu')}{(\omega-\bar{\alpha}_s(\mu_R)\chi(n,\nu))(\omega-\bar{\alpha}_s(\mu_R)\chi(n,\nu'))}i\frac{d}{d\nu'}\delta(\nu-\nu') \\ =\frac{1}{2}\int d\nu\int d\nu'\frac{\tilde{c}_1(z_1,\vec{p}_1,n,\nu)\tilde{c}_2(z_2,\vec{p}_2,n,\nu')\chi(n,\nu')}{(\omega-\bar{\alpha}_s(\mu_R)\chi(n,\nu))(\omega-\bar{\alpha}_s(\mu_R)\chi(n,\nu'))}i\frac{d}{d\nu'}\delta(\nu-\nu') \\ +\frac{\tilde{c}_1(z_1,\vec{p}_1,n,\nu')\tilde{c}_2(z_2,\vec{p}_2,n,\nu)\chi(n,\nu)}{(\omega-\bar{\alpha}_s(\mu_R)\chi(n,\nu'))(\omega-\bar{\alpha}_s(\mu_R)\chi(n,\nu))}i\frac{d}{d\nu}\delta(\nu'-\nu)\,, \tag{3.29}$$

and, thereafter, the following properties:

$$i\frac{d}{d\nu}\delta(\nu'-\nu)=-i\frac{d}{d\nu'}\delta(\nu'-\nu), \\ \int d\nu'\left(\frac{d}{d\nu'}\delta(\nu'-\nu)\right)f(\nu')=-f'(\nu')\big|_{\nu'=\nu}\,. \tag{3.30}$$

The resulting form for the term considered is

$$-\frac{i}{2}\int d\nu\left[\frac{\tilde{c}_1(z_1,\vec{p}_1,n,\nu)\tilde{c}_2'(z_2,\vec{p}_2,n,\nu)-\tilde{c}_1'(z_1,\vec{p}_1,n,\nu)\tilde{c}_2(z_2,\vec{p}_2,n,\nu)}{(\omega-\bar{\alpha}_s(\mu_R)\chi(n,\nu))^2}\chi(n,\nu)\right. \\ \left.+\frac{\tilde{c}_1(z_1,\vec{p}_1,n,\nu)\tilde{c}_2(z_2,\vec{p}_2,n,\nu)}{(\omega-\bar{\alpha}_s(\mu_R)\chi(n,\nu))^2}\chi'(n,\nu)\right], \tag{3.31}$$

that, using

$$\tilde{c}_1'(z_1,\vec{p}_1,n,\nu)\tilde{c}_2(z_2,\vec{p}_2,n,\nu)-\tilde{c}_1(z_1,\vec{p}_1,n,\nu)\tilde{c}_2'(z_2,\vec{p}_2,n,\nu) \\ =\tilde{c}_1(z_1,\vec{p}_1,n,\nu)\tilde{c}_2(z_2,\vec{p}_2,n,\nu)\frac{d}{d\nu}\ln\frac{\tilde{c}_1(z_1,\vec{p}_1,n,\nu)}{\tilde{c}_2(z_2,\vec{p}_2,n,\nu)}\,, \tag{3.32}$$

can be put in the following form:

$$-\frac{i}{2}\int d\nu\left[\frac{-\tilde{c}_1(z_1,\vec{p}_1,n,\nu)\tilde{c}_2(z_2,\vec{p}_2,n,\nu)\frac{d}{d\nu}\ln\frac{\tilde{c}_1(z_1,\vec{p}_1,n,\nu)}{\tilde{c}_2(z_2,\vec{p}_2,n,\nu)}}{(\omega-\bar{\alpha}_s(\mu_R)\chi(n,\nu))^2}\chi(n,\nu)\right. \\ \left.+\frac{\tilde{c}_1(z_1,\vec{p}_1,n,\nu)\tilde{c}_2(z_2,\vec{p}_2,n,\nu)}{(\omega-\bar{\alpha}_s(\mu_R)\chi(n,\nu))^2}\chi'(n,\nu)\right]. \tag{3.33}$$

Now, one can go back to the complete expression for the third term and use the residue theorem to obtain

$$\frac{1}{(2\pi)^2}\sum_{n=-\infty}^{\infty}\int d\nu\;\alpha_s^2(\mu_R)\tilde{c}_1(z_1,\vec{p}_1,n,\nu)\tilde{c}_2(z_2,\vec{p}_2,n,\nu)\left(\frac{\hat{s}}{s_0}\right)^{\bar{\alpha}_s(\mu_R)\chi(n,\nu)}\ln\left(\frac{\hat{s}}{s_0}\right)$$
$$\times\left[\bar{\alpha}_s^2(\mu_R)\frac{\beta_0}{8N_c}\chi(n,\nu)\left(i\frac{d}{d\nu}\ln\left(\frac{\tilde{c}_1(z_1,\vec{p}_1,n,\nu)}{\tilde{c}_2(z_2,\vec{p}_2,n,\nu)}\right)-i\frac{\chi'(n,\nu)}{\chi(n,\nu)}\right)\right]. \tag{3.34}$$

Summing the three terms, the result is

$$\frac{d\hat{\sigma}_{AB}(z_1,\vec{p}_1,z_2,\vec{p}_2,s)}{dz_1d^2\vec{p}_1dz_2d^2\vec{p}_2}=\frac{1}{(2\pi)^2}\sum_{n=-\infty}^{\infty}\int d\nu\left(\frac{\hat{s}}{s_0}\right)^{\bar{\alpha}_s(\mu_R)\chi(n,\nu)}\alpha_s^2(\mu_R)\tilde{c}_1(z_1,\vec{p}_1,n,\nu)\tilde{c}_2(z_2,\vec{p}_2,n,\nu)$$
$$\times\left[1+\alpha_s(\mu_R)\left(\frac{\tilde{c}_1^{(1)}(z_1,\vec{p}_1,n,\nu)}{\tilde{c}_1(z_1,\vec{p}_1,n,\nu)}+\frac{\tilde{c}_2^{(1)}(z_1,\vec{p}_1,n,\nu)}{\tilde{c}_2(z_1,\vec{p}_1,n,\nu)}\right)+\bar{\alpha}_s^2(\mu_R)\ln\left(\frac{\hat{s}}{s_0}\right)\right.$$
$$\left.\times\left\{\bar{\chi}(n,\nu)+\frac{\beta_0}{8N_c}\chi(n,\nu)\left(-\chi(n,\nu)+\frac{10}{3}+2\ln\mu_R^2+i\frac{d}{d\nu}\ln\frac{\tilde{c}_1(z_1,\vec{p}_1,n,\nu)}{\tilde{c}_2(z_2,\vec{p}_2,n,\nu)}\right)\right\}\right]. \tag{3.35}$$

The expression for the cross section given in Eq. (3.35) is valid both in the LLA and in the NLLA. However, it is not the only possible one. Actually, several NLA-equivalent expressions can be adopted; we use the *exponential representation*,

$$\frac{d\hat{\sigma}_{AB}(z_1,\vec{p}_1,z_2,\vec{p}_2,s)}{dz_1d^2\vec{p}_1dz_2d^2\vec{p}_2}=\frac{1}{(2\pi)^2}\sum_{n=-\infty}^{\infty}\int d\nu\left(\frac{\hat{s}}{s_0}\right)^{\bar{\alpha}_s(\mu_R)\chi(n,\nu)}$$
$$\times\left(\frac{\hat{s}}{s_0}\right)^{\bar{\alpha}_s^2(\mu_R)\left(\bar{\chi}(n,\nu)+\frac{\beta_0}{8N_c}\chi(n,\nu)\left(-\chi(n,\nu)+\frac{10}{3}+2\ln\frac{\mu_R^2}{\sqrt{s_1s_2}}\right)\right)}\alpha_s^2(\mu_R)\tilde{c}_1(z_1,\vec{p}_1,n,\nu)\tilde{c}_2(z_2,\vec{p}_2,n,\nu)$$
$$\times\left[1+\alpha_s(\mu_R)\left(\frac{\tilde{c}_1^{(1)}(z_1,\vec{p}_1,n,\nu)}{\tilde{c}_1(z_1,\vec{p}_1,n,\nu)}+\frac{\tilde{c}_2^{(1)}(z_1,\vec{p}_1,n,\nu)}{\tilde{c}_2(z_1,\vec{p}_1,n,\nu)}\right)+\bar{\alpha}_s^2(\mu_R)\ln\left(\frac{\hat{s}}{s_0}\right)\frac{\beta_0}{4N_c}\chi(n,\nu)f(\nu)\right], \tag{3.36}$$

where

$$2f(\nu)=i\frac{d}{d\nu}\ln\left(\frac{\tilde{c}_1(z_1,\vec{p}_1,n,\nu)}{\tilde{c}_2(z_2,\vec{p}_2,n,\nu)}\right)+2\ln\sqrt{s_1s_2}\,, \tag{3.37}$$

and s_1, s_2 denote here the hard scales which enter the impact factors $\tilde{c}_{1,2}$. We stress that the difference between the two representations is beyond the NLLA [92], as it can be easily checked.

3.1.2 From the partonic to the hadronic cross-section

What we saw in the previous subsection is correct for our *partonic* cross section. In this subsection, we want to understand how to pass to the *hadronic* cross section. In order to implement the hybrid factorization, we perform the following manipulation:

$$\left(\frac{x_1x_2s}{s_0}\right)^{\bar{\alpha}_s(\mu_R)\chi(n,\nu)} = \left(\frac{z_1z_2s}{s_0}\right)^{\bar{\alpha}_s(\mu_R)\chi(n,\nu)} \left(\frac{x_1}{z_1}\right)^{\bar{\alpha}_s(\mu_R)\chi(n,\nu)} \left(\frac{x_2}{z_2}\right)^{\bar{\alpha}_s(\mu_R)\chi(n,\nu)} , \quad (3.38)$$

and reabsorb the second (third) factor on the right hand side in the definition of the upper (lower) hadronic impact factor[30]. The impact of these corrective factors is seen at the sub-leading order[31]. In all next-to-leading terms, corrective factors produce sub-sub-leading effects and hence we can immediately perform the replacement $x_1x_2 \to z_1z_2$. Keeping in mind that the impact factors have been re-defined, we obtain

$$\frac{d\hat{\sigma}_{AB}(z_1,\vec{p}_1,z_2,\vec{p}_2,s)}{dz_1d^2\vec{p}_1dz_2d^2\vec{p}_2} = \frac{1}{(2\pi)^2}\sum_{n=-\infty}^{\infty}\int d\nu \left(\frac{z_1z_2s}{s_0}\right)^{\bar{\alpha}_s(\mu_R)\chi(n,\nu)}$$

$$\times \left(\frac{z_1z_2s}{s_0}\right)^{\bar{\alpha}_s^2(\mu_R)\left(\bar{\chi}(n,\nu)+\frac{\beta_0}{8N_c}\chi(n,\nu)\left(-\chi(n,\nu)+\frac{10}{3}+2\ln\frac{\mu_R^2}{\sqrt{s_1s_2}}\right)\right)} \alpha_s^2(\mu_R)\tilde{c}_1(z_1,\vec{p}_1,n,\nu)\tilde{c}_2(z_2,\vec{p}_2,n,\nu)$$

$$\times\left[1+\alpha_s(\mu_R)\left(\frac{\tilde{c}_1^{(1)}(z_1,\vec{p}_1,n,\nu)}{\tilde{c}_1(z_1,\vec{p}_1,n,\nu)}+\frac{\tilde{c}_2^{(1)}(z_1,\vec{p}_1,n,\nu)}{\tilde{c}_2(z_1,\vec{p}_1,n,\nu)}\right)+\bar{\alpha}_s^2(\mu_R)\ln\left(\frac{z_1z_2s}{s_0}\right)\frac{\beta_0}{4N_c}\chi(n,\nu)f(\nu)\right]. \quad (3.39)$$

If one calculates the impact factors at the next-to-leading order, the expression of the cross section is that of Eq. (3.39). Nonetheless, when the next-to-leading impact factors are unknown, some universal corrections may still be included. Indeed, if the impact factors were calculated up to the next-to-leading order, the dependence on the arbitrary scale, s_0, and on the renormalization scale[32], μ_R, would be next-to-next-to-leading. We can therefore add, to a prediction in which only the Green's function is known within the NLLA, some next-to-leading universal terms, coming from impact factors, which make the dependence on the scales sub-sub-leading. We adopt this scheme in the section devoted to Higgs production because the numerical implementation of the full next-to-leading Higgs impact factor is not yet available.

[30]This means that we include it when convoluting partonic impact factor with PDFs.

[31]Note that x_i and z_i are fractions of longitudinal momenta of particles that are in the same fragmentation region and, therefore, correction proportional to $\ln(x_i/z_i)$ are not large.

[32]In hadronic impact factors we also have the dependence on the factorization scale μ_F. The argument can be extended also to this latter scale.

3.1.3 Kinematics

For the tagged particles we introduce the standard Sudakov decomposition, using as light-cone basis the momenta k_A and k_B of the collinding protons,

$$p_1 = z_1 k_A + \frac{m_1^2 + \vec{p}_1^{\,2}}{z_1 s} k_B + p_{1\perp} \ , \quad p_2 = z_2 k_A + \frac{m_2^2 + \vec{p}_2^{\,2}}{z_1 s} k_B + p_{2\perp} \ ,$$

with $s = (k_A + k_B)^2 = 2k_A \cdot k_B = 4E_{k_A} E_{k_B}$, choosing the momenta of protons as

$$k_A = E_{k_A}(1, \vec{0}, 1) \ , \quad k_B = E_{k_B}(1, \vec{0}, -1) \ .$$

Now, we easily find that the rapidities of the two tagged particles are

$$y_1 = \ln\left(\frac{2z_1 E_{k_A}}{m_{1\perp}}\right) \ , \quad y_2 = -\ln\left(\frac{2z_2 E_{k_B}}{m_{2\perp}}\right) \ , \tag{3.40}$$

where $m_{i\perp} = \sqrt{m_i^2 + \vec{p}_i^{\,2}}$ denotes the transverse mass of the i_{th}-particle. The rapidity difference is given by

$$\Delta Y = y_1 - y_2 = \ln\left(\frac{z_1 z_2 s}{m_{1\perp} m_{2\perp}}\right) \tag{3.41}$$

For the semi-hard kinematics we have the requirement

$$\frac{e^{\Delta Y}}{z_1 z_2} = \frac{s}{m_{1\perp} m_{2\perp}} \gg 1 \ . \tag{3.42}$$

In what follows, we will need a cross section differential in the rapidities of the tagged particles. For this reason we adopt the change of variable

$$dz_1 dz_2 = \frac{e^{\Delta Y} m_{1\perp} m_{2\perp}}{s} dy_1 dy_2 \ .$$

If we set the scale $s_0 = m_{1\perp} m_{2\perp}$, we can write the cross-section as

$$\frac{d\hat{\sigma}_{AB}(y_1, \vec{p}_1, y_2, \vec{p}_2, s)}{dy_1 d|\vec{p}_1| d\phi_1 dy_2 d|\vec{p}_2| d\phi_2} = \frac{1}{(2\pi)^2} \frac{e^{\Delta Y} |\vec{p}_1||\vec{p}_2| m_{1\perp} m_{2\perp}}{s} \sum_{n=-\infty}^{\infty} \int d\nu e^{\Delta Y \bar{\alpha}_s(\mu_R)\chi(n,\nu)}$$

$$\times e^{\Delta Y \bar{\alpha}_s^2(\mu_R)\left(\bar{\chi}(n,\nu) + \frac{\beta_0}{8N_c}\chi(n,\nu)\left(-\chi(n,\nu) + \frac{10}{3} + 2\ln\frac{\mu_R^2}{\sqrt{s_1 s_2}}\right)\right)} \alpha_s^2(\mu_R) \tilde{c}_1(z_1, \vec{p}_1, n, \nu) \tilde{c}_2(z_2, \vec{p}_2, n, \nu)$$

$$\times \left[1 + \alpha_s(\mu_R)\left(\frac{\tilde{c}_1^{(1)}(z_1, \vec{p}_1, n, \nu)}{\tilde{c}_1(z_1, \vec{p}_1, n, \nu)} + \frac{\tilde{c}_2^{(1)}(z_1, \vec{p}_1, n, \nu)}{\tilde{c}_2(z_1, \vec{p}_1, n, \nu)}\right) + \bar{\alpha}_s^2(\mu_R) \Delta Y \frac{\beta_0}{4N_c} \chi(n,\nu) f(\nu)\right] \ . \tag{3.43}$$

The coefficients defining the impact factors projected in the (n, ν)-space have the form

$$\tilde{c}_1(z_1, \vec{p}_1, n, \nu) = e^{\phi_1} c_1(z_1, |\vec{p}_1|, n, \nu) \ , \quad \tilde{c}_2(z_2, \vec{p}_2, n, \nu) = e^{-\phi_2 - \pi} c_2(z_2, |\vec{p}_2|, n, \nu) \ . \tag{3.44}$$

Hence, the cross section (3.43) can be re-expressed as

$$\frac{d\hat{\sigma}_{AB}(y_1,\vec{p}_1,y_2,\vec{p}_2,s)}{dy_1 d|\vec{p}_1|d\phi_1 dy_2 d|\vec{p}_2|d\phi_2} = \frac{1}{(2\pi)^2}\left[\mathcal{C}_0 + 2\sum_{n=1}^{\infty}\cos(n\varphi)\,\mathcal{C}_n\right], \tag{3.45}$$

where

$$\mathcal{C}_n = \int_0^{2\pi} d\phi_1 \int_0^{2\pi} d\phi_2 \cos(n\varphi)\frac{d\hat{\sigma}_{AB}(y_1,\vec{p}_1,y_2,\vec{p}_2,s)}{dy_1 d|\vec{p}_1|d\phi_1 dy_2 d|\vec{p}_2|d\phi_2} = \frac{e^{\Delta Y}}{s}\int d\nu e^{\Delta Y\bar{\alpha}_s(\mu_R)\chi(n,\nu)}$$
$$\times e^{\Delta Y\bar{\alpha}_s^2(\mu_R)\left(\bar{\chi}(n,\nu)+\frac{\beta_0}{8N_c}\chi(n,\nu)\left(-\chi(n,\nu)+\frac{10}{3}+2\ln\frac{\mu_R^2}{\sqrt{s_1 s_2}}\right)\right)}\alpha_s^2(\mu_R)c_1(z_1,\vec{p}_1,n,\nu)c_2(z_2,\vec{p}_2,n,\nu)$$
$$\times\left[1+\alpha_s(\mu_R)\left(\frac{c_1^{(1)}(z_1,\vec{p}_1,n,\nu)}{c_1(z_1,\vec{p}_1,n,\nu)}+\frac{c_2^{(1)}(z_1,\vec{p}_1,n,\nu)}{c_2(z_1,\vec{p}_1,n,\nu)}\right)+\bar{\alpha}_s^2(\mu_R)\Delta Y\frac{\beta_0}{4N_c}\chi(n,\nu)f(\nu)\right] \tag{3.46}$$

and $\varphi = \phi_1 - \phi_2 - \pi$. Eq. (3.45) represents the final form of our fully differential cross-section and it is the starting point for the construction of all observables under investigation in this thesis. For illustration purposes, we have constructed the cross section using a single μ_R scale throughout. This is not the only possible choice for this scale and also completely asymmetrical choices can be made. More in general, this is true for all scales involved. The extension is trivial and, since we will consider several processes, we refer the reader to the original works for details [72, 80, 81, 82, 83].

3.2 Processes under investigation

3.2.1 Heavy flavor production in a VFNS

As it is well known, the treatment of the c and b quarks in pQCD is rather delicate. When we are in a perturbative regime, we have $Q^2 \gg \Lambda^2_{\rm QCD}$, where Q is the typical hard scale of the process and $\Lambda_{\rm QCD}$ is the QCD mass scale. For light quarks, this is sufficient to treat them as massless partons and to assume that they are always present in the initial state when introducing parton distribution functions. Instead, the presence in the initial state and the way one must treat the mass of an heavy quark ($Q = c, b$) depends on kinematical conditions. For this reason there are two main schemes for the treatment of an heavy quark:

- **Fixed-Flavor Number Scheme (FFNS)**[33], where the heavy quark is always treated as a massive particle and never as a massless parton irrespective of the value

[33] For more details see, *e.g.*, Ref. [98] and references therein.

of the scale Q. In this scheme, the heavy quark PDF is ignored and the number of active flavours is always kept fixed. This scheme takes into account heavy-quark mass effects in coefficient functions, but does not resum logarithmically enhanced terms of the form $\ln(Q^2/m_Q^2)$.

- **Zero-Mass Variable-Flavor Number scheme (ZM-VFNS)**[34], where all heavy-quark mass effects are ignored. These corresponds to neglect powers of the ratio m_Q^2/Q^2. On the other hand, since the heavy quark is treated here as a massless parton, the scheme allows us to resum potentially large logarithms of the type $\ln(Q^2/m_Q^2)$ into parton distribution functions and fragmentation functions. In this scheme, the heavy quark is present in the initial state above a fixed threshold.

It is clear that the two approaches work in complementary regimes. The ZM-VFNS is applicable when $Q^2 \gg m_Q^2$ holds. In these kinematic conditions, power mass corrections are suppressed and DGLAP-type logarithms are large. On the other hand, the FFNS, which allows us to include all finite quark mass corrections, is only accurate in the region $Q \lesssim m_Q$. It is clear that there is no exact natural separation between these two approaches and it is reasonable to think of a more complete description. This is provided by the so-called **General–Mass Variable Flavour Number scheme (GM–VFNS)**[35], which combines the advantage of the massive and massless calculations by means of an interpolated scheme which is valid for any value of the scale Q, and that matches the FFN and ZM–VFN schemes at small and large values of Q, respectively.

Currently, a complete next-to-leading order description of the impact factors contributing to the production of heavy quarks in adroproduction channels is not available. For example, the impact factor(s) for producing the J/Ψ have been computed in Ref. [109], using two different approaches for the description of the charmonium state: 1) **Color evaporation model (CEM)** [110, 111], 2) **Non-relativistic QCD (NRQCD) formalism** [112, 113, 114]. Even limiting ourselves to the first case, or only to the color octet production mechanism in the NRQCD formalism, the corrections are not known. At the level of gluon channel only, the diagrams to be calculated would be the same ones to be calculated for the next-to-leading order heavy-quark pair impact factor, shown at LO in the Appendix B and originally computed in Ref. [115]. This impact factor has

[34] See Refs. [99, 100, 101, 102, 100, 103].
[35] See Refs. [104, 105, 106, 107, 108].

been applied to the study of inclusive production of a heavy-light dijet system in Ref. [116].

The remaining part of this section is dedicated to the description of semi-hard reactions involving the production of heavy bound states in the ZM-VFNS, leaving the inclusion of mass effects for future projects. In this way, the final state transition from partons to hadrons is described by a usual fragmentation function which is suitably convoluted with the partonic impact factor and with the parton distribution function. The leading order expression of this impact factor, projected onto the eigenfunctions of the LO BFKL kernel, is

$$c_1(n,\nu,|\vec{p}_1|,z_1) = 2\sqrt{\frac{C_F}{C_A}}(|\vec{p}_1|^2)^{i\nu-1/2}\int_{z_1}^1 \frac{d\zeta}{\zeta}\left(\frac{\zeta}{z_1}\right)^{2i\nu-1} \times\left[\frac{C_A}{C_F}f_g(\zeta)D_g^{\mathcal{Q}}\left(\frac{z_1}{\zeta}\right)+\sum_{\alpha=q,\bar{q}} f_\alpha(\zeta)D_\alpha^{\mathcal{Q}}\left(\frac{z_1}{\zeta}\right)\right] , \tag{3.47}$$

while the next-to-leading corrections can be found in Ref. [70]. Within the same accuracy, the LO impact factor for producing a jet is

$$c_2(n,\nu,|\vec{p}_2|,z_2) = 2\sqrt{\frac{C_F}{C_A}}(|\vec{p}_2|^2)^{i\nu-1/2}\left(\frac{C_A}{C_F}f_g(z_2)+\sum_{\beta=q,\bar{q}} f_\beta(z_2)\right) , \tag{3.48}$$

while the next-to-leading corrections can be found in Ref. [77].

Using the aforementioned scheme, here, we analyze the following semi-hard reactions:

- $P(k_A)+P(k_B)\longrightarrow \Lambda_c^\pm(y_1,p_1)+X+\Lambda_c^\pm(y_2,p_2)$,
- $P(k_A)+P(k_B)\longrightarrow H_b(y_1,p_1)+X+\mathrm{jet}(y_2,p_2)$,
- $P(k_A)+P(k_B)\longrightarrow H_b(y_1,p_1)+X+H_b(y_2,p_2)$,
- $P(k_A)+P(k_B)\longrightarrow J/\psi(y_1,p_1)+X+\mathrm{jet}(y_2,p_2)$,

where we are inclusive on the baryon charge of the Λ_c particle, H_b stands for a generic bottomed flavored hadron[36].

[36]In our analysis we are inclusive on the production of all species of b-hadrons whose lowest Fock state contains either a b or $\bar{b}$ quark, but not both. Therefore, bottomed quarkonia are not considered. Furthermore, we ignore B_c mesons since their production rate is estimated to be at most 0.1% of b-hadrons (see, *e.g.*, Refs.[117, 118]). Our choice is in line with the b-hadron FF determination of Ref.[119].

Collinear PDFs are calculated via the `MMHT14` NLO PDF set [120] as provided by `LHAPDFv6.2.1` interpolator [121], and a two-loop running coupling with $\alpha_s(M_Z) = 0.11707$ and a dynamic-flavor threshold is chosen.

We describe jet emissions at NLO perturbative accuracy in terms of a reconstruction algorithm calculated within the "small-cone" approximation (SCA) [78, 79], *i.e.* for a small-jet cone aperture in the rapidity/azimuthal angle plane. More in particular, we adopt the version derived in Ref. [69], which is *infrared-safe* up to NLO perturbative and well-suited for numerical computations, with a cone-jet function selection [122] and for the jet-cone radius fixed at $\mathcal{R}_J = 0.5$, as usually done in recent experimental analyses at CMS [123]. The expression for the NLO jet vertex can be obtained, *e.g.*, by combining Eq. (36) of Ref. [77] with Eqs. (4.19)-(4.20) of Ref. [122].

Λ_c and b-hadrons fragmentation functions in VFNS

We described the parton fragmentation into Λ_c baryons in terms of the novel `KKSS19` NLO FF set [124] (see also Refs. [125, 126]), whose native implementation was directly linked to `JETHAD`. This parameterization mainly relies on a description *à la* Bowler [127] for c and b quark/antiquark flavors. Technical details on the fitting procedure are presented in Section IV of Ref. [124].

We depicted the parton fragmentation to b-hadrons by the hand of the `KKSS07` NLO FFs, that were originally extracted from data of inclusive B-meson emissions in e^+e^- annihilation [128]. In this parametrization the b flavor has its starting scale at $\mu_0 = 4.5$ GeV $\simeq m_b$ and is portrayed by a simple, three-parameter power-like *Ansatz* [129]

$$D^{H_b}(x, \mu_0) = \mathcal{N} x^a (1-x)^b \,, \tag{3.49}$$

whereas gluon and lighter quark (including c) FFs are generated through DGLAP evolution and vanish at $\mu_F = \mu_0$. Following Ref. [119], we obtained the b-hadron FFs from the B-meson ones by simply removing the branching fraction for the $b \to B^\pm$ transition, which was assumed as $f_u = f_d = 0.397$ (see also Ref. [128]).

We also show comparisons with predictions for lighter-hadron species (Λ hyperons, pions, kaons, and protons), these latter are described in terms `AKK08` NLO FFs [130], which are the closest in technology to `KKSS19`.

Quarkonium fragmentation functions

We build our NLO collinear FF sets for the *direct* J/ψ or Υ meson production by taking, as a starting point, the recent work done in Ref. [131]. There, a NLO calculation was performed for the heavy-quark FF depicting the transition $c \to J/\psi$ or the $b \to \Upsilon$ one, where c (b) indistinctly refer to the charm (bottom) quark and its antiquark. It essentially relies on the NRQCD factorization formalism taken with NLO accuracy (see, *e.g.*, Refs. [113, 114, 132, 133, 134, 135] and references therein), which allows us to write the FF function of a parton i fragmenting into a heavy quarkonium $\mathcal{Q}$ with longitudinal fraction z as

$$D_i^{\mathcal{Q}}(z,\mu_F) = \sum_{[n]} \mathcal{D}_i^{\mathcal{Q}}(z,\mu_F,[n]) \langle \mathcal{O}^{\mathcal{Q}}([n]) \rangle \; . \tag{3.50}$$

In Eq. (3.50), $\mathcal{D}_i(z,\mu_F,[n])$ denotes the perturbative short-distance coefficient containing terms proportional to $\ln(\mu_F/m_{\mathcal{Q}})$ (to be resummed via DGLAP evolution), $\langle \mathcal{O}^{\mathcal{Q}}([n]) \rangle$ stands for the non-perturbative NRQCD LDME, and $[n] \equiv {}^{2S+1}L_J^{(c)}$ represents the quarkonium quantum numbers in the spectroscopic notation (see, *e.g.*, Ref. [136]), the (c) superscript identifying the color state, singlet (1) or octet (8). Limiting ourselves to a spin-triplet (vector) and color-singlet quarkonium state, ${}^3S_1^{(1)}$, the analytic form of the initial-scale FF depicting the constituent heavy-quark to quarkonium transition, $Q \to \mathcal{Q}$ (we refer to $c \to J/\psi$ here[37] as well), reads (for details on its derivation, see Sections II and III of Ref. [131])

$$D_Q^{\mathcal{Q}}(z,\mu_F \equiv \mu_0) = D_Q^{\mathcal{Q},\mathrm{LO}}(z) + \frac{\alpha_s^3(3m_Q)}{m_Q^3} \, |\mathcal{R}_{\mathcal{Q}}(0)|^2 \, \Gamma_Q^{\mathcal{Q},\mathrm{NLO}}(z) \; , \tag{3.51}$$

with $m_c = 1.5$ GeV, and the NRQCD radial wave-function at the origin of the quarkonium state set to $|\mathcal{R}_{J/\psi}(0)|^2 = 0.810 \; \mathrm{GeV}^3$, according to potential-model calculations (Ref. [137] and references therein). The expression for the LO initial-scale FF was originally calculated in Ref. [138] and reads

$$D_Q^{\mathcal{Q},\mathrm{LO}}(z) = \frac{\alpha_s^2(3m_Q)}{m_Q^3} \, \frac{8z(1-z)^2}{27\pi(2-z)^6} \, |\mathcal{R}_{\mathcal{Q}}(0)|^2 \, (5z^4 - 32z^3 + 72z^2 - 32z + 16) \; , \tag{3.52}$$

and the polynomial function $\Gamma_Q^{\mathcal{Q},\mathrm{NLO}}(z)$ entering the expression for the NLO-FF correction is

$$\Gamma_Q^{J/\psi,\mathrm{NLO}}(z) \;\; = \;\; -9.01726z^{10} + 18.22777z^9 + 16.11858z^8 - 82.54936z^7$$

[37] In the original paper, Ref. [82], we consider the $b \to \Upsilon$

$$+ \quad 106.57565z^6 - 72.30107z^5 + 28.85798z^4 - 6.70607z^3$$
$$+ \quad 0.84950z^2 - 0.05376z - 0.00205 \tag{3.53}$$

Coefficients of z-powers in Eqs. (3.53) are obtained via a polynomial fit to the numerically-calculated NLO FFs. Starting from $\mu_F \equiv \mu_0 = 3m_Q$, in Ref. [131] a DGLAP-evolved formula for the $D_Q^{\mathcal{Q}}(z, \mu_F)$ function was derived and then applied to phenomenological studies of J/ψ production via e^+e^- single inclusive annihilation (SIA).

As pointed out in Ref. [139], both $(c \to J/\psi)$ and $(g \to J/\psi)$ fragmentation channels are similar in size. The relative weight of the heavy-quark and gluon contributions is also driven by the size of the hard scattering producing these partons. Therefore, the number of large p_T-gluons emitted could be of the same order, if not larger, than the heavy-quark one. Moreover, in a hadroproduction process such as the one considered in our study, the gluon FF is enhanced by the collinear convolution at LO with the corresponding gluon PDF (see Eq. (3.47)). Thus we expect, in our case, a stronger sensitivity on the gluon-fragmentation channel with respect to the case of a SIA-like reaction. Therefore, we include in our analysis also the contribution coming from the gluon fragmentation. The gluon to vector-quarkonium LO fragmentation mechanism starts at α_s^3, namely at the same order of the NLO correction to the heavy-quark FF in Eq. (3.51). The $(g \to {}^3S_1^{(1)} gg)$ fragmentation function was computed in Ref. [140] and reads

$$D_g^{\mathcal{Q}}(z, 2m_Q) = \frac{5}{36(2\pi)^2}\alpha_s^3(2m_Q)\frac{|\mathcal{R}_{\mathcal{Q}}(0)|^2}{m_{\mathcal{Q}}^3}\int_0^z d\xi \int_{(\xi+z^2)/2z}^{(1+\xi)/2} d\tau \frac{1}{(1-\tau)^2(\tau-\xi)^2(\tau^2-\xi)^2}$$
$$\sum_{i=1}^{2} z^i \left[f_i^{(g)}(\xi,\tau) + g_i^{(g)}(\xi,\tau)\frac{1+\xi-2\tau}{2(\tau-\xi)\sqrt{\tau^2-\xi}} \ln\left(\frac{\tau-\xi+\sqrt{\tau^2-\xi}}{\tau-\xi-\sqrt{\tau^2-\xi}}\right)\right], \tag{3.54}$$

with the six $f_i^{(g)}$ and $g_i^{(g)}$ functions being given in Eqs. (4)-(9) of Ref. [141]. We stress that the mechanism considered here is the *direct* production of the quarkonium from the parent gluon. Another contribution to J/ψ-meson production in high-energy processes, not considered in our analysis, is the production of a P-wave charmonium state χ_c, followed by its radiative decay $\chi_c \to J/\psi + \gamma$ (see Refs. [138, 142]).

The different initial energy scales at which quarks and gluons FF are taken is due to the production mechanism itself. The heavy-quark fragmentation involves at least three heavy quarks in the final state (Fig. 3.2, left panel), thus the running coupling in Eqs. (3.51) and (3.52) is calculated at $\mu_R = 3m_Q$. Conversely, the gluon fragmentation

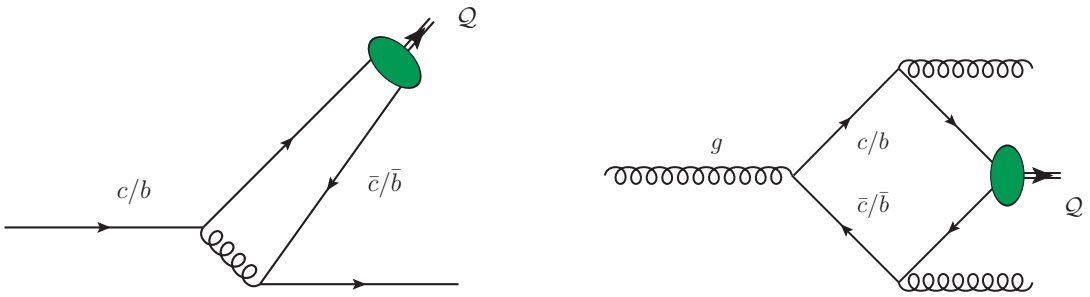

Figure 3.2: Left: one of the leading diagrams contributing to the heavy-quark fragmentation to a ${}^3S_1^{(1)}$ vector quarkonium $\mathcal{Q}$ at order α_s^2. Right: one of the leading diagrams contributing to the gluon fragmentation to ${}^3S_1^{(1)}$ vector quarkonium $\mathcal{Q}$ at order α_s^3. The green blob denotes the corresponding non-perturbative NRQCD LDME.

involves two heavy quarks only (Fig. 3.2, right panel), and this explains why the running coupling in Eq. (3.54) is taken at $\mu_R = 2m_Q$.

Starting from the initial-scale FFs in Eqs. (3.51, 3.54), we generate the corresponding functions for all parton species. This is a required step in order to perform analyses by means of our high-energy VFNS treatment. For a given quarkonium, J/ψ or Υ, we set the corresponding constituent heavy (anti-)quark FF, $D_c^{J/\psi} \equiv D_{\bar{c}}^{J/\psi}$ or $D_b^{\Upsilon} \equiv D_{\bar{b}}^{\Upsilon}$, to be equal to the parameterization given in Eq. (3.51) at the initial scale $\mu_0 = 3m_Q$ and we set the gluon FF, $D_g^{J/\psi}$ or D_g^{Υ}, to be equal to the parameterization given in Eq. (3.54) at the initial scale $\mu_0 = 2m_Q$. Then, we compute the DGLAP-evolved functions via the `APFEL++` library [143, 144, 145], thus getting a `LHAPDF` set of FFs that embodies all parton flavors. From now, according to names of Authors of Ref. [131], we will refer to these sets as the J/ψ `ZCW19`$^+$ NLO FF parameterizations[38].

3.2.2 Higgs plus jet/charmed-hadron

In Ref. [72, 83] the following semi-hard reactions

- $P(k_A) + P(k_B) \longrightarrow H(y_1, p_1) + X + \text{jet}(y_2, p_2)$,
- $P(k_A) + P(k_B) \longrightarrow H(y_1, p_1) + X + \Lambda_c(y_2, p_2)$,

[38] In Ref. [82] we named `ZCW19` the set which does not include the gluon FF at the initial scale $\mu_0 = 2m_Q$. In that set, also the gluon channel is purely generated by the evolution.

have been proposed as testified of BFKL dynamics. The setup of the PDFs, FFs and the jet reconstruction algorithm is identical to the one described in the previous subsection. As the implementation of the next-to-leading order level impact factor for the production of a forward Higgs boson from a colliding proton is not yet available, we use the leading order one (including finite top-mass contributions), which reads [72]

$$c_H(\kappa,\nu,|\vec{p}_1|,z_1)=\frac{1}{v^2}\frac{|\mathcal{H}_f(\vec{p}_1^{\,2})|^2}{128\pi^3\sqrt{2(N_c^2-1)}}\left(\vec{p}_1^{\,2}\right)^{i\nu+1/2} f_g(z_1,\mu_{F_1})\;, \tag{3.55}$$

where [146]

$$\mathcal{H}(\vec{p}_1^{\,2})=\frac{4m_t^2}{m_{H\perp}^2}$$
$$\times\left\{\left(\frac{1}{2}-\frac{2m_t^2}{m_{H\perp}^2}\right)\left[\Delta_h(\upsilon_2)^2-\Delta_h(\upsilon_1)^2\right]+\left(\frac{2\vec{p}_1^{\,2}}{m_{H\perp}^2}\right)\left[\sqrt{\upsilon_1}\,\Delta_h(\upsilon_1)-\sqrt{\upsilon_2}\,\Delta_h(\upsilon_2)\right]+2\right\}, \tag{3.56}$$

with $m_t=173.21$ GeV the top-quark mass, $\upsilon_1=1-4m_t^2/m_H^2$, $\upsilon_2=1+4m_t^2/\vec{p}_H^{\,2}$, the root $\sqrt{\upsilon_1}=i\sqrt{|\upsilon_1|}$ holding for negative values of υ_1. Moreover one has

$$\Delta_h(\upsilon)=\begin{cases}-2i\arcsin\dfrac{1}{\sqrt{1-\upsilon}}\;, & \upsilon<0\;;\\[2ex] \ln\dfrac{1+\sqrt{\upsilon}}{1-\sqrt{\upsilon}}-i\pi\;, & 0<\upsilon<1\;;\\[2ex] \ln\dfrac{1+\sqrt{\upsilon}}{\sqrt{\upsilon}-1}\;, & \upsilon>1\;.\end{cases} \tag{3.57}$$

In our study we consider a partial NLO implementation that includes the "universal" contributions to the Higgs impact factor, proportional to the corresponding LO impact factor. These terms are obtained on the basis of a renormalization group analysis, namely *via* the requirement of stability at NLO under variations of energy scales. Thus we have

$$c_H^{(1)}(\kappa,\nu,|\vec{p}_1|,z_1)\;=\;c_H(\kappa,\nu,|\vec{p}_1|,z_1)\left\{\frac{\beta_0}{2\pi}\left(\ln\frac{\mu_{R_1}}{|\vec{p}_1|}+\frac{5}{6}\right)+\chi\left(\kappa,\nu\right)\ln\left(\frac{\sqrt{s_0}}{m_{H\perp}}\right)+\frac{\beta_0}{2\pi}\ln\frac{\mu_{R_1}}{m_{H\perp}}\right.$$
$$\left.-\frac{1}{\pi f_g(z_1,\mu_{F_1})}\ln\left(\frac{\mu_{F_1}}{m_{H\perp}}\right)\int_{z_1}^1\frac{d\xi}{\xi}\left[P_{gg}(\xi)f_g\left(\frac{z_1}{\xi},\mu_{F_1}\right)+\sum_{a=q,\bar{q}}P_{ga}(\xi)f_a\left(\frac{z_1}{\xi},\mu_{F_1}\right)\right]\right\}\;. \tag{3.58}$$

3.3 Numerical results

The numerical elaboration of all the considered observables is done by making use of the `JETHAD` modular work package [84]. The sensitivity of our results on scale variation is

assessed by letting μ_R and μ_F to be around their *natural* values, up to a factor ranging from 1/2 to two. More specifically, we set[39]

$$\mu_R = \mu_F = \mu_N = \sqrt{m_{1\perp} m_{2\perp}}\,, \tag{3.59}$$

and the C_μ parameter entering plots as the ratio $\mu_{R,F}/\mu_N$ for all the consider processes, except the ones involving the production of a Higgs boson. In these latter cases, we use the geometrical mean in Eq. (3.59) only the exponential factor in Eq. (3.46), while the scale associated to each impact factor is chosen as

$$\mu_{R_i} = \mu_{F_i} = C_\mu \mu_{N_i} = C_\mu m_{i\perp}\,.$$

Error bands in our figures embody the combined effect of scale variation and phase-space multi-dimensional integration, the latter being steadily kept below 1% by the JETHAD integrators. All calculations of our observables is done in the $\overline{\rm MS}$ scheme. The kinematical cuts are always shown directly in plots, for more detailed discussion on these choices we refer to [72, 80, 81, 82, 83]. Furthermore, Refs. [72, 80, 81, 82, 83] contain for all the processes mentioned above, long and detailed studies, both at natural scales and at scales obtained through the *Brodsky-Lepage-Mackenzie* (BLM) *optimization* procedure [147, 148, 149, 150], which prescribes that the optimal scale value is the one that cancels the non-conformal β_0-terms in the considered observable. In the following, we want to provide a review of the observables that can be studied, focusing on the possibility of carrying out studies at natural scales. The reason for this choice is that, although the application of the BLM method led to a significant improvement of the agreement between predictions for azimuthal correlations of the two Mueller-Navelet jets and CMS data [123], the scale values found, much higher than the natural ones, generally bring to a substantial reduction of cross sections (observed for the first time in inclusive light charged dihadron emissions [151, 152]). This issue clearly hampers the possibility of doing precision studies.

3.3.1 Azimuthal-angle coefficients

The *azimuthal-angle coefficients*, are obtained by integrating coefficients $\mathcal{C}_n$ in Eq. (3.46) over the phase space of the outgoing particles, at fixed values of their mutual rapidity separation, ΔY. One has

$$C_n(\Delta Y, s) = \int_{p_1^{\rm min}}^{p_1^{\rm max}} d|\vec{p}_1| \int_{p_2^{\rm min}}^{p_2^{\rm max}} d|\vec{p}_2| \int_{y_1^{\rm min}}^{y_1^{\rm max}} dy_1 \int_{y_2^{\rm min}}^{y_2^{\rm max}} dy_2\, \delta\left(y_1 - y_2 - \Delta Y\right) \mathcal{C}_n\,. \tag{3.60}$$

[39] In case of jet or light hadrons the transverse mass coincide with the $|\vec{p}\,|$.

We investigate the ΔY-behavior of the φ-summed cross section (or ΔY-distribution), $C_0(\Delta Y, s)$, of the azimuthal-correlation moments, $R_{n0}(\Delta Y, s) = C_n/C_0 \equiv \langle \cos n\varphi \rangle$, and of their ratios, $R_{nm} = C_n/C_m$ [153, 154].

ΔY-distribution

In Fig. 3.3, we show the ΔY-behavior of C_0 for a series of different semi-hard reactions. The common feature is the downtrend exhibited by the cross section at increasing ΔY. It emerges as the interplay of two competing effects. On the one hand, the pure high-energy evolution leads to the well-known growth with energy of partonic cross sections. On the other hand, collinear parton distributions and fragmentation functions quench hadronic cross sections when ΔY increases. All the plots show a promising partial stabilization of the high-energy series.

Upper left panel of Fig. 3.3 shows the ΔY-dependence of the φ-summed cross section in the double Λ_c channel, together with corresponding predictions for detection of Λ hyperons, at NLLA. We note that NLA bands are almost nested (except for large values of ΔY, for which they overlap but are not fully nested) inside LLA ones and they are generally narrower in the Λ_c case. Since this analysis is performed around natural scales and without implementing any BLM optization, we claim that this is a clear effect of a (partially) reached stability of the high-energy series, for both hadron emissions. The fact that the stabilization effect is stronger for heavy species was corroborated in Ref. [80], observing that, while predictions for hyperons lose almost one order of magnitude when passing from natural scales to the expanded BLM ones, results for Λ_c baryons are much more stable, with the NLA band becoming even wider in the BLM case. Moreover, in Ref. [80] it was proposed that the stabilization effect is connected to the smooth and non-decreasing with μ_F FFs behavior of the Λ_c fragmentation functions. Subsequently, a similar behavior was observed for other hadronic species.

Another manifestation of stabilizing effects is shown in the upper right panel of Fig. 3.3, where we consider the $\Lambda_c + H$ channel. We perform phenomenological study by imposing realistic kinematic cuts of forthcoming experimental analyses at the LHC. In particular, we allow the charmed-hadron transverse momentum to be in the range $8\ \text{GeV} < p_{\mathcal{C}} < 20\ \text{GeV}$ and its rapidity in the ultraforward rapidity window $6 < y_{\mathcal{C}} < 7.5$. This choice is in line with nominal acceptances of FPF detector plans [155, 156]. We observe that the NLA

predictions are systematically contained inside LLA ones and the width of uncertainty bands considerably decreases when moving to the higher order. It should be specified that, even if this stabilization effect is very strong in the latter case, especially if one considers into the high rapidity-difference between the two detected objects, the analysis is only partial next-to-leading, due to the presence of the Higgs impact factor, whose complete next-to-leading implementation is not yet available[40].

Lastly, in lower panels of Fig. 3.3 we study, with the full NLLA, the ΔY-behavior of the cross section in the double J/ψ and J/ψ-plus-jet channels. Predictions are obtained by making use of the `ZCW19`$^+$ set. We note that values of C_0 are everywhere larger than 0.5 pb in the J/ψ-plus-jet channel. This leads to a very promising statistics, although being substantially lower than the one for heavy-baryon and heavy-light meson emissions [80, 81].

Azimuthal-correlation moments and their ratios

Azimuthal-correlation moments and their ratio are widely recognized as very sensitive to the BFKL dynamics. It is also well known that, in the Mueller-Navelet channel, the instabilities under higher order corrections and scale variations prevents any realistic analysis around natural values[41]. In Fig. 3.4, predictions for the R_{10}, R_{21} azimuthal ratios in the double Λ_c (upper panels) and in the double H_b (lower panels) channels, at natural scales, are presented. The downtrend of all these ratios when ΔY grows is a well know signal of the onset of high-energy dynamics. Larger rapidity distances heighten the weight of undetected gluons, thus leading to a decorrelation pattern in the azimuthal plane, which is more pronounced in pure LLA series.

Although, instabilities rising at natural scales are strong, they are milder than the ones observed in the Mueller-Navelet dijet channel. In the presented plots, the value of the R_{10} moment exceeds one in the small-ΔY region. This unphysical effect is fairly explained by the fact that contributions which are power-suppressed in energy and are not included in our BFKL treatment start to become relevant in those kinematic ranges, thus worsening the accuracy of our predictions.

[40] Nonetheless, we include all of the universal NLO terms presented in the previous section.

[41] At least for the pure azimuthal correlation moments.

The situation improves, when one considers ratio of azimuthal correlation moments. As firstly observed in Refs. [153, 154], the R_{21} ratios exhibits a fair stability under NLA corrections for both both final-state channels.

3.3.2 Azimuthal distribution

The *azimuthal distribution* of the two tagged particles, as a function of φ and at fixed values of ΔY, is

$$\frac{d\sigma_{pp}(\varphi, \Delta Y, s)}{\sigma_{pp} d\varphi} = \frac{1}{\pi} \left\{ \frac{1}{2} + \sum_{n=1}^{\infty} \cos(n\varphi) \langle \cos(n\varphi) \rangle \right\} \equiv \frac{1}{\pi} \left\{ \frac{1}{2} + \sum_{n=1}^{\infty} \cos(n\varphi) R_{n0} \right\} . \quad (3.61)$$

Proposed for the first time in the context for Mueller–Navelet studies [90, 157], this distribution represents one of the most directly accessible observables in experimental analyses. Indeed, experimental measurements hardly cover the whole azimuthal-angle plane due to limitations of the apparatus. Therefore, distributions differential on the azimuthal-angle difference, φ, could be easier compared with data.

In Fig. 3.5, we present predictions for the azimuthal distribution in the $\Lambda_c + H$ (left panels) and in the J/ψ + jet (right panels) channels, for three distinct values of the rapidity interval. LLA predictions are given in the upper panels, while NLA are found in the lower ones. In all cases the height of the peak visibly diminishes when ΔY grows, while the distribution width slightly widens. Again, at large values of ΔY the weight of gluons strongly ordered in rapidity predicted by BFKL increases, thus bringing to a reduction of the azimuthal correlation between the two detected objects, so that the number of back-to-back events lowers.

Focusing on patterns for the φ-distribution in the J/ψ + jet channel, we observe that at $\Delta Y = 1$ the LLA peak is much more pronounced than the corresponding NLA one, at $\Delta Y = 3$ the LLA and NLA peaks are similar in height, and at $\Delta Y = 5$ the LLA peak is beyond the NLA one. This behavior as a straightforward explanation. The small-ΔY range stays at the limit of applicability of the BFKL resummation, since the low values of the partonic center-of-mass energies reduces the phase space for secondary-gluon emissions. This leads to a stronger discrepancy between LLA and NLA results. Conversely, in the moderate-ΔY regime the high-energy series shows a fair stability when NLA corrections are switched on. Finally, the large-ΔY territory is very sensitive to the BFKL

dynamics, this reflecting in a stronger weight of the re-correlation effects, predicted by the NLA resummation, over pure LLA results.

The same pattern is observed in the $\Lambda_c + H$ channel. The only difference is that, from the lower ΔY value, the LLA predictions are below the NLLA ones. This is due to the fact that in this analysis we are considering ultra-forward kinematics, in fact, the first value of the rapidity difference is four. At these values, re-correlation effects, predicted by the NLA resummation, are already very strong.

3.3.3 Transverse-momentum distributions

Cross sections and azimuthal-angle correlations differential in the final-state rapidity interval, ΔY, are excellent testing grounds for the high-energy resummation. However, in order to probe regimes where other resummation dynamics are also relevant, more differential distributions in the p_T-spectrum are needed. Indeed, when the measured transverse momenta range in wider windows, other regions that are contiguous to the strict semi-hard one get probed. On one hand, when the transverse momenta are very large or their mutual distance is large, the weight of DGLAP-type logarithms as well as *threshold* contaminations [158, 159, 160] grows, thus making the description by our formalism inadequate. On the other hand, in the very low-p_T limit a pure high-energy treatment would also fail since large transverse-momentum logarithms entering the perturbative series are systematically neglected by BFKL. Therefore, in this section, rather than claiming to be able to describe the whole spectrum in p_T of the observables, we want to show that there exist kinematic windows in which high-energy resummation is relevant and in which therefore it must be taken into account in a serious precision program.

Single differential p_T-distribution

We start by studying the *transverse-momentum distribution* of one particle at fixed values of ΔY, *i.e.*

$$\frac{d\sigma_{pp}(|\vec{p}_1|, \Delta Y, s)}{d|\vec{p}_1| d\Delta Y} = \int_{p_2^{\min}}^{p_2^{\max}} d|\vec{p}_2| \int_{y_Q^{\min}}^{y_Q^{\max}} dy_1 \int_{y_J^{\min}}^{y_J^{\max}} dy_2 \, \delta\left(y_1 - y_2 - \Delta Y\right) \mathcal{C}_0. \tag{3.62}$$

We investigate this distribution in the Higgs + jet channel. Our calculation in the Born limit at $\Delta Y = 3$ (left panel of Fig. 3.6) is in fair agreement with the corresponding pattern in Ref. [146] (solid line in the left panel of Fig. 2), up to a factor two, due to the fact

that we restricted ΔY to be positive, which means that the Higgs particle is always more forward than the jet[42]. In our study, this calculation cannot exceed a given upper cut-off in the $|\vec{p}_H|$-range, say around 125 GeV. This is due to our choice for the final-state kinematic ranges, where consistency with experimental cuts in the rapidities of the detected objects would lead to $x_J > 1$ for sufficiently large jet transverse momenta.

Both the LLA (blue) and the NLA (red) series in upper panels of Fig. 3.6 show a peak (not present in the Born case) at $|\vec{p}_H|$ around 40 GeV for the two values of ΔY, and a decreasing behavior at large $|\vec{p}_H|$. For the sake of simplicity, we distinguish three kinematic subregions. The low-$|\vec{p}_H|$ region, *i.e.* $|\vec{p}_H| < 10$ GeV, has been excluded from our analysis, since it is dominated by large transverse-momentum logarithms, which call for the corresponding all-order resummation, not accounted by our formalism. To the intermediate-$|\vec{p}_H|$ region the set of configurations where $|\vec{p}_H|$ is of the same order of $|\vec{p}_J|$, which ranges from 35 to 60 GeV, corresponds. It is essentially the peak region plus the first part of the decreasing tail, where NLA bands are totally nested inside the LLA ones. Here, the impressive stability of the perturbative series unambiguously confirms the validity of our description at the hand of the BFKL resummation. Finally, in the large-$|\vec{p}_H|$ region represented by the long tail, NLA distributions decouple from LLA ones and exhibit an increasing sensitivity to scale variation. Here, DGLAP-type logarithms together with *threshold* effects start to become relevant, thus spoiling the convergence of the high-energy series. In Fig. 3.6 we present also the p_H-distributions at $\Delta Y = 3$ and 5, as obtained by a fixed-order NLO calculation through the POWHEG method [161, 162, 163], by suitably adapting the subroutines dedicated to the inclusive Higgs plus jet final state [164, 165]. It is interesting to observe that, both at $\Delta Y = 3$ and $\Delta Y = 5$, the NLO fixed-order prediction is systematically lower than the LLA- and NLA-BFKL ones and this is more evident at the larger ΔY, where the effect of resummation is expected to be more important. This observation provides with an interesting window for discrimination between fixed-order and high-energy-resummed approaches.

Finally, in lower panels of Fig. (3.6), we compare the p_T-distributions presented above with the corresponding ones obtained in the large top-mass limit, $M_t \to +\infty$. In Ref. [72], it was noted that, when this limit is taken, cross sections become at most $5 \div 7\,\%$ larger,

[42]Note that in Ref. [146] the Higgs mass is a free parameter. We compare our result with the corresponding one at $M_H = 120$ GeV.

whereas the effect on azimuthal correlations is very small or negligible. We do not show figures related with this comparison, since the bands related to the large top-mass limit are hardly distinguishable from the ones with physical top mass. The impact on the p_H-distribution is also quite small in the $|\vec{p}_H| \sim |\vec{p}_J|$ range, while it become more manifest when the value of $|\vec{p}_H|$ increases.

All these considerations brace the message that an exhaustive study of the $|\vec{p}_H|$-distribution would rely on a unified formalism where distinct resummations are concurrently embodied. In particular, the impact of the BFKL resummation could depend on the delicate interplay among the Higgs transverse mass, the Higgs transverse momentum and the jet transverse momentum entering, in logarithmic form, the expressions of partial NLO corrections to impact factors. Future studies including full higher-order corrections will allow us to further gauge the stability of our calculations.

Double differential p_T-distribution

Lastly, we also investigate the *double differential p_T-distribution* at fixed values of ΔY,

$$\frac{d\sigma_{pp}(|\vec{p}_1|, |\vec{p}_2|, \Delta Y, s)}{d|\vec{p}_1|d|\vec{p}_2|d\Delta Y} = \int_{y_1^{\min}}^{y_1^{\max}} dy_1 \int_{y_2^{\min}}^{y_2^{\max}} dy_2 \, \delta\left(y_1 - y_2 - \Delta Y\right) \mathcal{C}_0. \tag{3.63}$$

In Ref. [166] this study was proposed, without pretension of catching all the dominant features of this observable by the hand of our hybrid factorization, but rather to set the ground for futures studies where the interplay of different resummations (among all BFKL, Transverse momentum, and threshold one) can be deeply investigated. Results for our distributions in the H_b + jet channel at $\Delta Y = 3$ and 5 are presented in Fig. 3.7. In this analysis no BLM scale optimization is employed. We note that predictions fall off very fast when the two observable transverse momenta, $|\vec{p}_H|$ and $|\vec{p}_J|$, become larger or when their mutual distance grows. As generally predicted by the BFKL dynamics, LLA predictions (left panels) are always larger than NLA ones (right panels). Furthermore, we do not observe any peak, which could be present in the low-p_T region, namely where Transverse momentum-resummation effects are dominant and that it is excluded from our analysis.

3.4 Summary and outlook

In this chapter, we have proposed a series of new semi-hard reactions that can be studied at the LHC, presenting a whole series of observables useful for detecting high-energy effects. We believe that such effects should be included in the precision programs of the LHC and of future accelerators capable of reaching even higher center-of-mass energies.

There are several interesting future developments on the side of forward/backward phenomenology. The analysis presented here in the case of heavy-flavor production only partially covers the p_T-spectrum. In fact, as already said, in the region of small-p_T of the produced heavy-hadron a FFNS description is more reliable. The construction of predictions within this scheme (or in a full GM-VFNS), necessarily requires finding the NLO corrections to impact factors for the production of massive quarks (Q). The impact factor for the $Q \to Q$ transition is already known at next-to-leading order [167]. Nevertheless, the production of heavy-flavor involves other channels that are even dominanting. Among them, the contributions calculated at LO in the references [109, 115] are necessary to study the productions of quarkonia or heavy-light mesons. Another interesting channel in the context of forward/backward productions has been proposed in Ref. [168], *i.e.* forward Drell-Yan and backward jet production. In this case, a full NLL description, requires the calculation of the next-to-leading impact factor for the forward Drell-Yan production.

In the case of Higgs-plus-jet production, it is already possible to perform a full next-to-leading logarithmic analysis. Using the next-to-leading order result, for example obtained through POWHEG, it is also possible to implement a matching procedure to obtain a full next-to-leading order prediction supplemented by a complete resummation of high-energy logarithms. Through such a procedure it will be on the one hand clearer to distinguish the high-energy effects from those of the fixed order dynamics and on the other hand to provide valid predictions in a broader kinematic regime.

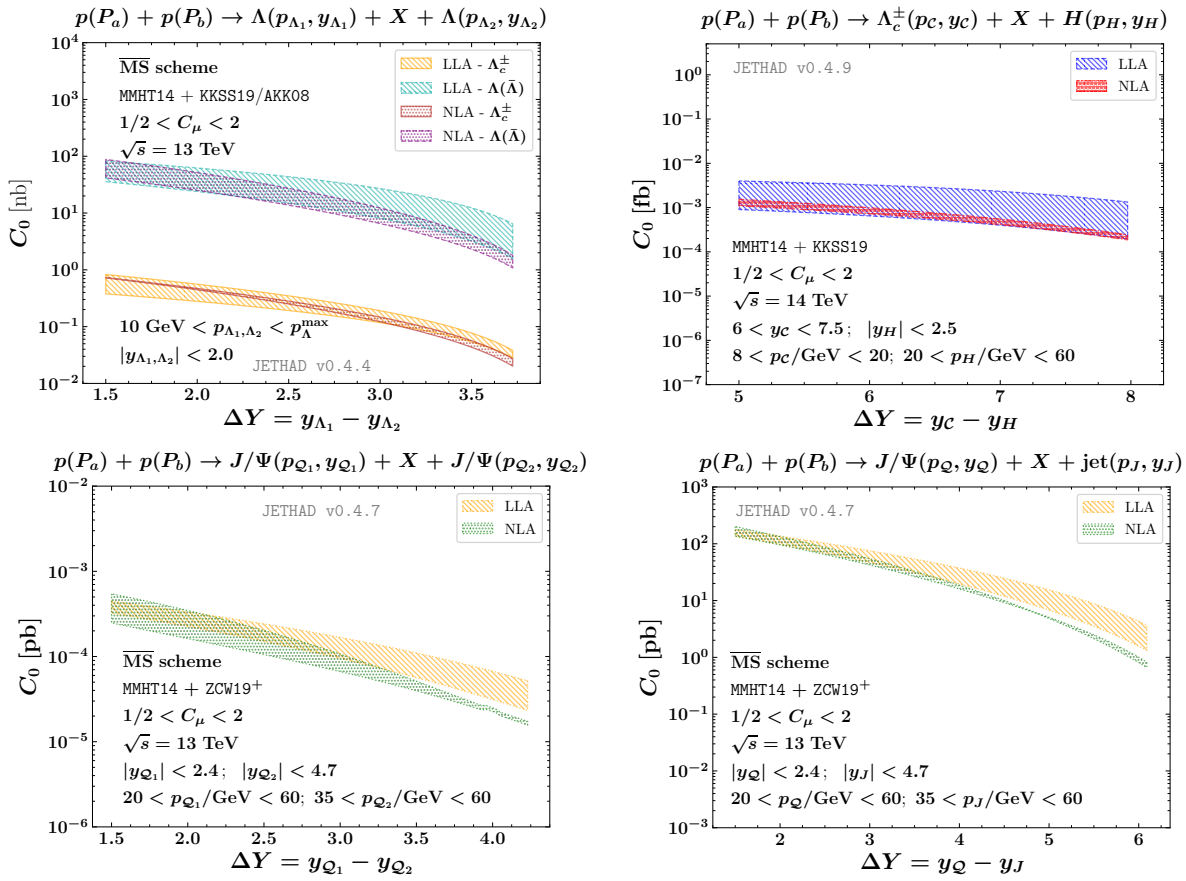

Figure 3.3: Behavior of the φ-summed cross section, C_0, as a function of ΔY, in the double Λ_c channel (upper left panel), in the Λ_c plus Higgs channel (upper right panel), in the double J/ψ (lower left panel) and in the J/ψ plus jet channel (lower right panel). $\sqrt{s} = 14$ for the Λ_c plus Higgs channel and $\sqrt{s} = 14$ in the remaining cases. Predictions for Λ_c emissions are compared with configurations where Λ hyperons are detected. Text boxes inside panels exhibit final-state kinematic cuts.

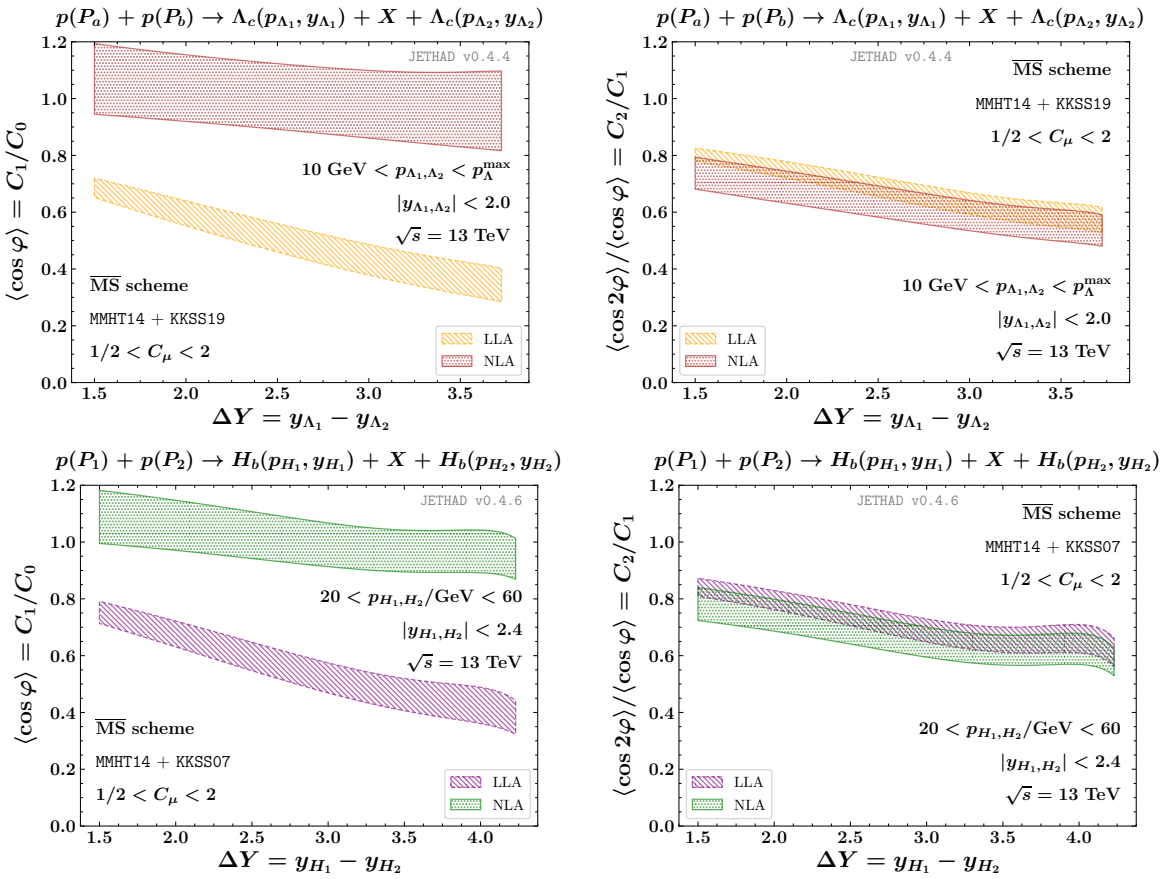

Figure 3.4: Behavior of azimuthal-correlation moments, $R_{nm} \equiv C_n/C_m$, as functions of ΔY, in the double Λ_c channel and in the double H_b channel, at natural scales, and for $\sqrt{s} = 13$ TeV. Text boxes inside panels exhibit final-state kinematic cuts.

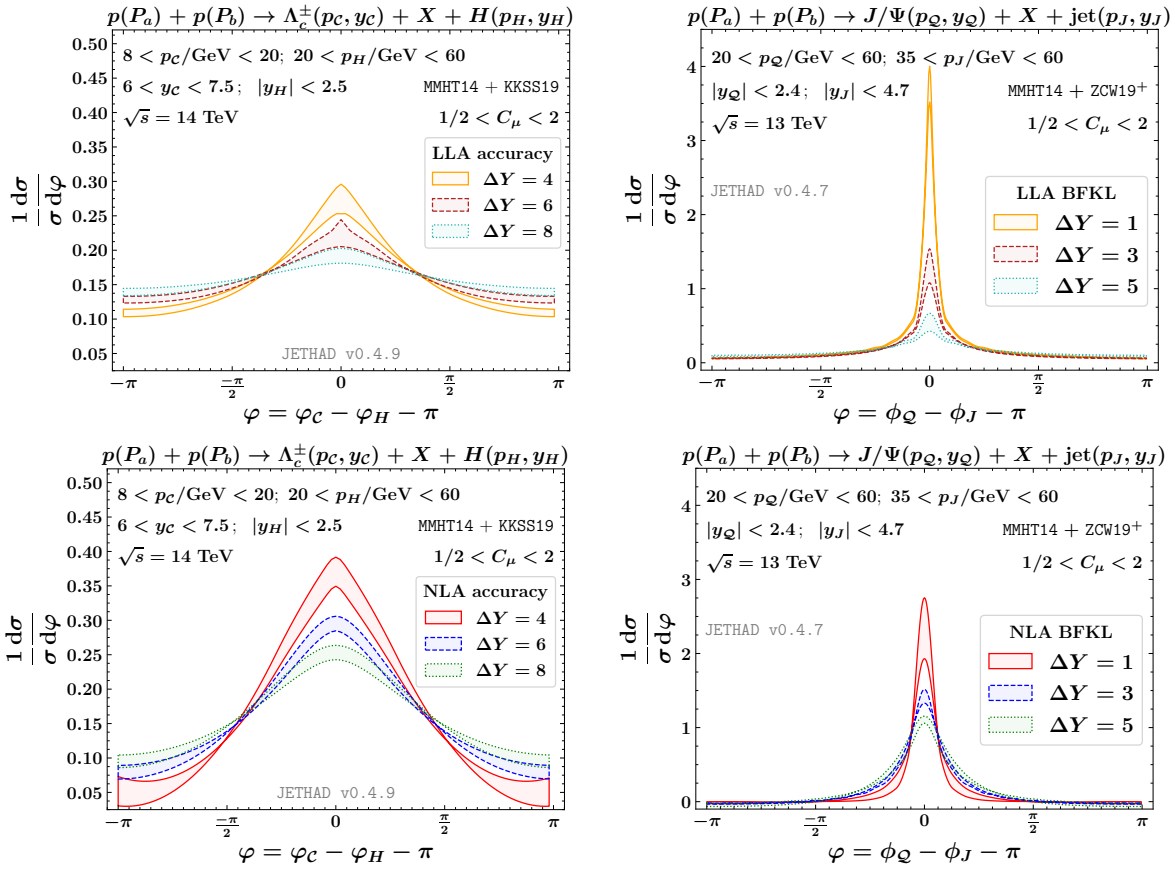

Figure 3.5: LLA (upper panels) and NLA (lower panels) predictions for the φ-distribution in the $\Lambda_c + H$ (left) and in the J/ψ + jet (right) channel, at $\sqrt{s} = 14$ TeV and $\sqrt{s} = 13$ TeV, respectively, and for three distinct values of ΔY. Text boxes inside panels exhibit final-state kinematic cuts.

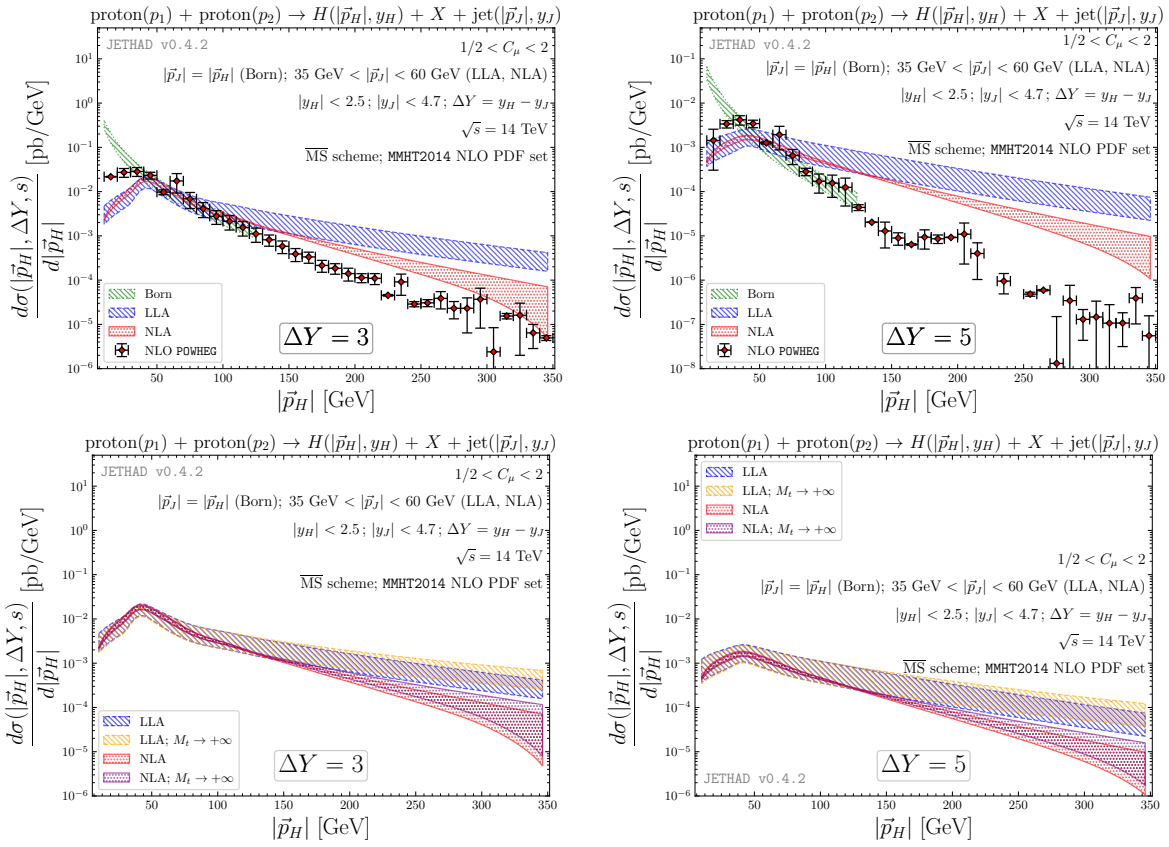

Figure 3.6: p_T-dependence of the cross section for the inclusive Higgs-jet hadroproduction for $\sqrt{s} = 14$ TeV and for $\Delta Y = 3, 5$. In the top panels, resumed predictions are compared to the fixed order result obtained through the POWHEG method. In the bottom panels, predictions in the standard case and in the large top-mass limit are compared. Text boxes inside panels exhibit final-state kinematic cuts.

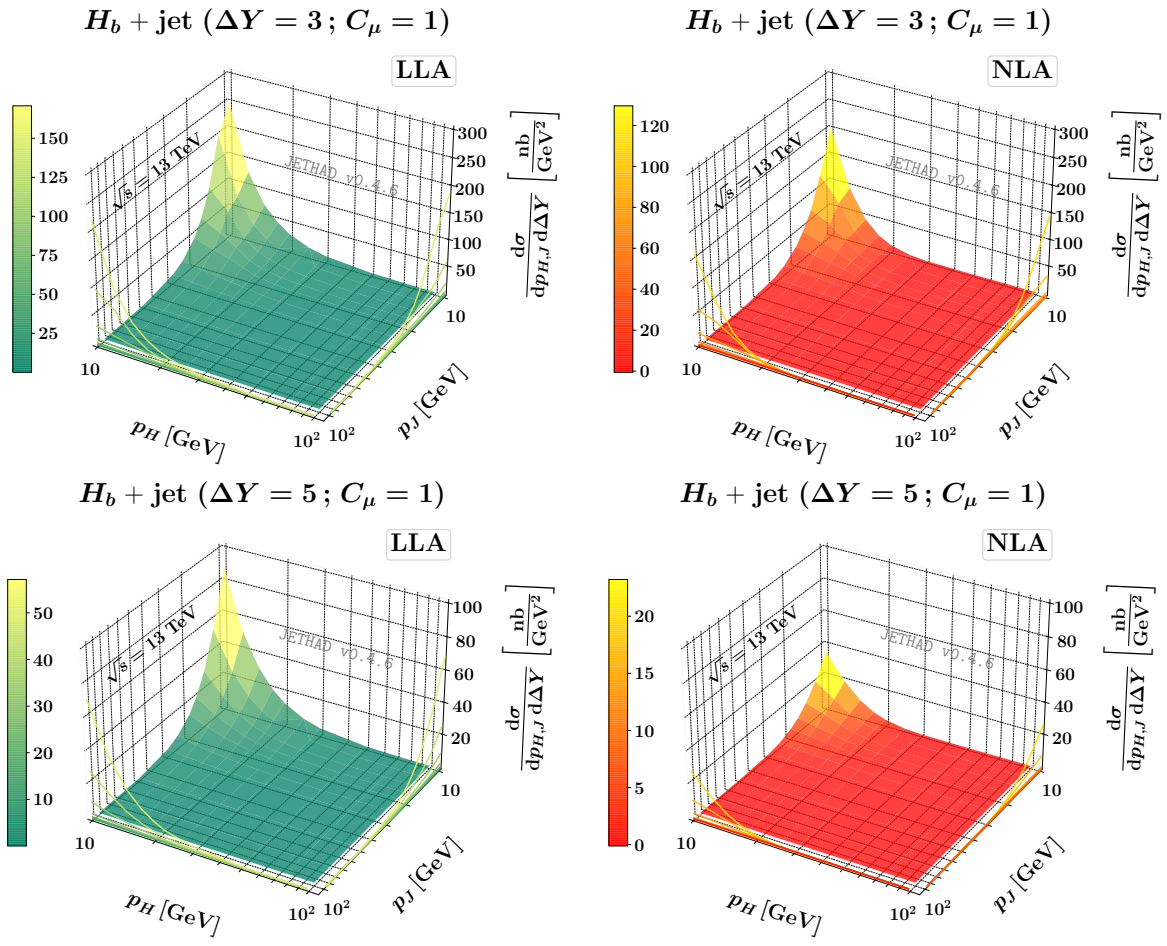

Figure 3.7: Double differential p_T-distribution for the H_b + jet channel at $\Delta Y = 3$ (top) and $\Delta Y = 5$ (bottom), $\sqrt{s} = 13$ TeV, and in the LLA (left) and NLA (right) resummation accuracy.

Part II
Beyond the NLLA

Chapter 4

Lipatov vertex in QCD with higher ϵ-accuracy

How can it be that mathematics, being after all a product of human thought which is independent of experience, is so admirably appropriate to the objects of reality?
Albert Einstein [169]

In this chapter, we deal with the computation of the Lipatov vertex with higher accuracy in the dimensional regularization parameter $\epsilon = (D-4)/2$. There are a number of reasons motivating the need of the NLO Lipatov effective vertex with higher ϵ-accuracy: first, it is the building block of the next-to-NLO contribution to the BFKL kernel from the production of one gluon in the collision of two Reggeons; second, it enters the expression of the impact factors for the Reggeon-gluon transition [170], which appear in the derivation of the bootstrap conditions for inelastic amplitudes; these discontinuities are needed in the derivation of the BFKL equation in the NNLLA; third, the discontinuities of multiple gluon production amplitudes in the MRK can be used [171] for a simple demonstration of violation of the ABDK-BDS (Anastasiou-Bern-Dixon-Kosower — Bern-Dixon-Smirnov) ansatz [172, 173] for amplitudes with maximal helicity violation in Yang-Mills theories with maximal super-symmetry ($\mathcal{N} = 4$ SYM) in the planar limit and for the calculations of the remainder functions to this ansatz. In the planar maximally supersymmetric $\mathcal{N} = 4$ Yang-Mills theory, the Lipatov vertex, within accuracy ϵ^2, has been computed in [174].

The chapter contains four sections. In the first, we briefly discuss the formulation of the BFKL approach in the NNLLA. In the second, we review the derivation of the Lipatov

vertex at one-loop. In the third, we compute the fundamental integrals appearing in the vertex up to the required accuracy. In the third and last section, we summarize and discuss future perspectives. The material of this chapter is based on Refs. [175, 176].

4.1 BFKL beyond NLLA

Extending BFKL beyond the NLLA is an extremely complex task. Let's summarize what we have seen in the previous chapters.

The s-channel discontinuities of the processes $A + B \to A' + B'$ are presented as the convolutions $\Phi_{AA'} \otimes G \otimes \Phi_{BB'}$, where the impact factors $\Phi_{AA'}$ and $\Phi_{BB'}$ describe transitions $A \to A'$ and $B \to B'$ due to interactions with Reggeized gluons and G is the Green's function for two interacting Reggeized gluons. The Mellin transform of the Green function, satisfy the BFKL equation (1.155)

$$\omega \hat{G}_\omega = 1 + \hat{\mathcal{K}} \hat{G}_\omega \ .$$

Energy dependence of scattering amplitudes is determined by the BFKL kernel, which is universal (process independent).
In the LLA, up to the required accuracy,

$$\hat{\mathcal{K}} = \hat{\omega}_1 + \hat{\mathcal{K}}_G^{(0)} \tag{4.1}$$

where $\hat{\omega}_1$ is the one-loop Regge trajectory and $\hat{\mathcal{K}}_G^{(0)}$ is the part of the kernel related to real production of one gluon.
In the NLLA, we can still rely on the previous program of computations, but the kernel, up to the required accuracy, is

$$\hat{\mathcal{K}} = \hat{\omega}_1 + \hat{\omega}_2 + \hat{\mathcal{K}}_G^{(0)} + \hat{\mathcal{K}}_G^{(1)} + \hat{\mathcal{K}}_{GG}^{(0)} + \hat{\mathcal{K}}_{Q\bar{Q}}^{(0)} \ , \tag{4.2}$$

where, in the "virtual" part, we have included the two-loop corrections to the Regge trajectory, while, in the real particle production part, we have included, together with the contribution from the one-gluon production in the RR collisions (this time calculated at one-loop accuracy), contributions from the two-gluon and quark-antiquark productions (these latter computed at Born level).

One might think that this scheme is applicable in the NNLLA as well. In this case it would be sufficient to calculate three-loop corrections to the trajectory, two-loop corrections to $\hat{\mathcal{K}}_G$, one-loop corrections to $\hat{\mathcal{K}}_{Q\bar{Q}}$ and $\hat{\mathcal{K}}_{GG}$ and to find in the Born approximation two new contributions, $\hat{\mathcal{K}}_{Q\bar{Q}G}$ and $\hat{\mathcal{K}}_{GGG}$. Unfortunately, the scheme based on the forms (1.14) and (1.104) does not provide a full resummation in the NNLLA. The reason is the need to take account of the contributions of Regge cuts and the imaginary parts of the amplitudes in the unitarity conditions (1.110).

The main difficult in the extention of BFKL beyond the NLLA is the appearance of three-Reggeon cut which invalidates the forms (1.14) in the NNLLA. This was first shown in [177] when considering the non-logarithmic terms in two-loop amplitudes for elastic scattering. A detailed consideration of the terms responsible for the breaking of the pole-Regge form in two- and three-loop amplitudes was performed in [178, 179, 180]. In [175, 181, 182] it was shown that the observed violation of the pole-Regge form can be explained by the contributions of the three-Reggeon cuts. A procedure for disentangling the Regge cut and Regge pole in QCD in all orders of perturbation theory has been suggested in [183]. Moreover, in deriving BFKL in the LLA, we have not emphasized much that the form of the inelastic amplitudes in Eq. (1.104) is strictly valid only for the real part of the amplitude. The reason is that only the real part is really needed in the LLA and in the NLLA. Indeed, the imaginary parts are suppressed by a power of $\ln s_i$ with respect to the real ones. In the LLA, no logarithm can be "lost" and hence only the real part is important. In the NLLA, in principle, the products of imaginary and real parts in the unitarity relations (1.110) are important, but they cancel due to summation of contributions complex conjugated to each other. In the NNLLA, we can "lose" two large logarithms and hence imaginary parts should be taken into account. At computational level, this is not very complicated since we need imaginary parts just in the main approximation. Nonetheless, this complicates the derivation of the BFKL equation and deprives it of its universality (see Ref. [175] for details).

In the following, as already mentioned, we focus our attention just on the one-loop Lipatov vertex, extending its knowledge in the ϵ-expansion up to the required accuracy for NNLL formulation of BFKL. In fact, the NNLLA formulation of BFKL requires not only two and three-loop calculations, but also higher ϵ-accuracy of the one-loop results. Thus, since the NLO RRG vertex has the singularity $1/\epsilon^2$, it must be known in general

up to terms of order ϵ^2 to ensure the accuracy ϵ^0 in the part of the kernel containing the product of two RRG vertices. Of course, in the region of small transverse momentum $\vec{p}$ of the produced gluon, the accuracy must be higher (ϵ^3). Fortunately, in this region the vertex was obtained in [184] exactly in ϵ.

4.2 Review of the Lipatov vertex at one-loop

4.2.1 The gluon production amplitude

The RRG vertex can be obtained from a generic $A+B \to A'+g+B'$ amplitude taken in MRK and with the gluon emitted in the central kinematical region. In this case we follow the construction in [47] and consider gluon-gluon collision. We will use the denotations p_A and p_B ($p_{A'}$ and $p_{B'}$) for the momenta of the incoming (outgoing) gluons, p and $e(p)$ for momentum and polarization vector of the produced gluon; $q_1 = p_A - p_{A'}$ and $q_2 = p_{B'} - p_B$ are the momentum transfers, so that $p = q_1 - q_2$. The denotations are the same as in [47], except that we use p for the "central" outgoing gluon, instead of k. The MRK kinematics is defined by the relations

$$s \gg s_1, s_2 \gg |t_1| \sim |t_2| \,, \tag{4.3}$$

where

$$s = (p_A + p_B)^2 \,, \qquad s_1 = (p_{A'} + p)^2 \,, \qquad s_2 = (p_{B'} + p)^2 \,, \qquad t_{1,2} = q_{1,2}^2 \,. \tag{4.4}$$

In terms of the parameters of the Sudakov decomposition

$$p = \beta_p \, p_A + \alpha_p \, p_B + p_\perp \,, \qquad\qquad q_i = \beta_i \, p_A + \alpha_i \, p_B + q_{i\perp} \,, \tag{4.5}$$

the relations (4.3) give

$$1 \gg \beta_p \approx \beta_1 \gg -\alpha_1 \simeq \frac{\vec{q}_1^{\,2}}{s} \,, \qquad\qquad 1 \gg \alpha_p \approx -\alpha_2 \gg \beta_2 \simeq \frac{\vec{q}_2^{\,2}}{s} \,,$$

$$s_1 \approx s \, \alpha_p \,, \qquad s_2 \approx s \, \beta_p \,, \qquad \vec{p}^{\,2} = -p_\perp^2 \approx \frac{s_1 s_2}{s} \,. \tag{4.6}$$

Here and below, the vector sign is used for the components of the momenta transverse to the plane of the momenta of the initial particles p_A and p_B.

To extract the RRG vertex, we can restrict ourselves to amplitudes with conservation of the helicities of the scattered gluons. The form of this amplitude is well known:

$$A_{2\to3} = 2s \, g^3 \, T^{c_1}_{A'A} \, \frac{1}{t_1} \, T^d_{c_2 c_1} \, \frac{1}{t_2} \, T^{c_2}_{B'B} \, e^*_\mu(p) \, \mathcal{A}^\mu(q_2, q_1) \,, \tag{4.7}$$

where T^a_{bc} are matrix elements of the colour group generator in the adjoint representation and the amplitude $\mathcal{A}^\mu$ in the Born approximation is equal to $C^\mu(q_2,q_1)$:

$$\mathcal{A}^\mu_{\rm Born} = C^\mu(q_2,q_1) = -{q_1}^\mu_\perp - {q_2}^\mu_\perp + \frac{p_A^\mu}{s_1}\,(\vec{p}^{\,2} - 2\vec{q}_1^{\,2}) - \frac{p_B^\mu}{s_2}\,(\vec{p}^{\,2} - 2\vec{q}_2^{\,2})\;. \tag{4.8}$$

It was shown in [39] that at one-loop order the amplitude can be presented in its gauge invariant form,

$$\mathcal{A}^\mu = C^\mu(q_2,q_1)(1+\bar{g}^2 r_C) + \mathcal{P}^\mu \bar{g}^2\, 2t_1 t_2\, r_{\mathcal{P}}\;, \tag{4.9}$$

where the terms proportional to p^μ were obviously omitted and

$$\bar{g} = \frac{N g^2 \Gamma(1-\epsilon)}{(4\pi)^{2+\epsilon}}\;,$$

$$\mathcal{P}^\mu = \frac{p_A^\mu}{s_1} - \frac{p_B^\mu}{s_2}\;,$$

$$\begin{aligned}
r_C = \Bigg\{ & t_1 t_2 \left(r_+ + \frac{\mathcal{F}_5}{2}\right) + t_2 \mathcal{I}_{4B} + \frac{\Gamma^2(\epsilon)}{\Gamma(2\epsilon)} (\vec{q}_1^{\,2})^\epsilon \left[-\frac{1}{2}\ln\left(\frac{s_1(-s_1)}{t_1^2}\right) + 2\psi(\epsilon) - \psi(2\epsilon) \right. \\
& \left. - \psi(1-\epsilon) + \frac{1}{2\epsilon(1+2\epsilon)(3+2\epsilon)} \left(-3(1+\epsilon) - \frac{\epsilon^2}{1+\epsilon} + \frac{t_1(3+14\epsilon+8\epsilon^2) - t_2(3+3\epsilon+\epsilon^2)}{t_1 - t_2} \right.\right. \\
& \left.\left. + \frac{\vec{p}^{\,2}\, t_1\, \epsilon}{(t_1-t_2)^3} \Big((2+\epsilon) t_2 - \epsilon\, t_1 \Big) \right] \Bigg\} + \Big\{ A \longleftrightarrow B \Big\}\;,
\end{aligned}$$

$$\begin{aligned}
r_{\mathcal{P}} = \Bigg\{ & (\vec{q}_1 \cdot \vec{q}_2) r_+ - \frac{t_1+t_2}{4}\mathcal{F}_5 - \frac{\mathcal{I}_{4B}}{2} + \frac{1}{2}\frac{\Gamma^2(\epsilon)}{\Gamma(2\epsilon)} (\vec{q}_1^{\,2})^{\epsilon-1} \left(-\frac{1}{2}\ln\left(\frac{s_1(-s_1)s_2(-s_2)}{s(-s)t_1^2}\right) + \psi(1) \right. \\
& \left. + \psi(\epsilon) - \psi(1-\epsilon) - \psi(2\epsilon) + \frac{t_1}{t_2\,(1+2\epsilon)(3+2\epsilon)} \left[\frac{t_2}{t_1-t_2}(11+7\epsilon) \right.\right. \\
& \left.\left. + \frac{\vec{p}^{\,2}}{(t_1-t_2)^3} \Big(t_2(t_1+t_2) - \epsilon\, t_1(t_1-t_2) \Big) + \frac{(\vec{p}^{\,2})^2}{(t_1-t_2)^3} \Big((2+\epsilon)t_2 - \epsilon\, t_1 \Big) \right] \right) \Bigg\} + \Big\{ A \longleftrightarrow B \Big\}.
\end{aligned} \tag{4.10}$$

The expression for the function r_+ appearing in the definition of $\mathcal{A}^\mu$ is

$$r_+ = \frac{f_-(\vec{q}_1^{\,2} - \vec{q}_2^{\,2}) - f_+ \vec{p}^{\,2}}{8(\vec{q}_1^{\,2}\vec{q}_2^{\,2} - (\vec{q}_1\vec{q}_2)^2)}\;, \tag{4.11}$$

with

$$\begin{aligned}
f_- \equiv & \left[-t_1\mathcal{F}_5 - \mathcal{I}_{4B} - \frac{\Gamma^2(\epsilon)}{\Gamma(2\epsilon)} (\vec{q}_2^{\,2})^{\epsilon-1} \left(\frac{1}{2}\ln\left(\frac{s_1(-s_1)s_2(-s_2)}{s(-s)t_2^2}\right) \right.\right. \\
& \left.\left. + \psi(1-\epsilon) - \psi(\epsilon) + \psi(2\epsilon) - \psi(1) \right) \right] - \Big[A \longleftrightarrow B \Big]\;,
\end{aligned} \tag{4.12}$$

$$f_+ \equiv \left\{ -t_1\mathcal{F}_5 - \mathcal{I}_{4B} - \frac{\Gamma^2(\epsilon)}{\Gamma(2\epsilon)} \left[(\vec{q}_2^{\,2})^{\epsilon-1} \left(\frac{1}{2}\ln\left(\frac{s_1(-s_1)s_2(-s_2)}{s(-s)t_2^2}\right) \right.\right.\right.$$

$$+\psi(1-\epsilon)-\psi(\epsilon)+\psi(2\epsilon)-\psi(1)\Big)$$

$$-(\vec{p}^{\,2})^{\epsilon-1}\left(\frac{1}{2}\ln\left(\frac{s_1(-s_1)s_2(-s_2)}{s(-s)(\vec{p}^{\,2})^2}\right)+\psi(1-\epsilon)-\psi(\epsilon)\right)\Bigg]\Bigg\}+\Big\{A\longleftrightarrow B\Big\}\,, \tag{4.13}$$

and

$$\mathcal{F}_5=\mathcal{I}_5-\mathcal{L}_3-\frac{1}{2}\ln\left(\frac{s(-s)(\vec{p}^{\,2})^2}{s_1(-s_1)s_2(-s_2)}\right)\mathcal{I}_3\,. \tag{4.14}$$

The total amplitude is given in terms of five structures $\mathcal{I}_3$, $\mathcal{L}_3$, $\mathcal{I}_{4B}$, $\mathcal{I}_{4A}$, $\mathcal{I}_5$, defined as [47]

$$\mathcal{I}_3=\int\frac{d^{2+2\epsilon}k}{\pi^{1+\epsilon}\Gamma(1-\epsilon)}\frac{1}{\vec{k}^{\,2}(\vec{k}-\vec{q}_1)^2(\vec{k}-\vec{q}_2)^2}\,, \tag{4.15}$$

$$\mathcal{L}_3=\int\frac{d^{2+2\epsilon}k}{\pi^{1+\epsilon}\Gamma(1-\epsilon)}\frac{1}{\vec{k}^{\,2}(\vec{k}-\vec{q}_1)^2(\vec{k}-\vec{q}_2)^2}\left[\ln\left(\frac{(\vec{k}-\vec{q}_1)^2(\vec{k}-\vec{q}_2)^2}{\vec{k}^{\,2}(\vec{q}_1-\vec{q}_2)^{\,2}}\right)\right]\,, \tag{4.16}$$

$$\mathcal{I}_{4B}=\int_0^1\frac{dx}{x}\int\frac{d^{2+2\epsilon}k}{\pi^{1+\epsilon}\Gamma(1-\epsilon)}$$

$$\times\left[\frac{1-x}{\Big(x\vec{k}^2+(1-x)(\vec{k}-\vec{q}_1)^2\Big)\,(\vec{k}-(1-x)(\vec{q}_1-\vec{q}_2))^2}-\frac{1}{(\vec{k}-\vec{q}_1)^2(\vec{k}-(\vec{q}_1-\vec{q}_2))^2}\right]\,, \tag{4.17}$$

$$\mathcal{I}_5=\int_0^1\frac{dx}{1-x}\int\frac{d^{2+2\epsilon}k}{\pi^{1+\epsilon}\Gamma(1-\epsilon)}\frac{1}{\vec{k}^{\,2}[(1-x)\vec{k}^{\,2}+x(\vec{k}-\vec{q}_1)^2]}$$

$$\times\left[\frac{x^2}{(\vec{k}-x(\vec{q}_1-\vec{q}_2))^2}-\frac{1}{(\vec{k}-\vec{q}_1+\vec{q}_2)^2}\right] \tag{4.18}$$

and $\mathcal{I}_{4A}=\mathcal{I}_{4B}(\vec{q}_1\leftrightarrow-\vec{q}_2)$.

4.2.2 The Lipatov vertex

Imposing general requirements of analyticity, unitarity and crossing symmetry, the production amplitude must take the Regge the form [39, 185]

$$8\,g^3\,\mathcal{A}^\mu=\Gamma(t_1;\vec{p}^{\,2})\Gamma(t_2;\vec{p}^{\,2})\left\{\left[\left(\frac{s_1}{\vec{p}^{\,2}}\right)^{\omega_1-\omega_2}+\left(\frac{-s_1}{\vec{p}^{\,2}}\right)^{\omega_1-\omega_2}\right]\left[\left(\frac{s}{\vec{p}^{\,2}}\right)^{\omega_2}+\left(\frac{-s}{\vec{p}^{\,2}}\right)^{\omega_2}\right]\,R^\mu\right.$$

$$\left.+\left[\left(\frac{s_2}{\vec{p}^{\,2}}\right)^{\omega_2-\omega_1}+\left(\frac{-s_2}{\vec{p}^{\,2}}\right)^{\omega_2-\omega_1}\right]\left[\left(\frac{s}{\vec{p}^{\,2}}\right)^{\omega_1}+\left(\frac{-s}{\vec{p}^{\,2}}\right)^{\omega_1}\right]\,L^\mu\right\}\,, \tag{4.19}$$

where $\omega_i=\omega(t_i)$ (we have chosen $\vec{p}^{\,2}$ as the scale of energy), $\Gamma(t_i;\vec{p}^{\,2})$ are the helicity conserving gluon-gluon-Reggeon vertices, R^μ and L^μ are the right and left RRG vertices, depending on $\vec{q}_1$ and $\vec{q}_2$. They are real in all physical channels, as well as $\Gamma(t_i;\vec{p}^{\,2})$.

In the one-loop approximation we have

$$\omega(t) = \omega^{(1)}(t) = -\overline{g}^2 \frac{\Gamma^2(\epsilon)}{\Gamma(2\epsilon)} (\vec{q}^{\,2})^{\epsilon} \,, \tag{4.20}$$

$$\Gamma(t;\vec{p}^{\,2}) = g\left(1 + \Gamma^{(1)}(t;\vec{p}^{\,2})\right) \,, \tag{4.21}$$

where

$$\Gamma^{(1)}(t;\vec{p}^{\,2}) = \overline{g}^2 \frac{\Gamma^2(\epsilon)}{\Gamma(2\epsilon)} (\vec{q}^{\,2})^{\epsilon} \left[\psi(\epsilon) - \frac{1}{2}\psi(1) - \frac{1}{2}\psi(1-\epsilon) \right.$$
$$\left. + \frac{9(1+\epsilon)^2 + 2}{4(1+\epsilon)(1+2\epsilon)(3+2\epsilon)} - \frac{1}{2}\ln\left(\frac{\vec{p}^{\,2}}{\vec{q}^{\,2}}\right)\right] \,. \tag{4.22}$$

In the same approximation we obtain from (4.19)

$$2g\left\{\mathcal{A}^{\mu} - C^{\mu}(q_2,q_1)\left[\Gamma^{(1)}(t_1;\vec{p}^{\,2}) + \Gamma^{(1)}(t_2;\vec{p}^{\,2}) + \frac{\omega_1}{2}\ln\left(\frac{s_1(-s_1)}{(\vec{p}^{\,2})^2}\right) + \frac{\omega_2}{2}\ln\left(\frac{s_2(-s_2)}{(\vec{p}^{\,2})^2}\right)\right.\right.$$
$$\left.\left. + \frac{\omega_1+\omega_2}{4}\ln\left(\frac{s(-s)(\vec{p}^{\,2})^2}{s_1(-s_1)s_2(-s_2)}\right)\right]\right\} = R^{\mu} + L^{\mu} + (R^{\mu} - L^{\mu})\frac{\omega_1 - \omega_2}{4}\ln\left(\frac{s_1(-s_1)s_2(-s_2)}{s(-s)(\vec{p}^{\,2})^2}\right) . \tag{4.23}$$

Since in all physical channels

$$\ln\left(\frac{s_1(-s_1)s_2(-s_2)}{s(-s)(\vec{p}^{\,2})^2}\right) = i\pi \,, \tag{4.24}$$

the combinations $R^{\mu} + L^{\mu}$ and $R^{\mu} - L^{\mu}$ are respectively related to the real and imaginary parts of the production amplitude. Using this we find that

$$R^{\mu} + L^{\mu} = 2g\left\{C^{\mu}(q_2,q_1) + \overline{g}^2\left(\frac{(\vec{q}_1\cdot\vec{q}_2)C^{\mu}(q_2,q_1) + 2\vec{q}_1^{\,2}\vec{q}_2^{\,2}\mathcal{P}^{\mu}}{2(\vec{q}_1^{\,2}\vec{q}_2^{\,2} - (\vec{q}_1\cdot\vec{q}_2)^2)}\left[\frac{\vec{q}_1^{\,2}\vec{q}_2^{\,2}\vec{p}^{\,2}}{2}(\mathcal{I}_5 - \mathcal{L}_3)\right.\right.\right.$$
$$-\vec{q}_2^{\,2}(\vec{q}_1\cdot\vec{p})\,\mathcal{I}_{4B} + \frac{\Gamma^2(\epsilon)}{\Gamma(2\epsilon)}\left(\frac{(\vec{p}^{\,2})^{\epsilon}}{2}(\vec{q}_1\cdot\vec{q}_2)\,(\psi(\epsilon) - \psi(1-\epsilon)) + (\vec{q}_1^{\,2})^{\epsilon}(\vec{q}_2\cdot\vec{p})\left(\ln\left(\frac{\vec{p}^{\,2}}{\vec{q}_1^{\,2}}\right) - \psi(1)\right.\right.$$
$$\left.\left.\left.\left.-\psi(\epsilon) + \psi(1-\epsilon) + \psi(2\epsilon)\right)\right)\right] + C^{\mu}(q_2,q_1)\left[-\frac{\vec{q}_2^{\,2}}{2}\mathcal{I}_{4B} + \frac{\Gamma^2(\epsilon)}{2\Gamma(2\epsilon)}\left(\frac{(\vec{p}^{\,2})^{\epsilon}}{2}(\psi(\epsilon) - \psi(1-\epsilon))\right.\right.$$
$$+(\vec{q}_1^{\,2})^{\epsilon}\left[\psi(\epsilon) - \psi(2\epsilon) + \frac{1}{2(1+2\epsilon)(3+2\epsilon)}\left(\frac{\vec{q}_1^{\,2} + \vec{q}_2^{\,2}}{\vec{q}_1^{\,2} - \vec{q}_2^{\,2}}(11+7\epsilon) + 2\epsilon\frac{\vec{p}^{\,2}\vec{q}_1^{\,2}}{(\vec{q}_1^{\,2} - \vec{q}_2^{\,2})^2}\right.\right.$$
$$\left.\left.\left.\left.-4\frac{\vec{p}^{\,2}\vec{q}_1^{\,2}\vec{q}_2^{\,2}}{(\vec{q}_1^{\,2} - \vec{q}_2^{\,2})^3}\right)\right]\right)\right] + \mathcal{P}^{\mu}\frac{\Gamma^2(\epsilon)(\vec{q}_1^{\,2})^{\epsilon}}{\Gamma(2\epsilon)(1+2\epsilon)(3+2\epsilon)}\left[\frac{\vec{q}_1^{\,2}\vec{q}_2^{\,2}}{\vec{q}_1^{\,2} - \vec{q}_2^{\,2}}(11+7\epsilon) + \epsilon\vec{p}^{\,2}\vec{q}_1^{\,2}\frac{\vec{q}_1^{\,2} - \vec{p}^{\,2}}{(\vec{q}_1^{\,2} - \vec{q}_2^{\,2})^2}\right.$$
$$\left.\left.\left.-\vec{p}^{\,2}\vec{q}_1^{\,2}\vec{q}_2^{\,2}\frac{\vec{q}_1^{\,2} + \vec{q}_2^{\,2} - 2\vec{p}^{\,2}}{(\vec{q}_1^{\,2} - \vec{q}_2^{\,2})^3}\right]\right) - \overline{g}^2\,(A \longleftrightarrow B)\right\} \tag{4.25}$$

and

$$R^\mu - L^\mu = \frac{2g\overline{g}^2}{\omega_1-\omega_2}\left\{-C^\mu(q_2,q_1)\frac{\Gamma^2(\epsilon)}{\Gamma(2\epsilon)}(\vec{p}^{\,2})^\epsilon + \frac{(\vec{q}_1\cdot\vec{q}_2)C^\mu(q_2,q_1)+2\vec{q}_1^{\,2}\vec{q}_2^{\,2}\mathcal{P}^\mu}{\vec{q}_1^{\,2}\vec{q}_2^{\,2}-(\vec{q}_1\cdot\vec{q}_2)^2}\right.$$

$$\left.\times\left[\vec{q}_1^{\,2}\vec{q}_2^{\,2}\vec{p}^{\,2}\mathcal{I}_3+\frac{\Gamma^2(\epsilon)}{\Gamma(2\epsilon)}\left((\vec{q}_1^{\,2})^\epsilon(\vec{q}_2\cdot\vec{p})-(\vec{q}_2^{\,2})^\epsilon(\vec{q}_1\cdot\vec{p})-(\vec{p}^{\,2})^\epsilon(\vec{q}_1\cdot\vec{q}_2)\right)\right]\right\}\,. \tag{4.26}$$

It is clear that, in order to know the Lipatov vertex at a certain order in the ϵ-expansion, we must calculate the integrals $\mathcal{I}_3$, $\mathcal{I}_{4A}$, $\mathcal{I}_{4B}$, and $\mathcal{I}_5-\mathcal{L}_3$ with the same accuracy.

In the region of small momenta of the central emitted gluon (the *soft region*, from now on) the vertex must be known to all orders in ϵ. The soft limit of integrals entering the vertex are computed in appendix C.4. By using Eqs. (C.45), (C.48) and (C.50), we easily find

$$R^\mu + L^\mu = 2gC^\mu(q_2,q_1)\left(1+\overline{g}^2\frac{\Gamma^2(\epsilon)}{2\Gamma(2\epsilon)}(\vec{p}^{\,2})^\epsilon\left[\psi(\epsilon)-\psi(1-\epsilon)\right]\right), \tag{4.27}$$

$$R^\mu - L^\mu = -\frac{2g\overline{g}^2}{\omega_1-\omega_2}C^\mu(q_2,q_1)\frac{\Gamma^2(\epsilon)}{\Gamma(2\epsilon)}(\vec{p}^{\,2})^\epsilon\,. \tag{4.28}$$

The last two equation confirm the result in [184, 186].

4.3 Fundamental integrals for the one-loop RRG vertex

In this section we present the result at ϵ^2-accuracy of the integrals in the transverse momentum space entering the one-loop RRG vertex, expanding expressions already available in the literature and, whenever possible, cross-checking them with an alternative calculation.

4.3.1 $\mathcal{I}_3$: Bern-Dixon-Kosower (BDK) method

We start from the integral

$$\mathcal{I}_3' \equiv \pi^{1+\epsilon}\Gamma(1-\epsilon)\,\mathcal{I}_3$$

$$= \int d^{2+2\epsilon}k\frac{1}{\vec{k}^2(\vec{k}-\vec{q}_1)^2(\vec{k}-\vec{q}_2)^2} = \int d^{2+2\epsilon}k_E\frac{1}{k_E^2(k_E-q_{1E})^2(k_E-q_{2E})^2}\,, \tag{4.29}$$

where k_E, q_{1E}, q_{2E} are Euclidean vectors in dimension $2+2\epsilon$ and $q_{1E}^2, q_{2E}^2, (q_{1E}-q_{2E})^2 \neq 0$. We can relate this Euclidean integral to a corresponding Minkowskian integral by Wick

rotation:

$$\int d^{2+2\epsilon}k_E \frac{1}{k_E^2(k_E-q_{1E})^2(k_E-q_{2E})^2} = i\int d^{2+2\epsilon}k \frac{1}{k^2(k-q_1)^2(k-q_2)^2} \ , \tag{4.30}$$

where $k=(ik_E^0,k_E^1)$, $q_1=(iq_{1E}^0,q_{1E}^1)$, $q_2=(iq_{2E}^0,q_{2E}^1)$. We note that

$$q_1^{\ 2}=-q_{1E}^2=-\vec{q}_1^{\,2}, \quad q_2^{\ 2}=-q_{2E}^2=-\vec{q}_2^{\,2} \ , \quad (q_1-q_2)^2=-(q_{1E}-q_{2E})^2=-(\vec{q}_1-\vec{q}_2)^{\,2}=-\vec{p}^{\,2}. \tag{4.31}$$

Hence, we need a triangular integral with three massive external legs. This result to all order in ϵ-expansion can be found in [187], taking care to apply the replacement $(\epsilon\to-\epsilon+1)$, because they calculated the integral in $d^{4-2\epsilon}k$, instead we need it in $d^{2+2\epsilon}k$. One finds that

$$\mathcal{I}_3' = \pi^{1+\epsilon}\alpha_1\alpha_2\alpha_3\left(-\frac{1}{2}\frac{\Gamma(2-\epsilon)\Gamma^2(\epsilon)}{\Gamma(2\epsilon-1)}\right)\frac{\hat{\Delta}_3^{1/2-\epsilon}}{(1-\epsilon)^2}\left[f\left(\delta_1\right)+f\left(\delta_2\right)+f\left(\delta_3\right)+c\right] \ , \tag{4.32}$$

where

$$\alpha_1=\sqrt{\frac{\vec{q}_2^{\,2}}{\vec{q}_1^{\,2}(\vec{q}_1-\vec{q}_2)^2}} \ , \quad \alpha_2=\sqrt{\frac{(\vec{q}_1-\vec{q}_2)^2}{\vec{q}_1^{\,2}\vec{q}_2^{\,2}}} \ , \quad \alpha_3=\sqrt{\frac{\vec{q}_1^{\,2}}{\vec{q}_2^{\,2}(\vec{q}_1-\vec{q}_2)^2}} \ , \tag{4.33}$$

$$\gamma_1=-\alpha_1+\alpha_2+\alpha_3 \ , \quad \gamma_2=\alpha_1-\alpha_2+\alpha_3 \ , \quad \gamma_3=\alpha_1+\alpha_2-\alpha_3 \ , \tag{4.34}$$

$$\delta_1=\frac{\gamma_1}{\sqrt{\hat{\Delta}_3}} \ , \quad \delta_2=\frac{\gamma_2}{\sqrt{\hat{\Delta}_3}} \ , \quad \delta_3=\frac{\gamma_3}{\sqrt{\hat{\Delta}_3}} \ , \tag{4.35}$$

$$\hat{\Delta}_3=-\alpha_1^2-\alpha_2^2-\alpha_3^2+2\alpha_1\alpha_2+2\alpha_2\alpha_3+2\alpha_1\alpha_3 \ , \tag{4.36}$$

$$c=-2\pi(1-\epsilon)\frac{\Gamma(2\epsilon-1)}{\Gamma^2(\epsilon)} \ , \tag{4.37}$$

$$\begin{aligned} f\left(\delta\right)=&\frac{1}{i}\left[\left(\frac{1+i\delta}{1-i\delta}\right)^{1-\epsilon}\ {}_2F_1\left(2-2\epsilon,1-\epsilon,2-\epsilon;-\left(\frac{1+i\delta}{1-i\delta}\right)\right)\right.\\ &\left.-\left(\frac{1-i\delta}{1+i\delta}\right)^{1-\epsilon}\ {}_2F_1\left(2-2\epsilon,1-\epsilon,2-\epsilon;-\left(\frac{1-i\delta}{1+i\delta}\right)\right)\right] \ . \end{aligned} \tag{4.38}$$

Using the expansion (C.11) and the definitions

$$z_i=-\left(\frac{1+i\delta_i}{1-i\delta_i}\right) \ , \tag{4.39}$$

we find

$$\mathcal{I}_3' = \pi^{1+\epsilon}\Gamma(1-\epsilon)\alpha_1\alpha_2\alpha_3\hat{\Delta}_3^{1/2-\epsilon}\frac{\Gamma^2(1+\epsilon)}{\Gamma(1+2\epsilon)}\frac{(1-2\epsilon)}{(1-\epsilon)}\left\{\frac{\alpha_1+\alpha_2+\alpha_3}{\sqrt{\hat{\Delta}_3}\epsilon}+\left(\pi+\sum_{i=1}^{3}\left[\frac{i\ z_i}{1-z_i}\right.\right.\right.$$

$$\times\left(1-\ln\left(-z_i\right)+\frac{1+z_i}{z_i}\ln\left(1-z_i\right)\right)-\left(z_i\to z_i^{-1}\right)\Bigg]\Bigg)+\Bigg(\pi+\sum_{i=1}^{3}\Bigg[\frac{i\,z_i}{1-z_i}$$
$$\times\left(2+\left(\frac{1+z_i}{z_i}\right)\ln\left(1-z_i\right)\ln\left((1-z_i)e\right)+\frac{1}{2}\ln^2\left(-z_i\right)-\frac{1-z_i}{z_i}\mathrm{Li}_2\left(z_i\right)\right.$$
$$\left.-\ln\left(-z_i\right)\left(1+\frac{1+z_i}{z_i}\ln\left(1-z_i\right)\right)\right)-\left(z_i\to z_i^{-1}\right)\Bigg]\Bigg)\epsilon+\Bigg(\pi(2+\zeta(2))$$
$$+\sum_i^3\Bigg[\frac{i\,z_i}{1-z_i}\Bigg(4+\ln(1-z_i)\Bigg(\frac{2(1+z_i)}{z_i}+\frac{2(1-z_i)}{z_i}\zeta(2)+\frac{\ln(1-z_i)}{3z_i}\big(3(1+z_i)$$
$$+2(1+z_i)\ln(1-z_i)-3(1-z_i)\ln z_i\big)-\frac{(1-z_i)}{z_i}(1+2\ln(1-z_i))\mathrm{Li}_2(z_i)-\frac{2(1-z_i)}{z_i}$$
$$\times\left(\mathrm{Li}_3(1-z_i)+\frac{\mathrm{Li}_3(z_i)}{2}-\zeta(3)\right)-\frac{\ln^3(-z_i)}{6}+\frac{\ln^2(-z_i)}{2}\left(1+\left(\frac{1+z_i}{z_i}\right)\ln(1-z_i)\right)$$
$$-\ln(-z_i)\left(2+\left(\frac{1+z_i}{z_i}\right)\ln\left(1-z_i\right)\ln\left((1-z_i)e\right)-\frac{1-z_i}{z_i}\mathrm{Li}_2\left(z_i\right)\right)\Bigg)-\left(z_i\to z_i^{-1}\right)\Bigg]\Bigg)\epsilon^2\Bigg\}\,. \tag{4.40}$$

Please note that $\delta_i\to-\delta_i$ is equivalent to $z_i\to z_i^{-1}$. We also observe that $\alpha_2=\alpha_1(\vec{q}_2\leftrightarrow\vec{q}_1-\vec{q}_2)$ and $\alpha_3=\alpha_1(\vec{q}_1\leftrightarrow\vec{q}_2)$. From this we realize that the second and the third term of the summation can be obtained from the first by two simple substitutions. We can rewrite:

$$\mathcal{I}_3'=\pi^{1+\epsilon}\Gamma(1-\epsilon)\alpha_1\alpha_2\alpha_3\hat{\Delta}_3^{1/2-\epsilon}\frac{\Gamma^2(1+\epsilon)}{\Gamma(1+2\epsilon)}\frac{(1-2\epsilon)}{(1-\epsilon)}\hat{\mathcal{S}}\Bigg\{\frac{\alpha_1}{\sqrt{\hat{\Delta}_3}\epsilon}+\Bigg(\pi+\Bigg[\frac{i\,z_1}{1-z_1}\left(1-\ln\left(-z_1\right)\right.$$
$$\left.+\frac{1+z_1}{z_1}\ln\left(1-z_1\right)\right)-\left(z_1\to z_1^{-1}\right)\Bigg]\Bigg)+\Bigg(\pi+\Bigg[\frac{i\,z_1}{1-z_1}\left(2+\left(\frac{1+z_1}{z_1}\right)\ln\left(1-z_1\right)\ln\left((1-z_1)e\right)\right.$$
$$\left.+\frac{1}{2}\ln^2\left(-z_1\right)-\frac{1-z_1}{z_1}\mathrm{Li}_2\left(z_1\right)-\ln\left(-z_1\right)\left(1+\frac{1+z_1}{z_1}\ln\left(1-z_1\right)\right)\right)-\left(z_1\to z_1^{-1}\right)\Bigg]\Bigg)\epsilon$$
$$+\Bigg(\pi(2+\zeta(2))+\Bigg[\frac{i\,z_1}{1-z_1}\Bigg(4+\ln(1-z_1)\Bigg(\frac{2(1+z_1)}{z_1}+\frac{2(1-z_1)}{z_1}\zeta(2)+\frac{\ln(1-z_1)}{3z_1}$$
$$\times\Bigg(3(1+z_1)+2(1+z_1)\ln(1-z_1)-3(1-z_1)\ln z_1\Bigg)\Bigg)-\frac{(1-z_1)}{z_1}(1+2\ln(1-z_1))\mathrm{Li}_2(z_1)$$
$$-\frac{2(1-z_1)}{z_1}\left(\mathrm{Li}_3(1-z_1)+\frac{\mathrm{Li}_3(z_1)}{2}-\zeta(3)\right)-\frac{\ln^3(-z_1)}{6}+\frac{\ln^2(-z_1)}{2}\left(1+\left(\frac{1+z_1}{z_1}\right)\ln(1-z_1)\right)$$
$$-\ln(-z_1)\left(2+\left(\frac{1+z_1}{z_1}\right)\ln\left(1-z_1\right)\ln\left((1-z_1)e\right)-\frac{1-z_1}{z_1}\mathrm{Li}_2\left(z_1\right)\right)-\left(z_1\to z_1^{-1}\right)\Bigg]\Bigg)\epsilon^2\Bigg\}\,, \tag{4.41}$$

where the operator $\hat{S}$ acts on a generic function $f(\vec{q}_1^{\,2},\vec{q}_2^{\,2},\vec{p}^{\,2})$ as

$$\hat{S}\left\{f\left(\vec{q}_1^{\,2},\vec{q}_2^{\,2},\vec{p}^{\,2}\right)\right\}=f\left(\vec{q}_1^{\,2},\vec{q}_2^{\,2},\vec{p}^{\,2}\right)+f\left(\vec{q}_1^{\,2},\vec{p}^{\,2},\vec{q}_2^{\,2}\right)+f\left(\vec{q}_2^{\,2},\vec{q}_1^{\,2},\vec{p}^{\,2}\right)\,. \tag{4.42}$$

4.3.2 $\mathcal{I}_3$: Alternative calculation

We verify the previous result through a different calculation procedure. We introduce the Feynman parametrization to get

$$\mathcal{I}_3 = (1-\epsilon)\int_0^1 dx \int_0^1 dy \frac{y^{\epsilon-1}}{(A-By)^{2-\epsilon}} \,, \tag{4.43}$$

where $A = x\vec{q}_1^{\,2} + (1-x)\vec{q}_2^{\,2}$ and $B = A - x(1-x)\vec{p}^{\,2}$. Now, it is convenient to perform the decomposition

$$\begin{aligned}\int_0^1 dx \int_0^1 dy \frac{y^{\epsilon-1}}{(A-By)^{2-\epsilon}} &= \int_0^1 dy \frac{y^{\epsilon}}{(A-By)^{-\epsilon}} \left[\frac{1/A^2}{y} + \frac{B/A^2}{A-By} + \frac{B/A}{(A-By)^2}\right] \\ &= \int_0^1 dy \left[\frac{y^{\epsilon-1}}{A^{2-\epsilon}}\left(1-\frac{B}{A}y\right)^{\epsilon} + \frac{By^{\epsilon}}{A^2(A-By)^{1-\epsilon}} + \frac{By^{\epsilon}}{A(A-By)^{2-\epsilon}}\right] .\end{aligned}$$

After this, we can safely expand $\left(1-\frac{B}{A}y\right)^{\epsilon}$ in the first term and y^{ϵ} in the second and third terms, getting

$$\begin{aligned}\mathcal{I}_3 = (1-\epsilon)\int_0^1 dx \int_0^1 dy \Bigg\{ &\frac{y^{\epsilon-1}}{A^{2-\epsilon}} + \frac{B}{A^2(A-By)^{1-\epsilon}} + \frac{B}{A(A-By)^{2-\epsilon}} + \epsilon\left(\frac{\ln\left(1-\frac{B}{A}y\right)}{A^2 y}\right. \\ &\left. + \frac{B\ln y}{A^2(A-By)} + \frac{B\ln y}{A(A-By)^2}\right) + \epsilon^2\left[\frac{\ln(1-\frac{B}{A}y)}{yA^2}\left(\frac{\ln(1-\frac{B}{A}y)}{2} + \ln A + \ln y\right)\right. \\ &\left.\left. + \frac{B\ln y}{A(A-By)}\left(\frac{\ln y}{2} + \ln(A-By)\right)\left(\frac{1}{A} + \frac{1}{A-By}\right)\right]\Bigg\} + \mathcal{O}(\epsilon^3) \,.\end{aligned}$$

Integrating over y, we obtain

$$\begin{aligned}\mathcal{I}_3 = \int_0^1 dx \Bigg\{ &\frac{(2-3\epsilon)}{\epsilon}\frac{1}{A^{2-\epsilon}} - \frac{(1-\epsilon)}{\epsilon}\frac{(A-B)^{\epsilon}}{A^2} + \frac{1}{A(A-B)^{1-\epsilon}} + \epsilon\left(\frac{1}{A^2}\ln\left(\frac{A-B}{A}\right)\right. \\ &\left.\left. - \frac{2}{A^2}\mathrm{Li}_2\left(\frac{B}{A}\right)\right)\Bigg\} + 2\epsilon^2\int_0^1 \frac{dx}{A^2}\left[2\,\mathrm{Li}_2\left(\frac{B}{A}\right) + \mathrm{S}_{1,2}\left(\frac{B}{A}\right)\right. \\ &\left. + \mathrm{Li}_3\left(\frac{B}{A}\right) + \frac{\ln A}{2}\left(\ln\left(\frac{A-B}{A}\right) - 2\,\mathrm{Li}_2\left(\frac{B}{A}\right)\right) + \frac{1}{4}\ln^2\left(\frac{A-B}{A}\right)\right] + \mathcal{O}(\epsilon^3) \,.\end{aligned} \tag{4.44}$$

In this form, all divergences are contained in the first three terms, which we can promptly compute, to get

$$\begin{aligned}\int_0^1 dx \frac{(2-3\epsilon)}{\epsilon A^{2-\epsilon}} = \frac{2}{ab}\Bigg[&\frac{1}{\epsilon} + \frac{a\ln b - b\ln a}{a-b} - \frac{1}{2} + \frac{\epsilon}{2}\left(\frac{a\ln^2 b - b\ln^2 a}{a-b} - \frac{a\ln b - b\ln a}{a-b} - 1\right) \\ &+ \frac{\epsilon^2}{6}\left(-3 - 3\frac{a\ln b - b\ln a}{a-b} - \frac{3}{2}\frac{a\ln^2 b - b\ln^2 a}{a-b} + \frac{a\ln^3 b - b\ln^3 a}{a-b}\right)\Bigg] + \mathcal{O}(\epsilon^3) \,,\end{aligned} \tag{4.45}$$

$$-\frac{(1-\epsilon)}{\epsilon}\int_0^1 dx\frac{(A-B)^\epsilon}{A^2}=-\frac{c^\epsilon}{ab}\left\{\frac{1}{\epsilon}-1-\frac{a+b}{a-b}\ln\left(\frac{a}{b}\right)-\epsilon\left[\zeta(2)+\frac{a+b}{a-b}\left(\mathrm{Li}_2\left(1-\frac{a}{b}\right)\right.\right.\right.$$
$$\left.-\mathrm{Li}_2\left(1-\frac{b}{a}\right)-\ln\left(\frac{a}{b}\right)\right)\Big]+\epsilon^2\left[\zeta(2)-\frac{a+b}{a-b}\ln\left(\frac{a}{b}\right)\left(\zeta(2)+\ln\left(\frac{a}{b}\right)\left(-\frac{1}{2}-\ln\left(1-\frac{a}{b}\right)\right.\right.\right.$$
$$\left.\left.\left.+\frac{1}{6}\ln\left(\frac{a}{b}\right)\right)\right)-\frac{4b}{a-b}\zeta(3)+2\frac{a+b}{a-b}\left(\mathrm{Li}_2\left(1-\frac{a}{b}\right)+2\mathrm{Li}_3\left(1-\frac{a}{b}\right)+\mathrm{Li}_3\left(\frac{a}{b}\right)\right)\Big]\right\}+\mathcal{O}(\epsilon^3), \tag{4.46}$$

$$\int_0^1 dx\frac{1}{A(A-B)^{1-\epsilon}}=\frac{1}{abc}\left\{\frac{a+b}{\epsilon}+(a+b)\ln c-(a-b)\ln\left(\frac{a}{b}\right)+\epsilon\left[\frac{(a+b)\ln^2 c}{2}\right.\right.$$
$$\left.-(a-b)\ln c\ln\left(\frac{a}{b}\right)-(a+b)\zeta(2)-(a-b)\left(\mathrm{Li}_2\left(1-\frac{a}{b}\right)-\mathrm{Li}_2\left(1-\frac{b}{a}\right)\right)\Big]+\epsilon^2\left[\frac{a+b}{6}\ln^3 c\right.$$
$$\left.-\frac{a-b}{2}\ln\left(\frac{a}{b}\right)\ln^2 c-\ln c\left((a+b)\zeta(2)+(a-b)\left(\mathrm{Li}_2\left(1-\frac{a}{b}\right)-\mathrm{Li}_2\left(1-\frac{b}{a}\right)\right)\right)+4b\zeta(3)\right.$$
$$\left.-(a-b)\left(\ln\left(\frac{a}{b}\right)\left(\zeta(2)-\ln\left(1-\frac{a}{b}\right)\ln\left(\frac{a}{b}\right)+\frac{1}{6}\ln^2\left(\frac{a}{b}\right)\right)-4\mathrm{Li}_3\left(1-\frac{a}{b}\right)-2\mathrm{Li}_3\left(\frac{a}{b}\right)\right)\Big]\right\}$$
$$+\mathcal{O}(\epsilon^3)\,, \tag{4.47}$$

where $a=\vec{q}_1^{\,2}$, $b=\vec{q}_2^{\,2}$, $c=\vec{p}^{\,2}$. Plugging into (4.44) the results given in (4.45)-(4.47), one gets an expression for $\mathcal{I}_3$, valid up to the order ϵ^2, in terms of finite one-dimensional integrals. A quick numerical comparison shows that this expression is perfectly equivalent to the one obtained in the previous section.

By limiting the accuracy to the order ϵ, we can express the result in a very compact form. We calculate the two residual one-dimensional integrals,

$$\int_0^1 dx\frac{1}{A^2}\ln\left(\frac{A-B}{A}\right)=-\frac{1}{2ab}\left[2-\ln\left(\frac{c^2}{ab}\right)+\frac{a+b}{a-b}\ln\left(\frac{a}{b}\right)\right]\,, \tag{4.48}$$

$$\int_0^1 dx\int_0^1 dy\frac{\ln\left(1-\frac{B}{A}y\right)}{yA^2}=\frac{1}{2ab}\left[2-2\zeta(2)-\ln\left(\frac{c^2}{ab}\right)+\frac{a+b}{a-b}\ln\left(\frac{a}{b}\right)+\frac{(a-b)^2-c(a+b)}{c(a-b)}\right.$$
$$\left.\times\left(\mathrm{Li}_2\left(1-\frac{a}{b}\right)-\mathrm{Li}_2\left(1-\frac{b}{a}\right)+\frac{1}{2}\ln\left(\frac{c^2}{ab}\right)\ln\left(\frac{a}{b}\right)\right)\right]+\frac{(a-b)^2-2c(a+b)+c^2}{2abc}I_{a,b,c}\,, \tag{4.49}$$

where

$$I_{a,b,c}=\int_0^1 dx\,\frac{1}{ax+b(1-x)-cx(1-x)}\ln\left(\frac{ax+b(1-x)}{cx(1-x)}\right)\,. \tag{4.50}$$

Various properties and representations of the integral (4.50), together with its explicit value for $I_{\vec{q}_1^{\,2},\vec{q}_2^{\,2}\vec{p}^{\,2}}$, are given in appendix C.2. Combining everything we find

$$\begin{aligned}\mathcal{I}_3 = \frac{\Gamma^2(1+\epsilon)}{\epsilon\Gamma(1+2\epsilon)}\Bigg[&(\vec{p}^{\,2})^\epsilon\left(\frac{1}{\vec{p}^{\,2}\vec{q}_1^{\,2}}+\frac{1}{\vec{p}^{\,2}\vec{q}_2^{\,2}}-\frac{1}{\vec{q}_1^{\,2}\vec{q}_2^{\,2}}\right)\\ &+(\vec{q}_1^{\,2})^\epsilon\left(\frac{1}{\vec{q}_1^{\,2}\vec{q}_2^{\,2}}+\frac{1}{\vec{q}_1^{\,2}\vec{p}^{\,2}}-\frac{1}{\vec{q}_2^{\,2}\vec{p}^{\,2}}\right)+(\vec{q}_2^{\,2})^\epsilon\left(\frac{1}{\vec{q}_2^{\,2}\vec{q}_1^{\,2}}+\frac{1}{\vec{q}_2^{\,2}\vec{p}^{\,2}}-\frac{1}{\vec{q}_1^{\,2}\vec{p}^{\,2}}\right)\\ &+\frac{\epsilon^2}{\vec{q}_1^{\,2}\vec{q}_2^{\,2}\vec{p}^{\,2}}((\vec{p}^{\,2})^2+(\vec{q}_1^{\,2})^2+(\vec{q}_2^{\,2})^2-2\vec{q}_1^{\,2}\vec{q}_2^{\,2}-2\vec{q}_1^{\,2}\vec{p}^{\,2}-2\vec{q}_2^{\,2}\vec{p}^{\,2})I_{\vec{q}_1^{\,2},\vec{q}_2^{\,2},\vec{p}^{\,2}}\Bigg]\,,\end{aligned} \tag{4.51}$$

or

$$\begin{aligned}\mathcal{I}_3 = &\frac{\Gamma^2(1+\epsilon)}{\epsilon\Gamma(1+2\epsilon)}\\ \times\hat{\mathcal{S}}\Bigg\{&(\vec{q}_2^{\,2})^\epsilon\left(\frac{1}{\vec{q}_2^{\,2}\vec{q}_1^{\,2}}+\frac{1}{\vec{q}_2^{\,2}\vec{p}^{\,2}}-\frac{1}{\vec{q}_1^{\,2}\vec{p}^{\,2}}\right)+\frac{\epsilon^2}{\vec{q}_1^{\,2}\vec{q}_2^{\,2}\vec{p}^{\,2}}((\vec{q}_2^{\,2})^2-\vec{q}_1^{\,2}\vec{q}_2^{\,2}-\vec{q}_2^{\,2}\vec{p}^{\,2})I_{\vec{q}_1^{\,2},\vec{q}_2^{\,2},\vec{p}^{\,2}}\Bigg\}\,.\end{aligned} \tag{4.52}$$

This result, after multiplication by the factor $\pi^{1+\epsilon}\Gamma(1-\epsilon)$ (see the definition (4.29)), is equivalent to (4.41) at the order ϵ.

4.3.3 $\mathcal{I}_{4B}$ and $\mathcal{I}_{4A}$: BDK method

The integral that has to be evaluated is

$$\begin{aligned}\mathcal{I}_{4B} = &\int_0^1\frac{dx}{x}\int\frac{d^{D-2}k}{\pi^{1+\epsilon}\Gamma(1-\epsilon)}\\ \times&\left[\frac{1-x}{\left(x\vec{k}^2+(1-x)(\vec{k}-\vec{q}_1)^2\right)(\vec{k}-(1-x)(\vec{q}_1-\vec{q}_2))^2}-\frac{1}{(\vec{k}-\vec{q}_1)^2(\vec{k}-(\vec{q}_1-\vec{q}_2))^2}\right]\,,\end{aligned} \tag{4.17}$$

Let's start from the integral I_{4B} defined as

$$I_{4B} = \frac{1}{i}\int d^Dk\frac{1}{(k^2+i\varepsilon)[(k+q_1)^2+i\varepsilon][(k+q_2)^2+i\varepsilon][(k-p_B)^2+i\varepsilon]}\,. \tag{4.53}$$

Using the BDK method and working in the Euclidean region ($s,s_1,s_2,t_1,t_2<0$) the result for this integral is [187]

$$\begin{aligned}I_{4B} =&\frac{\pi^{2+\epsilon}}{s_2t_2}\frac{\Gamma(1-\epsilon)\Gamma^2(1+\epsilon)}{\Gamma(1+2\epsilon)}\frac{2}{\epsilon^2}\Bigg[(-\alpha_4(\alpha_1-\alpha_5))^{-\epsilon}\,{}_2F_1\left(\epsilon,\epsilon,1+\epsilon;\frac{\alpha_1\alpha_4+\alpha_5\alpha_3-\alpha_5\alpha_4}{\alpha_4(\alpha_1-\alpha_5)}\right)\\ &+(-\alpha_5(\alpha_3-\alpha_4))^{-\epsilon}\,{}_2F_1\left(\epsilon,\epsilon,1+\epsilon;\frac{\alpha_1\alpha_4+\alpha_5\alpha_3-\alpha_5\alpha_4}{\alpha_5(\alpha_3-\alpha_4)}\right)\\ &-((\alpha_1-\alpha_5)(\alpha_3-\alpha_4))^{-\epsilon}\,{}_2F_1\left(\epsilon,\epsilon,1+\epsilon;-\frac{\alpha_1\alpha_4+\alpha_5\alpha_3-\alpha_5\alpha_4}{(\alpha_1-\alpha_5)(\alpha_3-\alpha_4)}\right)\Bigg]\,,\end{aligned} \tag{4.54}$$

where

$$\alpha_1 = \sqrt{-\frac{s_1 s_2}{s t_2 t_1}}\,, \quad \alpha_2 = \sqrt{-\frac{s_2 t_2}{s s_1 t_1}}\,, \quad \alpha_3 = \sqrt{-\frac{s t_2}{s_2 s_1 t_1}}\,,$$
$$\alpha_4 = \sqrt{-\frac{s t_1}{s_1 s_2 t_2}}\,, \quad \alpha_5 = \sqrt{-\frac{s_1 t_1}{s s_2 t_2}}\,. \tag{4.55}$$

We then have

$$\begin{aligned} I_{4B} =& \frac{\pi^{2+\epsilon}}{s_2 t_2}\frac{\Gamma(1-\epsilon)\Gamma^2(1+\epsilon)}{\Gamma(1+2\epsilon)}\frac{2}{\epsilon^2}\left[\frac{(-s_2)^\epsilon(-t_2)^\epsilon}{(s_2-t_1)^\epsilon}\,{}_2F_1\left(\epsilon,\epsilon,1+\epsilon;1-\frac{(-t_2)}{s_2-t_1}\right)\right. \\ &+\frac{(-s_2)^\epsilon(-t_2)^\epsilon}{(t_2-t_1)^\epsilon}\,{}_2F_1\left(\epsilon,\epsilon,1+\epsilon;1-\frac{s_2}{t_1-t_2}\right) \\ &\left.-\frac{(-s_2)^\epsilon(-t_2)^\epsilon(-t_1)^\epsilon}{(s_2-t_1)^\epsilon(t_2-t_1)^\epsilon}\,{}_2F_1\left(\epsilon,\epsilon,1+\epsilon;1-\frac{s_2 t_2}{(s_2-t_1)(t_2-t_1)}\right)\right]\,. \end{aligned} \tag{4.56}$$

Using (C.9), this result can be put in the following simpler form:

$$\begin{aligned} I_{4B} =& \frac{\pi^{2+\epsilon}}{s_2 t_2}\frac{\Gamma(1-\epsilon)\Gamma^2(1+\epsilon)}{\Gamma(1+2\epsilon)}\frac{2}{\epsilon^2}\left[(-s_2)^\epsilon\,{}_2F_1\left(1,\epsilon,1+\epsilon;1-\frac{s_2-t_1}{(-t_2)}\right)\right. \\ &\left.+(-t_2)^\epsilon\,{}_2F_1\left(1,\epsilon,1+\epsilon;1-\frac{t_1-t_2}{s_2}\right)-(-t_1)^\epsilon\,{}_2F_1\left(1,\epsilon,1+\epsilon;1-\frac{(s_2-t_1)(t_1-t_2)}{s_2(-t_2)}\right)\right]\,. \end{aligned} \tag{4.57}$$

We re-derive this result in appendix C.2.

For the first term in the square roots in (4.54) we have

$$(-t_2)^\epsilon\,(-s_2)^\epsilon\,(s_2-t_1)^{-\epsilon}\,{}_2F_1\left(\epsilon,\epsilon;1+\epsilon;1-\frac{(-t_2)}{s_2-t_1}\right)\,. \tag{4.58}$$

Analytically continuing the result in the region of positive s_2 by the replacement

$$(-s_2) \to e^{-i\pi} s_2\,, \tag{4.59}$$

using the MRK approximation to neglect $(-t_2)/(s_2-t_1)$ with respect to one in the argument of the hypergeometric function and recalling that

$${}_2F_1(\epsilon,\epsilon,1+\epsilon;1) = \Gamma(1-\epsilon)\Gamma(1+\epsilon) = \frac{\pi\epsilon}{\sin(\pi\epsilon)}\,, \tag{4.60}$$

we obtain

$$(-t_2)^\epsilon\,e^{-i\pi\epsilon}\Gamma(1-\epsilon)\Gamma(1+\epsilon) = (-t_2)^\epsilon\left[\cos(\pi\epsilon)\frac{\pi\epsilon}{\sin(\pi\epsilon)} - i\pi\epsilon\right]\,. \tag{4.61}$$

The second term,

$$\left(\frac{-t_2 s_2}{t_1-t_2}\right)^\epsilon\,{}_2F_1\left(\epsilon,\epsilon,1+\epsilon;1-\frac{s_2}{t_1-t_2}\right)\,, \tag{4.62}$$

with the help of (C.9) and (C.10) gives, assuming $t_1 > t_2$,

$$(-t_2)^\epsilon \, {}_2F_1\left(1, \epsilon, 1+\epsilon; 1-\frac{t_1-t_2}{s_2}\right) = (-t_2)^\epsilon \left(1 - \epsilon \ln\left(\frac{t_1-t_2}{s_2}\right) - \sum_{n=2}^{\infty} (-\epsilon)^n \zeta(n)\right) . \tag{4.63}$$

The third term,

$$-\left(\frac{t_1 t_2}{t_1-t_2}\right)^\epsilon \, {}_2F_1\left(\epsilon, \epsilon, 1+\epsilon; 1+\frac{t_2}{t_1-t_2}\right) , \tag{4.64}$$

using (C.9) and (C.10), again assuming $t_1 > t_2$, becomes

$$-(-t_1)^\epsilon \, {}_2F_1\left(1, \epsilon, 1+\epsilon; \frac{t_1}{t_2}\right) = -(-t_1)^\epsilon \left(1 - \epsilon \ln\left(1-\frac{t_1}{t_2}\right) - \sum_{n=2}^{\infty} (-\epsilon)^n \mathrm{Li}_n\left(\frac{t_1}{t_2}\right)\right) . \tag{4.65}$$

We finally obtain

$$\begin{aligned} I_{4B} = \frac{\pi^{2+\epsilon}}{s_2 t_2} \frac{\Gamma(1-\epsilon)\Gamma^2(1+\epsilon)}{\Gamma(1+2\epsilon)} \frac{2}{\epsilon^2} (-t_1)^\epsilon \Bigg[\left(\frac{t_2}{t_1}\right)^\epsilon \Bigg(e^{-i\pi\epsilon} \Gamma(1-\epsilon)\Gamma(1+\epsilon) \\ +1 - \epsilon \ln\left(\frac{t_1-t_2}{s_2}\right) - \sum_{n=2}^{\infty} (-\epsilon)^n \zeta(n) \Bigg) - 1 + \epsilon \ln\left(1-\frac{t_1}{t_2}\right) + \sum_{n=2}^{\infty} (-\epsilon)^n \mathrm{Li}_n\left(\frac{t_1}{t_2}\right) \Bigg] . \end{aligned} \tag{4.66}$$

Furthermore, starting from the integral in eq. (4.53), using the standard Sudakov decomposition for the 4-momentum k, one finds that, in the multi-Regge kinematics (see appendix C.3),

$$I_{4B} = -\frac{\pi^{2+\epsilon}\Gamma(1-\epsilon)}{s_2} \left[\frac{\Gamma^2(\epsilon)}{\Gamma(2\epsilon)} (-t_2)^{\epsilon-1} \left(\ln\left(\frac{-s_2}{-t_2}\right) + \psi(1-\epsilon) - 2\psi(\epsilon) + \psi(2\epsilon) \right) + \mathcal{I}_{4B} \right] , \tag{4.67}$$

where $\mathcal{I}_{4B}$ is exactly the integral defined in eq. (4.17). From this relation we can hence derive an expression for $\mathcal{I}_{4B}$ that, after some manipulations, can be cast in the following form:

$$\begin{aligned} \mathcal{I}_{4B} = \frac{\Gamma^2(1+\epsilon)}{\Gamma(1+2\epsilon)} \frac{2}{\epsilon^2} \frac{(-t_1)^\epsilon}{-t_2} \Bigg[\left(\frac{t_2}{t_1}\right)^\epsilon \Bigg(-\frac{1}{2} + \frac{\pi\epsilon}{\sin(\pi\epsilon)} \cos(\pi\epsilon) - \epsilon \ln\left(1-\frac{t_1}{t_2}\right) \\ + \sum_{n=2}^{\infty} \epsilon^n \zeta(n) \left(1 - (-1)^n \left(2^{n-1}-1\right)\right) \Bigg) - 1 + \epsilon \ln\left(1-\frac{t_1}{t_2}\right) + \sum_{n=2}^{\infty} (-\epsilon)^n \mathrm{Li}_n\left(\frac{t_1}{t_2}\right) \Bigg] . \end{aligned} \tag{4.68}$$

The result remains valid for $t_2 > t_1$. In particular, truncating the summation at $n = 4$ gives the desired result.

This result is completely equivalent to the one obtained by calculating directly $\mathcal{I}_{4B}$ introducing Feynman parameters (see the next subsection). The integral $\mathcal{I}_{4A}$ is defined similarly to $\mathcal{I}_{4B}$ in eq. (4.17), up to the replacement $q_1 \to -q_2$, implying that

$$\mathcal{I}_{4A} = \mathcal{I}_{4B}(t_1 \leftrightarrow t_2) \; . \tag{4.69}$$

4.3.4 $\mathcal{I}_{4B}$ and $\mathcal{I}_{4A}$: Alternative calculation

Starting from the expression

$$\mathcal{I}_{4B} = \int_0^1 \frac{dx}{x} \int \frac{d^{D-2}k}{\pi^{1+\epsilon}\Gamma(1-\epsilon)}$$

$$\times \left[\frac{1-x}{\left(x\vec{k}^2 + (1-x)(\vec{k}-\vec{q}_1)^2\right)(\vec{k}-(1-x)(\vec{q}_1-\vec{q}_2))^2} - \frac{1}{(\vec{k}-\vec{q}_1)^2(\vec{k}-(\vec{q}_1-\vec{q}_2))^2} \right] ,$$

introducing the Feynman parametrization and performing the integration over k, we obtain

$$\mathcal{I}_{4B} = \int_0^1 \frac{dx}{x} \left[\int_0^1 dz \frac{(1-x)}{[z(1-x)(ax+b(1-x)(1-z))]^{1-\epsilon}} - \int_0^1 dz \frac{1}{[bz(1-z)]^{1-\epsilon}} \right] . \tag{4.70}$$

Defining

$$a = \vec{q}_1^{\,2} = -t_1 \; , \quad b = \vec{q}_2^{\,2} = -t_2 \; , \quad c = 1 - \frac{a}{b} \; , \tag{4.71}$$

we can write $\mathcal{I}_{4B} \equiv b^{\epsilon-1} F(c)$, with

$$F(c) = \int_0^1 \frac{dx}{x} \left[\int_0^1 \frac{dz}{z} \frac{z^\epsilon (1-x)^\epsilon}{(1-xc-z(1-x))^{1-\epsilon}} - \int_0^1 dz \; z^{\epsilon-1}(1-z)^{\epsilon-1} \right] . \tag{4.72}$$

Performing the transformation $y = (1-x)z$ in the first term, we get

$$F(c) = \int_0^1 \frac{dx}{x} \left[\int_0^{1-x} \frac{dy}{y} \frac{y^\epsilon}{(1-xc-y)^{1-\epsilon}} - \int_0^1 dz \; z^{\epsilon-1}(1-z)^{\epsilon-1} \right] . \tag{4.73}$$

It is very simple to compute the integral for $c = 0$; we find

$$\begin{aligned} F(0) &= \int_0^1 \frac{dx}{x} \left[\int_0^{1-x} dy \; y^{\epsilon-1}(1-y)^{\epsilon-1} - \int_0^1 dz \; z^{\epsilon-1}(1-z)^{\epsilon-1} \right] \\ &= -\int_0^1 \frac{dx}{x} \int_{1-x}^1 dz \; z^{\epsilon-1}(1-z)^{\epsilon-1} = -\int_0^1 dz \; z^{\epsilon-1}(1-z)^{\epsilon-1} \int_{1-z}^1 \frac{dx}{x} \\ &= \int_0^1 dz \; z^{\epsilon-1}(1-z)^{\epsilon-1} \ln(1-z) = \frac{d}{d\delta} \left[\int_0^1 dz \; z^{\epsilon-1}(1-z)^{\delta-1} \right]_{\delta=\epsilon} . \end{aligned} \tag{4.74}$$

The function $F(c)$ in $c = 0$ is then

$$F(0) = \frac{\Gamma^2(\epsilon)}{\Gamma(2\epsilon)} \left(\psi(\epsilon) - \psi(2\epsilon)\right) \ . \tag{4.75}$$

We now compute the derivative with respect to c of the function F and get

$$\begin{aligned} F'(c) &= (1-\epsilon) \int_0^1 dx \int_0^{1-x} \frac{dy}{y} y^\epsilon (1-xc-y)^{\epsilon-2} = (1-\epsilon) \int_0^1 \frac{dy}{y} y^\epsilon \int_0^{1-y} dx (1-xc-y)^{\epsilon-2} \\ &= \frac{1}{c} \int_0^1 \frac{dy}{y} y^\epsilon \left(((1-c)(1-y))^{\epsilon-1} - (1-y)^{\epsilon-1}\right) = \frac{1}{c} \frac{\Gamma^2(\epsilon)}{\Gamma(2\epsilon)} \left((1-c)^{\epsilon-1} - 1\right) \ . \end{aligned} \tag{4.76}$$

Having this information, we can write

$$F(c) = F(0) + \int_0^c dx \ F'(x) = \frac{\Gamma^2(\epsilon)}{\Gamma(2\epsilon)} \left[\psi(\epsilon) - \psi(2\epsilon) + \int_0^c dx \left(\frac{(1-x)^{\epsilon-1} - 1}{x}\right)\right] \tag{4.77}$$

The integral on the right-hand side can be computed to all orders in ϵ:

$$\begin{aligned} &\int_0^c dx \left(\frac{(1-x)^{\epsilon-1} - 1}{x}\right) = \int_0^c dx \left[(1-x)^\epsilon \left(\frac{1}{1-x} + \frac{1}{x}\right) - \frac{1}{x}\right] \\ &= \frac{1}{\epsilon} \left[1 - (1-c)^\epsilon\right] + \int_0^c \frac{dx}{x} ((1-x)^\epsilon - 1) = \sum_{n=1}^\infty \left(\frac{\epsilon^n}{n!} \int_0^1 \frac{dx}{x} \ln^n(1-cx) - \epsilon^{n-1} \frac{\ln^n(1-c)}{n!}\right) . \end{aligned} \tag{4.78}$$

Using

$$\frac{1}{n!} \int_0^1 \frac{dx}{x} \ln^n(1-cx) = (-1)^n \ \mathrm{S}_{1,n}(c) \ , \tag{4.79}$$

we finally find

$$\int_0^c dx \left(\frac{(1-x)^{\epsilon-1} - 1}{x}\right) = \sum_{n=1}^\infty \epsilon^{n-1} \left(-\frac{\ln^n(1-c)}{n!} + \epsilon \ (-1)^n \ \mathrm{S}_{1,n}(c)\right) \ . \tag{4.80}$$

The final result for $\mathcal{I}_{4B}$ is then

$$\mathcal{I}_{4B} = \frac{\Gamma^2(\epsilon)}{\Gamma(2\epsilon)} (-t_2)^{\epsilon-1} \left[\psi(\epsilon) - \psi(2\epsilon) + \sum_{n=1}^\infty \epsilon^{n-1} \left(-\frac{\ln^n(t_1/t_2)}{n!} + \epsilon \ (-1)^n \ \mathrm{S}_{1,n}\left(1 - \frac{t_1}{t_2}\right)\right)\right] . \tag{4.81}$$

The expression (4.81) gives an alternative representation of $\mathcal{I}_{4B}$, which is completely equivalent to (4.68). Again, the complete ϵ^2 result is obtained truncating the series at $n = 4$.

We can achieve an alternative representation in terms of the hypergeometric function. In fact, we note that

$$\int_0^c \frac{dx}{x} \left((1-x)^\epsilon - 1\right) = \left((1-c)^\epsilon - 1\right) \ln c + \epsilon \left(\int_0^1 \frac{dy}{y} \ln(1-y) y^\epsilon - \int_0^{1-c} \frac{dy}{y} \ln(1-y) y^\epsilon\right)$$

$$= ((1-c)^\epsilon - 1)\ln c + \psi(1) - \psi(1+\epsilon) - \frac{(1-c)^\epsilon}{\epsilon}\Big({}_2F_1(1,\epsilon,1+\epsilon;1-c) - 1 + \epsilon\ln c\Big). \tag{4.82}$$

The last equality can be proved by using the explicit result for the first integral, *i.e.*

$$\int_0^1 \frac{dy}{y}\ln(1-y)y^\epsilon = \frac{d}{d\delta}\int_0^1 \frac{dy}{y}(1-y)^\delta y^\epsilon\Big|_{\delta=0} = \frac{d}{d\delta}\frac{\Gamma(1+\delta)\Gamma(\epsilon)}{\Gamma(1+\delta+\epsilon)}\Big|_{\delta=0} = \frac{1}{\epsilon}(\psi(1)-\psi(1+\epsilon))\ , \tag{4.83}$$

and the following expression for the second, in terms of the hypergeometric function,

$$\begin{aligned}{}_2F_1(1,\epsilon,1+\epsilon;1-c) &= \epsilon\int_0^1 \frac{dy}{y(1-y(1-c))}y^\epsilon = \epsilon\int_0^1 y^\epsilon d\ln\frac{y}{(1-y(1-c))}\\ &= -\epsilon\ln c - \epsilon^2\int_0^1 dy y^{\epsilon-1}\ln y + \epsilon^2\int_0^1 dy y^{\epsilon-1}\ln(1-y(1-c))\\ &= -\epsilon\ln c + 1 + \epsilon^2(1-c)^{-\epsilon}\int_0^{1-c} dy y^{\epsilon-1}\ln(1-y).\end{aligned} \tag{4.84}$$

Using (4.82), we obtain

$$\mathcal{I}_{4B} = \frac{\Gamma^2(\epsilon)}{\Gamma(2\epsilon)}b^{\epsilon-1}\left(\frac{1}{2\epsilon} + \psi(1) - \psi(1+2\epsilon) - \ln c - \frac{(1-c)^\epsilon}{\epsilon}{}_2F_1(1,\epsilon,1+\epsilon;1-c)\right)\ , \tag{4.85}$$

which is completely equivalent to both (4.68) and (4.81).

4.3.5 Combination $\mathcal{I}_5 - \mathcal{L}_3$

Let's start by considering the pentagonal integral I_5, defined as

$$I_5 = \frac{1}{i}\int d^Dk \frac{1}{(k^2+i\varepsilon)[(k+q_1)^2+i\varepsilon][(k+q_2)^2+i\varepsilon][(k+p_A)^2+i\varepsilon][(k-p_B)^2+i\varepsilon]}\ . \tag{4.86}$$

In multi-Regge kinematics (and in $D = 4+2\epsilon$), it is given by the following combination:

$$I_5 = \frac{\pi^{2+\epsilon}\Gamma(1-\epsilon)}{s}\left[\ln\left(\frac{(-s)(\vec{q}_1-\vec{q}_2)^2}{(-s_1)(-s_2)}\right)\mathcal{I}_3 + \mathcal{L}_3 - \mathcal{I}_5\right] \tag{4.87}$$

Inverting this relation, we obtain

$$\mathcal{I}_5 - \mathcal{L}_3 = \ln\left(\frac{(-s)(\vec{q}_1-\vec{q}_2)^2}{(-s_1)(-s_2)}\right)\mathcal{I}_3 - \frac{s}{\pi^{2+\epsilon}\Gamma(1-\epsilon)}I_5\ . \tag{4.88}$$

Hence, the integral I_5 can be used (together with $\mathcal{I}_3$) to calculate $\mathcal{I}_5 - \mathcal{L}_3$ (this combination is the one appearing in the Lipatov vertex [47]).

We start by working in the Euclidean region, defined by $s, s_1, s_2, t_1, t_2 < 0$, the analytical continuation to the physical region is obtained according to the prescriptions

$$(-s) \to e^{-i\pi} s \ , \qquad (-s_1) \to e^{-i\pi} s_1 \ , \qquad (-s_2) \to e^{-i\pi} s_2 \ . \tag{4.89}$$

We use the quantities α_i defined before, which we recall here:

$$\alpha_1 = \sqrt{-\frac{s_1 s_2}{s t_2 t_1}} \ , \quad \alpha_2 = \sqrt{-\frac{s_2 t_2}{s s_1 t_1}} \ , \quad \alpha_3 = \sqrt{-\frac{s t_2}{s_2 s_1 t_1}} \ ,$$

$$\alpha_4 = \sqrt{-\frac{s t_1}{s_1 s_2 t_2}} \ , \quad \alpha_5 = \sqrt{-\frac{s_1 t_1}{s s_2 t_2}} \ . \tag{4.55}$$

Let's define the reduced integral $\hat{I}_5$ in this way:

$$I_5 = -\pi^{D/2} \alpha_1 \alpha_2 \alpha_3 \alpha_4 \alpha_5 \hat{I}_5 \ . \tag{4.90}$$

In Ref. [187] it is shown that this integral is given by the recursive relation

$$\hat{I}_5 = \frac{1}{2} \left[\sum_{i=1}^{5} \gamma_i \hat{I}_4^{(i)} - 2\epsilon \Delta_5 \hat{I}_5^{(D=6+2\epsilon)} \right] \ , \tag{4.91}$$

where Δ_5 is the following quantity:

$$\Delta_5 = \sum_{i=1}^{5} (\alpha_i^2 - 2\alpha_i \alpha_{i+1} + 2\alpha_i \alpha_{i+2}) \ . \tag{4.92}$$

The γ_i's are

$$\gamma_1 = \alpha_1 - \alpha_2 + \alpha_3 + \alpha_4 - \alpha_5 \ , \tag{4.93}$$

$$\gamma_2 = -\alpha_1 + \alpha_2 - \alpha_3 + \alpha_4 + \alpha_5 \ , \tag{4.94}$$

$$\gamma_3 = \alpha_1 - \alpha_2 + \alpha_3 - \alpha_4 + \alpha_5 \ , \tag{4.95}$$

$$\gamma_4 = \alpha_1 + \alpha_2 - \alpha_3 + \alpha_4 - \alpha_5 \ , \tag{4.96}$$

$$\gamma_5 = -\alpha_1 + \alpha_2 + \alpha_3 - \alpha_4 + \alpha_5 \ . \tag{4.97}$$

$\hat{I}_4^{(i)}$ are the reduced version of $I_4^{(i)}$ (apart for a trivial $\pi^{2+\epsilon}$), *i.e.*

$$\hat{I}_4^{(i)} = \frac{\alpha_1 \alpha_2 \alpha_3 \alpha_4 \alpha_5}{\alpha_i} I_4^{(i)} \ . \tag{4.98}$$

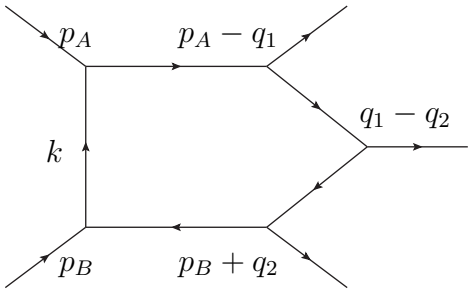

Figure 4.1: Schematic representation of the pentagonal integral. The arrows denote the direction of the momenta.

Box integrals part

The integrals $I_4^{(i)}$ are box integrals with all external legs on-shell, but one, which is off-shell. They can be obtained starting from I_5 (see Fig. 4.1) in this way (apart from a factor $\pi^{2+\epsilon}$):

- $I_4^{(1)}$
  Making the propagator between p_A and p_B "collapse", so that the two on-shell legs associated with p_A and p_B become a unique off-shell external leg with (incoming) momenta $p_A + p_B$.

- $I_4^{(2)}$
  Making the propagator between p_A and $p_{A'} = p_A - q_1$ "collapse", so that the two on-shell legs associated with p_A and $p_{A'}$ become a unique off-shell external leg with (incoming) momenta q_1.

- $I_4^{(3)}$
  Making the propagator between $p_{A'} = p_A - q_1$ and $q_1 - q_2$ "collapse", so that the two on-shell legs associated with $p_{A'}$ and $q_1 - q_2$ become a unique off-shell external leg with (outgoing) momenta $p_A - q_2$.

- $I_4^{(4)}$
  Making the propagator between $q_1 - q_2$ and $p_{B'} = p_B + q_2$ "collapse", so that the two on-shell legs associated with $q_1 - q_2$ and $p_{B'}$ become a unique off-shell external leg with (outgoing) momenta $p_B + q_1$.

- $I_4^{(5)}$
  Making the propagator between p_B and $p_{B'}$ "collapse", so that the two on-shell legs

associated with p_B and $p_{B'}$ become a unique off-shell external leg with (outgoing) momenta q_2.

The results for the reduced version of these integrals are

$$\begin{aligned}\hat{I}_4^{(1)}(s_1,s_2,s) =&\frac{2}{\epsilon^2}r_\Gamma\left[(-\alpha_3(\alpha_5-\alpha_4))^{-\epsilon}\,{}_2F_1\left(\epsilon,\epsilon,1+\epsilon;\frac{\alpha_5\alpha_3+\alpha_2\alpha_4-\alpha_4\alpha_3}{\alpha_3(\alpha_5-\alpha_4)}\right)\right.\\&+(-\alpha_4(\alpha_2-\alpha_3))^{-\epsilon}\,{}_2F_1\left(\epsilon,\epsilon,1+\epsilon;\frac{\alpha_5\alpha_3+\alpha_2\alpha_4-\alpha_4\alpha_3}{\alpha_4(\alpha_2-\alpha_3)}\right)\\&\left.-((\alpha_5-\alpha_4)(\alpha_2-\alpha_3))^{-\epsilon}\,{}_2F_1\left(\epsilon,\epsilon,1+\epsilon;-\frac{\alpha_5\alpha_3+\alpha_2\alpha_4-\alpha_4\alpha_3}{(\alpha_5-\alpha_4)(\alpha_2-\alpha_3)}\right)\right]\,,\end{aligned}\tag{4.99}$$

$$\begin{aligned}\hat{I}_4^{(2)}(s_2,t_2,t_1) =&\frac{2}{\epsilon^2}r_\Gamma\left[(-\alpha_4(\alpha_1-\alpha_5))^{-\epsilon}\,{}_2F_1\left(\epsilon,\epsilon,1+\epsilon;\frac{\alpha_1\alpha_4+\alpha_3\alpha_5-\alpha_4\alpha_5}{\alpha_4(\alpha_1-\alpha_5)}\right)\right.\\&+(-\alpha_5(\alpha_3-\alpha_4))^{-\epsilon}\,{}_2F_1\left(\epsilon,\epsilon,1+\epsilon;\frac{\alpha_1\alpha_4+\alpha_5\alpha_3-\alpha_5\alpha_4}{\alpha_5(\alpha_3-\alpha_4)}\right)\\&\left.-((\alpha_1-\alpha_5)(\alpha_3-\alpha_4))^{-\epsilon}\,{}_2F_1\left(\epsilon,\epsilon,1+\epsilon;-\frac{\alpha_1\alpha_4+\alpha_5\alpha_3-\alpha_5\alpha_4}{(\alpha_1-\alpha_5)(\alpha_3-\alpha_4)}\right)\right]\,,\end{aligned}\tag{4.100}$$

$$\begin{aligned}\hat{I}_4^{(3)}(s,s_1,t_2) =&\frac{2}{\epsilon^2}r_\Gamma\left[(-\alpha_5(\alpha_2-\alpha_1))^{-\epsilon}\,{}_2F_1\left(\epsilon,\epsilon,1+\epsilon;\frac{\alpha_2\alpha_5+\alpha_1\alpha_4-\alpha_1\alpha_5}{\alpha_5(\alpha_2-\alpha_1)}\right)\right.\\&+(-\alpha_1(\alpha_4-\alpha_5))^{-\epsilon}\,{}_2F_1\left(\epsilon,\epsilon,1+\epsilon;\frac{\alpha_2\alpha_5+\alpha_1\alpha_4-\alpha_1\alpha_5}{\alpha_1(\alpha_4-\alpha_5)}\right)\\&\left.-((\alpha_2-\alpha_1)(\alpha_4-\alpha_5))^{-\epsilon}\,{}_2F_1\left(\epsilon,\epsilon,1+\epsilon;-\frac{\alpha_2\alpha_5+\alpha_1\alpha_4-\alpha_1\alpha_5}{(\alpha_2-\alpha_1)(\alpha_4-\alpha_5)}\right)\right]\,,\end{aligned}\tag{4.101}$$

$$\begin{aligned}\hat{I}_4^{(4)}(s,s_2,t_1) =&\frac{2}{\epsilon^2}r_\Gamma\left[(-\alpha_1(\alpha_3-\alpha_2))^{-\epsilon}\,{}_2F_1\left(\epsilon,\epsilon,1+\epsilon;\frac{\alpha_1\alpha_3+\alpha_2\alpha_5-\alpha_2\alpha_1}{\alpha_1(\alpha_3-\alpha_2)}\right)\right.\\&+(-\alpha_2(\alpha_5-\alpha_1))^{-\epsilon}\,{}_2F_1\left(\epsilon,\epsilon,1+\epsilon;\frac{\alpha_1\alpha_3+\alpha_2\alpha_5-\alpha_2\alpha_1}{\alpha_2(\alpha_5-\alpha_1)}\right)\\&\left.-((\alpha_3-\alpha_2)(\alpha_5-\alpha_1))^{-\epsilon}\,{}_2F_1\left(\epsilon,\epsilon,1+\epsilon;-\frac{\alpha_1\alpha_3+\alpha_2\alpha_5-\alpha_2\alpha_1}{(\alpha_3-\alpha_2)(\alpha_5-\alpha_1)}\right)\right]\,,\end{aligned}\tag{4.102}$$

$$\hat{I}_4^{(5)}(s_1,t_1,t_2) = \frac{2}{\epsilon^2} r_\Gamma \left[(-\alpha_3(\alpha_1-\alpha_2))^{-\epsilon}\, {}_2F_1\left(\epsilon,\epsilon,1+\epsilon;\frac{\alpha_1\alpha_3+\alpha_2\alpha_4-\alpha_2\alpha_3}{\alpha_3(\alpha_1-\alpha_2)}\right) \right.$$
$$+(-\alpha_2(\alpha_4-\alpha_3))^{-\epsilon}\, {}_2F_1\left(\epsilon,\epsilon,1+\epsilon;\frac{\alpha_1\alpha_3+\alpha_2\alpha_4-\alpha_2\alpha_3}{\alpha_2(\alpha_4-\alpha_3)}\right)$$
$$\left.-((\alpha_1-\alpha_2)(\alpha_4-\alpha_3))^{-\epsilon}\, {}_2F_1\left(\epsilon,\epsilon,1+\epsilon;-\frac{\alpha_1\alpha_3+\alpha_2\alpha_4-\alpha_2\alpha_3}{(\alpha_1-\alpha_2)(\alpha_4-\alpha_3)}\right)\right] , \tag{4.103}$$

where

$$r_\Gamma = \frac{\Gamma(1-\epsilon)\Gamma^2(1+\epsilon)}{\Gamma(1+2\epsilon)} . \tag{4.104}$$

It is clear that with appropriate exchanges of the invariants s, s_1, s_2, t_1, t_2 they can be obtained from each other. In particular, as pointed out in [187], starting from one of these integrals the others can be obtained by cyclic permutations of the α_i's.

By expanding these results, in multi-Regge kinematics, we have

$$\hat{I}_4^{(1)}(s_1,s_2,s) \simeq \frac{\Gamma(1-\epsilon)\Gamma^2(1+\epsilon)}{\Gamma(1+2\epsilon)}\frac{2}{\epsilon^2}\left(\frac{(-s_1)(-s_2)}{(-s)}\right)^\epsilon \left\{1+\sum_{n=1}^{\infty}\epsilon^{2n}\,2\left(1-\frac{1}{2^{2n-1}}\right)\zeta(2n)\right\} , \tag{4.105}$$

$$\hat{I}_4^{(2)}(s_2,t_2,t_1) = \frac{\Gamma(1-\epsilon)\Gamma^2(1+\epsilon)}{\Gamma(1+2\epsilon)}\frac{2}{\epsilon^2}(-t_1)^\epsilon \left[\left(\frac{t_2}{t_1}\right)^\epsilon \left(e^{-i\pi\epsilon}\Gamma(1-\epsilon)\Gamma(1+\epsilon)\right.\right.$$
$$\left.\left.+1-\epsilon\ln\left(\frac{t_1-t_2}{s_2}\right)-\sum_{n=2}^{\infty}(-\epsilon)^n\zeta(n)\right)-1+\epsilon\ln\left(1-\frac{t_1}{t_2}\right)+\sum_{n=2}^{\infty}(-\epsilon)^n\mathrm{Li}_n\left(\frac{t_1}{t_2}\right)\right] . \tag{4.106}$$

$$\hat{I}_4^{(3)}(s,s_1,t_2) \simeq \frac{\Gamma(1-\epsilon)\Gamma^2(1+\epsilon)}{\Gamma(1+2\epsilon)}\frac{2}{\epsilon^2}(-t_2)^\epsilon \left\{1+\epsilon\ln\left(\frac{-s}{-s_1}\right)-\sum_{n=2}^{\infty}(-\epsilon)^n\zeta(n)\right\} , \tag{4.107}$$

$$\hat{I}_4^{(4)}(s,s_2,t_1) \simeq \frac{\Gamma(1-\epsilon)\Gamma^2(1+\epsilon)}{\Gamma(1+2\epsilon)}\frac{2}{\epsilon^2}(-t_1)^\epsilon \left\{1+\epsilon\ln\left(\frac{-s}{-s_2}\right)-\sum_{n=2}^{\infty}(-\epsilon)^n\zeta(n)\right\} , \tag{4.108}$$

$$\hat{I}_4^{(5)}(s_1,t_1,t_2) = \frac{\Gamma(1-\epsilon)\Gamma^2(1+\epsilon)}{\Gamma(1+2\epsilon)}\frac{2}{\epsilon^2}(-t_2)^\epsilon \left[\left(\frac{t_1}{t_2}\right)^\epsilon \left(e^{-i\pi\epsilon}\Gamma(1-\epsilon)\Gamma(1+\epsilon)\right.\right.$$
$$\left.\left.+1-\epsilon\ln\left(\frac{t_2-t_1}{s_1}\right)-\sum_{n=2}^{\infty}(-\epsilon)^n\zeta(n)\right)-1+\epsilon\ln\left(1-\frac{t_2}{t_1}\right)+\sum_{n=2}^{\infty}(-\epsilon)^n\mathrm{Li}_n\left(\frac{t_2}{t_1}\right)\right] . \tag{4.109}$$

Again, truncating the summation at $n=4$ gives the desired result. The integral $\hat{I}_4^{(2)}$, up to trivial factors, coincides with (4.66), as can be easily verified. Since we have computed

the integral $\mathcal{I}_{4B}$ through two independent methods, the integral $\hat{I}_4^{(2)}$ can be cross-checked. We can use the technique explained in appendix C.3 to obtain the relation (4.67) and then, by using the knowledge of $\mathcal{I}_{4B}$ integral from the alternative method explained in section 4.3.4, obtain an alternative expression for $\hat{I}_4^{(2)}$. This automatically verifies $\hat{I}_4^{(5)}$, that is obtained from $\hat{I}_4^{(2)}$ by the substitutions $s_2 \to s_1$ and $t_2 \leftrightarrow t_1$. The technique explained in appendix C.3 can be also applied to $\hat{I}_4^{(1)}$, $\hat{I}_4^{(3)}$, $\hat{I}_4^{(4)}$ in order to verify also the results. These latter cases are really much simpler with respect to the ones computed explicitly in appendix C.3. We can also verify these integrals using direct Feynman technique, as explained in C.2 for I_{4B}.

Del Duca, Duhr, Glover, Smirnov result for $\hat{I}_5^{D=6+2\epsilon}$ part

As it can be seen from eq. (4.91), beyond the constant order in the ϵ-expansion, the pentagon in dimension $D = 4 + 2\epsilon$ takes a contribution from the pentagon integral in dimension $D = 6+2\epsilon$. The latter pentagon integral is finite and hence does not contribute to the divergent and finite parts in (4.91). It starts to contribute at the order ϵ, and hence, if one wants to obtain the pentagon in $D = 4 + 2\epsilon$ up to ϵ^2 accuracy, the first two non-trivial orders of the pentagon in $D = 6 + 2\epsilon$ must be computed. There are different results in literature for the 6-dimensional pentagon integral [188, 189, 190, 191]; among these, the one obtained by Del Duca, Duhr, Glover, Smirnov (DDGS) is the most suitable for our aims, as it is calculated in multi-Regge kinematics and its ϵ-expansion up to the desired order is given. In [188] the integral is computed by two independent methods: 1) negative dimension approach and 2) Mellin-Barnes technique. The final result can be expressed in terms of transcendental double sums that, following Ref. [188], we denote by $\mathcal{M}$-functions; their definition is given in appendix A. Adapting their notation to ours, we define

$$x_1 \equiv \frac{st_1}{s_1 s_2} = \frac{t_1}{\vec{p}^{\,2}} , \quad x_2 = \frac{st_2}{s_1 s_2} = \frac{t_2}{\vec{p}^{\,2}} , \quad -\vec{p}^{\,2} = \frac{(-s_1)(-s_2)}{(-s)} , \quad y_1 \equiv \frac{1}{x_2} , \quad y_2 = \frac{x_1}{x_2} . \tag{4.110}$$

In Ref. [188] the three regions contributing to the pentagonal are identified as

- **Region I** : $\sqrt{x_1} + \sqrt{x_2} < 1$
- **Region II (a)** : $-\sqrt{x_1} + \sqrt{x_2} > 1$
- **Region II (b)** : $\sqrt{x_1} - \sqrt{x_2} > 1$

The solution in the **Region II (a)** is

$$\hat{I}_5^{(D=6+2\epsilon)} = -\frac{\Gamma(1-\epsilon)\Gamma^2(1+\epsilon)}{\Gamma(1+2\epsilon)}\sqrt{-\frac{s_1 s_2 t_1}{s t_2}}\left(\frac{(-s_1)(-s_2)}{(-s)}\right)^{\epsilon}\mathcal{I}^{II(a)}_{DDGS}(\vec{p}^{\,2},t_1,t_2)\;, \quad (4.111)$$

where

$$\mathcal{I}^{II(a)}_{DDGS}(\vec{p}^{\,2},t_1,t_2) = i_0^{II(a)}(y_1,y_2) - \epsilon\, i_1^{II(a)}(y_1,y_2) + \mathcal{O}(\epsilon^2)\;, \quad (4.112)$$

with

$$\begin{aligned}
i_0^{(IIa)}(y_1,y_2) &= (-8\ln y_1 - 4\ln y_2)\mathcal{M}\big(0,0,(1,1);-y_1,y_2\big) - 4\ln y_2\mathcal{M}\big((1,1),0,0;-y_1,y_2\big)\\
&+ 18\mathcal{M}\big(0,0,(1,2);-y_1,y_2\big) + 18\mathcal{M}\big(0,0,(2,1);-y_1,y_2\big) - 24\mathcal{M}\big(0,0,(1,1,1);-y_1,y_2\big)\\
&+ 8\mathcal{M}\big(0,1,(1,1);-y_1,y_2\big) + 16\mathcal{M}\big(1,0,(1,1);-y_1,y_2\big) - 8\mathcal{M}\big((1,1),0,1;-y_1,y_2\big)\\
&+ 8\mathcal{M}\big((1,1),1,0;-y_1,y_2\big) - \mathcal{M}\big(0,0,0;-y_1,y_2\big)\Big(\frac{\pi^2\ln y_1}{3} + \frac{\ln^2 y_1\ln y_2}{2} + \frac{\pi^2\ln y_2}{2} - 2\zeta(3)\Big)\\
&- \mathcal{M}\big(0,0,1;-y_1,y_2\big)\Big(2\ln y_1\ln y_2 + \ln^2 y_1 + \frac{5\pi^2}{3}\Big) + (6\ln y_1 + 3\ln y_2)\mathcal{M}\big(0,0,2;-y_1,y_2\big)\\
&+ \Big(2\ln y_1\ln y_2 + \frac{2\pi^2}{3}\Big)\mathcal{M}\big(1,0,0;-y_1,y_2\big) + (4\ln y_1 + 4\ln y_2)\mathcal{M}\big(1,0,1;-y_1,y_2\big)\\
&+ 4\ln y_1\mathcal{M}\big(0,1,1;-y_1,y_2\big) - 4\ln y_1\mathcal{M}\big(1,1,0;-y_1,y_2\big) + \Big(\ln^2 y_1 + \pi^2\Big)\mathcal{M}\big(0,1,0;-y_1,y_2\big)\\
&+ \ln y_2\mathcal{M}\big(2,0,0;-y_1,y_2\big) - 12\mathcal{M}\big(0,0,3;-y_1,y_2\big) - 6\mathcal{M}\big(0,1,2;-y_1,y_2\big)\\
&- 12\mathcal{M}\big(1,0,2;-y_1,y_2\big) - 8\mathcal{M}\big(1,1,1;-y_1,y_2\big) + 2\mathcal{M}\big(2,0,1;-y_1,y_2\big)\\
&- 2\mathcal{M}\big(2,1,0;-y_1,y_2\big), \qquad (4.113)
\end{aligned}$$

$$\begin{aligned}
i_1^{(IIa)}(y_1,y_2) &= \mathcal{M}\big(0,0,(1,1);-y_1,y_2\big)\Big(4\ln y_1\ln y_2 - 4\ln^2 y_1 + 2\ln^2 y_2 + 4\pi^2\Big)\\
&+ (2\ln^2 y_2 - 4\ln y_1\ln y_2)\mathcal{M}\big((1,1),0,0;-y_1,y_2\big) + (8\ln y_1 - 12\ln y_2)\mathcal{M}\big(1,0,(1,1);-y_1,y_2\big)\\
&+ (4\ln y_2 - 8\ln y_1)\mathcal{M}\big((1,1),0,1;-y_1,y_2\big) + (8\ln y_1 - 4\ln y_2)\mathcal{M}\big((1,1),1,0;-y_1,y_2\big)\\
&- 15\ln y_2\mathcal{M}\big(0,0,(1,2);-y_1,y_2\big) - 15\ln y_2\mathcal{M}\big(0,0,(2,1);-y_1,y_2\big)\\
&+ 20\ln y_2\mathcal{M}\big(0,0,(1,1,1);-y_1,y_2\big) - 4\ln y_2\mathcal{M}\big(0,1,(1,1);-y_1,y_2\big)\\
&- \ln y_2\mathcal{M}\big((1,2),0,0;-y_1,y_2\big) - \ln y_2\mathcal{M}\big((2,1),0,0;-y_1,y_2\big)\\
&+ 4\ln y_2\mathcal{M}\big((1,1,1),0,0;-y_1,y_2\big) + 32\mathcal{M}\big(0,0,(1,3);-y_1,y_2\big) + 36\mathcal{M}\big(0,0,(2,2);-y_1,y_2\big)\\
&+ 32\mathcal{M}\big(0,0,(3,1);-y_1,y_2\big) - 48\mathcal{M}\big(0,0,(1,1,2);-y_1,y_2\big) - 48\mathcal{M}\big(0,0,(1,2,1);-y_1,y_2\big)\\
&- 48\mathcal{M}\big(0,0,(2,1,1);-y_1,y_2\big) + 64\mathcal{M}\big(0,0,(1,1,1,1);-y_1,y_2\big) + 12\mathcal{M}\big(0,1,(1,2);-y_1,y_2\big)\\
&+12\mathcal{M}\big(0,1,(2,1);-y_1,y_2\big) - 16\mathcal{M}\big(0,1,(1,1,1);-y_1,y_2\big) + 18\mathcal{M}\big(1,0,(1,2);-y_1,y_2\big)\\
&+ 18\mathcal{M}\big(1,0,(2,1);-y_1,y_2\big) - 24\mathcal{M}\big(1,0,(1,1,1);-y_1,y_2\big) + 8\mathcal{M}\big(1,1,(1,1);-y_1,y_2\big)
\end{aligned}$$

$$
\begin{aligned}
&- 2\mathcal{M}\big((1,2),0,1;-y_1,y_2\big) + 2\mathcal{M}\big((1,2),1,0;-y_1,y_2\big) - 2\mathcal{M}\big((2,1),0,1;-y_1,y_2\big) \\
&+ 2\mathcal{M}\big((2,1),1,0;-y_1,y_2\big) + 8\mathcal{M}\big((1,1,1),0,1;-y_1,y_2\big) - 8\mathcal{M}\big((1,1,1),1,0;-y_1,y_2\big) \\
&+ \mathcal{M}\big(0,0,1;-y_1,y_2\big)\Big(\ln y_1 \ln^2 y_2 - \frac{\pi^2 \ln y_1}{3} - \frac{\ln^2 y_1 \ln y_2}{2} - \frac{2\ln^3 y_1}{3} + \frac{3\pi^2 \ln y_2}{2} - 6\zeta(3)\Big) \\
&+ \mathcal{M}\big(0,1,0;-y_1,y_2\big)\Big(\frac{\pi^2 \ln y_1}{3} - \frac{\ln^2 y_1 \ln y_2}{2} + \frac{2\ln^3 y_1}{3} - \frac{\pi^2 \ln y_2}{2} + 2\zeta(3)\Big) \\
&+ \mathcal{M}\big(1,0,0;-y_1,y_2\big)\Big(-\ln y_1 \ln^2 y_2 + \frac{\pi^2 \ln y_1}{3} + \frac{3\ln^2 y_1 \ln y_2}{2} - \frac{\pi^2 \ln y_2}{2} + 2\zeta(3)\Big) \\
&+ \mathcal{M}\big(0,0,2;-y_1,y_2\big)\Big(-3\ln y_1 \ln y_2 + 3\ln^2 y_1 - \frac{3\ln^2 y_2}{2} - 3\pi^2\Big) \\
&+ \mathcal{M}\big(0,1,1;-y_1,y_2\big)\Big(-2\ln y_1 \ln y_2 + 2\ln^2 y_1 - \frac{4\pi^2}{3}\Big) \\
&+ \mathcal{M}\big(1,1,0;-y_1,y_2\big)\Big(2\ln y_1 \ln y_2 - 3\ln^2 y_1 + \frac{\pi^2}{3}\Big) + (\ln y_2 - 2\ln y_1)\mathcal{M}\big(2,1,0;-y_1,y_2\big) \\
&+ \mathcal{M}\big(2,0,0;-y_1,y_2\big)\Big(\ln y_1 \ln y_2 - \frac{\ln^2 y_2}{2}\Big) + (9\ln y_2 - 6\ln y_1)\mathcal{M}\big(1,0,2;-y_1,y_2\big) \\
&+ (4\ln y_2 - 4\ln y_1)\mathcal{M}\big(1,1,1;-y_1,y_2\big) + (2\ln y_1 - \ln y_2)\mathcal{M}\big(2,0,1;-y_1,y_2\big) \\
&+ \mathcal{M}\big(0,0,0;-y_1,y_2\big)\Big(\frac{\ln^2 y_1 \ln^2 y_2}{4} - \frac{\pi^2 \ln^2 y_1}{6} - \frac{\ln^3 y_1 \ln y_2}{3} - 2\ln y_2 \zeta(3) + \frac{\pi^2 \ln^2 y_2}{4} + \frac{2\pi^4}{15}\Big) \\
&+ \Big(3\ln^2 y_1 - 2\ln^2 y_2 - \pi^2\Big)\mathcal{M}\big(1,0,1;-y_1,y_2\big) + 10\ln y_2 \mathcal{M}\big(0,0,3;-y_1,y_2\big) \\
&+ 3\ln y_2 \mathcal{M}\big(0,1,2;-y_1,y_2\big) - 20\mathcal{M}\big(0,0,4;-y_1,y_2\big) - 8\mathcal{M}\big(0,1,3;-y_1,y_2\big) \\
&- 12\mathcal{M}\big(1,0,3;-y_1,y_2\big) - 6\mathcal{M}\big(1,1,2;-y_1,y_2\big). \qquad (4.114)
\end{aligned}
$$

The solution in the **Region II (b)** is obtained by the replacement

$$\mathcal{I}^{II(a)}_{DDGS}(\vec{p}^{\,2},t_1,t_2) \to \mathcal{I}^{II(b)}_{DDGS}(\vec{p}^{\,2},t_1,t_2) = \frac{t_2}{t_1}\mathcal{I}^{II(a)}_{DDGS}(\vec{p}^{\,2},t_2,t_1) \qquad (4.115)$$

in eq. (4.111).

The solution in the **Region I** can be written as

$$\hat{I}_5^{(6+2\epsilon)} = -\frac{\Gamma(1-\epsilon)\Gamma^2(1+\epsilon)}{\Gamma(1+2\epsilon)}\sqrt{-\frac{st_1t_2}{s_1s_2}}\left(\frac{(-s_1)(-s_2)}{(-s)}\right)^{\epsilon}\mathcal{I}^{I}_{DDGS}(\vec{p}^{\,2},t_1,t_2)\,, \qquad (4.116)$$

where $\mathcal{I}^{I}_{DDGS}(\vec{p}^{\,2},t_1,t_2)$ can be obtained from $\mathcal{I}^{II(a)}_{DDGS}(\vec{p}^{\,2},t_1,t_2)$ by analytical continuation, according to the prescription $y_1 \to 1/y_1$.

4.4 Summary and outlook

We have calculated at the NLO the Reggeon-Reggeon-gluon (also called "Lipatov") effective vertex in QCD with accuracy up to the order ϵ^2, with $\epsilon = (D-4)/2$ and D the

space-time dimension. The NLO Lipatov effective vertex can be expressed in terms of a few integrals (triangle, boxes, pentagon), which we obtained at the required accuracy in a two-fold way: 1) taking their expressions, known at arbitrary ϵ, from the literature [187, 188] and expanding them to the required order; 2) calculating them from scratch[43], by an independent method. The purpose of the latter calculation is not only cross-checking, but also providing with an alternative, though equivalent, expression for the integrals, which could turn out to be more convenient for the uses of the NLO Lipatov effective vertex. For instance, the result up to order ϵ of the integral $\mathcal{I}_3$, calculated in section 4.3.2, is very compact compared to the result for the same integral computed in 4.3.1. It contains the structure $I_{\vec{q}_1^{\,2},\vec{q}_2^{\,2},\vec{p}^{\,2}}$ which has been extensively used in the BFKL literature (see *e.g.* [37]).

The integrals $\mathcal{I}_{4B}$, $\mathcal{I}_{4A}$ and $\hat{I}_4^{(i)}$ have been written as expansion to all orders in ϵ, in terms of polylogarithms. The integral $\mathcal{I}_3$ has been expanded up to the order ϵ^2, but can be expanded to higher orders, if needed. The residual and most complicated term is the one related to the pentagonal integral in dimension $6-2\epsilon$. Restricting to the order ϵ^2 in MRK, it is given in section 4.3.5. The knowledge of the one-loop Lipatov vertex in QCD at any successive order in the ϵ-expansion is completely reduced to the computation of this integral with higher ϵ-accuracy.

[43] With the exception of the part of the pentagon integral in $D = 4 + 2\epsilon$ which depends on the same integral in $D = 6+2\epsilon$. Nevertheless, in Ref. [188] this contribution was computed through two independent methods. In the case of $\mathcal{I}_3$ we have used an independent method valid just up to the order ϵ^2.

Part III
Beyond the linear regime: Saturation in the Shockwave formalism

Chapter 5

The Shockwave formalism

Physics is a very difficult thing; ...Unless you think that
physics is the most important thing in your life,
you should not do it. It takes passion, precision, patience.
S. Ting

In this chapter, the Shockwave formalism is introduced following [12, 192]. This approach, or equivalently his CGC formulation[44], applies when one consider the scattering of a dilute projectile on a dense target with high center-of-mass energy.
The chapter is organized in four sections. In the first section, we introduce the general picture of saturation. In the second section, we build the effective Lagrangian of the Shockwave approach. In the third, for pedagogical purposes, we derive the propagator of a quark crossing the Shockwave. Finally, in the last section, we derive the famous B-JIMWLK evolution equation for the dipole operator.

5.1 Saturation picture

The BFKL equation has gained much of its fame for being able to predict the rapid growth of the $\gamma^* p$ cross section at increasing center-of-mass energy s. In the large s limit, which in this context corresponds to the small Bjorken-x limit, the k_t-factorization is the most suitable scheme to investigate QCD processes.
If we consider the total cross section of Deep-Inelastic Scattering (DIS) through Eq. (1.158),

[44] CGC can be used also in the scattering of two dense systems.

we have

$$\sigma_{\gamma^* P}(x) = \frac{1}{(2\pi)^{D-2}} \int \frac{d^{D-2}k_\perp}{\vec{k}^2} \frac{\Phi_{\gamma^*\gamma^*}(\vec{k}\,)}{\vec{k}^2} \int \frac{d^{D-2}k'_\perp}{\vec{k}'^2} \frac{\Phi_{PP}(-\vec{k}')}{\vec{k}'^2} \int_{\delta-i\infty}^{\delta+i\infty} \frac{d\omega}{2\pi i} \left(\frac{1}{x}\right)^{\omega} G_\omega(\vec{q}_A, \vec{q}_B), \tag{5.1}$$

where $x = \frac{Q^2}{s}$. Obviously, it is important to make a clarification. Two impact factors appear in Eq. (5.1), one describing the γ^*-γ^* transition and the other describing the proton-proton transition. The second, clearly, contains non-perturbative information and cannot be defined and treated like the parton impact factors that we introduced in previous sections. Suppose we model it on the basis of reasonable physical arguments and define its convolution in the transverse momentum $\vec{k}'$ with the Green's function as $\mathcal{F}(x, \vec{k})$. We then have

$$\sigma_{\gamma^* P}(x) = \Phi_{\gamma^*\gamma^*}(\vec{k}\,) \otimes_{\vec{k}} \mathcal{F}(x, \vec{k}) \,, \tag{5.2}$$

where $\otimes_{\vec{k}}$ means convolution in the transverse momenta $\vec{k}$. The object we have denoted by $\mathcal{F}(x, \vec{k})$ is known as *unintegrated gluon density* and it is defined in such a way that the gluon collinear parton distribution function, f_g, is given by

$$f_g(x, Q^2) = \int \frac{d^2k}{\pi \vec{k}^{\,2}} \mathcal{F}(x, \vec{k}) \theta(Q^2 - \vec{k}^{\,2}) \,.$$

From Eq. (5.2) it is clear that the growth of cross sections that BFKL predicts is

$$\sigma_{\gamma^* P}(x) \sim \left(\frac{1}{x}\right)^{\omega_0} = \left(\frac{s}{Q^2}\right)^{\omega_0} \,.$$

This growth violates the Froissart bound [193],

$$\sigma_{tot} < c \ln^2 s,$$

where c is a constant. The violation cannot be removed by calculations of radiative corrections to a fixed $NNN...NL$ order and it is physically interpretable as an infinite growth of the UGD at low-x. The target appears to become a denser and denser gluon medium, until at some point it becomes infinitely dense.

It is clear that this scenario is incomplete and that some *saturation* effects must come into play in order to slow down this growth. The first idea to incorporate these effects was introduced by Gribov, Levin and Ryskin (GLR) [34] and it is based on a non-linear modification of the BFKL equation to incorporate recombination effects. This approach makes use of the double-log approximation, *i.e.* resummation of $\alpha_s \ln(s) \ln(Q^2)$ terms.

The most modern approach to saturation physics is based on a hierarchy of equations,

known under the name of Balitsky-JIMWLK (B-JIMWLK) equations. They were derived, in the so-called Shockwave approach, by Balitsky [12, 13, 14, 15] and, in the so-called Color Glass Condensate (CGC) approach, by Jalilian-Marian, Iancu, McLerran, Weigert, Leonidov and Kovner (JIMWLK) [16, 17, 18, 19, 20, 21, 22, 23, 24]. In the large N-limit, a closed equation, which is known as Balitsky-Kovchegov (BK), is obtained. This large-N truncation was recovered by Kovchegov using Mueller's dipole formalism [194, 195]. It can also be shown that, in the dipole operator case and in the double logarithmic limit, the GLR equation is recovered.

In saturation physics, a new dimensional scale is introduced, the so called *saturation scale*,

$$Q_s^2(x) \equiv (Ax^{-1})^{\frac{1}{3}} \Lambda^2_{\text{QCD}} \ , \tag{5.3}$$

where A is the mass number of the target. It is estimated that the CGC formalism (or equivalently Balitsky's shockwave formalism) must be applied instead of the BFKL formalism for

$$Q^2 < Q_s^2 \ .$$

Eq. (5.3) contains in itself extremely important information. The saturation scale grows not only with the inverse of the Bjorken-x, but also with the mass number of the target. Saturation effects are therefore emphasized in large nuclei. This is crucial, because it means that if very low values of x have to be reached for a proton to perceive these effects, for a large enough nucleus, these effects will be seen at larger x.

5.2 Boosted gluonic field and effective Lagrangian

5.2.1 Notation and conventions

We introduce the dimensionless Sudakov vectors n_1 and n_2, defined as

$$n_1 \equiv \frac{1}{\sqrt{2}}(1, 0_\perp, 1), \ \ n_2 \equiv \frac{1}{\sqrt{2}}(1, 0_\perp, -1) \ , \ \ n_1^+ = n_2^- = n_1 \cdot n_2 = 1 \ . \tag{5.4}$$

With these definitions, for any four-vector p, we can introduce the components

$$p^+ = p_- \equiv (p \cdot n_2) = \frac{1}{\sqrt{2}}(p^0 + p^3) \ , \qquad p_+ = p^- \equiv (p \cdot n_1) = \frac{1}{\sqrt{2}}(p^0 - p^3) \ ,$$

$$p = p^+ n_1 + p^- n_2 + p_\perp \ . \tag{5.5}$$

A generic scalar product can therefore be written as

$$(p \cdot k) = p^\mu k_\mu = p^+ k^- + p^- k^+ + (p_\perp \cdot k_\perp) \equiv p_+ k_- + p_- k_+ - (\vec{p} \cdot \vec{k}) \ . \tag{5.6}$$

We use the same notation for Dirac matrices, and denote

$$\gamma^+ = \gamma_- = \gamma^\mu n_{2,\mu} \,, \qquad \gamma^- = \gamma_+ = \gamma^\mu n_{1,\mu} \,. \tag{5.7}$$

Throughout the chapter we also use the notation

$$\gamma^\mu p_\mu = \hat{p} \,. \tag{5.8}$$

In the Regge limit, both the projectile and the target possess large components, respectively along the n_1 and along n_2, of the order

$$p_p^+ \sim p_t^- \sim \sqrt{\frac{s}{2}} \,. \tag{5.9}$$

Again, we work in a k_t-formalism, therefore the scattering amplitudes will be expressed as convolutions in transverse momenta between a projectile impact factor and a target impact factor. The gluons exchanged in the t-channel, describing the interaction between projectile and Shockwave field, are once again eikonal and carry an effective polarization proportional to n_2. Once again, we work in dimension $D = d + 2 = 4 + 2\epsilon$.

The fundamental idea of the Shockwave approach is to immediately exploit the Regge kinematics in such a way as to formulate the high-energy scattering problem in terms of the relevant degrees of freedom. In particular, since in Regge kinematics all the transverse momenta are of the same order of magnitude, but colliding particles strongly differ in rapidity, it is natural to factorize in the rapidity space (see Fig. 5.1). This type of factorization is achieved by introducing a rapidity cut-off, $e^\eta p_p^+$, which separates the "slow" modes from the "fast" modes. The interpretation of these modes as "fast" and "slow" is thought in the rest reference frame of the target. Gluons with +-momentum component below the cut-off act as an external *classical* field. The interaction between projectile and target is through these "slow" modes and, as we will see, it is described in terms of a Wilson-line operator. The B-JIMWLK evolution equations are the result of quantum corrections, due to "fast" gluons, to the Wilson line. Practically, in the spirit of the renormalization group, it is the dependence of the relevant matrix elements on the cut-off η which determines the high-energy behavior of the original amplitude.

One could reasonably ask why slow gluons can be treated classically. The answer lies in the fact that, in the saturation regime $Q^2 < Q_s^2(x)$, we are dealing with weakly coupled QCD, *i.e.*

$$\alpha_s(Q_s^2) \ll 1 \,. \tag{5.10}$$

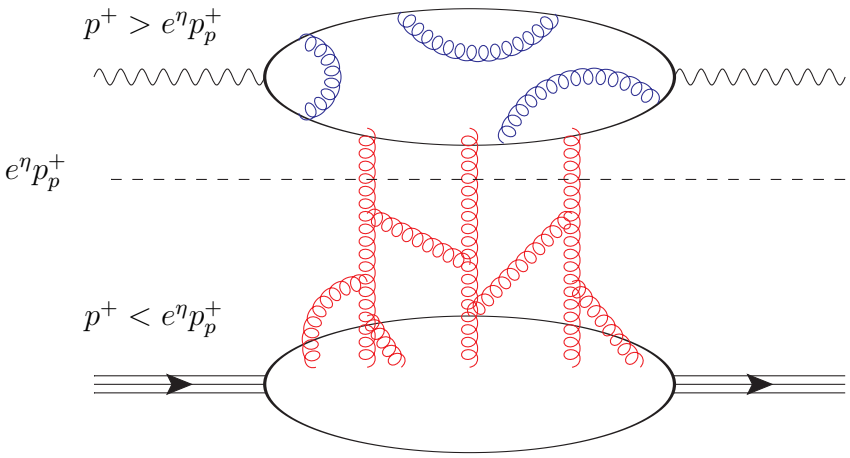

Figure 5.1: Schematic representation of the separation in the rapidity space between quantum "fast" modes (blue) and classical "slow" modes (red).

As it is well known, in the small-coupling regime, field theories are dominated by classical solutions. In this observation lies one of the most interesting aspects of saturation approaches. In fact, like other semi-classical approaches, they are able to describe interesting phenomena, which occur for small coupling, but for which approaches based on perturbation theory only are inadequate.

5.2.2 Boosted gluonic field

Let's consider a gluon field $b_0(\mu)$ in the target rest frame. Let's now perform a boost, with velocity β, along the z^+ axis to move to the projectile rest frame. The coordinate transformation is

$$(x^+, x^-, \vec{x}\,) \equiv \left(\frac{z^+}{\Lambda}, \Lambda z^-, \vec{x}\right) , \quad \text{with} \quad \Lambda = \sqrt{\frac{1+\beta}{1-\beta}} . \tag{5.11}$$

In the new frame, the gluonic field reads

$$\begin{aligned} b^+\left(x^+, x^-, \vec{x}\,\right) &= \frac{1}{\Lambda} b_0^+\left(\Lambda x^+, \frac{x^-}{\Lambda}, \vec{x}\right) , \\ b^-\left(x^+, x^-, \vec{x}\,\right) &= \Lambda b_0^-\left(\Lambda x^+, \frac{x^-}{\Lambda}, \vec{x}\right) , \\ b^{\,i}\left(x^+, x^-, \vec{x}\,\right) &= b_0^i\left(\Lambda x^+, \frac{x^-}{\Lambda}, \vec{x}\right) . \end{aligned} \tag{5.12}$$

Assuming that the field vanishes to infinity, and remembering that we are making a very large boost, the $+$ and i components of the field vanish. Hence, up to Λ^{-1} corrections,

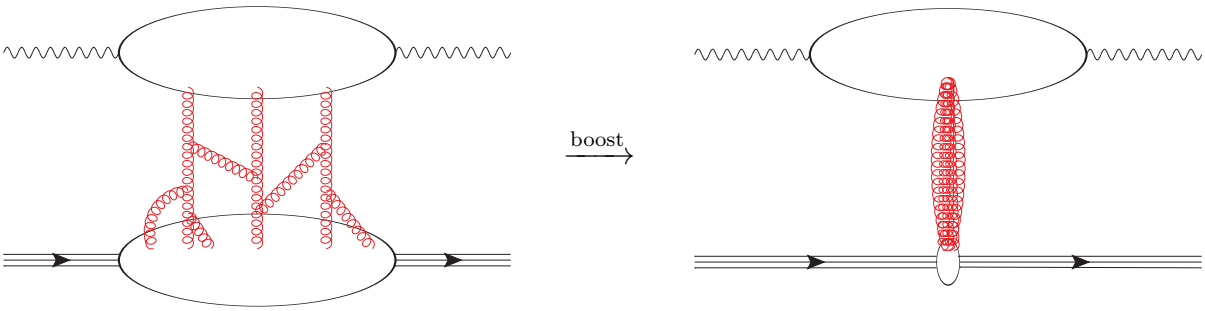

Figure 5.2: Schematic representation of the Shockwave approximation.

we get that

$$\begin{aligned} b^+\left(x^+,x^-,\vec{x}\,\right) &= 0\,, \\ b^-\left(x^+,x^-,\vec{x}\,\right) &= \Lambda b_0^-\left(\Lambda x^+,0,\vec{x}\right)\,, \\ b^{\,i}\left(x^+,x^-,\vec{x}\,\right) &= 0\,, \end{aligned} \tag{5.13}$$

where we note that, in this approximation, the surviving component of the field is always evaluated in $x^- = 0$. Exploiting that, for any integrable function F,

$$\lim_{\Lambda\to\infty} \Lambda F(\Lambda x) \propto \delta(x)\,, \tag{5.14}$$

we can write

$$b^\mu\left(x^+,x^-,\vec{x}\,\right) = b^-\left(x^+,\vec{x}\,\right) n_2^\mu \equiv \delta(x^+)\mathbf{B}(\vec{x}\,)n_2^\mu\,. \tag{5.15}$$

The last equation expresses precisely the idea of re-formulating the problem in terms of the relevant degrees of freedom. From the point of view of the projectile, the interaction takes place with an eikonal field (n_2^μ), well localized in the +-component ($\delta(x^+)$) and whose shape is described by a function depending on transverse coordinates only ($\mathbf{B}(\vec{x}\,)$). The effect of this transformation is depicted in Fig. (5.2).

Let's consider the collision of our projectile with a large momentum p_p along p^+ on a target with a large momentum p_t along p^- and with mass m_t. The energy of the target in the projectile's frame is

$$E = \frac{m_t}{\sqrt{1-\beta^2}} = \frac{p_t^+ + p_t^-}{\sqrt{2}} \sim \frac{p_t^-}{\sqrt{2}}\,. \tag{5.16}$$

From Eq. (5.16) it is simple to see that

$$\Lambda \sim \sqrt{\frac{s}{m_t^2}}\,,$$

when $p_p^+, p_t^- \sim \sqrt{\frac{s}{2}}$. Thus, the above approximation (neglecting Λ^{-1} corrections) is equivalent to neglect terms suppresed by $\frac{1}{\sqrt{s}}$ factor.

5.2.3 Effective Lagrangian

We now start from the QCD Lagrangian,

$$\mathcal{L} = -\frac{1}{4}\mathcal{F}_{a\mu\nu}\mathcal{F}^{a\mu\nu} + i\bar{\psi}\hat{D}\psi = \mathcal{L}_{\text{free}} + \mathcal{L}_{\text{int}} \,, \tag{5.17}$$

where we split the free and the interaction part; this latter reads

$$\mathcal{L}_{\text{int}} = -gf_{abc}\left(\partial_\mu \mathcal{A}^a_\nu\right)\left(\mathcal{A}^{\mu b}\mathcal{A}^{\nu c}\right) - \frac{1}{4}g^2 f_{abc}f_{ade}\left(\mathcal{A}^a_\mu \mathcal{A}^b_\nu \mathcal{A}^{\mu d}\mathcal{A}^{\nu e}\right) + i\bar{\psi}\left(-igt^a\hat{\mathcal{A}}^a\right)\psi \,. \tag{5.18}$$

In this interaction part, we write the total gluon field, $\mathcal{A}$, as the combination of the external field, b, and the usual gluon field A. The former describes the effective interaction of the projectile with the small-x gluons from the target, while the latter contributes to the quantum evolution of the system. We then have,

$$\mathcal{A}^a_\mu = A^a_\mu + b^a_\mu \,. \tag{5.19}$$

Using the fact that $b^\mu b_\mu \propto n_2^2 = 0$, we obtain

$$\begin{aligned}\mathcal{L}_{\text{int}} =& -gf_{abc}\left[\left(\left(A^b\cdot\partial\right)A^a + \left(b^b\cdot\partial\right)A^a\right)\cdot(A^c+b^c) + \left(\left(A^b\cdot\partial\right)b^a + \left(b^b\cdot\partial\right)b^a\right)\cdot A^c\right] \\ &- \frac{1}{4}g^2 f_{abc}f_{ade}\left[\left(\left(A^a\cdot A^d\right) + \left(b^d\cdot A^a\right)\right)\left(\left(A^b\cdot A^e\right) + \left(b^e\cdot A^b\right) + \left(b^b\cdot A^e\right)\right)\right. \\ &\left. + \left(b^a\cdot A^d\right)\left(\left(A^b\cdot A^e\right) + \left(b^e\cdot A^b\right) + \left(b^b\cdot A^e\right)\right)\right] + i\bar{\psi}\left[-igt^a\left(\hat{A}^a + \hat{b}^a\right)\right]\psi.\end{aligned} \tag{5.20}$$

In the lightcone gauge $A\cdot n_2 = 0$,

$$A\cdot b \propto A\cdot n_2 = 0$$

holds, and hence, Eq. (5.20) can be simplified. Therefore, in this case, unlike the formulation of the BFKL approach presented in the previous sections, it is essential to choose an axial gauge. In the aforementioned gauge, we then have

$$\begin{aligned}\mathcal{L}_{\text{int}} =& -gf_{abc}\left(A^b\cdot\partial\right)\left(A^a\cdot A^c\right) - \frac{1}{4}g^2 f_{abc}f_{ade}\left[\left(A^a\cdot A^d\right)\left(A^b\cdot A^e\right)\right] + i\bar{\psi}\left[-igt^a\hat{A}^a\right]\psi \\ &-gf_{abc}\left(b^b\cdot\partial\right)\left(A^a\cdot A^c\right) + gt^a\left(\bar{\psi}\hat{b}^a\psi\right).\end{aligned} \tag{5.21}$$

The first three terms describe the usual interactions of QCD, while the last two terms describe the interaction between the internal field and the Shockwave field. We denote this part of the Lagrangian as

$$\mathcal{L}^{\mathcal{S}}_{\text{int}} = -gf_{acb}b^{-c}g_{\alpha\beta}\left[A^a_\alpha\frac{\partial A^b_\beta}{\partial x^-}\right] + g\left(\bar{\psi}t^a\hat{b}^a\psi\right). \tag{5.22}$$

5.3 Quark propagator through the shockwave field

To give an explicit example of how Feynman rules describing the effective interaction can be found, let us re-derive the one for a quark propagator crossing the Shockwave.

5.3.1 Two gluons interaction

We start by considering the propagator interacting twice with the external field while propagating from a point z_0 (at negative light-cone time) to a point z_3 (at positive light-cone time). We have[45]

$$\begin{aligned}
&G\left(z_3,z_0\right)|_{z_3^+>0>z_0^+}\\
&=\int d^Dz_2d^Dz_1G_0\left(z_{32}\right)\left[igb^-\left(z_2\right)\gamma^+\right]G_0\left(z_{21}\right)\left[igb^-\left(z_1\right)\gamma^+\right]G_0\left(z_{10}\right)\\
&=\int d^Dz_2d^Dz_1\left[igb^-\left(z_2\right)igb^-\left(z_1\right)\right]\int\frac{d^Dp_3}{(2\pi)^D}\frac{d^Dp_2}{(2\pi)^D}\frac{d^Dp_1}{(2\pi)^D}G_0\left(p_3\right)\gamma^+G_0\left(p_2\right)\gamma^+G_0\left(p_1\right)\\
&\quad\times\exp\left[-i\left(p_3\cdot z_3\right)+i\left(p_3-p_2\right)\cdot z_2+i\left(p_2-p_1\right)\cdot z_1+i\left(p_1\cdot z_0\right)\right]\ ,
\end{aligned}\tag{5.23}$$

where we denote the free quark propagator by G_0. As explained before, the field $b^-(z)$ has no dependencies on z^-; this means that we can immediately integrate over z_1^-, z_2^-. These integrations produce two Dirac deltas which impose $p_3^+=p_2^+=p_1^+\equiv p^+$:

$$\begin{aligned}
&G\left(z_3,z_0\right)|_{z_3^+>0>z_0^+}=(2\pi)^2\int dz_2^+dz_1^+d^d\vec{z}_2d^d\vec{z}_1\left[igb^-\left(z_2^+,\vec{z}_2\right)igb^-\left(z_1^+,\vec{z}_1\right)\right]\\
&\times\int dp^+\int\frac{d^d\vec{p}_3}{(2\pi)^D}\frac{d^d\vec{p}_2}{(2\pi)^D}\frac{d^d\vec{p}_1}{(2\pi)^D}\exp\left[i\left(\vec{p}_3\cdot\vec{z}_{32}\right)+i\left(\vec{p}_2\cdot\vec{z}_{21}\right)+i\left(\vec{p}_1\cdot\vec{z}_{10}\right)-ip^+z_{30}^-\right]\\
&\times\int dp_3^-\frac{i\left(p^+\gamma^-+\hat{p}_{3\perp}\right)}{2p^+\left(p_3^--\frac{\vec{p}_3^{\,2}-i0}{2p^+}\right)}\exp\left[-ip_3^-z_{32}^+\right]\int dp_2^-\gamma^+\frac{i\left(p^+\gamma^-+\hat{p}_{2\perp}\right)}{2p^+\left(p_2^--\frac{\vec{p}_2^{\,2}-i0}{2p^+}\right)}\gamma^+\exp\left[-ip_2^-z_{21}^+\right]\\
&\times\int dp_1^-\frac{i\left(p^+\gamma^-+\hat{p}_{1\perp}\right)}{2p^+\left(p_1^--\frac{\vec{p}_1^{\,2}-i0}{2p^+}\right)}\exp\left[-ip_1^-z_{10}^+\right]\ .
\end{aligned}\tag{5.24}$$

In Eq. (5.24), we have already removed the γ^+ component in all quarks propagators exploiting $\gamma^+\gamma^+=0$. The integration over the three variables p_i^- can be preformed using Jordan's lemma. Due to the conditions imposed by theta functions, only the region $p^+>0$

[45] b^- contains the $SU(3)$ matrix in the fundamental representation.

gives a non-zero contribution:

$$
\begin{aligned}
&G\left(z_3,z_0\right)\big|_{z_3^+>0>z_0^+} = (2\pi)^5 \int dz_2^+ dz_1^+ d^d\vec{z}_2 d^d\vec{z}_1 \left[igb^-\left(z_2^+,\vec{z}_2\right) igb^-\left(z_1^+,\vec{z}_1\right)\right] \\
&\times \int dp^+ \theta\left(p^+\right)\theta\left(z_{32}^+\right)\theta\left(z_{21}^+\right)\theta\left(z_{10}^+\right)\exp\left[-ip^+ z_{30}^-\right] \\
&\times \int \frac{d^d\vec{p}_3}{(2\pi)^D}\frac{\left(p^+\gamma^- + \hat{p}_{3\perp}\right)}{2p^+}\exp\left[-i\frac{z_{32}^+}{2p^+}\left\{\left(\vec{p}_3 - \frac{p^+}{z_{32}^+}\vec{z}_{32}\right)^2 - \left(\frac{p^+}{z_{32}^+}\right)^2 \vec{z}_{32}^{\,2} - i0\right\}\right] \\
&\times \int \frac{d^d\vec{p}_2}{(2\pi)^D}\gamma^+ \exp\left[-i\frac{z_{21}^+}{2p^+}\left(\vec{p}_2^{\,2} - i0\right) + i\left(\vec{p}_2\cdot\vec{z}_{21}\right)\right] \\
&\times \int \frac{d^d\vec{p}_1}{(2\pi)^D}\frac{\left(p^+\gamma^- + \hat{p}_{1\perp}\right)}{2p^+}\exp\left[-i\frac{z_{10}^+}{2p^+}\left\{\left(\vec{p}_1 - \frac{p^+}{z_{10}^+}\vec{z}_{10}\right)^2 - \left(\frac{p^+}{z_{10}^+}\right)^2 \vec{z}_{10}^{\,2} - i0\right\}\right].
\end{aligned}
\tag{5.25}
$$

Up to corrections of order $\Lambda^{-1}\sim s^{-1/2}$, $b(z_i^+,\vec{z}_i)\propto\delta(z_i^+)$. This allows us to approximate the Gaussian integral over $\vec{p}_2$ by setting $z_{12}^+=0$ and getting therefore a $\delta(\vec{z}_{12})$. This is important, because it tells us that the interaction with the shockwave field occurs at a single transverse coordinate. We note that the remaining Gaussian integrals are always convergent since $\frac{z_{10}^+}{p^+},\frac{z_{32}^+}{p^+} > 0$. Observing that we can clearly rescale the pole prescription $i0$ by using an arbitrary positive quantity, we can make the following manipulation

$$
\begin{aligned}
&-i\frac{z_{32}^+}{2p^+}\left[\left(\vec{p}_3 - \frac{p^+}{z_{32}^+}\vec{z}_{32}\right)^2 - \left(\frac{p^+}{z_{32}^+}\right)^2 \vec{z}_{31}^{\,2} - i0\right] \\
&= -i\frac{z_{32}^+}{2p^+}\left[\left\{\left(\vec{p}_3 - \frac{p^+}{z_{32}^+}\vec{z}_{32}\right)^2 - i0\right\} - \left(\frac{p^+}{z_{32}^+}\right)^2\left(\vec{z}_{31}^{\,2} + i0\right)\right] \\
&= -i\frac{z_{32}^+}{2p^+}(1-i0)\left(\vec{p}_3 - \frac{p^+}{z_{32}^+}\vec{z}_{32}\right)^2 + i\frac{p^+}{2z_{32}^+}\left(\vec{z}_{31}^{\,2} + i0\right).
\end{aligned}
\tag{5.26}
$$

An analogous manipulation can be done for the exponent depending on p_1, and then both integrations can be performed to get

$$
\begin{aligned}
&G\left(z_3,z_0\right)\big|_{z_3^+>0>z_0^+} = \int dz_2^+ dz_1^+ d^d\vec{z}_2 d^d\vec{z}_1 \left[igb^-\left(z_2^+,\vec{z}_2\right) igb^-\left(z_1^+,\vec{z}_1\right)\right]\frac{\delta\left(\vec{z}_{21}\right)}{4(2\pi)^{2D-3}} \\
&\times\left(\gamma^- + \frac{\hat{z}_{31\perp}}{z_{32}^+}\right)\gamma^+\left(\gamma^- + \frac{\hat{z}_{10\perp}}{z_{10}^+}\right)\int dp^+\left(\frac{-2i\pi p^+}{z_{32}^+}\right)^{\frac{d}{2}}\left(\frac{-2i\pi p^+}{z_{10}^+}\right)^{\frac{d}{2}}\theta\left(p^+\right)\theta\left(z_{32}^+\right) \\
&\times\theta\left(z_{21}^+\right)\theta\left(z_{10}^+\right)\exp\left[-ip^+ z_{30}^- + i\frac{p^+}{2z_{32}^+}\left(\vec{z}_{31}^{\,2} + i0\right) + i\frac{p^+}{2z_{10}^+}\left(\vec{z}_{10}^{\,2} + i0\right)\right] \\
&= i\frac{\Gamma(D-1)}{4(2\pi)^{D-1}}\int dz_2^+ dz_1^+ d^d\vec{z}_1\left[igb^-\left(z_2^+,\vec{z}_1\right) igb^-\left(z_1^+,\vec{z}_1\right)\right] \\
&\times\frac{\left(z_3^+\gamma^- + \hat{z}_{31\perp}\right)\gamma^+\left(-z_0^+\gamma^- + \hat{z}_{10\perp}\right)}{\left(-z_3^+ z_0^+\right)^{\frac{D}{2}}}\frac{\theta\left(z_{32}^+\right)\theta\left(z_{21}^+\right)\theta\left(z_{10}^+\right)}{\left(-z_{30}^- + \frac{\vec{z}_{31}^{\,2}+i0}{2z_3^+} - \frac{\vec{z}_{10}^{\,2}+i0}{2z_0^+}\right)^{D-1}}.
\end{aligned}
\tag{5.27}
$$

Now, it is useful to define

$$U^{(2)}_{\vec{z}} = (ig)^2 \int dz_2^+ dz_1^+ \theta\left(z_{32}^+\right) \theta\left(z_{21}^+\right) \theta\left(z_{10}^+\right) b^-\left(z_2^+, \vec{z}\right) b^-\left(z_1^+, \vec{z}\right) \ , \tag{5.28}$$

and re-write the previous expression as

$$G\left(z_3, z_0\right)\big|_{z_3^+>0>z_0^+} = i\frac{\Gamma(D-1)}{4(2\pi)^{D-1}} \int d^d\vec{z}_1 U^{(2)}_{\vec{z}_1} \frac{\left(z_3^+\gamma^- + \hat{z}_{31\perp}\right)\gamma^+\left(-z_0^+\gamma^- + \hat{z}_{10\perp}\right)}{\left(-z_3^+ z_0^+\right)^{\frac{D}{2}}\left(-z_{30}^- + \frac{\vec{z}_{31}^2}{2z_3^+} - \frac{\vec{z}_{10}^2}{2z_0^+} + i0\right)^{D-1}} \ . \tag{5.29}$$

The physical interpretation of this expression is not immediate. We therefore introduce a representation which, as we shall see, is completely equivalent:

$$\tilde{G}\left(z_3, z_0\right)\Big|_{z_3^+>0>z_0^+} \equiv \int d^D z_1 \delta\left(z_1^+\right) G_0\left(z_{31}\right)\gamma^+ G_0\left(z_{10}\right)\theta\left(z_3^+\right)\theta\left(-z_0^+\right) U^{(2)}_{\vec{z}_1} \ . \tag{5.30}$$

From Eq. (5.30), the physical picture is clear: first the quark propagates from z_0 to z_1, then it interacts instantly at $z_1^+ = 0$ with the external field, then it propagates again from z_1 to z_3. Let's now prove that the expression we gave is completely equivalent. We first integrate over z_1^+ to get

$$\tilde{G}\left(z_3, z_0\right)\Big|_{z_3^+>0>z_0^+} = \left[\frac{\Gamma\left(\frac{D}{2}\right)}{2\pi^{\frac{D}{2}}}\right]^2 \int dz_1^- d^d\vec{z}_1 U^{(2)}_{\vec{z}_1} \frac{\left(z_3^+\gamma^- + \hat{z}_{31\perp}\right)\gamma^+\left(-z_0^+\gamma^- + \hat{z}_{10\perp}\right)}{\left(-2z_3^+ z_{31}^- + \vec{z}_{31}^2 + i0\right)^{\frac{D}{2}}\left(2z_0^+ z_{10}^- + \vec{z}_{10}^2 + i0\right)^{\frac{D}{2}}} \ , \tag{5.31}$$

and then we introduce the Schwinger representation for the denominators,

$$\frac{1}{(A \pm i0)^n} = \frac{(\mp i)^n}{\Gamma(n)} \int_0^{+\infty} d\alpha \left(\alpha^{n-1}\right) e^{\pm i\alpha(A \pm i0)} \ . \tag{5.32}$$

Performing the integration over z_1^- and then over one Schwinger parameter, we find

$$\begin{aligned}\tilde{G}\left(z_3, z_0\right)\Big|_{z_3^+>0>z_0^+} =& -\frac{(-i)^D}{4\pi^{D-1}} \int d^d\vec{z}_1 \left(-\frac{z_3^+}{z_0^+}\right)^{\frac{d}{2}} \frac{\left(z_3^+\gamma^- + \hat{z}_{31\perp}\right)\gamma^+\left(-z_0^+\gamma^- + \hat{z}_{10\perp}\right)}{z_0^+} \\ &\times U^{(2)}_{\vec{z}_1} \int_0^{+\infty} d\alpha_1 \left(\alpha_1\right)^d \exp\left[i\alpha_1\left(-2z_3^+ z_{30}^- + \vec{z}_{31}^2 - \frac{z_3^+}{z_0^+}\vec{z}_{10}^2 + i0\right)\right] .\end{aligned} \tag{5.33}$$

Integration with respect to the Schwinger parameter now gives

$$\begin{aligned}\tilde{G}\left(z_3, z_0\right)\Big|_{z_3^+>0>z_0^+} =& \frac{i\Gamma(D-1)}{4(2\pi)^{D-1}} \int d^d\vec{z}_1 \frac{\left(z_3^+\gamma^- + \hat{z}_{31\perp}\right)\gamma^+\left(-z_0^+\gamma^- + \hat{z}_{10\perp}\right)}{\left(-z_3^+ z_0^+\right)^{\frac{D}{2}}} \\ &\times \frac{\theta\left(z_3^+\right)\theta\left(-z_0^+\right) U^{(2)}_{z_1}}{\left(-z_{30}^- + \frac{\vec{z}_{31}^2}{2z_3^+} - \frac{\vec{z}_{10}^2}{2z_0^+} + i0\right)^{D-1}} .\end{aligned} \tag{5.34}$$

We have proved that

$$G\left(z_3, z_0\right)\big|_{z_3^+>0>z_0^+} = \tilde{G}\left(z_3, z_0\right)\Big|_{z_3^+>0>z_0^+} . \tag{5.35}$$

5.3.2 The appearance of the Wilson line

We would like to generalize what we saw previously and resum all possible interactions of the quark line with the external field b^μ. A great hint in this direction is given by form of $U^{(2)}_{\vec{z}}$ in Eq. (5.28). It is easy to see that it is the $(ig)^2$ term in the (ig)-expansion of the Wilson line (in the fundamental representation)

$$\left[z_3^+, z_0^+\right]_{\vec{z}} = \mathcal{P} \exp\left[ig \int_{z_0^+}^{z_3^+} dz^+ b^- \left(z^+, \vec{z}\right)\right] , \tag{5.36}$$

where $\mathcal{P}$ means time-ordered product. We want to establish that the generalization we seek is obtained by replacing $U^{(2)}_{\vec{z}}$ with the full Wilson line defined in Eq. (5.36), *i.e.*

$$G\left(z_3, z_0\right)\big|_{z_3^+>0>z_0^+} = \int d^D z_1 \delta\left(z_1^+\right) G_0\left(z_{31}\right) \gamma^+ G_0\left(z_{10}\right) \left[z_3^+, z_0^+\right]_{\vec{z}_1} . \tag{5.37}$$

We prove this by mathematical induction. We already proved that (5.37) is correct for $n = 2$, where n is the number of interactions, and for $n = 1$ is trivial. Let's prove the $n = 0$ case by setting the Wilson line to the identity in Eq. (5.33), we get

$$\begin{aligned} G^{(0)}\left(z_3, z_0\right)\big|_{z_3^+>0>z_0^+} = &- \frac{(-i)^D}{4\pi^{D-1}} \int d^d \vec{z}_1 \left(-\frac{z_3^+}{z_0^+}\right)^{\frac{d}{2}} \frac{\left(z_3^+\gamma^- + \hat{z}_{31\perp}\right)\gamma^+\left(-z_0^+\gamma^- + \hat{z}_{10\perp}\right)}{z_0^+} \\ &\times \int_0^{+\infty} d\alpha_1 \left(\alpha_1\right)^d \exp\left[i\alpha_1\left(-2z_3^+ z_{30}^- + \vec{z}_{31}^2 - \frac{z_3^+}{z_0^+}\vec{z}_{10}^2 + i0\right)\right] . \end{aligned} \tag{5.38}$$

A shift in the variable $\vec{z}_1$ allows us to have a Gaussian integral and hence to obtain

$$\begin{aligned} G^{(0)}\left(z_3, z_0\right)\big|_{z_3^+>0>z_0^+} = &- \frac{(-i)^D}{4\pi^{D-1} z_0^+} \left(-\frac{z_3^+}{z_0^+}\right)^{\frac{a}{2}} \int_0^{+\infty} d\alpha_1 \left(\alpha_1\right)^{\frac{d}{2}} \\ &\left[-2z_3^+ z_0^+ \left(\gamma^-\right) - 2\frac{z_3^+ z_0^+}{z_{30}^+}\left(\hat{z}_{30\perp}\right) - \frac{z_3^+ z_0^+ \vec{z}_{30}^2}{\left(z_{30}^+\right)^2}\left(\gamma^+\right) + i\frac{d}{2}\frac{z_0^+}{\alpha_1 z_{30}^+}\left(\gamma^+\right)\right] \\ &\times \exp\left[i\alpha_1\left(-2z_3^+ z_{30}^- + \frac{z_3^+}{z_{30}^+}\vec{z}_{30}^2 + i0\right)\right]\left(\frac{-i\pi z_0^+}{z_{30}^+}\right)^{\frac{d}{2}} . \end{aligned} \tag{5.39}$$

After the last integration we recover the usual free quark propagator in coordinates space:

$$G^{(0)}\left(z_3, z_0\right)\big|_{z_3^+>0>z_0^+} = \frac{i\Gamma\left(\frac{D}{2}\right)}{2\pi^{\frac{D}{2}}} \frac{\hat{z}_{30}}{\left(-z_{30}^2 + i0\right)^{\frac{D}{2}}} = G_0\left(z_3, z_0\right) . \tag{5.40}$$

To complete our proof, we only need to show that, assuming the result holds for n interactions, the case $n+1$ follows. If for n we have

$$G^{(n)}\left(z_3, z_0\right)\big|_{z_3^+>0>z_0^+} = \int d^D z_1 \delta\left(z_1^+\right) G_0\left(z_{31}\right) \gamma^+ G_0\left(z_{10}\right) \left[z_3^+, z_0^+\right]^{(n)}_{\vec{z}_1} , \tag{5.41}$$

then

$$G^{(n+1)}\left(z_3,z_0\right)\big|_{z_3^+>0>z_0^+} = \int d^D z_2 G_0\left(z_{32}\right)\left[ig\gamma^+ b^-\left(z_2\right)\right] G^{(n)}\left(z_2,z_0\right)$$
$$=(ig)\int d^D z_2 d^D z_1 b^-\left(z_2\right)\delta\left(z_1^+\right)\left[G_0\left(z_{32}\right)\gamma^+ G_0\left(z_{21}\right)\gamma^+ G_0\left(z_{10}\right)\right]\theta\left(z_2^+\right)\left[z_2^+,z_0^+\right]_{\vec{z}_1}^{(n)}. \tag{5.42}$$

The integration is performed as explained before and we get

$$G^{(n+1)}\left(z_3,z_0\right)\big|_{z_3^+>0>z_0^+} = \int d^D z_1 \delta\left(z_1^+\right)\left[G_0\left(z_{31}\right)\gamma^+ G_0\left(z_{10}\right)\right]$$
$$\times (ig)\int dz_2^+ \theta\left(z_{32}^+\right)\theta\left(z_2^+\right)\theta\left(-z_0^+\right) b^-\left(z_2^+,\vec{z}_1\right)\left[z_2^+,z_0^+\right]_{\vec{z}_1}^{(n)}. \tag{5.43}$$

This last expression can be immediately re-written as

$$G^{(n+1)}\left(z_3,z_0\right)\big|_{z_3^+>0>z_0^+} = \int d^D z_1 \delta\left(z_1^+\right)\left[G_0\left(z_{31}\right)\gamma^+ G_0\left(z_{10}\right)\right]\theta\left(z_3^+\right)\theta\left(-z_0^+\right)\left[z_3^+,z_0^+\right]_{\vec{z}_1}^{(n+1)}. \tag{5.44}$$

This completes our proof.
We want to make one last observation. Since the interaction is localized in light-cone time, we can have two situations:

- The integration boundaries z_0^+ and z_3^+ have the same sign. In this case the Wilson line reduces to the identity, the Shockwave is not crossed and we have a normal quark propagator.

- The integration boundaries z_0^+ and z_3^+ possess opposite sign. In this case the Wilson line is nontrivial and the Shockwave is crossed. It is clear that in this case, only the point $z^+ = 0$ of the entire integration domain contributes and that we can therefore extend the integration from $-\infty$ to $+\infty$.

We therefore define

$$U_{\vec{z}} \equiv [-\infty,+\infty]_{\vec{z}} = \mathcal{P}\exp\left[ig\int_{-\infty}^{+\infty} dz^+ b^-\left(z^+,\vec{z}\right)\right], \tag{5.45}$$

and its Fourier transform

$$U\left(p_\perp\right) \equiv \int d^d z_\perp e^{i(p_\perp\cdot z_\perp)} U_{\vec{z}}\,. \tag{5.46}$$

In defining the Feynman rules, we use these latter definitions. We avoid to report all of them here, they can be found in Ref. [192], where the notation is identical to the one used in the part of this thesis devoted to the Shockwave approach.

5.4 B-JIMWLK evoultion for the dipole operator

In this section, we want to study quantum corrections to the previous picture. As already anticipated, we will study the effect of a change in the cut-off η. We consider the external field at rapidity $\eta_1 = \eta + \Delta\eta$, where $\Delta\eta$ should be intended as a small deviation from η. We separate it as

$$b^-_{\eta+\Delta\eta}(z) = b^-_\eta(z) + b^-_{\Delta\eta}(z) \,, \tag{5.47}$$

where

$$b^-_{\Delta\eta}(z) \equiv \int \frac{d^D p}{(2\pi)^D} e^{-i(p\cdot z)} b^-(p) \theta\left(e^{\eta+\Delta\eta} p_p^+ - p^+\right) \theta\left(p^+ - e^\eta p_p^+\right) \tag{5.48}$$

contains gluons with +-momenta between $e^\eta p_p^+$ and $e^{\eta+\Delta\eta} p_p^+$. Let's consider now the Wilson line at rapidity η_1 for the propagation between the lightcone time x^+ and the lightcone time y^+. From Eq. (5.36), it can be written as

$$\left[x^+, y^+\right]^{\eta_1}_{\vec{z}} = \sum_N \int_{x^+}^{y^+} dz_1^+ (ig) b^-_{\eta_1}\left(z_1^+, \vec{z}\right) \int_{x^+}^{z_1^+} dz_2^+ (ig) b^-_{\eta_1}\left(z_2^+, \vec{z}\right) \ldots \int_{x^+}^{z_{N-1}} dz_N^+ (ig) b^-_{\eta_1}\left(z_N^+, \vec{z}\,\right) \,. \tag{5.49}$$

Now, we perform a perturbative expansion in the small parameter $ig\Delta\eta$ to show how the Wilson line at rapidity η is modified by the small perturbation. Using that $[z_i^+, z_j^+]^\eta_{\vec{z}} = 1$ if $z_i^+ z_j^+ > 0$, we find

$$\begin{aligned} \left[x^+, y^+\right]^{\eta+\Delta\eta}_{\vec{z}} =& \left[x^+, y^+\right]^\eta_{\vec{z}} + (ig) \int_{x^+}^{y} dz_1^+ \left[x^+, z_1^+\right]^\eta_{\vec{z}} b^-_{\Delta\eta}\left(z_1^+, \vec{z}\right) \left[z_1^+, y^+\right]^\eta_{\vec{z}} \\ &+ (ig)^2 \int_{x^+}^{y^+} dz_1^+ dz_2^+ \left[x^+, z_1^+\right]^\eta_{\vec{z}} b_{\Delta\eta}\left(z_1^+, \vec{z}\right) \left[z_1^+, z_2^+\right]^\eta_{\vec{z}} b_{\Delta\eta}\left(z_2^+, \vec{z}\right) \left[z_2^+, y^+\right]^\eta_{\vec{z}} \theta\left(z_{21}^+\right) . \end{aligned} \tag{5.50}$$

We study two eikonal lines propagating through the shockwave at rapidity $\eta_1 = \eta + \Delta$ and with a color singlet interaction with the external field. They interact "classically" with the part of the field generated by b^-_η. However, this *classical propagation* is modified by the quantum fluctuations generated by the field $b^-_{\Delta\eta}$. These quantum fluctuations lead to the evolution equation.

In the spirit of the expansion (5.50), taking into account these corrections is equivalent to considering the two lines that propagate in the part of the field generated by b^-_η with the possibility of emitting and reabsorbing a gluon which has a +-component of momenta strictly between $e^\eta p_p^+$ and $e^{\eta+\Delta\eta} p_p^+$ (see Figs. 5.3, 5.4).

The propagator of this gluon is built from $b^-_{\Delta\eta}$ and reads

$$\begin{aligned}\left(G^{\mu\nu}_{\Delta\eta}\right)^{ab} =&(-i)^d \int \frac{d^d\vec{z}_3}{(2\pi)^{d+1}} \left(U_{\vec{z}_3}\right)^{ab} \int_{e^\eta}^{e^{\eta+\Delta\eta}} dp^+ \frac{\left(p^+\right)^{d-1}}{2\left(-z_2^+ z_1^+\right)^{\frac{d}{2}+1}} \\ &\times \exp\left[-ip^+\left\{z_{21}^- - \frac{\vec{z}_{23}^{\,2}}{2z_2^+} + \frac{\vec{z}_{31}^{\,2}}{2z_1^+} - i0\right\}\right] \left(\vec{z}_{23}\cdot\vec{z}_{31}\right)\left(n_2^\mu n_2^\nu\right) \ ,\end{aligned} \tag{5.51}$$

where we want to remark the restriction on the +-component.

Before proceeding, we want to make a small digression to compare BFKL and Shockwave approach. Obviously, the physical picture is the same, there is a big rapidity gap between two interacting objects, and hence, there is phase space for gluon radiation strongly ordered in rapidity. In both cases, we are interested in resuming the large logarithmic corrections generated by these kinematic conditions. However, it is important to note that the way we want to construct the evolution is slightly different. For BFKL we had considered two lines of quarks strongly separated in rapidity which, precisely because of this separation, exchanged an infinite ladder of gluons. The effective polarization of gluons attached to the upper line was n_2^μ, while the one of gluons attached to the lower line was n_1^μ. In the present case, the two incoming lines represent the whole projectile; their longitudinal components are both of order p_p^+, *i.e.* they are in the same fragmentation region and there is no rapidity gap between them. The separation in rapidity is between this projectile and the gluons produced by the entire $b^\mu_{\eta_1}$ gluon field. This way of deriving evolution is closer in spirit to that of the Muller dipole, but, as we shall see, in the correct limit is equivalent to BFKL.

Let's move on to the calculation of corrections produced by the field $b^-_{\Delta\eta}$; they lead to ten Feynman diagrams. In four of these diagrams, the additional gluon crosses the Shockwave (see Fig. 5.3), and thus, this class of diagrams involves an additional adjoint Wilson line $\left(U^\eta_{\vec{z}_3}\right)^{ab}$. We refer to this part as *double dipole contribution*. In the remaining six, the Shockwave is crossed only by the eikonal lines (see Fig. 5.4), we refer to this part as *dipole contribution*.

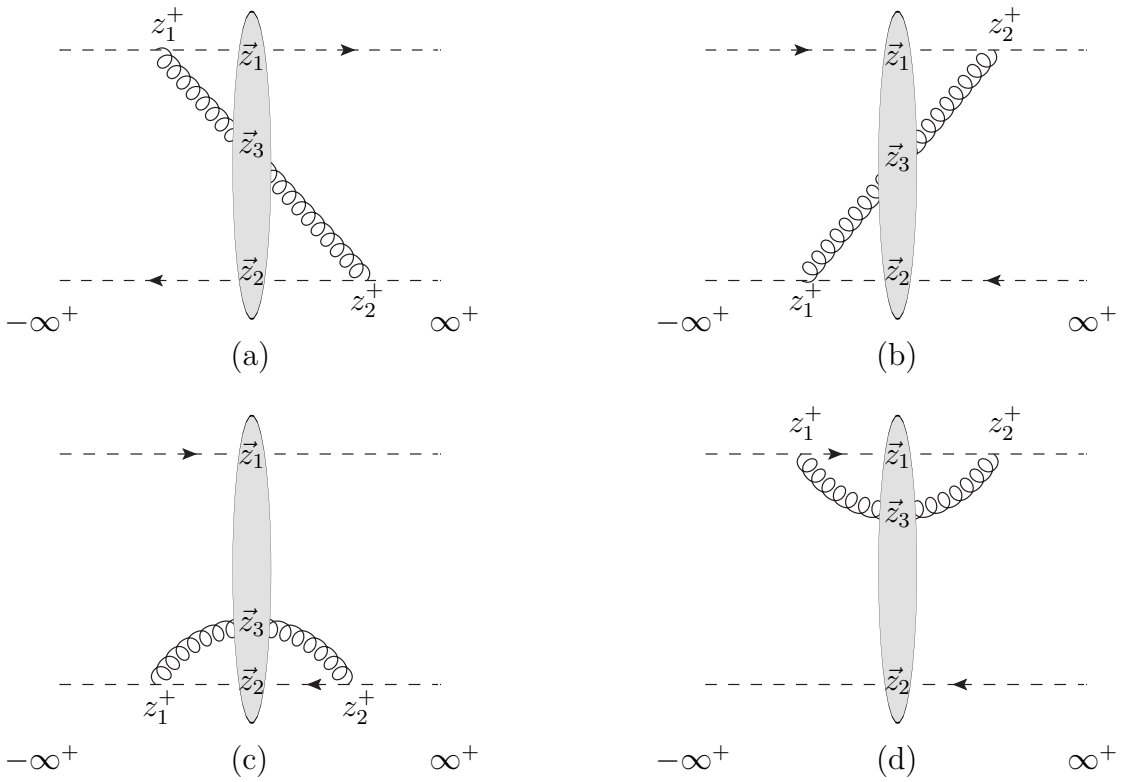

Figure 5.3: Double dipole contribution to the evolution. The Shockwave is always crossed at $z_3^+ = 0$.

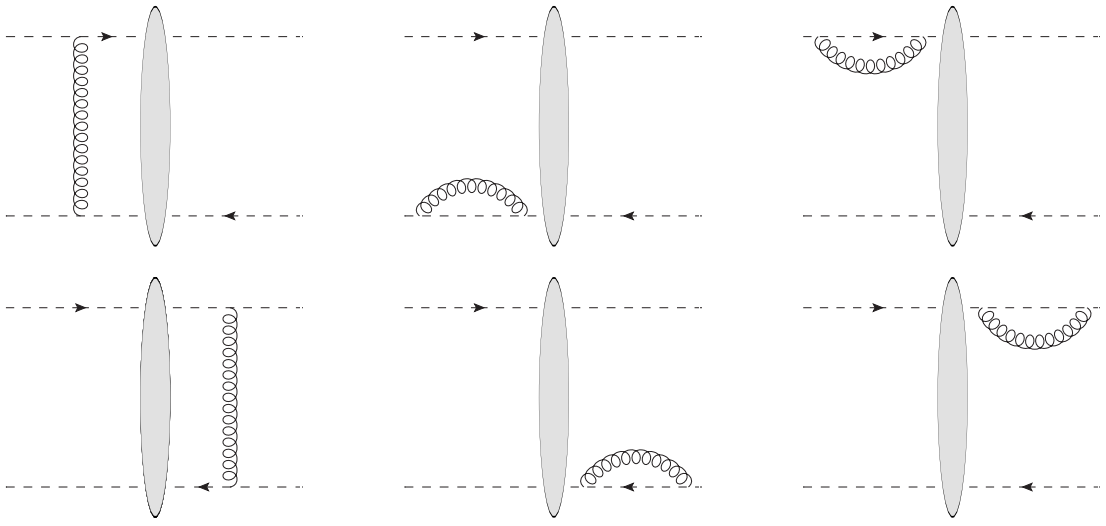

Figure 5.4: Dipole contribution to the evolution. The Shockwave is not crossed and hence only single dipole cntributions are generated.

We start by considering the diagram (a) in Fig. 5.3, it reads[46]

$$
\begin{aligned}
I_{(a)} &= (ig)(-ig)\mu^{-2\epsilon}\int_{-\infty}^{0} dz_1^+ \int_0^{+\infty} dz_2^+ \\
&\times \mathrm{Tr}\left(\left[+\infty, z_1^+\right]_{\vec{z}_1}^{\eta} t^b \left[z_1^+, -\infty\right]_{\vec{z}_1}^{\eta} \left[-\infty, z_2^+\right]_{\vec{z}_2}^{\eta} t^a \left[z_2^+, +\infty\right]_{\vec{z}_2}^{\eta}\right) \left(G_{\Delta\eta}\right)^{ab} \\
&= \frac{(-i)^d g^2 \mu^{-2\epsilon}}{2(2\pi)^{d+1}} \mathrm{Tr}\left(U_{\vec{z}_1}^{\eta} t^b U_{\vec{z}_2}^{\eta\dagger} t^a\right) \int d^d\vec{z}_3 \left(U_{\vec{z}_3}^{\eta}\right)^{ab} \int_{e^\eta}^{e^{\eta+\Delta\eta}} dp^+ \left(p^+\right)^{d-1} \\
&\times \int_{-\infty}^{0} \frac{dz_1^+}{\left(-z_1^+\right)^{\frac{d}{2}+1}} \int_0^{+\infty} \frac{dz_2^+}{\left(z_2^+\right)^{\frac{d}{2}+1}} \exp\left[-ip^+\left\{z_{21}^- - \frac{\vec{z}_{23}^{\,2}}{2z_2^+} + \frac{\vec{z}_{31}^{\,2}}{2z_1^+} - i0\right\}\right] \left(\vec{z}_{23}\cdot\vec{z}_{31}\right) \\
&= \frac{g^2\mu^{-2\epsilon} 2^d \left[\Gamma\left(\frac{d}{2}\right)\right]^2}{2(2\pi)^{d+1}} \int d^d\vec{z}_3 \frac{\left(\vec{z}_{23}\cdot\vec{z}_{31}\right)}{\left(\vec{z}_{23}^{\,2}\right)^{\frac{d}{2}} \left(\vec{z}_{31}^{\,2}\right)^{\frac{d}{2}}} \left[\mathrm{Tr}\left(U_{\vec{z}_1}^{\eta} t^b U_{\vec{z}_2}^{\eta\dagger} t^a\right)\left(U_{\vec{z}_3}^{\eta}\right)^{ab}\right] \int_{e^\eta}^{e^{n+\Delta_\eta}} dp^+ \frac{e^{-ip^+\left(z_{21}^- - i0\right)}}{p^+} \,.
\end{aligned}
\tag{5.52}
$$

This implies

$$
I_{(a)} \sim \frac{g^2\mu^{-2\epsilon} 2^d \left[\Gamma\left(\frac{d}{2}\right)\right]^2}{2(2\pi)^{d+1}} \int d^d\vec{z}_3 \frac{\left(\vec{z}_{23}\cdot\vec{z}_{31}\right)}{\left(\vec{z}_{23}^{\,2}\right)^{\frac{d}{2}} \left(\vec{z}_{31}^{\,2}\right)^{\frac{d}{2}}} \left[\mathrm{Tr}\left(U_{\vec{z}_1}^{\eta} t^b U_{\vec{z}_2}^{\eta\dagger} t^a\right)\left(U_{\vec{z}_3}^{\eta}\right)^{ab}\right](\Delta\eta) \,. \tag{5.53}
$$

The diagram (c) in Fig. 5.3 is computed similarly and gives

$$
I_{(c)} \sim \frac{g^2\mu^{-2\epsilon} \left[\Gamma\left(\frac{d}{2}\right)\right]^2 2^d}{2(2\pi)^{d+1}} \int d^d\vec{z}_3 \,\mathrm{Tr}\left(t^a U_{\vec{z}_2}^{\eta\dagger} t^b U_{\vec{z}_1}^{\eta}\right)\left(U_{\vec{z}_3}^{\eta}\right)^{ba} \frac{1}{\left(\vec{z}_{32}^{\,2} + i0\right)^{d-1}}(\Delta\eta) \,. \tag{5.54}
$$

Finally, diagram (b) and (d) are obtained from (a) and (c) respectively, by the substitutions $\vec{z}_1 \leftrightarrow \vec{z}_2$ and $ig \leftrightarrow -ig$. We have

$$
I_{(b)} \sim \frac{g^2\mu^{-2\epsilon} 2^d \left[\Gamma\left(\frac{d}{2}\right)\right]^2}{2(2\pi)^{d+1}} \int d^d\vec{z}_3 \frac{\left(\vec{z}_{23}\cdot\vec{z}_{31}\right)}{\left(\vec{z}_{23}^{\,2}\right)^{\frac{d}{2}} \left(\vec{z}_{31}^{\,2}\right)^{\frac{d}{2}}} \left[\mathrm{Tr}\left(U_{\vec{z}_1}^{\eta} t^b U_{\vec{z}_2}^{\eta\dagger} t^a\right)\left(U_{\vec{z}_3}^{\eta}\right)^{ab}\right](\Delta\eta) \,, \tag{5.55}
$$

$$
I_{(d)} \sim \frac{g^2\mu^{-2\epsilon} \left[\Gamma\left(\frac{d}{2}\right)\right]^2 2^d}{2(2\pi)^{d+1}} \int d^d\vec{z}_3 \,\mathrm{Tr}\left(t^a U_{\vec{z}_2}^{\eta\dagger} t^b U_{\vec{z}_1}^{\eta}\right)\left(U_{\vec{z}_3}^{\eta}\right)^{ba} \frac{1}{\left(\vec{z}_{31}^{\,2}\right)^{d-1}}(\Delta\eta) \,. \tag{5.56}
$$

We denote the sum of all these contributions by

$$
\begin{aligned}
I_R \equiv & \frac{\alpha_s \mu^{-2\epsilon} \Delta\eta \left[\Gamma\left(\frac{d}{2}\right)\right]^2}{\pi^d} \int d^d\vec{z}_3 \,\mathrm{Tr}\left(t^a U_{\vec{z}_1}^{\eta} t^b U_{\vec{z}_2}^{\eta\dagger}\right)\left(U_{\vec{z}_3}^{\eta}\right)^{ab} \\
& \times \left[\frac{2\left(\vec{z}_{23}\cdot\vec{z}_{31}\right)}{\left(\vec{z}_{23}^{\,2}\right)^{\frac{d}{2}} \left(\vec{z}_{31}^{\,2}\right)^{\frac{d}{2}}} + \frac{1}{\left(\vec{z}_{23}^{\,2}\right)^{d-1}} + \frac{1}{\left(\vec{z}_{31}^{\,2}\right)^{d-1}}\right] \,.
\end{aligned}
\tag{5.57}
$$

[46] Tr means trace with respect to the fundamental representation and it is needed in order to have a singlet exchange.

Now, we should compute the six diagrams without crossing. Instead of a direct computation, there is an elegant trick that allows to obtain directly the sum of all six contributions. Let's denote the sum of all these contributions as I_V. First, we observe that if we set all Wilson lines to the identity[47], we must have

$$\left(I_R + I_V\right)\big|_{U^\eta_{\vec{z}_{1,2,3}}\to 1} = 0 \implies I_R\big|_{U^\eta_{\vec{z}_{1,2,3}}\to 1} = -I_V\big|_{U^\eta_{\vec{z}_{1,2,3}}\to 1} . \tag{5.58}$$

Indeed, we are computing the linear term in the $\Delta\eta$ expansion of the dipole operator. When every Wilson line is set to one, any dependence on η disappears so this term in the expansion in exactly zero. Moreover, it is clear that

$$I_V \equiv C_V \operatorname{Tr}\left(U^\eta_{\vec{z}_1} U^{\eta\dagger}_{\vec{z}_2}\right) \implies I_V\big|_{U^\eta_{\vec{z}_{1,2,3}}\to 1} = C_V N_c . \tag{5.59}$$

Since

$$I_R\big|_{U^\eta_{\vec{z}_{1,2,3}}} = \frac{\alpha_s \mu^{-2\epsilon}\Delta\eta\left[\Gamma\left(\frac{d}{2}\right)\right]^2}{\pi^d}\frac{N_c-1}{2}\int d^d\vec{z}_3\left[\frac{2\left(\vec{z}_{23}\cdot\vec{z}_{31}\right)}{\left(\vec{z}_{23}^{\,2}\right)^{\frac{d}{2}}\left(\vec{z}_{31}^{\,2}\right)^{\frac{d}{2}}} + \frac{1}{\left(\vec{z}_{23}^{\,2}\right)^{d-1}} + \frac{1}{\left(\vec{z}_{31}^{\,2}\right)^{d-1}}\right] , \tag{5.60}$$

we immediately get

$$C_V = -\frac{\alpha_s \mu^{-2\epsilon}\Delta\eta\left[\Gamma\left(\frac{d}{2}\right)\right]^2}{\pi^d}\frac{N_c-1}{2N_c}\int d^d\vec{z}_3\left[\frac{2\left(\vec{z}_{23}\cdot\vec{z}_{31}\right)}{\left(\vec{z}_{23}^{\,2}\right)^{\frac{d}{2}}\left(\vec{z}_{31}^{\,2}\right)^{\frac{d}{2}}} + \frac{1}{\left(\vec{z}_{23}^{\,2}\right)^{d-1}} + \frac{1}{\left(\vec{z}_{31}^{\,2}\right)^{d-1}}\right] , \tag{5.61}$$

and hence the full dipole contribution, which reads

$$\begin{aligned} I_V = &-\frac{\alpha_s \mu^{-2\epsilon}\Delta\eta\left[\Gamma\left(\frac{d}{2}\right)\right]^2}{\pi^d}\frac{N_c^2-1}{2N_c} \\ &\times\int d^d\vec{z}_3\left[\frac{2\left(\vec{z}_{23}\cdot\vec{z}_{31}\right)}{\left(\vec{z}_{23}^{\,2}\right)^{\frac{d}{2}}\left(\vec{z}_{31}^{\,2}\right)^{\frac{d}{2}}} + \frac{1}{\left(\vec{z}_{23}^{\,2}\right)^{d-1}} + \frac{1}{\left(\vec{z}_{31}^{\,2}\right)^{d-1}}\right]\operatorname{Tr}\left(U^\eta_{\vec{z}_1} U^{\eta\dagger}_{\vec{z}_2}\right) . \end{aligned} \tag{5.62}$$

Considering together the dipole and double dipole contributions and taking the limit $\Delta\eta \to 0$, we get

$$\begin{aligned} \frac{\partial \operatorname{Tr}\left(U^\eta_{\vec{z}_1} U^{\eta\dagger}_{\vec{z}_2}\right)}{\partial\eta} = &\frac{\alpha_s \mu^{-2\epsilon}\left[\Gamma\left(\frac{d}{2}\right)\right]^2}{\pi^d}\int d^d\vec{z}_3\left[\operatorname{Tr}\left(U^\eta_{\vec{z}_1} t^b U^{\eta\dagger}_{\vec{z}_2} t^a\right)\left(U_{\vec{z}_3}\right)^{ab} - \frac{N_c^2-1}{2N_c}\operatorname{Tr}\left(U^\eta_{\vec{z}_1} U^{\eta\dagger}_{\vec{z}_2}\right)\right] \\ &\times\left[\frac{2\left(\vec{z}_{23}\cdot\vec{z}_{31}\right)}{\left(\vec{z}_{23}^{\,2}\right)^{\frac{d}{2}}\left(\vec{z}_{31}^{\,2}\right)^{\frac{d}{2}}} + \frac{1}{\left(\vec{z}_{23}^{\,2}\right)^{d-1}} + \frac{1}{\left(\vec{z}_{31}^{\,2}\right)^{d-1}}\right] . \end{aligned} \tag{5.63}$$

[47] From a physical point of view it clearly means that there is no interaction between the eikonal lines and the target.

We introduce now the dipole operators

$$\mathcal{U}_{ij}^{\eta} = \frac{1}{N_c}\,\mathrm{Tr}\left(U_{\vec{z}_i}^{\eta} U_{\vec{z}_j}^{\eta\dagger}\right) - 1\,, \tag{5.64}$$

Using the relation

$$\left(U_{\vec{z}_3}^{\eta}\right)^{ab} = 2\,\mathrm{Tr}\left(t^a U_{\vec{z}_3}^{\eta} t^b U_{\vec{z}_3}^{\eta\dagger}\right) \tag{5.65}$$

and the Fierz identity

$$\left(t_{ij}^a\right)\left(t_{kl}^a\right) = \frac{1}{2}\delta_{il}\delta_{jk} - \frac{1}{2N_c}\delta_{ij}\delta_{kl}\,, \tag{5.66}$$

we can immediately find

$$\begin{aligned}
&\mathrm{Tr}\left(U_{\vec{z}_1}^{\eta} t^b U_{\vec{z}_2}^{\eta\dagger} t^a\right)\left(U_{\vec{z}_3}^{\eta}\right)^{ab} - \frac{N_c^2-1}{2N_c}\,\mathrm{Tr}\left(U_{\vec{z}_1}^{\eta} U_{\vec{z}_2}^{\eta\dagger}\right)\\
=&2\,\mathrm{Tr}\left(t^a U_{\vec{z}_3}^{\eta} t^b U_{\vec{z}_3}^{\eta\dagger}\right)\mathrm{Tr}\left(t^a U_{\vec{z}_1}^{\eta} t^b U_{\vec{z}_2}^{\eta\dagger}\right) - \frac{N_c^2-1}{2N_c}\,\mathrm{Tr}\left(U_{\vec{z}_1}^{\eta} U_{\vec{z}_2}^{\eta\dagger}\right)\\
=&2\left[\frac{1}{2}\delta_{in}\delta_{jm} - \frac{1}{2N_c}\delta_{ij}\delta_{mn}\right]\left[\frac{1}{2}\delta_{kq}\delta_{pl} - \frac{1}{2N_c}\delta_{kl}\delta_{pq}\right]\\
&\times\left(U_{\vec{z}_3}^{\eta}\right)_{jk}\left(U_{\vec{z}_3}^{\eta\dagger}\right)_{li}\left(U_{\vec{z}_1}^{\eta}\right)_{np}\left(U_{\vec{z}_2}^{\eta\dagger}\right)_{qm} - \frac{N_c^2-1}{2N_c}\,\mathrm{Tr}\left(U_{\vec{z}_1}^{\eta} U_{\vec{z}_2}^{\eta\dagger}\right)\\
=&\frac{1}{2}\left[\mathrm{Tr}\left(U_{\vec{z}_1}^{\eta} U_{\vec{z}_3}^{\eta\dagger}\right)\mathrm{Tr}\left(U_{\vec{z}_3}^{\eta} U_{\vec{z}_2}^{\eta\dagger}\right) - N_c\,\mathrm{Tr}\left(U_{\vec{z}_1}^{\eta} U_{\vec{z}_2}^{\eta\dagger}\right)\right]\\
=&\frac{N_c^2}{2}\left[\mathcal{U}_{13}^{\eta} + \mathcal{U}_{32}^{\eta} - \mathcal{U}_{12}^{\eta} + \mathcal{U}_{13}^{\eta}\mathcal{U}_{32}^{\eta}\right].
\end{aligned} \tag{5.67}$$

Therefore, Eq. (5.63) in terms of the dipole operator takes the form

$$\begin{aligned}
\frac{\partial \mathcal{U}_{12}^{\eta}}{\partial\eta} =&\frac{\alpha_s N_c\left[\Gamma\left(\frac{d}{2}\right)\right]^2(\mu^2)^{1-\frac{d}{2}}}{2\pi^d}\\
&\times\int d^d\vec{z}_3\left[\mathcal{U}_{13}^{\eta} + \mathcal{U}_{32}^{\eta} - \mathcal{U}_{12}^{\eta} + \mathcal{U}_{13}^{\eta}\mathcal{U}_{32}^{\eta}\right]\left[\frac{2\left(\vec{z}_{23}\cdot\vec{z}_{31}\right)}{\left(\vec{z}_{23}^{\,2}\right)^{\frac{d}{2}}\left(\vec{z}_{31}^{\,2}\right)^{\frac{d}{2}}} + \frac{1}{\left(\vec{z}_{23}^{\,2}\right)^{d-1}} + \frac{1}{\left(\vec{z}_{31}^{\,2}\right)^{d-1}}\right],
\end{aligned} \tag{5.68}$$

which is the final evolution equation. Taking $D = 4$, one recovers the usual B-JIMWLK equation for the dipole operator

$$\frac{\partial \mathcal{U}_{12}^{\eta}}{\partial\eta} = \frac{\alpha_s N_c}{2\pi^2}\int d^2\vec{z}_3\left(\frac{\vec{z}_{12}^{\,2}}{\vec{z}_{23}^{\,2}\vec{z}_{31}^{\,2}}\right)\left[\mathcal{U}_{13}^{\eta} + \mathcal{U}_{32}^{\eta} - \mathcal{U}_{12}^{\eta} - \mathcal{U}_{13}^{\eta}\mathcal{U}_{32}^{\eta}\right]\,. \tag{5.69}$$

The operators constructed from the Wilson lines lead us to the physical scattering amplitudes when we consider the matrix elements between two (*in* and *out*) proton states. In this sense, the evolution equation for the dipole operator involves a double dipole operator. This second operator, involving four Wilson lines, in general, cannot be described

as a product of two dipole operators. For the latter a second evolution equation has to be written. This equation will depend on operators with higher number of Wilson lines. We thus obtain an infinite cascade of equations known as *Balitsky hierarchy*. We can recover the closed non-linear BK equation only in the large-N_c approximation ('t Hooft limit). In this case the double dipole operator becomes a product of dipoles. It is well known that the next-to-leading corrections in the large N_c approximation are of the order $1/N_c^2$ and hence, naively, we would expect corrections to BK dynamics to be of order 11%. However, saturation effects tend to play an important role in suppressing these corrections [196]. Finally, we observe that if we completely neglect the non-linear term (dilute approximation) in Eq. (5.69) we obtain the colour-dipole version of the BFKL equation (see *e.g.* [37]).

Chapter 6

Inclusive diffractive di-hadron production

Another roof, another proof.
Paul Erdős [197]

In this chapter, we consider again an hybrid high-energy/collinear factorization for the description of the semi-diffractive di-hadron production. This time, we rely on the Shock-wave formalism introduced in the previous chapter and on results obtained in Ref. [198]. The cancellation of divergences is explicitly shown, and the finite parts of the NLO differential cross-sections are found. We work in arbitrary kinematics such that both photoproduction and leptoproduction are considered. The results obtained, are usable to detect saturation effects, at both the future Electron-Ion-Collider (EIC) or already at LHC, using Ultra Peripheral Collisions (UPC).

The chapter contains six sections. In the first section, we set-up the general framework and we present the program of computations. In the second, we show counterterms coming from renormalization of FFs. In the third and fourth section we extract divergences from real and virtual corrections, respectively. In the fifth chapter we give all additional finite terms needed to construct the NLO cross section. Lastly, in the sixth section we summarize and discuss possible developments. The material of this chapter is based on Ref. [199].

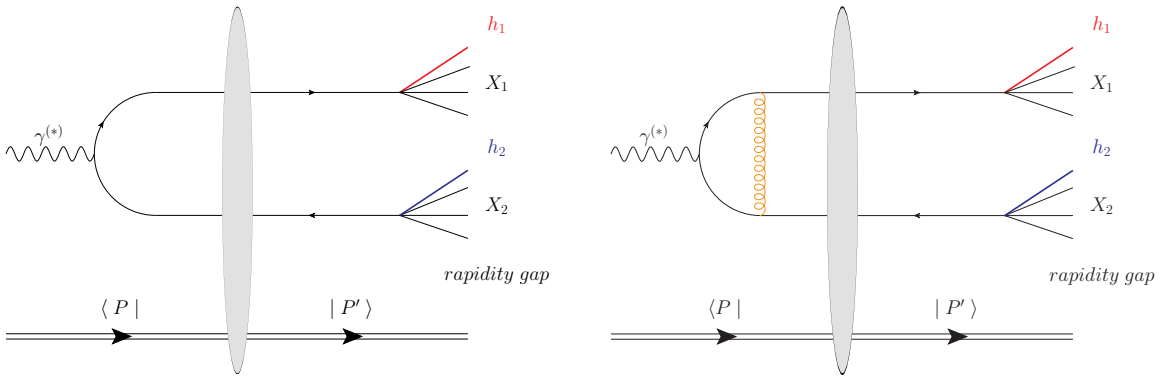

Figure 6.1: Left: Amplitude of the process (6.1) at LO. Right: An example of diagram contributing to the amplitude of the process (6.1) at NLO. The grey blob symbolizes the QCD shockwave. The double line symbolizes the target, which remains intact in the figure, but could just as well break. The quark and antiquark fragment into the systems $(h_1 X_1)$ and $(h_2 X_2)$. The two tagged hadrons h_1 and h_2 are drawn in red and blue.

6.1 Theoretical framework

6.1.1 Hybrid collinear/high-energy factorization

We want to perform a full NLO computation of the semi-inclusive diffractive di-hadron production in the high-energy limit:

$$\gamma^{(*)}(p_\gamma) + P(p_0) \to h_1(p_{h_1}) + h_2(p_{h_2}) + X + P'(p_0') \,, \tag{6.1}$$

where P is a nucleon or a nucleus target, generically called proton in the following. The initial photon plays the role of a probe (also named projectile). Our computation applies both to the photoproduction case (including ultraperipheral collisions) and to the electroproduction case (e.g. at EIC). A gap in rapidity is assumed between the outgoing nucleon/nucleus and the diffractive system $(X h_1 h_2)$. This is illustrated by Fig. 6.1.

We will be working in a combination of collinear factorization and small-x factorization, more precisely in the shockwave formalism for the latter.

Kinematics

We work in a reference frame such that the target moves ultra-relativistically and such that $s = (p_\gamma + p_0)^2 \sim 2 p_\gamma^+ p_0^- \gg \Lambda_{\text{QCD}}^2$, s also being larger than any other scale. Particles on the projectile side are moving in the n_1 (*i.e.* $+$) direction while particles on the target side have a large component along n_2 (*i.e.* $-$) direction.

We will use a kinematics such that the photon with virtuality Q is forward, and thus it does not carry any transverse momentum[48]:

$$\vec{p}_\gamma = 0, \quad p_\gamma^\mu = p_\gamma^+ n_1^\mu + \frac{p_\gamma^2}{2p_\gamma^+} n_2^\mu, \quad -p_\gamma^2 \equiv Q^2 \geq 0. \tag{6.2}$$

We will denote its transverse polarization ε_T. Its longitudinal polarization vector reads

$$\varepsilon_L^\alpha = \frac{1}{\sqrt{-p_\gamma^2}} \left(p_\gamma^+ n_1^\alpha - \frac{p_\gamma^2}{2p_\gamma^+} n_2^\alpha \right), \quad \varepsilon_L^+ = \frac{p_\gamma^+}{Q}, \quad \varepsilon_L^- = \frac{Q}{2p_\gamma^+}. \tag{6.3}$$

We write the momentum of the produced hadrons as

$$p_{h_i}^\mu = p_{h_i}^+ n_1^\mu + \frac{m_{h_i}^2 + \vec{p}_{h_i}^{\,2}}{2p_{h_i}^+} n_2^\mu + p_{h_i \perp}^\mu \quad (i = 1, 2)\,. \tag{6.4}$$

The momenta of the fragmenting quark of virtuality p_q^2 reads

$$p_q^\mu = p_q^+ n_1^\mu + \frac{p_q^2 + \vec{p}_q^{\,2}}{2p_q^+} n_2^\mu + p_{q\perp}^\mu \tag{6.5}$$

and similarly for an antiquark of virtuality $p_{\bar{q}}^2$,

$$p_{\bar{q}}^\mu = p_{\bar{q}}^+ n_1^\mu + \frac{p_{\bar{q}}^2 + \vec{p}_{\bar{q}}^{\,2}}{2p_{\bar{q}}^+} n_2^\mu + p_{\bar{q}\perp}^\mu\,. \tag{6.6}$$

From now, we will use the notation $p_{ij} = p_i - p_j$.

Collinear factorization

The kinematical region considered here is such that $\vec{p}_{h_1}^{\,2} \sim \vec{p}_{h_2}^{\,2} \gg \Lambda_{\rm QCD}^2$. The hadron momenta are the hard scale, making the use of perturbative QCD and collinear factorization possible. The constraint $\vec{p}^{\,2} \gg \vec{p}_{h_{1,2}}^{\,2}$, with $\vec{p}$ the relative transverse momentum of the two hadrons has also been considered. This means that the two produced hadrons have a large enough separation angle (or, in other words, a large enough invariant mass) so that it will not be necessary to consider the di-hadron unpolarized fragmentation functions: each hadron, typically pion, can be produced by two well-separated fragmentation cascades. The quark and antiquark in the hard part after collinear factorization will be treated as on-shell particles. For further use, we introduce the longitudinal momentum fraction x_q and $x_{\bar{q}}$ as

$$p_q^+ = x_q p_\gamma^+ \quad \text{and} \quad p_{\bar{q}}^+ = x_{\bar{q}} p_\gamma^+\,. \tag{6.7}$$

[48] Any transverse momentum in Euclidean space will be denoted with an arrow, while a $\perp$ index will be used in Minkowski space.

Similarly, we denote

$$p_{h_i}^+ = x_{h_i} p_\gamma^+ \,. \tag{6.8}$$

Shockwave approach

The small-x factorization applies here and the scattering amplitude is the convolution of the projectile impact factor and the non-perturbative matrix element of operators from the Wilson lines operators on the target states. One of such operators is the dipole operator, which in the fundamental representation of $SU(N_c)$ takes the form:

$$\left[\mathrm{Tr}\left(U_1 U_2^\dagger\right) - N_c\right](\vec{p}_1, \vec{p}_2) = \int d^d\vec{z}_1 d^d\vec{z}_{2\perp} e^{-i\vec{p}_1\cdot\vec{z}_1} e^{-i\vec{p}_2\cdot\vec{z}_2} \left[\mathrm{Tr}\left(U_{\vec{z}_1} U_{\vec{z}_2}^\dagger\right) - N_c\right] , \tag{6.9}$$

where $\vec{z}_{1,2}$ are the transverse positions of the $q, \bar{q}$ coming from the photon and $\vec{p}_{1,2}$ their respective transverse momentums kicks from the shockwave.

The proton matrix element should be parameterized. This can be done through a generic function F, following the definition of Ref. [198]

$$\begin{aligned} \left\langle P'\left(p_0'\right) \middle| T\left(\mathrm{Tr}\left(U_{\frac{z_\perp}{2}} U^\dagger{}_{-\frac{z_\perp}{2}}\right) - N_c\right) \middle| P\left(p_0\right)\right\rangle &\equiv 2\pi\delta\left(p_{00'}^-\right) F_{p_{0\perp}p_{0\perp}'}\left(z_\perp\right) \\ &\equiv 2\pi\delta\left(p_{00'}^-\right) F\left(z_\perp\right) \end{aligned} \tag{6.10}$$

and its Fourier Transform (FT) is

$$\int d^d z_\perp e^{i(z_\perp\cdot p_\perp)} F\left(z_\perp\right) \equiv \mathbf{F}\left(p_\perp\right). \tag{6.11}$$

Similar definitions exist for the double dipole operator and its action on proton states, as can be seen with eqs. (5.3) and (5.6) in [198], with

$$\begin{aligned} &\left\langle P'\left(p_0'\right) \middle| \left(\mathrm{Tr}\left(U_{\frac{z}{2}} U_x^\dagger\right) \mathrm{Tr}\left(U_x U^\dagger{}_{-\frac{z}{2}}\right) - N_c \,\mathrm{Tr}\left(U_{\frac{z}{2}} U^\dagger{}_{-\frac{z}{2}}\right)\right) \middle| P\left(p_0\right)\right\rangle \\ &\equiv 2\pi\delta\left(p_{00'}^-\right) \tilde{F}_{p_{0\perp}p_{0\perp}'}\left(z_\perp, x_\perp\right) \equiv 2\pi\delta\left(p_{00'}^-\right) \tilde{F}\left(z_\perp, x_\perp\right) \end{aligned} \tag{6.12}$$

and its FT is

$$\int d^d z_\perp d^d x_\perp e^{i(p_\perp\cdot x_\perp) + i(z_\perp\cdot q_\perp)} \tilde{F}\left(z_\perp, x_\perp\right) \equiv \tilde{\mathbf{F}}\left(q_\perp, p_\perp\right). \tag{6.13}$$

In this chapter, dimensional regularization will be used with $D = 2{+}d$, where $d = 2{+}2\epsilon$ is the transverse dimension.

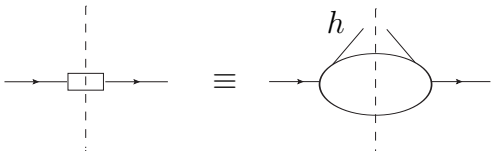

Figure 6.2: Graphical convention for the fragmentation function of a parton (here a quark for illustration) to a hadron h plus spectators. In the rest of this article, we will use the left-hand side of this drawing.

6.1.2 LO order

QCD collinear factorization stipulates that the total cross section, at leading twist and LO, reads, see ref [3] (chap. 12) and Ref. [200]

$$\frac{d\sigma_{0JI}^{h_1h_2}}{dx_{h_1}dx_{h_2}} = \sum_q \int_{x_{h_1}}^1 \frac{dx_q}{x_q} \int_{x_{h_2}}^1 \frac{dx_{\bar{q}}}{x_{\bar{q}}} D_q^{h_1}\left(\frac{x_{h_1}}{x_q}, \mu_F\right) D_{\bar{q}}^{h_2}\left(\frac{x_{h_2}}{x_{\bar{q}}}, \mu_F\right) \frac{d\hat{\sigma}_{JI}}{dx_q dx_{\bar{q}}} + (h_1 \leftrightarrow h_2)\,, \tag{6.14}$$

where q specifies the quark flavor types ($q = u, d, s, c, b$), and $J, I = L, T$ specify the photon polarization since we deal here with a modulus square amplitude (J labels the photon polarization in the complex conjugated amplitude and I in the amplitude). Here x_q and $x_{\bar{q}}$ are the longitudinal fractions of the photon momentum carried by the fragmenting partons, x_{h_1,h_2} are the longitudinal fraction of the photon momentum carried by the produced hadrons, μ_F is the factorization scale, $D^h_{q(\bar{q})}$ denotes the quark (antiquark) Fragmentation Function (FF) and $d\hat{\sigma}$ is the partonic cross section, i.e. the cross section for the subprocess

$$\gamma^{(*)}(p_\gamma) + P(p_0) \to q(p_q) + \bar{q}(p_{\bar{q}}) + P'(p_0')\,. \tag{6.15}$$

The graphical convention used in the present article for any fragmentation function is given in Fig. 6.2.

All detailed computations will be done considering only the first term in (6.14), remembering the second term is just simply obtained by the replacement $h_1 \leftrightarrow h_2$.

The partonic cross section (6.15) has been computed in the shockwave framework. The structure of the result for the whole process 6.1 at LO is illustrated in Fig. 6.3.

Collinear factorization means that the produced hadrons should fly collinearly to the fragmenting partons. This means here that the following constraints should be fulfilled

$$p_q^+ = \frac{x_q}{x_{h_1}} p_{h_1}^+, \quad \vec{p}_q = \frac{x_q}{x_{h_1}} \vec{p}_{h_1}\,, \tag{6.16}$$

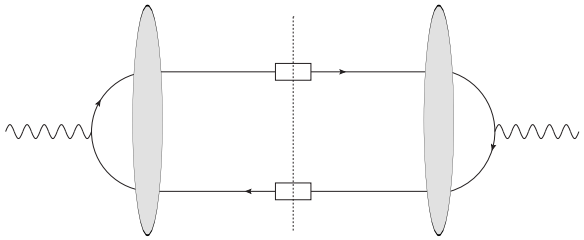

Figure 6.3: Diagram of the LO process at cross section level. The blob is the shockwave (we do not draw the coupling with the target for clarity) and the squares the FFs, see Fig. 6.2. The dashed line is to represent the integration over phase space.

$$p_{\bar{q}}^{+} = \frac{x_{\bar{q}}}{x_{h_2}} p_{h_2}^{+}, \quad \vec{p}_{\bar{q}} = \frac{x_{\bar{q}}}{x_{h_2}} \vec{p}_{h_2}\,. \tag{6.17}$$

Since the photon in the initial state can appear with different polarizations, we construct the density matrix

$$d\sigma_{JI} = \begin{pmatrix} d\sigma_{LL} & d\sigma_{LT} \\ d\sigma_{TL} & d\sigma_{TT} \end{pmatrix}, \qquad d\sigma_{TL} = d\sigma_{LT}^{*}. \tag{6.18}$$

Each element of this matrix has a LO contribution $d\sigma_0$. This Born order result, see Eq. (5.14) of Ref. [198], has the following structure:

$$\begin{aligned} d\sigma_{0JI} = {} & \frac{\alpha_{\rm em} Q_q^2}{(2\pi)^{4(d-1)} N_c} \frac{\left(p_0^-\right)^2}{2 x_q x_{\bar{q}} s^2} dx_q dx_{\bar{q}} d^d p_{q\perp} d^d p_{\bar{q}\perp} \delta\left(1 - x_q - x_{\bar{q}}\right) \left(\varepsilon_{I\beta} \varepsilon_{J\gamma}^{*}\right) \\ & \times \int d^d p_{1\perp} d^d p_{2\perp} d^d p_{1'\perp} d^d p_{2'\perp} \delta\left(p_{q1\perp} + p_{\bar{q}2\perp}\right) \delta\left(p_{11'\perp} + p_{22'\perp}\right) \\ & \times \sum_{\lambda_q, \lambda_{\bar{q}}} \Phi_0^{\beta}\left(p_{1\perp}, p_{2\perp}\right) \Phi_0^{\gamma *}\left(p_{1'\perp}, p_{2'\perp}\right) \mathbf{F}\left(\frac{p_{12\perp}}{2}\right) \mathbf{F}^{*}\left(\frac{p_{1'2'\perp}}{2}\right). \end{aligned} \tag{6.19}$$

Using the explicit expressions of the product $\Phi_0^{\beta}\Phi_0^{\gamma *}$, see Eq. (5.18-20) of Ref. [198], as well as Eq. (6.14), the LO cross sections are obtained and read for LL

$$\begin{aligned} \frac{d\sigma_{0LL}^{h_1 h_2}}{dx_{h_1} dx_{h_2} d^d p_{h_1\perp} d^d p_{h_2\perp}} = {} & \frac{4\alpha_{\rm em} Q^2}{(2\pi)^{4(d-1)} N_c} \sum_q \int_{x_{h_1}}^1 dx_q \int_{x_{h_2}}^1 dx_{\bar{q}}\, x_q x_{\bar{q}} \left(\frac{x_q}{x_{h_1}}\right)^d \left(\frac{x_{\bar{q}}}{x_{h_2}}\right)^d \\ \times \quad & \delta(1 - x_q - x_{\bar{q}}) Q_q^2 D_q^{h_1}\left(\frac{x_{h_1}}{x_q}\right) D_{\bar{q}}^{h_2}\left(\frac{x_{h_2}}{x_{\bar{q}}}\right) \mathcal{F}_{LL} + \left(h_1 \leftrightarrow h_2\right), \end{aligned} \tag{6.20}$$

where

$$\mathcal{F}_{LL} = \left| \int d^d p_{2\perp} \frac{\mathbf{F}\left(\frac{x_q}{2x_{h_1}} p_{h_1\perp} + \frac{x_{\bar{q}}}{2x_{h_2}} p_{h_2\perp} - p_{2\perp}\right)}{\left(\frac{x_{\bar{q}}}{x_{h_2}} \vec{p}_{h_2} - \vec{p}_2\right)^2 + x_q x_{\bar{q}} Q^2} \right|^2. \tag{6.21}$$

This LO cross section can be written differently, using transverse momentum conservation, see Eq. (6.19),

$$\frac{d\sigma_{0LL}^{h_1h_2}}{dx_{h_1}dx_{h_2}d^dp_{h_1\perp}d^dp_{h_2\perp}} = \frac{4\alpha_{\rm em}Q^2}{(2\pi)^{4(d-1)}N_c}\sum_q\int_{x_{h_1}}^1 dx_q\int_{x_{h_2}}^1 dx_{\bar q}\,x_qx_{\bar q}\left(\frac{x_q}{x_{h_1}}\right)^d\left(\frac{x_{\bar q}}{x_{h_2}}\right)^d$$
$$\times\quad \delta(1-x_q-x_{\bar q})Q_q^2D_q^{h_1}\left(\frac{x_{h_1}}{x_q}\right)D_{\bar q}^{h_2}\left(\frac{x_{h_2}}{x_{\bar q}}\right)\tilde{\mathcal{F}}_{LL}+(h_1\leftrightarrow h_2)\,, \tag{6.22}$$

where

$$\tilde{\mathcal{F}}_{LL} = \left|\int d^dp_{1\perp}\frac{\mathbf{F}\left(-\left(\frac{x_q}{2x_{h_1}}p_{h_1\perp}+\frac{x_{\bar q}}{2x_{h_2}}p_{h_2\perp}-p_{1\perp}\right)\right)}{\left(\frac{x_q}{x_{h_1}}\vec{p}_{h_1}-\vec{p}_1\right)^2+x_qx_{\bar q}Q^2}\right|^2. \tag{6.23}$$

Both forms can be used interchangeably in terms of NLO cross sections that are proportional to the LO cross sections, *i.e.* when dealing with the soft, virtual, and counterterm contribution to the NLO cross sections. For the collinear quark-gluon contribution, Eq. (6.20) will be used, while, for the collinear anti-quark-gluon contribution, Eq. (6.22) will be used.

Similarly, the non-diagonal interference term TL can be written in the two equivalent forms:

$$\frac{d\sigma_{0TL}^{h_1h_2}}{dx_{h_1}dx_{h_2}d^dp_{h_1\perp}d^dp_{h_2\perp}} = \frac{2\alpha_{\rm em}Q}{(2\pi)^{4(d-1)}N_c}\sum_q\int_{x_{h_1}}^1 dx_q\int_{x_{h_2}}^1 dx_{\bar q}\left(\frac{x_q}{x_{h_1}}\right)^d\left(\frac{x_{\bar q}}{x_{h_2}}\right)^d$$
$$\times\quad (x_{\bar q}-x_q)\delta(1-x_q-x_{\bar q})Q_q^2D_q^{h_1}\left(\frac{x_{h_1}}{x_q}\right)D_{\bar q}^{h_2}\left(\frac{x_{h_2}}{x_{\bar q}}\right)\mathcal{F}_{TL}+(h_1\leftrightarrow h_2)\,, \tag{6.24}$$

where

$$\begin{aligned}\mathcal{F}_{TL} = &\int d^dp_{2\perp}\frac{\mathbf{F}\left(\frac{x_q}{2x_{h_1}}p_{h_1\perp}+\frac{x_{\bar q}}{2x_{h_2}}p_{h_2\perp}-p_{2\perp}\right)}{\left(\frac{x_{\bar q}}{x_{h_2}}\vec{p}_{h_2}-\vec{p}_2\right)^2+x_qx_{\bar q}Q^2}\\ &\times\left[\int d^dp_{2'\perp}\frac{\mathbf{F}\left(\frac{x_q}{2x_{h_1}}p_{h_1\perp}+\frac{x_{\bar q}}{2x_{h_2}}p_{h_2\perp}-p_{2'\perp}\right)}{\left(\frac{x_{\bar q}}{x_{h_2}}\vec{p}_{h_2}-\vec{p}_{2'}\right)^2+x_qx_{\bar q}Q^2}\left(\frac{x_{\bar q}}{x_{h_2}}\vec{p}_{h_2}-\vec{p}_{2'}\right)\cdot\vec{\varepsilon}_T\right]^*\end{aligned} \tag{6.25}$$

and

$$\frac{d\sigma_{0TL}^{h_1h_2}}{dx_{h_1}dx_{h_2}d^dp_{h_1\perp}d^dp_{h_2\perp}} = \frac{2\alpha_{\rm em}Q}{(2\pi)^{4(d-1)}N_c}\sum_q\int_{x_{h_1}}^1 dx_q\int_{x_{h_2}}^1 dx_{\bar q}\left(\frac{x_q}{x_{h_1}}\right)^d\left(\frac{x_{\bar q}}{x_{h_2}}\right)^d$$
$$\times\quad (x_{\bar q}-x_q)\delta(1-x_q-x_{\bar q})Q_q^2D_q^{h_1}\left(\frac{x_{h_1}}{x_q}\right)D_{\bar q}^{h_2}\left(\frac{x_{h_2}}{x_{\bar q}}\right)\tilde{\mathcal{F}}_{TL}+(h_1\leftrightarrow h_2)\,, \tag{6.26}$$

where

$$\tilde{\mathcal{F}}_{TL} = \int d^d p_{1\perp} \frac{\mathbf{F}\left(-\left(\frac{x_q}{2x_{h_1}} p_{h_1\perp} + \frac{x_{\bar{q}}}{2x_{h_2}} p_{h_2\perp} - p_{1\perp}\right)\right)}{\left(\frac{x_q}{x_{h_1}}\vec{p}_{h_1} - \vec{p}_1\right)^2 + x_q x_{\bar{q}} Q^2} \times \left[\int d^d p_{1'\perp} \frac{\mathbf{F}\left(-\left(\frac{x_q}{2x_{h_1}} p_{h_1\perp} + \frac{x_{\bar{q}}}{2x_{h_2}} p_{h_2\perp} - p_{1'\perp}\right)\right)}{\left(\frac{x_q}{x_{h_1}}\vec{p}_{h_1} - \vec{p}_{1'}\right)^2 + x_q x_{\bar{q}} Q^2} \left(\frac{x_q}{x_{h_1}} p_{h_1} - p_{1'}\right) \cdot \varepsilon_T\right]^* . \tag{6.27}$$

The most complicated contribution TT reads

$$\frac{d\sigma_{0TT}^{h_1 h_2}}{dx_{h_1} dx_{h_2} d^d p_{h_1\perp} d^d p_{h_2\perp}} = \frac{\alpha_{\rm em}}{(2\pi)^{4(d-1)} N_c} \sum_q \int_{x_{h_1}}^1 \frac{dx_q}{x_q} \int_{x_{h_2}}^1 \frac{dx_{\bar{q}}}{x_{\bar{q}}} \left(\frac{x_q}{x_{h_1}}\right)^d \left(\frac{x_{\bar{q}}}{x_{h_2}}\right)^d \times \quad \delta(1 - x_q - x_{\bar{q}}) Q_q^2 D_q^{h_1}\left(\frac{x_{h_1}}{x_q}\right) D_{\bar{q}}^{h_2}\left(\frac{x_{h_2}}{x_{\bar{q}}}\right) \mathcal{F}_{TT} + (h_1 \leftrightarrow h_2) , \tag{6.28}$$

where

$$\mathcal{F}_{TT} = \left[(x_{\bar{q}} - x_q)^2 g_\perp^{ri} g_\perp^{lk} - g_\perp^{rk} g_\perp^{li} + g_\perp^{rl} g_\perp^{ik}\right] \times \int d^d p_{2\perp} \frac{\mathbf{F}\left(\frac{x_q}{2x_{h_1}} p_{h_1\perp} + \frac{x_{\bar{q}}}{2x_{h_2}} p_{h_2\perp} - p_{2\perp}\right)}{\left(\frac{x_{\bar{q}}}{x_{h_2}}\vec{p}_{h_2} - \vec{p}_2\right)^2 + x_q x_{\bar{q}} Q^2} \left(\frac{x_{\bar{q}}}{x_{h_2}} p_{h_2} - p_2\right)_r \varepsilon_{Ti} \times \left[\int d^d p_{2'\perp} \frac{\mathbf{F}\left(\frac{x_q}{2x_{h_1}} p_{h_1\perp} + \frac{x_{\bar{q}}}{2x_{h_2}} p_{h_2\perp} - p_{2'\perp}\right)}{\left(\frac{x_{\bar{q}}}{x_{h_2}}\vec{p}_{h_2} - \vec{p}_{2'}\right)^2 + x_q x_{\bar{q}} Q^2} \left(\frac{x_{\bar{q}}}{x_{h_2}} p_{h_2} - p_{2'}\right)_l \varepsilon_{Tk}\right]^* \tag{6.29}$$

or equivalently

$$\frac{d\sigma_{0TT}^{h_1 h_2}}{dx_{h_1} dx_{h_2} d^d p_{h_1\perp} d^d p_{h_2\perp}} = \frac{\alpha_{\rm em}}{(2\pi)^{4(d-1)} N_c} \sum_q \int_{x_{h_1}}^1 \frac{dx_q}{x_q} \int_{x_{h_2}}^1 \frac{dx_{\bar{q}}}{x_{\bar{q}}} \left(\frac{x_q}{x_{h_1}}\right)^d \left(\frac{x_{\bar{q}}}{x_{h_2}}\right)^d \times \quad \delta(1 - x_q - x_{\bar{q}}) Q_q^2 D_q^{h_1}\left(\frac{x_{h_1}}{x_q}\right) D_{\bar{q}}^{h_2}\left(\frac{x_{h_2}}{x_{\bar{q}}}\right) \tilde{\mathcal{F}}_{TT} + (h_1 \leftrightarrow h_2) , \tag{6.30}$$

where

$$\tilde{\mathcal{F}}_{TT} = \left[(x_{\bar{q}} - x_q)^2 g_\perp^{ri} g_\perp^{lk} - g_\perp^{rk} g_\perp^{li} + g_\perp^{rl} g_\perp^{ik}\right] \times \int d^d p_{1\perp} \frac{\mathbf{F}\left(-\left(\frac{x_q}{2x_{h_1}} p_{h_1\perp} + \frac{x_{\bar{q}}}{2x_{h_2}} p_{h_2\perp} - p_{1\perp}\right)\right)}{\left(\frac{x_q}{x_{h_1}}\vec{p}_{h_1} - \vec{p}_1\right)^2 + x_q x_{\bar{q}} Q^2} \left(\frac{x_q}{x_{h_1}} p_{h_1} - p_1\right)_r \varepsilon_{Ti} \times \left[\int d^d p_{1'\perp} \frac{\mathbf{F}\left(-\left(\frac{x_q}{2x_{h_1}} p_{h_1\perp} + \frac{x_{\bar{q}}}{2x_{h_2}} p_{h_2\perp} - p_{1'\perp}\right)\right)}{\left(\frac{x_q}{x_{h_1}}\vec{p}_{h_1} - \vec{p}_{1'}\right)^2 + x_q x_{\bar{q}} Q^2} \left(\frac{x_q}{x_{h_1}} p_{h_1} - p_{1'}\right)_l \varepsilon_{Tk}\right]^* . \tag{6.31}$$

Compared to the LL cross section, the TL cross section has the same form up to a factor of

$$\frac{1}{Q}\frac{x_{\bar{q}}-x_q}{2x_{\bar{q}}x_q}\left(\frac{x_{\bar{q}}}{x_{h_2}}\vec{p}_{h_2}-\vec{p}_{2'}\right)\cdot\vec{\varepsilon}_T^{\,*}$$

or

$$\frac{1}{Q}\frac{x_{\bar{q}}-x_q}{2x_{\bar{q}}x_q}\left(\frac{x_q}{x_{h_1}}p_{h_1}-p_{1'}\right)\cdot\varepsilon_T^{*}\,.$$

The TT cross section differs from the LL cross section by a factor of

$$\frac{1}{Q^2}\frac{1}{4x_q^2x_{\bar{q}}^2}\left[(x_{\bar{q}}-x_q)^2g_\perp^{ri}g_\perp^{lk}-g_\perp^{rk}g_\perp^{li}+g_\perp^{rl}g_\perp^{ik}\right]\left(\frac{x_q}{x_{h_1}}p_{h_1}-p_1\right)_r\varepsilon_{Ti}\left(\frac{x_q}{x_{h_1}}p_{h_1}-p_{1'}\right)_l\varepsilon_{Tk}^{*}$$

or

$$\frac{1}{Q^2}\frac{1}{4x_q^2x_{\bar{q}}^2}\left[(x_{\bar{q}}-x_q)^2g_\perp^{ri}g_\perp^{lk}-g_\perp^{rk}g_\perp^{li}+g_\perp^{rl}g_\perp^{ik}\right]\left(\frac{x_{\bar{q}}}{x_{h_2}}p_{h_2}-p_2\right)_r\varepsilon_{Ti}\left(\frac{x_{\bar{q}}}{x_{h_2}}p_{h_2}-p_{2'}\right)_l\varepsilon_{Tk}^{*}\,.$$

The factors of $1/Q$ and $1/Q^2$ come from the photon polarization while the other modifications come from the expression of the squared of the impact factors. Those modifications and additional factors between TL and TT cross section with respect to LL will remain true when going to NLO, for what concerns the extraction of divergences. This means that no additional detailed calculations are needed for those cases.

6.1.3 NLO computations in a nutshell

Different types of contributions in the dipole picture

At NLO, since we rely on the shockwave approach, it is convenient to separate the various contributions from the dipole point of view, as illustrated in Fig. 6.4. In this figure, we exhibit a few examples of diagrams, either virtual or real, as a representative of each five classes of diagrams. There are indeed five classes of contributions from the dipole point of view, namely $d\sigma_{iJI}\,(i=1,\cdots 5)$, so that the NLO density matrix can be written as

$$d\sigma_{JI}=d\sigma_{0JI}+d\sigma_{1JI}+d\sigma_{2JI}+d\sigma_{3JI}+d\sigma_{4JI}+d\sigma_{5JI}. \tag{6.32}$$

Now, we will shortly discuss each of these five NLO corrections.

For the virtual diagrams, there are two classes of diagrams: the diagrams in which the virtual gluon does not cross the shockwave, thus contributing to $d\sigma_{1IJ}$, purely made of dipole $\times$ dipole terms; the diagrams in which the virtual gluon does cross the shockwave, contributing both to $d\sigma_{1IJ}$, made of dipole $\times$ dipole terms, as well as to $d\sigma_{2IJ}$, made of double dipole $\times$ dipole (and dipole $\times$ double-dipole) terms.

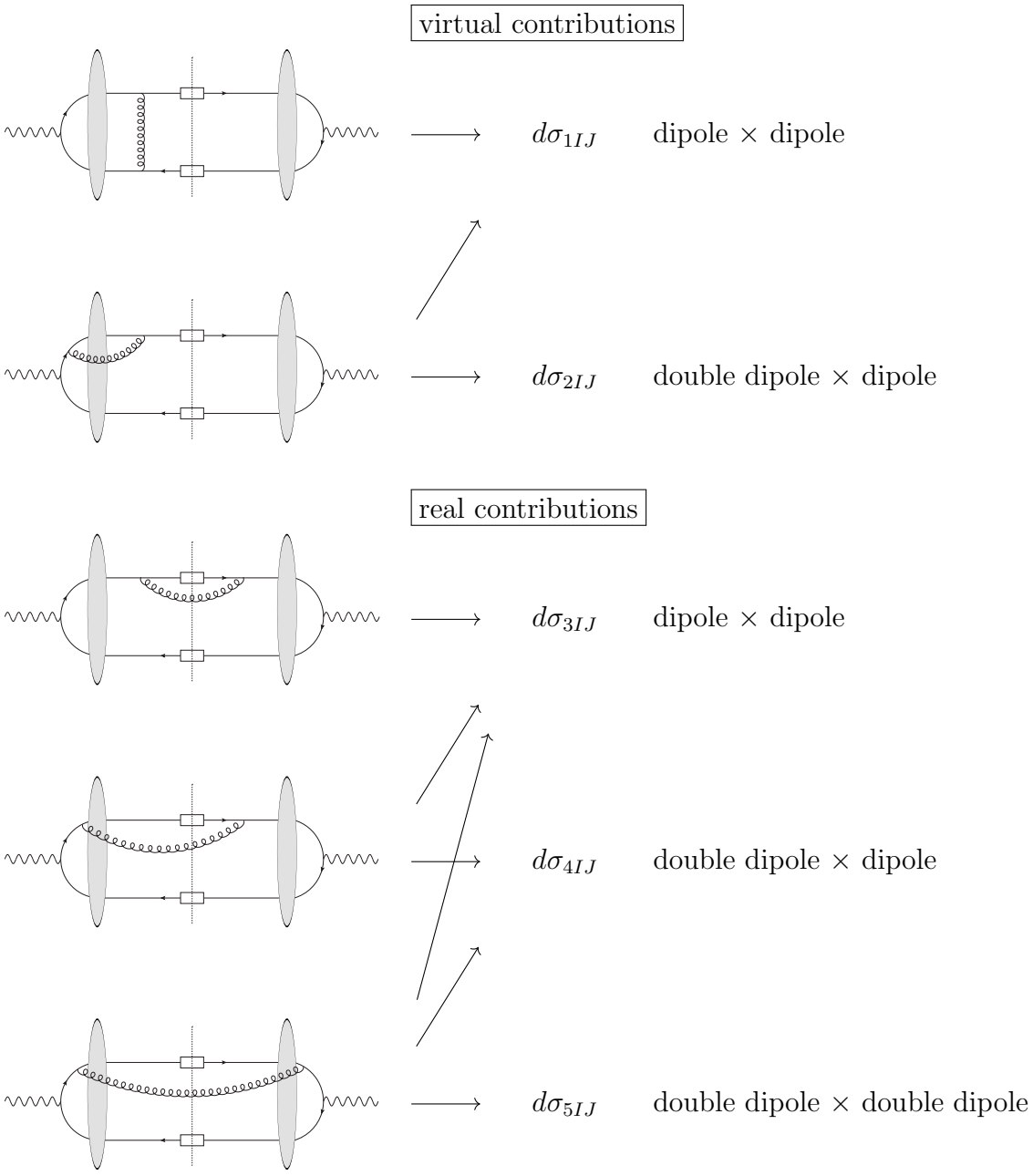

Figure 6.4: Illustration of the five kinds of contributions to the NLO cross section from the dipole point of view. Arrows show to which combination of dipole structures each type of diagrams contributes.

For the real diagrams, there are three classes of diagrams: the diagrams in which the real gluon does not cross the shockwave, thus contributing to $d\sigma_{3IJ}$, purely made of dipole $\times$ dipole terms; the diagrams in which the real gluon crosses exactly once the shockwave, contributing both to $d\sigma_{3IJ}$, made of dipole $\times$ dipole terms as well as to $d\sigma_{4IJ}$, made of double dipole $\times$ dipole (and dipole $\times$ double-dipole) terms; the diagrams in which the real gluon crosses exactly twice the shockwave, contributing to $d\sigma_{3IJ}$, made of dipole $\times$ dipole terms, to $d\sigma_{4IJ}$, made of double dipole $\times$ dipole (and dipole $\times$ double-dipole) terms, and to $d\sigma_{5IJ}$, made of double dipole $\times$ double dipole terms.

Overview of cancellation of divergences

Before providing technical details, let us sketch the way the computation will be done, putting emphasis on the infrared (IR) sector.

When generically decomposing any on-shell parton momentum in the Sudakov basis as[49]

$$p^\mu = zp^+ n_1^\mu + \frac{\vec{p}^2}{2zp^+} n_2^\mu + p_\perp^\mu \,, \tag{6.33}$$

in the IR sector, we face three kinds of divergences:

- Rapidity: z goes to zero and $p_\perp$ arbitrary.
- Soft: any component of the gluon momentum goes linearly to zero (obtained with both z and $p_\perp = z\tilde{p}_\perp \sim z$ going to zero).
- Collinear: parton's $p_\perp$ goes to zero, z being arbitrary.

Technically, since the z integration is regulated through a lower cut-off (named α), one should be careful with the fact that the appearance of $\ln \alpha$ may have originated from both rapidity or soft divergences.

The calculation goes as follows. First, the rapidity divergences, appearing only in the virtual corrections in the present computation, are taken care of at the amplitude level by absorbing them in the shockwave through one step of B-JIMWLK evolution. This removes part of terms with $\ln \alpha$ related to pure rapidity divergences.

Next, at the level of cross section, we separate the soft divergent contribution from the non-soft divergent terms. Combining real and virtual contributions, these soft divergent terms will disappear as guaranteed by the Kinoshita-Lee-Nauenberg theorem.

[49]Here p^+ is a large fixed momentum, eg p_γ^+ in our present case.

Finally, the remaining type of divergences, which are of purely collinear nature, will be absorbed into the fragmentation functions through one step of the Dokshitzer-Gribov-Lipatov-Altarelli-Parisi (DGLAP) evolution equation [5, 201, 7, 6].

Different fragmentation contributions to the NLO cross section

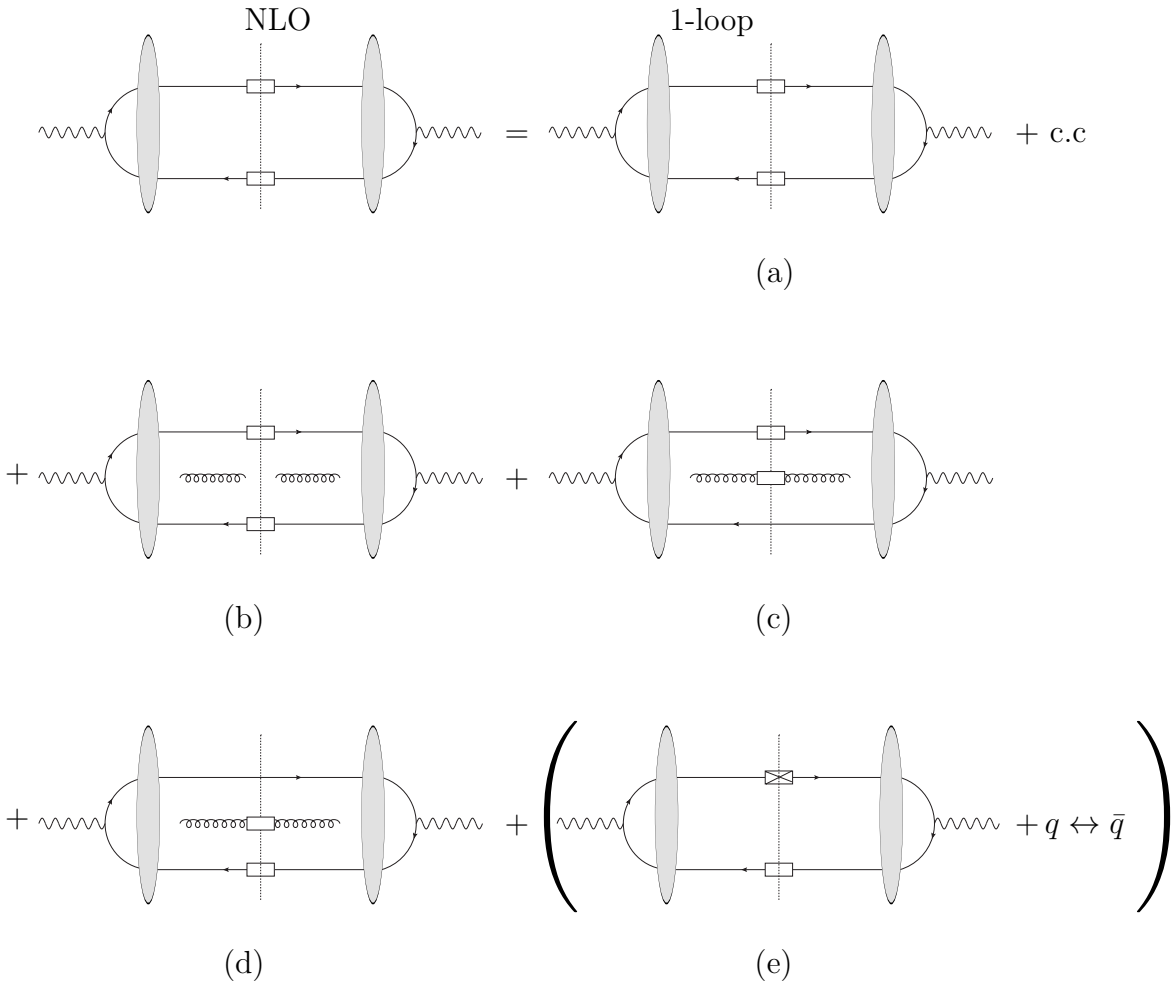

Figure 6.5: The five kinds of contributions to the NLO cross section.

At NLO, we have to deal with five kinds of contributions to the cross section, illustrated in Fig. 6.5:

(a) $\gamma^* + P \to h_1 + h_2 + X + P$ cross section at one loop (i.e. virtual contributions),

(b) $\gamma^* + P \to h_1 + h_2 + g + X + P$ cross section at Born level (i.e. real contributions),

(c) $\gamma^* + P \to h_1 + h_2 + \bar{q} + X + P$ cross section at Born level (i.e. real contributions),

(d) $\gamma^* + P \to h_1 + h_2 + q + X + P$ cross section at Born level (i.e. real contributions),

(e) FFs counterterms,

where X denotes the remnants of the fragmentation.

Contributions (a) and (e) are easy to treat since (a) is simply the convolution of a known one-loop result with fragmentation functions, while (e) is obtained from the Born result when one renormalizes the fragmentation functions. We just split them into finite and divergent parts.

For the real contributions (b), (c), (d), the treatment is less straightforward even if the partonic real corrections are also already known.

Contribution (b) is the most complicated one, it contains both soft and collinear divergences. When we square the amplitude contributing to (b), see Fig. 6.6, there is a series of finite contributions plus one, represented by the sum of contributions (1), (2), (3), (4) of Fig. 6.6, that contains all divergences, and that belongs only to the dipole-dipole contribution. We add and subtract to the latter its soft limit to obtain the following structure

$$\begin{aligned}\tilde{\sigma}_{(b)div} &= \sum_{\lambda_q,\lambda_g,\lambda_{\bar{q}}} |A_{q\bar{q},sing-dipole}|^2_{div} = \tilde{\sigma}_{(b)div,1} + \tilde{\sigma}_{(b)div,2} + \tilde{\sigma}_{(b)div,3} + \tilde{\sigma}_{(b)div,4} \\ &= \tilde{\sigma}^{soft}_{(b)div} + (\tilde{\sigma}_{(b)div,1} - \tilde{\sigma}^{soft}_{(b)div,1}) + (\tilde{\sigma}_{(b)div,2} - \tilde{\sigma}^{soft}_{(b)div,2}) + (\tilde{\sigma}_{(b)div,3} - \tilde{\sigma}^{soft}_{(b)div,3}) \\ &\quad + (\tilde{\sigma}_{(b)div,4} - \tilde{\sigma}^{soft}_{(b)div,4}) \end{aligned} \tag{6.34}$$

with the meaning that each of these four contributions is in one-to-one correspondence to the four diagrams (1), (2), (3), (4) in Fig. 6.6. Among these various terms, the terms $(\tilde{\sigma}_{(b)div,1} - \tilde{\sigma}^{soft}_{(b)div,1})$ and $(\tilde{\sigma}_{(b)div,3} - \tilde{\sigma}^{soft}_{(b)div,3})$ are collinearly divergent, while the terms $(\tilde{\sigma}_{(b)div,2} - \tilde{\sigma}^{soft}_{(b)div,2})$ and $(\tilde{\sigma}_{(b)div,4} - \tilde{\sigma}^{soft}_{(b)div,4})$ are finite.

In Fig. 6.7, the contribution with fragmentation from quark and gluon is considered. Again, we have

$$\tilde{\sigma}_{(c)div} = \sum_{\lambda_q,\lambda_g,\lambda_{\bar{q}}} |A_{qg,sing-dipole}|^2_{div} = \tilde{\sigma}_{(c)div,3}\,. \tag{6.35}$$

Here, one does not encounter any soft divergence. The only divergence comes from the contribution $\tilde{\sigma}_{(c)div,3}$ which has a collinear divergence when the fragmenting gluon and the antiquark are collinear.

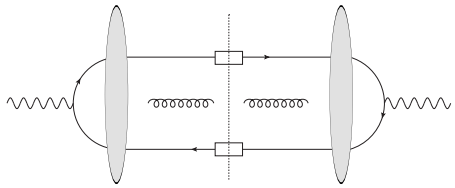

(b)

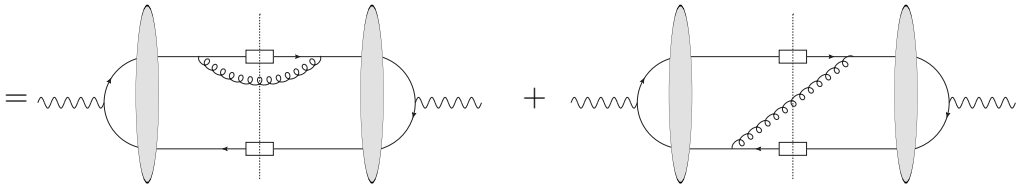

(1) (2)

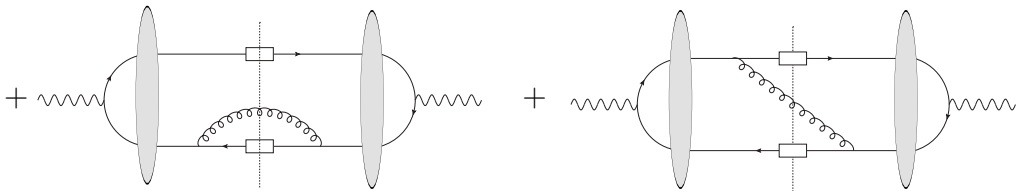

(3) (4)

+ finite contributions

Figure 6.6: NLO cross section in the case of fragmentation from the quark and the antiquark. We explicitly isolate the diagrams which contain divergences. Diagram (1) contains a collinear divergence between the fragmenting quark and the gluon as well as a soft gluon divergence. Diagram (2) contains a soft gluon divergence. Diagram (3) contains a collinear divergence between the fragmenting antiquark and the gluon as well as a soft gluon divergence. Diagram (4) contains a soft gluon divergence. By "finite terms", here, we mean all diagrams in which the gluon crosses the shockwave at least once.

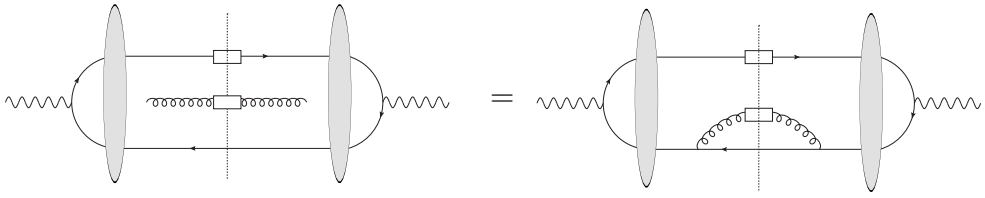

(c) (3)

+ finite contributions.

Figure 6.7: NLO cross section in the case of fragmentation from the gluon and the quark. We explicitly isolate the diagram which contains divergences, namely a collinear divergence between the fragmenting gluon and the antiquark.

The discussion for the fourth case, see Fig. 6.8, involving the fragmentation from antiquark and gluon goes along the same line: the only divergence comes from the contribution $\tilde{\sigma}_{(d)div,1}$ which has a collinear divergence when the fragmenting gluon and the quark are collinear.

6.2 Counterterms from FFs renormalization and evolution

The renormalization and evolution equations of FFs express the bare FFs in terms of dressed ones. In $\overline{\rm MS}$ scheme, at factorization scale μ_F, they take the form, following notations of Ref. [70]

$$
\begin{aligned}
D_q^h(x) &= D_q^h\left(x,\mu_F\right) - \frac{\alpha_s}{2\pi}\left(\frac{1}{\hat{\epsilon}} + \ln\frac{\mu_F^2}{\mu^2}\right)\int_x^1 \frac{dz}{z}\left[D_q^h\left(\frac{x}{z},\mu_F\right)P_{qq}(z) + D_g^h\left(\frac{x}{z},\mu_F\right)P_{gq}(z)\right],\\
D_g^h(x) &= D_g^h(x,\mu_F) - \frac{\alpha_s}{2\pi}\left(\frac{1}{\hat{\epsilon}} + \ln\frac{\mu_F^2}{\mu^2}\right)\int_x^1 \frac{dz}{z}\left[\sum_{q,\bar{q}} D_q^h\left(\frac{x}{z},\mu_F\right)P_{qg}(z) + D_g^h\left(\frac{x}{z},\mu_F\right)P_{gg}(z)\right],
\end{aligned}
\tag{6.36}
$$

where $\frac{1}{\hat{\epsilon}} = \frac{\Gamma(1-\epsilon)}{\epsilon(4\pi)^\epsilon} \sim \frac{1}{\epsilon} + \gamma_E - \ln(4\pi)$ and μ is the arbitrary parameter introduced by dimensional regularization. The LO splitting functions are given by

$$
P_{qq}(z) = C_F\left[\frac{1+z^2}{(1-z)_+} + \frac{3}{2}\delta(1-z)\right], \tag{6.37}
$$

$$
P_{gq}(z) = C_F\frac{1+(1-z)^2}{z}, \tag{6.38}
$$

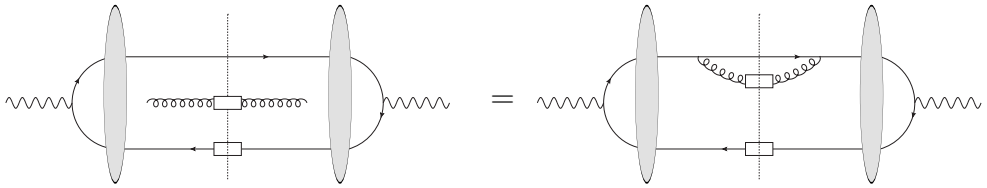

(d) (1)

+ finite contributions.

Figure 6.8: NLO cross section in the case of fragmentation from the gluon and the anti-quark. We explicitly isolate the diagram which contains divergences, namely a collinear divergence between the fragmenting gluon and the quark.

$$P_{qg}(z) = T_R\left[z^2+(1-z)^2\right] \quad \text{with} \quad T_R=\frac{1}{2}\,, \tag{6.39}$$

$$P_{gg}(z) = 2C_A\left[\frac{1}{(1-z)_+}+\frac{1}{z}-2+z(1-z)\right]+\left(\frac{11}{6}C_A-\frac{n_f}{3}\right)\delta(1-z)\,, \tag{6.40}$$

where the + prescription is defined as

$$\int_a^1 d\beta \frac{F(\beta)}{(1-\beta)_+} = \int_a^1 d\beta \frac{F(\beta)-F(1)}{(1-\beta)} - \int_0^a d\beta \frac{F(1)}{1-\beta}\,. \tag{6.41}$$

The collinear counterterms due to the renormalization of the bare FFs are calculated by inserting Eq. (6.36) in the contributions (6.20, 6.24, 6.28) to the LO cross section. This corresponds to the contribution (e) in Fig. 6.5. For the LL cross section, this counterterm takes the form

$$\begin{aligned}
&\left.\frac{d\sigma_{LL}^{q\bar{q}\to h_1h_2}}{dx_{h_1}d_{h_2}d^dp_{h_1\perp}d^dp_{h_2\perp}}\right|_{\rm ct}\\
&=\frac{4\alpha_{\rm em}Q^2}{(2\pi)^{4(d-1)}N_c}\sum_q\int_{x_{h_1}}^1 dx_q\int_{x_{h_2}}^1 dx_{\bar{q}}\; x_q x_{\bar{q}}\left(\frac{x_q}{x_{h_1}}\right)^d\left(\frac{x_{\bar{q}}}{x_{h_2}}\right)^d\delta(1-x_q-x_{\bar{q}})\\
&\times\mathcal{F}_{LL}\left(-\frac{\alpha_s}{2\pi}\right)\left(\frac{1}{\hat{\epsilon}}+\ln\frac{\mu_F^2}{\mu^2}\right)Q_q^2\left\{\int_{\frac{x_{h_1}}{x_q}}^1\frac{d\beta_1}{\beta_1}\left[P_{qq}(\beta_1)D_q^{h_1}\left(\frac{x_{h_1}}{\beta_1x_q},\mu_F\right)D_{\bar{q}}^{h_2}\left(\frac{x_{h_2}}{x_{\bar{q}}},\mu_F\right)\right.\right.\\
&\left.\left.+P_{gq}(\beta_1)D_g^{h_1}\left(\frac{x_{h_1}}{\beta_1x_q},\mu_F\right)D_{\bar{q}}^{h_2}\left(\frac{x_{h_2}}{x_{\bar{q}}},\mu_F\right)\right]\right.\\
&\left.+\int_{\frac{x_{h_2}}{x_{\bar{q}}}}^1\frac{d\beta_2}{\beta_2}\left[P_{qq}(\beta_2)D_q^{h_1}\left(\frac{x_{h_1}}{x_q},\mu_F\right)D_{\bar{q}}^{h_2}\left(\frac{x_{h_2}}{\beta_2x_{\bar{q}}},\mu_F\right)\right.\right.
\end{aligned}$$

$$
\begin{aligned}
&+P_{gq}(\beta_2)D_q^{h_1}\left(\frac{x_{h_1}}{x_q},\mu_F\right)D_g^{h_2}\left(\frac{x_{h_2}}{\beta_2 x_{\bar q}},\mu_F\right)\Bigg]\Bigg\}+(h_1\leftrightarrow h_2)\\
&=\left.\frac{d\sigma_{LL}^{h_1h_2}}{dx_{h_1}d_{h_2}d^dp_{h_1\perp}d^dp_{h_2\perp}}\right|_{\text{ct div}}+\left.\frac{d\sigma_{LL}^{h_1h_2}}{dx_{h_1}d_{h_2}d^dp_{h_1\perp}d^dp_{h_2\perp}}\right|_{\text{ct fin}}.
\end{aligned}
\tag{6.42}
$$

The divergent part is the one containing $1/\hat\epsilon$ and the finite term is the one with $\ln(\mu_F^2/\mu^2)$. The dependence on the arbitrary parameter μ disappears at the end when all finite terms are put together. We stress here that, for any separate term in the curly bracket, one can indifferently use $\mathcal{F}_{LL}$ or $\tilde{\mathcal{F}}_{LL}$. In particular, for the first two terms we can use $\mathcal{F}_{LL}$ and for the last two $\tilde{\mathcal{F}}_{LL}$. This simple observation is useful when observing the cancellation of divergences at the level of integrands. The same remark applies also for other transitions.

For cross sections involving other combinations of polarizations, we have

$$
\begin{aligned}
&\left.\frac{d\sigma_{TL}^{q\bar q\to h_1h_2}}{dx_{h_1}d_{h_2}d^dp_{h_1\perp}d^dp_{h_2\perp}}\right|_{\text{ct}}\\
&=\frac{2\alpha_{\text{em}}Q}{(2\pi)^{4(d-1)}N_c}\sum_q\int_{x_{h_1}}^1dx_q\int_{x_{h_2}}^1dx_{\bar q}\left(\frac{x_q}{x_{h_1}}\right)^d\left(\frac{x_{\bar q}}{x_{h_2}}\right)^d(x_{\bar q}-x_q)\,\delta(1-x_q-x_{\bar q})\\
&\times\mathcal{F}_{TL}\left(-\frac{\alpha_s}{2\pi}\right)\left(\frac{1}{\hat\epsilon}+\ln\frac{\mu_F^2}{\mu^2}\right)Q_q^2\Bigg\{\int_{\frac{x_{h_1}}{x_q}}^1\frac{d\beta_1}{\beta_1}\Bigg[P_{qq}(\beta_1)D_q^{h_1}\left(\frac{x_{h_1}}{\beta_1x_q},\mu_F\right)D_{\bar q}^{h_2}\left(\frac{x_{h_2}}{x_{\bar q}},\mu_F\right)\\
&+P_{gq}(\beta_1)D_g^{h_1}\left(\frac{x_{h_1}}{\beta_1x_q},\mu_F\right)D_{\bar q}^{h_2}\left(\frac{x_{h_2}}{x_{\bar q}},\mu_F\right)\Bigg]\\
&+\int_{\frac{x_{h_2}}{x_{\bar q}}}^1\frac{d\beta_2}{\beta_2}\Bigg[P_{qq}(\beta_2)D_q^{h_1}\left(\frac{x_{h_1}}{x_q},\mu_F\right)D_{\bar q}^{h_2}\left(\frac{x_{h_2}}{\beta_2x_{\bar q}},\mu_F\right)\\
&+P_{gq}(\beta_2)D_q^{h_1}\left(\frac{x_{h_1}}{x_q},\mu_F\right)D_g^{h_2}\left(\frac{x_{h_2}}{\beta_2x_{\bar q}},\mu_F\right)\Bigg]\Bigg\}+(h_1\leftrightarrow h_2)\\
&=\left.\frac{d\sigma_{TL}^{h_1h_2}}{dx_{h_1}d_{h_2}d^dp_{h_1\perp}d^dp_{h_2\perp}}\right|_{\text{ct div}}+\left.\frac{d\sigma_{TL}^{h_1h_2}}{dx_{h_1}d_{h_2}d^dp_{h_1\perp}d^dp_{h_2\perp}}\right|_{\text{ct fin}},
\end{aligned}
\tag{6.43}
$$

and

$$
\begin{aligned}
&\left.\frac{d\sigma_{TT}^{q\bar q\to h_1h_2}}{dx_{h_1}d_{h_2}d^dp_{h_1\perp}d^dp_{h_2\perp}}\right|_{\text{ct}}\\
&=\frac{\alpha_{\text{em}}}{(2\pi)^{4(d-1)}N_c}\sum_q\int_{x_{h_1}}^1\frac{dx_q}{x_q}\int_{x_{h_2}}^1\frac{dx_{\bar q}}{x_{\bar q}}\left(\frac{x_q}{x_{h_1}}\right)^d\left(\frac{x_{\bar q}}{x_{h_2}}\right)^d\delta(1-x_q-x_{\bar q})\\
&\times\mathcal{F}_{TT}\left(-\frac{\alpha_s}{2\pi}\right)\left(\frac{1}{\hat\epsilon}+\ln\frac{\mu_F^2}{\mu^2}\right)Q_q^2\Bigg\{\int_{\frac{x_{h_1}}{x_q}}^1\frac{d\beta_1}{\beta_1}\Bigg[P_{qq}(\beta_1)D_q^{h_1}\left(\frac{x_{h_1}}{\beta_1x_q},\mu_F\right)D_{\bar q}^{h_2}\left(\frac{x_{h_2}}{x_{\bar q}},\mu_F\right)
\end{aligned}
$$

$$
\begin{aligned}
&+P_{gq}(\beta_1)D_g^{h_1}\left(\frac{x_{h_1}}{\beta_1 x_q},\mu_F\right)D_{\bar q}^{h_2}\left(\frac{x_{h_2}}{x_{\bar q}},\mu_F\right)\Bigg]\\
&+\int_{\frac{x_{h_2}}{x_{\bar q}}}^1\frac{d\beta_2}{\beta_2}\Bigg[P_{qq}(\beta_2)D_q^{h_1}\left(\frac{x_{h_1}}{x_q},\mu_F\right)D_{\bar q}^{h_2}\left(\frac{x_{h_2}}{\beta_2 x_{\bar q}},\mu_F\right)\\
&+P_{gq}(\beta_2)D_q^{h_1}\left(\frac{x_{h_1}}{x_q},\mu_F\right)D_g^{h_2}\left(\frac{x_{h_2}}{\beta_2 x_{\bar q}},\mu_F\right)\Bigg]\Bigg\}+(h_1\leftrightarrow h_2)\\
&=\left.\frac{d\sigma_{TT}^{h_1h_2}}{dx_{h_1}d_{h_2}d^dp_{h_1\perp}d^dp_{h_2\perp}}\right|_{\text{ct div}}+\left.\frac{d\sigma_{TT}^{h_1h_2}}{dx_{h_1}d_{h_2}d^dp_{h_1\perp}d^dp_{h_2\perp}}\right|_{\text{ct fin}}.
\end{aligned}
\tag{6.44}
$$

The divergent parts are the ones containing $1/\hat\epsilon$ and the finite terms are the ones with $\ln(\mu_F^2/\mu^2)$. The dependence on the arbitrary parameter μ disappears at the end when all finite terms are put together.

6.3 NLO cross section: Virtual corrections

Here, we compute 1-loop virtual corrections to the leading order cross section. For sake of comprehension, we report the dipole-dipole virtual corrections to the $\gamma^*\to q\bar q$ cross section, as presented in (5.24) of [198], which we refer to as our partonic cross section. Adapting to our notation, we have

$$
\begin{aligned}
d\hat\sigma_{1LL}=&\frac{\alpha_s}{2\pi}\frac{\Gamma(1-\epsilon)}{(4\pi)^\epsilon}C_F\left(\frac{S_V+S_V^*}{2}\right)d\hat\sigma_{0LL}\\
&+\frac{\alpha_s Q^2}{4\pi}\left(\frac{N_c^2-1}{N_c}\right)\frac{\alpha_{\text{em}}Q_q^2}{(2\pi)^4N_c}dx_qdx_{\bar q}d^2p_{q\perp}d^2p_{\bar q\perp}\delta(1-x_q-x_{\bar q})\\
&\times\int d^2p_{1\perp}d^2p_{2\perp}d^2p'_{1\perp}d^2p'_{2\perp}\delta\left(p_{q1\perp}+p_{\bar q2\perp}\right)\frac{\delta\left(p_{11'\perp}+p_{22'\perp}\right)}{\vec p_{q1'}^{\,2}+x_qx_{\bar q}Q^2}\mathbf{F}\left(\frac{p_{12\perp}}{2}\right)\mathbf{F}^*\left(\frac{p_{1'2'\perp}}{2}\right)\\
&\times\Bigg[\frac{6x_q^2x_{\bar q}^2}{\vec p_{q1}^{\,2}+x_qx_{\bar q}Q^2}\ln\left(\frac{x_q^2x_{\bar q}^2\mu^4Q^2}{\left(x_q\vec p_{\bar q}-x_{\bar q}\vec p_q\right)^2\left(\vec p_{q1}^{\,2}+x_qx_{\bar q}Q^2\right)^2}\right)\\
&+\frac{\left(p_0^-\right)^2}{s^2p_\gamma^+}\text{tr}\left(\left(C_\parallel^4+C_{1\parallel}^5+C_{1\parallel}^6\right)\hat p_{\bar q}\gamma^+\hat p_q\right)\Bigg]+h.c.
\end{aligned}
\tag{6.45}
$$

in which the divergences are inside the contribution

$$
\begin{aligned}
\frac{S_V+S_V^*}{2}=&\frac{1}{\epsilon}\Bigg[-4\epsilon\ln(\alpha)\ln\left(\frac{x_q^2x_{\bar q}^2\mu^2}{\left(x_q\vec p_{\bar q}-x_{\bar q}\vec p_q\right)^2}\right)+4\ln(\alpha)+4\epsilon\ln^2(\alpha)-2\ln(x_qx_{\bar q})+3\\
&+2\epsilon\ln\left(\frac{x_qx_{\bar q}\mu^2}{\left(x_q\vec p_{\bar q}-x_{\bar q}\vec p_q\right)^2}\right)\ln(x_qx_{\bar q})+\epsilon\ln^2(x_qx_{\bar q})-3\epsilon\ln\left(\frac{x_qx_{\bar q}\mu^2}{\left(x_q\vec p_{\bar q}-x_{\bar q}\vec p_q\right)^2}\right)-\frac{\pi^2}{3}\epsilon+6\epsilon\Bigg],
\end{aligned}
\tag{6.46}
$$

where α is an infra-red cut-off imposed on the longitudinal fraction of gluon momenta in order to regularize rapidity divergences. In Eq. (6.45) the C functions have been parametrized using (5.25) and (5.26) in Ref. [198] as

$$\frac{(p_0^-)^2}{s^2 p_\gamma^+} tr(C_{||}^4 \hat{p}_{\bar{q}} \gamma^+ \hat{p}_q) = \int_0^x dz \left[(\phi_4)_{LL}\right]_+ + (q \leftrightarrow \bar{q}) \,, \tag{6.47}$$

and

$$\frac{(p_0^-)^2}{s^2 p_\gamma^+} tr(C_{1||}^n \hat{p}_{\bar{q}} \gamma^+ \hat{p}_q) = \int_0^x dz \left[(\phi_n)_{LL}\right]_+ |_{\vec{p}_3=\vec{0}} + (q \leftrightarrow \bar{q}) \,, \tag{6.48}$$

where $n = 5$ or 6, and $(q \leftrightarrow \bar{q})$ stands for $p_q \leftrightarrow p_{\bar{q}}$, $p_1^{(\prime)} \leftrightarrow p_2^{(\prime)}$, $x_q \leftrightarrow x_{\bar{q}}$. The expressions for $(\phi_n)_{LL}$ are given in Appendix D.1.

By using a factorization formula analogous to Eq. (6.14) and the expression (6.45), as well as the collinear constraints (6.16) and (6.17), we obtain the dipole-dipole virtual corrections to the full cross section. We split it into divergent part,

$$\begin{aligned}
&\left.\frac{d\sigma_{1LL}^{q\bar{q}\to h_1 h_2}}{dx_{h_1} d_{h_2} d^d p_{h_1\perp} d^d p_{h_2\perp}}\right|_{\rm div} \\
&= \frac{4\alpha_{\rm em} Q^2}{(2\pi)^{4(d-1)} N_c} \sum_q \int_{x_{h_1}}^1 dx_q \int_{x_{h_2}}^1 dx_{\bar{q}}\, x_q x_{\bar{q}} \left(\frac{x_q}{x_{h_1}}\right)^d \left(\frac{x_{\bar{q}}}{x_{h_2}}\right)^d \delta(1 - x_q - x_{\bar{q}}) \\
&\times Q_q^2 D_q^{h_1}\left(\frac{x_{h_1}}{x_q}, \mu_F\right) D_{\bar{q}}^{h_2}\left(\frac{x_{h_2}}{x_{\bar{q}}}, \mu_F\right) \mathcal{F}_{LL} \\
&\times \frac{\alpha_s}{2\pi} C_F \frac{1}{\hat{\epsilon}} \left[-4\epsilon \ln(\alpha) \ln\left(\frac{\mu^2}{\left(\frac{\vec{p}_{h_2}}{x_{h_2}} - \frac{\vec{p}_{h_1}}{x_{h_1}}\right)^2}\right) + 4\ln(\alpha) \right. \\
&\left. + 4\epsilon \ln^2(\alpha) - 2\ln(x_q x_{\bar{q}}) + 3\right] + (h_1 \leftrightarrow h_2)
\end{aligned} \tag{6.49}$$

and finite part,

$$\begin{aligned}
&\left.\frac{d\sigma_{1LL}^{q\bar{q}\to h_1 h_2}}{dx_{h_1} d_{h_2} d^d p_{h_1\perp} d^d p_{h_2\perp}}\right|_{\rm fin} \\
&= \frac{4\alpha_{\rm em} Q^2}{(2\pi)^{4(d-1)} N_c} \sum_q \int_{x_{h_1}}^1 dx_q \int_{x_{h_2}}^1 dx_{\bar{q}}\, x_q x_{\bar{q}} \left(\frac{x_q}{x_{h_1}}\right)^d \left(\frac{x_{\bar{q}}}{x_{h_2}}\right)^d \delta(1 - x_q - x_{\bar{q}}) \\
&\times Q_q^2 D_q^{h_1}\left(\frac{x_{h_1}}{x_q}, \mu_F\right) D_{\bar{q}}^{h_2}\left(\frac{x_{h_2}}{x_{\bar{q}}}, \mu_F\right) \mathcal{F}_{LL} \\
&\times \frac{\alpha_s}{2\pi} C_F \frac{1}{\hat{\epsilon}} \left[2\epsilon \ln\left(\frac{\mu^2}{x_q x_{\bar{q}} \left(\frac{\vec{p}_{h_2}}{x_{h_2}} - \frac{\vec{p}_{h_1}}{x_{h_1}}\right)^2}\right) \ln(x_q x_{\bar{q}}) \right.
\end{aligned}$$

$$
\begin{aligned}
&+\epsilon\ln^2(x_q x_{\bar q}) - 3\epsilon\ln\left(\frac{\mu^2}{x_q x_{\bar q}\left(\frac{\vec p_{h_2}}{x_{h_2}}-\frac{\vec p_{h_1}}{x_{h_1}}\right)^2}\right) - \frac{\pi^2}{3}\epsilon + 6\epsilon\Bigg] \\
&+ \frac{\alpha_s Q^2}{4\pi}\left(\frac{N_c^2-1}{N_c}\right)\frac{\alpha_{\rm em}}{(2\pi)^4 N_c}\sum_q\int_{x_{h_1}}^1\frac{dx_q}{x_q}\int_{x_{h_2}}^1\frac{dx_{\bar q}}{x_{\bar q}}\delta(1-x_q-x_{\bar q}) \\
&\times\left(\frac{x_q}{x_{h_1}}\right)^d\left(\frac{x_{\bar q}}{x_{h_2}}\right)^d Q_q^2 D_q^{h_1}\left(\frac{x_{h_1}}{x_q},\mu_F\right)D_{\bar q}^{h_2}\left(\frac{x_{h_2}}{x_{\bar q}},\mu_F\right) \\
&\times\int d^dp_{2\perp}\frac{\mathbf{F}\left(\frac{x_q}{2x_{h_1}}p_{h_1\perp}+\frac{x_{\bar q}}{2x_{h_2}}p_{h_2\perp}-p_{2\perp}\right)}{\left(\frac{x_{\bar q}}{x_{h_2}}\vec p_{h_2}-\vec p_2\right)^2+x_q x_{\bar q}Q^2}\int d^dp_{2'\perp}\frac{\mathbf{F}^*\left(\frac{x_q}{2x_{h_1}}p_{h_1\perp}+\frac{x_{\bar q}}{2x_{h_2}}p_{h_2\perp}-p_{2'\perp}\right)}{\left(\frac{x_{\bar q}}{x_{h_2}}\vec p_{h_2}-\vec p_{2'}\right)^2+x_q x_{\bar q}Q^2} \\
&\times\Bigg[6x_q^2x_{\bar q}^2\ln\left(\frac{\mu^4Q^2}{\left(\frac{\vec p_{h_2}}{x_{h_2}}-\frac{\vec p_{h_1}}{x_{h_1}}\right)^2\left(\left(\frac{x_{\bar q}}{x_{h_2}}\vec p_{h_2}-\vec p_2\right)^2+x_q x_{\bar q}Q^2\right)^2}\right)+\left(\int_0^{x_q}dz\left[(\phi_4)_{LL}\right]_+\right. \\
&\left.+\sum_{n=5,6}\left[(\phi_n)_{LL}\right]_+\Big|_{\vec p_3=\vec 0}+(q\leftrightarrow\bar q)\right)\left(\left(\frac{x_{\bar q}}{x_{h_2}}\vec p_{h_2}-\vec p_2\right)^2+x_q x_{\bar q}Q^2\right)\Bigg]+(h_1\leftrightarrow h_2)\,. \qquad (6.50)
\end{aligned}
$$

For the $d\sigma_{TL}$ element of the matrix (6.18), we get from (5.28) of [198]

$$
\begin{aligned}
&\frac{d\sigma_{1TL}^{q\bar q\to h_1h_2}}{dx_{h_1}d_{h_2}d^dp_{h_1\perp}d^dp_{h_2\perp}}\Big|_{\rm div} \\
&=\frac{2\alpha_{\rm em}Q}{(2\pi)^{4(d-1)}N_c}\sum_q\int_{x_{h_1}}^1dx_q\int_{x_{h_2}}^1dx_{\bar q}\left(\frac{x_q}{x_{h_1}}\right)^d\left(\frac{x_{\bar q}}{x_{h_2}}\right)^d(x_{\bar q}-x_q) \\
&\times\delta(1-x_q-x_{\bar q})Q_q^2D_q^{h_1}\left(\frac{x_{h_1}}{x_q},\mu_F\right)D_{\bar q}^{h_2}\left(\frac{x_{h_2}}{x_{\bar q}},\mu_F\right)\mathcal{F}_{TL} \\
&\times\frac{\alpha_s}{2\pi}C_F\frac{1}{\hat\epsilon}\Bigg[-4\epsilon\ln(\alpha)\ln\left(\frac{\mu^2}{\left(\frac{\vec p_{h_2}}{x_{h_2}}-\frac{\vec p_{h_1}}{x_{h_1}}\right)^2}\right)+4\ln(\alpha) \\
&+4\epsilon\ln^2(\alpha)-2\ln(x_qx_{\bar q})+3\Big]+(h_1\leftrightarrow h_2)\,, \qquad (6.51)
\end{aligned}
$$

and

$$
\begin{aligned}
&\frac{d\sigma_{1TL}^{q\bar q\to h_1h_2}}{dx_{h_1}d_{h_2}d^dp_{h_1\perp}d^dp_{h_2\perp}}\Big|_{\rm fin} \\
&=\frac{2\alpha_{\rm em}Q}{(2\pi)^{4(d-1)}N_c}\sum_q\int_{x_{h_1}}^1dx_q\int_{x_{h_2}}^1dx_{\bar q}\left(\frac{x_q}{x_{h_1}}\right)^d\left(\frac{x_{\bar q}}{x_{h_2}}\right)^d(x_{\bar q}-x_q) \\
&\times\delta(1-x_q-x_{\bar q})Q_q^2D_q^{h_1}\left(\frac{x_{h_1}}{x_q},\mu_F\right)D_{\bar q}^{h_2}\left(\frac{x_{h_2}}{x_{\bar q}},\mu_F\right)\mathcal{F}_{TL}
\end{aligned}
$$

$$
\times \frac{\alpha_s}{2\pi} C_F \frac{1}{\hat{\epsilon}} \left[2\epsilon \ln\left(\frac{\mu^2}{x_q x_{\bar{q}} \left(\frac{\vec{p}_{h_2}}{x_{h_2}} - \frac{\vec{p}_{h_1}}{x_{h_1}} \right)^2} \right) \ln(x_q x_{\bar{q}}) + \epsilon \ln^2(x_q x_{\bar{q}}) \right.
$$

$$
\left. -3\epsilon \ln\left(\frac{\mu^2}{x_q x_{\bar{q}} \left(\frac{\vec{p}_{h_2}}{x_{h_2}} - \frac{\vec{p}_{h_1}}{x_{h_1}} \right)^2} \right) - \frac{\pi^2}{3}\epsilon + 6\epsilon \right]
$$

$$
+ \frac{\alpha_s Q}{4\pi} \left(\frac{N_c^2 - 1}{N_c} \right) \frac{\alpha_{\rm em}}{(2\pi)^4 N_c} \sum_q \int_{x_{h_1}}^1 \frac{dx_q}{x_q} \int_{x_{h_2}}^1 \frac{dx_{\bar{q}}}{x_q} \, \delta(1 - x_q - x_{\bar{q}})
$$

$$
\times \left(\frac{x_q}{x_{h_1}} \right)^d \left(\frac{x_{\bar{q}}}{x_{h_2}} \right)^d Q_q^2 D_q^{h_1} \left(\frac{x_{h_1}}{x_q}, \mu_F \right) D_{\bar{q}}^{h_2} \left(\frac{x_{h_1}}{x_q}, \mu_F \right)
$$

$$
\times \int d^d p_{1\perp} d^d p_{2\perp} \mathbf{F}\left(\frac{p_{12\perp}}{2} \right) \delta\left(\frac{x_q}{x_{h_1}} p_{h_1\perp} - p_{1\perp} + \frac{x_{\bar{q}}}{x_{h_2}} p_{h_2\perp} - p_{2\perp} \right)
$$

$$
\times \int d^d p_{1'\perp} d^d p_{2'\perp} \mathbf{F}^*\left(\frac{p_{1'2'\perp}}{2} \right) \delta\left(\frac{x_q}{x_{h_1}} p_{h_1\perp} - p_{1'\perp} + \frac{x_{\bar{q}}}{x_{h_2}} p_{h_2\perp} - p_{2'\perp} \right) \varepsilon_{Ti}^*
$$

$$
\times \left[\frac{1}{\left(\frac{x_q}{x_{h_1}} \vec{p}_{h_1} - \vec{p}_1 \right)^2 + x_q x_{\bar{q}} Q^2} \left(\int_0^{x_q} \left[(\phi_4^i)_{TL} \right]_+ + \sum_{n=5,6} \int_0^{x_q} \left[(\phi_n^i)_{TL} \right]_+ \Big|_{\vec{p}_3 = \vec{0}} + (q \leftrightarrow \bar{q}) \right) \right]^\dagger
$$

$$
+ \frac{3 x_q x_{\bar{q}} (x_{\bar{q}} - x_q) \left(\frac{x_q}{x_{h_1}} p_{h_1\perp} - p_{1'\perp} \right)^i}{\left(\left(\frac{x_q}{x_{h_1}} \vec{p}_{h_1} - \vec{p}_1 \right)^2 + x_q x_{\bar{q}} Q^2 \right) \left(\left(\frac{x_q}{x_{h_1}} \vec{p}_{h_1} - \vec{p}_{1'} \right)^2 + x_q x_{\bar{q}} Q^2 \right)}
$$

$$
\times \left(\ln\left(\frac{Q^2 \mu^8 \left(\frac{\vec{p}_{h_2}}{x_{h_2}} - \frac{\vec{p}_{h_1}}{x_{h_1}} \right)^{-4}}{x_q x_{\bar{q}} \left(\left(\frac{x_q}{x_{h_1}} \vec{p}_{h_1} - \vec{p}_1 \right)^2 + x_q x_{\bar{q}} Q^2 \right) \left(\left(\frac{x_q}{x_{h_1}} \vec{p}_{h_1} - \vec{p}_{1'} \right)^2 + x_q x_{\bar{q}} Q^2 \right)} \right) \right.
$$

$$
\left. - \frac{x_q x_{\bar{q}} Q^2}{\left(\frac{x_q}{x_{h_1}} \vec{p}_{h_1} - \vec{p}_{1'} \right)^2} \ln\left(\frac{x_q x_{\bar{q}} Q^2}{\left(\frac{x_q}{x_{h_1}} \vec{p}_{h_1} - \vec{p}_{1'} \right)^2 + x_q x_{\bar{q}} Q^2} \right) \right) + \frac{1}{2 x_q x_{\bar{q}} \left(\left(\frac{x_q}{x_{h_1}} \vec{p}_{h_1} - \vec{p}_{1'} \right)^2 + x_q x_{\bar{q}} Q^2 \right)}
$$

$$
\times \left(\int_0^{x_q} \left[(\phi_4^i)_{LT} \right]_+ + \sum_{n=5,6} \int_0^{x_q} \left[(\phi_n^i)_{LT} \right]_+ \Big|_{\vec{p}_3 = \vec{0}} + (q \leftrightarrow \bar{q}) \right) \Bigg] + (h_1 \leftrightarrow h_2) \, . \tag{6.52}
$$

In the case of the TT transition, the result was obtained in Ref. [198] Eq. (5.35) and the divergent part is

$$
\left. \frac{d\sigma_{1TT}^{q\bar{q} \to h_1 h_2}}{dx_{h_1} d_{h_2} d^d p_{h_1\perp} d^d p_{h_2\perp}} \right|_{\rm div}
$$

$$
= \frac{\alpha_{\rm em}}{(2\pi)^{4(d-1)} N_c} \sum_q \int_{x_{h_1}}^1 \frac{dx_q}{x_q} \int_{x_{h_2}}^1 \frac{dx_{\bar{q}}}{x_{\bar{q}}} \left(\frac{x_q}{x_{h_1}} \right)^d \left(\frac{x_{\bar{q}}}{x_{h_2}} \right)^d \delta(1 - x_q - x_{\bar{q}})
$$

$$\times Q_q^2 D_q^{h_1}\left(\frac{x_{h_1}}{x_q},\mu_F\right) D_{\bar{q}}^{h_2}\left(\frac{x_{h_2}}{x_{\bar{q}}},\mu_F\right)\mathcal{F}_{TT}$$
$$\times \frac{\alpha_s}{2\pi}C_F\frac{1}{\hat{\epsilon}}\left[-4\epsilon\ln(\alpha)\ln\left(\frac{\mu^2}{\left(\frac{\vec{p}_{h_2}}{x_{h_2}}-\frac{\vec{p}_{h_1}}{x_{h_1}}\right)^2}\right)+4\ln(\alpha)\right.$$
$$\left.+4\epsilon\ln^2(\alpha)-2\ln(x_q x_{\bar{q}})+3\right]+(h_1\leftrightarrow h_2) \tag{6.53}$$

while the finite part reads

$$\left.\frac{d\sigma_{1TT}^{q\bar{q}\to h_1h_2}}{dx_{h_1}d_{h_2}d^dp_{h_1\perp}d^dp_{h_2\perp}}\right|_{\text{fin}}$$
$$=\frac{\alpha_{\text{em}}}{(2\pi)^{4(d-1)}N_c}\sum_q\int_{x_{h_1}}^1\frac{dx_q}{x_q}\int_{x_{h_2}}^1\frac{dx_{\bar{q}}}{x_{\bar{q}}}\left(\frac{x_q}{x_{h_1}}\right)^d\left(\frac{x_{\bar{q}}}{x_{h_2}}\right)^d\delta(1-x_q-x_{\bar{q}})$$
$$\times Q_q^2 D_q^{h_1}\left(\frac{x_{h_1}}{x_q},\mu_F\right) D_{\bar{q}}^{h_2}\left(\frac{x_{h_2}}{x_{\bar{q}}},\mu_F\right)\mathcal{F}_{TT}$$
$$\times\frac{\alpha_s}{2\pi}C_F\frac{1}{\hat{\epsilon}}\left[2\epsilon\ln\left(\frac{\mu^2}{x_qx_{\bar{q}}\left(\frac{\vec{p}_{h_2}}{x_{h_2}}-\frac{\vec{p}_{h_1}}{x_{h_1}}\right)^2}\right)\ln(x_qx_{\bar{q}})+\epsilon\ln^2(x_qx_{\bar{q}})\right.$$
$$\left.-3\epsilon\ln\left(\frac{\mu^2}{x_qx_{\bar{q}}\left(\frac{\vec{p}_{h_2}}{x_{h_2}}-\frac{\vec{p}_{h_1}}{x_{h_1}}\right)^2}\right)-\frac{\pi^2}{3}\epsilon+6\epsilon\right]$$
$$+\frac{\alpha_s}{4\pi}\left(\frac{N_c^2-1}{N_c}\right)\frac{\alpha_{\text{em}}}{(2\pi)^4N_c}\sum_q\int_{x_{h_1}}^1\frac{dx_q}{x_q}\int_{h_2}^1\frac{dx_{\bar{q}}}{x_{\bar{q}}}\,\delta(1-x_q-x_{\bar{q}})$$
$$\times\left(\frac{x_q}{x_{h_1}}\right)^d\left(\frac{x_{\bar{q}}}{x_{h_2}}\right)^d Q_q^2D_q^{h_1}\left(\frac{x_{h_1}}{x_q},\mu_F\right)D_{\bar{q}}^{h_2}\left(\frac{x_{h_2}}{x_{\bar{q}}},\mu_F\right)$$
$$\times\int d^dp_{1\perp}d^dp_{2\perp}\mathbf{F}\left(\frac{p_{12\perp}}{2}\right)\delta\left(\frac{x_q}{x_{h_1}}p_{h_1\perp}-p_{1\perp}+\frac{x_{\bar{q}}}{x_{h_2}}p_{h_2\perp}-p_{2\perp}\right)$$
$$\times\int d^dp_{1'\perp}d^dp_{2'\perp}\mathbf{F}^*\left(\frac{p_{1'2'\perp}}{2}\right)\delta\left(\frac{x_q}{x_{h_1}}p_{h_1\perp}-p_{1'\perp}+\frac{x_{\bar{q}}}{x_{h_2}}p_{h_2\perp}-p_{2'\perp}\right)$$
$$\times\varepsilon_{Ti}\bar{\varepsilon}^*_{Tk}\left\{\frac{3}{2}\frac{\left(\frac{x_q}{x_{h_1}}p_{h_1\perp}-p_{1\perp}\right)_r\left(\frac{x_q}{x_{h_1}}p_{h_1\perp}-p_{1'\perp}\right)_l}{\left(\left(\frac{x_q}{x_{h_1}}\vec{p}_{h_1}-\vec{p}_1\right)^2+x_qx_{\bar{q}}Q^2\right)\left(\left(\frac{x_q}{x_{h_1}}\vec{p}_{h_1}-\vec{p}_{1'}\right)^2+x_qx_{\bar{q}}Q^2\right)}\right.$$
$$\times\left[(x_{\bar{q}}-x_q)^2g_\perp^{ri}g_\perp^{lk}-g_\perp^{rk}g_\perp^{li}+g_\perp^{rl}g_\perp^{ik}\right]$$
$$\left.\times\left[\ln\left(\frac{\mu^4}{x_qx_{\bar{q}}\left(\frac{\vec{p}_{h_2}}{x_{h_2}}-\frac{\vec{p}_{h_1}}{x_{h_1}}\right)^2\left(\left(\frac{x_q}{x_{h_1}}\vec{p}_{h_1}-\vec{p}_1\right)^2+x_qx_{\bar{q}}Q^2\right)}\right)\right.$$

$$-\frac{x_q x_{\bar{q}} Q^2}{\left(\frac{x_q}{x_{h_1}}\vec{p}_{h_1}-\vec{p}_1\right)^2}\ln\left(\frac{x_q x_{\bar{q}} Q^2}{\left(\frac{x_q}{x_{h_1}}\vec{p}_{h_1}-\vec{p}_1\right)^2+x_q x_{\bar{q}} Q^2}\right)\Bigg] + \frac{1}{\left(\left(\frac{x_q}{x_{h_1}}\vec{p}_{h_1}-\vec{p}_{1'}\right)^2+x_q x_{\bar{q}} Q^2\right) x_q x_{\bar{q}}}$$
$$\times\left(\int_0^{x_q}\left[(\phi_4)^{ik}_{TT}\right]_+ + \sum_{n=5,6}\int_0^{x_q}\left[(\phi_n)^{ij}_{TT}\right]_+\Big|_{\vec{p}_3=\vec{0}} + (q\leftrightarrow\bar{q})\right) + h.c.\Big|_{1\leftrightarrow 1',i\leftrightarrow k}\Bigg\}$$
$$+(h_1\leftrightarrow h_2)\,. \tag{6.54}$$

6.4 NLO cross section: Real corrections

In this section, we will discuss the real corrections. Since, as explained above, the calculation is almost completely identical in the LL, TL, and TT cases (apart from factors that do not affect the general strategy), we will show the details of the LL case only. For the others, we will just report the final results.
The dipole-dipole partonic cross section is given by Eq. (6.6) of Ref. [198]:

$$\begin{aligned} d\hat{\sigma}_{3JI} = {} & \frac{\alpha_s}{\mu^{2\epsilon}}\left(\frac{N_c^2-1}{N_c}\right)\frac{\alpha_{\rm em}Q_q^2}{(2\pi)^{4(d-1)}N_c}\frac{(p_0^-)^2}{s^2 x'_q x'_{\bar{q}}}\varepsilon_{I\alpha}\varepsilon^*_{J\beta}dx'_q dx'_{\bar{q}}\delta(1-x'_q-x'_{\bar{q}}-x_g)d^dp_{q\perp}d^dp_{\bar{q}\perp} \\ & \times\frac{dx_g d^dp_{g\perp}}{x_g(2\pi)^d}\int d^dp_{1\perp}d^dp_{2\perp}\mathbf{F}\left(\frac{p_{12\perp}}{2}\right)\delta(p_{q1\perp}+p_{\bar{q}2\perp}+p_{g\perp}) \\ & \times\int d^dp_{1'\perp}d^dp_{2'\perp}\mathbf{F}^*\left(\frac{p_{1'2'\perp}}{2}\right)\delta(p_{q1'\perp}+p_{\bar{q}2'\perp}+p_{g\perp}) \\ & \times\Phi_3^\alpha(p_{1\perp},p_{2\perp})\Phi_3^{\beta*}(p_{1'\perp},p_{2'\perp})\,, \end{aligned} \tag{6.55}$$

where we introduce shorthand notation by suppressing summation over helicities of partons

$$\Phi_3^\alpha(p_{1\perp},p_{2\perp})\Phi_3^{\beta*}(p_{1'\perp},p_{2'\perp}) \equiv \sum_{\lambda_q,\lambda_g,\lambda_{\bar{q}}}\Phi_3^\alpha(p_{1\perp},p_{2\perp})\Phi_3^{\beta*}(p_{1'\perp},p_{2'\perp})\,. \tag{6.56}$$

The impact factor has the form $\Phi_3^\alpha = \Phi_4^\alpha|_{\vec{p}_3=0} + \tilde{\Phi}_3^\alpha$. Only the square of $\tilde{\Phi}_3^\alpha$ provides divergences in the cross section and it is given by (B.3) in Ref. [198]. The LL contribution

reads

$$
\begin{aligned}
&\tilde{\Phi}_3^+(\vec{p}_1,\vec{p}_2)\tilde{\Phi}_3^{+*}(\vec{p}_{1'},\vec{p}_{2'})\\
&=\frac{8x'_qx'_{\bar{q}}(p_\gamma^+)^4\left(dx_g^2+4x'_q(x'_q+x_g)\right)}{\left(Q^2+\frac{\vec{p}^{\,2}_{\bar{q}2'}}{x'_{\bar{q}}(1-x'_{\bar{q}})}\right)\left(Q^2+\frac{\vec{p}^{\,2}_{\bar{q}2'}}{x'_{\bar{q}}(1-x'_{\bar{q}})}\right)(x'_q\vec{p}_g-x_g\vec{p}_q)^2}\\
&-\frac{8x'_qx'_{\bar{q}}(p_\gamma^+)^4\left(2x_g-dx_g^2+4x'_qx'_{\bar{q}}\right)\left(x'_q\vec{p}_g-x_g\vec{p}_q\right)\cdot\left(x'_{\bar{q}}\vec{p}_g-x_g\vec{p}_{\bar{q}}\right)}{\left(Q^2+\frac{\vec{p}^{\,2}_{\bar{q}2'}}{x'_{\bar{q}}(1-x'_{\bar{q}})}\right)\left(Q^2+\frac{\vec{p}^{\,2}_{q1}}{x'_q(1-x'_q)}\right)\left(x'_q\vec{p}_g-x_g\vec{p}_q\right)^2\left(x'_{\bar{q}}\vec{p}_g-x_g\vec{p}_{\bar{q}}\right)^2}\\
&+\frac{8x'_qx'_{\bar{q}}(p_\gamma^+)^4\left(dx_g^2+4x'_{\bar{q}}(x'_{\bar{q}}+x_g)\right)}{\left(Q^2+\frac{\vec{p}^{\,2}_{q1}}{x'_q(1-x'_q)}\right)\left(Q^2+\frac{\vec{p}^{\,2}_{q1'}}{x'_q(1-x'_q)}\right)(x'_{\bar{q}}\vec{p}_g-x_g\vec{p}_{\bar{q}})^2}\\
&-\frac{8x'_qx'_{\bar{q}}(p_\gamma^+)^4\left(2x_g-dx_g^2+4x'_qx'_{\bar{q}}\right)\left(x'_q\vec{p}_g-x_g\vec{p}_q\right)\cdot\left(x'_{\bar{q}}\vec{p}_g-x_g\vec{p}_{\bar{q}}\right)}{\left(Q^2+\frac{\vec{p}^{\,2}_{q1'}}{x'_q(1-x'_q)}\right)\left(Q^2+\frac{\vec{p}^{\,2}_{\bar{q}2}}{x'_{\bar{q}}(1-x'_{\bar{q}})}\right)\left(x'_q\vec{p}_g-x_g\vec{p}_q\right)^2\left(x'_{\bar{q}}\vec{p}_g-x_g\vec{p}_{\bar{q}}\right)^2}\,.
\end{aligned}
\tag{6.57}
$$

The TL contribution is

$$
\begin{aligned}
&\tilde{\Phi}_3^+(\vec{p}_1,\vec{p}_2)\tilde{\Phi}_3^{i*}(\vec{p}_{1'},\vec{p}_{2'})\\
&=\frac{4x'_q\left(p_\gamma^+\right)^3}{\left(x'_q+x_g\right)\left(Q^2+\frac{\vec{p}^{\,2}_{\bar{q}2'}}{x'_{\bar{q}}\left(1-x'_{\bar{q}}\right)}\right)\left(Q^2+\frac{\vec{p}^{\,2}_{q1}}{x'_q\left(1-x'_q\right)}\right)}\left(\frac{\left(x'_qp_{g\perp}-x_gp_{q\perp}\right)_\mu\left(x'_{\bar{q}}p_{g\perp}-x_gp_{\bar{q}\perp}\right)_\nu}{\left(x'_q\vec{p}_g-x_g\vec{p}_q\right)^2\left(x'_{\bar{q}}\vec{p}_g-x_g\vec{p}_{\bar{q}}\right)^2}\right)\\
&\times\left[x_g\left(4x'_{\bar{q}}+x_gd-2\right)\left(p^\mu_{\bar{q}2'\perp}g^{i\nu}_\perp-p^\nu_{\bar{q}2'\perp}g^{\mu i}_\perp\right)-\left(2x'_{\bar{q}}-1\right)\left(4x'_qx'_{\bar{q}}+x_g\left(2-x_gd\right)\right)g^{\mu\nu}_\perp p^i_{\bar{q}2'\perp}\right]\\
&-\frac{4x'_q\left(p_\gamma^+\right)^3\left(2x'_{\bar{q}}-1\right)\left(x_g^2d+4x'_q\left(x'_q+x_g\right)\right)p^i_{\bar{q}2'\perp}}{\left(x'_q+x_g\right)\left(Q^2+\frac{\vec{p}^{\,2}_{\bar{q}2'}}{x'_{\bar{q}}\left(1-x'_{\bar{q}}\right)}\right)\left(Q^2+\frac{\vec{p}^{\,2}_{\bar{q}2}}{x'_{\bar{q}}\left(1-x'_{\bar{q}}\right)}\right)\left(x'_q\vec{p}_g-x_g\vec{p}_q\right)^2}+\left(q\leftrightarrow\bar{q}\right),
\end{aligned}
\tag{6.58}
$$

and finally, the TT contribution reads

$$
\begin{aligned}
&\tilde{\Phi}_3^i(\vec{p}_1,\vec{p}_2)\tilde{\Phi}_3^{k*}(\vec{p}_{1'},\vec{p}_{2'})\\
&=\frac{-2\left(p_\gamma^+\right)^2}{\left(x'_q+x_g\right)\left(x'_{\bar{q}}+x_g\right)\left(Q^2+\frac{\vec{p}^{\,2}_{\bar{q}2}}{x'_{\bar{q}}\left(1-x'_{\bar{q}}\right)}\right)\left(Q^2+\frac{\vec{p}^{\,2}_{q1'}}{x'_q\left(1-x'_q\right)}\right)}\\
&\times\left(\frac{\left(x'_qp_{g\perp}-x_gp_{q\perp}\right)_\mu\left(x'_{\bar{q}}p_{g\perp}-x_gp_{\bar{q}\perp}\right)_\nu}{\left(x'_q\vec{p}_g-x_g\vec{p}_q\right)^2\left(x'_{\bar{q}}\vec{p}_g-x_g\vec{p}_{\bar{q}}\right)^2}\right)\left\{x_g((d-4))x_g-2\right)\left[p^\nu_{q1'\perp}\left(p^\mu_{\bar{q}2\perp}g^{ik}_\perp+p^k_{\bar{q}2\perp}g^{\mu i}_\perp\right)\right.\\
&\left.+g^{\mu\nu}_\perp\left(\left(\vec{p}_{q1'}\cdot\vec{p}_{\bar{q}2}\right)g^{ik}_\perp+p^i_{q1'\perp}p^k_{\bar{q}2\perp}\right)-g^{\nu k}_\perp p^i_{q1'\perp}p^\mu_{\bar{q}2\perp}-g^{\mu i}_\perp g^{\nu k}_\perp\left(\vec{p}_{q1'}\cdot\vec{p}_{\bar{q}2}\right)\right]-g^{\mu\nu}_\perp\\
&\times\left[\left(2x'_q-1\right)\left(2x'_{\bar{q}}-1\right)p^k_{q1'\perp}p^i_{\bar{q}2\perp}\left(4x'_qx'_{\bar{q}}+x_g(2-x_gd)\right)+4x'_qx'_{\bar{q}}((\vec{p}_{q1'}\cdot\vec{p}_{\bar{q}2})g^{ik}_\perp+p^i_{q1'\perp}p^k_{\bar{q}2\perp})\right]\\
&+\left(p^\mu_{q1'\perp}p^\nu_{\bar{q}2\perp}g^{ik}_\perp-p^\mu_{q1'\perp}p^k_{\bar{q}2\perp}g^{\nu i}_\perp-p^i_{q1'\perp}p^\nu_{\bar{q}2\perp}g^{\mu k}_\perp-g^{\mu k}_\perp g^{\nu i}_\perp(\vec{p}_{q1'}\cdot\vec{p}_{\bar{q}2})\right)
\end{aligned}
$$

$$\times x_g((d-4)x_g+2)+x_g(2x'_{\bar q}-1)(x_g d+4x'_q-2)\left(g_\perp^{\mu k}p^\nu_{q1'\perp}-g_\perp^{\nu k}p^\mu_{q1'\perp}\right)p^i_{\bar q 2\perp}$$
$$+x_g(2x'_q-1)p^k_{q1'\perp}(4x'_{\bar q}+x_g d-2)\left(g_\perp^{\nu i}p^\mu_{\bar q 2\perp}-g_\perp^{\mu i}p^\nu_{\bar q 2\perp}\right)\}$$
$$-\frac{2x'_q(p^+_\gamma)^2(x_g^2 d+4x'_q(x'_q+x_g))\left((\vec p_{\bar q 2}\cdot\vec p_{\bar q 2'})g_\perp^{ik}-(1-2x'_{\bar q})^2 p^i_{\bar q 2\perp}p^k_{\bar q 2'\perp}+p^i_{\bar q 2'\perp}p^k_{\bar q 2\perp}\right)}{x'_{\bar q}(x'_q+x_g)^2\left(Q^2+\frac{\vec p^{\,2}_{\bar q 2}}{x'_{\bar q}(1-x'_{\bar q})}\right)\left(Q^2+\frac{\vec p^{\,2}_{\bar q 2'}}{x'_{\bar q}(1-x'_{\bar q})}\right)\left(x'_q\vec p_g-x_g\vec p_q\right)^2}$$
$$+(q\leftrightarrow\bar q)\,. \tag{6.59}$$

The divergent part of the LL partonic cross section from real emission is given by

$$\begin{aligned}
d\hat\sigma_{3LL}|_{div}=&\frac{4\alpha_{\rm em}Q^2}{(2\pi)^{4(d-1)}N_c}Q_q^2dx'_qdx'_{\bar q}\delta(1-x'_q-x'_{\bar q}-x_g)d^dp_{q\perp}d^dp_{\bar q\perp}\frac{\alpha_sC_F}{\mu^{2\epsilon}}\frac{dx_g}{x_g}\frac{d^dp_{g\perp}}{(2\pi)^d}\\
&\times\int d^dp_{1\perp}d^dp_{2\perp}\delta(p_{q1\perp}+p_{\bar q 2\perp}+p_{g\perp})\,\mathbf{F}\left(\frac{p_{12\perp}}{2}\right)\\
&\times\int d^dp_{1'\perp}d^dp_{2'\perp}\delta(p_{q1'\perp}+p_{\bar q 2'\perp}+p_{g\perp})\,\mathbf{F}^*\left(\frac{p_{1'2'\perp}}{2}\right)\\
&\times\left\{\frac{dx_g^2+4x'_q(x'_q+x_g)}{\left(Q^2+\frac{\vec p^{\,2}_{\bar q 2}}{x'_{\bar q}(1-x'_{\bar q})}\right)\left(Q^2+\frac{\vec p^{\,2}_{\bar q 2'}}{x'_{\bar q}(1-x'_{\bar q})}\right)(x'_q\vec p_g-x_g\vec p_q)^2}\right.\\
&-\frac{\left(2x_g-dx_g^2+4x'_qx'_{\bar q}\right)\left(x'_q\vec p_g-x_g\vec p_q\right)\cdot\left(x'_{\bar q}\vec p_g-x_g\vec p_{\bar q}\right)}{\left(Q^2+\frac{\vec p^{\,2}_{\bar q 2'}}{x'_{\bar q}(1-x'_{\bar q})}\right)\left(Q^2+\frac{\vec p^{\,2}_{q1}}{x'_q(1-x'_q)}\right)\left(x'_q\vec p_g-x_g\vec p_q\right)^2\left(x'_{\bar q}\vec p_g-x_g\vec p_{\bar q}\right)^2}\\
&+\frac{dx_g^2+4x'_{\bar q}(x'_{\bar q}+x_g)}{\left(Q^2+\frac{\vec p^{\,2}_{q1}}{x'_q(1-x'_q)}\right)\left(Q^2+\frac{\vec p^{\,2}_{q1'}}{x'_q(1-x'_q)}\right)(x'_{\bar q}\vec p_g-x_g\vec p_{\bar q})^2}\\
&\left.-\frac{\left(2x_g-dx_g^2+4x'_qx'_{\bar q}\right)\left(x'_q\vec p_g-x_g\vec p_q\right)\cdot\left(x'_{\bar q}\vec p_g-x_g\vec p_{\bar q}\right)}{\left(Q^2+\frac{\vec p^{\,2}_{q1'}}{x'_q(1-x'_q)}\right)\left(Q^2+\frac{\vec p^{\,2}_{\bar q 2}}{x'_{\bar q}(1-x'_{\bar q})}\right)\left(x'_q\vec p_g-x_g\vec p_q\right)^2\left(x'_{\bar q}\vec p_g-x_g\vec p_{\bar q}\right)^2}\right\}\,.
\end{aligned} \tag{6.60}$$

When two partons labeled i and j become collinear, the variable

$$\vec A_{ij}=x_i\vec p_j-x_j\vec p_i \tag{6.61}$$

vanishes. In the present case, the first term in the bracket of Eq. (6.60) gives the collinear divergences ($\vec A^2_{qg}\to 0$, i.e. quark-gluon channel) and the third ($\vec A^2_{\bar q g}\to 0$, i.e. antiquark-gluon channel).

For the LT, the relevant divergent squared impact factor is (6.58) and for the TT, it is (6.59).

6.4.1 Fragmentation from quark and anti-quark

As explained above, there are several contributions to the final cross section that contain divergences. In this section, we deal with extracting the soft and collinear divergences associated with the contribution (b) in Fig. 6.5. This contribution corresponds to the situation in which the quark and the anti-quark fragment and there is an additional emission of a gluon with respect to the LO case. Below,

- We compute the collinear divergence of the diagram (1) of Fig. 6.6 and show that it is removed by the + prescription part of the first term of Eq. (6.42).
- Similarly, we calculate the collinear divergence of the diagram (3) of Fig. 6.6 and show that it is removed by the + prescription part of the third term of Eq. (6.42).
- We extract the soft divergences of diagrams (1), (2), (3), (4) of Fig. 6.6 and discuss the complete cancellation of divergences of this contribution.

The calculations of the collinear divergences is done by Fourier transforming the $\mathbf{F}(\frac{p_{12\perp}}{2})$, as defined in (6.11), and by using the identity (see eg Ref. [202]):

$$\frac{1}{\mu^{2\epsilon}}\int d^{2+2\epsilon}q_\perp e^{-iq_\perp\cdot r_\perp}\frac{1}{q_\perp^2}=\pi\left(\frac{4\pi}{\mu^2 r_\perp^2}\right)^{\epsilon}\Gamma(\epsilon)\,. \tag{6.62}$$

We also have to change variables from the usual fraction of longitudinal photon momentum of the partons (x_i', x_g) with $i = q, \bar{q}$, in the spirit of the definition (6.7), as used in Eq. (6.60), to the variable of the fraction of longitudinal photon momentum of the parent parton x_i and longitudinal fraction β with respect to the parent parton and not with respect to the photon anymore:

$$(x_i', x_g)\to(x_i,\beta)\qquad\text{with}\qquad x_i'=\beta x_i\,. \tag{6.63}$$

Changing variables is necessary to be able to compare with (6.42), (6.43), and (6.44). Note that to make notations lighter, we will remove the apex ' when one particle is a spectator, see Figs. 6.9 and 6.10.

The Fourier transform of $\mathbf{F}\left(\frac{p_{12\perp}}{2}\right)$ is necessary in order to be able to integrate over the transverse momentum of the spectator parton, as it allows for the complete factorization of this momentum from this non-perturbative function.

Collinear contributions: q-g splitting

We use the kinematics illustrated in Fig. 6.9. The term in (6.57) considered for this collinear contribution is the first one in the bracket:

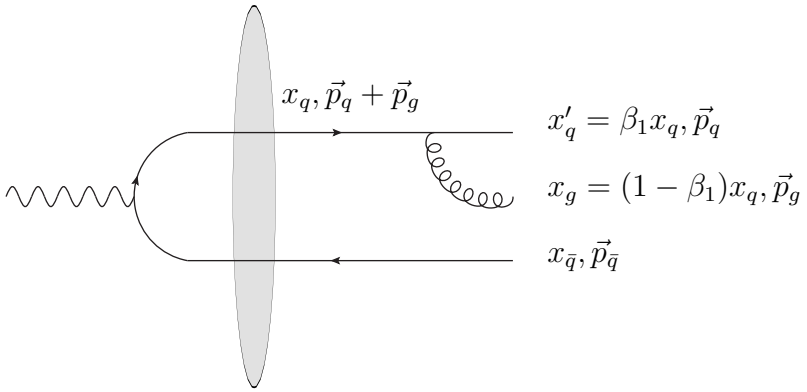

Figure 6.9: Kinematics for the $q - g$ splitting contribution. We indicate the longitudinal fraction of momentum carried by the partons as well as their transverse momenta.

$$
\begin{aligned}
&d\sigma_{3LL}^{q\bar{q}\to h_1 h_2}|_{\text{coll. qg}} \\
&= dx_{h_1} dx_{h_2} \frac{4\alpha_{\text{em}} Q^2}{(2\pi)^{4(d-1)} N_c} \sum_q \int_{x_{h_1}}^1 \frac{dx'_q}{x'_q} \int_{x_{h_2}}^1 \frac{dx_{\bar{q}}}{x_{\bar{q}}} \int_\alpha^1 \frac{dx_g}{x_g} \delta(1 - x'_q - x_{\bar{q}} - x_g) \\
&\times Q_q^2 D_q^{h_1}\left(\frac{x_{h_1}}{x'_q}, \mu_F\right) D_{\bar{q}}^{h_2}\left(\frac{x_{h_2}}{x_{\bar{q}}}, \mu_F\right) d^d p_{q\perp} d^d p_{\bar{q}\perp} \frac{\alpha_s}{\mu^{2\epsilon}} C_F \frac{d^d p_{g\perp}}{(2\pi)^d} \\
&\times \int d^d p_{1\perp} d^d p_{2\perp} \delta(p_{q1\perp} + p_{\bar{q}2\perp} + p_{g\perp})\, \mathbf{F}\left(\frac{p_{12\perp}}{2}\right) \\
&\times \int d^d p_{1'\perp} d^d p_{2'\perp} \delta(p_{q1'\perp} + p_{\bar{q}2'\perp} + p_{g\perp})\, \mathbf{F}^*\left(\frac{p_{1'2'\perp}}{2}\right) \\
&\times \frac{(dx_g^2 + 4x'_q(x'_q + x_g)) x_{\bar{q}}^2 (1 - x_{\bar{q}})^2}{\left(x_{\bar{q}}(1-x_{\bar{q}})Q^2 + \vec{p}_{\bar{q}2}^{\,2}\right)\left(x_{\bar{q}}(1-x_{\bar{q}})Q^2 + \vec{p}_{\bar{q}2'}^{\,2}\right)(x'_q \vec{p}_g - x_g \vec{p}_q)^2} + (h_1 \leftrightarrow h_2) \\
&= dx_{h_1} dx_{h_2} d^d p_{h_1\perp} d^d p_{h_2\perp} \frac{4\alpha_{\text{em}} Q^2}{(2\pi)^{4(d-1)} N_c} \sum_q \int_{x_{h_1}}^1 \frac{dx'_q}{x'_q} \int_\alpha^1 \frac{dx_g}{x_g} \int_{x_{h_2}}^1 \frac{dx_{\bar{q}}}{x_{\bar{q}}} \delta(1 - x'_q - x_{\bar{q}} - x_g) \\
&\times \left(\frac{x'_q}{x_{h_1}}\right)^d \left(\frac{x_{\bar{q}}}{x_{h_2}}\right)^d Q_q^2 D_q^{h_1}\left(\frac{x_{h_1}}{x'_q}, \mu_F\right) D_{\bar{q}}^{h_2}\left(\frac{x_{h_2}}{x_{\bar{q}}}, \mu_F\right) \frac{\alpha_s}{\mu^{2\epsilon}} C_F \frac{d^d p_{g\perp}}{(2\pi)^d} \\
&\times \int d^d p_{1\perp} d^d p_{2\perp} \delta\left(\frac{x'_q}{x_{h_1}} p_{h_1\perp} - p_{1\perp} + \frac{x_{\bar{q}}}{x_{h_2}} p_{h_2\perp} - p_{2\perp} + p_{g\perp}\right) \mathbf{F}\left(\frac{p_{12\perp}}{2}\right) \\
&\times \int d^d p_{1'\perp} d^d p_{2'\perp} \delta\left(\frac{x'_q}{x_{h_1}} p_{h_1\perp} - p_{1'\perp} + \frac{x_{\bar{q}}}{x_{h_2}} p_{h_2\perp} - p_{2'\perp} + p_{g\perp}\right) \mathbf{F}^*\left(\frac{p_{1'2'\perp}}{2}\right) \\
&\times \frac{(dx_g^2 + 4x'_q(x'_q + x_g)) x_{\bar{q}}^2 (1 - x_{\bar{q}})^2}{\left(x_{\bar{q}}(1-x_{\bar{q}})Q^2 + \left(\frac{x_{\bar{q}}}{x_{h_2}}\vec{p}_{h_2} - \vec{p}_2\right)^2\right)\left(x_{\bar{q}}(1-x_{\bar{q}})Q^2 + \left(\frac{x_{\bar{q}}}{x_{h_2}}\vec{p}_{h_2} - \vec{p}_{2'}\right)^2\right)\left(x'_q \vec{p}_g - x_g \frac{x'_q}{x_{h_1}} \vec{p}_{h_1}\right)^2} \\
&+ (h_1 \leftrightarrow h_2)
\end{aligned}
$$

$$
\begin{aligned}
&= dx_{h_1} dx_{h_2} d^d p_{h_1\perp} d^d p_{h_2\perp} \frac{4\alpha_{\rm em} Q^2}{(2\pi)^{4(d-1)} N_c} \sum_q \int_{x_{h_1}}^1 \frac{dx'_q}{x'_q} \int_\alpha^1 \frac{dx_g}{x_g} \int_{x_{h_2}}^1 \frac{dx_{\bar q}}{x_{\bar q}} \delta(1 - x'_q - x_{\bar q} - x_g) \\
&\times \left(\frac{x'_q}{x_{h_1}}\right)^d \left(\frac{x_{\bar q}}{x_{h_2}}\right)^d Q_q^2 D_q^{h_1}\left(\frac{x_{h_1}}{x'_q}, \mu_F\right) D_{\bar q}^{h_2}\left(\frac{x_{h_2}}{x_{\bar q}}, \mu_F\right) \frac{\alpha_s}{\mu^{2\epsilon}} C_F \frac{d^d p_{g\perp}}{(2\pi)^d} \\
&\times \int d^d p_{2\perp}\, \mathbf{F}\left(\frac{x'_q}{2x_{h_1}} p_{h_1\perp} + \frac{x_{\bar q}}{2x_{h_2}} p_{h_2\perp} - p_{2\perp} + \frac{p_{g\perp}}{2}\right) \\
&\times \int d^d p_{2'\perp}\, \mathbf{F}^*\left(\frac{x'_q}{2x_{h_1}} p_{h_1\perp} + \frac{x_{\bar q}}{2x_{h_2}} p_{h_2\perp} - p_{2'\perp} + \frac{p_{g\perp}}{2}\right) \\
&\times \frac{(dx_g^2 + 4x'_q(x'_q + x_g)) x_{\bar q}^2 (1 - x_{\bar q})^2}{\left(x_{\bar q}(1-x_{\bar q})Q^2 + \left(\frac{x_{\bar q}}{x_{h_2}}\vec p_{h_2} - \vec p_2\right)^2\right)\left(x_{\bar q}(1-x_{\bar q})Q^2 + \left(\frac{x_{\bar q}}{x_{h_2}}\vec p_{h_2} - \vec p_{2'}\right)^2\right)\left(x'_q \vec p_g - x_g \frac{x'_q}{x_{h_1}}\vec p_{h_1}\right)^2} \\
&+ (h_1 \leftrightarrow h_2)\,.
\end{aligned}
$$

After performing the change of variable

$$
\begin{aligned}
x'_q &= \beta_1 x_q \\
x_g &= (1 - \beta_1) x_q
\end{aligned}
$$

and using the Jacobian $dx'_q dx_g = x_q\, dx_q d\beta_1$ we can rewrite the longitudinal integration in the symbolic form

$$
\begin{aligned}
&\int_{x_{h_1}}^1 \frac{dx'_q}{x'_q} \int_{x_{h_2}}^1 \frac{dx_{\bar q}}{x_{\bar q}} \int_\alpha^1 \frac{dx_g}{x_g} \delta(1 - x'_q - x_{\bar q} - x_g) \\
&= \int_{x_{h_1}}^1 \frac{dx'_q}{x'_q} \int_\alpha^1 \frac{dx_g}{x_g} \int_{-\infty}^{+\infty} \frac{dx_{\bar q}}{x_{\bar q}} \theta(x_{\bar q} - x_{h_2}) \theta(1 - x_{\bar q}) \delta(1 - x'_q - x_{\bar q} - x_g) \\
&= \int_{x_{h_1}}^1 \frac{dx'_q}{x'_q} \int_\alpha^1 \frac{dx_g}{x_g} \theta(1 - x'_q - x_g - x_{h_2}) \theta(x'_q + x_g) \frac{1}{1 - x'_q - x_g} \\
&= \int_{x_{h_1}}^{1 - x_{h_2}} \frac{dx_q}{x_q} \frac{1}{1 - x_q} \int_{\frac{x_{h_1}}{x_q}}^{1 - \frac{\alpha}{x_q}} \frac{d\beta_1}{\beta_1(1 - \beta_1)}\,.
\end{aligned}
\tag{6.64}
$$

After this manipulation, we obtain

$$
\begin{aligned}
&\left.\frac{d\sigma_{3LL}^{q\bar q \to h_1 h_2}}{dx_{h_1} dx_{h_2} d^d p_{h_1\perp} d^d p_{h_2\perp}}\right|_{\rm coll\ qg} \\
&= \frac{4\alpha_{\rm em} Q^2}{(2\pi)^{4(d-1)} N_c} \sum_q \int_{x_{h_1}}^{1 - x_{h_2}} dx_q x_q (1 - x_q) \left(\frac{x_q}{x_{h_1}}\right)^d \left(\frac{1 - x_q}{x_{h_2}}\right)^d \\
&\times \int_{\frac{x_{h_1}}{x_q}}^{1 - \frac{\alpha}{x_q}} \frac{d\beta_1}{\beta_1} Q_q^2 D_q^{h_1}\left(\frac{x_{h_1}}{\beta_1 x_q}, \mu_F\right) D_{\bar q}^{h_2}\left(\frac{x_{h_2}}{1 - x_q}, \mu_F\right)
\end{aligned}
$$

$$\times \int d^d p_{2\perp} \int d^d z_{1\perp} \frac{e^{iz_{1\perp}\cdot\left(\frac{\beta_1 x_q}{2x_{h_1}} p_{h_1\perp} + \frac{1-x_q}{2x_{h_2}} p_{h_2\perp} - p_{2\perp}\right)} F(z_{1\perp})}{x_q(1-x_q)Q^2 + \left(\frac{1-x_q}{x_{h_2}}\vec{p}_{h_2} - \vec{p}_2\right)^2}$$

$$\times \int d^d p_{2'\perp} \int d^d z_{2\perp} \frac{e^{-iz_{2\perp}\cdot\left(\frac{\beta_1 x_q}{2x_{h_1}} p_{h_1\perp} + \frac{1-x_q}{2x_{h_2}} p_{h_2\perp} - p_{2'\perp}\right)} F^*(z_{2\perp})}{x_q(1-x_q)Q^2 + \left(\frac{1-x_q}{x_{h_2}}\vec{p}_{h_2} - \vec{p}_{2'}\right)^2}$$

$$\times \frac{2(1+\beta_1^2) + 2\epsilon(1-\beta_1)^2 + 4\epsilon(1+\beta_1^2)\ln\beta_1}{1-\beta_1}$$

$$\times e^{i\left(\frac{z_{1\perp}-z_{2\perp}}{2}\right)\cdot\frac{(1-\beta_1)x_q}{x_{h_1}} p_{h_1\perp}} \frac{\alpha_s}{\mu^{2\epsilon}} C_F \int \frac{d^d p_{g\perp}}{(2\pi)^d} \frac{e^{i\left(\frac{z_{1\perp}-z_{2\perp}}{2}\right)\cdot p_{g\perp}}}{\left(\vec{p}_g\right)^2} + (h_1 \leftrightarrow h_2). \tag{6.65}$$

The integral over $p_{g\perp}$ gives, using Eq. (6.62),

$$\begin{aligned}
\mu^{-2\epsilon} \int \frac{d^d p_{g\perp}}{(2\pi)^d} \frac{e^{i\left(\frac{z_{1\perp}-z_{2\perp}}{2}\right)\cdot p_{g\perp}}}{\left(\vec{p}_g\right)^2} &= \frac{1}{(2\pi)^d} \pi \mu^{-2\epsilon} \left[\frac{\left(\frac{z_{1\perp}-z_{2\perp}}{2}\right)^2}{4\pi}\right]^{-\epsilon} \Gamma(\epsilon) \\
&= \frac{1}{4\pi}\left(\frac{1}{\hat{\epsilon}} + \ln\left(\frac{c_0^2}{\left(\frac{z_{1\perp}-z_{2\perp}}{2}\right)^2 \mu^2}\right)\right) + O(\epsilon) \\
&= \frac{1}{4\pi}\frac{1}{\hat{\epsilon}}\left(\frac{c_0^2}{\left(\frac{z_{1\perp}-z_{2\perp}}{2}\right)^2 \mu^2}\right)^{\epsilon} + O(\epsilon)
\end{aligned} \tag{6.66}$$

where $c_0 = 2e^{-\gamma_E}$. This leads to

$$\begin{aligned}
&\left.\frac{d\sigma_{3LL}^{q\bar{q}\to h_1 h_2}}{dx_{h_1} dx_{h_2} d^d p_{h_1\perp} d^d p_{h_2\perp}}\right|_{\text{coll qg.}} \\
&= \frac{4\alpha_{\text{em}} Q^2}{(2\pi)^{4(d-1)} N_c} \sum_q \int_{x_{h_1}}^1 dx_q \int_{x_{h_2}}^1 dx_{\bar{q}} x_q x_{\bar{q}} \delta(1-x_q-x_{\bar{q}}) \left(\frac{x_q}{x_{h_1}}\right)^d \left(\frac{x_{\bar{q}}}{x_{h_2}}\right)^d \\
&\times \int d^d p_{2\perp} \int d^d z_{1\perp} \frac{e^{iz_{1\perp}\cdot\left(\frac{x_q}{2x_{h_1}} p_{h_1\perp} + \frac{1-x_q}{2x_{h_2}} p_{h_2\perp} - p_{2\perp}\right)} F(z_{1\perp})}{x_q(1-x_q)Q^2 + \left(\frac{1-x_q}{x_{h_2}}\vec{p}_{h_2} - \vec{p}_2\right)^2} \\
&\times \int d^d p_{2'\perp} \int d^d z_{2\perp} \frac{e^{-iz_{2\perp}\cdot\left(\frac{x_q}{2x_{h_1}} p_{h_1\perp} + \frac{1-x_q}{2x_{h_2}} p_{h_2\perp} - p_{2'\perp}\right)} F^*(z_{2\perp})}{x_q(1-x_q)Q^2 + \left(\frac{1-x_q}{x_{h_2}}\vec{p}_{h_2} - \vec{p}_{2'}\right)^2} \\
&\times \int_{\frac{x_{h_1}}{x_q}}^{1-\frac{\alpha}{x_q}} \frac{d\beta_1}{\beta_1} Q_q^2 D_q^{h_1}\left(\frac{x_{h_1}}{\beta_1 x_q}, \mu_F\right) D_{\bar{q}}^{h_2}\left(\frac{x_{h_2}}{1-x_q}, \mu_F\right) \\
&\times \frac{\alpha_s C_F}{2\pi}\left[\frac{1}{\hat{\epsilon}}\left(\frac{c_0^2}{\left(\frac{z_{1\perp}-z_{2\perp}}{2}\right)^2 \mu^2}\right)^{\epsilon} \frac{1+\beta_1^2}{1-\beta_1} + \frac{(1-\beta_1)^2 + 2(1+\beta_1^2)\ln\beta_1}{(1-\beta_1)}\right] + (h_1 \leftrightarrow h_2).
\end{aligned} \tag{6.67}$$

Here in Eq. (6.67) we have put back the integral in $x_{\bar{q}}$ using

$$\begin{aligned}\int_{x_{h_1}}^1 dx_q \int_{x_{h_2}}^1 dx_{\bar{q}}\,\delta(1-x_q-x_{\bar{q}}) &= \int_{x_{h_1}}^1 dx_q \int_{-\infty}^{+\infty} dx_{\bar{q}}\,\delta(1-x_q-x_{\bar{q}})\theta(1-x_{\bar{q}})\theta(x_{\bar{q}}-x_{h_2}) \\ &= \int_{x_{h_1}}^{1-x_{h_2}} dx_q\end{aligned} \tag{6.68}$$

in order to have the same form as in the LO cross section (6.20).

Now, to separate the collinear and soft contribution, we introduce the plus prescription, as defined in Eq. (6.41), and after, we expand the factor $\frac{1}{\epsilon}\left(\frac{c_0^2}{\left(\frac{z_{1\perp}-z_{2\perp}}{2}\right)^2\mu^2}\right)^{\epsilon}$ within accuracy of order ϵ^0, only in those terms whose integrand is safe in the limit $\beta_1 \to 1$:

$$\begin{aligned}
&\left.\frac{d\sigma_{3LL}^{q\bar{q}\to h_1h_2}}{dx_{h_1}dx_{h_2}d^dp_{h_1\perp}d^dp_{h_2\perp}}\right|_{\text{coll qg.}} \\
&= \frac{4\alpha_{\text{em}}Q^2}{(2\pi)^{4(d-1)}N_c}\sum_q \int_{x_{h_1}}^1 dx_q \int_{x_{h_2}}^1 dx_{\bar{q}}\; x_q x_{\bar{q}}\delta(1-x_q-x_{\bar{q}})\left(\frac{x_q}{x_{h_1}}\right)^d\left(\frac{x_{\bar{q}}}{x_{h_2}}\right)^d \\
&\times \int d^dp_{2\perp}\int d^dz_{1\perp}\frac{e^{iz_{1\perp}\cdot\left(\frac{x_q}{2x_{h_1}}p_{h_1\perp}+\frac{x_{\bar{q}}}{2x_{h_2}}p_{h_2\perp}-p_{2\perp}\right)}F(z_{1\perp})}{x_qx_{\bar{q}}Q^2+\left(\frac{x_{\bar{q}}}{x_{h_2}}\vec{p}_{h_2}-\vec{p}_2\right)^2} \\
&\times \int d^dp_{2'\perp}\int d^dz_{2\perp}\frac{e^{-iz_{2\perp}\cdot\left(\frac{x_q}{2x_{h_1}}p_{h_1\perp}+\frac{x_{\bar{q}}}{2x_{h_2}}p_{h_2\perp}-p_{2'\perp}\right)}F^*(z_{2\perp})}{x_qx_{\bar{q}}Q^2+\left(\frac{x_{\bar{q}}}{x_{h_2}}\vec{p}_{h_2}-\vec{p}_{2'}\right)^2} \\
&\times\Bigg\{\int_{\frac{x_{h_1}}{x_q}}^1 \frac{d\beta_1}{\beta_1}Q_q^2D_q^{h_1}\left(\frac{x_{h_1}}{\beta_1x_q},\mu_F\right)D_{\bar{q}}^{h_2}\left(\frac{x_{h_2}}{x_{\bar{q}}},\mu_F\right)\frac{\alpha_sC_F}{2\pi}\frac{1}{\hat{\epsilon}}\frac{1+\beta_1^2}{(1-\beta_1)_+} \\
&+\int_{\frac{x_{h_1}}{x_q}}^{1-\frac{\alpha}{x_q}} d\beta_1 Q_q^2D_q^{h_1}\left(\frac{x_{h_1}}{x_q},\mu_F\right)D_{\bar{q}}^{h_2}\left(\frac{x_{h_2}}{x_{\bar{q}}},\mu_F\right)\frac{\alpha_sC_F}{2\pi}\frac{1}{\hat{\epsilon}}\left(\frac{c_0^2}{\left(\frac{z_{1\perp}-z_{2\perp}}{2}\right)^2\mu^2}\right)^{\epsilon}\frac{2}{1-\beta_1} \\
&-Q_q^2D_q^{h_1}\left(\frac{x_{h_1}}{x_q},\mu_F\right)D_{\bar{q}}^{h_2}\left(\frac{x_{h_2}}{x_{\bar{q}}},\mu_F\right)\frac{\alpha_sC_F}{2\pi}\frac{1}{\hat{\epsilon}}2\ln\left(1-\frac{x_{h_1}}{x_q}\right) \\
&+\int_{\frac{x_{h_1}}{x_q}}^1 \frac{d\beta_1}{\beta_1}Q_q^2D_q^{h_1}\left(\frac{x_{h_1}}{\beta_1x_q},\mu_F\right)D_{\bar{q}}^{h_2}\left(\frac{x_{h_2}}{x_{\bar{q}}},\mu_F\right)\frac{\alpha_sC_F}{2\pi}\Bigg[\ln\left(\frac{c_0^2}{\left(\frac{z_{1\perp}-z_{2\perp}}{2}\right)^2\mu^2}\right)\frac{1+\beta_1^2}{(1-\beta_1)_+} \\
&+\frac{(1-\beta_1)^2+2(1+\beta_1^2)\ln\beta_1}{(1-\beta_1)}\Bigg]-Q_q^2D_q^{h_1}\left(\frac{x_{h_1}}{x_q},\mu_F\right)D_{\bar{q}}^{h_2}\left(\frac{x_{h_2}}{x_{\bar{q}}},\mu_F\right) \\
&\times\frac{\alpha_sC_F}{2\pi}2\ln\left(1-\frac{x_{h_1}}{x_q}\right)\ln\left(\frac{c_0^2}{\left(\frac{z_{1\perp}-z_{2\perp}}{2}\right)^2\mu^2}\right)\Bigg\}+(h_1\leftrightarrow h_2) \\
&= \left.\frac{d\sigma_{3LL}^{q\bar{q}\to h_1h_2}}{dx_{h_1}dx_{h_2}dp_{h_1\perp}d^dp_{h_2\perp}}\right|_{\text{coll. qg div}}+\left.\frac{d\sigma_{3LL}^{q\bar{q}\to h_1h_2}}{dx_{h_1}dx_{h_2}dp_{h_1\perp}d^dp_{h_2\perp}}\right|_{\text{coll. qg fin}},
\end{aligned} \tag{6.69}$$

where the term denoted by the label "coll. qg div" corresponds to the sum of the first three terms in the curly bracket, whereas the remaining terms in the curly bracket contribute to the term denoted "coll. qg fin".

This gives the following expression for the divergent part:

$$
\begin{aligned}
&\left.\frac{d\sigma_{3LL}^{q\bar{q}\to h_1h_2}}{dx_{h_1}dx_{h_2}dp_{h_1\perp}d^dp_{h_2\perp}}\right|_{\text{coll. qg div}}\\
&=\frac{4\alpha_{\rm em}Q^2}{(2\pi)^{4(d-1)}N_c}\sum_q\int_{x_{h_1}}^1 dx_q\int_{x_{h_2}}^1 dx_{\bar{q}}\;x_qx_{\bar{q}}\left(\frac{x_q}{x_{h_1}}\right)^d\left(\frac{x_{\bar{q}}}{x_{h_2}}\right)^d\delta(1-x_q-x_{\bar{q}})\\
&\times\int d^dp_{2\perp}\int d^dz_{1\perp}\frac{e^{iz_{1\perp}\cdot\left(\frac{x_q}{2x_{h_1}}p_{h_1\perp}+\frac{x_{\bar{q}}}{2x_{h_2}}p_{h_2\perp}-p_{2\perp}\right)}F(z_{1\perp})}{x_qx_{\bar{q}}Q^2+\left(\frac{x_{\bar{q}}}{x_{h_2}}\vec{p}_{h_2}-\vec{p}_2\right)^2}\\
&\times\int d^dp_{2'\perp}\int d^dz_{2\perp}\frac{e^{-iz_{2\perp}\cdot\left(\frac{x_q}{2x_{h_1}}p_{h_1\perp}+\frac{x_{\bar{q}}}{2x_{h_2}}p_{h_2\perp}-p_{2'\perp}\right)}F^*(z_{2\perp})}{x_qx_{\bar{q}}Q^2+\left(\frac{x_{\bar{q}}}{x_{h_2}}\vec{p}_{h_2}-\vec{p}_{2'}\right)^2}\\
&\times\frac{\alpha_s}{2\pi}\frac{1}{\hat{\epsilon}}Q_q^2\left[\int_{\frac{x_{h_1}}{x_q}}^1\frac{d\beta_1}{\beta_1}C_F\frac{1+\beta_1^2}{(1-\beta_1)_+}D_q^{h_1}\left(\frac{x_{h_1}}{\beta_1x_q},\mu_F\right)D_{\bar{q}}^{h_2}\left(\frac{x_{h_2}}{x_{\bar{q}}},\mu_F\right)\right.\\
&+\int_{\frac{x_{h_1}}{x_q}}^{1-\frac{\alpha}{x_q}}d\beta_1C_F\frac{2}{1-\beta_1}\left(\frac{c_0^2}{\left(\frac{z_{1\perp}-z_{2\perp}}{2}\right)^2\mu^2}\right)^{\epsilon}D_q^{h_1}\left(\frac{x_{h_1}}{x_q},\mu_F\right)D_{\bar{q}}^{h_2}\left(\frac{x_{h_2}}{x_{\bar{q}}},\mu_F\right)\\
&\left.-2C_F\ln\left(1-\frac{x_{h_1}}{x_q}\right)D_q^{h_1}\left(\frac{x_{h_1}}{x_q},\mu_F\right)D_{\bar{q}}^{h_2}\left(\frac{x_{h_2}}{x_{\bar{q}}},\mu_F\right)\right]+(h_1\leftrightarrow h_2)\,.
\end{aligned}
\tag{6.70}
$$

The first term in the bracket cancels part of the first term in the bracket in Eq. (6.42), *i.e.* the part involving the + prescription in the spitting function P_{qq}, and the remaining part of the P_{qq} term is cancelled by an analogous contribution in the virtual part. The second term in Eq. (6.70) has to be removed to avoid double counting as it corresponds to the soft contribution and will be taken into account later in the chapter. The third and last term, in Eq. (6.70), will compensate an analogous term in the soft contribution.

The finite part for the LL contribution takes the form

$$
\begin{aligned}
&\left.\frac{d\sigma_{3LL}^{q\bar{q}\to h_1h_2}}{dx_{h_1}dx_{h_2}dp_{h_1\perp}d^dp_{h_2\perp}}\right|_{\text{coll. qg fin}}\\
&=\frac{4\alpha_{\rm em}Q^2}{(2\pi)^{4(d-1)}N_c}\sum_q\int_{x_{h_1}}^1 dx_q\int_{x_{h_2}}^1 dx_{\bar{q}}\;x_qx_{\bar{q}}\delta(1-x_q-x_{\bar{q}})\left(\frac{x_q}{x_{h_1}}\right)^d\left(\frac{x_{\bar{q}}}{x_{h_2}}\right)^d\\
&\times\int d^dp_{2\perp}\int d^dz_{1\perp}\frac{e^{iz_{1\perp}\cdot\left(\frac{x_q}{2x_{h_1}}p_{h_1\perp}+\frac{x_{\bar{q}}}{2x_{h_2}}p_{h_2\perp}-p_{2\perp}\right)}F(z_{1\perp})}{x_qx_{\bar{q}}Q^2+\left(\frac{x_{\bar{q}}}{x_{h_2}}\vec{p}_{h_2}-\vec{p}_2\right)^2}
\end{aligned}
$$

$$
\begin{aligned}
&\times \int d^d p_{2'\perp} \int d^d z_{2\perp} \frac{e^{-iz_{2\perp}\cdot\left(\frac{x_q}{2x_{h_1}}p_{h_1\perp}+\frac{x_{\bar{q}}}{2x_{h_2}}p_{h_2\perp}-p_{2'\perp}\right)} F^*(z_{2\perp})}{x_q x_{\bar{q}} Q^2 + \left(\frac{x_{\bar{q}}}{x_{h_2}}\vec{p}_{h_2} - \vec{p}_{2'}\right)^2} \\
&\times \frac{\alpha_s C_F}{2\pi} \left\{ \int_{\frac{x_{h_1}}{x_q}}^1 \frac{d\beta_1}{\beta_1} Q_q^2 D_q^{h_1}\left(\frac{x_{h_1}}{\beta_1 x_q}, \mu_F\right) D_{\bar{q}}^{h_2}\left(\frac{x_{h_2}}{x_{\bar{q}}}, \mu_F\right) \right. \\
&\times \left[\ln\left(\frac{c_0^2}{\left(\frac{z_{1\perp}-z_{2\perp}}{2}\right)^2 \mu^2}\right) \frac{1+\beta_1^2}{(1-\beta_1)_+} + \frac{(1-\beta_1)^2 + 2(1+\beta_1^2)\ln\beta_1}{(1-\beta_1)} \right] \\
&\left. -2\ln\left(1-\frac{x_{h_1}}{x_q}\right) \ln\left(\frac{c_0^2}{\left(\frac{z_{1\perp}-z_{2\perp}}{2}\right)^2 \mu^2}\right) D_q^{h_1}\left(\frac{x_{h_1}}{x_q}, \mu_F\right) D_{\bar{q}}^{h_q}\left(\frac{x_{h_2}}{x_{\bar{q}}}, \mu_F\right) \right\} + (h_1 \leftrightarrow h_2)\,.
\end{aligned}
\tag{6.71}
$$

Similarly, one gets for the TL case

$$
\begin{aligned}
&\frac{d\sigma_{3TL}^{q\bar{q}\to h_1 h_2}}{dx_{h_1} dx_{h_2} dp_{h_1\perp} d^d p_{h_2\perp}}\bigg|_{\text{coll. qg}} \\
&= \frac{2\alpha_{\text{em}} Q}{(2\pi)^{4(d-1)} N_c} \sum_q \int_{x_{h_1}}^1 dx_q \int_{x_{h_2}}^1 dx_{\bar{q}}\, (x_{\bar{q}} - x_q)\delta(1-x_q-x_{\bar{q}}) \left(\frac{x_q}{x_{h_1}}\right)^d \left(\frac{x_{\bar{q}}}{x_{h_2}}\right)^d \\
&\times \int d^d p_{2\perp} \int d^d z_{1\perp} \frac{e^{iz_{1\perp}\cdot\left(\frac{x_q}{2x_{h_1}}p_{h_1\perp}+\frac{x_{\bar{q}}}{2x_{h_2}}p_{h_2\perp}-p_{2\perp}\right)} F(z_{1\perp})}{x_q x_{\bar{q}} Q^2 + \left(\frac{x_{\bar{q}}}{x_{h_2}}\vec{p}_{h_2} - \vec{p}_2\right)^2} \\
&\times \int d^d p_{2'\perp} \int d^d z_{2\perp} \frac{e^{-iz_{2\perp}\cdot\left(\frac{x_q}{2x_{h_1}}p_{h_1\perp}+\frac{x_{\bar{q}}}{2x_{h_2}}p_{h_2\perp}-p_{2'\perp}\right)} F^*(z_{2\perp})}{x_q x_{\bar{q}} Q^2 + \left(\frac{x_{\bar{q}}}{x_{h_2}}\vec{p}_{h_2} - \vec{p}_{2'}\right)^2} \left(\frac{x_{\bar{q}}}{x_{h_2}}\vec{p}_{h_2} - \vec{p}_{2'}\right)\cdot \vec{\varepsilon}_T^* \\
&\times \int_{\frac{x_{h_1}}{x_q}}^{1-\frac{\alpha}{x_q}} \frac{d\beta_1}{\beta_1} Q_q^2 D_q^{h_1}\left(\frac{x_{h_1}}{\beta_1 x_q}, \mu_F\right) D_{\bar{q}}^{h_2}\left(\frac{x_{h_2}}{x_{\bar{q}}}, \mu_F\right) \\
&\times \frac{\alpha_s C_F}{2\pi} \left[\frac{1}{\hat{\epsilon}} \left(\frac{c_0^2}{\left(\frac{z_{1\perp}-z_{2\perp}}{2}\right)^2 \mu^2}\right)^{\epsilon} \frac{1+\beta_1^2}{1-\beta_1} + \frac{(1-\beta_1)^2 + 2(1+\beta_1^2)\ln\beta_1}{(1-\beta_1)} \right] + (h_1 \leftrightarrow h_2) \\
&= \frac{d\sigma_{3TL}^{q\bar{q}\to h_1 h_2}}{dx_{h_1} dx_{h_2} dp_{h_1\perp} d^d p_{h_2\perp}}\bigg|_{\text{coll. qg div}} + \frac{d\sigma_{3TL}^{q\bar{q}\to h_1 h_2}}{dx_{h_1} dx_{h_2} dp_{h_1\perp} d^d p_{h_2\perp}}\bigg|_{\text{coll. qg fin}},
\end{aligned}
\tag{6.72}
$$

where

$$
\begin{aligned}
&\left.\frac{d\sigma_{3TL}^{q\bar{q}\to h_1h_2}}{dx_{h_1}dx_{h_2}dp_{h_1\perp}d^dp_{h_2\perp}}\right|_{\text{coll. qg div}}\\
&=\frac{2\alpha_{\text{em}}Q}{(2\pi)^{4(d-1)}N_c}\sum_q\int_{x_{h_1}}^1 dx_q\int_{x_{h_2}}^1 dx_{\bar{q}}\,(x_{\bar{q}}-x_q)\left(\frac{x_q}{x_{h_1}}\right)^d\left(\frac{x_{\bar{q}}}{x_{h_2}}\right)^d\delta(1-x_q-x_{\bar{q}})\\
&\times\int d^dp_{2\perp}\int d^dz_{1\perp}\frac{e^{iz_{1\perp}\cdot\left(\frac{x_q}{2x_{h_1}}p_{h_1\perp}+\frac{x_{\bar{q}}}{2x_{h_2}}p_{h_2\perp}-p_{2\perp}\right)}F(z_{1\perp})}{x_qx_{\bar{q}}Q^2+\left(\frac{x_{\bar{q}}}{x_{h_2}}\vec{p}_{h_2}-\vec{p}_2\right)^2}\\
&\times\int d^dp_{2'\perp}\int d^dz_{2\perp}\frac{e^{-iz_{2\perp}\cdot\left(\frac{x_q}{2x_{h_1}}p_{h_1\perp}+\frac{x_{\bar{q}}}{2x_{h_2}}p_{h_2\perp}-p_{2'\perp}\right)}F^*(z_{2\perp})}{x_qx_{\bar{q}}Q^2+\left(\frac{x_{\bar{q}}}{x_{h_2}}\vec{p}_{h_2}-\vec{p}_{2'}\right)^2}\left(\frac{x_{\bar{q}}}{x_{h_2}}\vec{p}_{h_2}-\vec{p}_{2'}\right)\cdot\vec{\varepsilon}_T^*\\
&\times\frac{\alpha_s}{2\pi}\frac{1}{\hat{\epsilon}}Q_q^2\left[\int_{\frac{x_{h_1}}{x_q}}^1\frac{d\beta_1}{\beta_1}C_F\frac{1+\beta_1^2}{(1-\beta_1)_+}D_q^{h_1}\left(\frac{x_{h_1}}{\beta_1x_q},\mu_F\right)D_{\bar{q}}^{h_2}\left(\frac{x_{h_2}}{x_{\bar{q}}},\mu_F\right)\right.\\
&+\int_{\frac{x_{h_1}}{x_q}}^{1-\frac{\alpha}{x_q}}d\beta_1C_F\frac{2}{1-\beta_1}\left(\frac{c_0^2}{\left(\frac{z_{1\perp}-z_{2\perp}}{2}\right)^2\mu^2}\right)^{\epsilon}D_q^{h_1}\left(\frac{x_{h_1}}{x_q},\mu_F\right)D_{\bar{q}}^{h_2}\left(\frac{x_{h_2}}{x_{\bar{q}}},\mu_F\right)\\
&\left.-2C_F\ln\left(1-\frac{x_{h_1}}{x_q}\right)D_q^{h_1}\left(\frac{x_{h_1}}{x_q},\mu_F\right)D_{\bar{q}}^{h_2}\left(\frac{x_{h_2}}{x_{\bar{q}}},\mu_F\right)\right]+(h_1\leftrightarrow h_2)\,,
\end{aligned}
$$

and

$$
\begin{aligned}
&\left.\frac{d\sigma_{3TL}^{q\bar{q}\to h_1h_2}}{dx_{h_1}dx_{h_2}dp_{h_1\perp}d^dp_{h_2\perp}}\right|_{\text{coll. qg fin}}\\
&=\frac{2\alpha_{\text{em}}Q}{(2\pi)^{4(d-1)}N_c}\sum_q\int_{x_{h_1}}^1 dx_q\int_{x_{h_2}}^1 dx_{\bar{q}}\,(x_{\bar{q}}-x_q)\delta(1-x_q-x_{\bar{q}})\left(\frac{x_q}{x_{h_1}}\right)^d\left(\frac{x_{\bar{q}}}{x_{h_2}}\right)^d\\
&\times\int d^dp_{2\perp}\int d^dz_{1\perp}\frac{e^{iz_{1\perp}\cdot\left(\frac{x_q}{2x_{h_1}}p_{h_1\perp}+\frac{x_{\bar{q}}}{2x_{h_2}}p_{h_2\perp}-p_{2\perp}\right)}F(z_{1\perp})}{x_qx_{\bar{q}}Q^2+\left(\frac{x_{\bar{q}}}{x_{h_2}}\vec{p}_{h_2}-\vec{p}_2\right)^2}\\
&\times\int d^dp_{2'\perp}\int d^dz_{2\perp}\frac{e^{-iz_{2\perp}\cdot\left(\frac{x_q}{2x_{h_1}}p_{h_1\perp}+\frac{x_{\bar{q}}}{2x_{h_2}}p_{h_2\perp}-p_{2'\perp}\right)}F^*(z_{2\perp})}{x_qx_{\bar{q}}Q^2+\left(\frac{x_{\bar{q}}}{x_{h_2}}\vec{p}_{h_2}-\vec{p}_{2'}\right)^2}\left(\frac{x_{\bar{q}}}{x_{h_2}}\vec{p}_{h_2}-\vec{p}_{2'}\right)\cdot\vec{\varepsilon}_T^*\\
&\times\frac{\alpha_sC_F}{2\pi}\left\{\int_{\frac{x_{h_1}}{x_q}}^1\frac{d\beta_1}{\beta_1}Q_q^2D_q^{h_1}\left(\frac{x_{h_1}}{\beta_1x_q},\mu_F\right)D_{\bar{q}}^{h_2}\left(\frac{x_{h_2}}{x_{\bar{q}}},\mu_F\right)\right.\\
&\times\left.\left[\ln\left(\frac{c_0^2}{\left(\frac{z_{1\perp}-z_{2\perp}}{2}\right)^2\mu^2}\right)\frac{1+\beta_1^2}{(1-\beta_1)_+}+\frac{(1-\beta_1)^2+2(1+\beta_1^2)\ln\beta_1}{(1-\beta_1)}\right]\right.
\end{aligned}
$$

$$-2\ln\left(1-\frac{x_{h_1}}{x_q}\right)\ln\left(\frac{c_0^2}{\left(\frac{z_{1\perp}-z_{2\perp}}{2}\right)^2\mu^2}\right)D_q^{h_1}\left(\frac{x_{h_1}}{x_q},\mu_F\right)D_{\bar{q}}^{h_q}\left(\frac{x_{h_2}}{x_{\bar{q}}},\mu_F\right)\Bigg\}+(h_1\leftrightarrow h_2)\,, \tag{6.73}$$

and finally, one obtains for the TT case

$$\begin{aligned}
&\frac{d\sigma_{3TT}^{q\bar{q}\to h_1h_2}}{dx_{h_1}dx_{h_2}dp_{h_1\perp}d^dp_{h_2\perp}}\bigg|_{\text{coll. qg}}\\
&=\frac{\alpha_{\text{em}}}{(2\pi)^{4(d-1)}N_c}\sum_q\int_{x_{h_1}}^1\frac{dx_q}{x_q}\int_{x_{h_2}}^1\frac{dx_{\bar{q}}}{x_{\bar{q}}}\delta(1-x_q-x_{\bar{q}})\left(\frac{x_q}{x_{h_1}}\right)^d\left(\frac{x_{\bar{q}}}{x_{h_2}}\right)^d\\
&\times\left[(x_{\bar{q}}-x_q)^2g_\perp^{ri}g_\perp^{lk}-g_\perp^{rk}g_\perp^{li}+g_\perp^{rl}g_\perp^{ik}\right]\\
&\times\int d^dp_{2\perp}\int d^dz_{1\perp}\frac{e^{iz_{1\perp}\cdot\left(\frac{x_q}{2x_{h_1}}p_{h_1\perp}+\frac{x_{\bar{q}}}{2x_{h_2}}p_{h_2\perp}-p_{2\perp}\right)}F(z_{1\perp})}{x_q(1-x_q)Q^2+\left(\frac{x_{\bar{q}}}{x_{h_2}}\vec{p}_{h_2}-\vec{p}_2\right)^2}\left(\frac{x_{\bar{q}}}{x_{h_2}}p_{h_2}-p_2\right)_r\varepsilon_{Ti}\\
&\times\int d^dp_{2'\perp}\int d^dz_{2\perp}\frac{e^{-iz_{2\perp}\cdot\left(\frac{x_q}{2x_{h_1}}p_{h_1\perp}+\frac{x_{\bar{q}}}{2x_{h_2}}p_{h_2\perp}-p_{2'\perp}\right)}F^*(z_{2\perp})}{x_qx_{\bar{q}}Q^2+\left(\frac{x_{\bar{q}}}{x_{h_2}}\vec{p}_{h_2}-\vec{p}_{2'}\right)^2}\left(\frac{x_{\bar{q}}}{x_{h_2}}p_{h_2}-p_{2'}\right)_l\varepsilon_{Tk}^*\\
&\times\int_{\frac{x_{h_1}}{x_q}}^{1-\frac{\alpha}{x_q}}\frac{d\beta_1}{\beta_1}Q_q^2D_q^{h_1}\left(\frac{x_{h_1}}{\beta_1x_q},\mu_F\right)D_{\bar{q}}^{h_2}\left(\frac{x_{h_2}}{x_{\bar{q}}},\mu_F\right)\\
&\times\frac{\alpha_sC_F}{2\pi}\left[\frac{1}{\hat{\epsilon}}\left(\frac{c_0^2}{\left(\frac{z_{1\perp}-z_{2\perp}}{2}\right)^2\mu^2}\right)^\epsilon\frac{1+\beta_1^2}{1-\beta_1}+\frac{(1-\beta_1)^2+2(1+\beta_1^2)\ln\beta_1}{(1-\beta_1)}\right]+(h_1\leftrightarrow h_2)\\
&=\frac{d\sigma_{3TT}^{q\bar{q}\to h_1h_2}}{dx_{h_1}dx_{h_2}dp_{h_1\perp}d^dp_{h_2\perp}}\bigg|_{\text{coll. qg div}}+\frac{d\sigma_{3TT}^{q\bar{q}\to h_1h_2}}{dx_{h_1}dx_{h_2}dp_{h_1\perp}d^dp_{h_2\perp}}\bigg|_{\text{coll. qg fin}}\,,
\end{aligned}\tag{6.74}$$

where

$$\begin{aligned}
&\frac{d\sigma_{3TT}^{q\bar{q}\to h_1h_2}}{dx_{h_1}dx_{h_2}dp_{h_1\perp}d^dp_{h_2\perp}}\bigg|_{\text{coll. qg div}}\\
&=\frac{\alpha_{\text{em}}}{(2\pi)^{4(d-1)}N_c}\sum_q\int_{x_{h_1}}^1\frac{dx_q}{x_q}\int_{x_{h_2}}^1\frac{dx_{\bar{q}}}{x_{\bar{q}}}\left(\frac{x_q}{x_{h_1}}\right)^d\left(\frac{x_{\bar{q}}}{x_{h_2}}\right)^d\delta(1-x_q-x_{\bar{q}})\\
&\times\left[(x_{\bar{q}}-x_q)^2g_\perp^{ri}g_\perp^{lk}-g_\perp^{rk}g_\perp^{li}+g_\perp^{rl}g_\perp^{ik}\right]\\
&\times\int d^dp_{2\perp}\int d^dz_{1\perp}\frac{e^{iz_{1\perp}\cdot\left(\frac{x_q}{2x_{h_1}}p_{h_1\perp}+\frac{x_{\bar{q}}}{2x_{h_2}}p_{h_2\perp}-p_{2\perp}\right)}F(z_{1\perp})}{x_qx_{\bar{q}}Q^2+\left(\frac{x_{\bar{q}}}{x_{h_2}}\vec{p}_{h_2}-\vec{p}_2\right)^2}\left(\frac{x_{\bar{q}}}{x_{h_2}}p_{h_2}-p_2\right)_r\varepsilon_{Ti}\\
&\times\int d^dp_{2'\perp}\int d^dz_{2\perp}\frac{e^{-iz_{2\perp}\cdot\left(\frac{x_q}{2x_{h_1}}p_{h_1\perp}+\frac{x_{\bar{q}}}{2x_{h_2}}p_{h_2\perp}-p_{2'\perp}\right)}F^*(z_{2\perp})}{x_qx_{\bar{q}}Q^2+\left(\frac{x_{\bar{q}}}{x_{h_2}}\vec{p}_{h_2}-\vec{p}_{2'}\right)^2}\left(\frac{x_{\bar{q}}}{x_{h_2}}p_{h_2}-p_{2'}\right)_l\varepsilon_{Tk}^*
\end{aligned}$$

$$
\begin{aligned}
&\times \frac{\alpha_s}{2\pi}\frac{1}{\hat{\epsilon}}Q_q^2\left[\int_{\frac{x_{h_1}}{x_q}}^1 \frac{d\beta_1}{\beta_1}C_F\frac{1+\beta_1^2}{(1-\beta_1)_+}D_q^{h_1}\left(\frac{x_{h_1}}{\beta_1 x_q},\mu_F\right)D_{\bar{q}}^{h_2}\left(\frac{x_{h_2}}{x_{\bar{q}}},\mu_F\right)\right.\\
&+\int_{\frac{x_{h_1}}{x_q}}^{1-\frac{\alpha}{x_q}} d\beta_1 C_F\frac{2}{1-\beta_1}\left(\frac{c_0^2}{\left(\frac{z_{1\perp}-z_{2\perp}}{2}\right)^2\mu^2}\right)^{\epsilon}D_q^{h_1}\left(\frac{x_{h_1}}{x_q},\mu_F\right)D_{\bar{q}}^{h_2}\left(\frac{x_{h_2}}{x_{\bar{q}}},\mu_F\right)\\
&\left.-2C_F\ln\left(1-\frac{x_{h_1}}{x_q}\right)D_q^{h_1}\left(\frac{x_{h_1}}{x_q},\mu_F\right)D_{\bar{q}}^{h_2}\left(\frac{x_{h_2}}{x_{\bar{q}}},\mu_F\right)\right]+(h_1\leftrightarrow h_2)\,,
\end{aligned}
$$

and

$$
\begin{aligned}
&\left.\frac{d\sigma_{3TT}^{q\bar{q}\to h_1h_2}}{dx_{h_1}dx_{h_2}dp_{h_1\perp}d^dp_{h_2\perp}}\right|_{\text{coll. qg fin}}\\
&=\frac{\alpha_{\text{em}}}{(2\pi)^{4(d-1)}N_c}\sum_q\int_{x_{h_1}}^1\frac{dx_q}{x_q}\int_{x_{h_2}}^1\frac{dx_{\bar{q}}}{x_{\bar{q}}}\delta(1-x_q-x_{\bar{q}})\left(\frac{x_q}{x_{h_1}}\right)^d\left(\frac{x_{\bar{q}}}{x_{h_2}}\right)^d\\
&\times\left[(x_{\bar{q}}-x_q)^2g_\perp^{ri}g_\perp^{lk}-g_\perp^{rk}g_\perp^{li}+g_\perp^{rl}g_\perp^{ik}\right]\\
&\times\int d^dp_{2\perp}\int d^dz_{1\perp}\frac{e^{iz_{1\perp}\cdot\left(\frac{x_q}{2x_{h_1}}p_{h_1\perp}+\frac{x_{\bar{q}}}{2x_{h_2}}p_{h_2\perp}-p_{2\perp}\right)}F(z_{1\perp})}{x_qx_{\bar{q}}Q^2+\left(\frac{x_{\bar{q}}}{x_{h_2}}\vec{p}_{h_2}-\vec{p}_2\right)^2}\left(\frac{x_{\bar{q}}}{x_{h_2}}p_{h_2}-p_2\right)_r\varepsilon_{Ti}\\
&\times\int d^dp_{2'\perp}\int d^dz_{2\perp}\frac{e^{-iz_{2\perp}\cdot\left(\frac{x_q}{2x_{h_1}}p_{h_1\perp}+\frac{x_{\bar{q}}}{2x_{h_2}}p_{h_2\perp}-p_{2'\perp}\right)}F^*(z_{2\perp})}{x_qx_{\bar{q}}Q^2+\left(\frac{x_{\bar{q}}}{x_{h_2}}\vec{p}_{h_2}-\vec{p}_{2'}\right)^2}\left(\frac{x_{\bar{q}}}{x_{h_2}}p_{h_2}-p_{2'}\right)_l\varepsilon_{Tk}^*\\
&\times\frac{\alpha_sC_F}{2\pi}\left\{\int_{\frac{x_{h_1}}{x_q}}^1\frac{d\beta_1}{\beta_1}Q_q^2D_q^{h_1}\left(\frac{x_{h_1}}{\beta_1x_q},\mu_F\right)D_{\bar{q}}^{h_2}\left(\frac{x_{h_2}}{x_{\bar{q}}},\mu_F\right)\right.\\
&\times\left[\ln\left(\frac{c_0^2}{\left(\frac{z_{1\perp}-z_{2\perp}}{2}\right)^2\mu^2}\right)\frac{1+\beta_1^2}{(1-\beta_1)_+}+\frac{(1-\beta_1)^2+2(1+\beta_1^2)\ln\beta_1}{(1-\beta_1)}\right]\\
&\left.-2\ln\left(1-\frac{x_{h_1}}{x_q}\right)\ln\left(\frac{c_0^2}{\left(\frac{z_{1\perp}-z_{2\perp}}{2}\right)^2\mu^2}\right)D_q^{h_1}\left(\frac{x_{h_1}}{x_q},\mu_F\right)D_{\bar{q}}^{h_q}\left(\frac{x_{h_2}}{x_{\bar{q}}},\mu_F\right)\right\}+(h_1\leftrightarrow h_2)\,.
\end{aligned}
\tag{6.75}
$$

Collinear contributions: $\bar{q}$-g splitting

Here the term in (6.57) to consider is the third one. The calculation proceeds in the same way as for the quark-gluon collinear contribution but this time the integration is performed over $p_{2\perp}$ and $p_{2'\perp}$. To observe the cancellation of these collinear divergences, one has to use the different representations we gave for the LO cross section, as explained before, see eqs. (6.22, 6.23) with respect to eqs. (6.20, 6.21).

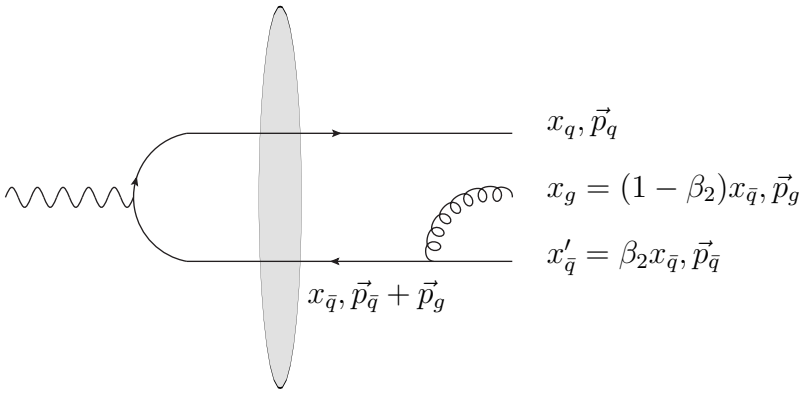

Figure 6.10: Kinematics for the $\bar{q} - g$ splitting contribution. We indicate the longitudinal fraction of momentum carried by the partons as well as their transverse momenta.

This time, the change of variable to be done is

$$\begin{aligned} x'_{\bar{q}} &= \beta_2 x_{\bar{q}}, \\ x_g &= (1-\beta_2) x_{\bar{q}}\,. \end{aligned} \tag{6.76}$$

This kinematics is illustrated in Fig. 6.10. The boundaries of integration for $(x_{\bar{q}}, \beta_2)$ are calculated in the same spirit as in eq (6.64).

Thus, after changes of variable and integrations, the third term in (6.57) takes the form

$$\begin{aligned} &\left.\frac{d\sigma_{3LL}^{q\bar{q}\to h_1 h_2}}{dx_{h_1} dx_{h_2} d^d p_{h_1\perp} d^d p_{h_2\perp}}\right|_{\text{coll. } \bar{q}g} \\ &= \frac{4\alpha_{\rm em} Q^2}{(2\pi)^{4(d-1)} N_c} \sum_q \int_{x_{h_1}}^1 dx_q \int_{x_{h_2}}^1 dx_{\bar{q}}\; x_q x_{\bar{q}} \delta(1-x_q-x_{\bar{q}}) \left(\frac{x_q}{x_{h_1}}\right)^d \left(\frac{x_{\bar{q}}}{x_{h_2}}\right)^d \\ &\times \int d^d p_{1\perp} \int d^d z_{1\perp} \frac{e^{iz_{1\perp}\cdot\left(-\frac{x_q}{2x_{h_1}} p_{h_1\perp} - \frac{x_{\bar{q}}}{2x_{h_2}} p_{h_2\perp} + p_{1\perp}\right)} F(z_{1\perp})}{x_q x_{\bar{q}} Q^2 + \left(\frac{x_q}{x_{h_1}} \vec{p}_{h_1} - \vec{p}_1\right)^2} \\ &\times \int d^d p_{1'\perp} \int d^d z_{2\perp} \frac{e^{-iz_{2\perp}\cdot\left(-\frac{x_q}{2x_{h_1}} p_{h_1\perp} - \frac{x_{\bar{q}}}{2x_{h_2}} p_{h_2\perp} + p_{1'\perp}\right)} F^*(z_{2\perp})}{x_q x_{\bar{q}} Q^2 + \left(\frac{x_q}{x_{h_1}} \vec{p}_{h_1} - \vec{p}_{1'}\right)^2} \\ &\times \int_{\frac{x_{h_2}}{x_{\bar{q}}}}^{1-\frac{\alpha}{x_{\bar{q}}}} \frac{d\beta_2}{\beta_2} Q_q^2 D_q^{h_1}\left(\frac{x_{h_1}}{x_q}, \mu_F\right) D_{\bar{q}}^{h_2}\left(\frac{x_{h_2}}{\beta_2 x_{\bar{q}}}, \mu_F\right) \\ &\times \frac{\alpha_s C_F}{2\pi} \left[\frac{1}{\hat{\epsilon}} \left(\frac{c_0^2}{\left(\frac{z_{2\perp}-z_{1\perp}}{2}\right)^2 \mu^2}\right)^{\epsilon} \frac{1+\beta_2^2}{1-\beta_2} + \frac{(1-\beta_2)^2 + 2(1+\beta_2^2)\ln\beta_2}{(1-\beta_2)}\right] + (h_1 \leftrightarrow h_2) \end{aligned}$$

$$= \left.\frac{d\sigma_{3LL}^{q\bar{q}\to h_1h_2}}{dx_{h_1}dx_{h_2}dp_{h_1\perp}d^dp_{h_2\perp}}\right|_{\text{coll. } \bar{q}g \text{ div}} + \left.\frac{d\sigma_{3LL}^{q\bar{q}\to h_1h_2}}{dx_{h_1}dx_{h_2}dp_{h_1\perp}d^dp_{h_2\perp}}\right|_{\text{coll. } \bar{q}g \text{ fin}} . \tag{6.77}$$

Adding the + prescription and expanding up to ϵ^0, just like for the collinear qg contribution, one gets the finite and divergent part of (6.77). The divergent part is

$$\begin{aligned}
&\left.\frac{d\sigma_{3LL}^{q\bar{q}\to h_1h_2}}{dx_{h_1}dx_{h_2}dp_{h_1\perp}d^dp_{h_2\perp}}\right|_{\text{coll. } \bar{q}g \text{ div}} \\
&= \frac{4\alpha_{\text{em}}Q^2}{(2\pi)^{4(d-1)}N_c}\sum_q \int_{x_{h_1}}^1 dx_q \int_{x_{h_2}}^1 dx_{\bar{q}}\; x_q x_{\bar{q}} \left(\frac{x_q}{x_{h_1}}\right)^d \left(\frac{x_{\bar{q}}}{x_{h_2}}\right)^d \delta(1-x_q-x_{\bar{q}}) \\
&\times \int d^dp_{1\perp} \int d^dz_{1\perp} \frac{e^{iz_{1\perp}\cdot\left(-\frac{x_q}{2x_{h_1}}p_{h_1\perp}-\frac{x_{\bar{q}}}{2x_{h_2}}p_{h_2\perp}+p_{1\perp}\right)}F(z_{1\perp})}{x_qx_{\bar{q}}Q^2+\left(\frac{x_q}{x_{h_1}}\vec{p}_{h_1}-\vec{p}_1\right)^2} \\
&\times \int d^dp_{1'\perp} \int d^dz_{2\perp} \frac{e^{-iz_{2\perp}\cdot\left(-\frac{x_q}{2x_{h_1}}p_{h_1\perp}-\frac{x_{\bar{q}}}{2x_{h_2}}p_{h_2\perp}+p_{1'\perp}\right)}F^*(z_{2\perp})}{x_qx_{\bar{q}}Q^2+\left(\frac{x_q}{x_{h_1}}\vec{p}_{h_1}-\vec{p}_{1'}\right)^2} \\
&\times \frac{\alpha_s}{2\pi}\frac{1}{\hat{\epsilon}}Q_q^2\left[\int_{\frac{x_{h_2}}{x_{\bar{q}}}}^1 \frac{d\beta_2}{\beta_2}C_F\frac{1+\beta_2^2}{(1-\beta_2)_+}D_q^{h_1}\left(\frac{x_{h_1}}{x_q},\mu_F\right)D_{\bar{q}}^{h_2}\left(\frac{x_{h_2}}{\beta_2x_{\bar{q}}},\mu_F\right)\right. \\
&+ \int_{\frac{x_{h_2}}{x_{\bar{q}}}}^{1-\frac{\alpha}{x_q}} d\beta_2 C_F\frac{2}{1-\beta_2}\left(\frac{c_0^2}{\left(\frac{z_{1\perp}-z_{2\perp}}{2}\right)^2\mu^2}\right)^{\epsilon} D_q^{h_1}\left(\frac{x_{h_1}}{x_q},\mu_F\right)D_{\bar{q}}^{h_2}\left(\frac{x_{h_2}}{x_{\bar{q}}},\mu_F\right) \\
&\left.-2C_F\ln\left(1-\frac{x_{h_2}}{x_{\bar{q}}}\right)D_q^{h_1}\left(\frac{x_{h_1}}{x_q},\mu_F\right)D_{\bar{q}}^{h_2}\left(\frac{x_{h_2}}{x_{\bar{q}}},\mu_F\right)\right] + (h_1\leftrightarrow h_2)\,.
\end{aligned} \tag{6.78}$$

The first term cancels with the + prescription term in the second P_{qq} in (6.42). We have to remove the second term to avoid double counting with the soft contribution. The third term is to be removed by the soft contribution.

The finite part is

$$\begin{aligned}
&\left.\frac{d\sigma_{3LL}^{q\bar{q}\to h_1h_2}}{dx_{h_1}dx_{h_2}dp_{h_1\perp}d^dp_{h_2\perp}}\right|_{\text{coll. } \bar{q}g \text{ fin}} \\
&= \frac{4\alpha_{\text{em}}Q^2}{(2\pi)^{4(d-1)}N_c}\sum_q \int_{x_{h_1}}^1 dx_q \int_{x_{h_2}}^1 dx_{\bar{q}}\; x_q x_{\bar{q}}\delta(1-x_q-x_{\bar{q}}) \left(\frac{x_q}{x_{h_1}}\right)^d \left(\frac{x_{\bar{q}}}{x_{h_2}}\right)^d \\
&\times \int d^dp_{1\perp} \int d^dz_{1\perp} \frac{e^{iz_{1\perp}\cdot\left(-\frac{x_q}{2x_{h_1}}p_{h_1\perp}-\frac{x_{\bar{q}}}{2x_{h_2}}p_{h_2\perp}+p_{1\perp}\right)}F(z_{1\perp})}{x_qx_{\bar{q}}Q^2+\left(\frac{x_q}{x_{h_1}}\vec{p}_{h_1}-\vec{p}_1\right)^2} \\
&\times \int d^dp_{1'\perp} \int d^dz_{2\perp} \frac{e^{-iz_{2\perp}\cdot\left(-\frac{x_q}{2x_{h_1}}p_{h_1\perp}-\frac{x_{\bar{q}}}{2x_{h_2}}p_{h_2\perp}+p_{1'\perp}\right)}F^*(z_{2\perp})}{x_qx_{\bar{q}}Q^2+\left(\frac{x_q}{x_{h_1}}\vec{p}_{h_1}-\vec{p}_{1'}\right)^2}
\end{aligned}$$

$$\times \frac{\alpha_s C_F}{2\pi}\left\{\int_{\frac{x_{h_2}}{x_{\bar{q}}}}^{1}\frac{d\beta_2}{\beta_2}Q_q^2 D_q^{h_1}\left(\frac{x_{h_1}}{x_q},\mu_F\right)D_{\bar{q}}^{h_2}\left(\frac{x_{h_2}}{\beta_2 x_{\bar{q}}},\mu_F\right)\right.$$
$$\times\left[\ln\left(\frac{c_0^2}{\left(\frac{z_{1\perp}-z_{2\perp}}{2}\right)^2\mu^2}\right)\frac{1+\beta_2^2}{(1-\beta_2)_+}+\frac{(1-\beta_2)^2+2(1+\beta_2^2)\ln\beta_2}{(1-\beta_2)_+}\right]$$
$$\left.-2\ln\left(1-\frac{x_{h_2}}{x_{\bar{q}}}\right)\ln\left(\frac{c_0^2}{\left(\frac{z_{1\perp}-z_{2\perp}}{2}\right)^2\mu^2}\right)D_q^{h_1}\left(\frac{x_{h_1}}{x_q},\mu_F\right)D_{\bar{q}}^{h_q}\left(\frac{x_{h_2}}{x_{\bar{q}}},\mu_F\right)\right\}+(h_1\leftrightarrow h_2)\,. \tag{6.79}$$

For the TL transition,

$$\begin{aligned}
&\left.\frac{d\sigma_{3TL}^{q\bar{q}\to h_1h_2}}{dx_{h_1}dx_{h_2}dp_{h_1\perp}d^dp_{h_2\perp}}\right|_{\text{coll. }\bar{q}g}\\
&=\frac{2\alpha_{\rm em}Q}{(2\pi)^{4(d-1)}N_c}\sum_q\int_{x_{h_1}}^1 dx_q\int_{x_{h_2}}^1 dx_{\bar{q}}\,(x_{\bar{q}}-x_q)\delta(1-x_q-x_{\bar{q}})\left(\frac{x_q}{x_{h_1}}\right)^d\left(\frac{x_{\bar{q}}}{x_{h_2}}\right)^d\\
&\times\int d^dp_{1\perp}\int d^dz_{1\perp}\frac{e^{iz_{1\perp}\cdot\left(-\frac{x_q}{2x_{h_1}}p_{h_1\perp}-\frac{x_{\bar{q}}}{2x_{h_2}}p_{h_2\perp}+p_{1\perp}\right)}F(z_{1\perp})}{x_qx_{\bar{q}}Q^2+\left(\frac{x_q}{x_{h_1}}\vec{p}_{h_1}-\vec{p}_1\right)^2}\\
&\times\int d^dp_{1'\perp}\int d^dz_{2\perp}\frac{e^{-iz_{2\perp}\cdot\left(-\frac{x_q}{2x_{h_1}}p_{h_1\perp}-\frac{x_{\bar{q}}}{2x_{h_2}}p_{h_2\perp}+p_{1'\perp}\right)}F^*(z_{2\perp})}{x_qx_{\bar{q}}Q^2+\left(\frac{x_q}{x_{h_1}}\vec{p}_{h_1}-\vec{p}_{1'}\right)^2}\left(\frac{x_q}{x_{h_1}}p_{h_1}-p_{1'}\right)\cdot\varepsilon_T^*\\
&\times\int_{\frac{x_{h_2}}{x_{\bar{q}}}}^{1-\frac{\alpha}{x_{\bar{q}}}}\frac{d\beta_2}{\beta_2}Q_q^2D_q^{h_1}\left(\frac{x_{h_1}}{x_q},\mu_F\right)D_{\bar{q}}^{h_2}\left(\frac{x_{h_2}}{\beta_2x_{\bar{q}}},\mu_F\right)\\
&\times\frac{\alpha_sC_F}{2\pi}\left[\frac{1}{\hat{\epsilon}}\left(\frac{c_0^2}{\left(\frac{z_{2\perp}-z_{1\perp}}{2}\right)^2\mu^2}\right)^{\epsilon}\frac{1+\beta_2^2}{1-\beta_2}+\frac{(1-\beta_2)^2+2(1+\beta_2^2)\ln\beta_2}{(1-\beta_2)}\right]+(h_1\leftrightarrow h_2)\\
&=\left.\frac{d\sigma_{3TL}^{q\bar{q}\to h_1h_2}}{dx_{h_1}dx_{h_2}dp_{h_1\perp}d^dp_{h_2\perp}}\right|_{\text{coll. }\bar{q}g\text{ div}}+\left.\frac{d\sigma_{3TL}^{q\bar{q}\to h_1h_2}}{dx_{h_1}dx_{h_2}dp_{h_1\perp}d^dp_{h_2\perp}}\right|_{\text{coll. }\bar{q}g\text{ fin}}
\end{aligned}\tag{6.80}$$

where

$$\begin{aligned}
&\left.\frac{d\sigma_{3TL}^{q\bar{q}\to h_1h_2}}{dx_{h_1}dx_{h_2}dp_{h_1\perp}d^dp_{h_2\perp}}\right|_{\text{coll. }\bar{q}g\text{ div}}\\
&=\frac{2\alpha_{\rm em}Q}{(2\pi)^{4(d-1)}N_c}\sum_q\int_{x_{h_1}}^1 dx_q\int_{x_{h_2}}^1 dx_{\bar{q}}(x_{\bar{q}}-x_q)\left(\frac{x_q}{x_{h_1}}\right)^d\left(\frac{x_{\bar{q}}}{x_{h_2}}\right)^d\delta(1-x_q-x_{\bar{q}})\\
&\times\int d^dp_{1\perp}\int d^dz_{1\perp}\frac{e^{iz_{1\perp}\cdot\left(-\frac{x_q}{2x_{h_1}}p_{h_1\perp}-\frac{x_{\bar{q}}}{2x_{h_2}}p_{h_2\perp}+p_{1\perp}\right)}F(z_{1\perp})}{x_qx_{\bar{q}}Q^2+\left(\frac{x_q}{x_{h_1}}\vec{p}_{h_1}-\vec{p}_1\right)^2}
\end{aligned}$$

$$\times \int d^d p_{1'\perp} \int d^d z_{2\perp} \frac{e^{-iz_{2\perp}\cdot\left(-\frac{x_q}{2x_{h_1}}p_{h_1\perp}-\frac{x_{\bar{q}}}{2x_{h_2}}p_{h_2\perp}+p_{1'\perp}\right)} F^*(z_{2\perp})}{x_q x_{\bar{q}} Q^2 + \left(\frac{x_q}{x_{h_1}}\vec{p}_{h_1} - \vec{p}_{1'}\right)^2} \left(\frac{x_q}{x_{h_1}} p_{h_1} - p_{1'}\right)\cdot\varepsilon_T^*$$

$$\times \frac{\alpha_s}{2\pi}\frac{1}{\hat{\epsilon}} Q_q^2 \left[\int_{\frac{x_{h_2}}{x_{\bar{q}}}}^1 \frac{d\beta_2}{\beta_2} C_F \frac{1+\beta_2^2}{(1-\beta_2)_+} D_q^{h_1}\left(\frac{x_{h_1}}{x_q},\mu_F\right) D_{\bar{q}}^{h_2}\left(\frac{x_{h_2}}{\beta_2 x_{\bar{q}}},\mu_F\right)\right.$$

$$+ \int_{\frac{x_{h_2}}{x_{\bar{q}}}}^{1-\frac{\alpha}{x_{\bar{q}}}} d\beta_2 C_F \frac{2}{1-\beta_2}\left(\frac{c_0^2}{\left(\frac{z_{1\perp}-z_{2\perp}}{2}\right)^2\mu^2}\right)^{\epsilon} D_q^{h_1}\left(\frac{x_{h_1}}{x_q},\mu_F\right) D_{\bar{q}}^{h_2}\left(\frac{x_{h_2}}{x_{\bar{q}}},\mu_F\right)$$

$$\left. -2C_F \ln\left(1-\frac{x_{h_2}}{x_{\bar{q}}}\right) D_q^{h_1}\left(\frac{x_{h_1}}{x_q},\mu_F\right) D_{\bar{q}}^{h_2}\left(\frac{x_{h_2}}{x_{\bar{q}}},\mu_F\right)\right] + (h_1 \leftrightarrow h_2)\,, \tag{6.81}$$

and

$$\left.\frac{d\sigma_{3TL}^{q\bar{q}\to h_1 h_2}}{dx_{h_1}dx_{h_2}dp_{h_1\perp}d^d p_{h_2\perp}}\right|_{\text{coll. } \bar{q}g \text{ fin}}$$

$$= \frac{2\alpha_{\text{em}} Q}{(2\pi)^{4(d-1)} N_c} \sum_q \int_{x_{h_1}}^1 dx_q \int_{x_{h_2}}^1 dx_{\bar{q}}\,(x_{\bar{q}}-x_q)\delta(1-x_q-x_{\bar{q}}) \left(\frac{x_q}{x_{h_1}}\right)^d \left(\frac{x_{\bar{q}}}{x_{h_2}}\right)^d$$

$$\times \int d^d p_{1\perp} \int d^d z_{1\perp} \frac{e^{iz_{1\perp}\cdot\left(-\frac{x_q}{2x_{h_1}}p_{h_1\perp}-\frac{x_{\bar{q}}}{2x_{h_2}}p_{h_2\perp}+p_{1\perp}\right)} F(z_{1\perp})}{x_q x_{\bar{q}} Q^2 + \left(\frac{x_q}{x_{h_1}}\vec{p}_{h_1} - \vec{p}_1\right)^2}$$

$$\times \int d^d p_{1'\perp} \int d^d z_{2\perp} \frac{e^{-iz_{2\perp}\cdot\left(-\frac{x_q}{2x_{h_1}}p_{h_1\perp}-\frac{x_{\bar{q}}}{2x_{h_2}}p_{h_2\perp}+p_{1'\perp}\right)} F^*(z_{2\perp})}{x_q x_{\bar{q}} Q^2 + \left(\frac{x_q}{x_{h_1}}\vec{p}_{h_1} - \vec{p}_{1'}\right)^2} \left(\frac{x_q}{x_{h_1}} p_{h_1} - p_{1'}\right)\cdot\varepsilon_T^*$$

$$\times \frac{\alpha_s C_F}{2\pi}\left\{\int_{\frac{x_{h_2}}{x_{\bar{q}}}}^1 \frac{d\beta_2}{\beta_2} Q_q^2 D_q^{h_1}\left(\frac{x_{h_1}}{x_q},\mu_F\right) D_{\bar{q}}^{h_2}\left(\frac{x_{h_2}}{\beta_2 x_{\bar{q}}},\mu_F\right)\right.$$

$$\times \left[\ln\left(\frac{c_0^2}{\left(\frac{z_{1\perp}-z_{2\perp}}{2}\right)^2\mu^2}\right)\frac{1+\beta_2^2}{(1-\beta_2)_+} + \frac{(1-\beta_2)^2+2(1+\beta_2^2)\ln\beta_2}{(1-\beta_2)_+}\right]$$

$$\left. -2\ln\left(1-\frac{x_{h_2}}{x_{\bar{q}}}\right)\ln\left(\frac{c_0^2}{\left(\frac{z_{1\perp}-z_{2\perp}}{2}\right)^2\mu^2}\right) D_q^{h_1}\left(\frac{x_{h_1}}{x_q},\mu_F\right) D_{\bar{q}}^{h_q}\left(\frac{x_{h_2}}{x_{\bar{q}}},\mu_F\right)\right\} + (h_1 \leftrightarrow h_2)\,. \tag{6.82}$$

For the TT case, we get

$$\left.\frac{d\sigma_{3TT}^{q\bar{q}\to h_1 h_2}}{dx_{h_1}dx_{h_2}dp_{h_1\perp}d^d p_{h_2\perp}}\right|_{\text{coll. } \bar{q}g}$$

$$= \frac{\alpha_{\text{em}}}{(2\pi)^{4(d-1)} N_c} \sum_q \int_{x_{h_1}}^1 \frac{dx_q}{x_q} \int_{x_{h_2}}^1 \frac{dx_{\bar{q}}}{x_{\bar{q}}}\delta(1-x_q-x_{\bar{q}}) \left(\frac{x_q}{x_{h_1}}\right)^d \left(\frac{x_{\bar{q}}}{x_{h_2}}\right)^d$$

$$
\begin{aligned}
&\times \left[(x_{\bar q}-x_q)^2 g_\perp^{ri} g_\perp^{lk} - g_\perp^{rk} g_\perp^{li} + g_\perp^{rl} g_\perp^{ik}\right] \\
&\times \int d^d p_{1\perp} \int d^d z_{1\perp} \frac{e^{iz_{1\perp}\cdot\left(-\frac{x_q}{2x_{h_1}}p_{h_1\perp}-\frac{x_{\bar q}}{2x_{h_2}}p_{h_2\perp}+p_{1\perp}\right)} F(z_{1\perp})}{x_q x_{\bar q} Q^2 + \left(\frac{x_q}{x_{h_1}}\vec p_{h_1} - \vec p_1\right)^2} \left(\frac{x_q}{x_{h_1}}p_{h_1} - p_1\right)_r \varepsilon_{Ti} \\
&\times \int d^d p_{1'\perp} \int d^d z_{2\perp} \frac{e^{-iz_{2\perp}\cdot\left(-\frac{x_q}{2x_{h_1}}p_{h_1\perp}-\frac{x_{\bar q}}{2x_{h_2}}p_{h_2\perp}+p_{1'\perp}\right)} F^*(z_{2\perp})}{x_q x_{\bar q} Q^2 + \left(\frac{x_q}{x_{h_1}}\vec p_{h_1} - \vec p_{1'}\right)^2} \left(\frac{x_q}{x_{h_1}}p_{h_1} - p_{1'}\right)_l \varepsilon^*_{Tk} \\
&\times \int_{\frac{x_{h_2}}{x_{\bar q}}}^{1-\frac{\alpha}{x_{\bar q}}} \frac{d\beta_2}{\beta_2} Q_q^2 D_q^{h_1}\left(\frac{x_{h_1}}{x_q},\mu_F\right) D_{\bar q}^{h_2}\left(\frac{x_{h_2}}{\beta_2 x_{\bar q}},\mu_F\right) \\
&\times \frac{\alpha_s C_F}{2\pi}\left[\frac{1}{\hat\epsilon}\left(\frac{c_0^2}{\left(\frac{z_{2\perp}-z_{1\perp}}{2}\right)^2\mu^2}\right)^{\epsilon}\frac{1+\beta_2^2}{1-\beta_2} + \frac{(1-\beta_2)^2+2(1+\beta_2^2)\ln\beta_2}{(1-\beta_2)}\right] + (h_1 \leftrightarrow h_2) \\
&= \left.\frac{d\sigma_{3TT}^{q\bar q\to h_1 h_2}}{dx_{h_1}dx_{h_2}dp_{h_1\perp}d^d p_{h_2\perp}}\right|_{\text{coll. } \bar q g \text{ div}} + \left.\frac{d\sigma_{3TT}^{q\bar q\to h_1 h_2}}{dx_{h_1}dx_{h_2}dp_{h_1\perp}d^d p_{h_2\perp}}\right|_{\text{coll. } \bar q g \text{ fin}},
\end{aligned}
\tag{6.83}
$$

where

$$
\begin{aligned}
&\left.\frac{d\sigma_{3TT}^{q\bar q\to h_1 h_2}}{dx_{h_1}dx_{h_2}dp_{h_1\perp}d^d p_{h_2\perp}}\right|_{\text{coll. } \bar q g \text{ div}} \\
&= \frac{\alpha_{\rm em}}{(2\pi)^{4(d-1)}N_c}\sum_q \int_{x_{h_1}}^1 \frac{dx_q}{x_q}\int_{x_{h_2}}^1 \frac{dx_{\bar q}}{x_{\bar q}}\left(\frac{x_q}{x_{h_1}}\right)^d\left(\frac{x_{\bar q}}{x_{h_2}}\right)^d \delta(1-x_q-x_{\bar q}) \\
&\times \left[(x_{\bar q}-x_q)^2 g_\perp^{ri} g_\perp^{lk} - g_\perp^{rk} g_\perp^{li} + g_\perp^{rl} g_\perp^{ik}\right] \\
&\times \int d^d p_{1\perp} \int d^d z_{1\perp} \frac{e^{iz_{1\perp}\cdot\left(-\frac{x_q}{2x_{h_1}}p_{h_1\perp}-\frac{x_{\bar q}}{2x_{h_2}}p_{h_2\perp}+p_{1\perp}\right)} F(z_{1\perp})}{x_q x_{\bar q} Q^2 + \left(\frac{x_q}{x_{h_1}}\vec p_{h_1} - \vec p_1\right)^2} \left(\frac{x_q}{x_{h_1}}p_{h_1} - p_1\right)_r \varepsilon_{Ti} \\
&\times \int d^d p_{1'\perp} \int d^d z_{2\perp} \frac{e^{-iz_{2\perp}\cdot\left(-\frac{x_q}{2x_{h_1}}p_{h_1\perp}-\frac{x_{\bar q}}{2x_{h_2}}p_{h_2\perp}+p_{1'\perp}\right)} F^*(z_{2\perp})}{x_q x_{\bar q} Q^2 + \left(\frac{x_q}{x_{h_1}}\vec p_{h_1} - \vec p_{1'}\right)^2} \left(\frac{x_q}{x_{h_1}}p_{h_1} - p_{1'}\right)_l \varepsilon^*_{Tk} \\
&\times \frac{\alpha_s}{2\pi}\frac{1}{\hat\epsilon}Q_q^2\left[\int_{\frac{x_{h_2}}{x_{\bar q}}}^1 \frac{d\beta_2}{\beta_2} C_F \frac{1+\beta_2^2}{(1-\beta_2)_+} D_q^{h_1}\left(\frac{x_{h_1}}{x_q},\mu_F\right) D_{\bar q}^{h_2}\left(\frac{x_{h_2}}{\beta_2 x_{\bar q}},\mu_F\right)\right. \\
&+ \int_{\frac{x_{h_2}}{x_{\bar q}}}^{1-\frac{\alpha}{x_{\bar q}}} d\beta_2 C_F \frac{2}{1-\beta_2}\left(\frac{c_0^2}{\left(\frac{z_{1\perp}-z_{2\perp}}{2}\right)^2\mu^2}\right)^{\epsilon} D_q^{h_1}\left(\frac{x_{h_1}}{x_q},\mu_F\right) D_{\bar q}^{h_2}\left(\frac{x_{h_2}}{x_{\bar q}},\mu_F\right) \\
&\left. -2C_F \ln\left(1-\frac{x_{h_2}}{x_{\bar q}}\right) D_q^{h_1}\left(\frac{x_{h_1}}{x_q},\mu_F\right) D_{\bar q}^{h_2}\left(\frac{x_{h_2}}{x_{\bar q}},\mu_F\right)\right] + (h_1 \leftrightarrow h_2)\,,
\end{aligned}
\tag{6.84}
$$

and

$$
\begin{aligned}
&\left.\frac{d\sigma_{3TT}^{q\bar{q}\to h_1h_2}}{dx_{h_1}dx_{h_2}dp_{h_1\perp}d^dp_{h_2\perp}}\right|_{\text{coll. } \bar{q}g \text{ fin}} \\
&= \frac{\alpha_{\text{em}}}{(2\pi)^{4(d-1)}N_c}\sum_q \int_{x_{h_1}}^1 \frac{dx_q}{x_q}\int_{x_{h_2}}^1 \frac{dx_{\bar{q}}}{x_{\bar{q}}}\delta(1-x_q-x_{\bar{q}})\left(\frac{x_q}{x_{h_1}}\right)^d\left(\frac{x_{\bar{q}}}{x_{h_2}}\right)^d \\
&\times\left[(x_{\bar{q}}-x_q)^2 g_\perp^{ri}g_\perp^{lk}-g_\perp^{rk}g_\perp^{li}+g_\perp^{rl}g_\perp^{ik}\right] \\
&\times\int d^dp_{1\perp}\int d^dz_{1\perp}\frac{e^{iz_{1\perp}\cdot\left(-\frac{x_q}{2x_{h_1}}p_{h_1\perp}-\frac{x_{\bar{q}}}{2x_{h_2}}p_{h_2\perp}+p_{1\perp}\right)}F(z_{1\perp})}{x_qx_{\bar{q}}Q^2+\left(\frac{x_q}{x_{h_1}}\vec{p}_{h_1}-\vec{p}_1\right)^2}\left(\frac{x_q}{x_{h_1}}p_{h_1}-p_1\right)_r\varepsilon_{Ti} \\
&\times\int d^dp_{1'\perp}\int d^dz_{2\perp}\frac{e^{-iz_{2\perp}\cdot\left(-\frac{x_q}{2x_{h_1}}p_{h_1\perp}-\frac{x_{\bar{q}}}{2x_{h_2}}p_{h_2\perp}+p_{1'\perp}\right)}F^*(z_{2\perp})}{x_qx_{\bar{q}}Q^2+\left(\frac{x_q}{x_{h_1}}\vec{p}_{h_1}-\vec{p}_{1'}\right)^2}\left(\frac{x_q}{x_{h_1}}p_{h_1}-p_{1'}\right)_l\varepsilon_{Tk}^* \\
&\times\frac{\alpha_sC_F}{2\pi}\left\{\int_{\frac{x_{h_2}}{x_{\bar{q}}}}^1\frac{d\beta_2}{\beta_2}Q_q^2D_q^{h_1}\left(\frac{x_{h_1}}{x_q},\mu_F\right)D_{\bar{q}}^{h_2}\left(\frac{x_{h_2}}{\beta_2x_{\bar{q}}},\mu_F\right)\right. \\
&\times\left[\ln\left(\frac{c_0^2}{\left(\frac{z_{1\perp}-z_{2\perp}}{2}\right)^2\mu^2}\right)\frac{1+\beta_2^2}{(1-\beta_2)_+}+\frac{(1-\beta_2)^2+2(1+\beta_2^2)\ln\beta_2}{(1-\beta_2)_+}\right] \\
&\left.-2\ln\left(1-\frac{x_{h_2}}{x_{\bar{q}}}\right)\ln\left(\frac{c_0^2}{\left(\frac{z_{1\perp}-z_{2\perp}}{2}\right)^2\mu^2}\right)D_q^{h_1}\left(\frac{x_{h_1}}{x_q},\mu_F\right)D_{\bar{q}}^{h_q}\left(\frac{x_{h_2}}{x_{\bar{q}}},\mu_F\right)\right\}+(h_1\leftrightarrow h_2)\,.
\end{aligned}
\tag{6.85}
$$

Soft contribution

To calculate the soft contribution of the divergent part of the real emission cross section, the soft limit of (6.60) is taken by setting $\vec{p}_g = x_g\vec{u}$, where $|\vec{u}| \sim |\vec{p}_h|$, which extracts the divergence on x_g.

$$
\begin{aligned}
&\left.\frac{d\sigma_{3LL}^{q\bar{q}\to h_1h_2}}{dx_{h_1}dx_{h_2}d^dp_{h_1\perp}dp_{h_2\perp}}\right|_{\text{soft}} \\
&= \frac{4\alpha_{\text{em}}Q^2}{(2\pi)^{4(d-1)}N_c}\sum_q\int_{x_{h_1}}^1\frac{dx_q'}{x_q'}\int_{x_{h_2}}^1\frac{dx_{\bar{q}}'}{x_{\bar{q}}'}Q_q^2D_q^{h_1}\left(\frac{x_{h_1}}{x_q'},\mu_F\right)D_{\bar{q}}^{h_2}\left(\frac{x_{h_2}}{x_{\bar{q}}'},\mu_F\right) \\
&\times\left(\frac{x_q'}{x_{h_1}}\right)^d\left(\frac{x_{\bar{q}}'}{x_{h_2}}\right)^d\int_\alpha^1\frac{dx_g}{x_g^{3-d}}\delta(1-x_q'-x_{\bar{q}}'-x_g)\frac{\alpha_sC_F}{\mu^{2\epsilon}}\int\frac{d^d\vec{u}}{(2\pi)^d} \\
&\times\int d^dp_{1\perp}d^dp_{2\perp}\,\mathbf{F}\left(\frac{p_{12\perp}}{2}\right)\delta\left(\frac{x_q'}{x_{h_1}}p_{h_1\perp}-p_{1\perp}+\frac{x_{\bar{q}}'}{x_{h_2}}p_{h_2\perp}-p_{2\perp}+x_gu_\perp\right) \\
&\times\int d^dp_{1'\perp}d^dp_{2'\perp}\,\mathbf{F}^*\left(\frac{p_{1'2'\perp}}{2}\right)\delta\left(\frac{x_q'}{x_{h_1}}p_{h_1\perp}-p_{1'\perp}+\frac{x_{\bar{q}}'}{x_{h_2}}p_{h_2\perp}-p_{2'\perp}+x_gu_\perp\right)
\end{aligned}
$$

$$
\times \left\{ \frac{dx_g^2 + 4x'_q(x'_q + x_g)}{\left(Q^2 + \frac{\left(\frac{x'_{\bar{q}}}{x_{h_2}}\vec{p}_{h_2} - \vec{p}_2\right)^2}{(1-x'_{\bar{q}})x'_{\bar{q}}}\right)\left(Q^2 + \frac{\left(\frac{x'_{\bar{q}}}{x_{h_2}}\vec{p}_{h_2} - \vec{p}_{2'}\right)^2}{(1-x'_{\bar{q}})x'_{\bar{q}}}\right) x'^2_q \left(\vec{u} - \frac{\vec{p}_{h_1}}{x_{h_1}}\right)^2} \right.
$$

$$
+ \frac{dx_g^2 + 4x'_{\bar{q}}(x'_{\bar{q}} + x_g)}{\left(Q^2 + \frac{\left(\frac{x'_{\bar{q}}}{x_{h_2}}\vec{p}_{h_2} - \vec{p}_2 + x_g\vec{u}\right)^2}{(1-x'_q)x'_q}\right)\left(Q^2 + \frac{\left(\frac{x'_{\bar{q}}}{x_{h_2}}\vec{p}_{h_2} - \vec{p}_{2'} + x_g\vec{u}\right)^2}{(1-x'_q)x'_q}\right) x'^2_{\bar{q}} \left(\vec{u} - \frac{\vec{p}_{h_2}}{x_{h_2}}\right)^2}
$$

$$
- \frac{[2x_g - dx_g^2 + 4x'_q x'_{\bar{q}}]\left(\vec{u} - \frac{\vec{p}_{h_1}}{x_{h_1}}\right)\cdot\left(\vec{u} - \frac{\vec{p}_{h_2}}{x_{h_2}}\right)}{\left(Q^2 + \frac{\left(\frac{x'_{\bar{q}}}{x_{h_2}}\vec{p}_{h_2} - \vec{p}_{2'}\right)^2}{(1-x'_{\bar{q}})x'_{\bar{q}}}\right)\left(Q^2 + \frac{\left(\frac{x'_{\bar{q}}}{x_{h_2}}\vec{p}_{h_2} - \vec{p}_2 + x_g\vec{u}\right)^2}{(1-x'_q)x'_q}\right) x'_q x'_{\bar{q}} \left(\vec{u} - \frac{\vec{p}_{h_1}}{x_{h_1}}\right)^2 \left(\vec{u} - \frac{\vec{p}_{h_2}}{x_{h_2}}\right)^2}
$$

$$
\left. - \frac{[2x_g - dx_g^2 + 4x'_q x'_{\bar{q}}]\left(\vec{u} - \frac{\vec{p}_{h_1}}{x_{h_1}}\right)\cdot\left(\vec{u} - \frac{\vec{p}_{h_2}}{x_{h_2}}\right)}{\left(Q^2 + \frac{\left(\frac{x'_{\bar{q}}}{x_{h_2}}\vec{p}_{h_2} - \vec{p}_2\right)^2}{(1-x'_{\bar{q}})x'_{\bar{q}}}\right)\left(Q^2 + \frac{\left(\frac{x'_{\bar{q}}}{x_{h_2}}\vec{p}_{h_2} - \vec{p}_{2'} + x_g\vec{u}\right)^2}{(1-x'_q)x'_q}\right) x'_q x'_{\bar{q}} \left(\vec{u} - \frac{\vec{p}_{h_1}}{x_{h_1}}\right)^2 \left(\vec{u} - \frac{\vec{p}_{h_2}}{x_{h_2}}\right)^2} \right\}
$$

$$
+ (h_1 \leftrightarrow h_2)\,.
$$

The limit $x_g \to 0$ in the F function and impact factor can be taken safely in the non-divergent terms of the cross section, as x'_q and $x'_{\bar{q}}$ are limited from below by x_{h_1}, x_{h_2} and so cannot be arbitrary small (ie of order x_g). The cross section in the soft limit becomes:

$$
\left.\frac{d\sigma_{3LL}^{q\bar{q}\to h_1 h_2}}{dx_{h_1}dx_{h_2}d^d p_{h_1\perp}dp_{h_2\perp}}\right|_{\text{soft}}
$$

$$
= \frac{4\alpha_{\text{em}}Q^2}{(2\pi)^{4(d-1)}N_c}\sum_q \int_{x_{h_1}}^1 \frac{dx'_q}{x'_q}\int_{x_{h_2}}^1 \frac{dx'_{\bar{q}}}{x'_{\bar{q}}} Q_q^2 D_q^{h_1}\left(\frac{x_{h_1}}{x'_q}, \mu_F\right) D_{\bar{q}}^{h_2}\left(\frac{x_{h_2}}{x'_{\bar{q}}}, \mu_F\right)
$$

$$
\times \left(\frac{x'_q}{x_{h_1}}\right)^d \left(\frac{x'_{\bar{q}}}{x_{h_2}}\right)^d \int_\alpha^1 \frac{dx_g}{x_g^{3-d}}\delta(1 - x'_q - x'_{\bar{q}} - x_g)\frac{\alpha_s C_F}{\mu^{2\epsilon}}\int \frac{d^d\vec{u}}{(2\pi)^d}
$$

$$
\times \int d^d p_{1\perp} d^d p_{2\perp}\ \mathbf{F}\left(\frac{p_{12\perp}}{2}\right)\delta\left(\frac{x'_q}{x_{h_1}}p_{h_1\perp} - p_{1\perp} + \frac{x'_{\bar{q}}}{x_{h_2}}p_{h_2\perp} - p_{2\perp}\right)
$$

$$
\times \int d^d p_{1'\perp} d^d p_{2'\perp}\ \mathbf{F}^*\left(\frac{p_{1'2'\perp}}{2}\right)\delta\left(\frac{x'_q}{x_{h_1}}p_{h_1\perp} - p_{1'\perp} + \frac{x'_{\bar{q}}}{x_{h_2}}p_{h_2\perp} - p_{2'\perp}\right)
$$

$$
\times \left\{ \frac{4}{\left(Q^2+\frac{\left(\frac{x'_{\bar{q}}}{x_{h_2}}\vec{p}_{h_2}-\vec{p}_2\right)^2}{(1-x'_{\bar{q}})x'_{\bar{q}}}\right)\left(Q^2+\frac{\left(\frac{x'_{\bar{q}}}{x_{h_2}}\vec{p}_{h_2}-\vec{p}_{2'}\right)^2}{(1-x'_{\bar{q}})x'_{\bar{q}}}\right)\left(\vec{u}-\frac{\vec{p}_{h_1}}{x_{h_1}}\right)^2} \right.
$$

$$
+\frac{4}{\left(Q^2+\frac{\left(\frac{x'_{\bar{q}}}{x_{h_2}}\vec{p}_{h_2}-\vec{p}_2\right)^2}{(1-x'_{q})x'_{q}}\right)\left(Q^2+\frac{\left(\frac{x'_{\bar{q}}}{x_{h_2}}\vec{p}_{h_2}-\vec{p}_{2'}\right)^2}{(1-x'_{q})x'_{q}}\right)\left(\vec{u}-\frac{\vec{p}_{h_2}}{x_{h_2}}\right)^2}
$$

$$
-\frac{4\left(\vec{u}-\frac{\vec{p}_{h_1}}{x_{h_1}}\right)\cdot\left(\vec{u}-\frac{\vec{p}_{h_2}}{x_{h_2}}\right)}{\left(Q^2+\frac{\left(\frac{x'_{\bar{q}}}{x_{h_2}}\vec{p}_{h_2}-\vec{p}_{2'}\right)^2}{(1-x'_{\bar{q}})x'_{\bar{q}}}\right)\left(Q^2+\frac{\left(\frac{x'_{\bar{q}}}{x_{h_2}}\vec{p}_{h_2}-\vec{p}_2\right)^2}{(1-x'_{q})x'_{q}}\right)\left(\vec{u}-\frac{\vec{p}_{h_1}}{x_{h_1}}\right)^2\left(\vec{u}-\frac{\vec{p}_{h_2}}{x_{h_2}}\right)^2}
$$

$$
\left. -\frac{4\left(\vec{u}-\frac{\vec{p}_{h_1}}{x_{h_1}}\right)\cdot\left(\vec{u}-\frac{\vec{p}_{h_2}}{x_{h_2}}\right)}{\left(Q^2+\frac{\left(\frac{x'_{\bar{q}}}{x_{h_2}}\vec{p}_{h_2}-\vec{p}_2\right)^2}{(1-x'_{\bar{q}})x'_{\bar{q}}}\right)\left(Q^2+\frac{\left(\frac{x'_{\bar{q}}}{x_{h_2}}\vec{p}_{h_2}-\vec{p}'_2\right)^2}{(1-x'_{q})x'_{q}}\right)\left(\vec{u}-\frac{\vec{p}_{h_1}}{x_{h_1}}\right)^2\left(\vec{u}-\frac{\vec{p}_{h_2}}{x_{h_2}}\right)^2} \right\} + (h_1 \leftrightarrow h_2)
$$

$$
= \frac{4\alpha_{\rm em}Q^2}{(2\pi)^{4(d-1)}N_c}\sum_q \int_{x_{h_1}}^1 \frac{dx'_q}{x'_q}\int_{x_{h_2}}^1 \frac{dx'_{\bar{q}}}{x'_{\bar{q}}} Q_q^2 D_q^{h_1}\left(\frac{x_{h_1}}{x'_q},\mu_F\right) D_{\bar{q}}^{h_2}\left(\frac{x_{h_2}}{x'_{\bar{q}}},\mu_F\right)
$$

$$
\times \left(\frac{x'_q}{x_{h_1}}\right)^d \left(\frac{x'_{\bar{q}}}{x_{h_2}}\right)^d \int_\alpha^1 \frac{dx_g}{x_g^{3-d}}\delta(1-x'_q-x'_{\bar{q}}-x_g)\frac{\alpha_s C_F}{\mu^{2\epsilon}}\int\frac{d^d\vec{u}}{(2\pi)^d}
$$

$$
\times \int d^d p_{1\perp} d^d p_{2\perp}\ \mathbf{F}\left(\frac{p_{12\perp}}{2}\right)\delta\left(\frac{x'_q}{x_{h_1}}p_{h_1\perp}-p_{1\perp}+\frac{x'_{\bar{q}}}{x_{h_2}}p_{h_2\perp}-p_{2\perp}\right)
$$

$$
\times \int d^d p_{1'\perp} d^d p_{2'\perp}\ \mathbf{F}^*\left(\frac{p_{1'2'\perp}}{2}\right)\delta\left(\frac{x'_q}{x_{h_1}}p_{h_1\perp}-p_{1'\perp}+\frac{x'_{\bar{q}}}{x_{h_2}}p_{h_2\perp}-p_{2'\perp}\right)
$$

$$
\times \frac{4}{\left(Q^2+\frac{\left(\frac{x'_{\bar{q}}}{x_{h_2}}\vec{p}_{h_2}-\vec{p}_2\right)^2}{(1-x'_{\bar{q}})x'_{\bar{q}}}\right)\left(Q^2+\frac{\left(\frac{x'_{\bar{q}}}{x_{h_2}}\vec{p}_{h_2}-\vec{p}_{2'}\right)^2}{(1-x'_{\bar{q}})x'_{\bar{q}}}\right)}\left\{\frac{1}{\left(\vec{u}-\frac{\vec{p}_{h_1}}{x_h}\right)^2}+\frac{1}{\left(\vec{u}-\frac{\vec{p}_{h_2}}{x_{h_2}}\right)^2}\right.
$$

$$
\left. -\frac{2\left(\vec{u}-\frac{\vec{p}_{h_1}}{x_{h_1}}\right)\cdot\left(\vec{u}-\frac{\vec{p}_{h_2}}{x_{h_2}}\right)}{\left(\vec{u}-\frac{\vec{p}_{h_1}}{x_{h_1}}\right)^2\left(\vec{u}-\frac{\vec{p}_{h_2}}{x_{h_2}}\right)^2}\right\} + (h_1 \leftrightarrow h_2)\ .
$$

Then, the cross section is divided into two parts in order to do two different changes of variables, which are the same changes as in eqs. (6.64, 6.76), in each part:

$$
x'_q = \beta_1 x_q\,, \qquad\qquad x_g = (1-\beta_1)x_q\,, \tag{6.86}
$$

$$x'_{\bar{q}} = \beta_2 x_{\bar{q}}\,, \qquad\qquad x_g = (1-\beta_2)x_{\bar{q}}\,, \tag{6.87}$$

where the integration boundaries are calculated following the steps in Eq. (6.64). This division and changes of variable respect the symmetry between diagrams (1) + (2) on one side, and (3) + (4) on the other side in Fig. 6.6. The limits $\beta_{1,2} \to 1$, corresponding to $x_g \to 0$ are then taken. The choice of splitting the cross section in this way, comes from the will to observe the cancellation of divergences at integrand level. The first term, after the transformation (6.86) and after taking the limit, gives

$$\begin{aligned}
&\left.\frac{d\sigma_{3LL}^{q\bar{q}\to h_1h_2}}{dx_{h_1}dx_{h_2}d^dp_{h_1\perp}dp_{h_2\perp}}\right|_{\text{soft }\beta_1}\\
&= \frac{2\alpha_{\rm em}Q^2}{(2\pi)^{4(d-1)}N_c}\sum_q\int_{x_{h_1}}^{1-x_{h_2}}\frac{dx_q}{x_q}\frac{1}{1-x_q}\left(\frac{x_q}{x_{h_1}}\right)^d\left(\frac{1-x_q}{x_{h_2}}\right)^d\\
&\times Q_q^2 D_q^{h_1}\left(\frac{x_{h_1}}{x_q},\mu_F\right)D_{\bar{q}}^{h_2}\left(\frac{x_{h_2}}{1-x_q},\mu_F\right)\\
&\times\int d^dp_{2\perp}\,\mathbf{F}\left(\frac{x_q}{2x_{h_1}}p_{h_1\perp}+\frac{1-x_q}{2x_{h_2}}p_{h_2\perp}-p_{2\perp}\right)\\
&\times\int d^dp_{2'\perp}\,\mathbf{F}^*\left(\frac{x_q}{2x_{h_1}}p_{h_1\perp}+\frac{1-x_q}{2x_{h_2}}p_{h_2\perp}-p_{2'\perp}\right)\\
&\times\int_{\frac{x_{h_1}}{x_q}}^{1-\frac{\alpha}{x_q}}\frac{d\beta_1}{(1-\beta_1)^{1-2\epsilon}x_q^{1-2\epsilon}}x_q\\
&\times\frac{4(1-x_q)^2x_q^2}{\left((1-x_q)x_qQ^2+\left(\frac{1-x_q}{x_{h_2}}\vec{p}_{h_2}-\vec{p}_2\right)^2\right)\left((1-x_q)x_qQ^2+\left(\frac{1-x_q}{x_{h_2}}\vec{p}_{h_2}-\vec{p}_{2'}\right)^2\right)}\\
&\times\frac{\alpha_sC_F}{\mu^{2\epsilon}}\int\frac{d^d\vec{u}}{(2\pi)^d}\left\{\frac{1}{\left(\vec{u}-\frac{\vec{p}_{h_1}}{x_{h_1}}\right)^2}+\frac{1}{\left(\vec{u}-\frac{\vec{p}_{h_2}}{x_{h_2}}\right)^2}-2\frac{\left(\vec{u}-\frac{\vec{p}_{h_1}}{x_{h_1}}\right)\cdot\left(\vec{u}-\frac{\vec{p}_{h_2}}{x_{h_2}}\right)}{\left(\vec{u}-\frac{\vec{p}_{h_1}}{x_{h_1}}\right)^2\left(\vec{u}-\frac{\vec{p}_{h_2}}{x_{h_2}}\right)^2}\right\}+(h_1\leftrightarrow h_2)\,.
\end{aligned}\tag{6.88}$$

In a similar fashion, the transformation (6.87) leads to second contribution, which reads

$$\begin{aligned}
&\left.\frac{d\sigma_{3LL}^{q\bar{q}\to h_1h_2}}{dx_{h_1}dx_{h_2}d^dp_{h_1\perp}dp_{h_2\perp}}\right|_{\text{soft }\beta_2}\\
&= \frac{2\alpha_{\rm em}Q^2}{(2\pi)^{4(d-1)}N_c}\sum_q\int_{x_{h_2}}^{1-x_{h_1}}\frac{dx_{\bar{q}}}{x_{\bar{q}}}\frac{1}{1-x_{\bar{q}}}\left(\frac{x_{\bar{q}}}{x_{h_2}}\right)^d\left(\frac{1-x_{\bar{q}}}{x_{h_1}}\right)^d\\
&\times Q_q^2 D_q^{h_1}\left(\frac{x_{h_1}}{1-x_{\bar{q}}},\mu_F\right)D_{\bar{q}}^{h_2}\left(\frac{x_{h_2}}{x_{\bar{q}}},\mu_F\right)\\
&\times\int d^dp_{2\perp}\,\mathbf{F}\left(\frac{1-x_{\bar{q}}}{2x_{h_1}}p_{h_1\perp}+\frac{x_{\bar{q}}}{2x_{h_2}}p_{h_2\perp}-p_{2\perp}\right)
\end{aligned}$$

$$
\begin{aligned}
&\times \int d^d p_{2'\perp}\, \mathbf{F}^* \left(\frac{1-x_{\bar{q}}}{2x_{h_1}} p_{h_1\perp} + \frac{x_{\bar{q}}}{2x_{h_2}} p_{h_2\perp} - p_{2'\perp} \right) \\
&\times \int_{\frac{x_{h_2}}{x_{\bar{q}}}}^{1-\frac{\alpha}{x_{\bar{q}}}} \frac{d\beta_2}{(1-\beta_2)^{1-2\epsilon} x_{\bar{q}}^{1-2\epsilon}} x_{\bar{q}} \\
&\times \frac{4(1-x_{\bar{q}})^2 x_{\bar{q}}^2}{\left((1-x_{\bar{q}}) x_{\bar{q}} Q^2 + \left(\frac{x_{\bar{q}}}{x_{h_2}} \vec{p}_{h_2} - \vec{p}_2 \right)^2 \right) \left((1-x_{\bar{q}}) x_{\bar{q}} Q^2 + \left(\frac{x_{\bar{q}}}{x_{h_2}} \vec{p}_{h_2} - \vec{p}_{2'} \right)^2 \right)} \\
&\times \frac{\alpha_s C_F}{\mu^{2\epsilon}} \int \frac{d^d \vec{u}}{(2\pi)^d} \left\{ \frac{1}{\left(\vec{u} - \frac{\vec{p}_{h_1}}{x_{h_1}} \right)^2} + \frac{1}{\left(\vec{u} - \frac{\vec{p}_{h_2}}{x_{h_2}} \right)^2} - 2 \frac{\left(\vec{u} - \frac{\vec{p}_{h_1}}{x_{h_1}} \right) \cdot \left(\vec{u} - \frac{\vec{p}_{h_2}}{x_{h_2}} \right)}{\left(\vec{u} - \frac{\vec{p}_{h_1}}{x_{h_1}} \right)^2 \left(\vec{u} - \frac{\vec{p}_{h_2}}{x_{h_2}} \right)^2} \right\} + (h_1 \leftrightarrow h_2)\,.
\end{aligned}
\tag{6.89}
$$

Next, we integrate over $\vec{u}$, which gives

$$
\begin{aligned}
I_u &= \frac{\alpha_s C_F}{\mu^{2\epsilon}} \int \frac{d^d \vec{u}}{(2\pi)^d} \left\{ \frac{1}{\left(\vec{u} - \frac{\vec{p}_{h_1}}{x_h} \right)^2} + \frac{1}{\left(\vec{u} - \frac{\vec{p}_{h_2}}{x_{h_2}} \right)^2} - 2 \frac{\left(\vec{u} - \frac{\vec{p}_{h_1}}{x_{h_1}} \right) \cdot \left(\vec{u} - \frac{\vec{p}_{h_2}}{x_{h_2}} \right)}{\left(\vec{u} - \frac{\vec{p}_{h_1}}{x_{h_1}} \right)^2 \left(\vec{u} - \frac{\vec{p}_{h_2}}{x_{h_2}} \right)^2} \right\} \\
&= \frac{\alpha_s C_F}{\mu^{2\epsilon}} \left(\frac{\vec{p}_{h_1}}{x_{h_1}} - \frac{\vec{p}_{h_2}}{x_{h_2}} \right)^2 \int \frac{d^d \vec{u}}{(2\pi)^d} \frac{1}{\left(\vec{u} - \frac{\vec{p}_{h_1}}{x_{h_1}} \right)^2 \left(\vec{u} - \frac{\vec{p}_{h_2}}{x_{h_2}} \right)^2} \\
&= \frac{\alpha_s C_F}{\mu^{2\epsilon}} \left(\frac{\vec{p}_{h_1}}{x_{h_1}} - \frac{\vec{p}_{h_2}}{x_{h_2}} \right)^2 \int \frac{d^d \vec{u}}{(2\pi)^d} \frac{1}{\vec{u}^2 \left(\vec{u} - \left(\frac{\vec{p}_{h_1}}{x_{h_1}} - \frac{\vec{p}_{h_2}}{x_{h_2}} \right) \right)^2} \\
&= \frac{\alpha_s C_F}{\mu^{2\epsilon}} \left(\frac{\vec{p}_{h_1}}{x_{h_1}} - \frac{\vec{p}_{h_2}}{x_{h_2}} \right)^2 \frac{1}{(2\pi)^d} \pi^{1+\epsilon} \Gamma(1-\epsilon) \beta(\epsilon, \epsilon) \left[\left(\frac{\vec{p}_{h_1}}{x_{h_1}} - \frac{\vec{p}_{h_2}}{x_{h_2}} \right)^2 \right]^{\epsilon-1} \\
&= \frac{\alpha_s}{2\pi} C_F \frac{1}{\hat{\epsilon}} \left[1 + \epsilon \ln \left(\frac{\left(\frac{\vec{p}_{h_1}}{x_{h_1}} - \frac{\vec{p}_{h_2}}{x_{h_2}} \right)^2}{\mu^2} \right) \right].
\end{aligned}
\tag{6.90}
$$

Finally, the integral over β leads to

$$
\begin{aligned}
\int_{\frac{x_h}{x}}^{1-\frac{\alpha}{x}} \frac{d\beta}{(1-\beta)^{3-d}} &= \int_{\frac{x_h}{x}}^{1-\frac{\alpha}{x}} \frac{d\beta}{1-\beta} \left[1 + 2\epsilon \ln(1-\beta) \right] \\
&= -\ln\left(\frac{\alpha}{x} \right) + \ln\left(1 - \frac{x_h}{x} \right) - \epsilon \ln^2\left(\frac{\alpha}{x} \right) + \epsilon \ln^2\left(1 - \frac{x_h}{x} \right) \\
&= -\ln\alpha + \ln x + \ln\left(1 - \frac{x_h}{x} \right) - \epsilon \left[\ln^2\alpha - 2\ln\alpha \ln x + \ln^2 x \right] \\
&\quad + \epsilon \ln^2\left(1 - \frac{x_h}{x} \right).
\end{aligned}
\tag{6.91}
$$

Combining both integrals over β (6.91) and over $\vec{u}$ (6.90) and keeping only the divergent

terms, eqs. (6.88) and (6.89) become respectively

$$
\begin{aligned}
&\left.\frac{d\sigma_{3LL}^{q\bar{q}\to h_1h_2}}{dx_{h_1}dx_{h_2}d^dp_{h_1\perp}dp_{h_2\perp}}\right|_{\text{soft }\beta_1}\\
&=\frac{2\alpha_{\text{em}}Q^2}{(2\pi)^{4(d-1)}N_c}\sum_q\int_{x_{h_1}}^1 dx_q\int_{x_{h_2}}^1 dx_{\bar{q}}\;x_qx_{\bar{q}}\left(\frac{x_q}{x_{h_1}}\right)^d\left(\frac{x_{\bar{q}}}{x_{h_2}}\right)^d\delta(1-x_q-x_{\bar{q}})\\
&\times Q_q^2D_q^{h_1}\left(\frac{x_{h_1}}{x_q},\mu_F\right)D_{\bar{q}}^{h_2}\left(\frac{x_{h_2}}{x_{\bar{q}}},\mu_F\right)\mathcal{F}_{LL}\frac{\alpha_SC_F}{2\pi}\frac{4}{\hat{\epsilon}}\left[-\ln\alpha+\ln x_q+\ln\left(1-\frac{x_{h_1}}{x_q}\right)\right.\\
&-\epsilon\ln^2\alpha-\epsilon\ln\alpha\ln\left(\frac{\left(\frac{\vec{p}_{h_1}}{x_{h_1}}-\frac{\vec{p}_{h_2}}{x_{h_2}}\right)^2}{\mu^2}\right)+\epsilon\ln x_q\left(\ln x_q+2\ln\left(1-\frac{x_{h_1}}{x_q}\right)\right.\\
&\left.\left.+\ln\left(\frac{\left(\frac{\vec{p}_{h_1}}{x_{h_1}}-\frac{\vec{p}_{h_2}}{x_{h_2}}\right)^2}{\mu^2}\right)\right)+\epsilon\ln\left(1-\frac{x_{h_1}}{x_q}\right)\left(\ln\left(\frac{\left(\frac{\vec{p}_{h_1}}{x_{h_1}}-\frac{\vec{p}_{h_2}}{x_{h_2}}\right)^2}{\mu^2}\right)+\ln\left(1-\frac{x_{h_1}}{x_q}\right)\right)\right]\\
&+(h_1\leftrightarrow h_2)\,,
\end{aligned}
$$

and

$$
\begin{aligned}
&\left.\frac{d\sigma_{3LL}^{q\bar{q}\to h_1h_2}}{dx_{h_1}dx_{h_2}d^dp_{h_1\perp}dp_{h_2\perp}}\right|_{\text{soft }\beta_2}\\
&=\frac{2\alpha_{\text{em}}Q^2}{(2\pi)^{4(d-1)}N_c}\sum_q\int_{x_{h_1}}^1 dx_q\int_{x_{h_2}}^1 dx_{\bar{q}}\;x_qx_{\bar{q}}\left(\frac{x_q}{x_{h_1}}\right)^d\left(\frac{x_{\bar{q}}}{x_{h_2}}\right)^d\delta(1-x_q-x_{\bar{q}})\\
&\times Q_q^2D_q^{h_1}\left(\frac{x_{h_1}}{x_q},\mu_F\right)D_{\bar{q}}^{h_2}\left(\frac{x_{h_2}}{x_{\bar{q}}},\mu_F\right)\mathcal{F}_{LL}\frac{\alpha_SC_F}{2\pi}\frac{4}{\hat{\epsilon}}\left[-\ln\alpha+\ln x_{\bar{q}}+\ln\left(1-\frac{x_{h_2}}{x_{\bar{q}}}\right)\right.\\
&-\epsilon\ln^2\alpha-\epsilon\ln\alpha\ln\left(\frac{\left(\frac{\vec{p}_{h_1}}{x_{h_1}}-\frac{\vec{p}_{h_2}}{x_{h_2}}\right)^2}{\mu^2}\right)+\epsilon\ln x_{\bar{q}}\left(\ln x_{\bar{q}}+2\ln\left(1-\frac{x_{h_2}}{x_{\bar{q}}}\right)\right.\\
&\left.\left.+\ln\left(\frac{\left(\frac{\vec{p}_{h_1}}{x_{h_1}}-\frac{\vec{p}_{h_2}}{x_{h_2}}\right)^2}{\mu^2}\right)\right)+\epsilon\ln\left(1-\frac{x_{h_2}}{x_{\bar{q}}}\right)\left(\ln\left(\frac{\left(\frac{\vec{p}_{h_1}}{x_{h_1}}-\frac{\vec{p}_{h_2}}{x_{h_2}}\right)^2}{\mu^2}\right)+\ln\left(1-\frac{x_{h_2}}{x_{\bar{q}}}\right)\right)\right]\\
&+(h_1\leftrightarrow h_2)\,.
\end{aligned}
$$

As said above, the total soft contribution expression is found by summing the two above equations. As usual, we split the final result into divergent and finite part. In the LL

case, we obtain

$$\begin{aligned}\left.\frac{d\sigma_{3LL}^{q\bar{q}\to h_1h_2}}{dx_{h_1}dx_{h_2}d^dp_{h_1\perp}dp_{h_2\perp}}\right|_{\text{soft div}} &= \frac{4\alpha_{\text{em}}Q^2}{(2\pi)^{4(d-1)}N_c}\sum_q\int_{x_{h_1}}^1 dx_q\int_{x_{h_2}}^1 dx_{\bar{q}}x_qx_{\bar{q}}\left(\frac{x_q}{x_{h_1}}\right)^d\left(\frac{x_{\bar{q}}}{x_{h_2}}\right)^d\\ &\times\delta(1-x_q-x_{\bar{q}})Q_q^2D_q^{h_1}\left(\frac{x_{h_1}}{x_q},\mu_F\right)D_{\bar{q}}^{h_2}\left(\frac{x_{h_2}}{x_{\bar{q}}},\mu_F\right)\mathcal{F}_{LL}\\ &\times\frac{\alpha_sC_F}{2\pi}\frac{1}{\hat{\epsilon}}\left[-4\ln\alpha+2\ln x_q+2\ln\left(1-\frac{x_{h_1}}{x_q}\right)-4\epsilon\ln^2\alpha\right.\\ &\left.-4\epsilon\ln\alpha\ln\left(\frac{\left(\frac{\vec{p}_{h_1}}{x_{h_1}}-\frac{\vec{p}_{h_2}}{x_{h_2}}\right)^2}{\mu^2}\right)+2\ln x_{\bar{q}}+2\ln\left(1-\frac{x_{h_2}}{x_{\bar{q}}}\right)\right]\\ &+(h_1\leftrightarrow h_2)\,.\end{aligned}\tag{6.92}$$

and

$$\begin{aligned}\left.\frac{d\sigma_{3LL}^{q\bar{q}\to h_1h_2}}{dx_{h_1}dx_{h_2}d^dp_{h_1\perp}dp_{h_2\perp}}\right|_{\text{soft fin}} &= \frac{4\alpha_{\text{em}}Q^2}{(2\pi)^{4(d-1)}N_c}\sum_q\int_{x_{h_1}}^1 dx_q\int_{x_{h_2}}^1 dx_{\bar{q}}x_qx_{\bar{q}}\left(\frac{x_q}{x_{h_1}}\right)^d\left(\frac{x_{\bar{q}}}{x_{h_2}}\right)^d\\ &\times\delta(1-x_q-x_{\bar{q}})Q_q^2D_q^{h_1}\left(\frac{x_{h_1}}{x_q},\mu_F\right)D_{\bar{q}}^{h_2}\left(\frac{x_{h_2}}{x_{\bar{q}}},\mu_F\right)\mathcal{F}_{LL}\\ &\times\frac{\alpha_sC_F}{\pi}\left[\ln x_q\left(\ln x_q+2\ln\left(1-\frac{x_{h_1}}{x_q}\right)+\ln\left(\frac{\left(\frac{\vec{p}_{h_1}}{x_{h_1}}-\frac{\vec{p}_{h_2}}{x_{h_2}}\right)^2}{\mu^2}\right)\right)\right.\\ &+\ln\left(1-\frac{x_{h_1}}{x_q}\right)\left(\ln\left(\frac{\left(\frac{\vec{p}_{h_1}}{x_{h_1}}-\frac{\vec{p}_{h_2}}{x_{h_2}}\right)^2}{\mu^2}\right)+\ln\left(1-\frac{x_{h_1}}{x_q}\right)\right)\\ &+\ln x_{\bar{q}}\left(\ln x_{\bar{q}}+2\ln\left(1-\frac{x_{h_2}}{x_{\bar{q}}}\right)+\ln\left(\frac{\left(\frac{\vec{p}_{h_1}}{x_{h_1}}-\frac{\vec{p}_{h_2}}{x_{h_2}}\right)^2}{\mu^2}\right)\right)\\ &\left.+\ln\left(1-\frac{x_{h_2}}{x_{\bar{q}}}\right)\left(\ln\left(\frac{\left(\frac{\vec{p}_{h_1}}{x_{h_1}}-\frac{\vec{p}_{h_2}}{x_{h_2}}\right)^2}{\mu^2}\right)+\ln\left(1-\frac{x_{h_2}}{x_{\bar{q}}}\right)\right)\right]\\ &+(h_1\leftrightarrow h_2)\,.\end{aligned}\tag{6.93}$$

For the TL and TT case, the calculation leads respectively to

$$\begin{aligned}\left.\frac{d\sigma_{3TL}^{q\bar{q}\to h_1h_2}}{dx_{h_1}dx_{h_2}d^dp_{h_1\perp}dp_{h_2\perp}}\right|_{\text{soft div}} &= \frac{2\alpha_{\text{em}}Q}{(2\pi)^{4(d-1)}N_c}\sum_q\int_{x_{h_1}}^1 dx_q\int_{x_{h_2}}^1 dx_{\bar{q}}(x_{\bar{q}}-x_q)\left(\frac{x_q}{x_{h_1}}\right)^d\left(\frac{x_{\bar{q}}}{x_{h_2}}\right)^d\\ &\times\delta(1-x_q-x_{\bar{q}})Q_q^2D_q^{h_1}\left(\frac{x_{h_1}}{x_q},\mu_F\right)D_{\bar{q}}^{h_2}\left(\frac{x_{h_2}}{x_{\bar{q}}},\mu_F\right)\mathcal{F}_{TL}\end{aligned}$$

$$
\begin{aligned}
&\times \frac{\alpha_s C_F}{2\pi}\frac{1}{\hat{\epsilon}}\left[-4\ln\alpha + 2\ln x_q + 2\ln\left(1-\frac{x_{h_1}}{x_q}\right) - 4\epsilon\ln^2\alpha\right.\\
&\left.-4\epsilon\ln\alpha\ln\left(\frac{\left(\frac{\vec{p}_{h_1}}{x_{h_1}}-\frac{\vec{p}_{h_2}}{x_{h_2}}\right)^2}{\mu^2}\right) + 2\ln x_{\bar{q}} + 2\ln\left(1-\frac{x_{h_2}}{x_{\bar{q}}}\right)\right]\\
&+ (h_1 \leftrightarrow h_2)\,, \qquad (6.94)
\end{aligned}
$$

$$
\begin{aligned}
\left.\frac{d\sigma_{3TL}^{q\bar{q}\to h_1h_2}}{dx_{h_1}dx_{h_2}d^dp_{h_1\perp}dp_{h_2\perp}}\right|_{\text{soft fin}} &= \frac{2\alpha_{\text{em}}Q}{(2\pi)^{4(d-1)}N_c}\sum_q\int_{x_{h_1}}^1 dx_q\int_{x_{h_2}}^1 dx_{\bar{q}}(x_{\bar{q}}-x_q)\left(\frac{x_q}{x_{h_1}}\right)^d\left(\frac{x_{\bar{q}}}{x_{h_2}}\right)^d\\
&\times \delta(1-x_q-x_{\bar{q}})Q_q^2 D_q^{h_1}\left(\frac{x_{h_1}}{x_q},\mu_F\right)D_{\bar{q}}^{h_2}\left(\frac{x_{h_2}}{x_{\bar{q}}},\mu_F\right)\mathcal{F}_{TL}\\
&\times \frac{\alpha_s C_F}{\pi}\left[\ln x_q\left(\ln x_q + 2\ln\left(1-\frac{x_{h_1}}{x_q}\right) + \ln\left(\frac{\left(\frac{\vec{p}_{h_1}}{x_{h_1}}-\frac{\vec{p}_{h_2}}{x_{h_2}}\right)^2}{\mu^2}\right)\right)\right.\\
&+\ln\left(1-\frac{x_{h_1}}{x_q}\right)\left(\ln\left(\frac{\left(\frac{\vec{p}_{h_1}}{x_{h_1}}-\frac{\vec{p}_{h_2}}{x_{h_2}}\right)^2}{\mu^2}\right)+\ln\left(1-\frac{x_{h_1}}{x_q}\right)\right)\\
&+\ln x_{\bar{q}}\left(\ln x_{\bar{q}} + 2\ln\left(1-\frac{x_{h_2}}{x_{\bar{q}}}\right) + \ln\left(\frac{\left(\frac{\vec{p}_{h_1}}{x_{h_1}}-\frac{\vec{p}_{h_2}}{x_{h_2}}\right)^2}{\mu^2}\right)\right)\\
&\left.+\ln\left(1-\frac{x_{h_2}}{x_{\bar{q}}}\right)\left(\ln\left(\frac{\left(\frac{\vec{p}_{h_1}}{x_{h_1}}-\frac{\vec{p}_{h_2}}{x_{h_2}}\right)^2}{\mu^2}\right)+\ln\left(1-\frac{x_{h_2}}{x_{\bar{q}}}\right)\right)\right]\\
&+ (h_1 \leftrightarrow h_2)\,. \qquad (6.95)
\end{aligned}
$$

and

$$
\begin{aligned}
\left.\frac{d\sigma_{3TT}^{q\bar{q}\to h_1h_2}}{dx_{h_1}dx_{h_2}d^dp_{h_1\perp}dp_{h_2\perp}}\right|_{\text{soft div}} &= \frac{\alpha_{\text{em}}}{(2\pi)^{4(d-1)}N_c}\sum_q\int_{x_{h_1}}^1\frac{dx_q}{x_q}\int_{x_{h_2}}^1\frac{dx_{\bar{q}}}{x_{\bar{q}}}\left(\frac{x_q}{x_{h_1}}\right)^d\left(\frac{x_{\bar{q}}}{x_{h_2}}\right)^d\\
&\times \delta(1-x_q-x_{\bar{q}})Q_q^2 D_q^{h_1}\left(\frac{x_{h_1}}{x_q},\mu_F\right)D_{\bar{q}}^{h_2}\left(\frac{x_{h_2}}{x_{\bar{q}}},\mu_F\right)\mathcal{F}_{TT}\\
&\times \frac{\alpha_s C_F}{2\pi}\frac{1}{\hat{\epsilon}}\left[-4\ln\alpha + 2\ln x_q + 2\ln\left(1-\frac{x_{h_1}}{x_q}\right) - 4\epsilon\ln^2\alpha\right.\\
&\left.-4\epsilon\ln\alpha\ln\left(\frac{\left(\frac{\vec{p}_{h_1}}{x_{h_1}}-\frac{\vec{p}_{h_2}}{x_{h_2}}\right)^2}{\mu^2}\right) + 2\ln x_{\bar{q}} + 2\ln\left(1-\frac{x_{h_2}}{x_{\bar{q}}}\right)\right]
\end{aligned}
$$

$$+ (h_1 \leftrightarrow h_2)\,, \tag{6.96}$$

$$\begin{aligned}
\left.\frac{d\sigma_{3TT}^{q\bar{q}\to h_1 h_2}}{dx_{h_1}dx_{h_2}d^d p_{h_1\perp}dp_{h_2\perp}}\right|_{\text{soft fin}} &= \frac{\alpha_{\text{em}}}{(2\pi)^{4(d-1)}N_c}\sum_q \int_{x_{h_1}}^1 \frac{dx_q}{x_q}\int_{x_{h_2}}^1 \frac{dx_{\bar{q}}}{x_{\bar{q}}}\left(\frac{x_q}{x_{h_1}}\right)^d\left(\frac{x_{\bar{q}}}{x_{h_2}}\right)^d \\
&\times \delta(1-x_q-x_{\bar{q}})Q_q^2 D_q^{h_1}\left(\frac{x_{h_1}}{x_q},\mu_F\right)D_{\bar{q}}^{h_2}\left(\frac{x_{h_2}}{x_{\bar{q}}},\mu_F\right)\mathcal{F}_{TT} \\
&\times \frac{\alpha_s C_F}{\pi}\left[\ln x_q\left(\ln x_q + 2\ln\left(1-\frac{x_{h_1}}{x_q}\right)+\ln\left(\frac{\left(\frac{\vec{p}_{h_1}}{x_{h_1}}-\frac{\vec{p}_{h_2}}{x_{h_2}}\right)^2}{\mu^2}\right)\right)\right. \\
&+\ln\left(1-\frac{x_{h_1}}{x_q}\right)\left(\ln\left(\frac{\left(\frac{\vec{p}_{h_1}}{x_{h_1}}-\frac{\vec{p}_{h_2}}{x_{h_2}}\right)^2}{\mu^2}\right)+\ln\left(1-\frac{x_{h_1}}{x_q}\right)\right) \\
&+\ln x_{\bar{q}}\left(\ln x_{\bar{q}}+2\ln\left(1-\frac{x_{h_2}}{x_{\bar{q}}}\right)+\ln\left(\frac{\left(\frac{\vec{p}_{h_1}}{x_{h_1}}-\frac{\vec{p}_{h_2}}{x_{h_2}}\right)^2}{\mu^2}\right)\right) \\
&\left.+\ln\left(1-\frac{x_{h_2}}{x_{\bar{q}}}\right)\left(\ln\left(\frac{\left(\frac{\vec{p}_{h_1}}{x_{h_1}}-\frac{\vec{p}_{h_2}}{x_{h_2}}\right)^2}{\mu^2}\right)+\ln\left(1-\frac{x_{h_2}}{x_{\bar{q}}}\right)\right)\right] \\
&+ (h_1 \leftrightarrow h_2)\,.
\end{aligned} \tag{6.97}$$

At this level, we are already able to observe the full cancellation of soft divergences (and hence the disappearance of $\ln\alpha$-terms). Consider, for instance, the longitudinal cross section. Combining the divergent soft contribution, coming from the real part, see Eq. (6.92), with the virtual contribution (6.49) we see the complete cancellation of these $\ln\alpha$-terms and also of $\frac{1}{\epsilon}\ln(x_q x_{\bar{q}})$-term. Moreover, surviving $\frac{1}{\epsilon}$ divergent terms cancel in combination with:

- Terms proportional to $\frac{3}{2}\delta(1-\beta_i)$ appearing inside the splitting functions in (6.42)
- Term proportional to $\ln\left(1-\frac{x_{h_1}}{x_q}\right)$ in Eq. (6.70)
- Term proportional to $\ln\left(1-\frac{x_{h_2}}{x_{\bar{q}}}\right)$ in (6.78)

Now, we are only left with collinearly divergent contributions related to the case of fragmentation from quark and gluon or from anti-quark and gluon. These should cancel the only two divergent contributions left in Eq. (6.42), i.e., the ones proportional to $P_{gq}(\beta_i)$.

6.4.2 Fragmentation from anti-quark and gluon

In this section, we deal with extracting the collinear divergences associated with the contribution (d) in Fig. 6.5. This contribution corresponds to the situation in which the anti-quark and the gluon fragment, while the quark plays the role of "spectator" emitted particle. This case is much simpler than before. We do not have to deal with any soft divergence and the only IR divergence that appears is when the fragmenting gluon is emitted by the quark line after the shockwave and the emitted quark and gluon become collinear. Hence, we can directly compute the contribution due to the first term of Eq. (6.60).

We emphasize the difference with the contribution calculated in section 6.4.1. Although at the level of hard computation the term that generates the present divergence is the same as the one that generates the collinear divergence in section 6.4.1, the situation is completely different. In the present case, we integrate out the quark kinematic variables and remain differential in the variable of the emitted gluon, while, in section 6.4.1 it was exactly the opposite.

Collinear contribution: q-g splitting

According to the above discussion, we should focus on the first term of Eq. (6.57), which exhibits a collinear pole, namely

$$
\begin{aligned}
&\left.\frac{d\sigma_{3LL}^{g\bar{q}\to h_1h_2}}{dx_{h_1}dx_{h_2}d^dp_{h_1\perp}d^dp_{h_2\perp}}\right|_{\text{coll qg}}\\
&=\frac{4\alpha_{\text{em}}Q^2}{(2\pi)^{4(d-1)}N_c}\sum_q\int_{x_{h_1}}^1\frac{dx_g}{x_g^2}\int_0^1dx'_q\int_{x_{h_2}}^1\frac{dx_{\bar{q}}}{x_{\bar{q}}}\delta(1-x'_q-x_{\bar{q}}-x_g)\\
&\times\left(\frac{x_g}{x_{h_1}}\right)^d\left(\frac{x_{\bar{q}}}{x_{h_2}}\right)^dQ_q^2D_g^{h_1}\left(\frac{x_{h_1}}{x_g},\mu_F\right)D_{\bar{q}}^{h_2}\left(\frac{x_{h_2}}{x_{\bar{q}}},\mu_F\right)\frac{\alpha_s}{\mu^{2\epsilon}}C_F\int\frac{d^dp_{q\perp}}{(2\pi)^d}\\
&\times\int d^dp_{2\perp}\mathbf{F}\left(\frac{p_{q\perp}}{2}+\frac{x_{\bar{q}}}{2x_{h_2}}p_{h_2\perp}-p_{2\perp}+\frac{x_g}{2x_{h_1}}p_{h_1\perp}\right)\\
&\times\int d^dp_{2'\perp}\mathbf{F}^*\left(\frac{p_{q\perp}}{2}+\frac{x_{\bar{q}}}{2x_{h_2}}p_{h_2\perp}-p_{2'\perp}+\frac{x_g}{2x_{h_1}}p_{h_1\perp}\right)\\
&\times\frac{1}{\left(x_{\bar{q}}(1-x_{\bar{q}})Q^2+\left(\frac{x_{\bar{q}}}{x_{h_2}}\vec{p}_{h_2}-\vec{p}_2\right)^2\right)\left(x_{\bar{q}}(1-x_{\bar{q}})Q^2+\left(\frac{x_{\bar{q}}}{x_{h_2}}\vec{p}_{h_2}-\vec{p}_{2'}\right)^2\right)}\\
&\times\frac{(dx_g^2+4x'_q(x'_q+x_g))x_{\bar{q}}^2(1-x_{\bar{q}})^2}{\left(x'_q\frac{x_g}{x_{h_1}}\vec{p}_{h_1}-x_g\vec{p}_q\right)^2}+(h_1\leftrightarrow h_2)\,.
\end{aligned}
$$

Using a change of variable similar to (6.64), here

$$x_g = \beta_1 x_q$$
$$x'_q = (1-\beta_1)x_q$$

with the Jacobian $dx'_q dx_g = dx_q d\beta_1 x_q$ and treating the integration over longitudinal fractions as follows

$$\begin{aligned}
&\int_{x_{h_1}}^1 \frac{dx_g}{x_g^2}\int_{x_{h_2}}^1 \frac{dx_{\bar q}}{x_{\bar q}}\int_0^1 dx'_q \delta(1-x'_q-x_{\bar q}-x_g)\\
&=\int_{x_{h_1}}^1 \frac{dx_g}{x_g^2}\int_0^1 dx'_q\int_{-\infty}^{+\infty}\frac{dx_{\bar q}}{x_{\bar q}}\theta(x_{\bar q}-x_{h_2})\theta(1-x_{\bar q})\delta(1-x'_q-x_{\bar q}-x_g)\\
&=\int_{x_{h_1}}^{1-x_{h_2}} dx_q \frac{1}{x_q(1-x_q)}\int_{\frac{x_{h_1}}{x_q}}^1 \frac{d\beta_1}{\beta_1^2}\,,
\end{aligned}$$

we get

$$\begin{aligned}
&\left.\frac{d\sigma_{3LL}^{g\bar q\to h_1h_2}}{dx_{h_1}dx_{h_2}dp_{h_1\perp}d^dp_{h_2\perp}}\right|_{\text{coll. qg}}\\
&=\frac{4\alpha_{\rm em}Q^2}{(2\pi)^{4(d-1)}N_c}\sum_q\int_{x_{h_1}}^{1-x_{h_2}}dx_q\int_{\frac{x_{h_1}}{x_q}}^1\frac{d\beta_1}{\beta_1}x_q(1-x_q)\left(\frac{x_q}{x_{h_1}}\right)^d\left(\frac{1-x_q}{x_{h_2}}\right)^d\\
&\times Q_q^2 D_g^{h_1}\left(\frac{x_{h_1}}{\beta_1 x_q},\mu_F\right)D_{\bar q}^{h_2}\left(\frac{x_{h_2}}{1-x_q},\mu_F\right)\\
&\times\int d^dp_{2\perp}\int d^dz_{1\perp}\frac{e^{iz_{1\perp}\cdot\left(\frac{1-x_q}{2x_{h_2}}p_{h_2\perp}-p_{2\perp}+\frac{\beta_1x_q}{2x_{h_1}}p_{h_1\perp}\right)}}{x_q(1-x_q)Q^2+\left(\frac{1-x_q}{x_{h_2}}\vec p_{h_2}-\vec p_2\right)^2}F(z_{1\perp})\\
&\times\int d^dp_{2'\perp}\int d^dz_{2\perp}\frac{e^{-iz_{2\perp}\cdot\left(\frac{1-x_q}{2x_{h_2}}p_{h_2\perp}-p_{2'\perp}+\frac{\beta_1x_q}{2x_{h_1}}p_{h_1\perp}\right)}}{x_q(1-x_q)Q^2+\left(\frac{1-x_q}{x_{h_2}}\vec p_{h_2}-\vec p_{2'}\right)^2}F^*(z_{2\perp})\\
&\times\frac{2((1-\beta_1)^2+1)+2\epsilon\beta_1^2}{\beta_1}\beta_1^{d-2}\frac{\alpha_s}{\mu^{2\epsilon}}C_F\int\frac{d^dp_{q\perp}}{(2\pi)^d}\frac{e^{i\left(\frac{z_{1\perp}-z_{2\perp}}{2}\right)\cdot p_{q\perp}}}{\left(\frac{(1-\beta_1)x_q}{x_{h_1}}\vec p_{h_1}-\vec p_q\right)^2}\\
&+(h_1\leftrightarrow h_2)\,.
\end{aligned}\tag{6.98}$$

Using Eq. (6.62) in Eq. (6.98) to perform the integration over quark transverse momenta, we obtain

$$
\begin{aligned}
&\left.\frac{d\sigma_{3LL}^{g\bar{q}\to h_1h_2}}{dx_{h_1}dx_{h_2}dp_{h_1\perp}d^dp_{h_2\perp}}\right|_{\text{coll. qg}}\\
&=\frac{4\alpha_{\text{em}}Q^2}{(2\pi)^{4(d-1)}N_c}\sum_q\int_{x_{h_1}}^{1-x_{h_2}}dx_q\int_{\frac{x_{h_1}}{x_q}}^1\frac{d\beta_1}{\beta_1}x_q(1-x_q)\left(\frac{x_q}{x_{h_1}}\right)^d\\
&\times\left(\frac{1-x_q}{x_{h_2}}\right)^d Q_q^2D_g^{h_1}\left(\frac{x_{h_1}}{\beta_1x_q},\mu_F\right)D_{\bar{q}}^{h_2}\left(\frac{x_{h_2}}{1-x_q},\mu_F\right)\\
&\times\int d^dp_{2\perp}\int d^dz_{1\perp}\frac{e^{iz_{1\perp}\cdot\left(\frac{1-x_q}{2x_{h_2}}p_{h_2\perp}-p_{2\perp}+\frac{\beta_1x_q}{2x_{h_1}}p_{h_1\perp}\right)}}{x_q(1-x_q)Q^2+\left(\frac{1-x_q}{x_{h_2}}\vec{p}_{h_2}-\vec{p}_2\right)^2}F(z_{1\perp})\\
&\times\int d^dp_{2'\perp}\int d^dz_{2\perp}\frac{e^{-iz_{2\perp}\cdot\left(\frac{1-x_q}{2x_{h_2}}p_{h_2\perp}-p_{2'\perp}+\frac{\beta_1x_q}{2x_{h_1}}p_{h_1\perp}\right)}}{x_q(1-x_q)Q^2+\left(\frac{1-x_q}{x_{h_2}}\vec{p}_{h_2}-\vec{p}_{2'}\right)^2}F^*(z_{2\perp})\\
&\times\frac{2((1-\beta_1)^2+1)+2\epsilon\beta_1^2+4\epsilon((1-\beta_1)^2+1)\ln\beta_1}{\beta_1}\\
&\times e^{i\left(\frac{z_{1\perp}-z_{2\perp}}{2}\right)\cdot\frac{(1-\beta_1)x_q}{x_{h_1}}p_{h_1\perp}}\frac{\alpha_sC_F}{4\pi}\left(\frac{1}{\hat{\epsilon}}+\ln\left(\frac{c_0^2}{\left(\frac{z_{1\perp}-z_{2\perp}}{2}\right)^2\mu^2}\right)\right)+(h_1\leftrightarrow h_2)\\
&=\frac{4\alpha_{\text{em}}Q^2}{(2\pi)^{4(d-1)}N_c}\sum_q\int_{x_{h_1}}^{1-x_{h_2}}dx_q\int_{\frac{x_{h_1}}{x_q}}^1\frac{d\beta_1}{\beta_1}x_q(1-x_q)\left(\frac{x_q}{x_{h_1}}\right)^d\\
&\times\left(\frac{1-x_q}{x_{h_2}}\right)^d Q_q^2D_g^{h_1}\left(\frac{x_{h_1}}{\beta_1x_q},\mu_F\right)D_{\bar{q}}^{h_2}\left(\frac{x_{h_2}}{1-x_q},\mu_F\right)\\
&\times\int d^dp_{2\perp}\int d^dz_{1\perp}\frac{e^{iz_{1\perp}\cdot\left(\frac{1-x_q}{2x_{h_2}}p_{h_2\perp}-p_{2\perp}+\frac{x_q}{2x_{h_1}}p_{h_1\perp}\right)}}{x_q(1-x_q)Q^2+\left(\frac{1-x_q}{x_{h_2}}\vec{p}_{h_2}-\vec{p}_2\right)^2}F(z_{1\perp})\\
&\times\int d^dp_{2'\perp}\int d^dz_{2\perp}\frac{e^{-iz_{2\perp}\cdot\left(\frac{1-x_q}{2x_{h_2}}p_{h_2\perp}-p_{2'\perp}+\frac{x_q}{2x_{h_1}}p_{h_1\perp}\right)}}{x_q(1-x_q)Q^2+\left(\frac{1-x_q}{x_{h_2}}\vec{p}_{h_2}-\vec{p}_{2'}\right)^2}F^*(z_{2\perp})\\
&\frac{\alpha_s}{2\pi}C_F\left[\frac{1}{\hat{\epsilon}}\frac{1+(1-\beta_1)^2}{\beta_1}+\beta_1+\frac{2(1+(1-\beta)^2)\ln\beta_1}{\beta_1}\right.\\
&\left.+\frac{1+(1-\beta_1)^2}{\beta_1}\ln\left(\frac{c_0^2}{\left(\frac{z_{1\perp}-z_{2\perp}}{2}\right)^2\mu^2}\right)\right]+(h_1\leftrightarrow h_2)\\
&=\left.\frac{d\sigma_{3LL}^{g\bar{q}\to h_1h_2}}{dx_{h_1}dx_{h_2}dp_{h_1\perp}d^dp_{h_2\perp}}\right|_{\text{coll. qg div}}+\left.\frac{d\sigma_{3LL}^{g\bar{q}\to h_1h_2}}{dx_{h_1}dx_{h_2}dp_{h_1\perp}d^dp_{h_2\perp}}\right|_{\text{coll.qg fin}},
\end{aligned}
\tag{6.99}
$$

where the term labeled with "div" contains the first term of the square bracket. Putting back $x_{\bar{q}}$ using Eq. (6.68), this divergent term takes the form:

$$\begin{aligned}
&\left.\frac{d\sigma_{3LL}^{g\bar{q}\to h_1h_2}}{dx_{h_1}dx_{h_2}dp_{h_1\perp}d^dp_{h_2\perp}}\right|_{\text{coll. qg div}}\\
&=\frac{4\alpha_{\rm em}Q^2}{(2\pi)^{4(d-1)}N_c}\sum_q\int_{x_{h_1}}^1 dx_q\int_{\frac{x_{h_2}}{x_q}}^1 dx_{\bar{q}}\;x_qx_{\bar{q}}\left(\frac{x_q}{x_{h_1}}\right)^d\left(\frac{x_{\bar{q}}}{x_{h_2}}\right)^d\\
&\times\delta(1-x_q-x_{\bar{q}})\mathcal{F}_{LL}\frac{\alpha_s}{2\pi}\frac{1}{\hat{\epsilon}}\int_{\frac{x_{h_1}}{x_q}}^1\frac{d\beta_1}{\beta_1}\\
&\times Q_q^2D_g^{h_1}\left(\frac{x_{h_1}}{\beta_1x_q},\mu_F\right)D_{\bar{q}}^{h_2}\left(\frac{x_{h_2}}{x_{\bar{q}}},\mu_F\right)C_F\frac{1+(1-\beta_1)^2}{\beta_1}+(h_1\leftrightarrow h_2)\,.
\end{aligned}\tag{6.100}$$

This is the term needed to cancel the divergent term proportional to $P_{gq}(\beta_1)$ in (6.42). Instead, the finite part in Eq. (6.99) reads

$$\begin{aligned}
&\left.\frac{d\sigma_{3LL}^{g\bar{q}\to h_1h_2}}{dx_{h_1}dx_{h_2}dp_{h_1\perp}d^dp_{h_2\perp}}\right|_{\text{coll. qg fin}}\\
&=\frac{4\alpha_{\rm em}Q^2}{(2\pi)^{4(d-1)}N_c}\sum_q\int_{x_{h_1}}^1 dx_q\int_{\frac{x_{h_2}}{x_q}}^1 dx_{\bar{q}}\;x_qx_{\bar{q}}\left(\frac{x_q}{x_{h_1}}\right)^d\left(\frac{x_{\bar{q}}}{x_{h_2}}\right)^d\\
&\times\delta(1-x_q-x_{\bar{q}})\int_{\frac{x_{h_1}}{x_q}}^1\frac{d\beta_1}{\beta_1}Q_q^2D_g^{h_1}\left(\frac{x_{h_1}}{\beta_1x_q},\mu_F\right)D_{\bar{q}}^{h_2}\left(\frac{x_{h_2}}{1-x_q},\mu_F\right)\\
&\times\int d^dp_{2\perp}\int d^dz_{1\perp}\frac{e^{iz_{1\perp}\cdot\left(\frac{1-x_q}{2x_{h_2}}p_{h_2\perp}-p_{2\perp}+\frac{x_q}{2x_{h_1}}p_{h_1\perp}\right)}}{x_q(1-x_q)Q^2+\left(\frac{1-x_q}{x_{h_2}}\vec{p}_{h_2}-\vec{p}_2\right)^2}F(z_{1\perp})\\
&\times\int d^dp_{2'\perp}\int d^dz_{2\perp}\frac{e^{-iz_{2\perp}\cdot\left(\frac{1-x_q}{2x_{h_2}}p_{h_2\perp}-p_{2'\perp}+\frac{x_q}{2x_{h_1}}p_{h_1\perp}\right)}}{x_q(1-x_q)Q^2+\left(\frac{1-x_q}{x_{h_2}}\vec{p}_{h_2}-\vec{p}_{2'}\right)^2}F^*(z_{2\perp})\\
&\times\frac{\alpha_s}{2\pi}C_F\Bigg[\beta_1+\frac{2(1+(1-\beta)^2)\ln\beta_1}{\beta_1}\\
&+\frac{1+(1-\beta_1)^2}{\beta_1}\ln\left(\frac{c_0^2}{\left(\frac{z_{1\perp}-z_{2\perp}}{2}\right)^2\mu^2}\right)\Bigg]+(h_1\leftrightarrow h_2)\,.
\end{aligned}\tag{6.101}$$

In a similar way, in the TL case, we get

$$\begin{aligned}
&\left.\frac{d\sigma_{3TL}^{g\bar{q}\to h_1h_2}}{dx_{h_1}dx_{h_2}dp_{h_1\perp}d^dp_{h_2\perp}}\right|_{\text{coll. qg}}\\
&=\frac{2\alpha_{\rm em}Q}{(2\pi)^{4(d-1)}N_c}\sum_q\int_{x_{h_1}}^1 dx_q\int_{x_{h_2}}^1 dx_{\bar{q}}\left(\frac{x_q}{x_{h_1}}\right)^d\left(\frac{x_{\bar{q}}}{x_{h_2}}\right)^d(x_{\bar{q}}-x_q)
\end{aligned}$$

$$
\begin{aligned}
&\times \delta(1-x_q-x_{\bar q}) \int_{\frac{x_{h_1}}{x_q}}^1 \frac{d\beta_1}{\beta_1} Q_q^2 D_g^{h_1}\left(\frac{x_{h_1}}{\beta_1 x_q},\mu_F\right) D_{\bar q}^{h_2}\left(\frac{x_{h_2}}{x_{\bar q}},\mu_F\right) \\
&\times \int d^d p_{2\perp} \int d^d z_{1\perp} \frac{e^{iz_{1\perp}\cdot\left(\frac{1-x_q}{2x_{h_2}}p_{h_2\perp}-p_{2\perp}+\frac{x_q}{2x_{h_1}}p_{h_1\perp}\right)}}{x_q(1-x_q)Q^2+\left(\frac{1-x_q}{x_{h_2}}\vec{p}_{h_2}-\vec{p}_2\right)^2} F(z_{1\perp}) \\
&\times \int d^d p_{2'\perp} \int d^d z_{2\perp} \frac{e^{-iz_{2\perp}\cdot\left(\frac{1-x_q}{2x_{h_2}}p_{h_2\perp}-p_{2'\perp}+\frac{x_q}{2x_{h_1}}p_{h_1\perp}\right)}}{x_q(1-x_q)Q^2+\left(\frac{1-x_q}{x_{h_2}}\vec{p}_{h_2}-\vec{p}_{2'}\right)^2} F^*(z_{2\perp}) \left(\frac{x_{\bar q}}{x_{h_2}}\vec{p}_{h_2}-\vec{p}_{2'}\right)\cdot\vec{\varepsilon}_T^{\,*} \\
&\times \frac{\alpha_s}{2\pi} C_F \left[\frac{1}{\hat\epsilon}\frac{1+(1-\beta_1)^2}{\beta_1}+\beta_1+\frac{2(1+(1-\beta)^2)\ln\beta_1}{\beta_1}\right. \\
&\left.+\frac{1+(1-\beta_1)^2}{\beta_1}\ln\left(\frac{c_0^2}{\left(\frac{z_{1\perp}-z_{2\perp}}{2}\right)^2\mu^2}\right)\right]+(h_1\leftrightarrow h_2) \\
&=\left.\frac{d\sigma_{3TL}^{g\bar q\to h_1h_2}}{dx_{h_1}dx_{h_2}dp_{h_1\perp}d^dp_{h_2\perp}}\right|_{\text{coll. qg div}}+\left.\frac{d\sigma_{3TL}^{g\bar q\to h_1h_2}}{dx_{h_1}dx_{h_2}dp_{h_1\perp}d^dp_{h_2\perp}}\right|_{\text{coll. qg fin}}. \qquad (6.102)
\end{aligned}
$$

Finally, in the TT case, we have

$$
\begin{aligned}
&\left.\frac{d\sigma_{3TT}^{g\bar q\to h_1h_2}}{dx_{h_1}dx_{h_2}dp_{h_1\perp}d^dp_{h_2\perp}}\right|_{\text{coll. qg}} \\
&=\frac{\alpha_{\text{em}}}{(2\pi)^{4(d-1)}N_c}\sum_q\int_{x_{h_1}}^1\frac{dx_q}{x_q}\int_{x_{h_2}}^1\frac{dx_{\bar q}}{x_{\bar q}}\left(\frac{x_q}{x_{h_1}}\right)^d\left(\frac{x_{\bar q}}{x_{h_2}}\right)^d\delta(1-x_q-x_{\bar q}) \\
&\times\int_{\frac{x_{h_1}}{x_q}}^1\frac{d\beta_1}{\beta_1}Q_q^2D_g^{h_1}\left(\frac{x_{h_1}}{\beta_1x_q},\mu_F\right)D_{\bar q}^{h_2}\left(\frac{x_{h_2}}{x_{\bar q}},\mu_F\right)\left[(x_{\bar q}-x_q)^2g_\perp^{ri}g_\perp^{lk}-g_\perp^{rk}g_\perp^{li}+g_\perp^{rl}g_\perp^{ik}\right] \\
&\times\int d^dp_{2\perp}\int d^dz_{1\perp}\frac{e^{iz_{1\perp}\cdot\left(\frac{1-x_q}{2x_{h_2}}p_{h_2\perp}-p_{2\perp}+\frac{x_q}{2x_{h_1}}p_{h_1\perp}\right)}}{x_q(1-x_q)Q^2+\left(\frac{1-x_q}{x_{h_2}}\vec{p}_{h_2}-\vec{p}_2\right)^2}F(z_{1\perp})\left(\frac{x_{\bar q}}{x_{h_2}}p_{h_2}-p_2\right)_r\varepsilon_{Ti} \\
&\times\int d^dp_{2'\perp}\int d^dz_{2\perp}\frac{e^{-iz_{2\perp}\cdot\left(\frac{1-x_q}{2x_{h_2}}p_{h_2\perp}-p_{2'\perp}+\frac{x_q}{2x_{h_1}}p_{h_1\perp}\right)}}{x_q(1-x_q)Q^2+\left(\frac{1-x_q}{x_{h_2}}\vec{p}_{h_2}-\vec{p}_{2'}\right)^2}F^*(z_{2\perp})\left(\frac{x_{\bar q}}{x_{h_2}}p_{h_2}-p_{2'}\right)_l\varepsilon_{Tk}^* \\
&\times\frac{\alpha_s}{2\pi}C_F\left[\frac{1}{\hat\epsilon}\frac{1+(1-\beta_1)^2}{\beta_1}+\beta_1+\frac{2(1+(1-\beta)^2)\ln\beta_1}{\beta_1}\right. \\
&\left.+\frac{1+(1-\beta_1)^2}{\beta_1}\ln\left(\frac{c_0^2}{\left(\frac{z_{1\perp}-z_{2\perp}}{2}\right)^2\mu^2}\right)\right]+(h_1\leftrightarrow h_2) \\
&=\left.\frac{d\sigma_{3TT}^{g\bar q\to h_1h_2}}{dx_{h_1}dx_{h_2}dp_{h_1\perp}d^dp_{h_2\perp}}\right|_{\text{coll. qg div}}+\left.\frac{d\sigma_{3TT}^{g\bar q\to h_1h_2}}{dx_{h_1}dx_{h_2}dp_{h_1\perp}d^dp_{h_2\perp}}\right|_{\text{coll. qg fin}}. \qquad (6.103)
\end{aligned}
$$

These results conclude the discussion of divergences in the case of fragmentation from antiquark and gluon.

6.4.3 Fragmentation from quark and gluon

In this section, we deal with extracting the collinear divergences associated with the contribution (c) in Fig. 6.5. This contribution corresponds to the situation in which the quark and the gluon fragment, while the anti-quark plays the role of the "spectator" emitted particle.

Collinear contribution: $\bar{q}$-g splitting

The term in Eq. (6.57) to consider is the third one. The calculation proceeds in the same way as for the anti-quark and gluon fragmentation, but this time the integration is over $p_{2,2'\perp}$ in the F function.

For the LL case, we get

$$
\begin{aligned}
&\left.\frac{d\sigma_{3LL}^{qg\to h_1h_2}}{dx_{h_1}dx_{h_2}dp_{h_1\perp}d^dp_{h_2\perp}}\right|_{\text{coll. }\bar{q}g}\\
&=\frac{4\alpha_{\text{em}}Q^2}{(2\pi)^{4(d-1)}N_c}\sum_q\int_{x_{h_1}}^1 dx_q\int_{x_{h_2}}^1 dx_{\bar{q}}\;x_qx_{\bar{q}}\delta(1-x_q-x_{\bar{q}})\left(\frac{x_q}{x_{h_1}}\right)^d\left(\frac{x_{\bar{q}}}{x_{h_2}}\right)^d\\
&\times\int_{\frac{x_{h_2}}{x_{\bar{q}}}}^1\frac{d\beta_2}{\beta_2}Q_q^2D_q^{h_2}\left(\frac{x_{h_1}}{x_q},\mu_F\right)D_g^{h_2}\left(\frac{x_{h_2}}{\beta_2x_{\bar{q}}},\mu_F\right)\\
&\times\int d^dp_{1\perp}\int d^dz_{1\perp}\frac{e^{iz_{1\perp}\cdot\left(-\frac{x_{\bar{q}}}{2x_{h_2}}p_{h_2\perp}+p_{1\perp}-\frac{x_q}{2x_{h_1}}p_{h_1\perp}\right)}}{x_qx_{\bar{q}}Q^2+\left(\frac{x_q}{x_{h_1}}\vec{p}_{h_1}-\vec{p}_1\right)^2}F(z_{1\perp})\\
&\times\int d^dp_{1'\perp}\int d^dz_{2\perp}\frac{e^{-iz_{2\perp}\cdot\left(-\frac{x_{\bar{q}}}{2x_{h_2}}p_{h_2\perp}-p_{1'\perp}-\frac{x_q}{2x_{h_1}}p_{h_1\perp}\right)}}{x_q(1-x_q)Q^2+\left(\frac{x_q}{x_{h_1}}\vec{p}_{h_1}-\vec{p}_{1'}\right)^2}F^*(z_{2\perp})\\
&\times\frac{\alpha_s}{2\pi}C_F\left[\frac{1}{\hat{\epsilon}}\frac{1+(1-\beta_2)^2}{\beta_2}+\beta_2+\frac{2(1+(1-\beta_2)^2)\ln\beta_2}{\beta_2}\right.\\
&\left.+\frac{1+(1-\beta_2)^2}{\beta_2}\ln\left(\frac{c_0^2}{\left(\frac{z_{2\perp}-z_{1\perp}}{2}\right)^2\mu^2}\right)\right]+(h_1\leftrightarrow h_2)\\
&=\left.\frac{d\sigma_{3LL}^{qg\to h_1h_2}}{dx_{h_1}dx_{h_2}dp_{h_1\perp}d^dp_{h_2\perp}}\right|_{\text{coll. }\bar{q}g\text{ div}}+\left.\frac{d\sigma_{3LL}^{qg\to h_1h_2}}{dx_{h_1}dx_{h_2}dp_{h_1\perp}d^dp_{h_2\perp}}\right|_{\text{coll. }\bar{q}g\text{ fin}}.
\end{aligned}
\tag{6.104}
$$

This term cancels the divergent term proportional to $P_{gq}(\beta_2)$ in (6.42). This is the last remaining cancellation of divergences, the rest of the cross section is now completely finite.

For the TL case, we get

$$\begin{aligned}
&\left.\frac{d\sigma_{3TL}^{qg\to h_1h_2}}{dx_{h_1}dx_{h_2}dp_{h_1\perp}d^dp_{h_2\perp}}\right|_{\text{coll. }\bar{q}g}\\
&=\frac{2\alpha_{\text{em}}Q}{(2\pi)^{4(d-1)}N_c}\sum_q\int_{x_{h_1}}^1 dx_q\int_{x_{h_2}}^1 dx_{\bar{q}}\,(x_{\bar{q}}-x_q)\delta(1-x_q-x_{\bar{q}})\left(\frac{x_q}{x_{h_1}}\right)^d\left(\frac{x_{\bar{q}}}{x_{h_2}}\right)^d\\
&\times\int_{\frac{x_{h_2}}{x_{\bar{q}}}}^1\frac{d\beta_2}{\beta_2}Q_q^2D_q^{h_2}\left(\frac{x_{h_1}}{x_q},\mu_F\right)D_g^{h_2}\left(\frac{x_{h_2}}{\beta_2x_{\bar{q}}},\mu_F\right)\\
&\times\int d^dp_{1\perp}\int d^dz_{1\perp}\frac{e^{iz_{1\perp}\cdot\left(-\frac{x_{\bar{q}}}{2x_{h_2}}p_{h_2\perp}+p_{1\perp}-\frac{x_q}{2x_{h_1}}p_{h_1\perp}\right)}}{x_qx_{\bar{q}}Q^2+\left(\frac{x_q}{x_{h_1}}\vec{p}_{h_1}-\vec{p}_1\right)^2}F(z_{1\perp})\\
&\times\int d^dp_{1'\perp}\int d^dz_{2\perp}\frac{e^{-iz_{2\perp}\cdot\left(-\frac{x_{\bar{q}}}{2x_{h_2}}p_{h_2\perp}-p_{1'\perp}-\frac{x_q}{2x_{h_1}}p_{h_1\perp}\right)}}{x_q(1-x_q)Q^2+\left(\frac{x_q}{x_{h_1}}\vec{p}_{h_1}-\vec{p}_{1'}\right)^2}F^*(z_{2\perp})\left(\frac{x_q}{x_{h_1}}p_{h_1}-p_{1'}\right)\cdot\varepsilon_T^*\\
&\times\frac{\alpha_s}{2\pi}C_F\left[\frac{1}{\hat{\epsilon}}\frac{1+(1-\beta_2)^2}{\beta_2}+\beta_2+\frac{2\ln\beta_2(1+(1-\beta_2)^2)}{\beta_2}\right.\\
&\left.+\frac{1+(1-\beta_2)^2}{\beta_2}\ln\left(\frac{c_0^2}{\left(\frac{z_{2\perp}-z_{1\perp}}{2}\right)^2\mu^2}\right)\right]+(h_1\leftrightarrow h_2)\\
&=\left.\frac{d\sigma_{3TL}^{qg\to h_1h_2}}{dx_{h_1}dx_{h_2}dp_{h_1\perp}d^dp_{h_2\perp}}\right|_{\text{coll. }\bar{q}g\text{ div}}+\left.\frac{d\sigma_{3TL}^{qg\to h_1h_2}}{dx_{h_1}dx_{h_2}dp_{h_1\perp}d^dp_{h_2\perp}}\right|_{\text{coll. }\bar{q}g\text{ fin}}.
\end{aligned}\tag{6.105}$$

Finally, for the TT case, we get

$$\begin{aligned}
&\left.\frac{d\sigma_{3TT}^{qg\to h_1h_2}}{dx_{h_1}dx_{h_2}dp_{h_1\perp}d^dp_{h_2\perp}}\right|_{\text{coll. }\bar{q}g}\\
&=\frac{\alpha_{\text{em}}}{(2\pi)^{4(d-1)}N_c}\sum_q\int_{x_{h_1}}^1\frac{dx_q}{x_q}\int_{x_{h_2}}^1\frac{dx_{\bar{q}}}{x_{\bar{q}}}\delta(1-x_q-x_{\bar{q}})\left(\frac{x_q}{x_{h_1}}\right)^d\left(\frac{x_{\bar{q}}}{x_{h_2}}\right)^d\\
&\times\int_{\frac{x_{h_2}}{x_{\bar{q}}}}^1\frac{d\beta_2}{\beta_2}Q_q^2D_q^{h_2}\left(\frac{x_{h_1}}{x_q},\mu_F\right)D_g^{h_2}\left(\frac{x_{h_2}}{\beta_2x_{\bar{q}}},\mu_F\right)\left[(x_{\bar{q}}-x_q)^2g_\perp^{ri}g_\perp^{lk}-g_\perp^{rk}g_\perp^{li}+g_\perp^{rl}g_\perp^{ik}\right]\\
&\times\int d^dp_{1\perp}\int d^dz_{1\perp}\frac{e^{iz_{1\perp}\cdot\left(-\frac{x_{\bar{q}}}{2x_{h_2}}p_{h_2\perp}+p_{1\perp}-\frac{x_q}{2x_{h_1}}p_{h_1\perp}\right)}}{x_qx_{\bar{q}}Q^2+\left(\frac{x_q}{x_{h_1}}\vec{p}_{h_1}-\vec{p}_1\right)^2}F(z_{1\perp})\left(\frac{x_q}{x_{h_1}}p_{h_1}-p_1\right)_r\varepsilon_{Ti}\\
&\times\int d^dp_{1'\perp}\int d^dz_{2\perp}\frac{e^{-iz_{2\perp}\cdot\left(-\frac{x_{\bar{q}}}{2x_{h_2}}p_{h_2\perp}-p_{1'\perp}-\frac{x_q}{2x_{h_1}}p_{h_1\perp}\right)}}{x_q(1-x_q)Q^2+\left(\frac{x_q}{x_{h_1}}\vec{p}_{h_1}-\vec{p}_{1'}\right)^2}F^*(z_{2\perp})\left(\frac{x_q}{x_{h_1}}p_{h_1}-p_{1'}\right)_l\varepsilon_{Tk}^*
\end{aligned}$$

$$\times \frac{\alpha_s}{2\pi} C_F \left[\frac{1}{\hat{\epsilon}} \frac{1+(1-\beta_2)^2}{\beta_2} + \beta_2 + \frac{2\ln\beta_2(1+(1-\beta_2)^2)}{\beta_2} \right.$$
$$\left. + \frac{1+(1-\beta_2)^2}{\beta_2} \ln\left(\frac{c_0^2}{\left(\frac{z_{2\perp}-z_{1\perp}}{2}\right)^2 \mu^2} \right) \right] + (h_1 \leftrightarrow h_2)$$
$$= \left. \frac{d\sigma_{3TT}^{qg\to h_1 h_2}}{dx_{h_1} dx_{h_2} dp_{h_1\perp} d^d p_{h_2\perp}} \right|_{\text{coll. } \bar{q}g \text{ div}} + \left. \frac{d\sigma_{3TT}^{qg\to h_1 h_2}}{dx_{h_1} dx_{h_2} dp_{h_1\perp} d^d p_{h_2\perp}} \right|_{\text{coll. } \bar{q}g \text{ fin}} . \tag{6.106}$$

6.5 Additional finite terms

Some of the finite terms of our calculation are presented in previous sections. They come as a result of the extraction of divergences. There are many other terms, completely disconnected from divergences, which however contribute to the final result. We proceed to list them, also emphasizing again what their nature is.

6.5.1 Virtual corrections: Dipole × double-dipole contribution

The 1-loop correction to the $\gamma^* \to q\bar{q}$ contains a dipole and double-dipole terms. The first one receives a contribution from all diagrams, while the second one gets contributions only from diagrams where the virtual gluon crosses the shockwave. At the cross section level there will therefore be two contributions:

- The one due to the interference between the dipole correction and the Born amplitude. This contains divergences and it is the one that we have completely computed in section 6.3.

- The one due to the interference between the double-dipole correction and the Born amplitude. Any rapidity divergence present in this term is completely reabsorbed into the renormalized Wilson operator, at the amplitude level, with the help of the B-JIMWLK evolution. After this operation, this contribution is finite and can be taken in convolution with FFs without any additional manipulation.

Starting from Eq. (5.34) of [198], we get

$$\frac{d\sigma_{2LL}^{q\bar{q}\to h_1 h_2}}{dx_{h_1} d^2 p_{h_1\perp} dx_{h_2} d^2 p_{h_2\perp}}$$
$$= \frac{\alpha_{\text{em}} \alpha_s Q^2}{(2\pi)^5 N_c x_{h_1}^2 x_{h_2}^2} \sum_q \frac{Q_q^2}{2} \int_{x_{h_1}}^1 dx_q \int_{x_{h_2}}^1 dx_{\bar{q}}\, x_q x_{\bar{q}}\, \delta(1-x_q-x_{\bar{q}}) D_q^{h_1}\left(\frac{x_{h_1}}{x_q}, \mu_F\right) D_{\bar{q}}^{h_2}\left(\frac{x_{h_2}}{x_{\bar{q}}}, \mu_F\right)$$

$$
\times \int d^2p_{1\perp}d^2p_{2\perp}d^2p_{1'\perp}d^2p_{2'\perp}\int\frac{d^2p_{3\perp}}{(2\pi)^2}\frac{\tilde{\mathbf{F}}\left(\frac{p_{12\perp}}{2},p_{3\perp}\right)\mathbf{F}^*\left(\frac{p_{1'2'\perp}}{2}\right)}{\left(\frac{x_q}{x_{h_1}}\vec{p}_{h_1}-\vec{p}_{1'}\right)^2+x_qx_{\bar{q}}Q^2}
$$

$$
\times\delta\left(\frac{x_q}{x_{h_1}}p_{h_1\perp}-p_{1\perp}+\frac{x_{\bar{q}}}{x_{h_2}}p_{h_2\perp}-p_{2\perp}-p_{3\perp}\right)\delta(p_{11'\perp}+p_{22'\perp}+p_{3\perp})
$$

$$
\times\left\{4x_qx_{\bar{q}}\left[\frac{x_qx_{\bar{q}}\left(\vec{p}_3^{\,2}-\left(\frac{x_{\bar{q}}}{x_{h_2}}\vec{p}_{h_2}-\vec{p}_2\right)^2-\left(\frac{x_q}{x_{h_1}}\vec{p}_{h_1}-\vec{p}_1\right)^2-2x_qx_{\bar{q}}Q^2\right)}{\left(\left(\frac{x_{\bar{q}}}{x_{h_2}}\vec{p}_{h_2}-\vec{p}_2\right)^2+x_qx_{\bar{q}}Q^2\right)\left(\left(\frac{x_q}{x_{h_1}}\vec{p}_{h_1}-\vec{p}_1\right)^2+x_qx_{\bar{q}}Q^2\right)-x_qx_{\bar{q}}Q^2\vec{p}_3^{\,2}}\right.
$$

$$
\times\ln\left(\frac{x_qx_{\bar{q}}}{e^{2\eta}}\right)\ln\left(\frac{\left(\left(\frac{x_{\bar{q}}}{x_{h_2}}\vec{p}_{h_2}-\vec{p}_2\right)^2+x_qx_{\bar{q}}Q^2\right)\left(\left(\frac{x_q}{x_{h_1}}\vec{p}_{h_1}-\vec{p}_1\right)^2+x_qx_{\bar{q}}Q^2\right)}{x_qx_{\bar{q}}Q^2\vec{p}_3^{\,2}}\right)
$$

$$
\left.-\left(\frac{2x_qx_{\bar{q}}}{Q^2x_qx_{\bar{q}}+\left(\frac{x_q}{x_{h_1}}\vec{p}_{h_1}-\vec{p}_1\right)^2}\ln\left(\frac{x_q}{e^{\eta}}\right)\ln\left(\frac{\vec{p}_3^{\,2}}{\mu^2}\right)+(q\leftrightarrow\bar{q})\right)\right]
$$

$$
\left.+\left[Q^2\int_0^{x_q}dz\left[(\phi_5+\phi_6)_{LL}\right]_+ +(q\leftrightarrow\bar{q})\right]\right\}+h.c.+(h_1\leftrightarrow h_2)\,. \tag{6.107}
$$

Concerning other transitions, we have

$$
\frac{d\sigma_{2TL}^{q\bar{q}\to h_1h_2}}{dx_{h_1}d^2p_{h_1\perp}dx_{h_2}d^2p_{h_2\perp}}
$$

$$
=\frac{\alpha_{\rm em}\alpha_sQ}{(2\pi)^5N_cx_{h_1}^2x_{h_2}^2}\sum_q\frac{Q_q^2}{2}\int_{x_{h_1}}^1dx_q\int_{x_{h_2}}^1dx_{\bar{q}}\,x_qx_{\bar{q}}\,\delta(1-x_q-x_{\bar{q}})
$$

$$
\times D_q^{h_1}\left(\frac{x_{h_1}}{x_q},\mu_F\right)D_{\bar{q}}^{h_2}\left(\frac{x_{h_2}}{x_{\bar{q}}},\mu_F\right)\int d^2p_{1\perp}d^2p_{2\perp}d^2p_{1'\perp}d^2p_{2'\perp}\frac{d^2p_{3\perp}d^2p_{3'\perp}}{(2\pi)^2}\varepsilon_{Ti}^*
$$

$$
\times\delta\left(\frac{x_q}{x_{h_1}}p_{h_1\perp}-p_{1\perp}+\frac{x_{\bar{q}}}{x_{h_2}}p_{h_2\perp}-p_{2\perp}-p_{3\perp}\right)\delta\left(p_{11'\perp}+p_{22'\perp}+p_{33'\perp}\right)
$$

$$
\times\left\{\delta(p_{3'\perp})\frac{\tilde{\mathbf{F}}\left(\frac{p_{12\perp}}{2},p_{3\perp}\right)\mathbf{F}^*\left(\frac{p_{1'2'\perp}}{2}\right)}{\left(\frac{x_q}{x_{h_1}}\vec{p}_{h_1}-\vec{p}_{1'}\right)^2+x_qx_{\bar{q}}Q^2}\left\{2(x_{\bar{q}}-x_q)\left(\frac{x_q}{x_{h_1}}p_{h_1}-p_{1'}\right)^i\right.\right.
$$

$$
\times\left[\frac{x_qx_{\bar{q}}\left(\vec{p}_3^{\,2}-\left(\frac{x_{\bar{q}}}{x_{h_2}}\vec{p}_{h_2}-\vec{p}_2\right)^2-\left(\frac{x_q}{x_{h_1}}\vec{p}_{h_1}-\vec{p}_1\right)^2-2x_qx_{\bar{q}}Q^2\right)}{\left(\left(\frac{x_{\bar{q}}}{x_{h_2}}\vec{p}_{h_2}-\vec{p}_2\right)^2+x_qx_{\bar{q}}Q^2\right)\left(\left(\frac{x_q}{x_{h_1}}\vec{p}_{h_1}-\vec{p}_1\right)^2+x_qx_{\bar{q}}Q^2\right)-x_qx_{\bar{q}}Q^2\vec{p}_3^{\,2}}\ln\left(\frac{x_qx_{\bar{q}}}{e^{2\eta}}\right)\right.
$$

$$
\left.\left.\times\ln\left(\frac{\left(\left(\frac{x_{\bar{q}}}{x_{h_2}}\vec{p}_{h_2}-\vec{p}_2\right)^2+x_qx_{\bar{q}}Q^2\right)\left(\left(\frac{x_q}{x_{h_1}}\vec{p}_{h_1}-\vec{p}_1\right)^2+x_qx_{\bar{q}}Q^2\right)}{x_qx_{\bar{q}}Q^2\vec{p}_3^{\,2}}\right)\right.
$$

$$
\begin{aligned}
&- \left(\frac{2x_q x_{\bar{q}}}{Q^2 x_q x_{\bar{q}} + \left(\frac{x_q}{x_{h_1}}\vec{p}_{h_1} - \vec{p}_1\right)^2} \ln\left(\frac{x_q}{e^\eta}\right) \ln\left(\frac{\vec{p}_3^{\,2}}{\mu^2}\right) + (q \leftrightarrow \bar{q}) \right) \Bigg] \\
&+ \left[\frac{1}{2x_q x_{\bar{q}}} \int_0^{x_q} dz \left[\left(\phi_5^i + \phi_6^i\right)_{TL} \right]_+ + (q \leftrightarrow \bar{q}) \right] \Bigg\} \\
&+ \delta(p_{3\perp}) \frac{\mathbf{F}\left(\frac{p_{12\perp}}{2}\right) \tilde{\mathbf{F}}^*\left(\frac{p_{1'2'\perp}}{2}, p_{3'\perp}\right)}{\left(\frac{x_q}{x_{h_1}}\vec{p}_{h_1} - \vec{p}_1\right)^2 + x_q x_{\bar{q}} Q^2} \Bigg\{ \Bigg[2x_q x_{\bar{q}} (x_{\bar{q}} - x_q) \left(\frac{x_q}{x_{h_1}} p_{h_1} - p_{1'}\right)^i \\
&\times \left(\frac{-2}{Q^2 x_q x_{\bar{q}} + \left(\frac{x_q}{x_{h_1}}\vec{p}_{h_1} - \vec{p}_{1'}\right)^2} \ln\left(\frac{x}{e^\eta}\right) \ln\left(\frac{\vec{p}_{3'}^{\,2}}{\mu^2}\right) \right. \\
&- \ln\left(\frac{x_q x_{\bar{q}}}{e^{2\eta}}\right) \frac{\left(\frac{x_{\bar{q}}}{x_{h_2}}\vec{p}_{h_2} - \vec{p}_{2'}\right)^2 + x_q x_{\bar{q}} Q^2}{\left(\left(\frac{x_{\bar{q}}}{x_{h_2}}\vec{p}_{h_2} - \vec{p}_{2'}\right)^2 + x_q x_{\bar{q}} Q^2\right)\left(\left(\frac{x_q}{x_{h_1}}\vec{p}_{h_1} - \vec{p}_{1'}\right)^2 + x_q x_{\bar{q}} Q^2\right) - x_q x_{\bar{q}} Q^2 \vec{p}_{3'}^{\,2}} \\
&\times \ln\left(\frac{\left(\left(\frac{x_{\bar{q}}}{x_{h_2}}\vec{p}_{h_2} - \vec{p}_{2'}\right)^2 + x_q x_{\bar{q}} Q^2\right)\left(\left(\frac{x_q}{x_{h_1}}\vec{p}_{h_1} - \vec{p}_{1'}\right)^2 + x_q x_{\bar{q}} Q^2\right)}{x_q x_{\bar{q}} Q^2 \vec{p}_{3'}^{\,2}} \right) \\
&+ \left. \frac{1}{\left(\frac{x_q}{x_{h_1}}\vec{p}_{h_1} - \vec{p}_{1'}\right)^2} \ln\left(\frac{x_q x_{\bar{q}}}{e^{2\eta}}\right) \ln\left(\frac{\left(\frac{x_q}{x_{h_1}}\vec{p}_{h_1} - \vec{p}_{1'}\right)^2 + x_q x_{\bar{q}} Q^2}{x_q x_{\bar{q}} Q^2} \right) \right) + (q \leftrightarrow \bar{q}) \Bigg] \\
&+ \left[\int_0^{x_q} dz \left[\left(\phi_5^{i*} + \phi_6^{i*}\right)_{LT} \right]_+ + (q \leftrightarrow \bar{q}) \right] \Bigg\} \Bigg\} \\
&+ (h_1 \leftrightarrow h_2) \,, \qquad (6.108)
\end{aligned}
$$

and

$$
\begin{aligned}
&\frac{d\sigma_{2TT}^{q\bar{q}\to h_1 h_2}}{dx_{h_1} d^2 p_{h_1\perp} dx_{h_2} d^2 p_{h_2\perp}} \\
&= \frac{\alpha_{\rm em}\alpha_s}{(2\pi)^5 N_c x_{h_1}^2 x_{h_2}^2} \sum_q \frac{Q_q^2}{2} \int_{x_{h_1}}^1 dx_q \int_{x_{h_2}}^1 dx_{\bar{q}}\, x_q x_{\bar{q}}\, \delta(1 - x_q - x_{\bar{q}}) D_q^{h_1}\left(\frac{x_{h_1}}{x_q}, \mu_F\right) D_{\bar{q}}^{h_2}\left(\frac{x_{h_2}}{x_{\bar{q}}}, \mu_F\right) \\
&\times \int d^2 p_{1\perp} d^2 p_{2\perp} \int \frac{d^2 p_{3\perp}}{(2\pi)^2} \int d^2 p_{1'\perp} d^2 p_{2'\perp} \frac{\varepsilon_{Ti} \varepsilon_{Tj}^*}{\left(\frac{x_q}{x_{h_1}}\vec{p}_{h_1} - \vec{p}_{1'}\right)^2 + x_q x_{\bar{q}} Q^2} \\
&\times \left[\delta\left(\frac{x_q}{x_{h_1}} p_{h_1\perp} - p_{1\perp} + \frac{x_{\bar{q}}}{x_{h_2}} p_{h_2\perp} - p_{2\perp} - p_{3\perp}\right) \delta\left(\frac{x_q}{x_{h_1}} p_{h_1\perp} - p_{1'\perp} + \frac{x_{\bar{q}}}{x_{h_2}} p_{h_2\perp} - p_{2'\perp}\right) \right. \\
&\times \tilde{\mathbf{F}}\left(\frac{p_{12\perp}}{2}, p_{3\perp}\right) \mathbf{F}^*\left(\frac{p_{1'2'\perp}}{2}\right) \left\{ \left[\left(\frac{x_q}{x_{h_1}} p_{h_1} - p_{1'}\right)_l \left(\frac{x_q}{x_{h_1}} p_{h_1} - p_1\right)_k \right. \right.
\end{aligned}
$$

$$\times \left((x_{\bar{q}}-x_q)^2 g_\perp^{ki} g_\perp^{lj} - g_\perp^{kj} g_\perp^{li} + g_\perp^{kl} g_\perp^{ij}\right) \left(\frac{-2}{Q^2 x_q x_{\bar{q}} + \left(\frac{x_q}{x_{h_1}}\vec{p}_{h_1} - \vec{p}_1\right)^2} \ln\left(\frac{x_q}{e^\eta}\right) \ln\left(\frac{\vec{p}_3^{\,2}}{\mu^2}\right) \right.$$

$$+ \frac{1}{\left(\frac{x_q}{x_{h_1}}\vec{p}_{h_1} - \vec{p}_1\right)^2} \ln\left(\frac{x_q x_{\bar{q}}}{e^{2\eta}}\right) \ln\left(\frac{\left(\frac{x_q}{x_{h_1}}\vec{p}_{h_1} - \vec{p}_1\right)^2 + x_q x_{\bar{q}} Q^2}{x_q x_{\bar{q}} Q^2} \right)$$

$$- \ln\left(\frac{x_q x_{\bar{q}}}{e^{2\eta}}\right) \frac{\left(\frac{x_{\bar{q}}}{x_{h_2}}\vec{p}_{h_2} - \vec{p}_2\right)^2 + x_q x_{\bar{q}} Q^2}{\left(\left(\frac{x_{\bar{q}}}{x_{h_2}}\vec{p}_{h_2} - \vec{p}_2\right)^2 + x_q x_{\bar{q}} Q^2\right)\left(\left(\frac{x_q}{x_{h_1}}\vec{p}_{h_1} - \vec{p}_1\right)^2 + x_q x_{\bar{q}} Q^2\right) - x_q x_{\bar{q}} Q^2 \vec{p}_3^{\,2}}$$

$$\left. \times \ln\left(\frac{\left(\left(\frac{x_{\bar{q}}}{x_{h_2}}\vec{p}_{h_2} - \vec{p}_2\right)^2 + x_q x_{\bar{q}} Q^2\right)\left(\left(\frac{x_q}{x_{h_1}}\vec{p}_{h_1} - \vec{p}_1\right)^2 + x_q x_{\bar{q}} Q^2\right)}{x_q x_{\bar{q}} Q^2 \vec{p}_3^{\,2}} \right) \right) + (q \leftrightarrow \bar{q}) \Bigg]$$

$$\left. + \frac{1}{x_q x_{\bar{q}}} \left[\int_0^{x_q} dz \left[\left(\phi_5^{ij} + \phi_6^{ij}\right)_{TT} \right]_+ dz + (q \leftrightarrow \bar{q}) \right] \right\} + h.c\Big|_{(p_1, p_3 \leftrightarrow p_{1'}, p_{3'}), (i \leftrightarrow j)} \Bigg]$$

$$+ (h_1 \leftrightarrow h_2)\,. \tag{6.109}$$

The ϕ function are defined in Appendix D.1.

6.5.2 Real corrections: Fragmentation from quark and anti-quark

In this case, we refer to the finite terms related to the contribution (b) of Fig. 6.5. In order to better understand what these contributions are, referring to Ref. [203], we recall that the impact factor for the transition $\gamma^* \to q\bar{q}g$ has a double dipole contribution ($\Phi_4^{(+,i)}$) and a single dipole ($\Phi_3^{(+,i)}$) contribution. The finite contributions which we obtain are

- Finite terms related to the dipole $\times$ dipole contribution.
- Dipole $\times$ double dipole contribution.
- Double dipole $\times$ double dipole contribution.

Finite part of dipole $\times$ dipole contribution

When we square the dipole contribution, using shorthand notation introduced in (6.56), we obtain the following structure:

$$\Phi_3^\alpha(\vec{p}_1, \vec{p}_2)\Phi_3^{\beta *}(\vec{p}_{1'}, \vec{p}_{2'}) = \tilde{\Phi}_3^\alpha(\vec{p}_1, \vec{p}_2)\tilde{\Phi}_3^{\beta *}(\vec{p}_{1'}, \vec{p}_{2'})$$

$$+\left(\tilde{\Phi}_3^{\alpha}(\vec{p}_1,\vec{p}_2)\Phi_4^{\beta *}(\vec{p}_{1'},\vec{p}_{2'},\vec{0})+\Phi_4^{\alpha}(\vec{p}_1,\vec{p}_2,\vec{0})\Phi_3^{\beta *}(\vec{p}_{1'},\vec{p}_{2'})\right)$$
$$+\Phi_4^{\alpha}(\vec{p}_1,\vec{p}_2,\vec{0})\Phi_4^{\beta *}(\vec{p}_{1'},\vec{p}_{2'},\vec{0})\,. \tag{6.110}$$

The first term in the RHS is the one containing divergences that we have considered in previous sections. After isolating soft and collinear divergences, finite terms remain. The finite contributions for $\tilde{\sigma}_{(b)div,1}$ and $\tilde{\sigma}_{(b)div,3}$ have been computed respectively in sections 6.4.1 and 6.4.1, see eqs. (6.71), (6.73), (6.75) and (6.79) (6.82) (6.85). Besides, the terms $(\tilde{\sigma}_{(b)div,2}-\tilde{\sigma}^{soft}_{(b)div,2})$ and $(\tilde{\sigma}_{(b)div,4}-\tilde{\sigma}^{soft}_{(b)div,4})$ in Eq. (6.34) are finite. Their contribution read

$$\left.\frac{d\sigma^{q\bar{q}\to h_1h_2}_{3LL}}{dx_{h_1}dx_{h_2}d^dp_{h_1\perp}d^dp_{h_2\perp}}\right|_{\text{finite, (b) 2,4}}$$
$$=\frac{\alpha_s C_F}{\mu^{2\epsilon}}\frac{4\alpha_{\rm em}Q^2}{(2\pi)^{4(d-1)}N_c\,x_{h_1}^d x_{h_2}^d}\sum_q\int_{x_{h_1}}^1\frac{dx_q}{x_q}\int_{x_{h_2}}^1\frac{dx_{\bar{q}}}{x_{\bar{q}}}\int_\alpha^1\frac{dx_g}{x_g^{3-d}}\left(x_qx_{\bar{q}}\right)^{d-1}\delta(1-x_q-x_{\bar{q}}-x_g)$$
$$\times Q_q^2 D_q^{h_1}\left(\frac{x_{h_1}}{x_q},\mu_F\right)D_{\bar{q}}^{h_2}\left(\frac{x_{h_2}}{x_{\bar{q}}},\mu_F\right)\int\frac{d^d\vec{u}}{(2\pi)^d}\int d^dp_{1\perp}d^dp_{2\perp}\mathbf{F}\left(\frac{p_{12\perp}}{2}\right)$$
$$\times\int d^dp_{1'\perp}d^dp_{2'\perp}\mathbf{F}^*\left(\frac{p_{1'2'\perp}}{2}\right)\delta\left(p_{11'\perp}+p_{22'\perp}\right)$$
$$\times\left\{\frac{8x_qx_{\bar{q}}\,\delta\left(\frac{x_q}{x_{h_1}}p_{h_1\perp}-p_{1\perp}+\frac{x_{\bar{q}}}{x_{h_2}}p_{h_2\perp}-p_{2\perp}\right)}{\left(Q^2+\frac{\left(\frac{x_{\bar{q}}}{x_{h_2}}\vec{p}_{h_2}-\vec{p}_{2'}\right)^2}{x_{\bar{q}}(1-x_{\bar{q}})}\right)\left(Q^2+\frac{\left(\frac{x_q}{x_{h_1}}\vec{p}_{h_1}-\vec{p}_1\right)^2}{x_q(1-x_q)}\right)}\frac{\left(\vec{u}-\frac{\vec{p}_{h_1}}{x_{h_1}}\right)\cdot\left(\vec{u}-\frac{\vec{p}_{h_2}}{x_{h_2}}\right)}{\left(\vec{u}-\frac{\vec{p}_{h_1}}{x_{h_1}}\right)^2\left(\vec{u}-\frac{\vec{p}_{h_2}}{x_{h_2}}\right)^2}\right.$$
$$-\frac{(2x_g-dx_g^2+4x_qx_{\bar{q}})\delta\left(\frac{x_q}{x_{h_1}}p_{h_1\perp}-p_{1\perp}+\frac{x_{\bar{q}}}{x_{h_2}}p_{h_2\perp}-p_{2\perp}+x_gu_\perp\right)}{\left(Q^2+\frac{\left(\frac{x_{\bar{q}}}{x_{h_2}}\vec{p}_{h_2}-\vec{p}_{2'}\right)^2}{x_{\bar{q}}(1-x_{\bar{q}})}\right)\left(Q^2+\frac{\left(\frac{x_q}{x_{h_1}}\vec{p}_{h_1}-\vec{p}_1\right)^2}{x_q(1-x_q)}\right)}\frac{\left(\vec{u}-\frac{\vec{p}_{h_1}}{x_{h_1}}\right)\cdot\left(\vec{u}-\frac{\vec{p}_{h_2}}{x_{h_2}}\right)}{\left(\vec{u}-\frac{\vec{p}_{h_1}}{x_{h_1}}\right)^2\left(\vec{u}-\frac{\vec{p}_{h_2}}{x_{h_2}}\right)^2}$$
$$-\frac{(2x_g-dx_g^2+4x_qx_{\bar{q}})\delta\left(\frac{x_q}{x_{h_1}}p_{h_1\perp}-p_{1\perp}+\frac{x_{\bar{q}}}{x_{h_2}}p_{h_2\perp}-p_{2\perp}+x_gu_\perp\right)}{\left(Q^2+\frac{\left(\frac{x_{\bar{q}}}{x_{h_2}}\vec{p}_{h_2}-\vec{p}_2\right)^2}{x_{\bar{q}}(1-x_{\bar{q}})}\right)\left(Q^2+\frac{\left(\frac{x_q}{x_{h_1}}\vec{p}_{h_1}-\vec{p}_{1'}\right)^2}{x_q(1-x_q)}\right)}$$
$$\left.\times\frac{\left(\vec{u}-\frac{\vec{p}_{h_1}}{x_{h_1}}\right)\cdot\left(\vec{u}-\frac{\vec{p}_{h_2}}{x_{h_2}}\right)}{\left(\vec{u}-\frac{\vec{p}_{h_1}}{x_{h_1}}\right)^2\left(\vec{u}-\frac{\vec{p}_{h_2}}{x_{h_2}}\right)^2}\right\}+(h_1\leftrightarrow h_2)\,, \tag{6.111}$$

in the LL case. The same contribution in the TL and TT cases is, respectively,

$$
\begin{aligned}
&\left.\frac{d\sigma_{3TL}^{q\bar{q}\to h_1h_2}}{dx_{h_1}dx_{h_2}d^dp_{h_1\perp}d^dp_{h_2\perp}}\right|_{\text{finite, (b) 2,4}}\\
&=\frac{\alpha_sC_F}{\mu^{2\epsilon}}\frac{2\alpha_{\rm em}Q}{(2\pi)^{4(d-1)}N_cx_{h_1}^dx_{h_2}^d}\sum_q\int_{x_{h_1}}^1\frac{dx_q}{x_q}\int_{x_{h_2}}^1\frac{x_{\bar q}}{x_{\bar q}}\int_\alpha^1\frac{dx_g}{x_g^{3-d}}(x_qx_{\bar q})^{d-1}\delta(1-x_q-x_{\bar q}-x_g)\\
&\times Q_q^2D_q^{h_1}\left(\frac{x_{h_1}}{x_q},\mu_F\right)D_{\bar q}^{h_2}\left(\frac{x_{h_2}}{x_{\bar q}},\mu_F\right)\int\frac{d^d\vec u}{(2\pi)^d}\int d^dp_{1\perp}d^dp_{2\perp}\mathbf{F}\left(\frac{p_{12\perp}}{2}\right)\\
&\times\int d^dp_{1'\perp}d^dp_{2'\perp}\mathbf{F}^*\left(\frac{p_{1'2'\perp}}{2}\right)\delta\left(p_{11'\perp}+p_{22'\perp}\right)\varepsilon_{Ti}^*\\
&\times\left\{\frac{\delta\left(\frac{x_q}{x_{h_1}}p_{h_1\perp}-p_{1\perp}+\frac{x_{\bar q}}{x_{h_2}}p_{h_2\perp}-p_{2\perp}+x_gu_\perp\right)}{\left(Q^2+\frac{\left(\frac{x_{\bar q}}{x_{h_2}}\vec p_{h_2}-\vec p_{2'}\right)^2}{x_{\bar q}(1-x_{\bar q})}\right)\left(Q^2+\frac{\left(\frac{x_q}{x_{h_1}}\vec p_{h_1}-\vec p_1\right)^2}{x_q(1-x_q)}\right)}\frac{\left(u_\perp-\frac{p_{h_1\perp}}{x_{h_1}}\right)_\mu\left(u_\perp-\frac{p_{h_2\perp}}{x_{h_2}}\right)_\nu}{\left(\vec u-\frac{\vec p_{h_1}}{x_{h_1}}\right)^2\left(\vec u-\frac{\vec p_{h_2}}{x_{h_2}}\right)^2}\right.\\
&\times\frac{1}{x_{\bar q}(x_q+x_g)}\left[x_g(4x_{\bar q}+dx_g-2)\left(\left(\frac{x_{\bar q}}{x_{h_2}}p_{h_2\perp}-p_{2'\perp}\right)^\mu g_\perp^{i\nu}-\left(\frac{x_{\bar q}}{x_{h_2}}p_{h_2\perp}-p_{2'\perp}\right)^\nu g_\perp^{i\mu}\right)\right.\\
&\left.-(2x_{\bar q}-1)(4x_{\bar q}x_q+x_g(2-x_gd))g_\perp^{\mu\nu}\left(\frac{x_{\bar q}}{x_{h_2}}p_{h_2\perp}-p_{2'\perp}\right)^i\right]\\
&+\frac{\delta\left(\frac{x_q}{x_{h_1}}p_{h_1\perp}-p_{1\perp}+\frac{x_{\bar q}}{x_{h_2}}p_{h_2\perp}-p_{2\perp}+x_gu_\perp\right)}{\left(Q^2+\frac{\left(\frac{x_q}{x_{h_1}}\vec p_{h_1}-\vec p_{1'}\right)^2}{x_q(1-x_q)}\right)\left(Q^2+\frac{\left(\frac{x_{\bar q}}{x_{h_2}}\vec p_{h_2}-\vec p_2\right)^2}{x_{\bar q}(1-x_{\bar q})}\right)}\frac{\left(u_\perp-\frac{p_{h_2\perp}}{x_{h_2}}\right)_\mu\left(u_\perp-\frac{p_{h_1\perp}}{x_{h_1}}\right)_\nu}{\left(\vec u-\frac{\vec p_{h_1}}{x_{h_1}}\right)^2\left(\vec u-\frac{\vec p_{h_2}}{x_{h_2}}\right)^2}\\
&\times\frac{1}{x_q(x_{\bar q}+x_g)}\left[x_g(4x_q+dx_g-2)\left(\left(\frac{x_q}{x_{h_1}}p_{h_1\perp}-p_{1'\perp}\right)^\mu g_\perp^{i\nu}-\left(\frac{x_q}{x_{h_1}}p_{h_1\perp}-p_{1'\perp}\right)^\nu g_\perp^{i\mu}\right)\right.\\
&\left.-(2x_q-1)(4x_{\bar q}x_q+x_g(2-x_gd))g_\perp^{\mu\nu}\left(\frac{x_q}{x_{h_2}}p_{h_1\perp}-p_{1'\perp}\right)^i\right]\\
&-\frac{8\,\delta\left(\frac{x_q}{x_{h_1}}p_{h_1\perp}-p_{1\perp}+\frac{x_{\bar q}}{x_{h_2}}p_{h_2\perp}-p_{2\perp}\right)}{\left(Q^2+\frac{\left(\frac{x_{\bar q}}{x_{h_2}}\vec p_{h_2}-\vec p_{2'}\right)^2}{x_{\bar q}(1-x_{\bar q})}\right)\left(Q^2+\frac{\left(\frac{x_q}{x_{h_1}}\vec p_{h_1}-\vec p_1\right)^2}{x_q(1-x_q)}\right)}\frac{\left(\vec u-\frac{\vec p_{h_1}}{x_{h_1}}\right)\cdot\left(\vec u-\frac{\vec p_{h_2}}{x_{h_2}}\right)}{\left(\vec u-\frac{\vec p_{h_1}}{x_{h_1}}\right)^2\left(\vec u-\frac{\vec p_{h_2}}{x_{h_2}}\right)^2}\\
&\left.\times\left(\frac{x_{\bar q}}{x_{h_2}}p_{h_2\perp}-p_{2'\perp}\right)^i(x_{\bar q}-x_q)\right\}+(h_1\leftrightarrow h_2)\,,
\end{aligned}
$$

and

$$\left.\frac{d\sigma_{3TT}^{q\bar{q}\to h_1h_2}}{dx_{h_1}dx_{h_2}d^dp_{h_1\perp}d^dp_{h_2\perp}}\right|_{\text{finite, (b) 2,4}}$$
$$=\frac{\alpha_sC_F}{\mu^{2\epsilon}}\frac{\alpha_{\rm em}}{(2\pi)^{4(d-1)}N_cx_{h_1}^dx_{h_2}^d}\sum_q\int_{x_{h_1}}^1\frac{dx_q}{x_q}\int_{x_{h_2}}^1\frac{dx_{\bar{q}}}{x_{\bar{q}}}\int_\alpha^1\frac{dx_g}{x_g^{3-d}}\delta(1-x_q-x_{\bar{q}}-x_g)(x_qx_{\bar{q}})^{d-1}$$
$$\times Q_q^2D_q^{h_1}\left(\frac{x_{h_1}}{x_q},\mu_F\right)D_{\bar{q}}^{h_2}\left(\frac{x_{h_2}}{x_{\bar{q}}},\mu_F\right)\int\frac{d^d\vec{u}}{(2\pi)^d}\int d^dp_{1\perp}d^dp_{2\perp}\mathbf{F}\left(\frac{p_{12\perp}}{2}\right)$$
$$\times\int d^dp_{1'\perp}d^dp_{2'\perp}\mathbf{F}^*\left(\frac{p_{1'2'\perp}}{2}\right)\delta(p_{11'\perp}+p_{22'\perp})\varepsilon_{Ti}\varepsilon_{Tk}^*$$
$$\times\left\{\left[\left[\left(-\frac{\delta\left(p_{q1\perp}+p_{\bar{q}2\perp}+x_gu_\perp\right)}{\left(Q^2+\frac{\vec{p}_{\bar{q}2}^{\,2}}{x_{\bar{q}}(1-x_{\bar{q}})}\right)\left(Q^2+\frac{\vec{p}_{q1'}^{\,2}}{x_q(1-x_q)}\right)}\frac{\left(u_\perp-\frac{p_{q\perp}}{x_q}\right)_\mu\left(u_\perp-\frac{p_{\bar{q}\perp}}{x_{\bar{q}}}\right)_\nu}{\left(\vec{u}-\frac{\vec{p}_q}{x_q}\right)^2\left(\vec{u}-\frac{p_{\bar{q}}}{x_{\bar{q}}}\right)^2}\right.\right.\right.$$
$$\times\frac{1}{(x_q+x_g)(x_{\bar{q}}+x_g)x_qx_{\bar{q}}}\left\{x_g((d-4))x_g-2\right)\left[p_{q1'\perp}^\nu\left(p_{\bar{q}2\perp}^\mu g_\perp^{ik}+p_{\bar{q}2\perp}^kg_\perp^{\mu i}\right)\right.$$
$$+g_\perp^{\mu\nu}\left((\vec{p}_{q1'}\cdot\vec{p}_{\bar{q}2})\,g_\perp^{ik}+p_{q1'\perp}^ip_{\bar{q}2\perp}^k\right)-g_\perp^{\nu k}p_{q1'\perp}^ip_{\bar{q}2\perp}^\mu-g_\perp^{\mu i}g_\perp^{\nu k}\,(\vec{p}_{q1'}\cdot\vec{p}_{\bar{q}2})\big]-g_\perp^{\mu\nu}$$
$$\times\big[(2x_q-1)\,(2x_{\bar{q}}-1)\,p_{q1'\perp}^kp_{\bar{q}2\perp}^i\,(4x_qx_{\bar{q}}+x_g(2-x_gd))+4x_qx_{\bar{q}}((\vec{p}_{q1'}\cdot\vec{p}_{\bar{q}2})g_\perp^{ik}+p_{q1'\perp}^ip_{\bar{q}2\perp}^k)\big]$$
$$+\left(p_{q1'\perp}^\mu p_{\bar{q}2\perp}^\nu g_\perp^{ik}-p_{q1'\perp}^\mu p_{\bar{q}2\perp}^kg_\perp^{\nu i}-p_{q1'\perp}^ip_{\bar{q}2\perp}^\nu g_\perp^{\mu k}-g_\perp^{\mu k}g_\perp^{\nu i}(\vec{p}_{q1'}\cdot\vec{p}_{\bar{q}2})\right)$$
$$\times x_g((d-4)x_g+2)+x_g(2x_{\bar{q}}-1)(x_gd+4x_q-2)\left(g_\perp^{\mu k}p_{q1'\perp}^\nu-g_\perp^{\nu k}p_{q1'\perp}^\mu\right)p_{\bar{q}2\perp}^i$$
$$+\ x_g(2x_q-1)p_{q1'\perp}^k(4x_{\bar{q}}+x_gd-2)\left(g_\perp^{\nu i}p_{\bar{q}2\perp}^\mu-g_\perp^{\nu k}p_{q1'\perp}^\nu\right)\}\big)+(q\leftrightarrow\bar{q})\big]$$
$$+\frac{8\,\delta(p_{q1\perp}+p_{\bar{q}2\perp})}{\left(Q^2+\frac{\vec{p}_{\bar{q}2}^{\,2}}{x_{\bar{q}}(1-x_{\bar{q}})}\right)\left(Q^2+\frac{\vec{p}_{q1'}^{\,2}}{x_q(1-x_q)}\right)}\frac{\left(\vec{u}-\frac{\vec{p}_q}{x_q}\right)\cdot\left(\vec{u}-\frac{\vec{p}_{\bar{q}}}{x_{\bar{q}}}\right)}{\left(\vec{u}-\frac{\vec{p}_q}{x_q}\right)^2\left(\vec{u}-\frac{\vec{p}_{\bar{q}}}{x_{\bar{q}}}\right)^2}$$
$$\times\frac{1}{x_qx_{\bar{q}}}\left[-(x_{\bar{q}}-x_q)^2g_\perp^{ri}g_\perp^{kl}+g_\perp^{il}g_\perp^{rk}-g_\perp^{rl}g_\perp^{ik}\right]p_{\bar{q}2\perp r}p_{q1'\perp l}\Big\}+(h_1\leftrightarrow h_2)\ .$$

In the above expression, the following replacement needs to be done:

$$p_{q\perp}=\frac{x_q}{x_{h_1}}p_{h_1\perp}\ ,\quad p_{\bar{q}\perp}=\frac{x_{\bar{q}}}{x_{h_2}}p_{h_2\perp}\ . \tag{6.112}$$

The remaining term in Eq. (6.110), for arbitrary polarization, is

$$\frac{d\sigma_{3JI}^{q\bar{q}\to h_1h_2}}{dx_{h_1}dx_{h_2}d^dp_{h_1}d^dp_{h_2}}$$
$$=\frac{2\alpha_s\alpha_{\rm em}C_F}{\mu^{2\epsilon}(2\pi)^{4(d-1)}N_c}\frac{(p_0^-)^2}{s^2x_{h_1}^dx_{h_2}^d}\sum_qQ_q^2\int_{x_{h_1}}^1\frac{dx_q}{x_q}\int_{x_{h_2}}^1\frac{dx_{\bar{q}}}{x_{\bar{q}}}\,(x_qx_{\bar{q}})^{d-1}D_q^{h_1}\left(\frac{x_{h_1}}{x_q},\mu_F\right)$$
$$\times D_{\bar{q}}^{h_2}\left(\frac{x_{h_2}}{x_{\bar{q}}},\mu_F\right)\int_0^1\frac{dx_g}{x_g}\int\frac{d^dp_{g\perp}}{(2\pi)^d}\delta(1-x_q-x_{\bar{q}}-x_g)\int d^dp_{1\perp}d^dp_{2\perp}d^dp_{1'\perp}d^dp_{2'\perp}$$

$$\times \mathbf{F}\left(\frac{p_{12\perp}}{2}\right)\mathbf{F}^*\left(\frac{p_{1'2'\perp}}{2}\right)\delta\left(\frac{x_q}{x_{h_1}}p_{h_1\perp}-p_{1\perp}+\frac{x_{\bar q}}{x_{h_2}}p_{h_2\perp}-p_{2\perp}+p_{g\perp}\right)\delta(p_{11'\perp}+p_{22'\perp})$$
$$\times \varepsilon_{I\alpha}\,\varepsilon^*_{J\beta}\left[\Phi_3^\alpha(p_{1\perp},p_{2\perp})\Phi_3^{\beta*}(p_{1'\perp},p_{2'\perp})-\tilde\Phi_3^\alpha(p_{1\perp},p_{2\perp})\tilde\Phi_3^{\beta*}(p_{1'\perp},p_{2'\perp})\right]$$
$$+(h_1\leftrightarrow h_2)\,. \tag{6.113}$$

Dipole × double-dipole contribution and double-dipole × double-dipole contribution

The dipole × double dipole contribution, for arbitrary polarization, is given by

$$\frac{d\sigma_{4JI}^{q\bar q\to h_1h_2}}{dx_{h_1}dx_{h_2}d^dp_{h_1\perp}d^dp_{h_2\perp}}$$
$$=\frac{\alpha_s\alpha_{\rm em}}{\mu^{2\epsilon}(2\pi)^{4(d-1)}N_c}\frac{(p_0^-)^2}{s^2x_{h_1}^dx_{h_2}^d}\sum_q Q_q^2\int_{x_{h_1}}^1\frac{dx_q}{x_q}\int_{x_{h_2}}^1\frac{dx_{\bar q}}{x_{\bar q}}\,(x_qx_{\bar q})^{d-1}D_q^{h_1}\left(\frac{x_{h_1}}{x_q},\mu_F\right)D_{\bar q}^{h_2}\left(\frac{x_{h_2}}{x_{\bar q}},\mu_F\right)$$
$$\times\int_0^1\frac{dx_g}{x_g}\int\frac{d^dp_{g\perp}}{(2\pi)^d}\delta(1-x_q-x_{\bar q}-x_g)\int d^dp_{1\perp}d^dp_{2\perp}d^dp'_{1\perp}d^dp'_{2\perp}\frac{d^dp_{3\perp}d^dp'_{3\perp}}{(2\pi)^d}$$
$$\times\delta\left(\frac{x_q}{x_{h_1}}p_{h_1\perp}-p_{1\perp}+\frac{x_{\bar q}}{x_{h_2}}p_{h_2\perp}-p_{2\perp}+p_{g3\perp}\right)\delta(p_{11'\perp}+p_{22'\perp}+p_{33'\perp})(\varepsilon_{I\alpha}\varepsilon^*_{J\beta})$$
$$\times\Big[\Phi_3^\alpha(p_{1\perp},p_{2\perp})\Phi_4^{\beta*}(p'_{1\perp},p'_{2\perp},p'_{3\perp})\mathbf{F}\left(\frac{p_{12\perp}}{2}\right)\tilde{\mathbf{F}}^*\left(\frac{p_{1'2'\perp}}{2},p'_{3\perp}\right)\delta(p_{3\perp}) \tag{6.114}$$
$$+\,\Phi_4^\alpha(p_{1\perp},p_{2\perp},p_{3\perp})\Phi_3^{\beta*}(p_{1'\perp},p_{2'\perp})\,\tilde{\mathbf{F}}\left(\frac{p_{12\perp}}{2},p_{3\perp}\right)\mathbf{F}^*\left(\frac{p_{1'2'\perp}}{2}\right)\delta(p'_{3\perp})\Big]+(h_1\leftrightarrow h_2)\,.$$

The double-dipole × double-dipole contribution, for arbitrary polarization, is given by

$$\frac{d\sigma_{5JI}^{q\bar q\to h_1h_2}}{dx_{h_1}dx_{h_2}d^dp_{h_1}d^dp_{h_2}}$$
$$=\frac{\alpha_s\alpha_{\rm em}(\varepsilon_{I\alpha}\varepsilon^*_{J\beta})}{\mu^{2\epsilon}(2\pi)^{4(d-1)}(N_c^2-1)}\frac{(p_0^-)^2}{s^2x_{h_1}^dx_{h_2}^d}\sum_q Q_q^2\int_{x_{h_1}}^1\frac{dx_q}{x_q}\int_{x_{h_2}}^1\frac{dx_{\bar q}}{x_{\bar q}}\,(x_qx_{\bar q})^{d-1}D_q^{h_1}\left(\frac{x_{h_1}}{x_q},\mu_F\right)$$
$$\times D_{\bar q}^{h_2}\left(\frac{x_{h_2}}{x_{\bar q}},\mu_F\right)\int_0^1\frac{dx_g}{x_g}\int\frac{d^dp_{g\perp}}{(2\pi)^d}\delta(1-x_q-x_{\bar q}-x_g)\int d^dp_{1\perp}d^dp_{2\perp}d^dp'_{1\perp}d^dp'_{2\perp}$$
$$\times\int\frac{d^dp_{3\perp}d^dp'_{3\perp}}{(2\pi)^{2d}}\delta\left(\frac{x_q}{x_{h_1}}p_{h_1\perp}-p_{1\perp}+\frac{x_{\bar q}}{x_{h_2}}p_{h_2\perp}-p_{2\perp}+p_{g3\perp}\right)\delta(p_{11'\perp}+p_{22'\perp}+p_{33'\perp})$$
$$\times\Phi_4^\alpha(p_{1\perp},p_{2\perp},p_{3\perp})\Phi_4^{\beta*}(p'_{1\perp},p'_{2\perp},p'_{3\perp})\tilde{\mathbf{F}}\left(\frac{p_{12\perp}}{2},p_{3\perp}\right)\tilde{\mathbf{F}}^*\left(\frac{p_{1'2'\perp}}{2},p'_{3\perp}\right)$$
$$+(h_1\leftrightarrow h_2)\,. \tag{6.115}$$

The expression for the squared impact factors can be found in Appendix D.2. They are written in terms of $p_q, p_{\bar q}, p_g, z$ and the following identification should be done:

$$p_{q\perp}=\frac{x_q}{x_{h_1}}p_{h_1\perp}\,,\quad p_{\bar q\perp}=\frac{x_{\bar q}}{x_{h_2}}p_{h_2\perp}\,,\quad z=x_g\,. \tag{6.116}$$

6.5.3 Real corrections: Fragmentation from anti-quark and gluon

Finite part of dipole × dipole contribution

When squaring the dipole contribution, we have also finite terms. This time we write separately for each polarization transition. In the LL case, we have

$$
\begin{aligned}
&\frac{d\sigma_{3LL}^{g\bar{q}\to h_1 h_2}}{dx_{h_1}dx_{h_2}d^dp_{h_1}d^dp_{h_2}} \\
&= \frac{2\alpha_s\alpha_{\rm em}C_F}{\mu^{2\epsilon}(2\pi)^{4(d-1)}N_c}\frac{(p_0^-)^2}{s^2x_{h_1}^dx_{h_2}^d}\sum_q Q_q^2\int_{x_{h_1}}^1\frac{dx_g}{x_g}\int_{x_{h_2}}^1\frac{dx_{\bar{q}}}{x_{\bar{q}}}\,(x_gx_{\bar{q}})^{d-1}D_g^{h_1}\left(\frac{x_{h_1}}{x_g},\mu_F\right) \\
&\times D_{\bar{q}}^{h_2}\left(\frac{x_{h_2}}{x_{\bar{q}}},\mu_F\right)\int_0^1\frac{dx_q}{x_q}\int\frac{d^dp_{q\perp}}{(2\pi)^d}\delta(1-x_q-x_{\bar{q}}-x_g)\int d^dp_{1\perp}d^dp_{2\perp}d^dp_{1'\perp}d^dp_{2'\perp} \\
&\times \mathbf{F}\left(\frac{p_{12\perp}}{2}\right)\mathbf{F}^*\left(\frac{p_{1'2'\perp}}{2}\right)\delta\left(p_{q1\perp}+\frac{x_{\bar{q}}}{x_{h_2}}p_{h_2\perp}-p_{2\perp}+\frac{x_g}{x_{h_1}}p_{h_1\perp}\right)\delta(p_{11'\perp}+p_{22'\perp})\frac{Q^2}{(p_\gamma^+)^2} \\
&\times\Bigg[\Phi_3^+(p_{1\perp},p_{2\perp})\Phi_3^{+*}(p_{1'\perp},p_{2'\perp})-\frac{8x_qx_{\bar{q}}(p_\gamma^+)^4\left(dx_g^2+4x_q(x_q+x_g)\right)}{\left(Q^2+\frac{\left(\frac{x_{\bar{q}}}{x_{h_2}}\vec{p}_{h_2}-\vec{p}_2\right)^2}{x_{\bar{q}}(1-x_{\bar{q}})}\right)\left(Q^2+\frac{\left(\frac{x_{\bar{q}}}{x_{h_2}}\vec{p}_{h_2}-\vec{p}_{2'}\right)^2}{x_{\bar{q}}(1-x_{\bar{q}})}\right)} \\
&\times\frac{1}{\left(x_q\frac{x_g}{x_{h_1}}\vec{p}_{h_1}-x_g\vec{p}_q\right)^2}\Bigg]+(h_1\leftrightarrow h_2)\,. \qquad (6.117)
\end{aligned}
$$

For the TL case, we have

$$
\begin{aligned}
&\frac{d\sigma_{3TL}^{g\bar{q}\to h_1 h_2}}{dx_{h_1}dx_{h_2}d^dp_{h_1}d^dp_{h_2}} \\
&= \frac{2\alpha_s\alpha_{\rm em}C_F}{\mu^{2\epsilon}(2\pi)^{4(d-1)}N_c}\frac{(p_0^-)^2}{s^2x_{h_1}^dx_{h_2}^d}\sum_q Q_q^2\int_{x_{h_1}}^1\frac{dx_g}{x_g}\int_{x_{h_2}}^1\frac{dx_{\bar{q}}}{x_{\bar{q}}}\,(x_gx_{\bar{q}})^{d-1}D_g^{h_1}\left(\frac{x_{h_1}}{x_g},\mu_F\right) \\
&\times D_{\bar{q}}^{h_2}\left(\frac{x_{h_2}}{x_{\bar{q}}},\mu_F\right)\int_0^1\frac{dx_q}{x_q}\int\frac{d^dp_{q\perp}}{(2\pi)^d}\delta(1-x_q-x_{\bar{q}}-x_g)\int d^dp_{1\perp}d^dp_{2\perp}d^dp_{1'\perp}d^dp_{2'\perp} \\
&\times \mathbf{F}\left(\frac{p_{12\perp}}{2}\right)\mathbf{F}^*\left(\frac{p_{1'2'\perp}}{2}\right)\delta\left(p_{q1\perp}+\frac{x_{\bar{q}}}{x_{h_2}}p_{h_2\perp}-p_{2\perp}+\frac{x_g}{x_{h_1}}p_{h_1\perp}\right)\delta(p_{11'\perp}+p_{22'\perp})\varepsilon_{Ti}^*\frac{Q}{p_\gamma^+}
\end{aligned}
$$

$$\times \Bigg[\Phi_3^+(p_{1\perp},p_{2\perp})\Phi_3^{i*}(p_{1'\perp},p_{2'\perp}) + \frac{4x_q\left(p_\gamma^+\right)^3(2x_{\bar q}-1)\left(x_g^2 d+4x_q\left(x_q+x_g\right)\right)}{\left(Q^2+\frac{\left(\frac{x_{\bar q}}{x_{h_2}}\vec{p}_{h_2}-\vec{p}_2\right)^2}{x_{\bar q}(1-x_{\bar q})}\right)\left(Q^2+\frac{\left(\frac{x_{\bar q}}{x_{h_2}}\vec{p}_{h_2}-\vec{p}_{2'}\right)^2}{x_{\bar q}(1-x_{\bar q})}\right)}$$

$$\times\frac{\left(\frac{x_{\bar q}}{x_{h_2}}p_{h_2\perp}-p_{2'\perp}\right)^i}{\left(x_q+x_g\right)\left(x_q\frac{x_g}{x_{h_1}}\vec{p}_{h_1}-x_g\vec{p}_q\right)^2}\Bigg] + (h_1\leftrightarrow h_2)\,. \tag{6.118}$$

Finally, for TT case, we obtain

$$\begin{aligned}
&\frac{d\sigma_{3TT}^{g\bar q\to h_1h_2}}{dx_{h_1}dx_{h_2}d^dp_{h_1}d^dp_{h_2}}\\
&=\frac{2\alpha_s\alpha_{\rm em}C_F}{\mu^{2\epsilon}(2\pi)^{4(d-1)}N_c}\frac{(p_0^-)^2}{s^2x_{h_1}^dx_{h_2}^d}\sum_q Q_q^2\int_{x_{h_1}}^1\frac{dx_g}{x_g}\int_{x_{h_2}}^1\frac{dx_{\bar q}}{x_{\bar q}}\,(x_gx_{\bar q})^{d-1}D_g^{h_1}\left(\frac{x_{h_1}}{x_g},\mu_F\right)\\
&\times D_{\bar q}^{h_2}\left(\frac{x_{h_2}}{x_{\bar q}},\mu_F\right)\int_0^1\frac{dx_q}{x_q}\int\frac{d^dp_{q\perp}}{(2\pi)^d}\delta(1-x_q-x_{\bar q}-x_g)\int d^dp_{1\perp}d^dp_{2\perp}\int d^dp_{1'\perp}d^dp_{2'\perp}\\
&\times\mathbf{F}\left(\frac{p_{12\perp}}{2}\right)\mathbf{F}^*\left(\frac{p_{1'2'\perp}}{2}\right)\delta\left(p_{q1\perp}+\frac{x_{\bar q}}{x_{h_2}}p_{h_2}-p_{2\perp}+\frac{x_g}{x_{h_1}}p_{h_1\perp}\right)\delta(p_{11'\perp}+p_{22'\perp})\varepsilon_{Ti}\,\varepsilon_{Tk}^*\\
&\times\Bigg[\Phi_3^i(p_{1\perp},p_{2\perp})\Phi_3^{k*}(p_{1'\perp},p_{2'\perp})-\frac{2x_q(p_\gamma^+)^2(x_g^2d+4x_q(x_q+x_g))}{\left(Q^2+\frac{\left(\frac{x_{\bar q}}{x_{h_2}}\vec{p}_{h_2}-\vec{p}_2\right)^2}{x_{\bar q}(1-x_{\bar q})}\right)\left(Q^2+\frac{\left(\frac{x_{\bar q}}{x_{h_2}}\vec{p}_{h_2}-\vec{p}_{2'}\right)^2}{x_{\bar q}(1-x_{\bar q})}\right)}\\
&\times\frac{\left((1-2x_{\bar q})^2g_\perp^{ri}g_\perp^{lk}-g_\perp^{li}g_\perp^{rk}+g_\perp^{rl}g_\perp^{ik}\right)\left(\frac{x_{\bar q}}{x_{h_2}}p_{h_2}-p_2\right)_r\left(\frac{x_{\bar q}}{x_{h_2}}p_{h_2}-p_{2'}\right)_l}{x_{\bar q}(x_q+x_g)^2\left(x_q\frac{x_g}{x_{h_1}}\vec{p}_{h_1}-x_g\vec{p}_q\right)^2}\Bigg]\\
&+(h_1\leftrightarrow h_2)\,.
\end{aligned}\tag{6.119}$$

Dipole × double-dipole contribution and double-dipole × double-dipole contribution

The dipole × double dipole contribution, for arbitrary polarization, is given by

$$
\begin{aligned}
&\frac{d\sigma_{4JI}^{g\bar{q}\to h_1h_2}}{dx_{h_1}dx_{h_2}d^dp_{h_1\perp}d^dp_{h_2\perp}}\\
&=\frac{\alpha_s\alpha_{\rm em}}{\mu^{2\epsilon}(2\pi)^{4(d-1)}N_c}\frac{(p_0^-)^2}{s^2x_{h_1}^dx_{h_2}^d}\sum_q Q_q^2\int_{x_{h_1}}^1\frac{dx_g}{x_g}\int_{x_{h_2}}^1\frac{dx_{\bar{q}}}{x_{\bar{q}}}\,(x_gx_{\bar{q}})^{d-1}D_g^{h_1}\left(\frac{x_{h_1}}{x_g},\mu_F\right)\\
&\times D_{\bar{q}}^{h_2}\left(\frac{x_{h_2}}{x_{\bar{q}}},\mu_F\right)\int_0^1\frac{dx_q}{x_q}\int\frac{d^dp_{q\perp}}{(2\pi)^d}\delta(1-x_q-x_{\bar{q}}-x_g)\int d^dp_{1\perp}d^dp_{2\perp}d^dp'_{1\perp}d^dp'_{2\perp}\\
&\times\frac{d^dp_{3\perp}d^dp'_{3\perp}}{(2\pi)^d}\delta\left(p_{q1\perp}+\frac{x_{\bar{q}}}{x_{h_2}}p_{h_2\perp}-p_{2\perp}+\frac{x_g}{x_{h_1}}p_{h_1\perp}-p_{3\perp}\right)\delta(p_{11'\perp}+p_{22'\perp}+p_{33'\perp})\\
&\times(\varepsilon_{I\alpha}\varepsilon^*_{J\beta})\left[\Phi_3^\alpha(p_{1\perp},p_{2\perp})\Phi_4^{\beta*}(p'_{1\perp},p'_{2\perp},p'_{3\perp})\mathbf{F}\left(\frac{p_{12\perp}}{2}\right)\tilde{\mathbf{F}}^*\left(\frac{p_{1'2'\perp}}{2},p'_{3\perp}\right)\delta(p_{3\perp})\right.\\
&\left.+\,\Phi_4^\alpha(p_{1\perp},p_{2\perp},p_{3\perp})\Phi_3^{\beta*}(p_{1'\perp},p_{2'\perp})\,\tilde{\mathbf{F}}\left(\frac{p_{12\perp}}{2},p_{3\perp}\right)\mathbf{F}^*\left(\frac{p_{1'2'\perp}}{2}\right)\delta(p'_{3\perp})\right]+(h_1\leftrightarrow h_2)\,.
\end{aligned}
\tag{6.120}
$$

The double-dipole × double-dipole contribution, for arbitrary polarization, is given by

$$
\begin{aligned}
&\frac{d\sigma_{5JI}^{g\bar{q}\to h_1h_2}}{dx_{h_1}dx_{h_2}d^dp_{h_1}d^dp_{h_2}}\\
&=\frac{\alpha_s\alpha_{\rm em}}{\mu^{2\epsilon}(2\pi)^{4(d-1)}(N_c^2-1)}\frac{(p_0^-)^2}{s^2x_{h_1}^dx_{h_2}^d}\sum_q Q_q^2\int_{x_{h_1}}^1\frac{dx_g}{x_g}\int_{x_{h_2}}^1\frac{dx_{\bar{q}}}{x_{\bar{q}}}\,(x_gx_{\bar{q}})^{d-1}D_g^{h_1}\left(\frac{x_{h_1}}{x_q},\mu_F\right)\\
&\times D_{\bar{q}}^{h_2}\left(\frac{x_{h_2}}{x_{\bar{q}}},\mu_F\right)\int_0^1\frac{dx_q}{x_q}\int\frac{d^dp_{q\perp}}{(2\pi)^d}\delta(1-x_q-x_{\bar{q}}-x_g)\int d^dp_{1\perp}d^dp_{2\perp}d^dp'_{1\perp}d^dp'_{2\perp}\\
&\times\int\frac{d^dp_{3\perp}d^dp'_{3\perp}}{(2\pi)^{2d}}\delta\left(p_{q1\perp}+\frac{x_{\bar{q}}}{x_{h_2}}p_{h_2\perp}-p_{2\perp}+\frac{x_g}{x_{h_1}}p_{h_1\perp}-p_{3\perp}\right)\delta(p_{11'\perp}+p_{22'\perp}+p_{33'\perp})\\
&\times(\varepsilon_{I\alpha}\varepsilon^*_{J\beta})\Phi_4^\alpha(p_{1\perp},p_{2\perp},p_{3\perp})\Phi_4^{\beta*}(p'_{1\perp},p'_{2\perp},p'_{3\perp})\tilde{\mathbf{F}}\left(\frac{p_{12\perp}}{2},p_{3\perp}\right)\tilde{\mathbf{F}}^*\left(\frac{p_{1'2'\perp}}{2},p'_{3\perp}\right)\\
&+(h_1\leftrightarrow h_2)\,.
\end{aligned}
\tag{6.121}
$$

Expression for the squared impact factors can be found in Appendix D.2. They are written in terms of $p_q, p_{\bar{q}}, p_g, z$ and the following identification should be done:

$$
p_{g\perp}=\frac{x_g}{x_{h_1}}p_{h_1\perp}\,,\quad p_{\bar{q}\perp}=\frac{x_{\bar{q}}}{x_{h_2}}p_{h_2\perp}\,,\quad z=x_g\,. \tag{6.122}
$$

6.5.4 Real corrections: Fragmentation from quark and gluon

Finite part of dipole × dipole contribution

When squaring the dipole contribution, one also gets finite terms. This time we write separately for each polarization transition. In the LL case, we have

$$
\begin{aligned}
&\frac{d\sigma_{3LL}^{qg\to h_1h_2}}{dx_{h_1}dx_{h_2}d^dp_{h_1}d^dp_{h_2}} \\
&= \frac{2\alpha_s\alpha_{\rm em}C_F}{\mu^{2\epsilon}(2\pi)^{4(d-1)}N_c}\frac{(p_0^-)^2}{s^2x_{h_1}^dx_{h_2}^d}\sum_q Q_q^2\int_{x_{h_1}}^1\frac{dx_q}{x_q}\int_{x_{h_2}}^1\frac{dx_g}{x_g}\,(x_qx_g)^{d-1}D_q^{h_1}\left(\frac{x_{h_1}}{x_q},\mu_F\right) \\
&\times D_g^{h_2}\left(\frac{x_{h_2}}{x_{\bar q}},\mu_F\right)\int_0^1\frac{dx_{\bar q}}{x_{\bar q}}\int\frac{d^dp_{\bar q\perp}}{(2\pi)^d}\delta(1-x_q-x_{\bar q}-x_g)\int d^dp_{1\perp}d^dp_{2\perp}\int d^dp_{1'\perp}d^dp_{2'\perp} \\
&\times \mathbf{F}\left(\frac{p_{12\perp}}{2}\right)\mathbf{F}^*\left(\frac{p_{1'2'\perp}}{2}\right)\delta\left(\frac{x_q}{x_{h_1}}p_{h_1\perp}-p_{1\perp}+p_{\bar q2\perp}+\frac{x_g}{x_{h_2}}p_{h_2\perp}\right)\delta(p_{11'\perp}+p_{22'\perp})\frac{Q^2}{(p_\gamma^+)^2} \\
&\times\Bigg[\Phi_3^+(p_{1\perp},p_{2\perp})\Phi_3^{+*}(p_{1'\perp},p_{2'\perp})-\frac{8x_qx_{\bar q}(p_\gamma^+)^4\left(dx_g^2+4x_{\bar q}(x_{\bar q}+x_g)\right)}{\left(Q^2+\frac{\left(\frac{x_q}{x_{h_1}}\vec p_{h_1}-\vec p_1\right)^2}{x_q(1-x_q)}\right)\left(Q^2+\frac{\left(\frac{x_q}{x_{h_1}}\vec p_{h_1}-\vec p_{1'}\right)^2}{x_q(1-x_q)}\right)} \\
&\times\frac{1}{\left(x_{\bar q}\frac{x_g}{x_{h_2}}\vec p_{h_2}-x_g\vec p_{\bar q}\right)^2}\Bigg]+(h_1\leftrightarrow h_2)\,. \qquad (6.123)
\end{aligned}
$$

For the TL case, we have

$$
\begin{aligned}
&\frac{d\sigma_{3TL}^{qg\to h_1h_2}}{dx_{h_1}dx_{h_2}d^dp_{h_1}d^dp_{h_2}} \\
&= \frac{2\alpha_s\alpha_{\rm em}C_F}{\mu^{2\epsilon}(2\pi)^{4(d-1)}N_c}\frac{(p_0^-)^2}{s^2x_{h_1}^dx_{h_2}^d}\sum_q Q_q^2\int_{x_{h_1}}^1\frac{dx_q}{x_q}\int_{x_{h_2}}^1\frac{dx_g}{x_g}\,(x_qx_g)^{d-1}D_q^{h_1}\left(\frac{x_{h_1}}{x_q},\mu_F\right) \\
&\times D_g^{h_2}\left(\frac{x_{h_2}}{x_g},\mu_F\right)\int_0^1\frac{dx_{\bar q}}{x_{\bar q}}\int\frac{d^dp_{\bar q\perp}}{(2\pi)^d}\delta(1-x_q-x_{\bar q}-x_g)\int d^dp_{1\perp}d^dp_{2\perp}d^dp_{1'\perp}d^dp_{2'\perp} \\
&\times \mathbf{F}\left(\frac{p_{12\perp}}{2}\right)\mathbf{F}^*\left(\frac{p_{1'2'\perp}}{2}\right)\delta\left(\frac{x_q}{x_{h_1}}p_{h_1\perp}-p_{1\perp}+p_{\bar q2\perp}+\frac{x_g}{x_{h_2}}p_{h_2\perp}\right)\delta(p_{11'\perp}+p_{22'\perp})\varepsilon_{Ti}^*\frac{Q}{p_\gamma^+} \\
&\times\Bigg[\Phi_3^+(p_{1\perp},p_{2\perp})\Phi_3^{i*}(p_{1'\perp},p_{2'\perp})+\frac{4x_{\bar q}\left(p_\gamma^+\right)^3(2x_q-1)\left(x_g^2d+4x_{\bar q}\left(x_{\bar q}+x_g\right)\right)}{\left(Q^2+\frac{\left(\frac{x_q}{x_{h_1}}\vec p_{h_1}-\vec p_1\right)^2}{x_q(1-x_q)}\right)\left(Q^2+\frac{\left(\frac{x_q}{x_{h_1}}\vec p_{h_1}-\vec p_{1'}\right)^2}{x_q(1-x_q)}\right)}
\end{aligned}
$$

$$\times \left.\frac{\left(\frac{x_q}{x_{h_1}}p_{h_1}-p_{1'}\right)^i}{(x_{\bar q}+x_g)\left(x_{\bar q}\frac{x_g}{x_{h_2}}\vec p_{h_2}-x_g\vec p_{\bar q}\right)^2}\right] + (h_1 \leftrightarrow h_2)\,. \tag{6.124}$$

Finally, for the TT case, we obtain

$$\begin{aligned}
&\frac{d\sigma_{3TT}^{qg\to h_1h_2}}{dx_{h_1}dx_{h_2}d^dp_{h_1}d^dp_{h_2}}\\
&=\frac{2\alpha_s\alpha_{\rm em}C_F}{\mu^{2\epsilon}(2\pi)^{4(d-1)}N_c}\frac{(p_0^-)^2}{s^2x_{h_1}^dx_{h_2}^d}\sum_q Q_q^2\int_{x_{h_1}}^1\frac{dx_q}{x_q}\int_{x_{h_2}}^1\frac{dx_g}{x_g}\,(x_qx_g)^{d-1}D_q^{h_1}\left(\frac{x_{h_1}}{x_q},\mu_F\right)\\
&\times D_g^{h_2}\left(\frac{x_{h_2}}{x_g},\mu_F\right)\int_0^1\frac{dx_{\bar q}}{x_{\bar q}}\int\frac{d^dp_{\bar q\perp}}{(2\pi)^d}\delta(1-x_q-x_{\bar q}-x_g)\int d^dp_{1\perp}d^dp_{2\perp}\int d^dp_{1'\perp}d^dp_{2'\perp}\\
&\times\mathbf{F}\left(\frac{p_{12\perp}}{2}\right)\mathbf{F}^*\left(\frac{p_{1'2'\perp}}{2}\right)\delta\left(\frac{x_q}{x_{h_1}}p_{h_1\perp}-p_{1\perp}+p_{\bar q2\perp}+\frac{x_g}{x_{h_2}}p_{h_2\perp}\right)\delta(p_{11'\perp}+p_{22'\perp})\varepsilon_{Ti}\,\varepsilon_{Tk}^*\\
&\times\left[\Phi_3^i(p_{1\perp},p_{2\perp})\Phi_3^{k*}(p_{1'\perp},p_{2'\perp})-\frac{2x_{\bar q}(p_\gamma^+)^2(x_g^2d+4x_{\bar q}(x_{\bar q}+x_g))}{\left(Q^2+\frac{\left(\frac{x_q}{x_{h_1}}\vec p_{h_1}-\vec p_1\right)^2}{x_q(1-x_q)}\right)\left(Q^2+\frac{\left(\frac{x_q}{x_{h_1}}\vec p_{h_1}-\vec p_{1'}\right)^2}{x_q(1-x_q)}\right)}\right.\\
&\left.\times\frac{\left((1-2x_q)^2g_\perp^{ir}g_\perp^{lk}-g_\perp^{il}g_\perp^{rl}+g_\perp^{ik}g_\perp^{lr}\right)\left(\frac{x_q}{x_{h_1}}p_{h_1}-p_1\right)_r\left(\frac{x_q}{x_{h_1}}p_{h_1}-p_{1'}\right)_l}{x_q(x_{\bar q}+x_g)^2\left(x_{\bar q}\frac{x_g}{x_{h_2}}\vec p_{h_2}-x_g\vec p_{\bar q}\right)^2}\right]\\
&+(h_1\leftrightarrow h_2)\,.
\end{aligned}\tag{6.125}$$

Dipole × double-dipole contribution and double-dipole × double-dipole contribution

The dipole × double dipole contribution is given, for arbitrary polarization, by

$$\begin{aligned}
&\frac{d\sigma_{4JI}^{q\bar q\to h_1h_2}}{dx_{h_1}dx_{h_2}d^dp_{h_1\perp}d^dp_{h_2\perp}}\\
&=\frac{\alpha_s\alpha_{\rm em}}{\mu^{2\epsilon}(2\pi)^{4(d-1)}N_c}\frac{(p_0^-)^2}{s^2x_{h_1}^dx_{h_2}^d}\sum_q Q_q^2\int_{x_{h_1}}^1\frac{dx_q}{x_q}\int_{x_{h_2}}^1\frac{dx_g}{x_g}\,(x_qx_g)^{d-1}D_q^{h_1}\left(\frac{x_{h_1}}{x_q},\mu_F\right)\\
&\times D_g^{h_2}\left(\frac{x_{h_2}}{x_g},\mu_F\right)\int_0^1\frac{dx_{\bar q}}{x_{\bar q}}\int\frac{d^dp_{\bar q\perp}}{(2\pi)^d}\delta(1-x_q-x_{\bar q}-x_g)\int d^dp_{1\perp}d^dp_{2\perp}d^dp'_{1\perp}d^dp'_{2\perp}\\
&\times\frac{d^dp_{3\perp}d^dp'_{3\perp}}{(2\pi)^d}\delta\left(\frac{x_q}{x_{h_1}}p_{h_1\perp}-p_{1\perp}+p_{\bar q2\perp}+\frac{x_g}{x_{h_2}}p_{h_2\perp}-p_{3\perp}\right)\delta(p_{11'\perp}+p_{22'\perp}+p_{33'\perp})\\
&\times(\varepsilon_{I\alpha}\varepsilon_{J\beta}^*)\left[\Phi_3^\alpha(p_{1\perp},p_{2\perp})\Phi_4^{\beta*}(p'_{1\perp},p'_{2\perp},p'_{3\perp})\mathbf{F}\left(\frac{p_{12\perp}}{2}\right)\tilde{\mathbf{F}}^*\left(\frac{p_{1'2'\perp}}{2},p'_{3\perp}\right)\delta(p_{3\perp})\right.
\end{aligned}\tag{6.126}$$

$$+\,\Phi_4^{\alpha}(p_{1\perp},p_{2\perp},p_{3\perp})\Phi_3^{\beta *}(p_{1'\perp},p_{2'\perp})\,\tilde{\mathbf{F}}\left(\frac{p_{12\perp}}{2},p_{3\perp}\right)\mathbf{F}^{*}\left(\frac{p_{1'2'\perp}}{2}\right)\delta(p'_{3\perp})\Big]+(h_1\leftrightarrow h_2)\,.$$

The double-dipole × double-dipole contribution is given, for arbitrary polarization, by

$$\begin{aligned}
&\frac{d\sigma_{5JI}^{q\bar{q}\to h_1h_2}}{dx_{h_1}dx_{h_2}d^dp_{h_1}d^dp_{h_2}}\\
&=\frac{\alpha_s\alpha_{\rm em}}{\mu^{2\epsilon}(2\pi)^{4(d-1)}(N_c^2-1)}\frac{(p_0^-)^2}{s^2x_{h_1}^dx_{h_2}^d}\sum_q Q_q^2\int_{x_{h_1}}^1\frac{dx_q}{x_q}\int_{x_{h_2}}^1\frac{dx_g}{x_g}\,(x_qx_g)^{d-1}D_q^{h_1}\left(\frac{x_{h_1}}{x_q},\mu_F\right)\\
&\times D_g^{h_2}\left(\frac{x_{h_2}}{x_g},\mu_F\right)\int_0^1\frac{dx_{\bar{q}}}{x_{\bar{q}}}\int\frac{d^dp_{\bar{q}\perp}}{(2\pi)^d}\delta(1-x_q-x_{\bar{q}}-x_g)\int d^dp_{1\perp}d^dp_{2\perp}d^dp'_{1\perp}d^dp'_{2\perp}\\
&\times\int\frac{d^dp_{3\perp}d^dp'_{3\perp}}{(2\pi)^{2d}}\delta\left(\frac{x_q}{x_{h_1}}p_{h_1\perp}-p_{1\perp}+p_{\bar{q}2\perp}+\frac{x_g}{x_{h_2}}p_{h_2\perp}-p_{3\perp}\right)\delta(p_{11'\perp}+p_{22'\perp}+p_{33'\perp})\\
&\times(\varepsilon_{I\alpha}\varepsilon^*_{J\beta})\Phi_4^{\alpha}(p_{1\perp},p_{2\perp},p_{3\perp})\Phi_4^{\beta *}(p'_{1\perp},p'_{2\perp},p'_{3\perp})\tilde{\mathbf{F}}\left(\frac{p_{12\perp}}{2},p_{3\perp}\right)\tilde{\mathbf{F}}^{*}\left(\frac{p_{1'2'\perp}}{2},p'_{3\perp}\right)\\
&+(h_1\leftrightarrow h_2)\,.
\end{aligned}\tag{6.127}$$

Expression for the squared impact factors can be found in Appendix D.2. They are written in terms of $p_q, p_{\bar{q}}, p_g, z$ and the following identification should be done:

$$p_{q\perp}=\frac{x_q}{x_{h_1}}p_{h_1\perp}\,,\quad p_{g\perp}=\frac{x_g}{x_{h_2}}p_{h_2\perp}\,,\quad z=x_g\,.\tag{6.128}$$

6.6 Summary and outlook

We have considered the diffractive production of a pair of hadrons at large p_T, in $\gamma^{(*)}$ nucleon/nucleus scattering, at NLO, in the most general kinematics in the eikonal approximation.

This new class of processes provides an access to precision physics of gluon saturation dynamics, with very promising future phenomenological studies both at the LHC in UPC (in photoproduction) and at the future EIC (both in photoproduction and leptoproduction). Our main result is the explicit finite result for the cross section at NLO, obtained after showing explicitly the cancellation of rapidity divergences (through the B-JIMWLK equation), soft divergences and collinear divergences between real, virtual contributions, and DGLAP evolution equation governing fragmentation functions. Finite contributions and purely divergent contributions have been separated and the sum of the latter has been shown to be zero. Hence, the collection of all terms labeled with "fin" in sections 6.2, 6.3, 6.4, plus all the formulas in section 6.5 give the final result. The natural continuation of this work is to evaluate the cross sections numerically, employing a model for the

description of the target, such as the McLerran Venugopalan (MV) [204, 205, 206] or the Golec-Biernat Wusthoff (GBW) [207] ones.

This NLO result adds a new piece in the list of processes which are very promising to probe gluonic saturation in nucleons and nuclei at NLO, including inclusive DIS [208, 209], photon-dijet production in DIS [210], dijets in DIS [211, 212], single hadron [213] and dihadrons production in DIS [214, 215], diffractive exclusive dijets [198, 203, 216] and exclusive light meson production [217, 218], exclusive quarkonium production [219, 220], and inclusive DDIS [221].

Chapter 7

Final thoughts and outlook

Deep questions answered, deeper questions posed.
Sir. Roger Penrose [222]

In the present work, we have presented a series of results aimed at reaching an era of precision in the high-energy factorization (HEF) framework, both in the linear and non-linear evolution regimes. To this aim we provided:

- The next-to-leading order correction to the impact factor (vertex) for the production of a forward Higgs boson, in the infinite top-mass limit. We obtained the result both in the momentum representation and as superposition of the eigenfunctions of the leading-order BFKL kernel. As already mentioned earlier, this impact factor allows to describe the inclusive hadroproduction of a forward Higgs in the limit of small Bjorken x, as well as the more interesting case of the inclusive forward emissions of a Higgs boson in association with a backward identified object.

- Predictions for a number of partially inclusive processes featuring a forward-plus-backward two-particle final-state configuration. They provide stringent tests for BFKL dynamics at the LHC.

- The computation of the Lipatov vertex in QCD within accuracy ϵ^2, which can be used for several purposes. The most important one is the computation of one of the contributions to the BFKL kernel in the NNLLA. Other include the proof of gluon Reggeization and the calculation of discontinuites of multiple production amplitudes in the MRK (which must be taken into account in the NNLLA).

- The next-to-leading order cross sections for the diffractive production of a pair of hadrons at large p_T, in $\gamma^{(*)}$ nucleon/nucleus scattering, at NLO, in the most general kinematics. This new class of processes gives access to precision physics of gluon saturation dynamics, with very promising phenomenological studies both at the LHC in UPC (in photoproduction) and at the future EIC (both in photoproduction and leptoproduction).

Since the pioneering works of Balitsky, Fadin, Kuraev and Lipatov, the BFKL approach (along with its extensions) and more in general the high-energy factorization framework have proven to be among the most powerful tools for understanding several aspects of QCD and more in general of QFTs, an incomplete list of them includes:

- The proton structure at small Bjorken-x and various class of processes featuring a forward-plus-backward two-particle final-state configuration [86].

- The asymptotic behaviour of partonic scattering amplitudes in QCD and in $\mathcal{N} = 4$ Super Yang-Mills theories [96, 97, 223, 224, 225].

- The connection between high-energy scattering and exactly solvable models [226, 227].

- The duality between the Pomeron in the maximally extended $\mathcal{N} = 4$ super symmetry and the Reggeized graviton in the 10-dimensional anti-de-Sitter space [228].

Regardless of the sheer elegance of its theoretical formulation, as shown in Chapter 3, the high-energy factorization is an important tool for achieving accuracy at modern accelerators such as the EIC and the LHC. The impact of high-energy resummation is expected to grow in the future and, as already shown in recent studies [229, 230, 231], important production channels at the new generation of colliders such as the FCC, will receive such large contributions that they will make the physics of those energies the BFKL physics.

In order to continue what started in this thesis and more generally by the scientific community of the sector, there are many developments that, in our opinion, it is necessary to consider in the near future.

Combined resummations and central productions

In Chapter 3, and especially when we discussed the p_T-distribution of the Higgs, we pointed out how different resummation mechanisms come into play in the description of this observable. It is important to note that while developing calculations at the frontier in high-energy resummation does not guarantee the absence of residual large logarithmic corrections, of a different nature, that can spoil the stability of the results and must therefore be resummed in a closed form. For example, the jet impact factor at NLO (projected onto the LO eigenfunctions of the BFKL kernel) has contributions of the type

$$\int_\alpha^1 \frac{d\zeta}{\zeta} f_q\left(\frac{\alpha}{\zeta}\right)\left(\frac{\ln(1-\zeta)}{1-\zeta}\right)_+ ,$$

where f_q is the quark PDF. These contributions are not divergent due to the +-prescription structure, but contain logarithmically large corrections at the threshold $\alpha \to 1$. Moreover, because of the +-prescription structure, these logarithms will multiply the derivative of the PDF (which is not small for $\alpha \to 1$). Similar contributions can also be found in the NLO hadron impact factor. Another example is represented by the forward Higgs boson cross section, at small transverse momentum. Here, we expect also Sudakov-type logarithmically large contributions. Perhaps, it would be extremely interesting to supplement the calculations with a resummation of such enhanced corrections in a Sudakov-like manner [232]. One of the great challenges for the future is precisely the construction of versatile formalisms that can accommodate different types of resummations.

In the thesis, we have extensively used the concept of *hybrid high-energy/collinear factorization*. It is important to stress that the present ansatz of factorization does not provide a complete interpolation between collinear and high-energy resummations. The underlying idea of this factorization is that even if collinear information is inserted for a correct treatment of the initial and/or final state IR-singularities, the dominant dynamic is that of BFKL-type logarithms. In this way, collinear dynamics is considered in the impact factors only. However, it is well known that collinearly enhanced NLO corrections to the BFKL kernel can be sizable. One of the approaches to improve this lack is the BLM procedure for the scale fixing [147, 148, 149, 150], that leads to a suppression of the NLO corrections. An alternative is an all order resummation of the collinearly enhanced terms, also called *collinear improvement* [233, 234, 235, 236, 237]. In the future, it would be interesting to consider the impact of collinear improvement on some of the observables seen in the thesis [85, 238].

Lastly, within the high-energy factorization, remarkable results have been produced in the context of forward and forward/backward productions. However, as highlighted in [229], at the next generation of accelerators, the high energy corrections will be large also in the central productions, making also the calculation of impact factors in the central region of rapidity very important. In this context, to date a single next-to-leading calculation has been performed [239] (the central jet). The calculation of these amplitudes requires evaluating $2 \to 3$ amplitudes, such as the one used to extract the Lipatov vertex.

Hypothesis on the remainder function of the BDS ansatz

In chapter 4 we computed the Lipatov vertex in QCD with the required ϵ-accuracy to construct one of the contribution to the BFKL kernel in the next-to-next-to leading logarithmic approximation. The result obtained is suitable for the purpose, since to obtain the part of the kernel containing the product of two one-loop RRG vertices, the integration over the phase space is that over a single particle and therefore completely trivial. This result is furthermore supplemented by the knowledge of the vertex at arbitrary ϵ in the soft limit of the emited particle.

However, we briefly mentioned at the beginning of the chapter that the discontinuities of multiple gluon production amplitudes in the MRK are interesting also from another point of view. They can be used [171] for a simple demonstration of violation of the ABDK-BDS (Anastasiou-Bern-Dixon-Kosower — Bern-Dixon-Smirnov) ansatz [172, 173] for amplitudes with maximal helicity violation (MHV) in Yang-Mills theories with maximal supersymmetry ($\mathcal{N} = 4$ SYM) in the planar limit and for the calculations of the remainder functions to this ansatz. There are two hypothesis about the remainder functions: the hypothesis of dual conformal invariance [240, 241], which asserts that the MHV amplitudes are given by products of the BDS amplitudes and that the remainder functions depend only on anharmonic ratios of kinematic invariants, and the hypothesis of scattering amplitude/Wilson loop correspondence [242, 243, 244, 245], according to which the remainder functions are given by expectation values of Wilson loops. Both these hypotheses are not proved. They can be tested by comparison of the BFKL discontinuities with the discontinuities calculated with the use of these hypothesis [246, 247].

To this aim, impact factors for the Reggeon-gluon transition, which are the natural

generalization of the impact factors for the particle-particle transitions, entering the discontinuities of elastic amplitudes, must be constructed with higher ϵ-accuracy. Again, the Lipatov vertex (in $\mathcal{N}=4$ SYM) will be part of these impact factors. Also in $\mathcal{N}=4$ SYM, the pentagon in $6+2\epsilon$ contributes to the vertex [174], which implies that the great complications that appear in QCD are also present in this theory. For the computation of the remainder functions non-trivial convolutions of impact factors are required, which impliy that a form as simple as possible of the vertex is required. Attacking this calculation, in our opinion, requires finding a more manageable expression of the second contribution in Eq. (4.91), which is one of our plans for the future.

BFKL vs B-JIMWLK and NNLL resummation

In this thesis, we presented works aimed at testing both BFKL and saturation dynamics. As explained in Chapter 5, the B-JIMWLK hierarchy of equations contains different aspects of small-x physics compared to the BFKL one. One of these is that saturation effects in large nuclei are emphasized, as can be understood from Eq. (5.3). Here, the atomic number dependence is due to presence of multiple re-scatterings in a large enough nucleus. This leads to an additional resummation parameters $\alpha_s^2 A^{1/3}$. The physical meaning of the parameter $\alpha_s^2 A^{1/3}$ is rather straightforward: at a given impact parameter the dipole interacts with $A^{1/3}$ nucleons, exchanging two gluons with each (two-gluon exchange is parametrically of order α_s^2). However, in small nuclei or a proton, the BFKL dynamics is expected to precede the onset of saturation physics. It is the opinion of the author and collaborators that considering observables in which predictions can be built both in the linear regime (à la BFKL) and in the effective Shockwave/CGC approaches, perhaps in a full NLLA, could help to find the point at which saturation effects modify the shape of BFKL predictions.

Last but not least, it is interesting to point out a different connection between the BFKL and the Shockwave approach. To date, after more than twenty-five years since the NLO corrections to BFKL were obtained, as explained in section 4.1, the problem of NNLO corrections remains opened and challenging. From a conceptual point of view, the main reason is that the pole Regge form of QCD amplitudes is violated in the NNLLA, as observed by direct computation at two-and three-loop. There exist two approaches for the explanation of this violation:

- The first has been developed in [175, 181] and employs the contribution of the cut alone to explain this phenomenon, considering triple Reggeon exchange.

- The second is an effective approach based on the Shockwave formalism (as formulated in [248]). In this approach, the phenomenon of gluon Reggeization, that we have discussed in Chapter 1 of the thesis essentially comes out from the fundamental ingredients of the Shockwave formalism: rapidity factorization and eikonal Wilson lines. It is revealed by expanding the Wilson lines close to the identity. In particular, the logarithm of a Wilson line is used as a gauge-invariant interpolating operator for a Reggeized gluon. In this context, the above violation is interpreted in terms of triple Reggeon exchange (Regge cut) and, in addition, its mixing with a single Reggeon [182].

Even not being a formal proof, the validity of these approaches may be confirmed or questioned in the four loop approximation [249], upon comparing their results with the results of four-loop calculations performed by the infrared-factorization method. In any case, the assertion that the QCD amplitudes with gluon quantum numbers in cross-channels and negative signature are given in the NNLLA, to all orders in perturbation theories, by the contributions of the Regge pole and the three-Reggeon cut (with or without mixing) is still only an hypothesis. It is our personal opinion that this problem undoubtedly represents one of the most fascinating aspects in the study of scattering amplitudes in non-Abelian gauge theories.

Appendix A

Further details on the Higgs impact factor

For consistency with individual papers, definitions of some special functions are repeated in different appendices.

A.1 Feynman rules of the gluon-Higgs effective field theory and definitions

In this Appendix we give more details about the gluon-Higgs effective theory. The Feynman rules associated to the Lagrangian (2.1) and used in this work are shown in Fig. A.1. The tensor structures appearing in Fig. A.1 are

$$H^{\mu\nu}(p_1, p_2) = g^{\mu\nu}(p_1 \cdot p_2) - p_1^\nu p_2^\mu \,, \tag{A.1}$$

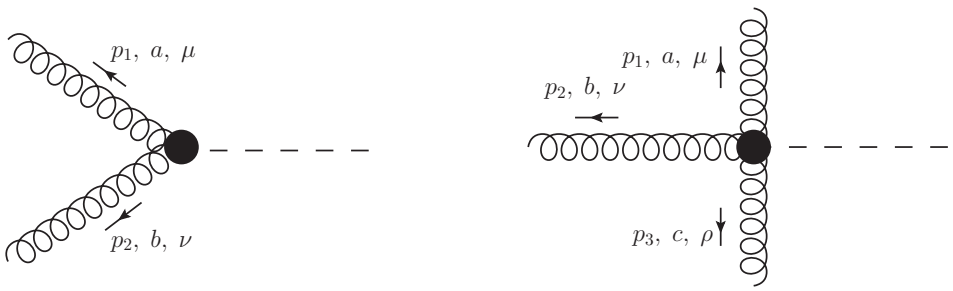

$(a)\ \ ig_H\delta^{ab}H^{\mu\nu}(p_1,p_2)$ $(b)\ \ g_H g f^{abc}V^{\mu\nu\rho}(p_1,p_2,p_3)$

Figure A.1: Feynman rule for the (a) ggH vertex and (b) $gggH$ vertex.

$$V^{\mu\nu\rho}(p_1,p_2,p_3) = (p_1-p_2)^\rho g^{\mu\nu} + (p_2-p_3)^\mu g^{\nu\rho} + (p_3-p_1)^\nu g^{\rho\mu} \ . \tag{A.2}$$

It is important to note that, as in QCD, in using Feynman rules for this theory, symmetry factors must be taken into account correctly. In particular, the first and second diagram in the Fig. 2.7 require a symmetry factor $S = 1/2$.
We also define here some useful functions used in the main text:

$$\psi(z) = \frac{\Gamma'(z)}{\Gamma(z)} \ , \quad \psi'(z) = \frac{d}{dz}\psi(z) \ , \quad H_n = \gamma_E + \psi(n+1) \ , \tag{A.3}$$

$$\mathrm{Li}_2(z) = -\int_0^z \frac{\ln(1-t)}{t}dt = -\int_0^1 \frac{\ln(1-zt)}{t}dt \ , \tag{A.4}$$

$${}_2F_1(a,b,c,z) = \frac{1}{\mathcal{B}(b,c-b)}\int_0^1 dx\, x^{b-1}(1-x)^{c-b-1}(1-zx)^{-a} \quad \text{for} \quad \Re\mathrm{e}\{\mathrm{c}\} > \Re\mathrm{e}\{\mathrm{b}\} > 0 \ , \tag{A.5}$$

where $\mathcal{B}$ is the Euler beta function and z is not a real number such that it is greater than or equal to 1. It is useful to show the behaviour for $z \to 1^-$ of the hypergeometric function:

- If $\Re e\{c\} > \Re e\{a+b\}$, then

$${}_2F_1(a,b,c,1) = \frac{\Gamma(c)\Gamma(c-a-b)}{\Gamma(c-a)\Gamma(c-b)} \ . \tag{A.6}$$

- If $\Re e\{c\} = \Re e\{a+b\}$, then

$$\lim_{z\to 1^-} \frac{{}_2F_1(a,b,a+b,z)}{-\ln(1-z)} = \frac{\Gamma(a+b)}{\Gamma(a)\Gamma(b)} \quad \text{for} \ \ c = a+b \ , \tag{A.7}$$

  and

$$\lim_{z\to 1^-} (1-z)^{a+b-c}\left({}_2F_1(a,b,c,z) - \frac{\Gamma(c)\Gamma(c-a-b)}{\Gamma(c-a)\Gamma(c-b)}\right) = \frac{\Gamma(c)\Gamma(a+b-c)}{\Gamma(a)\Gamma(b)} \tag{A.8}$$

  for $c \neq a+b$.

- If $\Re e\{c\} < \Re e\{a+b\}$, then

$$\lim_{z\to 1^-} \frac{{}_2F_1(a,b,c,z)}{(1-z)^{c-a-b}} = \frac{\Gamma(c)\Gamma(a+b-c)}{\Gamma(a)\Gamma(b)} \ . \tag{A.9}$$

A.2 Integrals for the virtual corrections

We give here definition and result of Feynman integrals that appear in the calculation of the virtual corrections. The integrals B_0 and C_0 can be found also in the Appendix A of Ref. [47], the integral D_0 in Ref. [250] (see also Ref. [251]).[50] Concerning integrals with two denominators, we have

$$B_0(-\vec{q}^{\,2}) = \int \frac{d^Dk}{i(2\pi)^D}\frac{1}{k^2(k+q)^2} = -\frac{1}{(4\pi)^{2-\epsilon}}\frac{\Gamma(1+\epsilon)\Gamma^2(-\epsilon)}{2(1-2\epsilon)\Gamma(-2\epsilon)}(\vec{q}^{\,2})^{-\epsilon}\,, \tag{A.10}$$

$$B_0(m_H^2) = \int \frac{d^Dk}{i(2\pi)^D}\frac{1}{k^2(k+p_H)^2} = -\frac{1}{(4\pi)^{2-\epsilon}}\frac{\Gamma(1+\epsilon)\Gamma^2(-\epsilon)}{2(1-2\epsilon)\Gamma(-2\epsilon)}(-m_H^2)^{-\epsilon}\,. \tag{A.11}$$

Independent integrals with three denominators appearing in the computation are

$$C_0(m_H^2,0,-\vec{q}^{\,2}) = C_0(0,-\vec{q}^{\,2},m_H^2) = \int \frac{d^Dk}{i(2\pi)^D}\frac{1}{k^2(k+q)^2(k+p_H)^2}$$

$$= \frac{1}{(4\pi)^{2-\epsilon}}\frac{\Gamma(1+\epsilon)\Gamma^2(-\epsilon)}{2\Gamma(-2\epsilon)}\frac{1}{\epsilon}\frac{\left((\vec{q}^{\,2})^{-\epsilon}-(-m_H^2)^{-\epsilon}\right)}{m_H^2+\vec{q}^{\,2}}\,, \tag{A.12}$$

$$C_0(0,0,-\vec{q}^{\,2}) = \int \frac{d^Dk}{i(2\pi)^D}\frac{1}{k^2(k+q)^2(k+k_2)^2} = \frac{1}{(4\pi)^{2-\epsilon}}\frac{\Gamma(1+\epsilon)\Gamma^2(-\epsilon)}{2\Gamma(-2\epsilon)}\frac{1}{\epsilon}(\vec{q}^{\,2})^{-\epsilon-1}\,, \tag{A.13}$$

$$C_0(m_H^2,0,s) = \int \frac{d^Dk}{i(2\pi)^D}\frac{1}{k^2(k+p_H)^2(k+k_1+k_2)^2}$$

$$\simeq -\frac{1}{(4\pi)^{2-\epsilon}}\frac{\Gamma(1+\epsilon)\Gamma^2(-\epsilon)}{2\Gamma(-2\epsilon)}\frac{1}{\epsilon}\frac{\left((-s)^{-\epsilon}-(-m_H^2)^{-\epsilon}\right)}{s}\,, \tag{A.14}$$

$$C_0(0,0,s) = \int \frac{d^Dk}{i(2\pi)^D}\frac{1}{k^2(k-k_1)^2(k+k_2)^2} = \frac{1}{(4\pi)^{2-\epsilon}}\frac{\Gamma(1+\epsilon)\Gamma^2(-\epsilon)}{2\Gamma(-2\epsilon)}\frac{1}{\epsilon}(-s)^{-\epsilon-1}\,, \tag{A.15}$$

There is only one relevant four-denominator integral,

$$D_0(m_H^2,0,0,0;-\vec{q}^{\,2},s) = \int \frac{d^Dk}{i(2\pi)^D}\frac{1}{k^2(k+p_H)^2(k+q)^2(k-k_2')^2}$$

$$= \frac{\Gamma(1+\epsilon)\Gamma^2(-\epsilon)}{(4\pi)^{2-\epsilon}\vec{q}^{\,2}s}\frac{1}{\epsilon\Gamma(-2\epsilon)}\Big[(\vec{q}^{\,2})^{-\epsilon}+(-s)^{-\epsilon}-\left(-m_H^2\right)^{-\epsilon} \tag{A.16}$$

[50] In our notation the subscript 0 means that all propagators appearing in the integral are massless. The arguments in the definitions of B_0 and C_0 integrals below represent the squared of the external momenta on which they depend. D_0, in addition to the four squared of the external momenta, depends also on the two independent Mandelstam variables typical of a $2 \to 2$ process.

$$-\epsilon^2\left(\mathrm{Li}_2\left(1+\frac{m_H^2}{\vec{q}^{\,2}}\right)+\frac{1}{2}\ln^2\left(-\frac{\vec{q}^{\,2}}{s}\right)+\frac{\pi^2}{3}\right)\Bigg]+\mathcal{O}(\epsilon)\ ,$$

where $k_2' = k_2 - q$ and $(p_H + k_2')^2 = (k_1 + k_2)^2 = s$. The definition of the integrals $C_0(m_H^2, 0, -s)$, $C_0(0, 0, -s)$, $D_0(m_H^2, 0, 0, 0; -\vec{q}^{\,2}, -s)$ can be obtained by exchanging k_2 and $-k_2'$; the result for these integrals is obviously obtained through the $s \to -s$ transformation. We observe that what said above is valid in the Regge limit; it allows us to neglect m_H^2 and $\vec{q}^{\,2}$ when these appear summed to s.

A.3 Master Integrals for the projection

For the projection onto the eigenfunctions of the BFKL kernel we just need the following integrals:

$$I_1(\gamma_1,\gamma_2,n,\nu)=\int\frac{d^{2-2\epsilon}\vec{q}}{\pi\sqrt{2}}(\vec{q}^{\,2})^{i\nu-\frac{3}{2}}e^{in\phi}(\vec{q}^{\,2})^{-\gamma_1}\left[(\vec{q}-\vec{p}_H)^2\right]^{-\gamma_2}\ ,$$

$$I_2(\gamma_1,n,\nu)=\int\frac{d^{2-2\epsilon}\vec{q}}{\pi\sqrt{2}}(\vec{q}^{\,2})^{i\nu-\frac{3}{2}}e^{in\phi}(\vec{q}^{\,2})^{-\gamma_1}\frac{1}{[(\vec{q}-\vec{p}_H)^2]\left[(1-z_H)m_H^2+(\vec{p}_H-z_H\vec{q})^2\right]}\ ,$$

$$I_3(\gamma_1,\gamma_2,n,\nu)=\int\frac{d^{2-2\epsilon}\vec{q}}{\pi\sqrt{2}}(\vec{q}^{\,2})^{i\nu-\frac{3}{2}}e^{in\phi}(\vec{q}^{\,2})^{-\gamma_1}\left[(1-z_H)m_H^2+(\vec{p}_H-z_H\vec{q})^2\right]^{-\gamma_2}\ .$$

We note that

$$\lim_{z_H\to 1} I_2(\gamma_1,n,\nu) = I_1(\gamma_1,2,n,\nu)\ , \tag{A.17}$$

$$\lim_{z_H\to 1} I_3(\gamma_1,\gamma_2,n,\nu) = I_1(\gamma_1,\gamma_2,n,\nu)\ . \tag{A.18}$$

We show here the explicit calculation of the most complicated one, I_2 and just quote the result for the other two. First, we introduce the vector $l \equiv (1, i)$ and write

$$e^{in\phi}=(\cos\phi+i\sin\phi)^n=\left(\frac{q_x+iq_y}{|\vec{q}\,|}\right)^n=\frac{(\vec{q}\cdot\vec{l}\,)^n}{(\vec{q}^{\,2})^{\frac{n}{2}}}\ . \tag{A.19}$$

Then, after Feynman parameterization and the shift

$$\vec{q}\to\vec{q}+\left(x+\frac{y}{z_H}\right)\vec{p}_H \tag{A.20}$$

one finds

$$I_2(\gamma_1,n,\nu)=\frac{1}{z_H^2}\frac{\Gamma\left(\frac{7}{2}+\gamma_1+\frac{n}{2}-i\nu\right)}{\Gamma\left(\frac{3}{2}+\gamma_1+\frac{n}{2}-i\nu\right)}\int\frac{d^{2-2\epsilon}\vec{q}}{\pi\sqrt{2}}\int_0^1 dx\int_0^{1-x}dy(1-x-y)^{\frac{1}{2}+\gamma_1+\frac{n}{2}-i\nu}$$

$$\frac{\left[\vec{q}\cdot\vec{l}+\left(x+\frac{y}{z_H}\right)\vec{p}_H\cdot\vec{l}\right]^n}{\left[\vec{q}^{\,2}-\left(x+\frac{y}{z_H}\right)^2\vec{p}_H^{\,2}+x\vec{p}_H^{\,2}+y\left(\tilde{m}_H^2+\frac{\vec{p}_H^{\,2}}{z_H^2}\right)\right]^{\frac{7}{2}+\gamma_1+\frac{n}{2}-i\nu}}\ , \tag{A.21}$$

where $\tilde{m}_H^2=\frac{(1-z_H)m_H^2}{z_H^2}$. Now, we expand the binomial in the numerator as

$$\left[\vec{q}\cdot\vec{l}+\left(x+\frac{y}{z_H}\right)\vec{p}_H\cdot\vec{l}\right]^n=\sum_{j=0}^{n}\binom{n}{j}(\vec{q}\cdot\vec{l})^j\left(x+\frac{y}{z_H}\right)^{n-j}(\vec{p}_H\cdot\vec{l})^{n-j} \tag{A.22}$$

and observe that only the term with $j=0$ survives. At this point, we are able to obtain the simple form,

$$I_2(\gamma_1,n,\nu)=\frac{(\vec{p}_H^{\,2})^{\frac{n}{2}}e^{in\phi_H}}{z_H^2}\frac{\Gamma\left(\frac{7}{2}+\gamma_1+\frac{n}{2}-i\nu\right)}{\Gamma\left(\frac{3}{2}+\gamma_1+\frac{n}{2}-i\nu\right)}$$
$$\times\int_0^1 dx\int_0^{1-x}dy(1-x-y)^{\frac{1}{2}+\gamma_1+\frac{n}{2}-i\nu}\left(x+\frac{y}{z_H}\right)^n\int\frac{d^{2-2\epsilon}\vec{q}}{\pi\sqrt{2}}\frac{1}{[\vec{q}^{\,2}+L]^{\frac{7}{2}+\gamma_1+\frac{n}{2}-i\nu}}\ , \tag{A.23}$$

where

$$L=x\vec{p}_H^{\,2}+y\left(\tilde{m}_H^2+\frac{\vec{p}_H^{\,2}}{z_H^2}\right)-\left(x+\frac{y}{z_H}\right)^2\vec{p}_H^{\,2}\ . \tag{A.24}$$

Finally, we can integrate over $\vec{q}$ and then make the change of variables

$$x=\lambda\Delta\ ,\quad y=\lambda(1-\Delta)\ , \tag{A.25}$$

to obtain

$$I_2(\gamma_1,n,\nu)=\frac{(\vec{p}_H^{\,2})^{\frac{n}{2}}e^{in\phi_H}}{z_H^2\sqrt{2}\pi^\epsilon}\frac{\Gamma\left(\frac{5}{2}+\gamma_1+\frac{n}{2}-i\nu+\epsilon\right)}{\Gamma\left(\frac{3}{2}+\gamma_1+\frac{n}{2}-i\nu\right)}\int_0^1 d\Delta\left(\Delta+\frac{(1-\Delta)}{z_H}\right)^n\ ,$$
$$\left[\left(\Delta+\frac{(1-\Delta)}{z_H^2}\right)\vec{p}_H^{\,2}+(1-\Delta)\tilde{m}_H^{\,2}\right]^{-\frac{5}{2}-\gamma_1-\frac{n}{2}+i\nu-\epsilon}\int_0^1 d\lambda\ \lambda^{-\frac{3}{2}-\gamma_1+\frac{n}{2}+i\nu-\epsilon}$$
$$\times(1-\lambda)^{\frac{1}{2}+\gamma_1+\frac{n}{2}-i\nu}(1-\lambda\zeta)^{-\frac{5}{2}-\gamma_1-\frac{n}{2}+i\nu-\epsilon}\ , \tag{A.26}$$

where

$$\zeta=\frac{\left(\Delta+\frac{(1-\Delta)}{z_H}\right)^2\vec{p}_H^{\,2}}{\left[\left(\Delta+\frac{(1-\Delta)}{z_H^2}\right)\vec{p}_H^{\,2}+\frac{(1-\Delta)(1-z_H)m_H^2}{z_H^2}\right]}\ . \tag{A.27}$$

It is easy to see that the integral over λ gives a representation of the hypergeometric function. By using Eq. (A.5) we arrive at the final form

$$I_2(\gamma_1,n,\nu)=\frac{(\vec{p}_H^{\,2})^{\frac{n}{2}}e^{in\phi_H}}{z_H^2\sqrt{2}\pi^\epsilon}\left[\frac{\Gamma\left(\frac{5}{2}+\gamma_1+\frac{n}{2}-i\nu+\epsilon\right)\Gamma\left(-\frac{1}{2}-\gamma_1+\frac{n}{2}+i\nu-\epsilon\right)}{\Gamma\left(1+n-\epsilon\right)}\right]$$

$$\times \int_0^1 d\Delta \left(\Delta + \frac{(1-\Delta)}{z_H}\right)^n \left[\left(\Delta + \frac{(1-\Delta)}{z_H^2}\right)\vec{p}_H^{\,2} + \frac{(1-\Delta)(1-z_H)m_H^2}{z_H^2}\right]^{-\frac{5}{2}-\gamma_1+i\nu-\frac{n}{2}-\epsilon}$$
$$\times {}_2F_1\left(-\frac{1}{2}-\gamma_1+\frac{n}{2}+i\nu-\epsilon, \frac{5}{2}+\gamma_1-i\nu+\frac{n}{2}+\epsilon, 1+n-\epsilon, \zeta\right) . \quad (A.28)$$

It is very important to note that this integral is indeed divergent for every $\epsilon > -1$ (see the asymptotic behaviors of the hypergeometric function in Appendix A). It is important to extract the divergent contribution of the integral I_2 in the form of a pole in ϵ. For this purpose, we take the limit $\Delta \to 1$ in the integrand of I_2. Using Eq. (A.9), we have, up to terms $\mathcal{O}(\epsilon)$,

$$I_{2,\text{as}}(\gamma_1, n, \nu) = \frac{(\vec{p}_H^{\,2})^{-\frac{3}{2}-\gamma_1+i\nu-\epsilon} e^{in\phi_H}\Gamma(1+\epsilon)}{(1-z_H)\sqrt{2}\pi^\epsilon} \frac{1}{(m_H^2+(1-z_H)\vec{p}_H^{\,2})} \int_0^1 d\Delta (1-\Delta)^{-\epsilon-1}$$
$$= -\frac{1}{\epsilon}\frac{(\vec{p}_H^{\,2})^{-\frac{3}{2}-\gamma_1+i\nu-\epsilon} e^{in\phi_H}\Gamma(1+\epsilon)}{(1-z_H)\sqrt{2}\pi^\epsilon} \frac{1}{(m_H^2+(1-z_H)\vec{p}_H^{\,2})} \quad (A.29)$$

This simpler integral has the same singular behavior of I_2, therefore the combination

$$I_{2,\text{reg}} \equiv I_2 - I_{2,\text{as}} = \frac{(\vec{p}_H^{\,2})^{\frac{n}{2}} e^{in\phi_H}}{z_H^2\sqrt{2}} \left[\frac{\Gamma\left(\frac{5}{2}+\gamma_1+\frac{n}{2}-i\nu\right)\Gamma\left(-\frac{1}{2}-\gamma_1+\frac{n}{2}+i\nu\right)}{\Gamma(1+n)}\right]$$
$$\times \int_0^1 d\Delta \left(\Delta + \frac{(1-\Delta)}{z_H}\right)^n \left[\left(\Delta + \frac{(1-\Delta)}{z_H^2}\right)\vec{p}_H^{\,2} + \frac{(1-\Delta)(1-z_H)m_H^2}{z_H^2}\right]^{-\frac{5}{2}-\gamma_1+i\nu-\frac{n}{2}}$$
$$\times \left\{ {}_2F_1\left(-\frac{1}{2}-\gamma_1+\frac{n}{2}+i\nu, \frac{5}{2}+\gamma_1-i\nu+\frac{n}{2}, 1+n, \zeta\right) - \frac{z_H^2(\vec{p}_H^{\,2})^{-\frac{3}{2}-\gamma_1-\frac{n}{2}+i\nu}}{(m_H^2+(1-z_H)\vec{p}_H^{\,2})} \right.$$
$$\left. \times \frac{\Gamma(1+n)}{\Gamma(\frac{5}{2}+\gamma_1+\frac{n}{2}-i\nu)\Gamma(-\frac{1}{2}-\gamma_1+\frac{n}{2}+i\nu)} \frac{1}{(1-\Delta)(1-z_H)} \right\} , \quad (A.30)$$

is not divergent and has a finite $\epsilon \to 0$ limit.

The other two integrals can be computed by using the same technique:

$$I_1(\gamma_1, \gamma_2, n, \nu) = \int \frac{d^{2-2\epsilon}\vec{q}}{\pi\sqrt{2}} (\vec{q}^{\,2})^{i\nu-\frac{3}{2}} e^{in\phi} (\vec{q}^{\,2})^{-\gamma_1} \left[(\vec{q}-\vec{p}_H)^2\right]^{-\gamma_2} = \frac{(\vec{p}_H^{\,2})^{-\frac{1}{2}+i\nu-\epsilon-\gamma_1-\gamma_2} e^{in\phi_H}}{\sqrt{2}\pi^\epsilon}$$
$$\times \left[\frac{\Gamma\left(\frac{1}{2}+\gamma_1+\gamma_2+\frac{n}{2}-i\nu+\epsilon\right)\Gamma\left(-\frac{1}{2}-\gamma_1+\frac{n}{2}+i\nu-\epsilon\right)\Gamma(1-\gamma_2-\epsilon)}{\Gamma\left(\frac{3}{2}+\gamma_1+\frac{n}{2}-i\nu\right)\Gamma\left(\frac{1}{2}-\gamma_1-\gamma_2+\frac{n}{2}+i\nu-2\epsilon\right)\Gamma(\gamma_2)}\right] , \quad (A.31)$$

note that for $\gamma_2 \geq 1$ and integer, we cannot put $\epsilon = 0$ because the integral is divergent;

$$I_3(\gamma_1, \gamma_2, n, \nu) = \int \frac{d^{2-2\epsilon}\vec{q}}{\pi\sqrt{2}} (\vec{q}^{\,2})^{i\nu-\frac{3}{2}} e^{in\phi} (\vec{q}^{\,2})^{-\gamma_1} \left[(1-z_H)m_H^2 + (\vec{p}_H - z_H\vec{q})^2\right]^{-\gamma_2}$$

$$= \frac{(\vec{p}_H^{\,2})^{\frac{n}{2}} e^{in\phi_H}}{(z_H^2)^{\gamma_2+\frac{n}{2}}\sqrt{2}\pi^\epsilon} \left(\frac{\vec{p}_H^{\,2}}{z_H^2} + \frac{(1-z_H)m_H^2}{z_H^2}\right)^{-\frac{1}{2}-\gamma_1-\gamma_2-\frac{n}{2}+i\nu-\epsilon} \tag{A.32}$$

$$\times \left[\frac{\Gamma\left(\frac{1}{2}+\gamma_1+\gamma_2+\frac{n}{2}-i\nu+\epsilon\right)\Gamma(-\frac{1}{2}-\gamma_1+\frac{n}{2}+i\nu-\epsilon)\Gamma(\frac{3}{2}+\frac{n}{2}+\gamma_1-i\nu)}{\Gamma\left(\frac{3}{2}+\gamma_1+\frac{n}{2}-i\nu\right)\Gamma\left(\gamma_2\right)\Gamma(1+n-\epsilon)}\right]$$

$$\times {}_2F_1\left(-\frac{1}{2}-\gamma_1+\frac{n}{2}+i\nu-\epsilon, \frac{1}{2}+\gamma_1+\gamma_2+\frac{n}{2}-i\nu+\epsilon, 1+n-\epsilon, \xi\right) ,$$

where

$$\xi = \frac{1}{1+\frac{(1-z_H)m_H^2}{\vec{p}_H^{\,2}}} . \tag{A.33}$$

Appendix B

Heavy-quark pair impact factor

B.1 Impact factor in the transverse momentum space

In this Section we give the expression of the leading-order impact factor, together with the functional form of the amplitude for the $g + R \to q\bar{q}$ subprocess, where R here means "Reggeized gluon". The leading-order impact factor is defined as [35]

$$d\Phi_{gg}^{\{Q\bar{Q}\}}(z_Q, \vec{p}_Q, \vec{q}) = \frac{\langle cc'|\widehat{\mathcal{P}}|0\rangle}{2\left(N^2-1\right)} \times \sum_{\lambda_Q \lambda_{\bar{Q}} \lambda_G} \sum_{Q\bar{Q}a} \int \frac{ds_{gR}}{2\pi} d\rho_{\{Q\bar{Q}\}} \Gamma^{ca}_{g\to\{Q\bar{Q}\}}\left(\vec{q}\right) \left(\Gamma^{ac'}_{g\to\{Q\bar{Q}\}}\left(\vec{q}\right)\right)^* , \tag{B.1}$$

where

$$\langle cc'|\widehat{\mathcal{P}}|0\rangle = \frac{\delta^{cc'}}{\sqrt{N^2-1}} \tag{B.2}$$

is the projector on the singlet state. We take the sum over helicities, $\{\lambda_Q, \lambda_{\bar{Q}}\}$, and over color indices, $\{Q, \bar{Q}\}$, of the two produced particles (quark and antiquark) and average over polarization and color states of the incoming gluon. In Eq. (B.1), s_{gR} denotes the invariant squared mass of the gluon-Reggeon system, while $d\rho_{\{Q\bar{Q}\}}$ is the differential phase space of the outgoing particles. The amplitude $\Gamma^{ca}_{g\to\{Q\bar{Q}\}}$ describes the production of quark-antiquark pair in a collision between a gluon and a Reggeon. The latter, as before, can be treated as an ordinary gluon in the "nonsense" polarization state $\epsilon_R^\mu = -k_2^\mu/s$. Having two particles produced in the intermediate state, one can write

$$\frac{ds_{gR}}{2\pi} d\rho_{\{Q\bar{Q}\}} = \frac{1}{2\left(2\pi\right)^3} \delta\left(1 - z_Q - z_{\bar{Q}}\right) \delta^{(2)}\left(\vec{q} - \vec{p}_Q - \vec{p}_{\bar{Q}}\right) \frac{dz_Q dz_{\bar{Q}}}{z_Q z_{\bar{Q}}} d^2\vec{p}_Q \, d^2\vec{p}_{\bar{Q}} \, , \tag{B.3}$$

with $p_{\bar{Q}}$ the antiquark momentum, and $z_{\bar{Q}}$ its longitudinal momentum fraction (with respect to the incoming gluon). Summing over the three contributions, $\{\mathcal{M}_{1,2,3}\}$, of

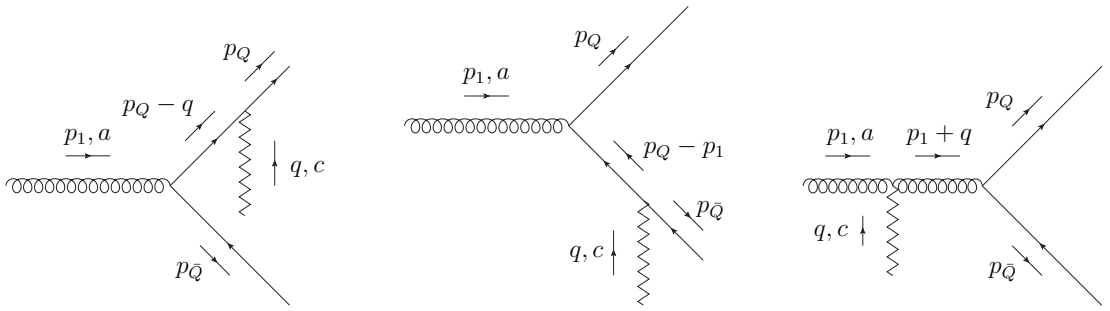

$\mathcal{M}_1$ $\mathcal{M}_2$ $\mathcal{M}_3$

Figure B.1: Feynman diagrams relevant for the calculation of the impact factor for the heavy-quark pair hadroproduction.

Fig. B.1, one gets

$$\begin{aligned}\Gamma^{ca}_{g\to\{Q\bar{Q}\}} = &-ig^2\left(t^a t^c\right)\bar{u}\left(p_Q\right)\left(mR\not{\epsilon} - 2z_Q\vec{P}\cdot\vec{\epsilon} - \not{\vec{P}}\not{\epsilon}\right)\frac{\not{k}_2}{s}v\left(p_{\bar{Q}}\right)\\ &- ig^2\left(t^c t^a\right)\bar{u}\left(p_Q\right)\left(m\bar{R}\not{\epsilon} - 2z_Q\vec{\bar{P}}\cdot\vec{\epsilon} - \not{\vec{\bar{P}}}\not{\epsilon}\right)\frac{\not{k}_2}{s}v\left(p_{\bar{Q}}\right)\ ,\end{aligned} \tag{B.4}$$

where ϵ^μ identifies the gluon polarization vector, $\{t\}$ are the $SU(3)$ color matrices and $R, \bar{R}, \vec{P}, \vec{\bar{P}}$ are defined as

$$R = \frac{1}{m_Q^2 + \vec{p}_Q^{\,2}} - \frac{1}{m_Q^2 + (\vec{p}_Q - z_Q\vec{q})^2}\ , \tag{B.5}$$

$$\bar{R} = \frac{1}{m_Q^2 + (\vec{p}_Q - z_Q\vec{q})^2} - \frac{1}{m_Q^2 + (\vec{p}_Q - \vec{q})^2}\ , \tag{B.6}$$

$$\vec{P} = \frac{\vec{p}_Q}{m_Q^2 + \vec{p}_Q^{\,2}} - \frac{\vec{p}_Q - z_Q\vec{q}}{m_Q^2 + (\vec{p}_Q - z_Q\vec{q})^2}\ , \tag{B.7}$$

$$\vec{\bar{P}} = \frac{\vec{p}_Q - z_Q\vec{q}}{m_Q^2 + (\vec{p}_Q - z_Q\vec{q})^2} - \frac{\vec{p}_Q - \vec{q}}{m_Q^2 + (\vec{p}_Q - \vec{q})^2}\ . \tag{B.8}$$

Using Eq. (B.4) together with Eq. (B.1) and performing sums and integrations (the latter ones only on the antiquark variables), our final result reads

$$\begin{aligned}d\Phi^{\{Q\bar{Q}\}}_{gg}(z_Q, \vec{p}_Q, \vec{q}) = \frac{\alpha_s^2\sqrt{N^2-1}}{2\pi N}\Bigg[&\left(m_Q^2\left(R+\bar{R}\right)^2 + \left(z_Q^2 + z_{\bar{Q}}^2\right)\left(\vec{P}+\vec{\bar{P}}\right)^2\right)\\ &-\frac{N^2}{N^2-1}\left(2m_Q^2 R\bar{R} + \left(z_Q^2 + z_{\bar{Q}}^2\right)2\vec{P}\cdot\vec{\bar{P}}\right)\Bigg]\ d^2\vec{p}_Q\ dz_Q\ .\end{aligned} \tag{B.9}$$

B.2 Projection onto the eigenfunction of the LO BFKL kernel

In the following we compute the projection of the impact factors onto the eigenfunctions of the leading-order BFKL kernel, to get the (n,ν)-representation. We get

$$\frac{d\Phi_{gg}^{\{Q\bar{Q}\}}\left(n,\nu,\vec{p}_Q,z_Q\right)}{d^2\vec{p}_Q\,dz_Q} \equiv \int \frac{d^2\vec{q}}{\pi\sqrt{2}}(\vec{q}^{\,2})^{i\nu-\frac{3}{2}}e^{in\phi}\frac{d\Phi_{gg}^{\{Q\bar{Q}\}}(\vec{q},\vec{p}_Q,z_Q)}{d^2\vec{p}_Q\,dz_Q} = \frac{\alpha_s^2\sqrt{N^2-1}}{2\pi N}$$

$$\times\left\{m_Q^2\left(J_3-2\frac{J_2(0)}{m_Q^2+\vec{p}_Q^{\,2}}\right)+(z_Q^2+z_{\bar{Q}}^2)\left(-m_Q^2\left(J_3-2\frac{J_2(0)}{m_Q^2+\vec{p}_Q^{\,2}}\right)+\frac{J_2(1)}{m_Q^2+\vec{p}_Q^{\,2}}\right)\right.$$

$$-\frac{N^2}{N^2-1}\left[2m_Q^2\left[\left(z_Q^2+z_{\bar{Q}}^2-1\right)\left(1-\left(z_Q^2\right)^{\frac{1}{2}-i\nu}\right)\right]\frac{J_2(0)}{m_Q^2+\vec{p}_Q^{\,2}}+\left[2m_Q^2(z_Q^2+z_{\bar{Q}}^2-1)\left(z_Q^2\right)^{\frac{1}{2}-i\nu}\right]\right.$$

$$\left.\left.\left(J_3-\frac{J_4(0)}{\left(z_Q^2\right)^{\frac{1}{2}-i\nu}}\right)-(z_Q^2+z_{\bar{Q}}^2)\left[(1-z_Q)^2J_4(1)-\frac{\left(1-\left(z_Q^2\right)^{\frac{1}{2}-i\nu}\right)}{m_Q^2+\vec{p}_Q^{\,2}}J_2(1)\right]\right]\right\}\,, \quad \text{(B.10)}$$

where $J_2(\lambda)$, J_3 and $J_4(\lambda)$ read

$$\begin{aligned}J_2\left(\lambda\right) &\equiv \int\frac{d^2\vec{q}}{\pi\sqrt{2}}(\vec{q}^{\,2})^{i\nu-\frac{3}{2}}e^{in\phi}\frac{(\vec{q}^{\,2})^{\lambda}}{m_Q^2+(\vec{p}_Q-\vec{q})^2}\\ &= \frac{\left(\vec{p}_Q^{\,2}\right)^{\frac{n}{2}}e^{in\phi_Q}}{\sqrt{2}}\frac{1}{\left(m_Q^2+\vec{p}_Q^{\,2}\right)^{\frac{3}{2}+\frac{n}{2}-i\nu-\lambda}}\frac{\Gamma\left(\frac{1}{2}+\frac{n}{2}+i\nu+\lambda\right)\Gamma\left(\frac{1}{2}+\frac{n}{2}-i\nu-\lambda\right)}{\Gamma\left(1+n\right)}\\ &\times\frac{\left(\frac{1}{2}+\frac{n}{2}-i\nu-\lambda\right)}{\left(-\frac{1}{2}+\frac{n}{2}+i\nu+\lambda\right)}\,{}_2F_1\left(-\frac{1}{2}+\frac{n}{2}+i\nu+\lambda,\frac{3}{2}+\frac{n}{2}-i\nu-\lambda,1+n,\chi\right)\,,\end{aligned} \quad \text{(B.11)}$$

$$\begin{aligned}J_3 &\equiv \int\frac{d^2\vec{q}}{\pi\sqrt{2}}(\vec{q}^{\,2})^{i\nu-\frac{3}{2}}e^{in\phi}\frac{1}{\left(m_Q^2+(\vec{p}_Q-\vec{q})^2\right)^2}\\ &= \frac{\left(\vec{p}_Q^{\,2}\right)^{\frac{n}{2}}e^{in\phi_Q}}{\sqrt{2}}\frac{1}{\left(m_Q^2+\vec{p}_Q^{\,2}\right)^{\frac{5}{2}+\frac{n}{2}-i\nu}}\frac{\Gamma\left(\frac{1}{2}+\frac{n}{2}+i\nu\right)\Gamma\left(\frac{1}{2}+\frac{n}{2}-i\nu\right)}{\Gamma\left(1+n\right)}\frac{\left(\frac{1}{2}+\frac{n}{2}-i\nu\right)}{\left(-\frac{1}{2}+\frac{n}{2}+i\nu\right)}\\ &\times\left(\frac{3}{2}+\frac{n}{2}-i\nu\right)\,{}_2F_1\left(-\frac{1}{2}+\frac{n}{2}+i\nu,\frac{5}{2}+\frac{n}{2}-i\nu,1+n,\chi\right)\,,\end{aligned} \quad \text{(B.12)}$$

$$
\begin{aligned}
J_4\left(\lambda\right) &\equiv \int \frac{d^2\vec{q}}{\pi\sqrt{2}} (\vec{q}^{\,2})^{i\nu-\frac{3}{2}} e^{in\phi} \frac{(\vec{q}^{\,2})^{\lambda}}{(m_Q^2+(\vec{p}_Q-\vec{q})^2)(m_Q^2+(\vec{p}_Q-z_Q\vec{q})^2)} \\
&= \frac{\left(\vec{p}_Q^{\,2}\right)^{\frac{n}{2}} e^{in\phi_Q}}{z_Q^2\sqrt{2}} \frac{\left(\frac{3}{2}-i\nu-\lambda+\frac{n}{2}\right)}{\left(m_Q^2+\vec{p}_Q^{\,2}\right)^{\frac{5}{2}-i\nu-\lambda+\frac{n}{2}}} \frac{\Gamma\left(\frac{1}{2}+\frac{n}{2}+i\nu+\lambda\right)\Gamma\left(\frac{1}{2}+\frac{n}{2}-i\nu-\lambda\right)}{\Gamma\left(1+n\right)} \\
&\times \frac{\left(\frac{1}{2}+\frac{n}{2}-i\nu-\lambda\right)}{\left(-\frac{1}{2}+\frac{n}{2}+i\nu+\lambda\right)} \int_0^1 d\Delta \left(1+\frac{\Delta}{z}-\Delta\right)^n \left(1+\frac{\Delta}{z^2}-\Delta\right)^{-\frac{5}{2}+i\nu+\lambda-\frac{n}{2}} \\
&\times \ {}_2F_1\left(-\frac{1}{2}+i\nu+\lambda+\frac{n}{2}, \frac{5}{2}-i\nu-\lambda+\frac{n}{2}, 1+n, \chi\,\frac{\left(1+\frac{\Delta}{z}-\Delta\right)^2}{\left(1+\frac{\Delta}{z^2}-\Delta\right)}\right) ,
\end{aligned}
\tag{B.13}
$$

and $\chi \equiv \frac{\vec{p}_Q^{\,2}}{m_Q^2+\vec{p}_Q^{\,2}}$; the azimuthal angles ϕ and ϕ_Q are defined as $\cos\phi \equiv q_x/|\vec{q}|$ and $\cos\phi_Q \equiv p_{Q,x}/|\vec{p}_Q|$.

Appendix C

Further details on the Lipatov vertex

C.1 Polylogarithms, Hypergeometric functions and Nested harmonic sums

In this appendix we give some usual definitions and useful relations.

Polylogarithms [252]

We define polylogarithms as

$$\mathrm{Li}_{a+1}(z) = \frac{(-1)^a\, z}{a!} \int_0^1 dt \frac{\ln^a(t)}{1-tz} \tag{C.1}$$

and Nielsen generalized polylogarithms as

$$\mathrm{S}_{a,b}(z) = \frac{(-1)^{a+b-1}}{(a-1)!b!} \int_0^1 dt \frac{\ln^{a-1} t \ln^b(1-zt)}{t} \;, \quad \mathrm{S}_{a,1}(z) = \mathrm{Li}_{a+1}(z) \;, \tag{C.2}$$

where a and b are integers. During calculations, the following inversion and reflection formulas for polylogarithms are useful [252],

$$\mathrm{Li}_n(z) + (-1)^n \mathrm{Li}_n\left(\frac{1}{z}\right) = -\frac{1}{n!}\ln^n(-z) - \sum_{j=0}^{n-2} \frac{1}{j!}(1+(-1)^{n-j})(1-2^{1-n+j})\zeta(n-j)\ln^j(-z) \;,$$

$$\mathrm{S}_{n,p}(z) = \sum_{j=0}^{n-1} \frac{\ln^j z}{j!} \left\{ s_{n-j,p} - \sum_{k=0}^{p-1} \frac{(-1)^k \ln^k(1-z)}{k!} \mathrm{S}_{p-k,n-j}(1-z) \right\} + \frac{(-1)^p}{n!p!} \ln^n z \ln^p(1-z) \,,$$

where

$$s_{n,p} = S_{n,p}(1) \;.$$

In particular, from these relations, we obtain

$$\mathrm{Li}_2(z) = -\mathrm{Li}_2\left(\frac{1}{z}\right) - \zeta(2) - \frac{1}{2}\ln^2(-z)\,, \quad \mathrm{Li}_3(z) = \mathrm{Li}_3\left(\frac{1}{z}\right) - \zeta(2)\ln(-z) - \frac{1}{6}\ln^3(-z)\,,$$

$$\mathrm{Li}_4(z) = -\mathrm{Li}_4\left(\frac{1}{z}\right) - \frac{7}{4}\zeta(4) - \frac{1}{2}\zeta(2)\ln^2(-z) - \frac{1}{4!}\ln^4(-z)\,,$$

$$\mathrm{Li}_2(z) = \zeta(2) - \mathrm{Li}_2(1-z) - \ln z \ln(1-z)\,,$$

$$\mathrm{Li}_3(z) = -\mathrm{Li}_3(1-z) - \mathrm{Li}_3\left(1-\frac{1}{z}\right) + \zeta(3) + \frac{1}{6}\ln^3 z + \zeta(2)\ln z - \frac{1}{2}\ln^2 z \ln(1-z)\,,$$

$$\mathrm{Li}_4(z) = \zeta(4) - \mathrm{S}_{1,3}(1-z) + \ln z(\zeta(3) - \mathrm{S}_{1,2}(1-z)) + \frac{\ln^2 z}{2}(\zeta(2) - \mathrm{Li}_2(1-z)) - \frac{1}{6}\ln^3 z \ln(1-z)\,.$$

It is also useful to know that,

$$\frac{d}{dy}\mathrm{Li}_2(y) = -\frac{\ln(1-y)}{y}\,, \quad \frac{d}{dy}\mathrm{Li}_3(y) = \frac{\mathrm{Li}_2(y)}{y}\,, \quad \frac{d}{dy}\mathrm{S}_{1,2}(y) = \frac{\ln^2(1-y)}{2y}\,, \tag{C.3}$$

$$\Im\{\mathrm{Li}_2(y+i\varepsilon)\} = \pi\theta(y-1)\ln(y)\,, \quad \Im\{\mathrm{Li}_3(y+i\varepsilon)\} = \pi\theta(y-1)\frac{\ln^2(y)}{2}\,, \tag{C.4}$$

$$\Im\{\mathrm{S}_{1,2}(y+i\varepsilon)\} = \pi\theta(y-1)\left[\zeta(2) - \mathrm{Li}_2\left(\frac{1}{y}\right) - \frac{\ln^2(y)}{2}\right]\,. \tag{C.5}$$

Hypergeometric function ${}_2F_1$

We can represent the hypergeometric function ${}_2F_1$ as

$${}_2F_1(a,b,c;z) = \frac{1}{B(b,c-b)}\int_0^1 dx\, x^{b-1}(1-x)^{c-b-1}(1-zx)^{-a}\,, \tag{C.6}$$

for $\Re\{c\} > \Re\{b\} > 0$. The definition is valid in the entire complex z-plane with a cut along the real axis from 1 to infinity. Using the integral representation (C.6) and performing the transformation

$$x = -\frac{y}{z\left[1 - \left(1+\frac{1}{z}\right)y\right]}\,, \tag{C.7}$$

one can prove the following identity

$${}_2F_1(a,b,1+b;1+z) = (-z)^{-b}\,{}_2F_1\left(1+b-a,b,1+b;1+z^{-1}\right)\,. \tag{C.8}$$

Choosing $a = b = \epsilon$, we get

$${}_2F_1(1,\epsilon,1+\epsilon;1+z) = \,(-z)^{-\epsilon}\,{}_2F_1(\epsilon,\epsilon,1+\epsilon;1+z^{-1})\,. \tag{C.9}$$

One can also prove the following expansions [253]

$${}_2F_1(1,-\epsilon,1-\epsilon;z) = 1 - \sum_{i=1}^{\infty}\epsilon^i\mathrm{Li}_i(z)\,, \tag{C.10}$$

$$
\begin{aligned}
{}_2F_1(2-2\epsilon,1-\epsilon,2-\epsilon;z) = \frac{1}{1-z}\Bigg\{1 + \left[1+\left(\frac{1+z}{z}\right)\ln(1-z)\right]\epsilon \\
+\left[2+\left(\frac{1+z}{z}\right)\ln(1-z)\ln((1-z)e) - \left(\frac{1-z}{z}\right)\mathrm{Li}_2(z)\right]\epsilon^2 \\
+\Bigg[4+\ln(1-z)\left(\frac{2(1+z)}{z}+\frac{2(1-z)}{z}\zeta(2)+\frac{\ln(1-z)}{3z}\right. \\
\left.\times\left(3(1+z)+2(1+z)\ln(1-z)-3(1-z)\ln z\right)\right) - \frac{1-z}{z}\mathrm{Li}_2(z)\left(1+2\ln(1-z)\right) \\
-\frac{2(1-z)}{z}\left(\mathrm{Li}_3(1-z)+\frac{\mathrm{Li}_3(z)}{2}-\zeta(3)\right)\Bigg]\epsilon^3\Bigg\} + \mathcal{O}(\epsilon^4)\ . \qquad \text{(C.11)}
\end{aligned}
$$

Nested harmonic sums and $\mathcal{M}$ functions [188]

The nested harmonic sums are defined recursively by

$$
S_i(n) = \sum_{k=1}^{n}\frac{1}{k^i}\ , \qquad S_{i\vec{j}}(n) = \sum_{k=1}^{n}\frac{S_{\vec{j}}(k)}{k^i}\ , \qquad \text{(C.12)}
$$

while the $\mathcal{M}$-functions are defined by the double series

$$
\mathcal{M}(\vec{i},\vec{j},\vec{k};x_1,x_2) = \sum_{n_1=0}^{\infty}\sum_{n_2=0}^{\infty}\binom{n_1+n_2}{n_1}^2 S_{\vec{i}}(n_1)S_{\vec{j}}(n_2)S_{\vec{k}}(n_1+n_2)x_1^{n_1}x_2^{n_2}\ . \qquad \text{(C.13)}
$$

C.2 Some useful integrals

The integral $I_{a,b,c}$

The integral

$$
I_{a,b,c} = \int_0^1 dx\ \frac{1}{ax+b(1-x)-cx(1-x)}\ln\left(\frac{ax+b(1-x)}{cx(1-x)}\right) \qquad (4.50)
$$

is invariant with respect to any permutation of its arguments, as it can be seen from the representation

$$
I_{a,b,c} = \int_0^1 dx_1\int_0^1 dx_2\int_0^1 dx_3\ \frac{\delta(1-x_1-x_2-x_3)}{(ax_1+bx_2+cx_3)(x_1x_2+x_1x_3+x_2x_3)}\ . \qquad \text{(C.14)}
$$

To prove that (4.50) and (C.14) are equivalent, we first integrate over x_3 and then perform the change of variables

$$
x = \frac{x_2}{x_1+x_2}\ , \qquad z = \frac{x_1x_2}{(1-x_1)x_1+(1-x_2)x_2-x_1x_2}\ ,
$$

$$x_1 = \frac{(1-x)z}{z+x(1-x)(1-z)}\,, \quad x_2 = \frac{xz}{z+x(1-x)(1-z)}\,, \quad x_3 = \frac{x(1-x)(1-z)}{z+x(1-x)(1-z)},$$

with Jacobian

$$J = \frac{xz(1-x)}{[z+x(1-x)(1-z)]^3}\,. \tag{C.15}$$

We obtain

$$\begin{aligned} I_{a,b,c} &= \int_0^1 dx \int_0^\infty dz\, \frac{\Theta\left(\frac{x(1-x)(1-z)}{z+x(1-x)(1-z)}\right)}{az(1-x)+bxz+cx(1-x)(1-z)} \\ &= \int_0^1 dx\, \frac{1}{a(1-x)+bx-cx(1-x)} \ln\left(\frac{bx+a(1-x)}{cx(1-x)}\right)\,, \end{aligned} \tag{C.16}$$

which is equal to (4.50) after the trivial change of variables $x \leftrightarrow 1-x$.
Another useful representation of immediate proof is

$$I_{a,b,c} = \int_0^1 dx \int_1^\infty dt\, \frac{1}{t\,[ax(1-x)(t-1)+b(1-x)+cx]}\,. \tag{C.17}$$

In the case when $a = \vec{q}_1^{\,2}$, $b = \vec{q}_2^{\,2}$ and $c = (\vec{q}_1 - \vec{q}_2)^2 \equiv \vec{p}^{\,2}$, the explicit solution of the integral is [254]

$$\begin{aligned} I_{\vec{q}_1^{\,2},\vec{q}_2^{\,2},\vec{p}^{\,2}} &= \int_0^1 dx \frac{1}{\vec{q}_1^{\,2}x+\vec{q}_2^{\,2}(1-x)-\vec{p}^{\,2}x(1-x)} \ln\left(\frac{\vec{q}_1^{\,2}x+\vec{q}_2^{\,2}(1-x)}{\vec{p}^{\,2}x(1-x)}\right) \\ &= -\frac{2}{|\vec{q}_1||\vec{q}_2|\sin\phi}\left[\ln\rho\arctan\left(\frac{\rho\sin\phi}{1-\rho\cos\phi}\right)+\Im\left(-\mathrm{Li}_2(\rho e^{i\phi})\right)\right]\,, \end{aligned} \tag{C.18}$$

where ϕ is the angle between $\vec{q}_1$, $\vec{q}_2$ and $\rho = \min\left(\frac{|\vec{q}_1|}{|\vec{q}_2|}, \frac{|\vec{q}_2|}{|\vec{q}_1|}\right)$.

The box integral with one external mass

Here, we derive the result for I_{4B} in Eq. (4.54), *i.e.* a box integral with massless propagators and one external mass, using direct Feynman technique. The integral is

$$I_{4B} = \frac{1}{i}\int d^D k \frac{1}{(k^2+i\varepsilon)[(k+q_1)^2+i\varepsilon][(k+q_2)^2+i\varepsilon][(k-p_B)^2+i\varepsilon]}\,. \tag{4.53}$$

Defining

$$d_1 = k^2+i\varepsilon\,, \quad d_2 = (k+q_1)^2+i\varepsilon\,, \quad d_3 = (k+q_2)^2+i\varepsilon\,, \quad d_4 = (k-p_B)^2+i\varepsilon\,, \tag{C.19}$$

we can write

$$\frac{1}{d_1 d_4} = \int_0^1 dx \frac{1}{\left((1-x)d_1+xd_4\right)^2}\,, \quad \frac{1}{d_2 d_3} = \int_0^1 dy \frac{1}{\left((1-y)d_2+yd_3\right)^2}\,, \tag{C.20}$$

and hence

$$\frac{1}{d_1 d_2 d_3 d_4} = \Gamma(4) \int_0^1 dy \int_0^1 dx \int_0^1 dz \frac{z(1-z)}{\left[(1-z)\left((1-x)d_1 + x d_4\right) + z\left((1-y)d_2 + y d_3\right)\right]^4} \,. \tag{C.21}$$

After integration in the $d^D k$, we obtain for I_{4B},

$$I_{4B} = \pi^{D/2}\Gamma(4-D/2)$$
$$\times \int_0^1 dz \int_0^1 dx \int_0^1 dy \frac{z(1-z)}{\left[z(1-z)\left(-s_2 x(1-y) + (by + a(1-y))(1-x)\right) - i0\right]^{4-D/2}} \,, \tag{C.22}$$

where $a = -t_1,\ b = -t_2$. Performing the trivial integrations over z and x, we have

$$I_{4B} = \pi^{D/2}\Gamma(1-\epsilon)\frac{\Gamma^2(\epsilon)}{\Gamma(2\epsilon)}$$
$$\times \int_0^1 \frac{dy}{s_2(1-y) + by + a(1-y)} \left[(-s_2(1-y) - i0)^{\epsilon-1} - (by + a(1-y))^{\epsilon-1}\right] . \tag{C.23}$$

The first term in the square bracket gives

$$(-s_2 - i0)^{\epsilon-1} \int_0^1 dy \frac{(1-y)^{\epsilon-1}}{(s_2+a)(1-y) + by} = (-s_2 - i0)^{\epsilon-1} \frac{1}{b} \int_0^1 dx \frac{x^{\epsilon-1}}{1 - x\left(1 - (s_2+a)/b\right)}$$
$$= (-s_2 - i0)^{\epsilon-1} \frac{1}{b}\frac{1}{\epsilon}\ {}_2F_1\left(1, \epsilon, 1+\epsilon; 1 - \frac{(s_2+a)}{b}\right) . \tag{C.24}$$

In the second term, denoting $t = by + a(1-y)$, one can organize the integral as

$$\int_a^b dt = \int_0^b dt - \int_0^a dt = b\int_0^1 dx - a\int_0^1 dx \,. \tag{C.25}$$

In this way, we obtain

$$\int_0^1 \frac{dy}{s_2(1-y) + by + a(1-y)} (by + a(1-y))^{\epsilon-1} = \frac{b^\epsilon}{s_2 b} \int_0^1 dx \frac{x^{\epsilon-1}}{1 - x\left(1 - (b-a)/s_2\right)}$$
$$-\frac{a^\epsilon}{s_2 b} \int_0^1 dx \frac{x^{\epsilon-1}}{1 - x\left(1 - (b-a)(s_2+a)/(s_2 b)\right)} = \frac{b^\epsilon}{s_2 b\epsilon} {}_2F_1\left(1, \epsilon, 1+\epsilon; 1 - \frac{(b-a)}{s_2}\right)$$
$$-\frac{a^\epsilon}{s_2 b\epsilon} {}_2F_1\left(1, \epsilon, 1+\epsilon; 1 - \frac{(b-a)(s_2+a)}{(s_2 b)}\right) . \tag{C.26}$$

Finally, restoring t_1 and t_2, we have

$$I_{4B} = \frac{\pi^{2+\epsilon}}{s_2 t_2} \frac{\Gamma(1-\epsilon)\Gamma^2(1+\epsilon)}{\Gamma(1+2\epsilon)} \frac{2}{\epsilon^2} \Bigg[(-s_2 - i0)^\epsilon\ {}_2F_1\left(1, \epsilon, 1+\epsilon; 1 - \frac{(s_2 - t_1)}{(-t_2)}\right) \tag{C.27}$$

$$+(-t_2)^{\epsilon}{}_2F_1\left(1,\epsilon,1+\epsilon;1-\frac{(t_1-t_2)}{s_2}\right)-(-t_1)^{\epsilon}{}_2F_1\left(1,\epsilon,1+\epsilon;1-\frac{(s_2-t_1)\,(t_1-t_2)}{s_2(-t_2)}\right)\Bigg].$$

This result is exact and coincides with that in (4.57).

Feynman integrals with logarithms

In the calculation it happens to come across momentum integrals that have logarithms in the numerator. We explain below how to evaluate them, considering the example

$$\int d^{D-2}k\frac{\ln\vec{k}^{\,2}}{\vec{k}^{\,2}(\vec{k}+\vec{q}_2)^2}\,. \tag{C.28}$$

Using $\ln\vec{k}^{\,2}=\frac{\partial}{\partial\alpha}(\vec{k}^{\,2})^{\alpha}\big|_{\alpha=0}$ and exchanging the order of integration and derivative, we get

$$\begin{aligned}&\frac{\partial}{\partial\alpha}\left[\int d^{D-2}k\frac{1}{(\vec{k}^{\,2})^{1-\alpha}(\vec{k}+\vec{q}_2)^2}\right]_{\alpha=0}\\&=\pi^{1+\epsilon}(\vec{q}_2^{\,2})^{-1+\epsilon}\frac{\partial}{\partial\alpha}\left[(\vec{q}_2^{\,2})^{\alpha}\frac{\Gamma(1-\alpha-\epsilon)\Gamma(\epsilon)\Gamma(\alpha+\epsilon)}{\Gamma(1-\alpha)\Gamma(2\epsilon+\alpha)}\right]_{\alpha=0}\\&=\pi^{1+\epsilon}(\vec{q}_2^{\,2})^{-1+\epsilon}\frac{\Gamma(1-\epsilon)\Gamma^2(\epsilon)}{\Gamma(2\epsilon)}\left[\ln\vec{q}_2^{\,2}+\psi(1)+\psi(\epsilon)-\psi(1-\epsilon)-\psi(2\epsilon)\right].\end{aligned} \tag{C.29}$$

C.3 Relation between Euclidean and Minkowskian integrals

In this appendix, we give an explicit derivation of the following relations:

$$I_5=\frac{\pi^{2+\epsilon}\Gamma(1-\epsilon)}{s}\left[\ln\left(\frac{(-s)(\vec{q}_1-\vec{q}_2)^2}{(-s_1)(-s_2)}\right)\mathcal{I}_3+\mathcal{L}_3-\mathcal{I}_5\right]\,, \tag{4.87}$$

$$I_{4B}=-\frac{\pi^{2+\epsilon}\Gamma(1-\epsilon)}{s_2}\left[\frac{\Gamma^2(\epsilon)}{\Gamma(2\epsilon)}(-t_2)^{\epsilon-1}\left(\ln\left(\frac{-s_2}{-t_2}\right)+\psi(1-\epsilon)-2\psi(\epsilon)+\psi(2\epsilon)\right)+\mathcal{I}_{4B}\right]\,. \tag{4.67}$$

- Let's start from the definition of I_5:

$$I_5=\frac{1}{i}\int d^Dk\frac{1}{(k^2+i\varepsilon)[(k+q_1)^2+i\varepsilon][(k+q_2)^2+i\varepsilon][(k+p_A)^2+i\varepsilon][(k-p_B)^2+i\varepsilon]}\,.$$

We introduce the standard Sudakov decomposition for momenta,

$$k=\alpha p_B+\beta p_A+k_\perp\,,\qquad d^Dk=\frac{s}{2}d\alpha d\beta d^{D-2}k_\perp\,, \tag{C.30}$$

$$q_1 = p_A - p_{A'} = -\frac{\vec{q}_1^{\,2}}{s} p_B + \frac{s_2}{s} p_A + q_{1\perp} \ , \quad q_2 = p_{B'} - p_B = -\frac{s_1}{s} p_B + \frac{\vec{q}_2^{\,2}}{s} p_A + q_{2\perp} \ . \tag{C.31}$$

By expressing denominators in terms of Sudakov variables, we can reduce the integration over α to a simple computation of residues in the complex plane. We have the following five simple poles:

$$\alpha_1 = \frac{\vec{k}^{\,2} - i\varepsilon}{\beta s} \ , \quad \alpha_2 = \frac{(k+\vec{q}_1)^2 - i\varepsilon}{s(\beta + \frac{s_2}{s})} + \frac{\vec{q}_1^{\,2}}{s} \ , \quad \alpha_3 = \frac{(k+\vec{q}_2)^2 - i\varepsilon}{s(\beta + \frac{\vec{q}_2^{\,2}}{s})} + \frac{s_1}{s} \ , \tag{C.32}$$

$$\alpha_4 = \frac{\vec{k}^2 - i\varepsilon}{(1+\beta)s} \ , \quad \alpha_5 = \frac{\vec{k}^2 - i\varepsilon}{\beta s} + 1 \ . \tag{C.33}$$

We observe that in the region $\Omega = \{\beta < -1 \quad \vee \quad \beta > 0\}$ the integral always vanishes, since all poles are on the same side with respect to the real α-axis; in the region $\bar{\Omega} = \{-1 < \beta < 0\}$ we have contributions from three poles lying in the lower real α-axis: α_4 in the whole region $-1 < \beta < 0$, α_2 in the region $-\frac{s_2}{s} < \beta < 0$ and α_3 in the region $-\frac{\vec{q}_2^{\,2}}{s} < \beta < 0$. The integral can therefore be expressed as

$$\begin{aligned}
I_5 = &-\pi \int_{-1}^{0} \frac{d\beta}{1+\beta} \int d^{D-2}k \frac{1}{\Big[\alpha_4 \beta s - \vec{k}^2 + i\varepsilon\Big]} \frac{1}{\Big[(\alpha_4 - \frac{\vec{q}_1^{\,2}}{s})(\beta + \frac{s_2}{s})s - (k+\vec{q}_1)^2 + i\varepsilon\Big]} \\
&\times \frac{1}{\Big[(\alpha_4 - 1)\beta s - \vec{k}^2 + i\varepsilon\Big]} \frac{1}{\Big[(\alpha_4 - \frac{s_1}{s})(\beta + \frac{\vec{q}_2^{\,2}}{s})s - (\vec{k}+\vec{q}_2)^2 + i\varepsilon\Big]} \\
&-\pi \int_{-\frac{s_2}{s}}^{0} \frac{d\beta}{\beta + \frac{s_2}{s}} \int d^{D-2}k \frac{1}{\Big[\alpha_2 \beta s - \vec{k}^2 + i\varepsilon\Big]} \frac{1}{\Big[(\alpha_2 - \frac{s_1}{s})(\beta + \frac{\vec{q}_2^{\,2}}{s})s - (\vec{k}+\vec{q}_2)^2 + i\varepsilon\Big]} \\
&\times \frac{1}{\Big[\alpha_2(1+\beta)s - \vec{k}^2 + i\varepsilon\Big]} \frac{1}{\Big[(\alpha_2 - 1)\beta s - \vec{k}^2 + i\varepsilon\Big]} \\
&-\pi \int_{-\frac{\vec{q}_2^{\,2}}{s}}^{0} \frac{d\beta}{\beta + \frac{\vec{q}_2^{\,2}}{s}} \int d^{D-2}k \frac{1}{\Big[\alpha_3 \beta s - \vec{k}^2 + i\varepsilon\Big]} \frac{1}{\Big[(\alpha_3 - \frac{\vec{q}_1^{\,2}}{s})(\beta + \frac{s_2}{s})s - (\vec{k}+\vec{q}_1)^2 + i\varepsilon\Big]} \\
&\times \frac{1}{\Big[\alpha_3(1+\beta)s - \vec{k}^2 + i\varepsilon\Big]} \frac{1}{\Big[(\alpha_3 - 1)\beta s - \vec{k}^2 + i\varepsilon\Big]} \ .
\end{aligned} \tag{C.34}$$

Substituting the explicit values of poles and doing simple algebric manipulations, we end up with (omitting the $i\varepsilon$'s in the denominators)

$$I_5 \simeq -\pi \int_0^1 d\beta \beta^3 \int d^{D-2}k \frac{1}{\vec{k}^{\,2}(\vec{k} + \beta\vec{q}_1)^2[(\vec{k} + \beta\vec{q}_2)^2 + \beta(1-\beta)(-s_1)][\vec{k}^{\,2} + \beta(1-\beta)(-s)]}$$

$$+\pi\int_0^1 d\beta\beta^3\int d^{D-2}k\left(\frac{s_2}{s}\right)\frac{1}{(\vec{k}+\vec{q}_1)^2(\vec{k}+(1-\beta)\vec{q}_1+\beta\vec{q}_2)^2[(\vec{k}+(1-\beta)\vec{q}_1)^2+\beta(1-\beta)\vec{q}_1^{\,2}]}$$
$$\times\frac{1}{[(\vec{k}+(1-\beta)\vec{q}_1)^2+\beta(1-\beta)(-s_2)]}$$
$$-\pi\int_0^1 d\beta(1-\beta)^3\int d^{D-2}k\frac{(\vec{q}_2^{\,2})^2}{s_2 s}\frac{1}{[(\vec{k}+\vec{q}_2)^2]^2(\vec{k}+\beta\vec{q}_2)^2[(\vec{k}+\beta\vec{q}_2)^2+\beta(1-\beta)\vec{q}_2^{\,2}]}\,. \tag{C.35}$$

The third integral is suppressed in the high-energy approximation; as for the other two, they can be calculated by first performing the change of variable $\vec{k}\to\beta\vec{k}$ in the integration over $\vec{k}$ and then integrating some terms in β by using the following integral:

$$\int_0^1 d\beta\frac{(1-\beta)^{D-n}}{\delta+\beta}=\int_0^1 d\beta\frac{(1-\beta)^{D-n}-1}{\delta+\beta}+\int_0^1 d\beta\frac{1}{\delta+\beta}$$
$$\simeq\int_0^1 d\beta\frac{(1-\beta)^{D-n}-1}{\beta}+\int_0^1 d\beta\frac{1}{\delta+\beta}\simeq\psi(1)-\psi(D-n-1)-\ln\delta\,, \tag{C.36}$$

where δ is a generic quantity tending to zero, like $\vec{k}^{\,2}/s$ for instance, and $n=5$ and 6 in the cases we are interested in. We obtain

$$I_5=\frac{\pi}{s}\int d^{D-2}k\frac{1}{\vec{k}^{\,2}(\vec{k}+\vec{q}_1)^2(\vec{k}+\vec{q}_2)^2}\left[\ln\left(\frac{(k+\vec{q}_2)^2(-s)}{(-s_1)(-s_2)}\right)-(\psi(1)-\psi(D-5))\right]$$
$$+\pi\,\frac{\vec{q}_1^{\,2}}{s}\int_0^1 d\beta\beta^3\int d^{D-2}k\frac{1}{\vec{k}^{\,2}(\vec{k}+\beta\vec{q}_1)^2(\vec{k}+\beta\vec{q}_2)^2[\vec{k}^{\,2}+\beta(1-\beta)\vec{q}_1^{\,2}]}\,. \tag{C.37}$$

To get the desired form, we rewrite the last two terms in the square bracket as an integral over β,

$$\psi(1)-\psi(D-5)=\int_0^1 d\beta\,\frac{(1-\beta)^{D-6}-1}{\beta}=\int_0^1 d\beta\,\frac{\beta^{D-6}}{1-\beta}-\int_0^1 d\beta\,\frac{1}{\beta}\,,$$

and combine with the last term of the full expression, to get

$$I_5=\frac{\pi}{s}\int d^{D-2}k\frac{1}{\vec{k}^{\,2}(\vec{k}+\vec{q}_1)^2(\vec{k}+\vec{q}_2)^2}\ln\left(\frac{(k+\vec{q}_2)^2(-s)}{(-s_1)(-s_2)}\right)$$
$$-\frac{\pi}{s}\int_0^1\frac{d\beta}{1-\beta}\int\frac{d^{D-2}k}{\vec{k}^{\,2}}\left[\frac{\beta^2}{(\vec{k}-\beta(\vec{q}_1-\vec{q}_2))^2[(1-\beta)\vec{k}^{\,2}+\beta(\vec{k}-\vec{q}_1)^2]}-\frac{1}{(\vec{k}-\vec{q}_1+\vec{q}_2)^2(\vec{k}-\vec{q}_1)^2}\right]$$
$$=\frac{\pi}{s}\int d^{D-2}k\frac{1}{\vec{k}^{\,2}(\vec{k}-\vec{q}_1)^2(\vec{k}-\vec{q}_2)^2}\left[\ln\left(\frac{(-s)(\vec{q}_1-\vec{q}_2)^2}{(-s_1)(-s_2)}\right)+\ln\left(\frac{(\vec{k}-\vec{q}_1)^2(\vec{k}-\vec{q}_2)^2}{\vec{k}^{\,2}(\vec{q}_1-\vec{q}_2)^{\,2}}\right)\right]$$

$$-\frac{\pi}{s}\int_0^1\frac{d\beta}{1-\beta}\int\frac{d^{D-2}k}{\vec{k}^{\,2}}\left[\frac{\beta^2}{(\vec{k}-\beta(\vec{q}_1-\vec{q}_2))^2[(1-\beta)\vec{k}^{\,2}+\beta(\vec{k}-\vec{q}_1)^2]}-\frac{1}{(\vec{k}-\vec{q}_1+\vec{q}_2)^2(\vec{k}-\vec{q}_1)^2}\right]$$
$$+\frac{\pi}{s}\int d^{D-2}k\frac{1}{\vec{k}^{\,2}(\vec{k}-\vec{q}_1)^2(\vec{k}-\vec{q}_2)^2}\left[\ln\left(\frac{\vec{k}^{\,2}}{(\vec{k}-\vec{q}_1)^2}\right)\right]\ .$$

Expressing the term in the last line as

$$\frac{\pi}{s}\int_0^1 d\beta\frac{1}{1-\beta}\int d^{D-2}k\frac{1}{(\vec{k}-\vec{q}_1)^2(\vec{k}-\vec{q}_2)^2}\left[\frac{1}{\beta\vec{k}^{\,2}+(1-\beta)(\vec{k}-\vec{q}_1)^{\,2}}-\frac{1}{\vec{k}^{\,2}}\right]\ ,$$

and performing simple manipulations, we get

$$I_5=\ \frac{\pi}{s}\int d^{D-2}k\frac{1}{\vec{k}^{\,2}(\vec{k}-\vec{q}_1)^2(\vec{k}-\vec{q}_2)^2}\left[\ln\left(\frac{(-s)(\vec{q}_1-\vec{q}_2)^2}{(-s_1)(-s_2)}\right)\right]$$
$$+\frac{\pi}{s}\int d^{D-2}k\frac{1}{\vec{k}^{\,2}(\vec{k}-\vec{q}_1)^2(\vec{k}-\vec{q}_2)^2}\left[\ln\left(\frac{(\vec{k}-\vec{q}_1)^2(\vec{k}-\vec{q}_2)^2}{\vec{k}^{\,2}(\vec{q}_1-\vec{q}_2)^{\,2}}\right)\right]$$

$$-\frac{\pi}{s}\ \int_0^1 d\beta\frac{1}{1-\beta}\int d^{D-2}k\frac{1}{\vec{k}^{\,2}[(1-\beta)\vec{k}^{\,2}+\beta(\vec{k}-\vec{q}_1)^2]}\left[\frac{\beta^2}{(\vec{k}-\beta(\vec{q}_1-\vec{q}_2))^2}-\frac{1}{(\vec{k}-\vec{q}_1+\vec{q}_2)^2}\right],$$

which, by using definitions (4.15), (4.16), (4.18), leads exactly to eq. (4.87).

- Let's prove the second relation; again we start from the definition of I_{4B}:

$$I_{4B}=\frac{1}{i}\int d^Dk\frac{1}{(k^2+i\varepsilon)[(k+q_1)^2+i\varepsilon][(k+q_2)^2+i\varepsilon][(k-p_B)^2+i\varepsilon]}\ . \tag{C.38}$$

We again introduce the Sudakov decomposition (C.30)-(C.31) and observe that we have four poles:

$$\beta_1=\frac{\vec{k}^{\,2}-i\varepsilon}{\alpha s}\ ,\quad \beta_2=\frac{(\vec{k}+\vec{q}_1)^2-i\varepsilon}{(\alpha-\frac{\vec{q}_1^{\,2}}{s})s}-\frac{s_2}{s}\ ,\quad \beta_3=\frac{(\vec{k}+\vec{q}_2)^2-i\varepsilon}{(\alpha-\frac{s_1}{s})s}-\frac{\vec{q}_2^{\,2}}{s}\ ,\quad \beta_4=\frac{\vec{k}^{\,2}-i\varepsilon}{(\alpha-1)s}\ .$$

In the region $\Omega=\{\alpha<0\ \ \vee\ \ \alpha>1\}$ the integral always vanishes, while, in the region $\bar{\Omega}=\{0<\alpha<1\}$, if we close the integration path over β in the half-plane $\Im\beta>0$ and use the residue theorem, we have

$$I_{4B}=-\pi\int_0^1\frac{d\alpha}{1-\alpha}\int d^{D-2}k\ \frac{1}{(\alpha\beta_4 s-\vec{k}^2+i\varepsilon)}$$
$$\times\frac{1}{[\alpha(\beta_4+\frac{s_2}{s})s-(\vec{k}+\vec{q}_1)^2+i\varepsilon][(\alpha-\frac{s_1}{s})(\beta_4+\frac{\vec{q}_2^{\,2}}{s})s-(\vec{k}+\vec{q}_2)^2+i\varepsilon]}$$

$$+\pi\int_0^{\frac{s_1}{s}}\frac{d\alpha}{\alpha-\frac{s_1}{s}}\int\frac{d^{D-2}k}{(\alpha\beta_3 s-\vec{k}^2+i\varepsilon)[\alpha(\beta_3+\frac{s_2}{s})s-(\vec{k}+\vec{q}_1)^2+i\epsilon][(\alpha-1)\beta_3 s-\vec{k}^2+i\varepsilon]}\,. \tag{C.39}$$

In the last expression, we neglected the contribution of the pole β_2, which is present in the region $\Omega'=\{0<\alpha<\vec{q}_1^{\,2}/s\}$, since it is suppressed in the MRK. For the same reason, in the previous integrals we approximated $\alpha-\vec{q}_1^{\,2}/s$ with α. Substituting the explicit values of β_3 and β_4, one gets (recalling that $s_1s_2/s=(\vec{q}_1-\vec{q}_2)^2$ and taking the high-energy limit)

$$I_{4B}=\pi\int_0^1 d\alpha\alpha^2\int d^{D-2}k\frac{1}{\vec{k}^2(\vec{k}+\alpha\vec{q}_2)^2[(\vec{k}+\alpha\vec{q}_1)^2+\alpha(1-\alpha)(-s_2-i\varepsilon)]} \tag{C.40}$$

$$-\pi\frac{(\vec{q}_1-\vec{q}_2)^2}{s_2}\int_0^1 d\alpha\;\alpha^2\int\frac{d^{D-2}k}{(\vec{k}+\vec{q}_2)^2[(\vec{k}+(1-\alpha)\vec{q}_2)^2+\alpha(1-\alpha)\vec{q}_2^{\,2}](\vec{k}+(1-\alpha)\vec{q}_2+\alpha\vec{q}_1)^2}\,.$$

Manipulating the first term and using the integral in eq. (C.36), one can obtain the following form:

$$\begin{aligned}I_{4B}=&\frac{\pi^{2+\epsilon}}{s_2t_2}\frac{\Gamma(1-\epsilon)\Gamma^2(\epsilon)}{\Gamma(2\epsilon)}(\vec{q}_2^{\,2})^\epsilon\left[\ln\left(\frac{-s_2}{-t_2}\right)+\psi(1-\epsilon)-\psi(\epsilon)\right]\\&+\frac{\pi}{s_2}\int_0^1\frac{d\alpha}{\alpha}\int d^{D-2}k\frac{1}{(\vec{k}-\vec{q}_1)^2(\vec{k}-(\vec{q}_1-\vec{q}_2))^2}\\&-\frac{\pi}{s_2}\int_0^1\frac{d\alpha}{1-\alpha}\int d^{D-2}k\frac{1}{(\vec{k}+\vec{q}_2)^2\left[\alpha\vec{k}^2+(1-\alpha)(\vec{k}+\vec{q}_1)^2\right]}\\&-\pi\frac{(\vec{q}_1-\vec{q}_2)^2}{s_2}\int_0^1 d\alpha\;\alpha^2\int d^{D-2}k\frac{1}{\vec{k}^2[(\vec{k}+\alpha\vec{q}_2)^2+\alpha(1-\alpha)\vec{q}_2^{\,2}](\vec{k}+\alpha(\vec{q}_2-\vec{q}_1))^2}\,.\end{aligned} \tag{C.41}$$

In the last integral we perform the transformation

$$\vec{k}\to\vec{k}'=\vec{k}-\vec{p}\,,\qquad\alpha\to\alpha'=\frac{\alpha\vec{k'}^{\,2}}{(1-\alpha)\vec{k}^2+\alpha\vec{k'}^{\,2}}\quad\text{with}\quad\vec{p}\equiv\vec{q}_1-\vec{q}_2\,,$$

and get

$$\begin{aligned}I_{4B}=&\frac{\pi^{2+\epsilon}}{s_2t_2}\frac{\Gamma(1-\epsilon)\Gamma^2(\epsilon)}{\Gamma(2\epsilon)}(\vec{q}_2^{\,2})^\epsilon\left[\ln\left(\frac{-s_2}{-t_2}\right)+\psi(1-\epsilon)-\psi(\epsilon)\right]\\&+\frac{\pi}{s_2}\int_0^1\frac{d\alpha}{\alpha}\int d^{D-2}k\frac{1}{(\vec{k}-\vec{q}_1)^2(\vec{k}-(\vec{q}_1-\vec{q}_2))^2}\\&-\frac{\pi}{s_2}\int_0^1\frac{d\alpha}{1-\alpha}\int d^{D-2}k\frac{1}{(\vec{k}+\vec{q}_2)^2\left[\alpha\vec{k}^2+(1-\alpha)(\vec{k}+\vec{q}_1)^2\right]}\end{aligned}$$

$$-\frac{\pi}{s_2}\int_0^1 d\alpha \int d^{D-2}k \frac{\alpha^2 \vec{p}^{\,2}}{(\vec{k}+\alpha\vec{p})^2[(\vec{k}+\alpha\vec{p})^2+\alpha(1-\alpha)\vec{p}^{\,2}][(1-\alpha)\vec{k}^2+\alpha(\vec{k}+\vec{q}_1)^2]} \,. \tag{C.42}$$

The last two terms can be shown to lead to

$$-\frac{\pi}{s_2}\int_0^1 \frac{d\alpha}{\alpha}\int d^{D-2}k \frac{1-\alpha}{(\vec{k}-(1-\alpha)(\vec{q}_1-\vec{q}_2))^2[\alpha\vec{k}^{\,2}+(1-\alpha)(\vec{k}-\vec{q}_1)^2]}$$
$$+\frac{\pi^{2+\epsilon}}{s_2 t_2}\frac{\Gamma(1-\epsilon)\Gamma^2(\epsilon)}{\Gamma(2\epsilon)}(\vec{q}_2^{\,2})^{\epsilon}(\psi(2\epsilon)-\psi(\epsilon)) \,, \tag{C.43}$$

so that we finally find

$$I_{4B} = -\frac{\pi^{2+\epsilon}\Gamma(1-\epsilon)}{s_2}\left[\frac{\Gamma^2(\epsilon)}{\Gamma(2\epsilon)}(-t_2)^{\epsilon-1}\left(\ln\left(\frac{-s_2}{-t_2}\right)+\psi(1-\epsilon)-2\psi(\epsilon)+\psi(2\epsilon)\right)\right]$$
$$-\frac{\pi^{2+\epsilon}\Gamma(1-\epsilon)}{s_2}\int_0^1\frac{d\alpha}{\alpha}\int\frac{d^{D-2}k}{\pi^{1+\epsilon}\Gamma(1-\epsilon)}$$
$$\times\left[\frac{1-\alpha}{\left[\alpha\vec{k}^2+(1-\alpha)(\vec{k}-\vec{q}_1)^2\right](\vec{k}-(1-\alpha)(\vec{q}_1-\vec{q}_2))^2}-\frac{1}{(\vec{k}-\vec{q}_1)^2(\vec{k}-(\vec{q}_1-\vec{q}_2))^2}\right] \,, \tag{C.44}$$

which is exactly eq. (4.67).

C.4 Soft limit

In this appendix we evaluate the soft limit ($\vec{p}\to 0$) of the integrals considered so far. We start from $\mathcal{I}_3$, given by eq. (4.15). In the soft limit, the dominant contribution comes from the region $\vec{k}\simeq\vec{q}_1\simeq\vec{q}_2$; hence we can make the replacement

$$\frac{1}{\vec{k}^{\,2}}\to\frac{1}{\vec{Q}^{\,2}} \quad \text{with} \quad \vec{Q}\equiv\frac{\vec{q}_1+\vec{q}_2}{2}$$

and obtain

$$\mathcal{I}_3 \simeq \frac{1}{\vec{Q}^2}\frac{1}{\pi^{1+\epsilon}\Gamma(1-\epsilon)}\int d^{2+2\epsilon}k\frac{1}{\vec{k}^{\,2}(\vec{k}+\vec{p})^2} = \frac{1}{\vec{Q}^2}\frac{\Gamma^2(\epsilon)}{\Gamma(2\epsilon)}(\vec{p}^{\,2})^{\epsilon-1} \,. \tag{C.45}$$

To obtain the soft limit of $\mathcal{I}_{4B}$, eq. (4.17), we restart from the representation

$$\mathcal{I}_{4B} = \int_0^1\frac{dx}{x}(J_B(x)-J_B(0)) \,,$$

where

$$J_B(x) = \int_0^1 dz\frac{1-x}{[z(1-x)(ax+b(1-x)(1-z))]^{1-\epsilon}} \,, \qquad a=\vec{q}_1^{\,2},\ b=\vec{q}_2^{\,2} \,. \tag{C.46}$$

and we observe that, in the soft region

$$\vec{q}_1 \simeq \vec{q}_2 \simeq \frac{\vec{q}_1 + \vec{q}_2}{2} = \vec{Q} \,,$$

$J_B(x)$ becomes

$$J_B(x) \simeq \frac{1}{(\vec{Q}^2)^{1-\epsilon}} \int_0^1 dz \frac{1}{z^{1-\epsilon}(1-x)^{-\epsilon}[1-z(1-x)]^{1-\epsilon}} = \frac{1}{(\vec{Q}^2)^{1-\epsilon}} \int_0^{1-x} dz \; [z(1-z)]^{\epsilon-1}$$

and

$$\mathcal{I}_{4B} = -\frac{1}{(\vec{Q}^2)^{1-\epsilon}} \int_0^1 \frac{dx}{x} \int_{1-x}^1 dz \; [z(1-z)]^{\epsilon-1} = -\frac{1}{(\vec{Q}^2)^{1-\epsilon}} \int_0^1 dz \; [z(1-z)]^{\epsilon-1} \int_{1-z}^1 \frac{dx}{x}$$

$$= \frac{\Gamma^2(\epsilon)}{\Gamma(2\epsilon)} \frac{1}{(\vec{Q}^2)^{1-\epsilon}} (\psi(\epsilon) - \psi(2\epsilon)) \,.$$

Alternatively one can use the property of the Euler-Beta function to find

$$\mathcal{I}_{4B} = -\frac{1}{(\vec{Q}^2)^{1-\epsilon}} \int_0^1 \frac{dx}{x} \int_{1-x}^1 dz \; [z(1-z)]^{\epsilon-1} = -\frac{1}{(\vec{Q}^2)^{1-\epsilon}} \int_0^1 \frac{dx}{x} \left[B(\epsilon,\epsilon) - B(1-x,\epsilon,\epsilon) \right] \,,$$

where $B(x,a,b)$ is the incomplete Euler beta function and $B(a,b) = B(1,a,b)$. Introducing the regularized Euler beta function,

$$I_{1-x}(\epsilon,\epsilon) = \frac{B(1-x,\epsilon,\epsilon)}{B(\epsilon,\epsilon)} \,, \tag{C.47}$$

and using the property $1 - I_{1-x}(\epsilon,\epsilon) = I_x(\epsilon,\epsilon)$, we find

$$\mathcal{I}_{4B} = -\frac{B(\epsilon,\epsilon)}{(\vec{Q}^2)^{1-\epsilon}} \int_0^1 \frac{dx}{x} I_x(\epsilon,\epsilon) = \frac{\Gamma^2(\epsilon)}{\Gamma(2\epsilon)} \frac{1}{(\vec{Q}^2)^{1-\epsilon}} (\psi(\epsilon) - \psi(2\epsilon)) \,. \tag{C.48}$$

The soft limit of the pentagon integral, eq. (4.86), can be immediately obtained and reads [47]

$$I_5 \simeq \frac{\pi^{2+\epsilon}\Gamma(1-\epsilon)}{s} \frac{\Gamma^2(\epsilon)}{\Gamma(2\epsilon)} \frac{(\vec{p}^{\,2})^{\epsilon-1}}{\vec{Q}^2} (\psi(\epsilon) - \psi(1-\epsilon) + i\pi) \,. \tag{C.49}$$

From this, by using eq. (4.87), we obtain

$$\mathcal{I}_5 - \mathcal{L}_3 \simeq \frac{\Gamma^2(\epsilon)}{\Gamma(2\epsilon)} \frac{(\vec{p}^{\,2})^{\epsilon-1}}{\vec{Q}^2} (\psi(1-\epsilon) - \psi(\epsilon)) \,. \tag{C.50}$$

Appendix D

Further details on the di-hadron production

D.1 Finite parts of virtual corrections

D.1.1 Building-block integrals

$$I_1^k(\vec{q}_1,\,\vec{q}_2,\,\Delta_1,\,\Delta_2) \;\equiv\; \frac{1}{\pi}\int \frac{d^d\vec{l}\,(l_\perp^k)}{\Big[(\vec{l}-\vec{q}_1)^2+\Delta_1\Big]\Big[(\vec{l}-\vec{q}_2)^2+\Delta_2\Big]\,\vec{l}^{\,2}}, \tag{D.1}$$

$$I_2(\vec{q}_1,\,\vec{q}_2,\,\Delta_1,\,\Delta_2) \;\equiv\; \frac{1}{\pi}\int \frac{d^d\vec{l}}{\Big[(\vec{l}-\vec{q}_1)^2+\Delta_1\Big]\Big[(\vec{l}-\vec{q}_2)^2+\Delta_2\Big]}, \tag{D.2}$$

$$I_3^k(\vec{q}_1,\,\vec{q}_2,\,\Delta_1,\,\Delta_2) \;\equiv\; \frac{1}{\pi}\int \frac{d^d\vec{l}\,(l_\perp^k)}{\Big[(\vec{l}-\vec{q}_1)^2+\Delta_1\Big]\Big[(\vec{l}-\vec{q}_2)^2+\Delta_2\Big]}, \tag{D.3}$$

$$I^{jk}(\vec{q}_1,\,\vec{q}_2,\,\Delta_1,\,\Delta_2) \;\equiv\; \frac{1}{\pi}\int \frac{d^d\vec{l}\,(l_\perp^j l_\perp^k)}{\Big[(\vec{l}-\vec{q}_1)^2+\Delta_1\Big]\Big[(\vec{l}-\vec{q}_2)^2+\Delta_2\Big]\,\vec{l}^{\,2}}\,. \tag{D.4}$$

The arguments of these integrals will be different for each diagram so we will write them explicitly before giving the expression of each diagram, but we will omit them in the equations for the reader's convenience.

Explicit results for the first three integrals in (D.1-D.4) are obtained by a straightforward Feynman parameter integration. We will express them using the following variables:

$$\rho_1 \;\equiv\; \frac{(\vec{q}_{12}^{\,2}+\Delta_{12})-\sqrt{(\vec{q}_{12}^{\,2}+\Delta_{12})^2+4\vec{q}_{12}^{\,2}\Delta_2}}{2\vec{q}_{12}^{\,2}}, \tag{D.5}$$

$$\rho_2 \equiv \frac{(\vec{q}_{12}^{\,2}+\Delta_{12})+\sqrt{(\vec{q}_{12}^{\,2}+\Delta_{12})^2+4\vec{q}_{12}^{\,2}\Delta_2}}{2\vec{q}_{12}^{\,2}}\,, \tag{D.6}$$

where $\Delta_{ij}=\Delta_i-\Delta_j$.
One gets

$$\begin{aligned} I_1^k &= \frac{q_{1\perp}^k}{2\left[\vec{q}_{12}^{\,2}\left(\vec{q}_1^{\,2}+\Delta_1\right)\left(\vec{q}_2^{\,2}+\Delta_2\right)-\left(\vec{q}_1^{\,2}-\vec{q}_2^{\,2}+\Delta_{12}\right)\left(\vec{q}_1^{\,2}\Delta_2-\vec{q}_2^{\,2}\Delta_1\right)\right]} \\ &\times \left\{\frac{\left(\vec{q}_2^{\,2}+\Delta_2\right)\vec{q}_{12}^{\,2}+\vec{q}_2^{\,2}\left(\Delta_1+\Delta_2\right)+\Delta_2\left(\Delta_{21}-2\vec{q}_1^{\,2}\right)}{\left(\rho_1-\rho_2\right)\vec{q}_{12}^{\,2}}\ln\left[\left(\frac{-\rho_1}{1-\rho_1}\right)\left(\frac{1-\rho_2}{-\rho_2}\right)\right]\right. \\ &\times \left.\left(\vec{q}_2^{\,2}+\Delta_2\right)\ln\left[\frac{\Delta_2\left(\vec{q}_1^{\,2}+\Delta_1\right)^2}{\Delta_1\left(\vec{q}_2^{\,2}+\Delta_2\right)^2}\right]+(1\leftrightarrow 2)\right\}\,, \end{aligned} \tag{D.7}$$

$$I_2 = \frac{1}{\vec{q}_{12}^{\,2}\left(\rho_1-\rho_2\right)}\ln\left[\left(\frac{-\rho_1}{1-\rho_1}\right)\left(\frac{1-\rho_2}{-\rho_2}\right)\right]\,, \tag{D.8}$$

and

$$\begin{aligned} I_3^k &= \frac{\left(\vec{q}_{12}^{\,2}+\Delta_{12}\right)q_1^k+\left(\vec{q}_{21}^{\,2}+\Delta_{21}\right)q_2^k}{2\left(\rho_1-\rho_2\right)\left(\vec{q}_{12}^{\,2}\right)^2}\ln\left[\left(\frac{-\rho_1}{1-\rho_1}\right)\left(\frac{1-\rho_2}{-\rho_2}\right)\right] \\ &- \frac{q_{12}^k}{2\vec{q}_{12}^{\,2}}\ln\left(\frac{\Delta_1}{\Delta_2}\right)\,. \end{aligned} \tag{D.9}$$

Please note that in some cases the real part of Δ_1 or Δ_2 will be negative so the previous results can acquire an imaginary part from the imaginary part $\pm i0$ of the arguments.
The last integral in (D.4) can be expressed in terms of the other ones by writing

$$I^{jk}=I_{11}\left(q_{1\perp}^j q_{1\perp}^k\right)+I_{12}\left(q_{1\perp}^j q_{2\perp}^k+q_{2\perp}^j q_{1\perp}^k\right)+I_{22}\left(q_{2\perp}^j q_{2\perp}^k\right)\,, \tag{D.10}$$

with

$$\begin{aligned} I_{11} &= -\frac{1}{2}\frac{\left[\vec{q}_2^{\,2}q_{1\perp k}-\left(\vec{q}_1\cdot\vec{q}_2\right)q_{2\perp k}\right]}{\left[\vec{q}_1^{\,2}\vec{q}_2^{\,2}-\left(\vec{q}_1\cdot\vec{q}_2\right)^2\right]^2} \\ &\times\left[\left(\frac{\vec{q}_1\cdot\vec{q}_2}{\vec{q}_1^{\,2}}\right)\ln\left(\frac{\vec{q}_1^{\,2}+\Delta_1}{\Delta_1}\right)q_{1\perp}^k+\left(\vec{q}_2\cdot\vec{q}_{21}\right)I_3^k+\left\{\vec{q}_2^{\,2}\left(\vec{q}_1\cdot\vec{q}_{12}\right)+\Delta_1\vec{q}_2^{\,2}-\Delta_2\left(\vec{q}_1\cdot\vec{q}_2\right)\right\}I_1^k\right]\,, \\ I_{12} &= \frac{-1}{4\left[\vec{q}_1^{\,2}\vec{q}_2^{\,2}-\left(\vec{q}_1\cdot\vec{q}_2\right)^2\right]}\ln\left(\frac{\vec{q}_1^{\,2}+\Delta_1}{\Delta_1}\right) \\ &+\frac{\vec{q}_2^{\,2}\left(\vec{q}_1\cdot\vec{q}_2\right)}{2\left[\vec{q}_1^{\,2}\vec{q}_2^{\,2}-\left(\vec{q}_1\cdot\vec{q}_2\right)^2\right]^2}\left[\left(\vec{q}_1^{\,2}+\Delta_1\right)\left(q_{1\perp k}I_1^k\right)+\left(q_{1\perp k}I_3^k\right)\right] \end{aligned} \tag{D.11}$$

$$- \frac{(\vec{q}_1^{\,2}\vec{q}_2^{\,2}) + (\vec{q}_1\cdot\vec{q}_2)^2}{4\left[\vec{q}_1^{\,2}\vec{q}_2^{\,2} - (\vec{q}_1\cdot\vec{q}_2)^2\right]^2}\left[\left(\vec{q}_2^{\,2}+\Delta_2\right)\left(q_{1\perp k}I_1^k\right) + \left(q_{1\perp k}I_3^k\right)\right] + (1\leftrightarrow 2), \tag{D.12}$$

$$I_{22} = I_{11}|_{1\leftrightarrow 2}\,. \tag{D.13}$$

In what follows, for the ϕ's functions we use the variables $x, \bar{x}$. In the main text these should be identified as $x = x_q$ and $\bar{x} = x_{\bar{q}}$.

D.1.2 ϕ_4

The arguments in the integrals of D.1.1 are

$$\begin{aligned}
\vec{q}_1 &= \vec{p}_1 - \left(\frac{x-z}{x}\right)\vec{p}_q, \qquad \vec{q}_2 = \left(\frac{x-z}{x}\right)(x\vec{p}_{\bar{q}} - \bar{x}\vec{p}_q)\,, \\
\Delta_1 &= (x-z)(\bar{x}+z)\,Q^2, \quad \Delta_2 = -\frac{x\,(\bar{x}+z)}{\bar{x}\,(x-z)}\vec{q}^{\,2} - i0\,.
\end{aligned}$$

Let us write the impact factors in terms of these variables.
They read:

(longitudinal NLO) $\times$ (longitudinal LO) contribution:

$$(\phi_4)_{LL} = -\frac{4(x-z)(\bar{x}+z)}{z}[-\bar{x}(x-z)(z+1)I_2 + q_{2\perp k}(2x^2-(2x-z)(z+1))I_1^k]\,, \tag{D.14}$$

(longitudinal NLO) $\times$ (transverse LO) contribution:

$$(\phi_4)^j_{LT} = (1-2x)p_{q1'}{}^j_{\perp}\,(\phi_4)_{LL} - 4(x-z)(\bar{x}+z)(1-2x+z)[(\vec{q}\cdot\vec{p}_{q1'})g^j_{\perp k} + q^j_{2\perp}p_{q1'\perp k}]I_1^k\,, \tag{D.15}$$

(transverse NLO) $\times$ (longitudinal LO) contribution:

$$\begin{aligned}
(\phi_4)^i_{TL} = 2\{&[(x-\bar{x}-z)q^i_{2\perp}q_{1\perp k} + (-8x\bar{x}-6xz+2z^2+3z+1)q^j_{1\perp}q_{2\perp k}]I_1^k \\
&- 2[4x^2 - x(3z+5) + (z+1)^2]q_{2\perp k}I^{ik} + (x-\bar{x}-z)\,(\vec{q}_2\cdot\vec{q}_1)\,I^i \\
&+ I_2[(x-\bar{x}-z)q^i_{2\perp} + \bar{x}(2(x-z)^2 - 5x + 3z + 1)q^i_{1\perp}] \\
&- \bar{x}[2(x-z)^2 - 5x + 3z + 1]I_3^i \\
&+ \frac{x\bar{x}(1-2x)}{z}[2q_{2\perp k}I^{ik} + I_3^i - q^i_{1\perp}(2q_{2\perp k}I_1^k + I_2)]\}\,,
\end{aligned} \tag{D.16}$$

(transverse NLO) $\times$ (transverse LO) contribution:

$$\begin{aligned}
(\phi_4)^{ij}_{TT} &= \left[(x-\bar{x}-2z)(x-\bar{x}-z)(\vec{q}_2\cdot\vec{p}_{q1'})q^i_{1\perp} + (z+1)((\vec{q}_1\cdot\vec{q}_2)\,p^i_{q1'\perp} - (\vec{q}_1\cdot\vec{p}_{q1'})q^i_{2\perp})\right]I_1^j \\
&+ 2\bar{x}[q_{2\perp k} - (x-z)q_{1\perp k}](p^i_{q1'\perp}I^{jk} - g^{ij}_{\perp}p_{q1'\perp l}I^{kl})
\end{aligned}$$

$$
\begin{aligned}
&+ \quad 2(x-z)[(2\bar{x}+z)(\vec{q}_2\cdot\vec{p}_{q1'}) - \bar{x}(\vec{q}_1\cdot\vec{p}_{q1'})]I^{ij} \\
&+ \quad [(1-z)((\vec{q}_1\cdot\vec{p}_{q1'})q^j_{2\perp} - (\vec{q}_2\cdot\vec{p}_{q1'})q^j_{1\perp}) - (1-2x)(\bar{x}-x+z)\,(\vec{q}_1\cdot\vec{q}_2)\,p^j_{q1'\perp}]I^i_1 \\
&- \quad 2\left[(x-z)(\bar{x}q^j_{1\perp} - (2\bar{x}+z)q^j_{2\perp})p_{q1'\perp k}\right. \\
&+ \quad \left.(1-2x)\left(4x^2-(3z+5)x+(z+1)^2\right)q_{2\perp k}{p_{q1'}}^j_{\perp}\right]I^{ik} \\
&- \quad \bar{x}\,(\bar{x}-x)\left(2(x-z)^2-5x+3z+1\right)p^j_{q1'\perp}I^i_3 \\
&+ \quad \bar{x}\,(\bar{x}+z)\,(p^i_{q1'\perp}I^j_3 - g^{ij}_{\perp}p_{q1'\perp k}I^k_3) \\
&+ \quad I_2\left[g^{ij}_{\perp}\,((1-z)(\vec{q}_2\cdot\vec{p}_{q1'}) - \bar{x}(1+x-z)(\vec{q}_1\cdot\vec{p}_{q1'}))\right. \\
&+ \quad ((1-z)q^j_{2\perp} - \bar{x}(1+x-z)q^j_{1\perp}){p_{q1'}}^i_{\perp} \\
&- \quad \left.(\bar{x}-x)\left((\bar{x}-x+z)q^i_{2\perp} - \bar{x}\left(2(x-z)^2-5x+3z+1\right)q^i_{1\perp}\right){p_{q1'}}^j_{\perp}\right] \\
&+ \quad I^k_1\left[g^{ij}_{\perp}\,((x-\bar{x}+z)(\vec{q}_1\cdot\vec{p}_{q1'})q_{2\perp k} + (1-z)(\vec{q}_2\cdot\vec{p}_{q1'})q_{1\perp k} - (z+1)\,(\vec{q}_1\cdot\vec{q}_2)\,p_{q1'\perp k})\right. \\
&+ \quad q^j_{1\perp}((x-\bar{x}+z)q_{2\perp k}p^i_{q1'\perp} - (z+1)q^i_{2\perp}p_{q1'\perp k}) \\
&+ \quad q^j_{2\perp}((x-\bar{x}-2z)(x-\bar{x}-z)q^i_{1\perp}p_{q1'\perp k} + (1-z)q_{1\perp k}{p_{q1'}}^i_{\perp}) \\
&- \quad \left.(1-2x)((1-2x+z)q^i_{2\perp}q_{1\perp k} - (2z^2+3z-x(8\bar{x}+6z)+1)q^i_{1\perp}q_{2\perp k}){p_{q1'}}^j_{\perp}\right] \\
&+ \quad \frac{x\bar{x}}{z}\left[(x-\bar{x})^2p^j_{q1'\perp}(2q_{2\perp k}I^{ik} + I^i_3 - q^i_{1\perp}(I_2 + 2q_{2\perp k}I^k_1))\right. \\
&+ \quad p^i_{q1'\perp}(q^j_{1\perp}(I_2 + 2q_{2\perp k}I^k_1) - 2q_{2\perp k}I^{jk} - I^j_3) \\
&+ \quad \left.g^{ij}_{\perp}((\vec{q}_1\cdot\vec{p}_{q1'})(I_2 + 2q_{2\perp k}I^k_1) + p_{q1'\perp k}(2q_{2\perp l}I^{kl} + I^k_3))\right]\,. \qquad \text{(D.17)}
\end{aligned}
$$

D.1.3 ϕ_5

Here the integrals from D.1.1 will have the following arguments :

$$\vec{q}_1 = \left(\frac{x-z}{x}\right)\vec{p}_3 - \frac{z}{x}\vec{p}_1, \quad \vec{q}_2 = \vec{p}_{q1} - \frac{z}{x}\vec{p}_q\,, \qquad \text{(D.18)}$$

$$\Delta_1 = \frac{z(x-z)}{x^2\bar{x}}(\vec{p}^{\,2}_{\bar{q}2} + x\bar{x}Q^2), \quad \Delta_2 = (x-z)(\bar{x}+z)Q^2\,. \qquad \text{(D.19)}$$

With such variables, it is easy to see that the argument in the square roots in (D.6) are full squares. In terms of the variables in (D.18), the impact factors read,

(longitudinal NLO) $\times$ (longitudinal LO):

$$(\phi_5)_{LL} = \frac{4(x-z)(-2x(\bar{x}+z)+z^2+z)}{xz}\left[\bar{x}(x-z)I_2 - (zq_{1\perp k} - x\,(\bar{x}+z)\,q_{2\perp k})\,I^k_1\right]\,, \qquad \text{(D.20)}$$

(longitudinal NLO) $\times$ (transverse LO) :

$$(\phi_5)^j_{LT} = (\bar{x}-x)p^j_{q1'\perp}\,(\phi_5)_{LL} \qquad \text{(D.21)}$$

$$+\frac{4(x-z)(x-\bar{x}-z)}{x}\left(zq_{1\perp}^{k}-x(\bar{x}+z)q_{2\perp}^{k}\right)p_{q1'\perp l}\left(g_{\perp k}^{j}I_1^{l}+I_1^{j}\right)\,,$$

(transverse NLO) × (longitudinal LO) :

$$\begin{aligned}
(\phi_5)_{TL}^{i} &= 2\left[(x-\bar{x}-z)\,(\vec{q}_1\cdot\vec{q}_2)-\bar{x}(x-z)^2Q^2+(\frac{z}{x}-x)\vec{q}_1^{\,2}\right]I_1^{i}\\
&+\frac{2}{x}\left[xq_{2\perp k}(-8x\bar{x}-6xz+2z^2+3z+1)+2q_{1\perp k}(2xz-2x^2+x-z^2)\right]q_{1\perp}^{i}I_1^{k}\\
&+2q_{2\perp}^{i}q_{1\perp k}(x-\bar{x}-z)I_1^{k}+2\frac{\bar{x}}{x}(x(8x-3)-6xz+2z^2+z)I_1^{i}\\
&+\frac{2}{x}\left[xq_{2\perp}^{i}(x-\bar{x}-z)+q_{1\perp}^{i}(8x^3-6x^2(z+2)+x(z+3)(2z+1)-2z^2)\right]I_2\\
&-\frac{4}{x}\left[(x-z)(\bar{x}+z)q_{1\perp k}+x(4x^2-x(3z+5)+(z+1)^2)q_{2\perp k}\right]I^{ik}\\
&-\frac{4}{z}x\bar{x}(x-\bar{x})\left[q_{2\perp k}I^{ik}+I_3^{i}-q_{1\perp}^{i}\left(q_{2\perp k}I_1^{k}+I_2\right)\right]\,,
\end{aligned}\tag{D.22}$$

(transverse NLO) × (transverse LO) :

$$\begin{aligned}
(\phi_5)_{TT}^{ij} &= -2(x-z)\left[\frac{z}{x}(\vec{q}_1\cdot\vec{p}_{q1'})-(2\bar{x}+z)(\vec{q}_2\cdot\vec{p}_{q1'})\right]I^{ij}\\
&+\left[-\bar{x}(x-z)^2Q^2p_{q1'\perp}^{i}+(\bar{x}-x+2z)(\bar{x}-x+z)(\vec{q}_2\cdot\vec{p}_{q1'})q_{1\perp}^{i}\right.\\
&-(\vec{q}_1\cdot\vec{p}_{q1'})((z+1)q_{2\perp}^{i}-2\frac{z}{x}(2x-z)q_{1\perp}^{i})\\
&\left.+((z+1)\,(\vec{q}_1\cdot\vec{q}_2)-\left(x+\frac{z}{x}\right)\vec{r}^{\,2})p_{q1'\perp}^{i}\right]I_1^{j}\\
&-2\frac{\bar{x}}{x}(xq_{2\perp k}+(x-z)q_{1\perp k})\left(g_{\perp}^{ij}p_{q1'\perp l}I^{kl}-p_{q1'}{}_{\perp}^{i}I^{jk}\right)\\
&+\left[\bar{x}\,(x-\bar{x})\,(x-z)^2Q^2p_{q1'\perp}^{j}-(z-1)(\vec{q}_1\cdot\vec{p}_{q1'})q_{2\perp}^{j}\right.\\
&\left.+(z-1)(\vec{q}_2\cdot\vec{p}_{q1'})q_{1\perp}^{j}+\frac{x-\bar{x}}{x}\left((x^2-z)\vec{q}_1^{\,2}+x(\bar{x}-x+z)(\vec{q}_1\cdot\vec{q}_2)\right)p_{q1'\perp}^{k}\right]I_1^{i}\\
&+2\left[\frac{x-\bar{x}}{x}\left(x(4x^2-(3z+5)x+(z+1)^2)q_{2\perp k}+(x-z)(\bar{x}+z)q_{1\perp k}\right)p_{q1'\perp}^{j}\right.\\
&\left.-\frac{x-z}{x}\left(x(2x-z-2)q_{2\perp}^{j}+zq_{1\perp}^{j}\right)p_{q1'\perp k}\right]I^{ik}\\
&+\frac{\bar{x}\,(\bar{x}-x)}{x}\left(2z^2-6xz+z+x(8x-3)\right)p_{q1'\perp}^{j}I_3^{i}\\
&+\left[(x-\bar{x})\left((\bar{x}-x+z)q_{2\perp}^{i}+\left(6(z+2)x-8x^2-(z+3)(2z+1)+2\frac{z^2}{x}\right)q_{1\perp}^{i}r_{\perp}^{i}\right)p_{q1'\perp}^{j}\right.\\
&\left.+(1-z)(g_{\perp}^{ij}(\vec{q}_2\cdot\vec{p}_{q1'})+q_{2\perp}^{k}p_{q1'\perp}^{i})+(2x+z-3)(g_{\perp}^{ik}(\vec{q}_1\cdot\vec{p}_{q1'})+q_{1\perp}^{k}p_{q1'\perp}^{i})\right]I_2\\
&+\left(3\bar{x}+z-\frac{z}{x}\right)p_{q1'\perp}^{i}I_3^{k}-\frac{\bar{x}}{x}(3x-z)g_{\perp}^{ij}p_{q1'\perp k}I_3^{k}\\
&+\left[(x-\bar{x})p_{q1'\perp}^{j}\left\{(\bar{x}-x+z)q_{2\perp}^{i}q_{1\perp k}-(2z^2-6xz+3z-8x\bar{x}+1)q_{2\perp k}q_{1\perp}^{i}\right.\right.
\end{aligned}$$

$$
\begin{aligned}
&- 2(\bar{x}-x+2z-\frac{z^2}{x})q_{1\perp k}q^i_{1\perp}\Big\} + \bar{x}(x-z)^2Q^2 g^{ij}_\perp p_{q1'\perp k} \\
&+ (1-z)q_{1\perp k}(g^{ij}_\perp(\vec{q}_2\cdot\vec{p}_{q1'}) + q^j_{2\perp}p^i_{q1'\perp}) \\
&+ ((x-\bar{x}+z)q_{2\perp k} - 2q_{1\perp k})\left(g^{ij}_\perp(\vec{q}_1\cdot\vec{p}_{q1'}) + q^j_{1\perp}p^i_{q1'\perp}\right) \\
&+ g^{ij}_\perp\left(\left(x+\frac{z}{x}\right)\vec{q}_1^{\,2} - (z+1)(\vec{q}_1\cdot\vec{q}_2)\right)p_{q1'\perp k} \\
&+ \left((x-\bar{x}-2z)(x-\bar{x}-z)q^i_{1\perp}q^j_{2\perp} - (z+1)q^i_{2\perp}q^j_{1\perp} + 2(2x-z)\frac{z}{x}q^i_{1\perp}q^j_{1\perp}\right)p_{q1'\perp k}\Big] I^k_1 \\
&+ \frac{2x\bar{x}}{z}\left[(x-\bar{x})^2 p^j_{q1'\perp}(q_{2\perp k}I^{ik} + I^i_3) - p^i_{q1'\perp}(q_{2\perp k}I^{jk} + I^k_3) + g^{ij}_\perp p_{q1'\perp k}(q_{2\perp l}I^{kl} + I^k_3)\right. \\
&\left.+ (I_2 + q_{2\perp k}I^k_1)\left(g^{ij}_\perp(\vec{q}_1\cdot\vec{p}_{q1'}) + q^j_{1\perp}p^i_{q1'\perp} - (1-2x)^2 q^i_{1\perp}p^j_{q1'\perp}\right)\right]. \qquad \text{(D.23)}
\end{aligned}
$$

D.1.4 ϕ_6

We will use the variable

$$\vec{q} = \left(\frac{x-z}{x}\right)\vec{p}_3 - \frac{z}{x}\vec{p}_1\,. \qquad \text{(D.24)}$$

In terms of these variable we have (longitudinal NLO) $\times$ (longitudinal NLO) :

$$(\phi_6)_{LL} = -4x\bar{x}^2 J_0\,, \qquad \text{(D.25)}$$

(longitudinal NLO) $\times$ (transverse NLO) :

$$(\phi_6)^j_{LT} = (1-2x)p^j_{q1'\perp}(\phi_6)_{LL}\,, \qquad \text{(D.26)}$$

(transverse NLO) $\times$ (longitudinal NLO) :

$$(\phi_6)^i_{TL} = 2\bar{x}\left[(1-2x)p^i_{\bar{q}2\perp}J_0 - J^i_{1\perp}\right], \qquad \text{(D.27)}$$

(transverse NLO) $\times$ (transverse NLO) :

$$
\begin{aligned}
(\phi_6)^{ij}_{TT} = {}& \bar{x}\left[(x-\bar{x})^2 p^i_{\bar{q}2\perp}p^j_{q1'\perp} - g^{ij}_\perp(\vec{p}_{\bar{q}2}\cdot\vec{p}_{q1'}) - p^i_{q1'\perp}p^j_{\bar{q}2\perp}\right]J_0 \\
&+ \bar{x}\left[(x-\bar{x})p^j_{q1'\perp}g^i_{\perp k} - p_{q1'\perp k}g^{ij}_\perp + p^i_{q1'\perp}g^j_{\perp k}\right]J^k_{1\perp}\,. \qquad \text{(D.28)}
\end{aligned}
$$

We introduced

$$J^k_{1\perp} = \frac{(x-z)^2}{x^2}\frac{q^k_\perp}{\vec{q}^{\,2}}\ln\left(\frac{\vec{p}^{\,2}_{\bar{q}2} + x\bar{x}Q^2}{\vec{p}^{\,2}_{\bar{q}2} + x\bar{x}Q^2 + \frac{x^2\bar{x}}{z(x-z)}\vec{q}^{\,2}}\right), \qquad \text{(D.29)}$$

and

$$J_0 = \frac{z}{x(\vec{p}^{\,2}_{\bar{q}2} + x\bar{x}Q^2)} - \frac{2x(x-z)+z^2}{xz(\vec{p}^{\,2}_{\bar{q}2} + x\bar{x}Q^2)}\ln\left(\frac{x^2\bar{x}\mu^2}{z(x-z)(\vec{p}^{\,2}_{\bar{q}2} + x\bar{x}Q^2) + x^2\bar{x}\vec{q}^{\,2}}\right). \qquad \text{(D.30)}$$

D.2 Finite part of squared impact factors

In this section, we present the finite part of squared impact factors for the real corrections case.

D.2.1 LL transition

The double-dipole × double-dipole contribution is

$$\Phi_4^+(p_{1\perp},p_{2\perp},p_{3\perp})\Phi_4^{+*}(p'_{1\perp},p'_{2\perp},p'_{3\perp}) = \frac{8p_\gamma^{+4}}{z^2\left(\frac{\vec{p}^{\,2}_{\bar{q}2'}}{x_{\bar{q}}(1-x_{\bar{q}})}+Q^2\right)\left(Q^2+\frac{\vec{p}^{\,2}_{q1'}}{x_q}+\frac{\vec{p}^{\,2}_{\bar{q}2'}}{x_{\bar{q}}}+\frac{\vec{p}^{\,2}_{g3'}}{z}\right)}$$
$$\times\left[\frac{x_{\bar{q}}\left(dz^2+4x_q\left(x_q+z\right)\right)\left(x_q\vec{p}_{g3}-z\vec{p}_{q1}\right)\left(x_q\vec{p}_{g3'}-z\vec{p}_{q1'}\right)}{x_q\left(x_q+z\right)^2\left(\frac{(\vec{p}_{g3}+\vec{p}_{q1})^2}{x_{\bar{q}}(x_q+z)}+Q^2\right)\left(\frac{(\vec{p}_{g3}+\vec{p}_{q1})^2}{x_{\bar{q}}}+\frac{\vec{p}^{\,2}_{g3}}{z}+\frac{\vec{p}^{\,2}_{q1}}{x_q}+Q^2\right)}\right.$$
$$\left.-\frac{(4x_qx_{\bar{q}}+2z-dz^2)(x_{\bar{q}}\vec{p}_{g3}-z\vec{p}_{\bar{q}2})(x_q\vec{p}_{g3'}-z\vec{p}_{q1'})}{\left(x_{\bar{q}}+z\right)\left(x_q+z\right)\left(\frac{(\vec{p}_{\bar{q}2}+\vec{p}_{g3})^2}{x_q(x_{\bar{q}}+z)}+Q^2\right)\left(\frac{(\vec{p}_{\bar{q}2}+\vec{p}_{g3})^2}{x_q}+\frac{\vec{p}^{\,2}_{g3}}{z}+\frac{\vec{p}^{\,2}_{\bar{q}2}}{x_{\bar{q}}}+Q^2\right)}\right]+(q\leftrightarrow\bar{q}). \quad \text{(D.31)}$$

The interference term in the dipole × dipole contribution reads

$$\left(\tilde{\Phi}_3^+(\vec{p}_1,\vec{p}_2)\Phi_4^{+*}(\vec{p}_{1'},\vec{p}_{2'},\vec{0})+\Phi_4^+(\vec{p}_1,\vec{p}_2,\vec{0})\tilde{\Phi}_3^{+*}(\vec{p}_{1'},\vec{p}_{2'})\right)$$
$$=\left[\frac{8p_\gamma^{+4}}{z\left(x_q+z\right)\left(\frac{\vec{p}^{\,2}_{\bar{q}2'}}{x_{\bar{q}}(x_q+z)}+Q^2\right)\left(\frac{\vec{p}^{\,2}_{q1'}}{x_q}+\frac{\vec{p}^{\,2}_{\bar{q}2'}}{x_{\bar{q}}}+\frac{\vec{p}_g^{\,2}}{z}+Q^2\right)}\right.$$
$$\times\left\{\frac{\left(4x_qx_{\bar{q}}+z(2-dz)\right)\left(\vec{p}_g-\frac{z}{x_{\bar{q}}}\vec{p}_{\bar{q}}\right)\left(x_q\vec{p}_g-z\vec{p}_{q1'}\right)}{\left(\vec{p}_g-\frac{z\vec{p}_{\bar{q}}}{x_{\bar{q}}}\right)^2\left(\frac{\vec{p}^{\,2}_{q1'}}{x_q(x_{\bar{q}}+z)}+Q^2\right)}\right.$$
$$\left.\left.-\frac{x_{\bar{q}}\left(dz^2+4x_q\left(x_q+z\right)\right)\left(\vec{p}_g-\frac{z}{x_q}\vec{p}_q\right)\left(\vec{p}_g-\frac{z}{x_q}\vec{p}_{q1'}\right)}{\left(\vec{p}_g-\frac{z\vec{p}_q}{x_q}\right)^2\left(\frac{\vec{p}^{\,2}_{\bar{q}2}}{x_{\bar{q}}(x_q+z)}+Q^2\right)}\right\}+(q\leftrightarrow\bar{q})\right]$$
$$+(1\leftrightarrow1',2\leftrightarrow2'). \quad \text{(D.32)}$$

The double-dipole × dipole contribution has the form

$$\Phi_4^+(\vec{p}_1,\vec{p}_2,\vec{p}_3)\,\Phi_3^{+*}(\vec{p}_{1'},\vec{p}_{2'})=\Phi_4^+(\vec{p}_1,\vec{p}_2,\vec{p}_3)\Phi_4^{+*}(\vec{p}_{1'},\vec{p}_{2'},\vec{0})+\Phi_4^+(\vec{p}_1,\vec{p}_2,\vec{p}_3)\tilde{\Phi}_3^{+*}(\vec{p}_{1'},\vec{p}_{2'}), \quad \text{(D.33)}$$

where

$$\Phi_4^+(\vec{p}_1,\vec{p}_2,\vec{p}_3)\tilde{\Phi}_3^{+*}(\vec{p}_{1'},\vec{p}_{2'}) = \frac{8p_\gamma^{+4}}{z\,(x_q+z)\left(\frac{\vec{p}_{\bar{q}2}^{\,2}}{x_{\bar{q}}(x_q+z)}+Q^2\right)\left(\frac{\vec{p}_{q1}^{\,2}}{x_q}+\frac{\vec{p}_{\bar{q}2}^{\,2}}{x_{\bar{q}}}+\frac{\vec{p}_{g3}^{\,2}}{z}+Q^2\right)}$$
$$\times\left\{\frac{(4x_qx_{\bar{q}}+z(2-dz))\,(\vec{p}_g-\frac{z}{x_{\bar{q}}}\vec{p}_{\bar{q}})(x_q\vec{p}_{g3}-z\vec{p}_{q1})}{(\vec{p}_g-\frac{z\vec{p}_{\bar{q}}}{x_{\bar{q}}})^2\left(\frac{\vec{p}_{q1'}^{\,2}}{x_q(x_{\bar{q}}+z)}+Q^2\right)}\right.$$
$$\left.-\frac{x_{\bar{q}}\,(dz^2+4x_q\,(x_q+z))\,(\vec{p}_g-\frac{z}{x_q}\vec{p}_q)(\vec{p}_{g3}-\frac{z}{x_q}\vec{p}_{q1})}{(\vec{p}_g-\frac{z\vec{p}_q}{x_q})^2\left(\frac{\vec{p}_{\bar{q}2'}^{\,2}}{x_{\bar{q}}(x_q+z)}+Q^2\right)}\right\}+(q\leftrightarrow\bar{q}). \quad \text{(D.34)}$$

For the dipole × double-dipole contribution, one just has to complex conjugate (D.34) and also invert the name of the momenta i.e. $1',2'\leftrightarrow 1,2$.

D.2.2 LT/TL transition

The double-dipole × double-dipole contribution is

$$\Phi_4^i(p_{1\perp},p_{2\perp},p_{3\perp})\Phi_4^{+*}(p'_{1\perp},p'_{2\perp},p'_{3\perp})$$
$$=\frac{-4p_\gamma^{+3}}{\left(Q^2+\frac{\vec{p}_{g3}^{\,2}}{z}+\frac{\vec{p}_{q1}^{\,2}}{x_q}+\frac{\vec{p}_{\bar{q}2}^{\,2}}{x_{\bar{q}}}\right)\left(Q^2+\frac{\vec{p}_{g3'}^{\,2}}{z}+\frac{\vec{p}_{q1'}^{\,2}}{x_q}+\frac{\vec{p}_{\bar{q}2'}^{\,2}}{x_{\bar{q}}}\right)}$$
$$\times\left(\frac{z\left((\vec{P}\cdot\vec{p}_{q1})G_\perp^i-(\vec{G}\cdot\vec{p}_{q1})P_\perp^i\right)(dz+4x_q-4)-(\vec{G}\cdot\vec{P})p_{q1\perp}^i\,(2x_q-1)\,(4\,(x_q-1)\,x_{\bar{q}}-dz^2)}{z^2x_{\bar{q}}\,(z+x_{\bar{q}})^{\,3}\left(Q^2+\frac{\vec{p}_{q1}^{\,2}}{x_q(z+x_{\bar{q}})}\right)\left(Q^2+\frac{\vec{p}_{q1'}^{\,2}}{x_q(z+x_{\bar{q}})}\right)}\right.$$
$$+\frac{z\left((\vec{P}\cdot\vec{p}_{q1})H_\perp^i-(\vec{H}\cdot\vec{p}_{q1})P_\perp^i\right)(dz+4x_q-2)-(\vec{H}\cdot\vec{P})p_{q1\perp}^i\,(2x_q-1)\,(z(2-dz)+4x_qx_{\bar{q}})}{z^2x_q\,(z+x_q)\,(z+x_{\bar{q}})^{\,2}\left(Q^2+\frac{\vec{p}_{\bar{q}2'}^{\,2}}{(z+x_q)x_{\bar{q}}}\right)\left(Q^2+\frac{\vec{p}_{q1}^{\,2}}{x_q(z+x_{\bar{q}})}\right)}$$
$$\left.+\frac{H_\perp^i\,(z(zd+d-2)+x_q\,(2-4x_{\bar{q}}))\,x_{\bar{q}}}{z\,(z+x_q)^{\,2}\,(z+x_{\bar{q}})\left(Q^2+\frac{\vec{p}_{\bar{q}2'}^{\,2}}{(z+x_q)x_{\bar{q}}}\right)}\right)+(q\leftrightarrow\bar{q}). \quad \text{(D.35)}$$

Here,

$$G_\perp^i=x_{\bar{q}}p_{g3'\perp}^i-zp_{\bar{q}2'\perp}^i,\quad H_\perp^i=x_qp_{g3'\perp}^i-zp_{q1'\perp}^i,\quad P_\perp^i=x_{\bar{q}}p_{g3\perp}^i-zp_{\bar{q}2\perp}^i. \quad \text{(D.36)}$$

The interference term in the dipole × dipole contribution reads

$$\left(\Phi_4^i(\vec{p}_1,\vec{p}_2,\vec{0})\tilde{\Phi}_3^{+*}(\vec{p}_{1'},\vec{p}_{2'})+\tilde{\Phi}_3^i(\vec{p}_1,\vec{p}_2)\Phi_4^{+*}(\vec{p}_{1'},\vec{p}_{2'},\vec{0})\right)$$

$$
\begin{aligned}
&= 4p_\gamma^{+3}\left(\frac{\Delta_{q\perp}^i x_q x_{\bar q}\left(dz^2+dz-2z+2x_q-4x_qx_{\bar q}\right)}{\vec\Delta_q^2\left(z+x_q\right)^2\left(z+x_{\bar q}\right)\left(Q^2+\frac{\vec p_g^{\,2}}{z}+\frac{\vec p_{q1}^{\,2}}{x_q}+\frac{\vec p_{\bar q2}^{\,2}}{x_{\bar q}}\right)\left(Q^2+\frac{\vec p_{\bar q2'}^{\,2}}{(z+x_q)x_{\bar q}}\right)}\right.\\
&-\frac{(\vec J\cdot\vec\Delta_q)p^i_{\bar q2\perp}\left(dz^2+4x_q\left(z+x_q\right)\right)\left(1-2x_{\bar q}\right)+z\left((\vec J\cdot\vec p_{\bar q2})\Delta^i_{q\perp}-(\vec p_{\bar q2}\cdot\vec\Delta_q)J^i_\perp\right)\left(dz+4x_{\bar q}-4\right)}{z\left(z+x_q\right)^3\vec\Delta_q^2\left(Q^2+\frac{\vec p_g^{\,2}}{z}+\frac{\vec p_{q1'}^{\,2}}{x_q}+\frac{\vec p_{\bar q2'}^{\,2}}{x_{\bar q}}\right)\left(Q^2+\frac{\vec p_{\bar q2}^{\,2}}{(z+x_q)x_{\bar q}}\right)\left(Q^2+\frac{\vec p_{\bar q2'}^{\,2}}{(z+x_q)x_{\bar q}}\right)}\\
&-\frac{x_q\left(z\left((\vec K\cdot\vec p_{\bar q2})\Delta^i_{q\perp}-(\vec p_{\bar q2}\cdot\vec\Delta_q)K^i_\perp\right)\left(dz+4x_{\bar q}-2\right)+(\vec K\cdot\vec\Delta_q)p^i_{\bar q2\perp}\left(1-2x_{\bar q}\right)\left(z(dz-2)-4x_qx_{\bar q}\right)\right)}{z\left(z+x_q\right)^2x_{\bar q}\left(z+x_{\bar q}\right)\vec\Delta_q^2\left(Q^2+\frac{\vec p_g^{\,2}}{z}+\frac{\vec p_{q1'}^{\,2}}{x_q}+\frac{\vec p_{\bar q2'}^{\,2}}{x_{\bar q}}\right)\left(Q^2+\frac{\vec p_{\bar q2}^{\,2}}{(z+x_q)x_{\bar q}}\right)\left(Q^2+\frac{\vec p_{q1'}^{\,2}}{x_q(z+x_{\bar q})}\right)}\\
&-\frac{z\left((\vec p_{q1}\cdot\vec\Delta_q)X^i_\perp-(\vec X\cdot\vec p_{q1})\Delta^i_{q\perp}\right)\left(dz+4x_q-2\right)+(\vec X\cdot\vec\Delta_q)p^i_{q1\perp}\left(1-2x_q\right)\left(z(dz-2)-4x_qx_{\bar q}\right)}{z\vec\Delta_q^2\left(z+x_q\right)\left(z+x_{\bar q}\right)^2\left(Q^2+\frac{\vec p_g^{\,2}}{z}+\frac{\vec p_{q1}^{\,2}}{x_q}+\frac{\vec p_{\bar q2}^{\,2}}{x_{\bar q}}\right)\left(Q^2+\frac{\vec p_{\bar q2'}^{\,2}}{(z+x_q)x_{\bar q}}\right)\left(Q^2+\frac{\vec p_{q1}^{\,2}}{x_q(z+x_{\bar q})}\right)}\\
&\left.+\frac{z\left((\vec X\cdot\vec p_{q1})\Delta^i_{\bar q\perp}-(\vec p_{q1}\cdot\vec\Delta_{\bar q})X^i_\perp\right)\left(dz+4x_q-4\right)-(\vec X\cdot\vec\Delta_{\bar q})p^i_{q1\perp}\left(2x_q-1\right)\left(4\left(x_q-1\right)x_{\bar q}-dz^2\right)}{z\left(z+x_{\bar q}\right)^3\vec\Delta_{\bar q}^2\left(Q^2+\frac{\vec p_g^{\,2}}{z}+\frac{\vec p_{q1}^{\,2}}{x_q}+\frac{\vec p_{\bar q2}^{\,2}}{x_{\bar q}}\right)\left(Q^2+\frac{\vec p_{q1}^{\,2}}{x_q(z+x_{\bar q})}\right)\left(Q^2+\frac{\vec p_{q1'}^{\,2}}{x_q(z+x_{\bar q})}\right)}\right)\\
&+(q\leftrightarrow\bar q)\,,
\end{aligned}
\tag{D.37}
$$

where

$$
\vec\Delta_q=\frac{x_q\vec p_g-x_g\vec p_q}{x_q+x_g}\,,\qquad \vec\Delta_{\bar q}=\frac{x_{\bar q}\vec p_g-x_g\vec p_{\bar q}}{x_q+x_g}\,,
\tag{D.38}
$$

$$
\begin{aligned}
X^i_\perp=x_{\bar q}p^i_{g\perp}-zp^i_{\bar q2\perp}=&P^i_\perp|_{p_3=0},\quad J^i_\perp=x_qp^i_{g\perp}-zp^i_{q1'\perp}=H^i_\perp|_{p'_3=0},\\
&K^i_\perp=x_{\bar q}p^i_{g\perp}-zp^i_{\bar q2'\perp}=G^i_\perp|_{p'_3=0}.
\end{aligned}
\tag{D.39}
$$

The TL transition is obtained from above by complex conjugation and inverting the naming of the different momenta in (D.37) and (D.35).

The double-dipole × dipole have, respectively, the form

$$
\Phi_4^i(\vec p_1,\vec p_2,\vec p_3)\Phi_3^{+*}(\vec p_{1'},\vec p_{2'})=\Phi_4^i(\vec p_1,\vec p_2,\vec p_3)\Phi_4^{+*}(\vec p_{1'},\vec p_{2'},0)+\Phi_4^i(\vec p_1,\vec p_2,\vec p_3)\tilde\Phi_3^{+*}(\vec p_{1'},\vec p_{2'})\,,
\tag{D.40}
$$

$$
\Phi_4^+(\vec p_1,\vec p_2,\vec p_3)\Phi_3^{i*}(\vec p_{1'},\vec p_{2'})=\Phi_4^+(\vec p_1,\vec p_2,\vec p_3)\Phi_4^{i*}(\vec p_{1'},\vec p_{2'},\vec 0)+\Phi_4^+(\vec p_1,\vec p_2,\vec p_3)\tilde\Phi_3^{i*}(\vec p_{1'},\vec p_{2'})\,,
\tag{D.41}
$$

where

$$
\Phi_4^i(\vec p_1,\vec p_2,\vec p_3)\tilde\Phi_3^{+*}(\vec p_{1'},\vec p_{2'})=\frac{4p_\gamma^{+3}}{(x_q+z)\,\vec\Delta_q^2\left(\frac{\vec p_{\bar q2'}^{\,2}}{x_{\bar q}(x_q+z)}+Q^2\right)\left(\frac{\vec p_{q1}^{\,2}}{x_q}+\frac{\vec p_{\bar q2}^{\,2}}{x_{\bar q}}+\frac{\vec p_{g3}^{\,2}}{z}+Q^2\right)}
$$

$$\times \left\{ \frac{x_q x_{\bar{q}} \Delta_q^i \left(dz(z+1) - 2\left(1-2x_q\right)\left(x_q+z\right)\right)}{\left(x_q+z\right)\left(x_{\bar{q}}+z\right)} + \frac{\left(dz+4x_q-2\right)\left(\Delta_q^i \vec{P}\cdot\vec{p}_{q1} - P^i \vec{p}_{q1}\cdot\vec{\Delta}_q\right)}{\left(x_{\bar{q}}+z\right)^2\left(\frac{\vec{p}_{q1}^{\,2}}{x_q(x_{\bar{q}}+z)}+Q^2\right)} \right.$$

$$+ \frac{\left(2x_q-1\right)p_{q1}^i \vec{P}\cdot\vec{\Delta}_q\left(z(dz-2)-4x_q x_{\bar{q}}\right)}{z\left(x_{\bar{q}}+z\right)^2\left(\frac{\vec{p}_{q1}^{\,2}}{x_q(x_{\bar{q}}+z)}+Q^2\right)} - \frac{\left((d-4)z-4x_q\right)\left(W^i \vec{p}_{\bar{q}2}\cdot\vec{\Delta}_q - \Delta_q^i \vec{W}\cdot\vec{p}_{\bar{q}2}\right)}{\left(x_q+z\right)^2\left(\frac{\vec{p}_{\bar{q}2}^{\,2}}{x_{\bar{q}}(x_q+z)}+Q^2\right)}$$

$$\left. + \frac{\left(2x_{\bar{q}}-1\right)\left(dz^2+4x_q\left(x_q+z\right)\right)p_{\bar{q}2}^i \vec{W}\cdot\vec{\Delta}_q}{z\left(x_q+z\right)^2\left(\frac{\vec{p}_{\bar{q}2}^{\,2}}{x_{\bar{q}}(x_q+z)}+Q^2\right)} \right\} + \left(q \leftrightarrow \bar{q}\right), \tag{D.42}$$

and

$$\Phi_4^+(\vec{p}_1,\vec{p}_2,\vec{p}_3)\tilde{\Phi}_3^{i*}(\vec{p}_{1'},\vec{p}_{2'}) = \frac{4p_\gamma^{+3}}{z\vec{\Delta}_q^2\left(x_q+z\right)^2\left(Q^2+\frac{\vec{p}_{g3}^{\,2}}{z}+\frac{\vec{p}_{q1}^{\,2}}{x_q}+\frac{\vec{p}_{\bar{q}2}^{\,2}}{x_{\bar{q}}}\right)\left(Q^2+\frac{\vec{p}_{\bar{q}2'}^{\,2}}{(z+x_q)x_{\bar{q}}}\right)}$$

$$\times \left[\frac{x_q z\left(\left((d-4)z-4x_q+2\right)\left(P^i\left(\vec{p}_{\bar{q}2'}\cdot\vec{\Delta}_q\right)-\Delta_q^i\left(\vec{P}\cdot\vec{p}_{\bar{q}2'}\right)\right)\right.}{x_{\bar{q}}\left(x_{\bar{q}}+z\right)\left(\frac{\vec{p}_{q1}^{\,2}}{x_q(x_{\bar{q}}+z)}+Q^2\right)} \right.$$

$$- \frac{x_q\left(x_q-x_{\bar{q}}+z\right)p_{\bar{q}2'}^i\left(\vec{P}\cdot\vec{\Delta}_q\right)\left(z(dz-2)-4x_q x_{\bar{q}}\right)}{x_{\bar{q}}\left(x_{\bar{q}}+z\right)\left(\frac{\vec{p}_{q1}^{\,2}}{x_q(x_{\bar{q}}+z)}+Q^2\right)}$$

$$- \frac{\left(x_q-x_{\bar{q}}+z\right)\left(dz^2+4x_q\left(x_q+z\right)\right)p_{\bar{q}2'}^i\left(\vec{W}\cdot\vec{\Delta}_q\right)}{\left(x_q+z\right)\left(\frac{\vec{p}_{\bar{q}2}^{\,2}}{x_{\bar{q}}(x_q+z)}+Q^2\right)}$$

$$\left. - \frac{z\left(\left(d-4\right)z-4x_q\right)\left(\Delta_q^i\left(\vec{W}\cdot\vec{p}_{\bar{q}2'}\right)-W^i\left(\vec{p}_{\bar{q}2'}\cdot\vec{\Delta}_q\right)\right)}{\left(x_q+z\right)\left(\frac{\vec{p}_{\bar{q}2}^{\,2}}{x_{\bar{q}}(x_q+z)}+Q^2\right)} \right] + \left(q \leftrightarrow \bar{q}\right). \tag{D.43}$$

Here, we introduced

$$W_\perp^i = x_q p_{g3\perp}^i - z p_{q1\perp}^i. \tag{D.44}$$

D.2.3 TT transition

The double-dipole × double-dipole contribution is

$$\Phi_4^i(p_{1\perp},p_{2\perp},p_{3\perp})\Phi_4^k(p'_{1\perp},p'_{2\perp},p'_{3\perp})^* = \left(\frac{p_\gamma^{+2}}{\left(Q^2+\frac{\vec{p}_{g3}^{\,2}}{z}+\frac{\vec{p}_{q1}^{\,2}}{x_q}+\frac{\vec{p}_{\bar{q}2}^{\,2}}{x_{\bar{q}}}\right)\left(Q^2+\frac{\vec{p}_{g3'}^{\,2}}{z}+\frac{\vec{p}_{q1'}^{\,2}}{x_q}+\frac{\vec{p}_{\bar{q}2'}^{\,2}}{x_{\bar{q}}}\right)} \right.$$

$$
\begin{aligned}
&\times \Bigg[-\frac{g_\perp^{ik} x_q x_{\bar q}\,(z d + d - 2 + 2x_{\bar q})}{(z+x_q)^2\,(z+x_{\bar q})} - \frac{2P_\perp^k p_{q1\perp}^i\,(1-2x_q)}{z\,(z+x_{\bar q})^2\left(Q^2+\frac{\vec p_{q1}^{\,2}}{x_q(z+x_{\bar q})}\right)}\left(\frac{(d-2)z-2x_{\bar q}}{z+x_{\bar q}}+\frac{dz+2x_{\bar q}}{z+x_q}\right)\\
&- \frac{2\left(g_\perp^{ik}(\vec P\cdot\vec p_{q1}) + P_\perp^i p_{q1\perp}{}^k\right)}{z\,(z+x_{\bar q})^2\left(Q^2+\frac{\vec p_{q1}^{\,2}}{x_q(z+x_{\bar q})}\right)}\left(\frac{(d-4)z-2x_{\bar q}}{z+x_q}+\frac{(d-2)z-2x_{\bar q}}{z+x_{\bar q}}\right)\\
&- \frac{1}{z^2 x_q\,(z+x_q)^2\,x_{\bar q}\,(z+x_{\bar q})^2\left(Q^2+\frac{\vec p_{\bar q2'}^{\,2}}{(z+x_q)x_{\bar q}}\right)\left(Q^2+\frac{\vec p_{q1}^{\,2}}{x_q(z+x_{\bar q})}\right)}\Big\{(\vec H\cdot\vec P)\left[p_{q1\perp}^i p_{\bar q2'\perp}^k\,(1-2x_q)\right.\\
&\times(1-2x_{\bar q})\,(z(2-dz)+4x_q x_{\bar q}) + (g_\perp^{ik}(\vec p_{q1}\cdot\vec p_{\bar q2'}) + p_{q1\perp}^k p_{\bar q2'\perp}^i)\,(z(2-(d-4)z)+4x_q x_{\bar q})\Big]\\
&+((d-4)z-2)\left[z(\vec H\cdot\vec p_{\bar q2'})(g_\perp^{ik}(\vec P\cdot\vec p_{q1}) + P_\perp^i p_{q1\perp}^k) + zH_\perp^k\left((\vec P\cdot\vec p_{q1})p_{\bar q2'\perp}^i - (\vec p_{q1}\cdot\vec p_{\bar q2'})P_\perp^i\right)\right]\\
&+((d-4)z+2)\left[zH^i\left((\vec P\cdot\vec p_{\bar q2'})p_{q1\perp}^k - (\vec p_{q1}\cdot\vec p_{\bar q2'})P_\perp^k\right) + z(\vec H\cdot\vec p_{q1})(g_\perp^{ik}(\vec P\cdot\vec p_{\bar q2'}) + P_\perp^k p_{\bar q2'\perp}^i)\right]\\
&+2z\left((\vec H\cdot\vec p_{\bar q2'})P_\perp^k - (\vec P\cdot\vec p_{\bar q2'})H_\perp^k\right)p_{q1\perp}{}^i\,(1-2x_q)\,(dz+4x_{\bar q}-2)\Big\}\\
&- \frac{1}{z^2 x_q x_{\bar q}\,(z+x_{\bar q})^4\left(Q^2+\frac{\vec p_{q1}^{\,2}}{x_q(z+x_{\bar q})}\right)\left(Q^2+\frac{\vec p_{q1'}^{\,2}}{x_q(z+x_{\bar q})}\right)}\Big\{z\,((d-4)z-4x_{\bar q})\\
&\times\Big[g_\perp^{ik}\left((\vec G\cdot\vec p_{q1'})(\vec P\cdot\vec p_{q1}) - (\vec G\cdot\vec p_{q1})(\vec P\cdot\vec p_{q1'})\right) + (\vec p_{q1}\cdot\vec p_{q1'})\left(G_\perp^i P_\perp^k - G_\perp^k P_\perp^i\right)\\
&+2(\vec G\cdot\vec p_{q1'})\left(P_\perp^i p_{q1\perp}^k + P_\perp^k p_{q1\perp}^i\,(1-2x_q)\right) - 2(\vec G\cdot\vec p_{q1})\left(P_\perp^k p_{q1'\perp}^i + P_\perp^i p_{q1'\perp}^k\,(1-2x_q)\right)\Big]\\
&+\left.(\vec G\cdot\vec P)\left[p_{q1\perp}^k p_{q1'\perp}^i - p_{q1\perp}^i p_{q1'\perp}^k\,(1-2x_q)^2 + g_\perp^{ik}\,(\vec p_{q1}\cdot\vec p_{q1'})\right]\left(dz^2+4x_{\bar q}\,(z+x_{\bar q})\right)\Big\}\right]\\
&+\left.(1\leftrightarrow 1', 2\leftrightarrow 2', 3\leftrightarrow 3', i\leftrightarrow k)\right) + (q\leftrightarrow\bar q). \qquad \text{(D.45)}
\end{aligned}
$$

The interference term in the dipole × dipole contribution reads

$$
\begin{aligned}
&\left(\tilde\Phi_3^i(\vec p_1,\vec p_2)\Phi_4^{k*}(\vec p_{1'},\vec p_{2'},\vec 0) + \Phi_4^i(\vec p_1,\vec p_2,\vec 0)\tilde\Phi_3^{k*}(\vec p_{1'},\vec p_{2'})\right)\\
&= \Bigg(\frac{2p_\gamma^{+2}}{\vec\Delta_q^2\left(Q^2+\frac{\vec p_g^{\,2}}{z}+\frac{\vec p_{q1}^{\,2}}{x_q}+\frac{\vec p_{\bar q2}^{\,2}}{x_{\bar q}}\right)\left(Q^2+\frac{\vec p_{\bar q2'}^{\,2}}{(z+x_q)x_{\bar q}}\right)}\\
&\times\left[\frac{((d-2)z-2x_q)\,x_q}{(z+x_q)^3}\left(g_\perp^{ik}(\vec p_{\bar q2'}\cdot\vec\Delta_q) + p_{\bar q2'}{}^i{}_\perp\Delta_{q\perp}^k + p_{\bar q2'\perp}^k\Delta_{q\perp}^i\,(1-2x_{\bar q})\right)\right.\\
&+\frac{x_q\left(((d-4)z-2x_q)\left(g_\perp^{ik}(\vec p_{\bar q2'}\cdot\vec\Delta_q) + p_{\bar q2'\perp}^i\Delta_{q\perp}^k\right) + p_{\bar q2'\perp}^k\Delta_{q\perp}^i\,(dz+2x_q)\,(1-2x_{\bar q})\right)}{(z+x_q)^2\,(z+x_{\bar q})}\\
&-\frac{1}{z\,(z+x_q)^2 x_{\bar q}\,(z+x_{\bar q})^2\left(Q^2+\frac{\vec p_{q1}^{\,2}}{x_q(z+x_{\bar q})}\right)}\Big\{z((d-4)z+2)
\end{aligned}
$$

$$
\begin{aligned}
&\times\Big[{p_{q1}}^{i}_{\perp}\left((\vec{p}_{\bar{q}2'}\cdot\vec{\Delta}_q)X^k_\perp-(\vec{X}\cdot\vec{p}_{\bar{q}2'})\Delta^k_{q\perp}\right)(2x_q-1)-(\vec{X}\cdot\vec{p}_{\bar{q}2'})\left(g^{ik}_\perp(\vec{p}_{q1}\cdot\vec{\Delta}_q)+p^k_{q1\perp}\Delta^i_{q\perp}\right)\\
&-X^k_\perp\left((\vec{p}_{q1}\cdot\vec{\Delta}_q)p^i_{\bar{q}2'\perp}-(\vec{p}_{q1}\cdot\vec{p}_{\bar{q}2'})\Delta_q{}^i_\perp\right)\Big]+4x_qz\,(1-2x_q)\,p^i_{q1\perp}\Big((\vec{p}_{\bar{q}2'}\cdot\vec{\Delta}_q)X^k_\perp-(\vec{X}\cdot\vec{p}_{\bar{q}2'})\Delta^k_{q\perp}\Big)\\
&+z\,(1-2x_{\bar{q}})\,(dz+4x_q-2)\,p^k_{\bar{q}2'\perp}\left((\vec{p}_{q1}\cdot\vec{\Delta}_q)X^i_\perp-(\vec{X}\cdot\vec{p}_{q1})\Delta^i_{q\perp}\right)-z((d-4)z-2)\\
&\times\left[\left(g^{ik}_\perp(\vec{X}\cdot\vec{p}_{q1})+X^i_\perp p^k_{q1\perp}\right)(\vec{p}_{\bar{q}2'}\cdot\vec{\Delta}_q)+\left((\vec{X}\vec{p}_{q1})p_{\bar{q}2'}{}^i_\perp-(\vec{p}_{q1}\vec{p}_{\bar{q}2'})X^i_\perp\right)\Delta^k_{q\perp}\right]\\
&+(\vec{X}\cdot\vec{\Delta}_q)p^i_{q1\perp}p^k_{\bar{q}2'\perp}\,(1-2x_q)\,(1-2x_{\bar{q}})\,(z(dz-2)-4x_qx_{\bar{q}})\\
&-(\vec{X}\cdot\vec{\Delta}_q)\left(g^{ik}_\perp(\vec{p}_{q1}\cdot\vec{p}_{\bar{q}2'})+p^k_{q1\perp}p^i_{\bar{q}2'\perp}\right)(z(2-(d-4)z)+4x_qx_{\bar{q}})\Big\}\\
&-\frac{1}{z\,(z+x_q)^{\,4}\left(Q^2+\frac{\vec{p}^{\,2}_{\bar{q}2}}{(z+x_q)x_{\bar{q}}}\right)x_{\bar{q}}}\Big\{z\,(dz+4x_{\bar{q}}-4)\Big[(1-2x_{\bar{q}})\\
&\times\left(p^k_{\bar{q}2'\perp}\left((\vec{p}_{\bar{q}2}\cdot\vec{\Delta}_q)V^i_\perp-(\vec{V}\cdot\vec{p}_{\bar{q}2})\Delta^i_{q\perp}\right)+p^i_{\bar{q}2\perp}\left((\vec{V}\vec{p}_{\bar{q}2'})\Delta^k_{q\perp}-(\vec{p}_{\bar{q}2'}\cdot\vec{\Delta}_q)V^k_\perp\right)\right)\\
&+V^k_\perp\left((\vec{p}_{\bar{q}2}\cdot\vec{\Delta}_q)p^i_{\bar{q}2'\perp}-(\vec{p}_{\bar{q}2}\cdot\vec{p}_{\bar{q}2'})\Delta^i_{q\perp}\right)+\left((\vec{p}_{\bar{q}2}\cdot\vec{p}_{\bar{q}2'})V^i_\perp-(\vec{V}\cdot\vec{p}_{\bar{q}2})p^i_{\bar{q}2'\perp}\right)\Delta^k_{q\perp}\\
&+g^{ik}_\perp\left((\vec{V}\cdot\vec{p}_{\bar{q}2'})(\vec{p}_{\bar{q}2}\cdot\vec{\Delta}_q)-(\vec{V}\cdot\vec{p}_{\bar{q}2})(\vec{p}_{\bar{q}2'}\cdot\vec{\Delta}_q)\right)+p^k_{\bar{q}2\perp}\left((\vec{V}\cdot\vec{p}_{\bar{q}2'})\Delta^i_{q\perp}-(\vec{p}_{\bar{q}2'}\cdot\vec{\Delta}_q)V^i_\perp\right)\Big]\\
&+(\vec{V}\cdot\vec{\Delta}_q)\left(p^i_{\bar{q}2\perp}p^k_{\bar{q}2'\perp}\,(1-2x_{\bar{q}})^2-g^{ik}_\perp(\vec{p}_{\bar{q}2}\cdot\vec{p}_{\bar{q}2'})-p^k_{\bar{q}2\perp}p^i_{\bar{q}2'\perp}\right)\left(dz^2-4x_q\,(x_{\bar{q}}-1)\right)\Big\}\Big]\\
&+(1\leftrightarrow1',2\leftrightarrow2',i\leftrightarrow k)\Big)+(q\leftrightarrow\bar{q}).
\end{aligned}
\tag{D.46}
$$

Here,

$$
V^i_\perp=x_qp^i_{g\perp}-zp^i_{q1\perp}. \tag{D.47}
$$

The double-dipole × dipole contribution has the form

$$
\Phi^i_4(\vec{p}_1,\vec{p}_2,\vec{p}_3)\,\Phi^{k*}_3(\vec{p}_{1'},\vec{p}_{2'})=\Phi^i_4(\vec{p}_1,\vec{p}_2,\vec{p}_3)\Phi^{k*}_4(\vec{p}_{1'},\vec{p}_{2'},\vec{0})+\Phi^i_4(\vec{p}_1,\vec{p}_2,\vec{p}_3)\tilde{\Phi}^{k*}_3(\vec{p}_{1'},\vec{p}_{2'}), \tag{D.48}
$$

where

$$
\begin{aligned}
&\Phi^i_4(\vec{p}_1,\vec{p}_2,\vec{p}_3)\tilde{\Phi}^{k*}_3(\vec{p}_{1'},\vec{p}_{2'})\\
&=\frac{2p^{+2}_\gamma}{\vec{\Delta}^2_q\left(Q^2+\frac{\vec{p}^{\,2}_{g3}}{z}+\frac{\vec{p}^{\,2}_{q1}}{x_q}+\frac{\vec{p}^{\,2}_{\bar{q}2}}{x_{\bar{q}}}\right)\left(Q^2+\frac{\vec{p}^{\,2}_{\bar{q}2'}}{(z+x_q)x_{\bar{q}}}\right)}\\
&\times\left[\frac{((d-2)z-2x_q)\,x_q}{(z+x_q)^{\,3}}\left(g^{ik}_\perp(\vec{p}_{\bar{q}2'}\vec{\Delta}_q)+p_{\bar{q}2'}{}^i_\perp\Delta_{q\perp}{}^k+p_{\bar{q}2'\perp}{}^k\Delta_{q\perp}{}^i\,(1-2x_{\bar{q}})\right)\right.\\
&\left.+\frac{x_q\left(((d-4)z-2x_q)\left(g^{ik}_\perp(\vec{p}_{\bar{q}2'}\vec{\Delta}_q)+p^i_{\bar{q}2'\perp}\Delta^k_{q\perp}\right)+p^k_{\bar{q}2'\perp}\Delta^i_{q\perp}\,(dz+2x_q)\,(1-2x_{\bar{q}})\right)}{(z+x_q)^{\,2}\,(z+x_{\bar{q}})}\right]\\
&-\frac{1}{z\,(z+x_q)^{\,2}x_{\bar{q}}\,(z+x_{\bar{q}})^{\,2}\left(Q^2+\frac{\vec{p}^{\,2}_{q1}}{x_q(z+x_{\bar{q}})}\right)}\Big\{z((d-4)z+2)
\end{aligned}
$$

$$
\begin{aligned}
&\times \Big[p_{q1}{}^{i}_{\perp} \left((\vec{p}_{\bar{q}2'} \vec{\Delta}_q) P^k_\perp - (\vec{P}\vec{p}_{\bar{q}2'}) \Delta_q{}^k_\perp \right) (2x_q - 1) - (\vec{P}\vec{p}_{\bar{q}2'}) \left(g^{ik}_\perp (\vec{p}_{q1}\vec{\Delta}_q) + p_{q1}{}^k_\perp \Delta_q{}^i_\perp \right) \\
&- P^k_\perp \Big((\vec{p}_{q1}\vec{\Delta}_q) p_{\bar{q}2'}{}^i_\perp - (\vec{p}_{q1}\vec{p}_{\bar{q}2'}) \Delta_q{}^i_\perp \Big) \Big] + 4x_q z\,(1-2x_q)\, p_{q1}{}^i_\perp \Big((\vec{p}_{\bar{q}2'}\vec{\Delta}_q) P^k_\perp - (\vec{P}\vec{p}_{\bar{q}2'}) \Delta_q{}^k_\perp \Big) \\
&+ z\,(1-2x_{\bar{q}})\,(dz + 4x_q - 2)\, p_{\bar{q}2'}{}^k_\perp \left((\vec{p}_{q1}\vec{\Delta}_q) P^i_\perp - (\vec{P}\vec{p}_{q1}) \Delta_q{}^i_\perp \right) - z((d-4)z - 2) \\
&\times \Big[\Big(g^{ik}_\perp (\vec{P}\vec{p}_{q1}) + P^i_\perp p_{q1}{}^k_\perp \Big) (\vec{p}_{\bar{q}2'}\vec{\Delta}_q) + \Big((\vec{P}\vec{p}_{q1}) p_{\bar{q}2'}{}^i_\perp - (\vec{p}_{q1}\vec{p}_{\bar{q}2'}) P^i_\perp \Big) \Delta_q{}^k_\perp \Big] \\
&+ (\vec{P}\vec{\Delta}_q) p_{q1}{}^i_\perp p_{\bar{q}2'}{}^k_\perp\, (1-2x_q)\,(1-2x_{\bar{q}})\,(z(dz-2) - 4x_q x_{\bar{q}}) \\
&- (\vec{P}\vec{\Delta}_q) \left(g^{ik}_\perp (\vec{p}_{q1}\vec{p}_{\bar{q}2'}) + p_{q1}{}^k_\perp p_{\bar{q}2'}{}^i_\perp \right) (z(2-(d-4)z) + 4x_q x_{\bar{q}}) \Big\} \ . \qquad \text{(D.49)}
\end{aligned}
$$

As above, the dipole $\times$ double-dipole contribution is obtained by complex conjugation and changing the momenta.

Bibliography

[1] Joachim Bartels, Victor Fadin, Evgeny Levin, Aharon Levy, Victor Kim, and Agustin Sabio-Vera, eds. *From the Past to the Future*. World Scientific, Dec. 2021. ISBN: 978-981-12-3111-7, 978-981-12-3113-1. DOI: 10.1142/12127.

[2] Eugene Levin. "Chapter 2: Lev Lipatov: My Friend and Renowned Physicist". In: *From the Past to the Future*. Ed. by Joachim Bartels, Victor Fadin, Evgeny Levin, Aharon Levy, Victor Kim, and Agustin Sabio-Vera. 2021, pp. 25–55. DOI: 10.1142/9789811231124_0002. arXiv: 1909.11452 [physics.hist-ph].

[3] John Collins. "Foundations of perturbative QCD". In: *Camb. Monogr. Part. Phys. Nucl. Phys. Cosmol.* 32 (2011), pp. 1–624.

[4] H. Fritzsch, Murray Gell-Mann, and H. Leutwyler. "Advantages of the Color Octet Gluon Picture". In: *Phys. Lett. B* 47 (1973), pp. 365–368. DOI: 10.1016/0370-2693(73)90625-4.

[5] V.N. Gribov and L.N. Lipatov. "Deep inelastic e p scattering in perturbation theory". In: *Sov. J. Nucl. Phys.* 15 (1972), pp. 438–450.

[6] Yuri L. Dokshitzer. "Calculation of the Structure Functions for Deep Inelastic Scattering and e+ e- Annihilation by Perturbation Theory in Quantum Chromodynamics." In: *Sov. Phys. JETP* 46 (1977), pp. 641–653.

[7] Guido Altarelli and G. Parisi. "Asymptotic Freedom in Parton Language". In: *Nucl. Phys. B* 126 (1977), pp. 298–318. DOI: 10.1016/0550-3213(77)90384-4.

[8] Victor S. Fadin, E.A. Kuraev, and L.N. Lipatov. "On the Pomeranchuk Singularity in Asymptotically Free Theories". In: *Phys. Lett. B* 60 (1975), pp. 50–52. DOI: 10.1016/0370-2693(75)90524-9.

[9] E. A. Kuraev, L. N. Lipatov, and Victor S. Fadin. "Multi - Reggeon Processes in the Yang-Mills Theory". In: *Sov. Phys. JETP* 44 (1976), pp. 443–450.

[10] E.A. Kuraev, L.N. Lipatov, and Victor S. Fadin. "The Pomeranchuk Singularity in Nonabelian Gauge Theories". In: *Sov. Phys. JETP* 45 (1977), pp. 199–204.

[11] I.I. Balitsky and L.N. Lipatov. "The Pomeranchuk Singularity in Quantum Chromodynamics". In: *Sov. J. Nucl. Phys.* 28 (1978), pp. 822–829.

[12] Ian Balitsky. "Effective field theory for the small x evolution". In: *Phys. Lett. B* 518 (2001), pp. 235–242. DOI: 10.1016/S0370-2693(01)01041-3. arXiv: hep-ph/0105334.

[13] I. Balitsky. "Operator expansion for high-energy scattering". In: *Nucl. Phys. B* 463 (1996), pp. 99–160. DOI: 10.1016/0550-3213(95)00638-9. arXiv: hep-ph/9509348.

[14] I. Balitsky. "Factorization for high-energy scattering". In: *Phys. Rev. Lett.* 81 (1998), pp. 2024–2027. DOI: 10.1103/PhysRevLett.81.2024. arXiv: hep-ph/9807434.

[15] Ian Balitsky. "Factorization and high-energy effective action". In: *Phys. Rev. D* 60 (1999), p. 014020. DOI: 10.1103/PhysRevD.60.014020. arXiv: hep-ph/9812311.

[16] Jamal Jalilian-Marian, Alex Kovner, Andrei Leonidov, and Heribert Weigert. "The BFKL equation from the Wilson renormalization group". In: *Nucl. Phys. B* 504 (1997), pp. 415–431. DOI: 10.1016/S0550-3213(97)00440-9. arXiv: hep-ph/9701284.

[17] Jamal Jalilian-Marian, Alex Kovner, Andrei Leonidov, and Heribert Weigert. "The Wilson renormalization group for low x physics: Towards the high density regime". In: *Phys. Rev. D* 59 (1998), p. 014014. DOI: 10.1103/PhysRevD.59.014014. arXiv: hep-ph/9706377.

[18] Jamal Jalilian-Marian, Alex Kovner, and Heribert Weigert. "The Wilson renormalization group for low x physics: Gluon evolution at finite parton density". In: *Phys. Rev. D* 59 (1998), p. 014015. DOI: 10.1103/PhysRevD.59.014015. arXiv: hep-ph/9709432.

[19] Jamal Jalilian-Marian, Alex Kovner, Andrei Leonidov, and Heribert Weigert. "Unitarization of gluon distribution in the doubly logarithmic regime at high density". In: *Phys. Rev. D* 59 (1999). [Erratum: Phys.Rev.D 59, 099903 (1999)], p. 034007. DOI: 10.1103/PhysRevD.59.034007. arXiv: hep-ph/9807462.

[20] Alex Kovner, J. Guilherme Milhano, and Heribert Weigert. "Relating different approaches to nonlinear QCD evolution at finite gluon density". In: *Phys. Rev. D* 62 (2000), p. 114005. DOI: 10.1103/PhysRevD.62.114005. arXiv: hep-ph/0004014.

[21] Heribert Weigert. "Unitarity at small Bjorken x". In: *Nucl. Phys. A* 703 (2002), pp. 823–860. DOI: 10.1016/S0375-9474(01)01668-2. arXiv: hep-ph/0004044.

[22] Edmond Iancu, Andrei Leonidov, and Larry D. McLerran. "Nonlinear gluon evolution in the color glass condensate. 1." In: *Nucl. Phys. A* 692 (2001), pp. 583–645. DOI: 10.1016/S0375-9474(01)00642-X. arXiv: hep-ph/0011241.

[23] Edmond Iancu, Andrei Leonidov, and Larry D. McLerran. "The Renormalization group equation for the color glass condensate". In: *Phys. Lett. B* 510 (2001), pp. 133–144. DOI: 10.1016/S0370-2693(01)00524-X. arXiv: hep-ph/0102009.

[24] Elena Ferreiro, Edmond Iancu, Andrei Leonidov, and Larry McLerran. "Nonlinear gluon evolution in the color glass condensate. 2." In: *Nucl. Phys. A* 703 (2002), pp. 489–538. DOI: 10.1016/S0375-9474(01)01329-X. arXiv: hep-ph/0109115.

[25] Steven Weinberg. *The First Three Minutes. A Modern View of the Origin of the Universe*. 1977. ISBN: 978-0-465-02437-7.

[26] J. R. Forshaw and D. A. Ross. *Quantum Chromodynamics and the Pomeron*. Cambridge Lecture Notes in Physics. Cambridge University Press, 1997. DOI: 10.1017/CBO9780511524387.

[27] P. D. B. Collins. *An Introduction to Regge Theory and High Energy Physics*. Cambridge Monographs on Mathematical Physics. Cambridge University Press, 1977. DOI: 10.1017/CBO9780511897603.

[28] V. S. Fadin. "BFKL news". In: *LAFEX International School on High-Energy Physics (LISHEP 98) Session A: Particle Physics for High School Teachers - Session B: Advanced School in HEP - Session C: Workshop on Diffractive Physics*. July 1998, pp. 742–776. arXiv: hep-ph/9807528.

[29] A. Duncan. *The Conceptual Framework of Quantum Field Theory*. Oxford University Press, Aug. 2012. ISBN: 9780199573264. DOI: 10.1093/acprof:oso/9780199573264.001.0001. URL: https://doi.org/10.1093/acprof:oso/9780199573264.001.0001.

[30] T. E. Regge. "Introduction to complex orbital momenta". In: *Il Nuovo Cimento (1955-1965)* 14 (1959), pp. 951–976.

[31] A. Sommerfeld. *Partial differential equations in physics*. Pure and Applied Mathematics - Academic Press. Acad. Press, 1961. ISBN: 9788187169499. URL: https://books.google.fr/books?id=xHW3%5C_2TcbOAC.

[32] I. Y. Pomeranchuck. In: *Sov. Phys.* **3** (1956), p. 306.

[33] L. F. Foldy and Peierls. In: *Phys. Rev.* **130** (1963), p. 1585.

[34] L.V. Gribov, E.M. Levin, and M.G. Ryskin. "Semihard Processes in QCD". In: *Phys. Rept.* 100 (1983), pp. 1–150. DOI: 10.1016/0370-1573(83)90022-4.

[35] V. S. Fadin and R. Fiore. "The Generalized nonforward BFKL equation and the 'bootstrap' condition for the gluon Reggeization in the NLLA". In: *Phys. Lett. B* 440 (1998), pp. 359–366. DOI: 10.1016/S0370-2693(98)01099-5.

[36] V. S. Fadin and L. N. Lipatov. "High-Energy Production of Gluons in a Quasi-multiRegge Kinematics". In: *JETP Lett.* 49 (1989), p. 352.

[37] B. L. Ioffe, V. S. Fadin, and L. N. Lipatov. *Quantum chromodynamics: Perturbative and nonperturbative aspects*. Cambridge Univ. Press, 2010. DOI: 10.1017/CBO9780511711817.

[38] V. S. Fadin and R. Fiore. "Quark contribution to the gluon-gluon - reggeon vertex in QCD". In: *Phys. Lett. B* 294 (1992), pp. 286–292. DOI: 10.1016/0370-2693(92)90696-2.

[39] V.S. Fadin and L.N. Lipatov. "Radiative corrections to QCD scattering amplitudes in a multi-Regge kinematics". In: *Nuclear Physics B* 406.1 (1993), pp. 259–292. ISSN: 0550-3213. DOI: https://doi.org/10.1016/0550-3213(93)90168-O. URL: https://www.sciencedirect.com/science/article/pii/055032139390168O.

[40] Victor S. Fadin, R. Fiore, and A. Quartarolo. "Radiative corrections to quark quark reggeon vertex in QCD". In: *Phys. Rev. D* 50 (1994), pp. 2265–2276. DOI: 10.1103/PhysRevD.50.2265. arXiv: hep-ph/9310252.

[41] Victor S. Fadin, R. Fiore, and A. Quartarolo. "Quark contribution to the reggeon - reggeon - gluon vertex in QCD". In: *Phys. Rev. D* 50 (1994), pp. 5893–5901. DOI: 10.1103/PhysRevD.50.5893. arXiv: hep-th/9405127.

[42] V. S. Fadin, R. Fiore, and A. Quartarolo. "Reggeization of quark quark scattering amplitude in QCD". In: *Phys. Rev. D* 53 (1996), pp. 2729–2741. DOI: 10.1103/PhysRevD.53.2729. arXiv: hep-ph/9506432.

[43] Victor S. Fadin. "Two loop correction to the gluon trajectory in QCD". In: *Phys. Atom. Nucl.* 58 (1995), pp. 1762–1766.

[44] M. I. Kotsky and Victor S. Fadin. "Reggeization of the amplitude of gluon-gluon scattering". In: *Phys. Atom. Nucl.* 59 (1996), pp. 1035–1045.

[45] Victor S. Fadin, M. I. Kotsky, and R. Fiore. "Gluon Reggeization in QCD in the next-to-leading order". In: *Phys. Lett. B* 359 (1995), pp. 181–188. DOI: 10.1016/0370-2693(95)01016-J.

[46] Victor S. Fadin, R. Fiore, and M. I. Kotsky. "Gluon Regge trajectory in the two loop approximation". In: *Phys. Lett. B* 387 (1996), pp. 593–602. DOI: 10.1016/0370-2693(96)01054-4. arXiv: hep-ph/9605357.

[47] Victor S. Fadin, R. Fiore, and A. Papa. "One loop Reggeon-Reggeon gluon vertex at arbitrary space-time dimension". In: *Phys. Rev. D* 63 (2001), p. 034001. DOI: 10.1103/PhysRevD.63.034001. arXiv: hep-ph/0008006.

[48] Victor S. Fadin and L. N. Lipatov. "Next-to-leading corrections to the BFKL equation from the gluon and quark production". In: *Nucl. Phys. B* 477 (1996), pp. 767–808. DOI: 10.1016/0550-3213(96)00334-3. arXiv: hep-ph/9602287.

[49] Victor S. Fadin, M. I. Kotsky, and L. N. Lipatov. "Gluon pair production in the quasimulti - Regge kinematics". In: (Dec. 1996). arXiv: hep-ph/9704267.

[50] S. Catani, M. Ciafaloni, and F. Hautmann. "GLUON CONTRIBUTIONS TO SMALL x HEAVY FLAVOR PRODUCTION". In: *Phys. Lett. B* 242 (1990), pp. 97–102. DOI: 10.1016/0370-2693(90)91601-7.

[51] S. Catani, M. Ciafaloni, and F. Hautmann. "High-energy factorization and small x heavy flavor production". In: *Nucl. Phys. B* 366 (1991), pp. 135–188. DOI: 10.1016/0550-3213(91)90055-3.

[52] G. Camici and M. Ciafaloni. "NonAbelian q anti-q contributions to small x anomalous dimensions". In: *Phys. Lett. B* 386 (1996), pp. 341–349. DOI: 10.1016/0370-2693(96)00962-8. arXiv: hep-ph/9606427.

[53] G. Camici and M. Ciafaloni. "k factorization and small-x anomalous dimensions". In: *Nucl. Phys. B* 496 (1997). [Erratum: Nucl.Phys.B 607, 431–432 (2001)], pp. 305–336. DOI: 10.1016/S0550-3213(97)00261-7. arXiv: hep-ph/9701303.

[54] Victor S. Fadin, R. Fiore, A. Flachi, and M. I. Kotsky. "Quark - anti-quark contribution to the BFKL kernel". In: *Phys. Lett. B* 422 (1998), pp. 287–293. DOI: 10.1016/S0370-2693(98)00044-6. arXiv: hep-ph/9711427.

[55] Francesco Giovanni Celiberto, Michael Fucilla, Dmitry Yu. Ivanov, Mohammed M. A. Mohammed, and Alessandro Papa. "The next-to-leading order Higgs impact factor in the infinite top-mass limit". In: *JHEP* 08 (2022), p. 092. DOI: 10.1007/JHEP08(2022)092. arXiv: 2205.02681 [hep-ph].

[56] Michael Fucilla. "The Higgs impact factor at next-to-leading order". In: (Dec. 2022). arXiv: 2212.01794 [hep-ph].

[57] John R. Ellis, Mary K. Gaillard, and Dimitri V. Nanopoulos. "A Phenomenological Profile of the Higgs Boson". In: *Nucl. Phys. B* 106 (1976), p. 292. DOI: 10.1016/0550-3213(76)90382-5.

[58] Mikhail A. Shifman, A. I. Vainshtein, M. B. Voloshin, and Valentin I. Zakharov. "Low-Energy Theorems for Higgs Boson Couplings to Photons". In: *Sov. J. Nucl. Phys.* 30 (1979), pp. 711–716.

[59] S. Dawson. "Radiative corrections to Higgs boson production". In: *Nucl. Phys. B* 359 (1991), pp. 283–300. DOI: 10.1016/0550-3213(91)90061-2.

[60] V. Ravindran, J. Smith, and W.L. van Neerven. "Next-to-leading order QCD corrections to differential distributions of Higgs boson production in hadron–hadron collisions". In: *Nucl. Phys. B* 634.1–2 (July 2002), pp. 247–290. DOI: 10.1016/s0550-3213(02)00333-4.

[61] Martin Hentschinski, Krzysztof Kutak, and Andreas van Hameren. "Forward Higgs production within high energy factorization in the heavy quark limit at next-to-leading order accuracy". In: *Eur. Phys. J. C* 81.2 (2021). [Erratum: Eur. Phys. J. C 81, 262 (2021)], p. 112. DOI: 10.1140/epjc/s10052-021-08902-6. arXiv: 2011.03193 [hep-ph].

[62] Victor S. Fadin, Dmitry Yu. Ivanov, and M. I. Kotsky. "Photon Reggeon interaction vertices in the NLA". In: *Phys. Atom. Nucl.* 65 (2002), pp. 1513–1527. DOI: 10.1134/1.1501664. arXiv: hep-ph/0106099.

[63] Victor S. Fadin and R. Fiore. "Calculation of Reggeon vertices in QCD". In: *Phys. Rev. D* 64 (2001), p. 114012. DOI: 10.1103/PhysRevD.64.114012. arXiv: hep-ph/0107010.

[64] R. Mertig, M. Böhm, and A. Denner. "Feyn Calc - Computer-algebraic calculation of Feynman amplitudes". In: *Comput. Physics Commun.* 64.3 (1991), pp. 345–359.

[65] Vladyslav Shtabovenko, Rolf Mertig, and Frederik Orellana. "New developments in FeynCalc 9.0". In: *Comput. Physics Commun.* 207 (2016), pp. 432–444.

[66] Victor S. Fadin and Alan D. Martin. "Infrared safety of impact factors for colorless particle interactions". In: *Phys. Rev. D* 60 (1999), p. 114008. DOI: 10.1103/PhysRevD.60.114008. arXiv: hep-ph/9904505.

[67] Carl R. Schmidt. "H —> g g g (g q anti-q) at two loops in the large M(t) limit". In: *Phys. Lett. B* 413 (1997), pp. 391–395. DOI: 10.1016/S0370-2693(97)01102-7. arXiv: hep-ph/9707448.

[68] Maxim A. Nefedov. "Computing one-loop corrections to effective vertices with two scales in the EFT for Multi-Regge processes in QCD". In: *Nucl. Phys. B* 946 (2019), p. 114715. DOI: 10.1016/j.nuclphysb.2019.114715. arXiv: 1902.11030 [hep-ph].

[69] Dmitry Yu. Ivanov and A. Papa. "The next-to-leading order forward jet vertex in the small-cone approximation". In: *JHEP* 05 (2012), p. 086. DOI: 10.1007/JHEP05(2012)086. arXiv: 1202.1082 [hep-ph].

[70] Dmitry Yu. Ivanov and Alessandro Papa. "Inclusive production of a pair of hadrons separated by a large interval of rapidity in proton collisions". In: *JHEP* 07 (2012), p. 045. DOI: 10.1007/JHEP07(2012)045. arXiv: 1205.6068 [hep-ph].

[71] Francesco Giovanni Celiberto, Michael Fucilla, Dmitry Yu. Ivanov, Mohammed M. A. Mohammed, Maxim Nefedov, and Alessandro Papa. In: (in preparation).

[72] Francesco Giovanni Celiberto, Dmitry Yu. Ivanov, Mohammed M. A. Mohammed, and Alessandro Papa. "High-energy resummed distributions for the inclusive Higgs-plus-jet production at the LHC". In: *Eur. Phys. J. C* 81.4 (2021), p. 293. DOI: 10.1140/epjc/s10052-021-09063-2. arXiv: 2008.00501 [hep-ph].

[73] R. S. Pasechnik, O. V. Teryaev, and A. Szczurek. "Scalar Higgs boson production in a fusion of two off-shell gluons". In: *Eur. Phys. J. C* 47 (2006), pp. 429–435. DOI: 10.1140/epjc/s2006-02586-6. arXiv: hep-ph/0603258.

[74] E. Segrè. *Enrico Fermi, fisico: una biografia scientifica*. Le Ellissi. Zanichelli, 1987. ISBN: 9788808022387. URL: https://books.google.fr/books?id=RiTUAAAACAAJ.

[75] J. Bartels, D. Colferai, and G. P. Vacca. "The NLO jet vertex for Mueller-Navelet and forward jets: The Quark part". In: *Eur. Phys. J. C* 24 (2002), pp. 83–99. DOI: 10.1007/s100520200919. arXiv: hep-ph/0112283.

[76] J. Bartels, D. Colferai, and G. P. Vacca. "The NLO jet vertex for Mueller-Navelet and forward jets: The Gluon part". In: *Eur. Phys. J. C* 29 (2003), pp. 235–249. DOI: 10.1140/epjc/s2003-01169-5. arXiv: hep-ph/0206290.

[77] Francesco Caporale, Dmitry Yu. Ivanov, Beatrice Murdaca, and Alessandro Papa. "Mueller-Navelet small-cone jets at LHC in next-to-leading BFKL". In: *Nucl. Phys. B* 877 (2013), pp. 73–94. DOI: 10.1016/j.nuclphysb.2013.09.013. arXiv: 1211.7225 [hep-ph].

[78] M. Furman. "Study of a Nonleading {QCD} Correction to Hadron Calorimeter Reactions". In: *Nucl. Phys. B* 197 (1982), pp. 413–445. DOI: 10.1016/0550-3213(82)90452-7.

[79] F. Aversa, P. Chiappetta, Mario Greco, and J. P. Guillet. "QCD Corrections to Parton-Parton Scattering Processes". In: *Nucl. Phys. B* 327 (1989), p. 105. DOI: 10.1016/0550-3213(89)90288-5.

[80] Francesco Giovanni Celiberto, Michael Fucilla, Dmitry Yu. Ivanov, and Alessandro Papa. "High-energy resummation in Λ_c baryon production". In: *Eur. Phys. J. C* 81.8 (2021), p. 780. DOI: 10.1140/epjc/s10052-021-09448-3. arXiv: 2105.06432 [hep-ph].

[81] Francesco Giovanni Celiberto, Michael Fucilla, Dmitry Yu. Ivanov, Mohammed M. A. Mohammed, and Alessandro Papa. "Bottom-flavored inclusive emissions in the variable-flavor number scheme: A high-energy analysis". In: *Phys. Rev. D* 104.11 (2021), p. 114007. DOI: 10.1103/PhysRevD.104.114007. arXiv: 2109.11875 [hep-ph].

[82] Francesco Giovanni Celiberto and Michael Fucilla. "Diffractive semi-hard production of a J/ψ or a Υ from single-parton fragmentation plus a jet in hybrid factorization". In: *Eur. Phys. J. C* 82.10 (2022), p. 929. DOI: 10.1140/epjc/s10052-022-10818-8. arXiv: 2202.12227 [hep-ph].

[83] Francesco Giovanni Celiberto, Michael Fucilla, Mohammed M. A. Mohammed, and Alessandro Papa. "Ultraforward production of a charmed hadron plus a Higgs boson in unpolarized proton collisions". In: *Phys. Rev. D* 105.11 (2022), p. 114056. DOI: 10.1103/PhysRevD.105.114056. arXiv: 2205.13429 [hep-ph].

[84] Francesco Giovanni Celiberto. "Hunting BFKL in semi-hard reactions at the LHC". In: *Eur. Phys. J. C* 81.8 (2021), p. 691. DOI: 10.1140/epjc/s10052-021-09384-2. arXiv: 2008.07378 [hep-ph].

[85] Francesco Giovanni Celiberto. "High-energy emissions of light mesons plus heavy flavor at the LHC and the Forward Physics Facility". In: *Phys. Rev. D* 105.11 (2022), p. 114008. DOI: 10.1103/PhysRevD.105.114008. arXiv: 2204.06497 [hep-ph].

[86] Alfred H. Mueller and H. Navelet. "An Inclusive Minijet Cross-Section and the Bare Pomeron in QCD". In: *Nucl. Phys. B* 282 (1987), pp. 727–744. DOI: 10.1016/0550-3213(87)90705-X.

[87] Francesco Giovanni Celiberto. "High-energy resummation in semi-hard processes at the LHC". PhD thesis. Università della Calabria and INFN-Cosenza, 2017. arXiv: 1707.04315 [hep-ph].

[88] Francesco Giovanni Celiberto and Alessandro Papa. "Mueller-Navelet jets at the LHC: Hunting data with azimuthal distributions". In: *Phys. Rev. D* 106.11 (2022), p. 114004. DOI: 10.1103/PhysRevD.106.114004. arXiv: 2207.05015 [hep-ph].

[89] Dimitri Colferai, Florian Schwennsen, Lech Szymanowski, and Samuel Wallon. "Mueller Navelet jets at LHC - complete NLL BFKL calculation". In: *JHEP* 12 (2010), p. 026. DOI: 10.1007/JHEP12(2010)026. arXiv: 1002.1365 [hep-ph].

[90] Bertrand Ducloué, Lech Szymanowski, and Samuel Wallon. "Confronting Mueller-Navelet jets in NLL BFKL with LHC experiments at 7 TeV". In: *JHEP* 05 (2013), p. 096. DOI: 10.1007/JHEP05(2013)096. arXiv: 1302.7012 [hep-ph].

[91] Betrand Ducloué, Lech Szymanowski, and Samuel Wallon. "Evidence for high-energy resummation effects in Mueller-Navelet jets at the LHC". In: *Phys. Rev. Lett.* 112 (2014), p. 082003. DOI: 10.1103/PhysRevLett.112.082003. arXiv: 1309.3229 [hep-ph].

[92] Francesco Caporale, Dmitry Yu. Ivanov, Beatrice Murdaca, and Alessandro Papa. "Mueller–Navelet jets in next-to-leading order BFKL: theory versus experiment". In: *Eur. Phys. J. C* 74.10 (2014). [Erratum: Eur.Phys.J.C 75, 535 (2015)], p. 3084. DOI: 10.1140/epjc/s10052-015-3754-5. arXiv: 1407.8431 [hep-ph].

[93] Francesco Giovanni Celiberto, Dmitry Yu. Ivanov, Beatrice Murdaca, and Alessandro Papa. "Mueller–Navelet Jets at LHC: BFKL Versus High-Energy DGLAP". In: *Eur. Phys. J. C* 75.6 (2015), p. 292. DOI: 10.1140/epjc/s10052-015-3522-6. arXiv: 1504.08233 [hep-ph].

[94] Francesco Giovanni Celiberto, Dmitry Yu. Ivanov, Beatrice Murdaca, and Alessandro Papa. "Mueller–Navelet jets at 13 TeV LHC: dependence on dynamic constraints in the central rapidity region". In: *Eur. Phys. J. C* 76.4 (2016), p. 224. DOI: 10.1140/epjc/s10052-016-4053-5. arXiv: 1601.07847 [hep-ph].

[95] Andreas van Hameren, Leszek Motyka, and Grzegorz Ziarko. "Hybrid k_T-factorization and impact factors at NLO". In: *JHEP* 11 (2022), p. 103. DOI: 10.1007/JHEP11(2022)103. arXiv: 2205.09585 [hep-ph].

[96] A. V. Kotikov and L. N. Lipatov. "NLO corrections to the BFKL equation in QCD and in supersymmetric gauge theories". In: *Nucl. Phys. B* 582 (2000), pp. 19–43. DOI: 10.1016/S0550-3213(00)00329-1. arXiv: hep-ph/0004008.

[97] A. V. Kotikov and L. N. Lipatov. "DGLAP and BFKL equations in the $N = 4$ supersymmetric gauge theory". In: *Nucl. Phys. B* 661 (2003). [Erratum: Nucl.Phys.B 685, 405–407 (2004)], pp. 19–61. DOI: 10.1016/S0550-3213(03)00264-5. arXiv: hep-ph/0208220.

[98] S. Alekhin, J. Blumlein, S. Klein, and S. Moch. "The 3, 4, and 5-flavor NNLO Parton from Deep-Inelastic-Scattering Data and at Hadron Colliders". In: *Phys. Rev. D* 81 (2010), p. 014032. DOI: 10.1103/PhysRevD.81.014032. arXiv: 0908.2766 [hep-ph].

[99] B. Mele and P. Nason. "The Fragmentation function for heavy quarks in QCD". In: *Nucl. Phys. B* 361 (1991). [Erratum: Nucl.Phys.B 921, 841–842 (2017)], pp. 626–644. DOI: 10.1016/0550-3213(91)90597-Q.

[100] Matteo Cacciari and Mario Greco. "Large p_T hadroproduction of heavy quarks". In: *Nucl. Phys. B* 421 (1994), pp. 530–544. DOI: 10.1016/0550-3213(94)90515-0. arXiv: hep-ph/9311260.

[101] M. Buza, Y. Matiounine, J. Smith, and W. L. van Neerven. "Charm electroproduction viewed in the variable flavor number scheme versus fixed order perturbation theory". In: *Eur. Phys. J. C* 1 (1998), pp. 301–320. DOI: 10.1007/BF01245820. arXiv: hep-ph/9612398.

[102] Isabella Bierenbaum, Johannes Blumlein, and Sebastian Klein. "Mellin Moments of the O(alpha**3(s)) Heavy Flavor Contributions to unpolarized Deep-Inelastic Scattering at Q**2 >> m**2 and Anomalous Dimensions". In: *Nucl. Phys. B* 820 (2009), pp. 417–482. DOI: 10.1016/j.nuclphysb.2009.06.005. arXiv: 0904.3563 [hep-ph].

[103] J. Binnewies, Bernd A. Kniehl, and G. Kramer. "Predictions for D*+- - photoproduction at HERA with new fragmentation functions from LEP-1". In: *Phys. Rev. D* 58 (1998), p. 014014. DOI: 10.1103/PhysRevD.58.014014. arXiv: hep-ph/9712482.

[104] Michael Krämer, Fredrick I. Olness, and Davison E. Soper. "Treatment of heavy quarks in deeply inelastic scattering". In: *Phys. Rev. D* 62 (2000), p. 096007. DOI: 10.1103/PhysRevD.62.096007. arXiv: hep-ph/0003035.

[105] Stefano Forte, Eric Laenen, Paolo Nason, and Juan Rojo. "Heavy quarks in deep-inelastic scattering". In: *Nucl. Phys. B* 834 (2010), pp. 116–162. DOI: 10.1016/j.nuclphysb.2010.03.014. arXiv: 1001.2312 [hep-ph].

[106] J. Blümlein, A. De Freitas, C. Schneider, and K. Schönwald. "The Variable Flavor Number Scheme at Next-to-Leading Order". In: *Phys. Lett. B* 782 (2018), pp. 362–366. DOI: 10.1016/j.physletb.2018.05.054. arXiv: 1804.03129 [hep-ph].

[107] M. A. G. Aivazis, John C. Collins, Fredrick I. Olness, and Wu-Ki Tung. "Leptoproduction of heavy quarks. 2. A Unified QCD formulation of charged and neutral current processes from fixed target to collider energies". In: *Phys. Rev. D* 50 (1994), pp. 3102–3118. DOI: 10.1103/PhysRevD.50.3102. arXiv: hep-ph/9312319.

[108] R. S. Thorne and R. G. Roberts. "An Ordered analysis of heavy flavor production in deep inelastic scattering". In: *Phys. Rev. D* 57 (1998), pp. 6871–6898. DOI: 10.1103/PhysRevD.57.6871. arXiv: hep-ph/9709442.

[109] Renaud Boussarie, Bertrand Ducloué, Lech Szymanowski, and Samuwl Wallon. "Forward J/ψ and very backward jet inclusive production at the LHC". In: *Phys.*

Rev. D 97.1 (2018), p. 014008. DOI: 10.1103/PhysRevD.97.014008. arXiv: 1709.01380 [hep-ph].

[110] Harald Fritzsch. "Producing Heavy Quark Flavors in Hadronic Collisions: A Test of Quantum Chromodynamics". In: *Phys. Lett. B* 67 (1977), pp. 217–221. DOI: 10.1016/0370-2693(77)90108-3.

[111] F. Halzen. "Cvc for Gluons and Hadroproduction of Quark Flavors". In: *Phys. Lett. B* 69 (1977), pp. 105–108. DOI: 10.1016/0370-2693(77)90144-7.

[112] W. E. Caswell and G. P. Lepage. "Effective Lagrangians for Bound State Problems in QED, QCD, and Other Field Theories". In: *Phys. Lett. B* 167 (1986), pp. 437–442. DOI: 10.1016/0370-2693(86)91297-9.

[113] B. A. Thacker and G. Peter Lepage. "Heavy quark bound states in lattice QCD". In: *Phys. Rev. D* 43 (1991), pp. 196–208. DOI: 10.1103/PhysRevD.43.196.

[114] Geoffrey T. Bodwin, Eric Braaten, and G. Peter Lepage. "Rigorous QCD analysis of inclusive annihilation and production of heavy quarkonium". In: *Phys. Rev. D* 51 (1995). [Erratum: Phys.Rev.D 55, 5853 (1997)], pp. 1125–1171. DOI: 10.1103/PhysRevD.55.5853. arXiv: hep-ph/9407339.

[115] Andrèe Dafne Bolognino, Francesco Giovanni Celiberto, Michael Fucilla, Dmitry Yu. Ivanov, and Alessandro Papa. "High-energy resummation in heavy-quark pair hadroproduction". In: *Eur. Phys. J. C* 79.11 (2019), p. 939. DOI: 10.1140/epjc/s10052-019-7392-1. arXiv: 1909.03068 [hep-ph].

[116] Andrèe Dafne Bolognino, Francesco Giovanni Celiberto, Michael Fucilla, Dmitry Yu. Ivanov, and A. Papa. "Inclusive production of a heavy-light dijet system in hybrid high-energy and collinear factorization". In: *Phys. Rev. D* 103.9 (2021), p. 094004. DOI: 10.1103/PhysRevD.103.094004. arXiv: 2103.07396 [hep-ph].

[117] Roel Aaij et al. "Precision measurement of CP violation in $B_s^0 \to J/\psi K^+K^-$ decays". In: *Phys. Rev. Lett.* 114.4 (2015), p. 041801. DOI: 10.1103/PhysRevLett.114.041801. arXiv: 1411.3104 [hep-ex].

[118] Roel Aaij et al. "Measurement of the b-quark production cross-section in 7 and 13 TeV pp collisions". In: *Phys. Rev. Lett.* 118.5 (2017). [Erratum: Phys.Rev.Lett. 119, 169901 (2017)], p. 052002. DOI: 10.1103/PhysRevLett.118.052002. arXiv: 1612.05140 [hep-ex].

[119] G. Kramer and H. Spiesberger. "b-hadron production in the general-mass variable-flavour-number scheme and LHC data". In: *Phys. Rev. D* 98.11 (2018), p. 114010. DOI: 10.1103/PhysRevD.98.114010. arXiv: 1809.04297 [hep-ph].

[120] L.A. Harland-Lang, A.D. Martin, P. Motylinski, and R.S. Thorne. "Parton distributions in the LHC era: MMHT 2014 PDFs". In: *Eur. Phys. J. C* 75.5 (2015), p. 204. DOI: 10.1140/epjc/s10052-015-3397-6. arXiv: 1412.3989 [hep-ph].

[121] Andy Buckley, James Ferrando, Stephen Lloyd, Karl Nordström, Ben Page, Martin Rüfenacht, Marek Schönherr, and Graeme Watt. "LHAPDF6: parton density access in the LHC precision era". In: *Eur. Phys. J. C* 75 (2015), p. 132. DOI: 10.1140/epjc/s10052-015-3318-8. arXiv: 1412.7420 [hep-ph].

[122] Dimitri Colferai and Alessnadro Niccoli. "The NLO jet vertex in the small-cone approximation for kt and cone algorithms". In: *JHEP* 04 (2015), p. 071. DOI: 10.1007/JHEP04(2015)071. arXiv: 1501.07442 [hep-ph].

[123] Vardan Khachatryan et al. "Azimuthal decorrelation of jets widely separated in rapidity in pp collisions at $\sqrt{s} = 7$ TeV". In: *JHEP* 08 (2016), p. 139. DOI: 10.1007/JHEP08(2016)139. arXiv: 1601.06713 [hep-ex].

[124] B. A. Kniehl, G. Kramer, I. Schienbein, and H. Spiesberger. "$\Lambda_c^{\pm}$ production in pp collisions with a new fragmentation function". In: *Phys. Rev. D* 101.11 (2020), p. 114021. DOI: 10.1103/PhysRevD.101.114021. arXiv: 2004.04213 [hep-ph].

[125] Bernd A. Kniehl and Gustav Kramer. "D0, D+, D+(s), and Lambda+(c) fragmentation functions from CERN LEP1". In: *Phys. Rev. D* 71 (2005), p. 094013. DOI: 10.1103/PhysRevD.71.094013. arXiv: hep-ph/0504058.

[126] B. A. Kniehl, G. Kramer, I. Schienbein, and H. Spiesberger. "Inclusive Charmed-Meson Production at the CERN LHC". In: *Eur. Phys. J. C* 72 (2012), p. 2082. DOI: 10.1140/epjc/s10052-012-2082-2. arXiv: 1202.0439 [hep-ph].

[127] M. G. Bowler. "e+ e- Production of Heavy Quarks in the String Model". In: *Z. Phys. C* 11 (1981), p. 169. DOI: 10.1007/BF01574001.

[128] Bernd A. Kniehl, Gustav Kramer, Ingo Schienbein, and Hubert Spiesberger. "Finite-mass effects on inclusive B meson hadroproduction". In: *Phys. Rev. D* 77 (2008), p. 014011. DOI: 10.1103/PhysRevD.77.014011. arXiv: 0705.4392 [hep-ph].

[129] V. G. Kartvelishvili and A. K. Likhoded. "Structure Functions and Leptonic Widths of Heavy Mesons". In: *Yad. Fiz.* 42 (1985), pp. 1306–1308.

[130] S. Albino, B. A. Kniehl, and G. Kramer. "AKK Update: Improvements from New Theoretical Input and Experimental Data". In: *Nucl. Phys. B* 803 (2008), pp. 42–104. DOI: 10.1016/j.nuclphysb.2008.05.017. arXiv: 0803.2768 [hep-ph].

[131] Xu-Chang Zheng, Chao-Hsi Chang, and Xing-Gang Wu. "NLO fragmentation functions of heavy quarks into heavy quarkonia". In: *Phys. Rev. D* 100.1 (2019), p. 014005. DOI: 10.1103/PhysRevD.100.014005. arXiv: 1905.09171 [hep-ph].

[132] N. Brambilla et al. "Heavy quarkonium physics". In: (Dec. 2004). DOI: 10.5170/CERN-2005-005. arXiv: hep-ph/0412158.

[133] N. Brambilla et al. "Heavy Quarkonium: Progress, Puzzles, and Opportunities". In: *Eur. Phys. J. C* 71 (2011), p. 1534. DOI: 10.1140/epjc/s10052-010-1534-9. arXiv: 1010.5827 [hep-ph].

[134] Antonio Pineda. "Review of Heavy Quarkonium at weak coupling". In: *Prog. Part. Nucl. Phys.* 67 (2012), pp. 735–785. DOI: 10.1016/j.ppnp.2012.01.038. arXiv: 1111.0165 [hep-ph].

[135] Nora Brambilla, Hee Sok Chung, and Antonio Vairo. "Inclusive Hadroproduction of P-Wave Heavy Quarkonia in Potential Nonrelativistic QCD". In: *Phys. Rev. Lett.* 126.8 (2021), p. 082003. DOI: 10.1103/PhysRevLett.126.082003. arXiv: 2007.07613 [hep-ph].

[136] Lars Bugge. "EXPERIMENTAL HEAVY QUARKONIUM PHYSICS: INTRODUCTION AND SURVEY". In: Lectures presented at the Trondheim Workshop 1984 in Theoretical Physics: Quantum ChromoDynamics in Theory and Experiment. Trondheim, Norway. *Report Number: OSLO-86-20* (Aug. 1986).

[137] Estia J. Eichten and Chris Quigg. "Mesons with beauty and charm: Spectroscopy". In: *Phys. Rev. D* 49 (1994), pp. 5845–5856. DOI: 10.1103/PhysRevD.49.5845. arXiv: hep-ph/9402210.

[138] Eric Braaten, King-man Cheung, and Tzu Chiang Yuan. "Z0 decay into charmonium via charm quark fragmentation". In: *Phys. Rev. D* 48 (1993), pp. 4230–4235. DOI: 10.1103/PhysRevD.48.4230. arXiv: hep-ph/9302307.

[139] Eric Braaten, Michael A. Doncheski, Sean Fleming, and Michelangelo L. Mangano. "Fragmentation production of J/ψ and ψ' at the Tevatron". In: *Phys. Lett. B* 333 (1994), pp. 548–554. DOI: 10.1016/0370-2693(94)90182-1. arXiv: hep-ph/9405407.

[140] Eric Braaten and Tzu Chiang Yuan. "Gluon fragmentation into heavy quarkonium". In: *Phys. Rev. Lett.* 71 (1993), pp. 1673–1676. DOI: 10.1103/PhysRevLett.71.1673. arXiv: hep-ph/9303205.

[141] Eric Braaten and Tzu Chiang Yuan. "Gluon fragmentation into spin triplet S wave quarkonium". In: *Phys. Rev. D* 52 (1995), pp. 6627–6629. DOI: 10.1103/PhysRevD.52.6627. arXiv: hep-ph/9507398.

[142] Tzu Chiang Yuan. "Perturbative QCD fragmentation functions for production of P wave mesons with charm and beauty". In: *Phys. Rev. D* 50 (1994), pp. 5664–5675. DOI: 10.1103/PhysRevD.50.5664. arXiv: hep-ph/9405348.

[143] Valerio Bertone, Stefano Carrazza, and Juan Rojo. "APFEL: A PDF Evolution Library with QED corrections". In: *Comput. Phys. Commun.* 185 (2014), pp. 1647–1668. DOI: 10.1016/j.cpc.2014.03.007. arXiv: 1310.1394 [hep-ph].

[144] Stefano Carrazza, Alfio Ferrara, Daniele Palazzo, and Juan Rojo. "APFEL Web: a web-based application for the graphical visualization of parton distribution functions". In: *J. Phys. G* 42.5 (2015), p. 057001. DOI: 10.1088/0954-3899/42/5/057001. arXiv: 1410.5456 [hep-ph].

[145] Valerio Bertone. "APFEL++: A new PDF evolution library in C++". In: *PoS* DIS2017 (2018). Ed. by Uta Klein, p. 201. DOI: 10.22323/1.297.0201. arXiv: 1708.00911 [hep-ph].

[146] V. Del Duca, W. Kilgore, C. Oleari, C. R. Schmidt, and D. Zeppenfeld. "Kinematical limits on Higgs boson production via gluon fusion in association with jets". In: *Phys. Rev. D* 67 (2003), p. 073003. DOI: 10.1103/PhysRevD.67.073003. arXiv: hep-ph/0301013.

[147] S. J. Brodsky, F. Hautmann, and D. E. Soper. "Probing the QCD pomeron in e+ e- collisions". In: *Phys. Rev. Lett.* 78 (1997). [Erratum: Phys.Rev.Lett. 79, 3544 (1997)], pp. 803–806. DOI: 10.1103/PhysRevLett.78.803. arXiv: hep-ph/9610260.

[148] S. J. Brodsky, F. Hautmann, and D. E. Soper. "Virtual photon scattering at high-energies as a probe of the short distance pomeron". In: *Phys. Rev. D* 56 (1997), pp. 6957–6979. DOI: 10.1103/PhysRevD.56.6957. arXiv: hep-ph/9706427.

[149] Stanley J. Brodsky, Victor S. Fadin, Victor T. Kim, Lev N. Lipatov, and Grigorii B. Pivovarov. "The QCD pomeron with optimal renormalization". In: *JETP Lett.* 70 (1999), pp. 155–160. DOI: 10.1134/1.568145. arXiv: hep-ph/9901229.

[150] Stanley J. Brodsky, Victor S. Fadin, Victor T. Kim, Lev N. Lipatov, and Grigorii B. Pivovarov. "High-energy QCD asymptotics of photon-photon collisions". In: *JETP Lett.* 76 (2002), pp. 249–252. DOI: 10.1134/1.1520615. arXiv: hep-ph/0207297.

[151] Francesco Giovanni Celiberto, Dmitry Yu. Ivanov, Beatrice Murdaca, and Alessandro Papa. "High energy resummation in dihadron production at the LHC". In: *Phys. Rev. D* 94.3 (2016), p. 034013. DOI: 10.1103/PhysRevD.94.034013. arXiv: 1604.08013 [hep-ph].

[152] Francesco Giovanni Celiberto, Dmitry Yu. Ivanov, Beatrice Murdaca, and Alessandro Papa. "Dihadron production at the LHC: full next-to-leading BFKL calculation". In: *Eur. Phys. J. C* 77.6 (2017), p. 382. DOI: 10.1140/epjc/s10052-017-4949-8. arXiv: 1701.05077 [hep-ph].

[153] Agustin Sabio Vera. "The Effect of NLO conformal spins in azimuthal angle decorrelation of jet pairs". In: *Nucl. Phys. B* 746 (2006), pp. 1–14. DOI: 10.1016/j.nuclphysb.2006.04.004. arXiv: hep-ph/0602250.

[154] Agustin Sabio Vera and Florian Schwennsen. "The Azimuthal decorrelation of jets widely separated in rapidity as a test of the BFKL kernel". In: *Nucl. Phys. B* 776 (2007), pp. 170–186. DOI: 10.1016/j.nuclphysb.2007.03.050. arXiv: hep-ph/0702158.

[155] Luis A. Anchordoqui et al. "The Forward Physics Facility: Sites, experiments, and physics potential". In: *Phys. Rept.* 968 (2022), pp. 1–50. DOI: 10.1016/j.physrep.2022.04.004. arXiv: 2109.10905 [hep-ph].

[156] Jonathan L. Feng et al. "The Forward Physics Facility at the High-Luminosity LHC". In: *J. Phys. G* 50.3 (2023), p. 030501. DOI: 10.1088/1361-6471/ac865e. arXiv: 2203.05090 [hep-ex].

[157] C. Marquet and C. Royon. "Azimuthal decorrelation of Mueller-Navelet jets at the Tevatron and the LHC". In: *Phys. Rev. D* 79 (2009), p. 034028. DOI: 10.1103/PhysRevD.79.034028. arXiv: 0704.3409 [hep-ph].

[158] Roberto Bonciani, Stefano Catani, Michelangelo L. Mangano, and Paolo Nason. "Sudakov resummation of multiparton QCD cross-sections". In: *Phys. Lett. B* 575 (2003), pp. 268–278. DOI: 10.1016/j.physletb.2003.09.068. arXiv: hep-ph/0307035.

[159] D. de Florian, A. Kulesza, and W. Vogelsang. "Threshold resummation for high-transverse-momentum Higgs production at the LHC". In: *JHEP* 02 (2006), p. 047. DOI: 10.1088/1126-6708/2006/02/047. arXiv: hep-ph/0511205.

[160] Claudio Muselli, Stefano Forte, and Giovanni Ridolfi. "Combined threshold and transverse momentum resummation for inclusive observables". In: *JHEP* 03 (2017), p. 106. DOI: 10.1007/JHEP03(2017)106. arXiv: 1701.01464 [hep-ph].

[161] Paolo Nason. "A New method for combining NLO QCD with shower Monte Carlo algorithms". In: *JHEP* 11 (2004), p. 040. DOI: 10.1088/1126-6708/2004/11/040. arXiv: hep-ph/0409146.

[162] Stefano Frixione, Paolo Nason, and Carlo Oleari. "Matching NLO QCD computations with Parton Shower simulations: the POWHEG method". In: *JHEP* 11 (2007), p. 070. DOI: 10.1088/1126-6708/2007/11/070. arXiv: 0709.2092 [hep-ph].

[163] Simone Alioli, Paolo Nason, Carlo Oleari, and Emanuele Re. "A general framework for implementing NLO calculations in shower Monte Carlo programs: the POWHEG BOX". In: *JHEP* 06 (2010), p. 043. DOI: 10.1007/JHEP06(2010)043. arXiv: 1002.2581 [hep-ph].

[164] John M. Campbell, R. Keith Ellis, Rikkert Frederix, Paolo Nason, Carlo Oleari, and Ciaran Williams. "NLO Higgs Boson Production Plus One and Two Jets Using the POWHEG BOX, MadGraph4 and MCFM". In: *JHEP* 07 (2012), p. 092. DOI: 10.1007/JHEP07(2012)092. arXiv: 1202.5475 [hep-ph].

[165] Keith Hamilton, Paolo Nason, Carlo Oleari, and Giulia Zanderighi. "Merging H/W/Z + 0 and 1 jet at NLO with no merging scale: a path to parton shower + NNLO matching". In: *JHEP* 05 (2013), p. 082. DOI: 10.1007/JHEP05(2013)082. arXiv: 1212.4504 [hep-ph].

[166] Francesco Giovanni Celiberto, Dmitry Yu. Ivanov, Mohammed. M. A. Mohammed, and Alessandro Papa. "High-energy resummation in inclusive hadroproduction

of Higgs plus jet". In: *SciPost Phys. Proc.* 8 (2022), p. 039. DOI: 10.21468/SciPostPhysProc.8.039. arXiv: 2107.13037 [hep-ph].

[167] Grigorios Chachamis, Michal Deak, and German Rodrigo. "Heavy quark impact factor in kT-factorization". In: *JHEP* 12 (2013), p. 066. DOI: 10.1007/JHEP12(2013)066. arXiv: 1310.6611 [hep-ph].

[168] Krzysztof Golec-Biernat, Leszek Motyka, and Tomasz Stebel. "Forward Drell-Yan and backward jet production as a probe of the BFKL dynamics". In: *JHEP* 12 (2018), p. 091. DOI: 10.1007/JHEP12(2018)091. arXiv: 1811.04361 [hep-ph].

[169] Albert Einstein. "Geometry and Experience (1921)". In: *Beyond Geometry: Classic Papers from Riemann to Einstein* (Jan. 2007), pp. 147–.

[170] J. Bartels, V.S. Fadin, and R. Fiore. "The bootstrap conditions for the gluon reggeization". In: *Nuclear Physics B* 672.1-2 (Nov. 2003), pp. 329–356. DOI: 10.1016/j.nuclphysb.2003.08.034. URL: https://doi.org/10.1016%2Fj.nuclphysb.2003.08.034.

[171] V.S. Fadin. "Discontinuities of multi-Regge amplitudes". In: *AIP Conference Proceedings*. AIP Publishing LLC, 2015. DOI: 10.1063/1.4915996. URL: https://doi.org/10.1063%2F1.4915996.

[172] C. Anastasiou, L. Dixon, Z. Bern, and D. A. Kosower. "Planar Amplitudes in Maximally Supersymmetric Yang-Mills Theory". In: *Physical Review Letters* 91.25 (Dec. 2003). DOI: 10.1103/physrevlett.91.251602. URL: https://doi.org/10.1103%2Fphysrevlett.91.251602.

[173] Zvi Bern, Lance J. Dixon, and Vladimir A. Smirnov. "Iteration of planar amplitudes in maximally supersymmetric Yang-Mills theory at three loops and beyond". In: *Physical Review D* 72.8 (Oct. 2005). DOI: 10.1103/physrevd.72.085001. URL: https://doi.org/10.1103%2Fphysrevd.72.085001.

[174] Vittorio Del Duca, Claude Duhr, and E. W. Nigel Glover. "The Five-gluon amplitude in the high-energy limit". In: *JHEP* 12 (2009), p. 023. DOI: 10.1088/1126-6708/2009/12/023. arXiv: 0905.0100 [hep-th].

[175] V. S. Fadin. "Particularities of the NNLLA BFKL". In: *AIP Conf. Proc.* 1819.1 (2017). Ed. by Marcella Capua, Roberto Fiore, Alessandro Papa, Marco Rossi, Ada Solano, and Enrico Tassi, p. 060003. DOI: 10.1063/1.4977159. arXiv: 1612.04481 [hep-ph].

[176] Victor S. Fadin, Michael Fucilla, and Alessandro Papa. "One-loop Lipatov vertex in QCD with higher ϵ-accuracy". In: *JHEP* 04 (2023), p. 137. DOI: 10.1007/JHEP04(2023)137. arXiv: 2302.09868 [hep-ph].

[177] Vittorio Del Duca and E. W. Nigel Glover. "The High-energy limit of QCD at two loops". In: *JHEP* 10 (2001), p. 035. DOI: 10.1088/1126-6708/2001/10/035. arXiv: hep-ph/0109028.

[178] Vittorio Del Duca, Giulio Falcioni, Lorenzo Magnea, and Leonardo Vernazza. "High-energy QCD amplitudes at two loops and beyond". In: *Phys. Lett. B* 732 (2014), pp. 233–240. DOI: 10.1016/j.physletb.2014.03.033. arXiv: 1311.0304 [hep-ph].

[179] Vittorio Del Duca, Giulio Falcioni, Lorenzo Magnea, and Leonardo Vernazza. "Beyond Reggeization for two- and three-loop QCD amplitudes". In: *PoS* RADCOR2013 (2013), p. 046. DOI: 10.22323/1.197.0046. arXiv: 1312.5098 [hep-ph].

[180] Vittorio Del Duca, Giulio Falcioni, Lorenzo Magnea, and Leonardo Vernazza. "Analyzing high-energy factorization beyond next-to-leading logarithmic accuracy". In: *JHEP* 02 (2015), p. 029. DOI: 10.1007/JHEP02(2015)029. arXiv: 1409.8330 [hep-ph].

[181] V. S. Fadin and L. N. Lipatov. "Reggeon cuts in QCD amplitudes with negative signature". In: *Eur. Phys. J. C* 78.6 (2018), p. 439. DOI: 10.1140/epjc/s10052-018-5910-1. arXiv: 1712.09805 [hep-ph].

[182] Simon Caron-Huot, Einan Gardi, and Leonardo Vernazza. "Two-parton scattering in the high-energy limit". In: *JHEP* 06 (2017), p. 016. DOI: 10.1007/JHEP06(2017)016. arXiv: 1701.05241 [hep-ph].

[183] Giulio Falcioni, Einan Gardi, Niamh Maher, Calum Milloy, and Leonardo Vernazza. "Disentangling the Regge Cut and Regge Pole in Perturbative QCD". In: *Phys. Rev. Lett.* 128.13 (2022), p. 132001. DOI: 10.1103/PhysRevLett.128.132001. arXiv: 2112.11098 [hep-ph].

[184] V.S. Fadin, R. Fiore, and M. I. Kotsky. "Gribov's theorem on soft emission and the Reggeon-Reggeon-gluon vertex at small transverse momentum". In: *Physics Letters B* 389.4 (Dec. 1996), pp. 737–741. DOI: 10.1016/s0370-2693(96)01331-7. URL: https://doi.org/10.1016%2Fs0370-2693%2896%2901331-7.

[185] J. Bartels. "High-energy behaviour in a non-abelian gauge theory (II). First corrections to Tn→m beyond the leading In s approximation". In: *Nuclear Physics B* 175.3 (1980), pp. 365–401. ISSN: 0550-3213. DOI: https://doi.org/10.1016/0550-3213(80)90019-X. URL: https://www.sciencedirect.com/science/article/pii/055032138090019X.

[186] Vittorio Del Duca and Carl R. Schmidt. "Virtual next-to-leading corrections to the Lipatov vertex". In: *Phys. Rev. D* 59 (1999), p. 074004. DOI: 10.1103/PhysRevD.59.074004. arXiv: hep-ph/9810215.

[187] Zvi Bern, Lance Dixon, and David A. Kosower. "Dimensionally-regulated pentagon integrals". In: *Nuclear Physics B* 412.3 (Jan. 1994), pp. 751–816. DOI: 10.1016/0550-3213(94)90398-0. URL: https://doi.org/10.1016%2F0550-3213%2894%2990398-0.

[188] Vittorio Del Duca, Claude Duhr, E. W. Nigel Glover, and Vladimir A. Smirnov. "The One-loop pentagon to higher orders in epsilon". In: *JHEP* 01 (2010), p. 042. DOI: 10.1007/JHEP01(2010)042. arXiv: 0905.0097 [hep-th].

[189] Bernd A. Kniehl and Oleg V. Tarasov. "Analytic result for the one-loop scalar pentagon integral with massless propagators". In: *Nucl. Phys. B* 833 (2010), pp. 298–319. DOI: 10.1016/j.nuclphysb.2010.03.006. arXiv: 1001.3848 [hep-th].

[190] Mikhail G. Kozlov and Roman N. Lee. "One-loop pentagon integral in d dimensions from differential equations in ϵ-form". In: *JHEP* 02 (2016), p. 021. DOI: 10.1007/JHEP02(2016)021. arXiv: 1512.01165 [hep-ph].

[191] Nikolaos Syrrakos. "Pentagon integrals to arbitrary order in the dimensional regulator". In: *JHEP* 06 (2021), p. 037. DOI: 10.1007/JHEP06(2021)037. arXiv: 2012.10635 [hep-ph].

[192] Renaud Boussarie. "Perturbative study of selected exclusive QCD processes at high and moderate energies". PhD thesis. Orsay, LPT, 2016.

[193] Marcel Froissart. "Asymptotic behavior and subtractions in the Mandelstam representation". In: *Phys. Rev.* 123 (1961), pp. 1053–1057. DOI: 10.1103/PhysRev.123.1053.

[194] Yuri V. Kovchegov. "Small x F(2) structure function of a nucleus including multiple pomeron exchanges". In: *Phys. Rev. D* 60 (1999), p. 034008. DOI: 10.1103/PhysRevD.60.034008. arXiv: hep-ph/9901281.

[195] Yuri V. Kovchegov. "Unitarization of the BFKL pomeron on a nucleus". In: *Phys. Rev. D* 61 (2000), p. 074018. DOI: 10.1103/PhysRevD.61.074018. arXiv: hep-ph/9905214.

[196] Yuri V. Kovchegov and Eugene Levin. *Quantum chromodynamics at high energy*. Vol. 33. Cambridge University Press, Aug. 2012. ISBN: 978-0-521-11257-4, 978-1-139-55768-9. DOI: 10.1017/CBO9781139022187.

[197] *A Tribute to Paul Erdos*. Cambridge University Press, 1990. DOI: 10.1017/CBO9780511983917.

[198] R. Boussarie, A. V. Grabovsky, L. Szymanowski, and S. Wallon. "On the one loop $\gamma^{(*)} \to q\bar{q}$ impact factor and the exclusive diffractive cross sections for the production of two or three jets". In: *JHEP* 11 (2016), p. 149. DOI: 10.1007/JHEP11(2016)149. arXiv: 1606.00419 [hep-ph].

[199] Michael Fucilla, Andrey V. Grabovsky, Emilie Li, Lech Szymanowski, and Samuel Wallon. "NLO computation of diffractive di-hadron production in a saturation framework". In: *JHEP* 03 (2023), p. 159. DOI: 10.1007/JHEP03(2023)159. arXiv: 2211.05774 [hep-ph].

[200] Guido Altarelli, R. Keith Ellis, G. Martinelli, and So-Young Pi. "Processes Involving Fragmentation Functions Beyond the Leading Order in QCD". In: *Nucl. Phys. B* 160 (1979), pp. 301–329. DOI: 10.1016/0550-3213(79)90062-2.

[201] L. N. Lipatov. "The parton model and perturbation theory". In: *Yad. Fiz.* 20 (1974), pp. 181–198.

[202] Giovanni A. Chirilli, Bo-Wen Xiao, and Feng Yuan. "Inclusive Hadron Productions in pA Collisions". In: *Phys. Rev. D* 86 (2012), p. 054005. DOI: 10.1103/PhysRevD.86.054005. arXiv: 1203.6139 [hep-ph].

[203] R. Boussarie, A. V. Grabovsky, L. Szymanowski, and S. Wallon. "Impact factor for high-energy two and three jets diffractive production". In: *JHEP* 09 (2014), p. 026. DOI: 10.1007/JHEP09(2014)026. arXiv: 1405.7676 [hep-ph].

[204] Larry D. McLerran and Raju Venugopalan. "Computing quark and gluon distribution functions for very large nuclei". In: *Phys. Rev. D* 49 (1994), pp. 2233–2241. DOI: 10.1103/PhysRevD.49.2233. arXiv: hep-ph/9309289.

[205] Larry D. McLerran and Raju Venugopalan. "Gluon distribution functions for very large nuclei at small transverse momentum". In: *Phys. Rev. D* 49 (1994), pp. 3352–3355. DOI: 10.1103/PhysRevD.49.3352. arXiv: hep-ph/9311205.

[206] Larry D. McLerran and Raju Venugopalan. "Green's functions in the color field of a large nucleus". In: *Phys. Rev. D* 50 (1994), pp. 2225–2233. DOI: 10.1103/PhysRevD.50.2225. arXiv: hep-ph/9402335.

[207] Krzysztof J. Golec-Biernat and M. Wusthoff. "Saturation effects in deep inelastic scattering at low Q**2 and its implications on diffraction". In: *Phys. Rev.* D59 (1998), p. 014017. DOI: 10.1103/PhysRevD.59.014017. arXiv: hep-ph/9807513 [hep-ph].

[208] G. Beuf, T. Lappi, and R. Paatelainen. "Massive Quarks at One Loop in the Dipole Picture of Deep Inelastic Scattering". In: *Phys. Rev. Lett.* 129.7 (2022), p. 072001. DOI: 10.1103/PhysRevLett.129.072001. arXiv: 2112.03158 [hep-ph].

[209] G. Beuf, T. Lappi, and R. Paatelainen. "Massive quarks in NLO dipole factorization for DIS: Transverse photon". In: *Phys. Rev. D* 106.3 (2022), p. 034013. DOI: 10.1103/PhysRevD.106.034013. arXiv: 2204.02486 [hep-ph].

[210] Kaushik Roy and Raju Venugopalan. "NLO impact factor for inclusive photon+dijet production in $e + A$ DIS at small x". In: *Phys. Rev. D* 101.3 (2020), p. 034028. DOI: 10.1103/PhysRevD.101.034028. arXiv: 1911.04530 [hep-ph].

[211] Paul Caucal, Farid Salazar, and Raju Venugopalan. "Dijet impact factor in DIS at next-to-leading order in the Color Glass Condensate". In: *JHEP* 11 (2021), p. 222. DOI: 10.1007/JHEP11(2021)222. arXiv: 2108.06347 [hep-ph].

[212] Paul Caucal, Farid Salazar, Björn Schenke, and Raju Venugopalan. "Back-to-back inclusive dijets in DIS at small x: Sudakov suppression and gluon saturation at NLO". In: *JHEP* 11 (2022), p. 169. DOI: 10.1007/JHEP11(2022)169. arXiv: 2208.13872 [hep-ph].

[213] Filip Bergabo and Jamal Jalilian-Marian. "Single inclusive hadron production in DIS at small x: next to leading order corrections". In: *JHEP* 01 (2023), p. 095. DOI: 10.1007/JHEP01(2023)095. arXiv: 2210.03208 [hep-ph].

[214] Filip Bergabo and Jamal Jalilian-Marian. "One-loop corrections to dihadron production in DIS at small x". In: *Phys. Rev. D* 106.5 (2022), p. 054035. DOI: 10.1103/PhysRevD.106.054035. arXiv: 2207.03606 [hep-ph].

[215] Edmond Iancu and Yair Mulian. "Dihadron production in DIS at NLO: the real corrections". In: (Nov. 2022). arXiv: 2211.04837 [hep-ph].

[216] R. Boussarie, A. V. Grabovsky, L. Szymanowski, and S. Wallon. "Towards a complete next-to-logarithmic description of forward exclusive diffractive dijet electroproduction at HERA: real corrections". In: *Phys. Rev. D* 100.7 (2019), p. 074020. DOI: 10.1103/PhysRevD.100.074020. arXiv: 1905.07371 [hep-ph].

[217] R. Boussarie, A. V. Grabovsky, D. Yu. Ivanov, L. Szymanowski, and S. Wallon. "Next-to-Leading Order Computation of Exclusive Diffractive Light Vector Meson Production in a Saturation Framework". In: *Phys. Rev. Lett.* 119.7 (2017), p. 072002. DOI: 10.1103/PhysRevLett.119.072002. arXiv: 1612.08026 [hep-ph].

[218] Heikki Mäntysaari and Jani Penttala. "Exclusive production of light vector mesons at next-to-leading order in the dipole picture". In: *Phys. Rev. D* 105.11 (2022), p. 114038. DOI: 10.1103/PhysRevD.105.114038. arXiv: 2203.16911 [hep-ph].

[219] Heikki Mäntysaari and Jani Penttala. "Exclusive heavy vector meson production at next-to-leading order in the dipole picture". In: *Phys. Lett. B* 823 (2021), p. 136723. DOI: 10.1016/j.physletb.2021.136723. arXiv: 2104.02349 [hep-ph].

[220] Heikki Mäntysaari and Jani Penttala. "Complete calculation of exclusive heavy vector meson production at next-to-leading order in the dipole picture". In: *JHEP* 08 (2022), p. 247. DOI: 10.1007/JHEP08(2022)247. arXiv: 2204.14031 [hep-ph].

[221] G. Beuf, H. Hänninen, T. Lappi, Y. Mulian, and H. Mäntysaari. "Diffractive deep inelastic scattering at NLO in the dipole picture: The $q\bar{q}g$ contribution". In: *Phys. Rev. D* 106.9 (2022), p. 094014. DOI: 10.1103/PhysRevD.106.094014. arXiv: 2206.13161 [hep-ph].

[222] Roger Penrose. *The Road to Reality : A Complete Guide to the Laws of the Universe*. London: Random House, 2005. URL: https://www.worldcat.org/title/tthe-road-to-reality-a-complete-guide-to-the-laws-of-the-universe/oclc/1088817197&referer=brief_results.

[223] V. S. Fadin and R. Fiore. "The Dipole form of the BFKL kernel in supersymmetric Yang-Mills theories". In: *Phys. Lett. B* 661 (2008), pp. 139–144. DOI: 10.1016/j.physletb.2008.01.046. arXiv: 0712.3901 [hep-ph].

[224] V. S. Fadin, R. Fiore, and A. V. Grabovsky. "Matching of the low-x evolution kernels". In: *Nucl. Phys. B* 831 (2010), pp. 248–261. DOI: 10.1016/j.nuclphysb.2010.01.017. arXiv: 0911.5617 [hep-ph].

[225] Ian Balitsky and Giovanni A. Chirilli. "High-energy amplitudes in N=4 SYM in the next-to-leading order". In: *Phys. Lett. B* 687 (2010), pp. 204–213. DOI: 10.1016/j.physletb.2010.02.084. arXiv: 0911.5192 [hep-ph].

[226] L. N. Lipatov. "Asymptotic behavior of multicolor QCD at high energies in connection with exactly solvable spin models". In: *JETP Lett.* 59 (1994), pp. 596–599. arXiv: hep-th/9311037.

[227] L. D. Faddeev and G. P. Korchemsky. "High-energy QCD as a completely integrable model". In: *Phys. Lett. B* 342 (1995), pp. 311–322. DOI: 10.1016/0370-2693(94)01363-H. arXiv: hep-th/9404173.

[228] A. V. Kotikov and L. N. Lipatov. "Pomeron in the N=4 supersymmetric gauge model at strong couplings". In: *Nucl. Phys. B* 874 (2013), pp. 889–904. DOI: 10.1016/j.nuclphysb.2013.06.018. arXiv: 1301.0882 [hep-th].

[229] Marco Bonvini and Simone Marzani. "Double resummation for Higgs production". In: *Phys. Rev. Lett.* 120.20 (2018), p. 202003. DOI: 10.1103/PhysRevLett.120.202003. arXiv: 1802.07758 [hep-ph].

[230] Francesco Giovanni Celiberto, Michael Fucilla, Luigi Delle Rose, Gabriele Gatto, and Alessandro Papa. "High-energy resummed Higgs-plus-jet distributions at NLL/NLO* with POWHEG+JETHAD". In: (in preparation).

[231] Francesco Giovanni Celiberto and Alessandro Papa. "The high-energy QCD dynamics from Higgs-plus-jet correlations at the FCC". In: (May 2023). arXiv: 2305.00962 [hep-ph].

[232] Bo-Wen Xiao and Feng Yuan. "BFKL and Sudakov Resummation in Higgs Boson Plus Jet Production with Large Rapidity Separation". In: *Phys. Lett. B* 782 (2018), pp. 28–33. DOI: 10.1016/j.physletb.2018.04.070. arXiv: 1801.05478 [hep-ph].

[233] G. P. Salam. "A Resummation of large subleading corrections at small x". In: *JHEP* 07 (1998), p. 019. DOI: 10.1088/1126-6708/1998/07/019. arXiv: hep-ph/9806482.

[234] M. Ciafaloni, D. Colferai, and G. P. Salam. "A collinear model for small x physics". In: *JHEP* 10 (1999), p. 017. DOI: 10.1088/1126-6708/1999/10/017. arXiv: hep-ph/9907409.

[235] M. Ciafaloni, D. Colferai, and G. P. Salam. "Renormalization group improved small x equation". In: *Phys. Rev. D* 60 (1999), p. 114036. DOI: 10.1103/PhysRevD.60.114036. arXiv: hep-ph/9905566.

[236] M. Ciafaloni, D. Colferai, G. P. Salam, and A. M. Stasto. "Renormalization group improved small x Green's function". In: *Phys. Rev. D* 68 (2003), p. 114003. DOI: 10.1103/PhysRevD.68.114003. arXiv: hep-ph/0307188.

[237] Agustin Sabio Vera. "An 'All-poles' approximation to collinear resummations in the Regge limit of perturbative QCD". In: *Nucl. Phys. B* 722 (2005), pp. 65–80. DOI: 10.1016/j.nuclphysb.2005.06.003. arXiv: hep-ph/0505128.

[238] Francesco Caporale, Alessandro Papa, and Agustin Sabio Vera. "Collinear improvement of the BFKL kernel in the electroproduction of two light vector mesons". In: *Eur. Phys. J. C* 53 (2008), pp. 525–532. DOI: 10.1140/epjc/s10052-007-0481-6. arXiv: 0707.4100 [hep-ph].

[239] J. Bartels, Agustin Sabio Vera, and F. Schwennsen. "NLO inclusive jet production in k_T-factorization". In: *JHEP* 11 (2006), p. 051. DOI: 10.1088/1126-6708/2006/11/051. arXiv: hep-ph/0608154.

[240] Zvi Bern, Michael Czakon, Lance J. Dixon, David A. Kosower, and Vladimir A. Smirnov. "Four-loop planar amplitude and cusp anomalous dimension in maximally supersymmetric Yang-Mills theory". In: *Physical Review D* 75.8 (Apr. 2007). DOI: 10.1103/physrevd.75.085010. URL: https://doi.org/10.1103%2Fphysrevd.75.085010.

[241] Dung Nguyen, Marcus Spradlin, and Anastasia Volovich. "New dual conformally invariant off-shell integrals". In: *Physical Review D* 77.2 (Jan. 2008). DOI: 10.1103/physrevd.77.025018. URL: https://doi.org/10.1103%2Fphysrevd.77.025018.

[242] J.M. Drummond, G.P. Korchemsky, and E. Sokatchev. "Conformal properties of four-gluon planar amplitudes and Wilson loops". In: *Nuclear Physics B* 795.1-2 (May 2008), pp. 385–408. DOI: 10.1016/j.nuclphysb.2007.11.041. URL: https://doi.org/10.1016%2Fj.nuclphysb.2007.11.041.

[243] J.M. Drummond, J. Henn, G.P. Korchemsky, and E. Sokatchev. "On planar gluon amplitudes/Wilson loops duality". In: *Nuclear Physics B* 795.1-2 (May 2008), pp. 52–68. DOI: 10.1016/j.nuclphysb.2007.11.007. URL: https://doi.org/10.1016%2Fj.nuclphysb.2007.11.007.

[244] Andreas Brandhuber, Paul Heslop, and Gabriele Travaglini. "MHV amplitudes in super-Yang–Mills and Wilson Loops". In: *Nuclear Physics B* 794.1-2 (May 2008), pp. 231–243. DOI: 10.1016/j.nuclphysb.2007.11.002. URL: https://doi.org/10.1016%2Fj.nuclphysb.2007.11.002.

[245] J.M. Drummond, J. Henn, G.P. Korchemsky, and E. Sokatchev. "Hexagon Wilson loop = six-gluon MHV amplitude". In: *Nuclear Physics B* 815.1-2 (July 2009), pp. 142–173. DOI: 10.1016/j.nuclphysb.2009.02.015. URL: https://doi.org/10.1016%2Fj.nuclphysb.2009.02.015.

[246] L. N. Lipatov and A. Prygarin. "Mandelstam cuts and lightlike Wilson loops in $\mathcal{N} = 4$ supersymmetry". In: *Physical Review D* 83.4 (Feb. 2011). DOI: 10.1103/physrevd.83.045020. URL: https://doi.org/10.1103%2Fphysrevd.83.045020.

[247] V.S. Fadin and L.N. Lipatov. "BFKL equation for the adjoint representation of the gauge group in the next-to-leading approximation at N=4 SUSY". In: *Physics Letters B* 706.4-5 (Jan. 2012), pp. 470–476. DOI: 10.1016/j.physletb.2011.11.048. URL: https://doi.org/10.1016%2Fj.physletb.2011.11.048.

[248] Simon Caron-Huot. "When does the gluon reggeize?" In: *JHEP* 05 (2015), p. 093. DOI: 10.1007/JHEP05(2015)093. arXiv: 1309.6521 [hep-th].

[249] V. S. Fadin. "Higher-Order Contributions to QCD Amplitudes in Regge Kinematics (Scientific Summary)". In: *JETP Lett.* 111.1 (2020), pp. 1–7. DOI: 10.1134/S0021364020010026.

[250] Zvi Bern, Lance J. Dixon, and David A. Kosower. "Dimensionally regulated pentagon integrals". In: *Nucl. Phys. B* 412 (1994), pp. 751–816. DOI: 10.1016/0550-3213(94)90398-0. arXiv: hep-ph/9306240.

[251] R. Keith Ellis and Giulia Zanderighi. "Scalar one-loop integrals for QCD". In: *JHEP* 2008.02 (Feb. 2008), pp. 002–002. DOI: 10.1088/1126-6708/2008/02/002.

[252] K. S. Kölbig. "Nielsen's Generalized Polylogarithms". In: *SIAM Journal on Mathematical Analysis* 17.5 (1986), pp. 1232–1258. DOI: 10.1137/0517086. eprint: https://doi.org/10.1137/0517086. URL: https://doi.org/10.1137/0517086.

[253] Mikhail Yu Kalmykov. "Gauss hypergeometric function: reduction, ϵ-expansion for integer/half-integer parameters and Feynman diagrams". In: *Journal of High Energy Physics* 2006.04 (Apr. 2006), pp. 056–056. DOI: 10.1088/1126-6708/2006/04/056. URL: https://doi.org/10.1088%2F1126-6708%2F2006%2F04%2F056.

[254] Victor S. Fadin and D. A. Gorbachev. "Nonforward color octet BFKL kernel". In: *JETP Lett.* 71 (2000), pp. 222–226. DOI: 10.1134/1.568320.